12th International Conference on
Management of Innovative Technologies
&
4th International Conference on
Sustainable Life in Manufacturing

General sponsors

22nd-24th of September 2013, Fiesa - Slovenia

Proceedings of the

12th International Conference on

Management of Innovative Technologies

&

4th International Conference on

Sustainable Life in Manufacturing

MIT&SLIM 2013

Fiesa, Slovenia
22th – 24th September 2013

Editors:

Mihael Junkar
Janez Kopač
Paul R. Levy
Oguz Colak

Title:	Proceedings of the 12th International Conference on Management of Innovative Technologies and 4th International Conference on Sustainable Life in Manufacturing, MIT&SLIM 2013	
Editors:	**Mihael Junkar**,	University of Ljubljana, Slovenia
	Janez Kopač,	University of Ljubljana, Slovenia
	Paul R. Levy,	University of Brighton, UK
	Oguz Colak,	Süleyman Demirel University, Turkey
Programme committee:	**D. Kramar, J. Valentinčič, M. Jerman**, University of Ljubljana, Slovenia.	
Organizers:	**TAVO**, Slovene Society for Abrasive Water Jet Technology, Slovenia **Laboratory for Alternative Technologies**, Univ. of Ljubljana, Slovenia **Laboratory for Cutting**, Univ. of Ljubljana, Slovenia **CAD/CAM Reseach and Application Center**, Suleyman Demirel University (SUD), Turkey **Centre for Research in Innovation Management**, University of Brighton, UK	
General sponsors:	**BHDT**, Austria **SECO Tools**, Slovenia	
Sponsors:	**BTS** Company, Slovenia **TEXIMP**, Slovenia **TITAN**, Slovenia	
Design:	**D. Kramar**, **M. Jerman**, University of Ljubljana, Slovenia.	
Publishers:	**TAVO** - Slovene Society for Abrasive Water Jet Technology, Slovenia, **LAT** - Laboratory for Alternative Technologies, Univ. of Ljubljana, Slovenia. **LABOD** - Laboratory for Cutting, Univ. of Ljubljana, Slovenia.	
Note:	This is an extended version of the conference proceedings published only in digital form and distributed on USB keys.	

CIP - Kataložni zapis o publikaciji
Narodna in univerzitetna knjižnica, Ljubljana

005:001.895(082)
621:502.131.1(082)

INTERNATIONAL Conference on Management of Innovative Technologies (12 ; 2013 ; Piran)
MIT & SLIM 2013 [Elektronski vir] : proceedings of the 12th International Conference on Management of Innovative Technologies & 4th International Conference on Sustainable Life in Manufacturing, Fiesa, Slovenia, 22th-24th September 2013 / [organizers TAVO Slovene Society for Abrasive Water Jet Technology ... et al.] ; editors Mihael Junkar ... [et al.]. - Ljubljana : TAVO - Slovene Society for Abrasive Water Jet Technology : LAT - Laboratory for Alternative Technologies, Faculty of Mechanical Engineering : LABOD - Laboratory for Cutting, 2013

ISBN 978-961-6536-67-7 (Fakulteta za strojništvo)
1. Gl. stv. nasl. 2. Junkar, Mihael 3. International Conference on Sustainable Life in Manufacturing (4 ; 2013 ; Piran) 4. TAVO, Društvo za tehnologije abrazivne in vodne obdelave (Ljubljana)
269878528

The Editors and the Conference Committee believe that the subject of the papers to be presented are in line with the objectives of the conference, but it is not responsible for any data or any other information dispensed in the Proceedings.

All papers have been peer reviewed by the members of Scientific Committee.

Preface

Previous MIT (Management of Innovative Technologies) - SLIM (Sustainable Life in Manufacturing) have seen world economic boom and subsequent collapse. Our conferences have explored technological innovation and technology management from multi-disciplinary perspectives. That has been the unique contribution of our previous eleven conference - bringing together academics and practitioners from different fields to exchange ideas, knowledge and experience that can impact significantly on cross-disciplinary research and also stimulate innovation in practice.

Human factors, "technosophy" (the wise application of technology) and sustainability have been key areas of interest for many of the conference's contributors and now, as we announce our call for contributions to the 12th MIT and 4th SLIM Conference in 2013, in a year of continuing global recession, financial and environmental challenges, our conference seems as relevant and important as ever.

In the beautiful setting of Fiesa, Slovenia, bordering with Croatia and Italy and within driving distance of many other countries, we are glad our conference sits as the borderland of different cultures, just as our program sits at the border of different disciplines, interests and perspectives. This year we welcome contributions that address regeneration in times of recession. We welcome contributions that examine the role of technological innovation in the development of sustainable businesses, organisations, communities and economies.

It is our hope that the conference will generate insights that will directly contribute to our emerge from economic crisis, in our respective sectors, industries, economies and as a world community. We welcome case studies and stories, as well as sessions which, may lead to inter-disciplinary research.

Mihael Junkar

Paul Levy

Janez Kopač

Oguz Colak

International Scientific Committee:

Chairmen:

Mihael Junkar	University of Ljubljana	(Slovenia)
Janez Kopač	University of Ljubljana	(Slovenia)

Co-Chairmen:

Oguz Colak	Suleyman Demirel University	(Turkey)
Paul Levy	University of Brighton	(UK)

Members:

Samuel Bigot	Cardiff University	(UK)
Giuliano Bissacco	Technical University of Denmark	(Denmark)
Halil Caliskan	University of Bartin	(Turkey)
Costel Emil Cotet	University “Politehnica” of Bucharest	(Romania)
Franci Čuš	University of Maribor	(Slovenia)
Stefan Dimov	Universty of Birmingham	(UK)
Anselmo Diniz	University of Campinas, São Paulo	(Brazil)
Davorin Kramar	University of Ljubljana	(Slovenia)
G. Lakić-Globocki	University of Banja Luka	(Bosnia & Herzegovina)
Gorazd Lampič	University of Ljubljana	(Slovenia)
Andrej Lebar	University of Ljubljana	(Slovenia)
Cédric Masclet	University of Grenoble	(France)
Henri Orbanić	University of Ljubljana	(Slovenia)
Frank Pude	University of App. Sci. NW Switzerland	(Switzerland)
Franci Pušavec	University of Ljubljana	(Slovenia)
Maria H. Robert	University of Campinas	(Brazil)
Joel Rech	University of Lyon	(France)
Alojz Sluga	University of Ljubljana	(Slovenia)
Milenko Sekulić	University of Novi Sad	(Serbia)
Mirko Soković	University of Ljubljana	(Slovenia)
Franz Trieb	BHDT GmbH	(Austria)
Joško Valentinčič	University of Ljubljana	(Slovenia)
Sencer Yeralan	University of Florida	(USA)

Organizing committee:

Mihael Junkar (Slovenia)
Janez Kopač (Slovenia)
Oguz Colak (Turkey)
Paul Levy (UK)
Davorin Kramar (Slovenia)
Marko Jerman (Slovenia)
Joško Valentinčič (Slovenia)

Content

SESSION 2B

Process modelling and measurements

Method of measuring the water jet diameter
J. Gil Cano, A. Lebar, M. Jerman

Modelling of the main cutting force in high-pressure jet assisted turning process by genetic algorithm
V. Pucovsky, D. Kramar, M. Sekulić

A Novel Method for Material Machinability Evaluation
B. Sredanović, G. Globočki - Lakić, Đ. Čiča, S. Borojević

Further development of the spatial cutting tool wear measurement system
L. Čerče, F. Pušavec, J. Dugar, J. Kopač

3D foot surface scanning for the purpose of foot orthotics production
K. Obrovac, T. Udiljak, J. Vuković Obrovac, J. Nižetić, A. Mutka

An investigation into roller burnishing process
B. Žabkar, J. Kopač

SESSION 3

Industrial session

Mass production of the Step Lock Bolt
N. Sase, T. Takahashi, K. Tamura

SESSION 4A

Innovative technologies

Electronic component cleaning by supercritical CO2
M. Bauer, S. Schweinstig, S. Thäter, R. Steinhilper

Radio Frequency Communication – A new (service-) interface for electronic control units
R. Steinhilper, J. Kleylein-Feuerstein, A. Reger

Numerical simulations: An Indispensable Tool in Piezoelectric Micropumps Research
B. Pečar, D. Križaj, D. Vrtačnik, D. Resnik, M. Možek, U. Aljančič, T. Dolžan, S. Amon

Process chain for microreactor monomere replication in polymer
I. Sabotin, J. Valentinčič

Design of vario-therm tempering systems for injection moulding of micro-parts
D. Kobold, A. Glojek, A. Hančič

SESSION 4B

Advanced technologies

Powerled Life Test System
B. Uslu, İ.S. Üncü

Chip Formation Analysis of High Pressure Jet Assisted Machining of Ti6Al4V
L. Yunlu, O. Çolak, C. Kurbanoğlu

Experimental Study on Machinability of AISI H13 Tool Steel
B. Yalcin, K. Kıran, E. Aykan, O. Çolak

Feeding the ultrasonic devices used in boats with solar energy by using logic switching method
R. Abdulla, F.G.K. Abdulla

Technologies for tube sampling in nuclear power plant heat exchangers
J. Valentinčič, M. Resnik, M. Frankovič

Application of Vortex tube for tool cooling
M. Duspara, B. Kosec, M. Stoić, D. Kramar, A. Stoić

Burr Formation after Face Milling of Compacted Graphite Iron used in Diesel Engine Blocks
M.O. dos Santos, G. F. Batalha, M. Stipkovic Filho, E. C. Bordinassi

Groove rolling of a round bar
T. Pepelnjak, S. Štarkel

Keynote lectures

An Exploration of the Dimensions of Conscious Business and Consideration of The Notion of Toxic Business Consciousness

Paul Levy, Senior Lecturer, CENTRIM, University of Brighton UK

and

Professor Mihael Junkar, Faculty of Mechanical Engineering, University of Ljubljana, Slovenia

Abstract

This discussion paper draws upon two years' research into the field of Conscious Business. The paper attempts to elaborate the dimensions of a conscious business, describing the elements of a business that claims to be conscious. Conscious Business is a term that has increasingly developed out of the Conscious Capitalism movement and the sustainable business field. This paper takes a more neutral look at consciousness in business and also explores the more radical phenomenon of toxicity in business consciousness.

Introduction

There are a vast number of definitions of consciousness. In science, consciousness is a function of the brain. In metaphysics and the "New age" movement, the brain is an element or even a function of consciousness! Explanations abound, and it is easy to get lost in the mire of thought and application. The scientific establishment is disdainful of anyone who claims consciousness exists beyond the brain and there is even a growing view that consciousness itself is a kind of functional illusion created by chemical and electrical brain activity. The self, apparently, is an illusion. (See here. And here. And here).

"Conscious" Business would suggest that a business can be more or less conscious, and can behave in more or less and different ways. So, the definition of what conscious means is rather important.

In the currently established view of "conscious" in conscious business, the definition tends to suggest that a more conscious business takes into account social, ethical, and environmental issues that is was previously less conscious off. So a more "conscious" business is more aware of its social, ethical and environmental responsibilities. This then modifies its approach to the practice of capitalism rendering it into a more "consciously capitalist" organisation.

So, in this definition, a conscious business is a better corporate citizen in a way that a more conscious neighbour is one who is more aware of the impact of the noise they make on neighbours, or in a way that a child is a more "conscious" child when he or she stands up for an elderly person on a crowded bus. In the mainstream of Conscious Business, consciousness is about waking up to one's social responsibility. Being aware only of the process of money making is a "Lower" or "lesser" form of consciousness. Being aware of issues beyond the process of pure money making is viewed and defined as being of 'higher' or 'greater' consciousness.

As a result of this, conscious business tends to sit mostly in the fields of "green" behaviours, as well as corporate and social responsibility, and also in the field of more human-centred approaches to management, leadership and organisation.

From a more “pure” conceptual view, this is a kind of benevolently intended misuse, or perhaps partial use of the term “conscious”. Indeed, most of the philosophical, scientific and even esoteric definitions of consciousness do not top slice the definition of the word conscious and then claim it as the sole territory of the “good”. In scientific definitions, consciousness is either value-free or beyond value. Consciousness is a state of awareness, awakeness, alertness. It is a state in which sensory data is optimised through a combination of accurate sense perception and clear cognition. In many new age philosophies, the natural state of the universe is “good” or benevolent, and when consciousness is raised it realises this in itself, and this self-realisation is a realisation of one’s duty to do the good, as this harmonises with natural law. At the other, more socially Darwinistic extreme, doing the good is functionally useful to survival, and nothing more. There’s huge diversity of view, much disagreement, and little or no proof one way or the other.

The Narrow Focus on Conscious Business as Sustainability and Social Responsibility.

It doesn’t surprise us that “conscious business” has been defined in terms of social and ethical responsibility because:

1. This is a neat definition

2. This is a nice new badge for the ailing fields of “green” and corporate social responsibility

3. The recent global meltdown is being described as a failure of capitalism, pointing to a lack of consciousness of all factors, especially in the banking sector.

What interests me, is that, whether one takes an esoteric/metaphysical view or a natural scientific/materialistic view of consciousness in business, a number of useful dimensions can be identified which fit well with a benevolent, “goodness”-based definition, and also something much broader where consciousness is simply a form of heightened awakeness and awareness.

There are some of the dimensions I’ve identified so far. Most, if not all, a transpositions of consciousness in a human being. The main difference is that in a business, consciousness can vary in extent and quality in different parts of the business. Often the leaders are seen as the “head”, but this metaphor only works partly, especially in highly networked and fluid business structures. Here, the head can move location, within and even outside of the main body!

The Dimensions of consciousness in a business

One can view consciousness in business along a number of dimensions. These dimensions can view business consciousness in terms of…

1. A state of being awake or asleep

Positive: The business is fully aware of internal and external dynamics and is energised to proact and react

Negative: The business remains in a state of unchange, cut off what either experience or decision-making

2. A state of awareness or ignorance

Positive: The business is aware of all internal and external dynamics and may also be aware of its sleep state

Negative: The business is ignorant of internal and external dynamics and isn't even aware it is in a state of unchange

3. A state of high or lower sense of alertness (hearing, seeing, touching etc)

Positive: The business has high and clear visibility of its internal and external dynamics through clear and real time pictures and data

Negative: The business lacks visibility with no clear vision, data on performance and in a way is working blind or blurred

4. A state of broad or narrow focus, deep or surface focus

Positive: The business is aware of its broad context but is also able to reach root causes and focus and prioritise when necessary on what needs to be done

Negative: The business either too generalist and superficial, or has become fixated on one market, one product or one strategy

5. A holistic or partial awareness

Positive: The business has a clear awareness of the whole system, and how it fits into the "big picture", The business can take a helicopter view and adapt as necessary based on that view

The business has a bias on its leadership team – for example an over-focus on marketing at the expense of product development and innovation. The business is "biased" in a way that distorts its ability to gain objective overview.

6. A clear or blurred view

Positive: The business has a culture of truthfulness based on honesty and accurate information. Data is real time and logical thinking works in partnership with insight and intuition.

Negative: The business has distorted information systems, out of date or not properly collected data and analysis. Subjectivity is often mistaken for fact.

7. A high to low degree of self-awareness

Positive: The business is aware of its core motives and values. It knows that is motivating it and how its historical and present biases impact on it. It knows the difference between forecasting and wishful thinking.

Negative: The business's motives are often hidden from it, sometimes by interest groups, sometimes because the business is simply superficially reactive or has confused "spin" with core values.

8. A state of primitive or childish versus evolved or adult consciousness

Positive: The business is able to be patient, to give and take criticism, to make informed decisions, to learn from failure and to commit over the long term. The business has awareness of its place and impact around it in the social and environmental space around it.

Negative: The business is naive, often reacts on emotion rather than knowledge and a contextualised need. It's view of profit and growth is short term and superficial. It sees business as war. The business can even sulk and block when criticised. The business is centred mostly on itself, ignorant of its impact socially and environmentally except it ways that benefit it narrowly

These are tentatively written dimensions and I'll be developing them further over time.

A conscious business can therefore be described differently based on the underpinning definition of the word 'conscious'. Personally, I feel the view of conscious as "green and good" is too narrow and limiting. It is possible to be conscious and to be neither green nor good. But if we do want to be green and good, it helps to be conscious along the above dimensions.

Further exploration - Going Deeper and Darker

One of the unique aspects to the definition of conscious business we presented earlier is that a business can be highly conscious and be hugely damaging, cynical and even corrupt.

The mainstream definitions of conscious business take a view that being "conscious" means being benevolent, and it isn't surprising that the words "ethical" and "sustainable" are attached to many "conscious" businesses. So, a conscious business is one that is more socially and ethically aware and applies these into a more "conscious" approach to what they do. In essence, a conscious business is a "conscience business"!

This is a very laudable approach because the use of the term conscious to signify social responsibility is a timely and needed antidote to much of the greed, socially and environmentally insensitive, win-lose-obsessed capitalism that has brought about the recent global economic collapse. Greed is seen as short-term, short-sighted, and ultimately narrow-minded. A conscious business improves its awareness by improving its behaviour! Essentially the organisation wakes up to itself and its social responsibility and impact.

And yet it is quite possible to be very aware of one's actions that are harmful of others. In literature, in film, in religious and mythological traditions, the "devil" is a very conscious being – clever, sharp and aware of all the scenarios. True, some businesses lack consciousness when they behave unethically, but others are very sharply conscious, aware of all the variables, impacts, and even the laws they are breaking, and still they decide to act, cleverly managing and masking those actions. A conscious business can be good or evil.

So, when a business reaches a high level of consciousness, it could be playing the law in ways that undermine the spirit of that law, manipulating customers, suppliers, employees and stakeholders in all kinds of damaging ways that maximise its own profits. It can be spinning the truth into a tissue of clever, within-the-law (or not) lies, it can be playing one group off against another, it can even be cheating, creating addiction and dependency, polluting and distorting, all by design, all as part of a set of highly self-aware conscious choices.

A business can be highly conscious and using that consciousness to become a good citizen in the local or global economy. Or it could be deploying that consciousness in devilish ways that poison humanity, leaving it, as a corporate being, largely untouched and unharmed in at least the medium term. A conscious business can be nourishing or toxic for its stakeholders. It may even know that part of its toxic behaviour is also poisoning itself, but has developed clever and smart defences and ways of ensuring it remains largely able to continue. This is the key issue. The dominant view of conscious businesses sees consciously unethical behaviour as being ultimately a sign of lack of consciousness because, in the end, it was all come back on the corporation engaging in unethical activity. Not always so. The genius that come with high consciousness can allow corporate entities to develop that can become very resilient to their own partly self-inflicted toxic behaviour. They can bear court cases, customer backlashes in the short-term, employee rebellions, and still continue in the long-term. They know how to take the hit for a longer term self-beneficial game plan.

So, in our model of conscious business, we do not see "goodness" or "sustainability" as in input to the model. It is a possible output – but not always. Increasing business consciousness can indeed raise awareness in a corporation of the impact of its actions on its communities in ways that make it modify its behaviour to be more benevolent. But, equally, it can wake up a business to its potential to become sharply and cleverly poisonous in ways that can maximise profit. Examples include creating entanglement and addiction in customers and employees, suppliers and collaborators. It can pollute environments in ways that leave it legally untouched at least for years) and can also pollute minds with half-truths, manipulative messages and processes which corrupt aspects of its value chain into helping it to maximise profit and minimal cost to itself. And it remains entirely and deeply self-aware of what it is doing.

So, our model can begin to audit the level and quality of consciousness in a business. But a new dimension is also added that attempts to identify the toxicity of that consciousness in terms of its impact on its internal and external stakeholders. It isn't enough to sat a conscious business is a good business. Too many sharply toxic and very conscious businesses know very well how to dress up that toxicity as benevolence. There are already some emerging definitions of toxic business. See Forbes, for example, which focuses on a toxic business as one of weak culture, distortion and lacking in truth (I'd call that a particular form of poison that weakens and starves of truth). Fast Company view toxic business as one that is a poor employer and which has a cold philosophy. In both cases the toxicity arises out of a certain lack of consciousness. A more academic viewpoints to the self-poisoning that can happen at the top of the business: "Egocentric, or "narcissistic" managers can easily perpetuate a self-reinforcing pattern of behavior, one in which the conquered subordinate is transformed into an enabler, or an obsequious follower who willingly serves the boss." (Reference here.). The authors contrast toxicity with "collaboration". Collaboration tends to reduce toxicity. Of course, but only if that collaboration is genuine and not a smokescreen for skilled, conscious, underlying toxic behaviour such as hidden agendas and manipulation.

There's a simple checklist for a toxic workplace here, which ranges across conflict, poor management and demotivated employees. Once again, the definition doesn't take in the possibility that the highest form of toxicity is the Monkshood of management and leadership – the poisonous behaviours that can't be detected. The issue here is that, in some very conscious businesses, toxic behaviours are designed, and are specifically designed to be undetectable.

Here are a few of my own, admittedly anecdotal, examples of conscious toxic business behaviour (where consciousness here refers to being aware of both behaviour and motive in the actor, who still decides to proceed with the action):

* the poisoning of minds through direct deception, distortion and economy with the truth

* the poisoning of human bodies and physical environment through the distortion of product, service or process description and performance feedback

* the starvation of people, environment, or process in ways detrimental, in ways that are undetectable- this can include greed with resources, but also starvation of choice or of information that can create a greater sense of freedom of thought, feeling of action

* the manipulation of the behaviour of others in ways that harms their physical or mental well being – employees, customers, suppliers, stakeholders (for example, create fear in employees who work beyond their paid hours in order not to get fired or have their "card marked" – this is often dressed up as "ambitious leadership"

* the exploitation of work forces or customer groups in ways that harm their physical, mental or social well being in ways that also "spin" legality

* the creation of collusions of mediocrity where openness and honesty are framed always a dysfunctional behaviour and "troublemaking", thus starving people and situations of truthfulness

* the creation of entanglement through contracting and pressured expectation that leaves employees feeling imprisoned at work, customers and suppliers tied in ways that make them feel "chained". Conscious businesses often frame this cleverly as "benevolent" entanglement.

* the creation of technological, future shock, putting people into trance states where lack of understanding and lethargy create zombie-like compliance, and where they feel overwhelmed by technological change that leaves them feeling drained by apparent choice and information overload

Just as physical poisoning involves the introduction of substances harmful to the human being into it, toxic business can involve the physical poisoning of people and environments. But it can also involve the creation and implementation of systems and business processes that starve people and groups of truthfulness, poison minds and understanding, manipulate truth, hide one process or substance as another, to pretend something is beneficial when it is harmful, to create lethargy, addiction and paralysis, to engender conflict via manipulation and distortion. And also to create stress and pressure that harms humans in ways that could have been avoided. Toxic business is a new variable in highly conscious businesses. Of course, a business can be very low in consciousness and be toxic. It can also be non-toxic! Here the focus is on the fact that with self-awareness comes responsibility, but also comes the possibility and potential to abuse that newly won consciousness and to become toxic – poisonous to the "other".

So, our model tries to measure and assess consciousness, but it also adds the possibility of an extra dimension – the toxicity of the conscious business.

And what then, if anything, can be done?

The most conscious toxic businesses will be attempting to fly under the radar of detection. They will be skilled at lowering the consciousness of individuals, groups, even whole communities around them so that the poison remains undetected, ideally in perpetuity. Here detection becomes about legal investigation, of “smoking out”, of “outing”, of bringing that which is hidden out in the open – naming the devil with evidence. And, like Moriarty, the most conscious toxic businesses will be a match even for Sherlock Holmes himself. But here, detoxification has to come from confrontation.

There will also be conscious and toxic businesses who, though highly conscious businesses, have started to self-poison. Here the toxicity turns in on the organisation. The business, for example, can start to believe its own lies, and public scandal or even physical disasters such as an oil spill or a train crash can then force the toxicity out into the gaze of public inquiry. Here detoxification comes from scrutiny and public exorcism.

There will then also be highly conscious businesses who have elements within (shareholders, certain leaders and influencers) and also from outside who (consultants, the media and customer groups) who start to draw attention to the worst elements of the toxicity. The business may go into internal conflict as certain toxic behaviours are outed as unacceptable. Here the business needs to shift towards a wish to detoxify. This can arise from customer protest, from a public scandal or an accident that snaps the business out of its one form of sleep – the sleep in which it isn’t entirely aware of its toxic impact. Here the moral conscience awakens in all or part of the leadership in a kind of Ebeneezer Scrooge-like awakening. It can still be that the really toxic conscious business pretends at moral awakening in order to minimise damage to profits over the longer term. Often apparent changes in behaviour simply revert and fade back to toxicity over the longer term game. But some companies will detoxify through moral purging and specific changes to values, policies and practices, with independent scrutiny or external and internal validation. The business transforms to become benevolently conscious rather than toxically conscious.

It all boils down to whether the business is aware of its deepest motives for action. If these motives are based purely on profit at ANY cost, then the toxic business will simply attempt to continually enhance its consciousness in order to maintain its profits and growth, leveraging toxicity always to that end. It will only behave benevolently when this serves short term profitability, never from an authentically experienced sense of a wish to do the good without being toxic. It will even play the game of ethics, social responsibility and environmentalism, but purely as a calculating move in its game to maximise its own economic power and resource achievement. But where there is even a hint that the toxic behaviour isn’t entirely intended, and that a critical mass of people inside the business are only behaving in toxic ways out of fear, trance or manipulation, then there are seeds for a possible shift to detoxification. But it might take massive intervention to achieve that. And sometimes it needs only a minimal intervention that sends the whole toxic tower of cards crashing down.

Source Material

http://consc.net/online
http://consc.net/online/8.3b
http://www.quantumconsciousness.org/documents/fnint-06-0009321.pdf
http://sciwrite.org/glj/reviews.dennett.html
http://rationalmadness.wordpress.com/treasures/conscious-business-realm/

Improving the over-all efficiency of mold and dies by functionalizing surfaces

F. Bleicher[1], C. Lechner[1], M. Obermair[1], C. Habersohn[1]

[1] *Vienna University of Technology, Institute of Production Engineering and Laser Technology, Vienna*

Abstract

The process of machine hammer peening (MHP) is based on an actuator, which moves an axially guided carbide metal ball with an oscillating motion to a workpiece surface. This actuator could be attached to any kind of machine tool, even to a robot. Due to well-directed impacts it is possible to structure and modify the material and its surface in various ways. The surface treatment by machine hammer peening can be applied in order to functionalize surfaces made of different materials. Especially in mold and die making high potentials can be found by improved tribological properties. The main positive effects of machine hammer peening are the induction of compressive residual stresses, the hardness increase of the upper surface layer and a reduction of surface roughness up to mirror-like qualities. Furthermore an embedding of WC-particles into the near-surface zones of tool steel materials can be realized, which offers new possibilities to improve the tribological performance of components.

Keywords: Cold forming, surface modification, machine hammer peening.

1 Introduction

Modern tool and mold making comes along with an increasing cost and pricing pressure. Due to globalized markets it is necessary to reduce the manufacturing throughput time dramatically. Contrary the industry and its customers demand for higher geometric accuracy and surface quality of tools [1]. As a consequence toolmakers are forced to look for new innovative technologies.

As illustrated in Fig. 1 (see [2, 3]) the conventional process chain of tool and mold making starts with rough milling, pre-finishing and finishing operations. Subsequently these milling operations are followed by a hardening process. Typically the tool surface gets a final finishing to achieve the requested surface quality (see Fig. 1c). The latter is mainly done by manual operation. Machine hammer peening (MHP) can be used to widely substitute the time-consuming and cost-intensive surface finishing operation [4]. By adjusting the MHP process parameters (see Fig. 2c and Tab. 1) appropriately it is possible to influence the surface quality and the functionality of tools and molds in order to achieve either polished-like surfaces or an enhanced wear resistance.

The process itself is based on the oscillating motion of an axially guided plunger [3, 4, 5]. The actuator can be attached to a machine tool or even to a robot. Due to the NC-controlled positioning of the hammering tip it is possible to machine the surface by well-directed impacts (Fig. 2b).

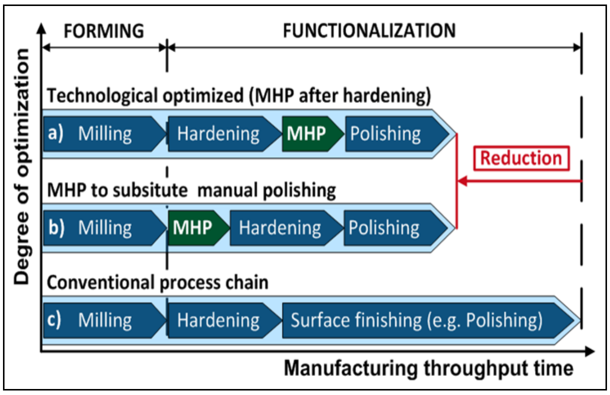

Figure 1 Optimization of the production process chain in the tool and mold making by the use of MHP of hardened materials

Especially tool and mold makers have to deal with the machining of free-form surfaces. Processing complex surface topographies by MHP requires non-orthogonal hits. Thus the system behavior has to be investigated. Besides the surface burnishing effect, experimental results show a significant increase in hardness and the implementation of compressive residual stresses into the near surface areas. This will lead to an increase in wear resistance, particularly if MHP is performed after thermal hardening. Consequently higher tool life can be expected. This paper is based on experimental tests to show the influence of orthogonal and non-orthogonal MHP hits and their effect on the surface roughness as well as on the increase of the material´s hardness in the surface near area. Further investigations presented in this paper show that MHP offers an additional new field of application. Tungsten carbide powder has been processed into the surface of a 1.2379 tool steel material. This functionalization can be used to enhance the abrasive wear resistance of tools.

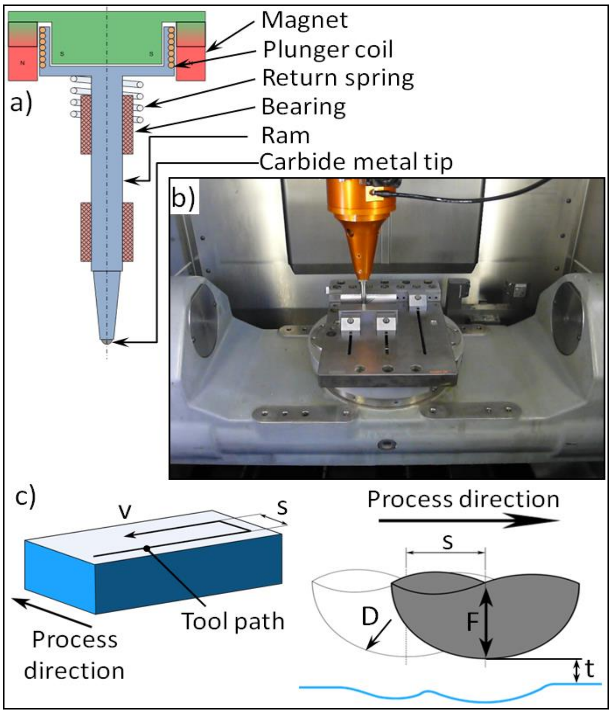

Figure 2 Technology of machine hammer peening: a) Design of the electro-magnetic actuator, b) Experimental set up at a Hermle 5-axis machining center, c) Illustration of important process parameters (described in Tab. 1).

Table 1 Adjustable process parameters.

Parameter	Unit	Description
Diameter D	[mm]	Diameter of the spherical plunger tip
Distance t	[mm]	Distance between surface and plunger tip, equivalent to impact energy
Side Step s	[mm]	Distance between two MHP tool paths
Frequency F	[Hz]	frequency of the oscillating movement
Feed Rate v	[mm/min]	provided by the machine tool

2 Experimental Work

In order to derive a comprehensive understanding of the mechanism for surface modification by MHP and to be able to verify the applicability of this technology various experiments have been carried out. The experimental results of these investigations will further be used to validate process models. The electro-magnetic actuator system is able to provide an operating frequency up to 500Hz. To perform the experiments the actuator was attached to a Hermle C20U five axis milling machine (see Fig. 2b).

2.1 Surface modification

In order to determine the mechanism of surface modification single peening lines of different length have been machined with various side step values (0,1 mm, 0,3 mm and 0,5 mm) on a C45E (1.1191) specimen. The distance t used for accelerating the ram and therefore equivalent to impact energy has been varied in a range of 0,2 mm up to 1,2 mm using a sphere diameter of 8 mm. The surface topography of the specimen has been measured by the 3D-measurement device Infinite-Focus (Alicona). Based on these results profiles could be extracted (Fig. 5). Thus it was possible to calculate the differences in areas of material after each line and get an overview of the material displacement process.

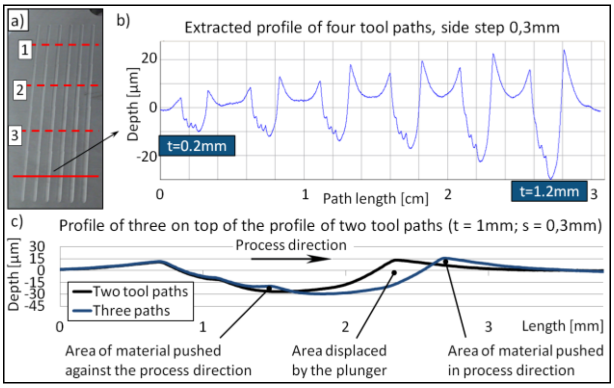

Figure 3 Evaluation of single peening lines: a) Measurement positions to extract the profiles of a single tool path (1), two (2), three (3) up to four tool paths, b) Extracted profile of four tool paths with given side step of 0,3mm (peening distance t is varied from t = 0,2 mm on the left up to t = 1,2 mm on the right), c) Arrangement of two profiles to calculate the difference in areas of material.

Regarding the cross section view it is evident that the material displaced by the plunger tip is pushed in as well as against the process direction. The direct dependency of the peening distance *t* and the impact energy could be observed (Fig. 3b). The measurement of the difference in areas illustrates that the material distribution directly depends on the chosen side step *s*. Because of the observed back flow displaced workpiece material partly fills up the previous tool path line.

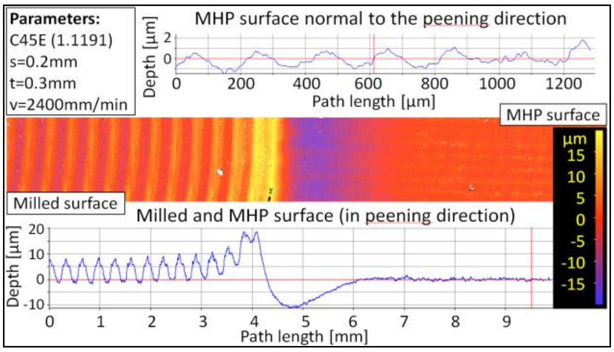

Figure 4 Measured surface topography and extracted profiles.

Due to this effect it is possible to optimize the process parameters in order to get hardly any difference in height between a peened and an unpeened surface as can be presented in Fig. 4. These results could be obtained by using a sphere diameter of 8 mm and reduced impact energy.

2.2 Residual compressive stresses

The physical state of high-duty workpieces has to be described precisely. This includes the knowledge of residual stresses in the component and especially in its surface layers [6]. However, the investigation of compressive residual stresses induced by the MHP process has been a main focus of the experimental tests.

To answer the questions, whether the induction of residual stress shows work-direction dependency or multiple machining can increase the induced residual compressive stress, a milled C45E (1.1191) specimen was machined in different directions one and in parts two times (Fig. 5).

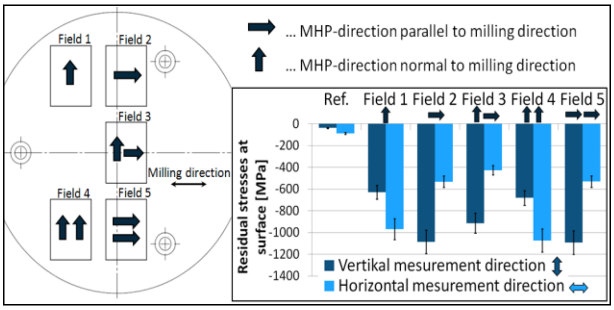

Figure 5 Specimen with different machined fields and results of the residual stress measurement.

The X-ray diffraction method was used to measure residual stresses at the surface of the investigated areas and the milled reference surface. Fig. 5 shows a significant induction of compressive residual stresses in each machined field. An increase of stresses induced by a second peening step could not be observed. Moreover the measured data indicate that the value of compressive stress induced in a specific direction depends on the peening feed direction. The residual compressive stress induction normal to the peening direction is higher than in peening feed direction. As the evaluation of field 3 in Fig. 5 shows, the peening direction of the last peening step determines the final distribution of induced residual stresses.

2.3 Surface burnishing

Another focus is the investigation of the surface topography and roughness depending on the chosen process parameters. During a number of experiments the influence of the main process parameters could be identified. As an example Fig. 6 shows the influence of the feed rate.

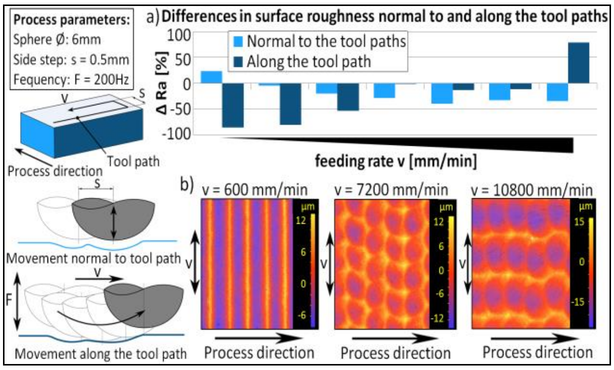

Figure 6 Surface topography depending on the feed rate v: a) R_a-value difference of the hammer peened surface expressed as a percentage of the initial R_a-value of the milled surface measured in the given direction, b) Measured surface topographies (10x magnification).

In the presented experiment the feed rate has been varied in a range of 600 mm/min up to 10.800 mm/min to machine the surface of a C45E (1.1911) specimen with a preliminarily face milled surface. Based on the investigations of surface topography and using the presented hammering parameters it could be observed that the material is mainly pushed to the side of each tool path.

In reference to the tests in Fig. 5 the resulting surface topography shows nearly the same characteristics as the surface illustrated on the left side of Fig. 6b (v = 600 mm/min). It can be assumed that a massive material displacement normal to the peening direction causes a higher induction of residual stresses. The surface roughness normal to and along the hammering tool path was evaluated by the use of the tactile roughness measurement device MahrSurf PS1. Later on the changes in surface roughness between each hammered and the milled reference surface have been calculated for both directions and are given in Fig. 6a.

Furthermore different surface topographies have been observed by the use of the 3D surface measurement device Infinite-Focus (Alicona). Three investigated topographies are shown in Fig. 6b, where a significant direction depending difference of the R_a-values measured normal to and along the tool paths can be observed. Regarding the results of the surface measurements it has to be concluded that this phenomenon cannot be explained by a stiffness problem due to a bearing clearance of the hammering device as presented in [4]. The 3D surface measurements (Fig. 6b) show that the side step between the tool paths is constant and very accurate with reference to the obliged value of the side step parameter. The observed differences clearly depend on the chosen feed rate and consequently on the distance between the single impacts along the tool path.

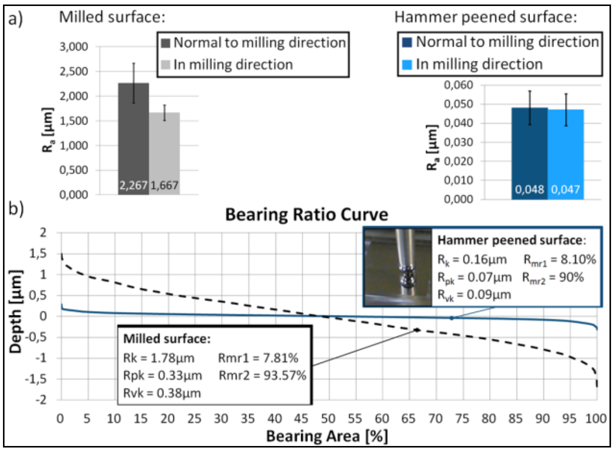

Figure 7 Evaluation of surface roughness in X3CrNiMo13-4: a) R_a-values of the surface before and after hammer peening (average value and deviation of six single measurements), b) Bearing ratio curve before and after machining measured with the measurement device Infinite-Focus (Alicona).

Table 2 Process parameters applied in pre-machining and in MHP process steps, using a frequency F = 200 Hz and sphere diameter D = 10 mm

Pre-machining parameters	1st peening step	2nd peening step
End milling cutter: Ø16 mm	side step: 0,2 mm	side step: 0,05 mm
Spindle speed: 1592 rpm	distance t: 1,2 mm	distance t: 0,2 mm
Feed rate v: 509 mm/min	v: 2400 mm/min	v: 600 mm/min

Further results reveal that apart from the feeding rate the sphere diameter of the plunger tip, the side step between the peening paths and the impact energy depending on the surface/hammer-tip distance *t* are significant parameters for surface refinement. As an example for the capabilities of MHP technology in surface refinement Fig. 7 shows the differences between a milled and a hammer peened surface of an X3CrNiMo13-4 (1.4313) specimen. After peening using a two steps process even a surface roughness value of $R_a < 0{,}05$ µm for both directions (normal to and in direction of the previous milling step) could be determined.

2.4 Non-orthogonal alignment

The investigations were performed on X155CrVMo12-1 (1.2379) tool steel samples. This type of highly alloyed tool steel is characterized by an increased strength and wear resistance and therefore used in a wide variety of tool making applications.

Typical applications include punching and blanking dies for stainless steel sheet metals, brass, copper, zinc and hard abrasive materials in general. Other applications suitable for this tool steel include deep drawing dies, cupping and forming dies. As a reference material again plain carbon steel C45E (1.1191) was tested for the conducted force and acceleration measurements. Both materials were investigated in unhardened and hardened conditions. Tab. 3 and Tab. 4 show the chemical composition and the mechanical properties of the investigated materials.

As part of previous investigations presented in [3, 5] a good agreement between a simplified unidirectional Matlab-Simulink model and the real system could be demonstrated for orthogonal hits. It can be anticipated that the impact direction of MHP as part of a tool-making procedure is restricted by the geometry of the workpiece. Thus the influence of various impact angles on the peening force and the mechanical behavior of the system have to be analyzed. In order to gain first insights an acceleration sensor as well as plungers equipped with strain gauge measuring devices were used to measure force and acceleration in different tilted directions, depending on varied impact angles and peening distances. Fig. 8 presents the forces measured in axial and radial directions of the peening tool for a peening distance of 0,5 mm and different impact angles. As it can be seen, a significant decrease of the axial force component occurs in an impact angle range from 10° up to 30°.

Table 3 Chemical composition of the tested materials.

%	C	Si	Mn	Cr	Ni	Mo	W	V
1.2379	1.55	0.3	0.3	12	0.18	0.7	0.18	0.8
1.1191	0.45	0.25	0.65					

Table 4 Mechanical properties of X155CrVMo12-1 and C45E.

Mechanical property	Unit	X155CrVMo12-1 (1.2379)	C45E (1.1191)
Young´s modulus *E*	N/mm^2	210	210
Yield strength $R_{p0.2}$	N/mm^2	420	430
Tensile strength R_m	N/mm^2	870	700
Hardness unhardened	HV	250	230
Hardness hardened	HV	650	570

For large angles like α > 30° the force components remained almost at a constant value. Moreover non-orthogonal hits lead to resulting radial force components. The radial forces raised in a non-proportional dimension in the range from 10° to 30°. Above all the radial force is nearly proportional to the impact angle. In addition the measurements proved that both force components are found to be increasing if a higher peening distance is used for machining.

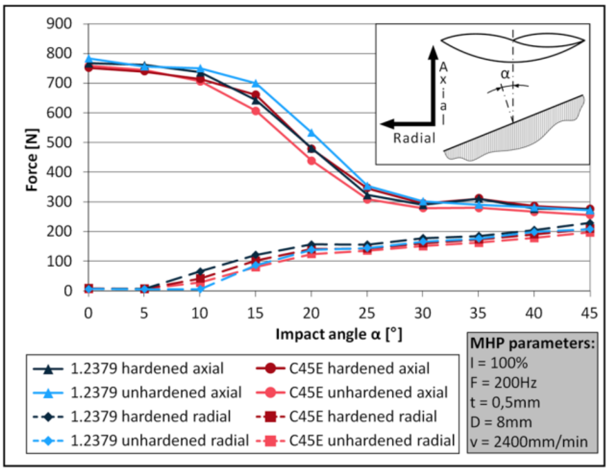

Figure 8 Investigation of impact forces, measured in axial and radial direction of the plunger tool (illustration gives the positive measurement directions).

The investigation of the acceleration measurement results, presented in Fig. 9a, shows a significant change in the dynamic behavior of the plunger depending on the impact angle. At an angle of less than 10° the time between the kickback at the actuator housing and the workpiece impact is higher than half of a period. In this case the force of the plunger coil has to pull the tool away from the surface after each single impact. Within the range of angles showing a significant decrease of the axial force (10° to 30°) the impact time shifts to the moment of previous kickback.

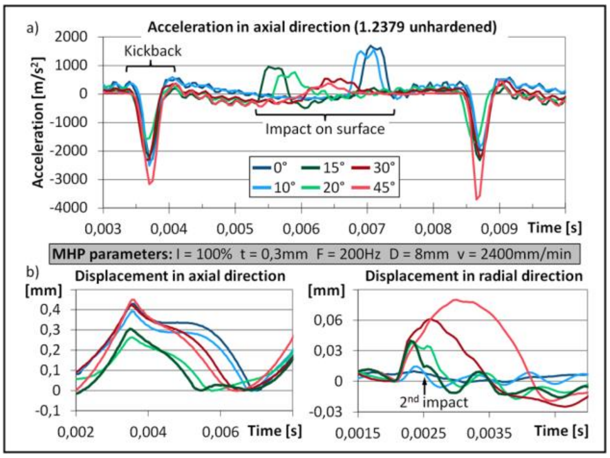

Figure 9 Investigation of dynamic system behavior: a) Acceleration measured in axial direction, b) Displacement in axial and radial direction.

Hence, the plunger coil force presses the tool in direction of the surface during and after the impact moment, which may even lead to a second impact as seen in Fig. 9b (displacement in radial direction; impact angle 15°). At an impact angle of more than 25° the time of contact to the workpiece drifts again to an interval higher than half of the period. Fig. 9b shows that the radial displacement rises with increasing impact angle. This effect is based on the increased radial force, which induces a deviation of the hammering device and machine tool structure.

2.5 Investigation of non-orthogonal hits in terms of surface finishing

Previous results show that the technology of MHP is suitable for inducing compressive residual stresses into the material [3, 5]. Moreover the treatment leads to an increase in surface hardness. However, it has to be expected that these positive effects disappear if thermal hardening takes place after MHP. Based on the results of experiments which were focused on the peening distance influence on surface hardening of 1.2379 tool steel with varying initial hardness, it can be pointed out that MHP leads to a significant increase in hardness in the order of ~5% up to ~14% for both unhardened and hardened samples (Fig. 10).

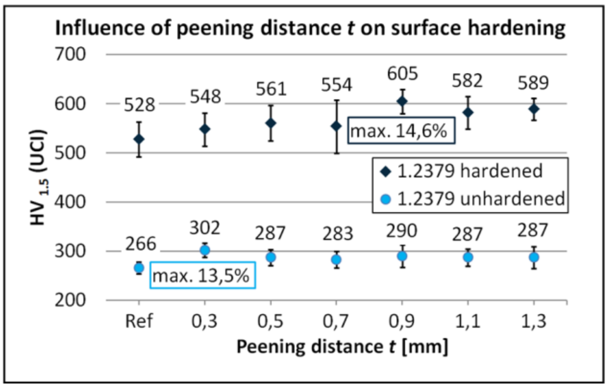

Figure 10 Surface hardening by MHP for tool steel, mean value of nine measurements on the surface with standard deviation. Highest hardness increase is given in percentage.

In order to derive a statement about the possibility of smoothing hardened steel surfaces with initial roughness in comparison with pre-finished forming tools two types of samples, hardened and unhardened ones, were used to determine the influence of impact angle and peening distance on the resulting surface topography. The samples´ surfaces were prepared by milling and afterwards peened using the same feed direction as chosen for the milling process. The applied MHP parameter setting, given in Fig. 11, was chosen based on previous findings [3]. It was expected to generate a surface roughness of $R_a \leq 0.3$ µm, which is generally required e.g. for sheet metal forming tools. Although the initial milling structures of the unhardened samples are rougher than those of the hardened ones it can be illustrated in Fig. 11 that a significant reduction of roughness in hardened and unhardened samples took place due to the MHP treatment. A higher impact force, which is significantly influenced by the peening distance value, is needed for optimized burnishing of the hardened material.

In contrast the surface roughness of the unhardened samples is increasing when treated with an increased peening distance due to a higher depth of the single indentations. Impacts produced during the MHP process dominate the topography of this sample. The influence of the peening distance on the resulting surface roughness decreases, especially for the unhardened sample, with increasing impact angle. Thus it can be concluded that an increased impact angle leads to an optimized burnishing of soft materials regardless of the chosen peening distance value. For the smoothing of hard materials high orthogonal forces are needed to flatten the groves resulting from the previous milling operation.

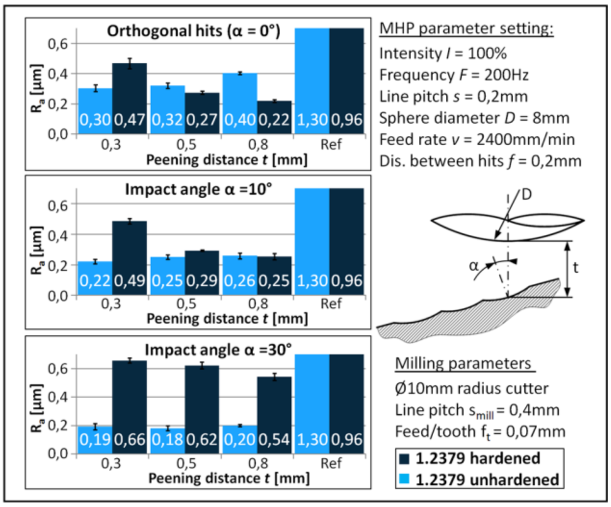

Figure 11 Surface roughness values for different impact angles and peening distances, each column represents the average of six measurements across the peening (milling) direction with standard deviation.

However, based on the presented experimental results it can be deduced that a significant surface burnishing of the investigated hardened tool steel material is possible by fulfilling the above mentioned requirements.

3 Embedding of hard materials

Another approach of experimental tests focuses on the investigation of mechanical alloying by the use of the MHP process. During a number of distinctive experiments the fundamental suitability of embedding coating and hard materials was proven for the aluminum alloy AlMgSi0,5 (3.3206) as well as for the brass material CuZn39Pb3 (2.0401). One of the main topics of the presented work is the investigation of the machinability to embed tungsten carbide (WC) particles into the near surface zone of 1.2379 tool steel.

Two tungsten carbide powders consisting of different grain sizes were used (WC 2µm-4µm and WC/W2C 45µm-90µm). Each powder was mixed in a suspension using oil (46 [mm²/s]/40°C) applied to the face milled sample surface. Subsequently, the prepared surfaces were treated with MHP two times applying the peening parameter setting given in Tab. 5. In addition to these two types of mechanically alloyed samples a milled reference sample as well as a hammer peened reference surface were machined and investigated.

Table 5 Parameter setting used for embedding of tungsten carbide.

Parameter	Unit	Value	Description
Diameter *D*	mm	8	Of the spherical plunger tip
Distance *t*	mm	0.8	between surface and plunger tip
Line pitch *s*	mm	0.2	between two MHP tool paths
Frequ. *F*	Hz	200	of the oscillating movement
Feed rate *v*	mm/ min	2400	provided by the machine tool
Peening feed direction	1st peening step: longitudinal direction of the specimen 2nd peening step: transverse direction of the specimen		

As presented in Fig. 12a an almost homogeneous layer of embedded tungsten carbide could have been generated. Depending on the grain size of the used WC particles the surface roughness is significantly increasing as shown in Fig 12b.

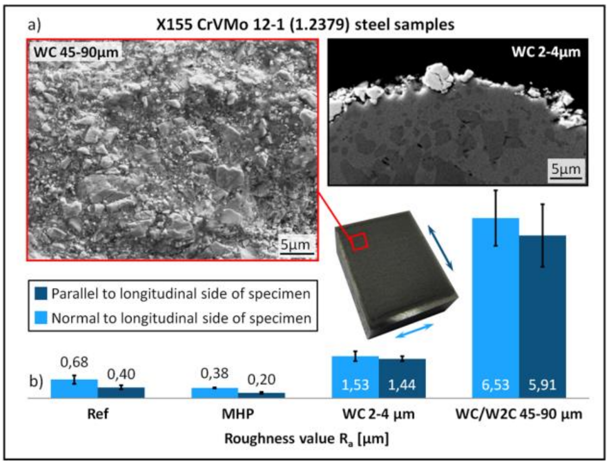

Figure 12 Embedding of WC particles: a) SEM images of the surface and the cross-section, b) Surface roughness measurements.

To analyze the tribological performance of the generated surfaces the samples were tested with a SRV® tribometer under reciprocating sliding conditions using a ball-on-flat configuration. A standard 10 mm diameter 100Cr6 (1.3505) bearing steel ball with an applied normal load of 10 N was used as counterbody. The contact zone was lubricated using fully synthetic PAO-8 additive-free oil (see Fig. 13b). During the test, the friction force was measured and the performances of the 1.2379 samples with embedded WC were compared with those of conventional not peened and machine hammer peened samples.

The results show that the coefficient of friction (COF) for the samples with embedded WC particles is identical to and independent of the particle size. Compared to the MHP and unpeened sample the COF is slightly higher. After the test, the morphology and depth of the wear track was analyzed using white light confocal microscopy (Fig 13c).

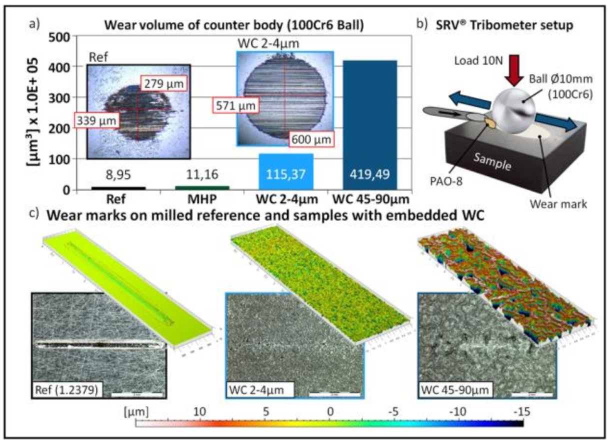

Figure 13 Tribological investigations: a) Wear volume of counterbody including two microscope images of the counterbody wear zone with given diameter of the wear mark, b) Used test setup. c) Wear marks on mechanically alloyed and milled reference samples.

The wear scar of the not peened and the MHP samples was clearly visible and each had a similar width and depth. In contrast the samples with embedded WC particles showed an increased wear resistance. Irrespective of the particle size the wear scar was not measurable. Furthermore the removed wear volume of the counterbody was analyzed by means of microscopy techniques. A significantly higher removed wear volume was measured for the balls which faced the samples with embedded particles (Fig. 13a).

4 Conclusions

This paper presents the results of experimental tests of machine hammer peening technology. The electro-mechanically operating actuator can be attached to a machining center and a robot, respectively. Thus the intensity and allocation of the penetration on the workpiece surface can be discretely controlled by CNC and process parameters of the actuator control system.

Correlations are made between the material flow of the micro-forming process, the process parameters and the surface modification. It was shown that previous tool path lines are partially or fully filled up with material displaced by the following tool path depending on the process parameters. The phenomenon could also be used to describe an observed dependency of the induced compressive residual stresses. By machining and testing specimen made of 100Cr6 material according to the extensive Round Robin Study in [7] associated residual stresses in a range of more than -1000 MPa and a depth of penetration of up to 1 mm were detected. By the application of the MHP process on multi-axis machining centers complex workpiece geometries like free-form surfaces can be machined. Hence, the technology of machine hammer peening offers various application opportunities in the fields of tool and die making industries [4].

Compared to the conventional process chain, the polishing process time can be significantly reduced by using MHP. Good surface finishing results of hardened tool steel were shown.

An additional application of MHP as part of a mechanical alloying process was presented. The coated tool steel material showed a significant reduction in wear during tribometer tests. Thus the MHP process offers the opportunity to generate wear protection layers at defined areas of a component. Compared to thermal coating this technology can be performed at room temperature and under atmospheric pressure in the same setup as the previous milling operation. Experimental results show a high potential for wear-intensive manufacturing processes, for example in the production of core boxes where erosive wear damage is caused by blown silica sand [3,8].

The increase in productivity, the achieved surface hardness and the induction of compressive residual stresses lead to an enhanced tool and mold life cycle by expanding the life time of the tool, which entails a reduction in the average costs per piece as addressed in Fig. 14.

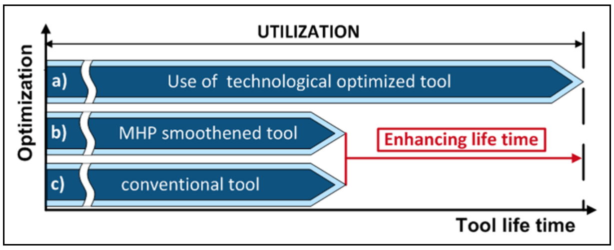

Figure 14 Optimized utilization and life cycle of tools and molds by surface modification.

The basic findings presented in this paper are currently being tested on real tools to investigate the application of the technological improvement to mold and die making. Further steps in research focus in process modelling using FEM or smoothed particle simulation.

References

[1] T. Altan, B.W. Lilly, Y.C. Yen: Manufacturing of dies and molds. In Annals of the 50th CIRP Conference on Manufacturing Technology, pp. 2/405-423, 2001.

[2] P. Groche, M. Engels, M. Steitz, C. Müller, J. Scheil, M. Heilmeier: Potential of mechanical surface treatment for mold and die production. In Int. Journal of Materials Research, pp. 103/783-789.

[3] F. Bleicher, C. Lechner, C. Habersohn, M. Obermair, F. Heindl, M. R. Ripoli: Improving the tribological characteristics of tool and mold surfaces by machine hammer peening. In Annals of the 62nd CIRP Conference on Manufacturing Technology, 1/239-242, 2013.

[4] J. Wied: Oberflächenbehandlung von Umformwerkzeugen durch Festklopfen. In PhD Dissertation, Technical University of Darmstadt, 2011.

[5] F. Bleicher, C. Lechner, C. Habersohn, E. Kozeschnik, B. Adjassoho, H. Kaminski: Mechanism of surface modification using machine hammer peening. In Annals of the 61st CIRP Conference on Manufacturing Technology, pp. 1/375-378, 2012.

[6] E. Brinksmeier, J.T. Cammett, W. König, P. Leskovar, J. Peters, H.K. Tönshoff: Residual Stresses - Measurement and Causes in Machining Processes. In Annals of the 31st CIRP Conference on Manufacturing Technology 2/491-510, 1982.

[7] I.S. Jawahir, E. Brinksmeier, R. M´Saoubi, D.K. Aspinwall, J.C. Quteiro, D. Meyer, D. Umbrello, A.D. Jayal: Surface integrity in material removal processes: Recent advances. In Annals of the 60th CIRP Conference on Manufacturing Technology, 2/603-626, 2011.

[8] J. Rodríguez, D. Martinez, A. Perez, R. González, E. Rodríguez, S. Veltierra: Erosion wear in heat treated tool steels used in core boxes at automotive foundries. In Proc. of 16th Int. Conf. on Wear Materials, Vol. 263, pp. 1-6/301-308, 2007.

Alternative brand building and product development

E. Halilović[1], N. Matjaž[2],

[1] *ONDU d.o.o.; elvis@ondu.si; www.ondu.si*
[2] *Faculty of mechanical engineering, University of Ljubljana, Slovenia*

Abstract

In this era of the so called wikinomics where customer is no longer only the king but a co-creator and contributor too, a new perspective on creating brands is of great importance (if not already overdue). With the power of the Internet – probably one of the greatest tools ever invented – at our hands, there are new opportunities to tap into being created every day. How do we make the customer an important part of the creative process and how does his involvement benefit the brand awareness and the brand itself? New channels like social media and crowdfunding platforms are creating massive paradigm shifts by emphasizing the interconnected nature of the internet which gives new power to small and upcoming brands such as ours.

Influence of MQL on friction coefficient and workmaterial adhesion during machining of cast aluminium with various cutting tool substrates made of PCD, HSS

J. Rech[1], P. Faverjon[1],

[1] *ENISE, University of Lyon, Laboratoire de Tribologie et Dynamique des Systèmes, France*

Abstract

Due to the increasing account taken of environmental constraints, industry works on how to limit the massive use of lubricants by using the micro-pulverization of oil in machining processes. The success of a machining operation is dependent on a friction coefficient and weak adhesion with the tool-work material interface. This paper aims at identifying the influence of cutting tool substrates (High Speed Steel / HSS, PCD) and of Minimum Quantity Lubrication (MQL) on the friction coefficient and on adhesion in tribological conditions corresponding to the ones observed in the cutting of aluminium alloys (sliding velocity : 20 – 1500 m/min). An open tribometer, especially designed to simulate these tribological conditions, has been used.
It has been shown that HSS and carbide substrates lead to large friction coefficients (0.8-1) and substantial adhesion in dry conditions, whereas PCD substrates lead to friction coefficient average values (0.4-0.5) and very limited adhesion, which proves the necessity to use PCD tools in the dry machining of aluminium. It has also been shown that the application of MQL leads to a large decrease of the friction coefficient (0.1-0.2) and eliminates almost all traces of adhesions on pins for any substrates, which shows that MQL is an interesting compromise between dry machining and flood cooling.

Keywords: MQL, Sustainable machining, Aluminium, Friction, Adhesion, Tribology.

1 Introduction

Production lines in the automotive industry today use conventional lubrication based on straight oil or emulsion. The role of cutting fluids is to provide cooling of both machine-tool and workpiece by minimizing the heat generated during cutting, to lubricate the tool-chip interface in order to limit the tool wear and also to enhance the chip removal [1]. In the case of aluminium machining, such as in the automotive industry, the lubricant plays one more important part: to prevent aluminium from sticking to cutting tools. Cutting fluids are crucial for machining but at the same time, they cause trouble in the sanitary field (allergies, work atmosphere…) and in the domain of maintenance [2]. Supply systems such as tanks, pipes, pumps, filters, centrifuges often break down which decrease the efficiency of production plants. One way of improvement is the Minimum Quantity Lubrication (MQL). This lubrication mode is often considered sustainable for machining [3] [4] [5]. However, the replacement of several hundred of litters per minute by some millilitres per hour induces many changes for both machine-tools and manufacturing processes. The process must be carefully designed to take into account the oil flow decreasing (thousands of times less in MQL than in conventional lubrication). Some functions of conventional lubrication are not provided anymore under MQL conditions: e.g. global cooling of the workpiece and machine tool. Some other functions may be uncertain e.g. cutting lubrication and aluminium sticking limitation.
Several methods may be undertaken to analyse the influence of a cutting fluid on machining process. The most common way is to run cutting tests and to compare macroscopic measurements such as forces and torque. The most common are the tapping torque test (ASTMD-5619) and drilling tests (ASTMA830-85) [6]. These methods are based on comparative statements and do not permit to understand what happens at the tool / workmaterial interface. Additionally they are only convenient for tapping or drilling and extension on other cutting operations need punctual developments as it was done by Cakir et al. [7] and Jayal and Balaji [8] for turning and Vieira et al. [9] in milling.
A lot of authors prefers running cutting wear tests and analysing the impact of lubrication on tool life time. Such tests are expensive, very sensitive to little variation of any parameter [10], and time consuming: especially in the case of MQL where

tool life can be higher than in conventional lubrication [11] [12] [13]. Alternative methods such as the use of tribometer can be used since the analysis of friction coefficient remains an issue in tribology [10]. Several frictional set-ups already exist or have been developed. The most widely known set-up is the pin-on-disc system, which is unfortunately not able to simulate the contact conditions in cutting, since the conditions (temperature, pressure) are not relevant to those observed in reality [14]. Workmaterial slides on rake face (chip) and on the flank face (machined surface) but never comes back i.e. the tool always cuts virgin aluminium. This is commonly called an open tribo-system. So as to be able to analyse what is happening at the tool/chip/workmaterial interface in cutting, open tribometers should be used.
Aluminium machinability and especially coolant strategy have been largely investigated [3][4][5][15][16]. As example, Braga et al. [3] studied the impact of MQL on aluminium by power monitoring and tool wear examination. Itoigawa et al. [4] analysed the impact of MQL on aluminium machinability through end milling tests but again does not investigate friction phenomenon at the tool/chip/workpiece interface. Bhowmick et al. [5] investigated the impact of MQL on cutting forces and torque. Kishawy et al. [15] and Lopez de Lacalle et al. [16] studied the impact of MQL providing on tool wear. Generally, a lack of tribo-investigations at the tool/chip/workpiece interface appears and leads to the need of fundamental understanding in tribology during machining of aluminium under MQL conditions.
This paper aims at determining the influence of MQL on friction and aluminium sticking compared to dry conditions by using an open tribometer.

2 Methodology

2.1 The tribometer

For being able to compare MQL and dry machining effects on both friction and aluminium sticking, an open tribometer was used. This basically consists in sliding a pin on a bar fixed onto a CNC lathe chuck, see Figure 1.

The kinematic of the lathe allows to reach sliding speeds up to 1500 m/min and local pressures at the tube / pin interface of about 1 GPa. This pressure is generated by a constant piloted normal force FN of 200 N. AlSi7 aluminium (84 HB) was cast in tubes and longitudinally turned with cutting speed of 500 m/min, feed of 0,15 mm/rev and depth of cut of 0,5 mm. The pin is cylindrical Ø8 mm and has a

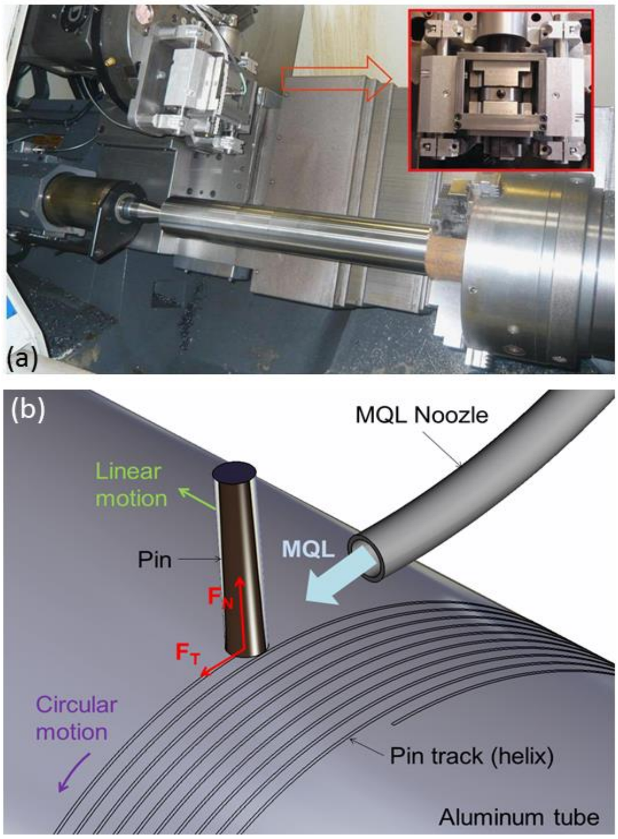

Figure 1 Tribometer [14] and MQL providing**.**

Ø34 mm spherical polished extremity. The substrate and eventual coating are fixed for being representative of cutting tools normally used for machining in the automotive industry. Four various pins were tested for this study. HSS pins were TiN or TiCN coated while PCD pins were uncoated. The granulometry of PCD was 2 and 10 µm. A tridimensional dynamometer records forces and calculates the apparent coefficient of friction µ as related in the following equation (1). This actually corresponds to the macroscopic friction coefficient which cannot be directly identified as interfacial friction coefficient meaning that post treatments would be necessary for being used in numerical simulations. On the contrary, the apparent friction coefficient µ is convenient for determining experimentally the influence of MQL on friction and workmaterial adhesion on tools.

$$\mu = \frac{F_T}{F_N} \tag{1}$$

Where FT is the tangential force and FN is the normal force as shown on figure 1. The sliding speeds have to be chosen in accordance with the normal cutting conditions of the tool. Every test was run under dry and MQL conditions, replicated three times each.

2.2 Mist generation

The CNC lathe was equipped with a mist generator LubriLean referenced VarioSuper from the SKF-Vögel company. This device was supplied with air pressured at 6,5 bar. Different levels of lubrication are available, the lowest one was used which corresponds to a flow rate of approximately 50 l/min with a noozle Ø8 mm. MQL is provided at the pin/work material interface as shown on figure 1.
The lubricant was the EcoCut Mikro Plus 20 from Fuchs. This is a straight oil fully biodegradable for which main characteristics are resumed in table 1.

Table 1 Fuchs oil characteristics.

Characteristic	Temp. [°C]	Unit	Value
density	15	kg / m^3	0,842
viscosity	40	mm² / s	27
flash point	-	°C	> 188

3 Results and discussion

3.1 Friction

The first output of this experimental setup is the apparent friction coefficient μ. The mean value of friction coefficient is considered during the stable period of sliding. Then the friction coefficient is plotted for different pins, sliding conditions, and lubrication conditions.

HSS pins are representative of tapping tools. Uncoated HSS is commonly used for cut tapping whereas TiCN coated HSS is used for form tapping. For these operations in aluminium alloy, thread machining speed is typically about 30 m/min with often higher speed in return. Figure 3 shows the coefficient of friction for HSS pins from 20 to 100 m/min under dry and MQL conditions. First of all, it has to be noticed that there was a lot of aluminium stuck on pins under dry conditions which led to extreme severe sliding (see Figure 4(b) and 4(c)) and coefficient of friction μ > 1. Under dry conditions, TiCN HSS pin has a friction coefficient on average 10% lower than the uncoated one decreasing slowly when sliding speed rises.
It appears clearly that MQL has a beneficial effect on friction, decreasing it by about 4. Under MQL conditions, TiCN HSS and uncoated HSS pins have exactly the same friction coefficient. It means that considering friction, TiCN coating has no beneficial effect.

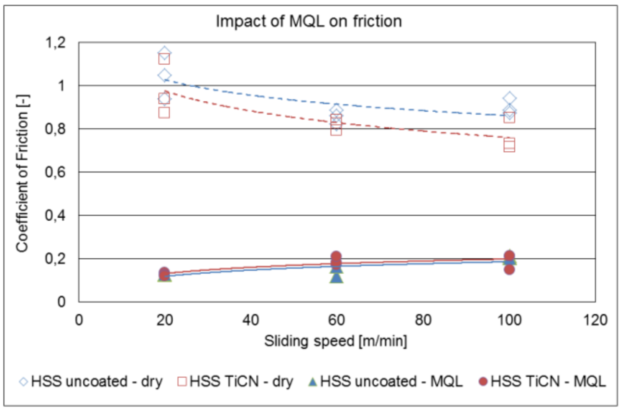

Figure 2 Impact of MQL on friction vs. dry conditions with HSS pins.

2μm PCD pins represent boring tools while 10μm PCD pins characterize milling cutters. Here the sliding speeds are going from 20 to 1500 m/min which corresponds to the maximum on this lathe. Industrial cutting conditions can go four times higher: up to 6000 m/min. The figure 3 shows that even under dry conditions, the friction coefficient is lower with PCD than with HSS pins. Moreover, the faster the sliding speed, the lower the friction coefficient. At 1500 m/min, μ=0,22 with both kinds of pins and it can be expected that it would be the same at higher sliding speeds i.e. industrial cutting conditions. It means that MQL has no effect over 1500 m/min because of non-penetration of oil mist at the pin/work material interface. These results have been highlight by Claudin et al. [10].

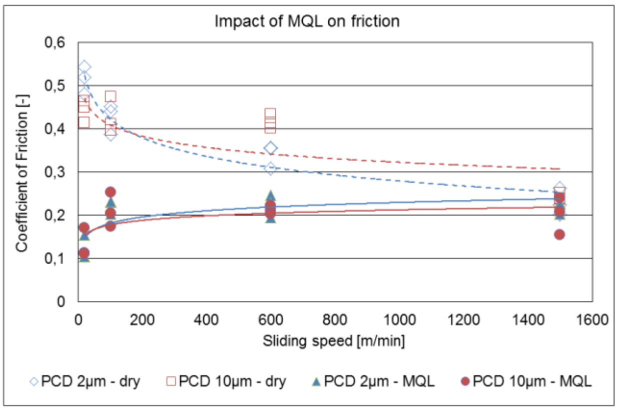

Figure 3 Impact of MQL on friction vs. dry conditions with PCD pins.

On the contrary, when the interface is properly lubricated, the coefficient of friction is of about 0,2. PCD tools are often used at high cutting speed; it means that MQL has only a beneficial impact for central cutters e.g. reaming operations (where cutting speeds approach 0) and not for peripheral cutters (where high cutting speeds appear). In reaming, speed along cutting edge is going from 0 up to 6000 m/min so MQL would reduce friction around the center but such machining operations are continuous and Claudin et al. [10] have shown that lubrication is only effective the first tenths of seconds at slow sliding speeds and is immediately evacuated at high sliding speeds. So, considering that industrial cutting speeds are between 1500 and 6000 m/min, MQL is not appropriate for PCD tools. Finally, there is no difference between both 2µm- and 10µm-PCD from friction point of view.

To sum up, it has been shown that considering friction, MQL is of great interest with HSS tools and at slow sliding speeds with PCD tools.

3.2 Aluminium sticking

In the case of aluminium machining, the most difficult task is to prevent tools from aluminium sticking especially under MQL condition. So as to be able to match the impact of MQL compared to dry condition, pins have been analysed after tribotests. This consists in measuring the quantity of aluminium stuck on pins on photographs taken with a binocular microscope as shown in Fig. 5. This extreme case of adhered aluminium occurs with HSS tools only and can be limited by MQL employment. There is absolutely no sticking on PCD pins under both dry and MQL conditions.

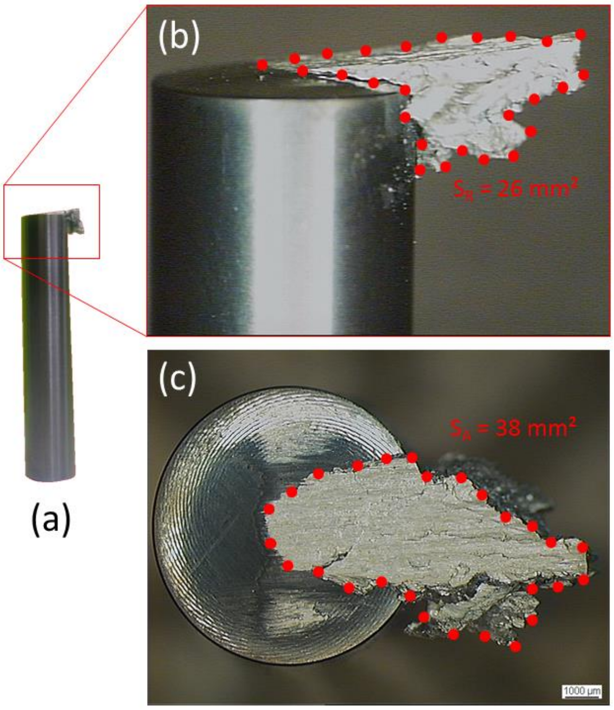

Figure 4 Aluminium sticking on a pin.

The figures 5 and 6 sum up the amount of adhered workmaterial SA and SR as shown on Fig 5 (c).

It appears clearly on Figure 5 that the quantity of aluminium stuck on HSS pins after tribotests is almost the same whatever the sliding speed under dry conditions. On the contrary, the amount of workmaterial adhered on pins is seriously reduced by using MQL.

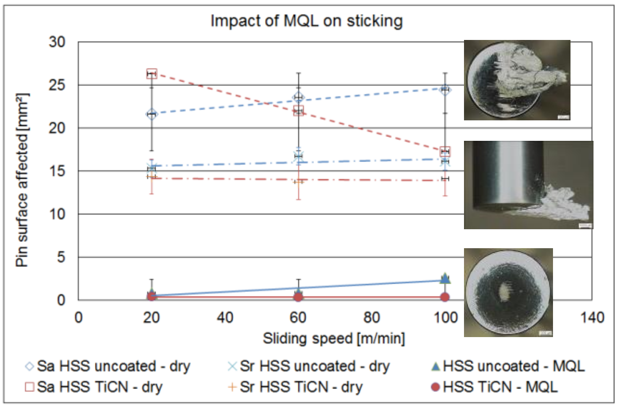

Figure 5 Impact of MQL on adhered workmaterial vs. dry conditions with HSS pins**.**

Contrary to HSS, PCD does not get stuck under dry conditions and employment of MQL is not helpful from adhesion point of view, see Fig 6. There is no sticking even at slow sliding speed.

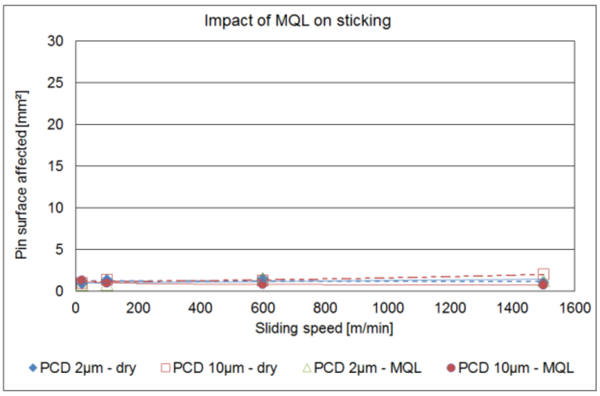

Figure 6 Impact of MQL on adhered workmaterial vs. dry conditions with HSS pins

4 Conclusion, perspectives

4.1 Conclusion

This study analyses the influence of MQL on friction and workmaterial adhesion on cutting tools. It has been shown that:

- The friction phenomena is highly decreased by using of MQL for HSS tools and for PCD tools when sliding speed is lower than 1500 m/min.

- HSS tools do need to be lubricated for limiting aluminium adhesion. On the contrary, PCD tools never get stuck. MQL is convenient for HSS and is not needed for PCD.
- There is no difference in friction and adhesion between 2 and 10 μm grain size PCD.

4.2 Further work

Some effects of MQL were investigated in this study. It would be attractive to complete this work by:

- Running tribotests at higher sliding speeds and extend investigations on tap quality.
- Identifying wear mechanisms for optimizing tool life.
- Testing other pin materials: firstly uncoated cemented carbides representative of drills.
- Using an atmosphere controlled tribometer so as to catch the influence of temperature on friction and workmaterial adhesion.

References

[1] Trent, E.M., 1991 Metal Cutting, Butter worth Heinemann, ISBN 0-7506-1068-9.

[2] Boyer, H.F., Waremme, J., Bourdiol, J.L., Delaunay, D., 2011, A study about energy consumption and cutting fluid used to clutch case machining, Mécanique & Industries 12:389–393.

[3] Braga, D.U., Diniz, A.E., Miranda, G.W.A., Coppini, N.L., 2002, Using a minimum quantity of lubricant (MQL) and a diamond coated tool in the drilling of aluminium–silicon alloys, Journal of Materials Processing Technology 122:127–138.

[4] Itoigawa, F., Childs, T.H.C., Nakamura, T., Belluco, W., 2006, Effects and mechanisms in minimal quantity lubrication machining of an aluminium alloy, Wear 260:339–344.

[5] Bhowmick, S., Alpas, A., 2008, Minimum quantity lubrication drilling of aluminium–silicon alloys in water using diamond-like carbon coated drills, International Journal of Machine Tools & Manufacture 48:1429–1443.

[6] Pawlak, Z., Klamecki, B.E., Rauckyte, T., Shpenkov, G.P., Kopkowski, A., 2005, The tribo-chemical and micellar espects of cutting fluids, Tribology International, 38:1–4.

[7] Cakir, O., Kiyak, M., Altan, E., 2004, Comparison of gases applications to wet and dry cuttings in turning, Journal of Materials Processing Technology 153–154:35–41.

[8] Jayal,A.D., Balaji, A.K., 2009, Effects of cutting fluid application on tool wear in machining: interaction with tool-coatings and tool surface features, Wear 267:1723–1730.

[9] Vieira, J.M., Machado, A.R., Ezugwu, E.O., 2001, Performance of cutting fluids during face milling of steels, Journal for Materials Processing and Technology, 116(2–3):244–251.

[10] Claudin, C., Mondelin, A., Rech, J., Fromentin, G., 2010, Effects of a straight oil on friction at the tool–work material interface in machining, International Journal of Machine Tools & Manufacture 50:681–688.

[11] Dhar, N.R., Kamruzzaman, M., Ahmed, M., 2006, Effect of minimum quantity lubrication (MQL) on tool wear and surface roughness in turning AISI-4340 steel, Journal of Materials Processing Technology 172:299–304.

[12] Kamata, Y., Obikawa., T, 2007, High speed MQL finish-turning of Inconel 718 with different coated tools, Journal of Materials Processing Technology 192–193:281–286.

[13] Khan, M.M.A., Mithu, M.A.H., Dhar, N.R., 2009, Effects of minimum quantity lubrication on turning AISI 9310 alloy steel using vegetable oil-based cutting fluid, Journal of Materials Processing Technology 209:5573–5583.

[14] Bonnet, C., Valiorgue, F., Rech, J, Claudin, C., Hamdi, H., Bergheau, J.M., Gilles, P., 2008, Identification of a friction model—Application to the context of dry cutting of an AISI 316L austenitic stainless steel with a TiN coated carbide tool, International Journal of Machine Tools & Manufacture 48:1211–1223.

[15] Kishawy, H.A., Dumitrescu, M., Ng, E.G., Elbestawi, M.A., 2005, Effect of coolant strategy on tool performance, chip morphology and surface quality during high-speed machining of A356 aluminium alloy, International Journal of Machine Tools & Manufacture 45: 219–227.

[16] Lopez de Lacalle, L.N., Angulo, C., Lamikiz, A., Sanchez, J.A., 2006, Experimental and numerical investigation of the effect of spray cutting fluids in high speed milling, Journal of Materials Processing Technology 172: 11–15.

Sustainability

Technology that 5 Billion People Need
What can engineers do for sustaining our sphere?

Hiroshi Fujii[1] and Naoki Sase[2]

[1] *Gifu University, Japan*
[2] *Toyama National College of Technology, Japan*

Abstract

One of the most serious threatening to the future of the world is an increase in the population of human beings. The population of 6.8 billion in 2010 will become 9.3 billion in 2050. The people who have no land, no job and no house are flowing into big cities with the last glimmer of hope. According to the prospect by United Nations, about 5 billion of people will be living under critical condition forty years later. Unless we improve the quality of life of those people, we will not be able to sustain the environment of the world. Electric power plants, road constructions, mobile phone systems, tunnels and bridges are all necessary. On top of those, much simpler machines which work every day beside the people are badly and urgently needed. Some of mechanical engineers have to work for them. The authors intend to draw engineers' attention to this problem in this paper. Those will include;
Incinerator: In many countries, people are living buried with litters. We need a small incinerator to burn waists from several families every day at site.
Cooking stove: Collecting fuels as like as branches of trees and animal droppings has been getting harder. An efficient cooking stove will be a great help especially in the arid regions. Parabolic disk with a reflection surface can also be applied in many parts of the world.
Hydraulic Turbines which can generate electricity with the least amount of water*;* Even traditional Water Wheel should be reevaluated, redesigned and supplied to the rural areas.
Simple method to obtain the safe water to drink: Solar water disinfection and an equipment for distilling water are discussed.
Regeneration of forest: A lack of water for drinking and irrigation is already a serious issue. There is no simple way to solve it. The authors like to show a project of the recovery of forest lead by Dr. Yasuo Abe, in Nepal.
Mini-excavator: Small and trouble-free excavator should also be produced.

Keywords: population explosion of the world, 50 billion people living in slums, machines and equipment for everyday life, to sustain present environment

1 Introduction

The word "population explosion" started appearing often in media in 1960s. The appeal was supposed to be seriously received and be responded immediately. However, the United Nations is still giving us the same warning, more and more seriously.

The 2012 Revision of World Population Prospects [1] is presented by the Population Division of the Department of Economic and Social Affairs of the United Nations Secretariat. It is available both on the web-site and PDF. It says as follows in its conclusion:

"In late 2011, the world's population surpassed the 7 billion mark and it is currently growing by an additional 78 million persons every year. By 2050, the world's population is likely to reach an unprecedented size between 8.1 billion and 10.6 billion people. Most of the future population growth will occur in developing countries, particularly in least developed countries. Presently, many developing countries still have population growth rates that, if sustained, would undermine their development and put pressure on future generations."

The other report [2] says that, in 2050 – only 40 years later from now – a half of population on the earth will be living in slum condition. This acute increase in world population results in all sorts of problems in the world. Shortages of energy resources, global warming, insufficient food for children, deficiency of drinking water etc. will be caused, obviously or inherently, by the excessive number of ourselves.

Every country is working out with numerous counter measures in order to deal with the problems. Those include: developments of new energy resources, efforts to reach a worldwide agreement for global warming, changes in taxation law of agricultural products between countries, improvements of riverbanks and beaches and constructions of irrigation system, economical assistances to less developed countries and so on and on. The United Nations is also carrying out many projects to lower the fertility. Politicians, experts of development and university professors have kept on discussing about what we should do.

These are all necessary. There is no doubt about it. But, we know that those big projects cannot necessarily directly contribute to extremely poor people for improving their everyday life. Some of us, as engineers, certainly could do some more to them.

The authors would like to show some simple ideas of machines and equipment that can work every day beside the people. Our society has developed so many types of machines during the past centuries and left them behind. New technologies are always attractive and exciting for us. But, if we look back at some fundamental technology again, we will be able to find many things that can improve the life of the people.

2 Incinerator and cooking stove for the people

The report [1] quoted above provides the population of every country and area. **Figure 1** shows the reproduction of the data of 1950 and 2010 and the projected population to 2050. It is clear that the most increase of 2.6 billion from now will occur in Asia and Africa.

So, the next question is where the increased people will live. Mark R. Montgomery's analysis is shown in **Figure 2**. During the 3rd quarter and the 4th quarter of the last century, the population of the rural area in developing countries was increased by about 750 billion. But, during the term from 2000 to 2030, the population in the rural area will not increase [1] any more. Instead, the population in the urban area will mark an unprecedented increase. The urban population in developing countries will increase by 2 billion. Which means that all cultivatable lands have been fully utilized already. In the rural areas, mostly farming areas, there are no more room for the increased population or not enough food to support any extra family. The people, who have no land, no house, no job and no money, can do nothing but flow into big cities with the last glimmer of hope.

What kind of environment is waiting for them? An analysis to answer the question has been published as a United Nations Report. In the report titled "Seven Billion and Growing: The Role of Population Policy in Achieving Sustainability" [4], the author of the report tries to estimate the number of people who live in slums presently. We must admit that it is not easy to define the "slum". Regardless the difficulty and arguments, the figure helps us obtain a rough idea of how many people are living in great difficulty.

Figure 3 shows the present slum population, classified according to the area. There are about 900 million people living in slums. On top of this number, extra 2 billion people will join within only 3 decades, as we just saw in **Figure 2**, and another 2 billion or little more within 2030-'50. As a whole, the population who live in slums will be 5 billion all together in 2050. This is the threatening to the world.

Regardless if we could reach the reasonable fertility level by then or not, about 5 billion people will be living in the slum condition soon or later.

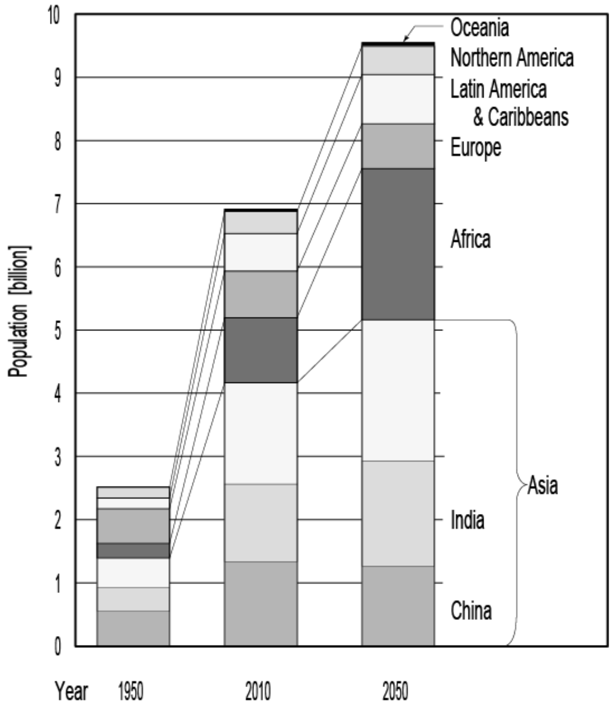

Figure 1 Prospect of population of the world

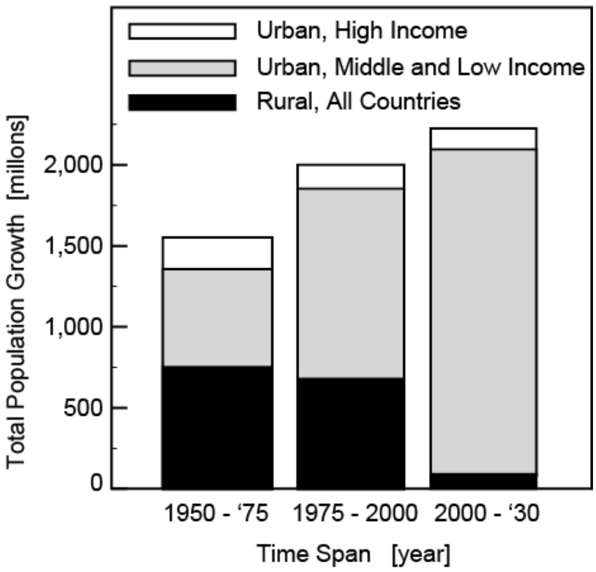

Figure 2 Growth of urban population

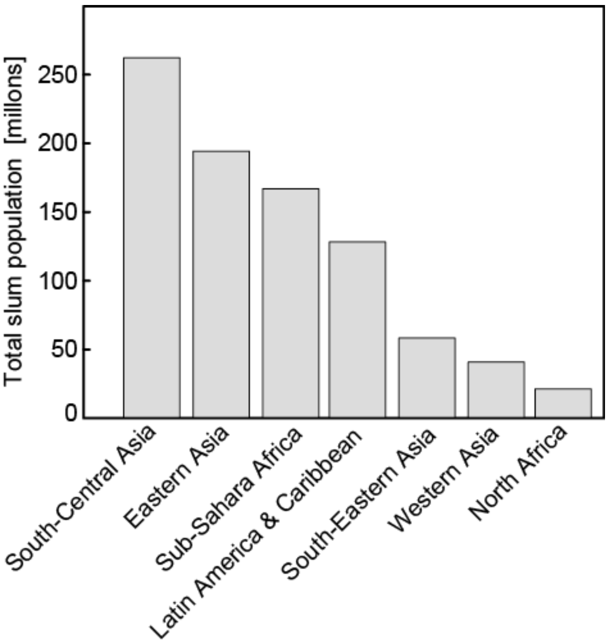

Figure 3 Estimated population living in slums

2.1 Incinerator

Even now already, the people in slums are living among litters and garbage in many countries. If you live being buried by wastes and garbage, you will lose your pride and, soon or later, your moral code will be collapsed. This is the problem. Poverty itself is not a big matter. Many people in many countries have experienced it. But, in the present slums, there is no hope because it is made so as a part of the social structure. That is why the problem becomes serious.

In most developing countries, cities and towns have no budget for having the garage collectors or no budget to operate them. Even if the collection is done somehow, they often throw the garbage to a big throwing area and pile them up. There is no technical and social solution to deal with those mountains of garbage.

One of what people need under this condition is a simple incinerator. If each family could burn out flammable items and garbage together, they can keep their surrounding tidy. A sophisticated electric incinerator is not needed.

The authors like to propose to produce two parts shown in **Figure 4** and deliver them to the people. The ones who receive them are requested to construct a square wall of 80cm both in width and depth and 1.2m in height. A grid to hold the material to be burnt is placed inside the structure and the structure is covered with a lid with chimney on it.

The structure may be made by rocks, concrete blocks, clay or anything else inflammable. People can dig a hole with a big opening at the bottom, too.

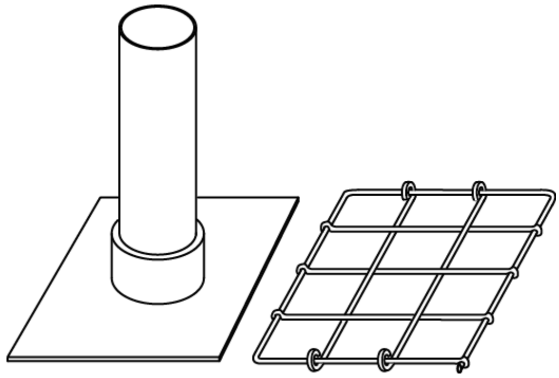

Figure 4 Parts for constructing a simple incinerator

Before the people use this kind of incinerators, they have to learn to separate rubbish into burnable and non-burnable items. Glasses and metals should be separated first. These can be recycled, if some collection system is introduced. Garbage can be turned into compost in many ways. The rest can be burned out by any simple incinerator as like as the one shown above as an example.

Environment enthusiasts might say that this causes air pollution when every family in a country starts using personal incinerators at the same time. Of course it may happen. But, it is more important for the society that the people wish to live in better surroundings. It will give the governments a good chance to invest to cleaning facilities.

2.2 Cooking stove

In the world today, at least 3 billion people have no gas nor electricity for cooking. This number will be doubled in coming 40 years. The people are collecting dropped branches of trees, dried grasses, dungs of animals, woods from broken houses and all kinds of burnable materials. They make fire with them to cook meals and make tea. If they run out of those fuels, they will cut leaves, branches or even trees at the end. Nobody has a right to stop them.

It is sad to know that in many parts of the world vast areas of forests are being lost. This is a process continuing for the last thousands of years. King Solomon built a beautiful palace using hundreds of huge Lebanon cedars. Now this area is almost a desert. Deserts in Africa are expanding. In the arid region in Central Asia, the pasture land is shrinking every year.

That is why we need to develop an efficient cooking stove from which the people can get the thermal energy from grasses and trees. Such a stove will help adults and children use their time and labour for more creative purposes. In addition to that, we can expect to be able to save a considerable area of forests.

In these days, many manufacturers of outdoor gears are producing such cooking stoves. A company in Japan sells a stove with which you can get 1 litter of boiling water from a few sheet of A4 papers. Unfortunately, however, these products are either too expensive or too big. They sometimes requires electricity. These are no use for poor people.

Technologies required for an efficient combustion have been well established. Theoretical approaches to the efficient combustion are well discussed and checked by experiments and practices. The key to high efficiency is considered to be the design of the second combustion chamber in a limited space. Only obstacle to be overcome is to make them simple and cheap. If it is not possible, governments can buy those efficient cooking stoves and deliver the stoves to the people.

In the arid regions, plants is not and will not be collectable in future. Instead, plenty of solar energy is available there. For solar voltaic, solar panels, controllers, inverters and batteries are needed. But, in many countries, the government cannot deliver them to the people in free of charge. And, people cannot buy them.

Under this situation, a parabolic thermal collector is a promising equipment. **Figure 5** shows an example which is actually used at Mukhtinat (3,900m above the sea level, west of Mount Annapulna,) in Nepal. Considerable amount of water can be kept hot while the sun shines.

This type of concentrating solar cooker was first invented by a retired surveyor, John wilfrid Wright [5]. He made it with rattan and Aluminium foil in his kitchen.

When an engineer see this, he/she will start thinking what kind of sensor is useful to distinguish the direction of the sun and what kind of mechanism is the best to rotate the collector in order to follow the sun accurately. Don't think it in that way here, but think how to make it cheaper without lowering the fundamental features.

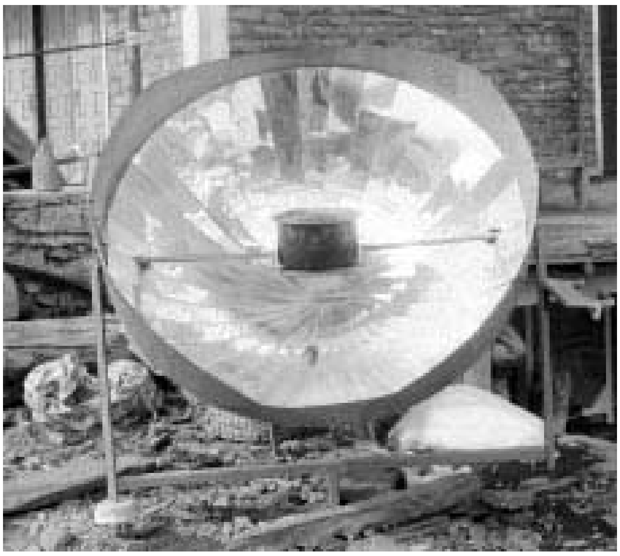

Figure 5 A parabolic solar cooker with segmented reflectors used in Nepal

3 To secure safe water

3.1 Solar water disinfection

It is a matter of life or death whether safe water is available or not. It is becoming more and more difficult to obtain safe water in many countries. This situation will be accelerated in near future.

WHO (World Health Organization) of the United Nations is responsible for providing leadership on global health matters. WHO recommends a simple, cheap and effective method for solar water disinfection. The method is just to put water in PET bottles and to expose them to the sunlight (ultraviolet). This method is very efficient and has been already applied in numerous developing countries.

However, disinfection may not make all kinds of water safe to drink due to non-biological agents such as toxic chemicals or heavy metals. Consequently, additional steps beyond disinfection may be necessary to make water clean enough to drink, in many parts of the world.

3.2 Distillation of water

There are numerous places where only muddy water, sea water or water contaminated by harmful substances is accessible in the world. Poor people cannot afford the water in PET bottle. For those people, distillation of unhealthy water is only possible solution to survive.

Figure 6 shows a proposal of home appliance to distil unhealthy water. A container ⑤ in the figure holds bad water. It is heated by fire or whatever means available. Vapour goes up through the holes of the strainer ④. On the other hand, ① is simply a basket with wood chips, straws, dried leaves, etc. in it. The whole basket is made wet by water and dried. The water kept in the bottle ② is cooled down by the latent heat of evaporation from the basket Part 1and becomes much cooler than the water in the pot ⑤. Consequently, the vapour touched with ② is condensed and accumulated in the container ③.

The authors wish any company to produce a great number of this set as like as one million sets or more. It will make it possible to sell the set in really cheap price.

There are many people who are drinking toxic water. They can drink safe water in this way. There are many fishermen who are dehydrated so often and suffer from kidney disease because of the shortage of safe water. They can drink distilled sea water. A lot of children will be saved by such a simple device.

An American man, Mr. Garth Johnson, made a distillation equipment [5]. It is called Bailey's "Photon Bottle Distillation Apparatus." He made it being inspired by Alchemist's vessels, as well as the drawings of Leonardo da Vinci. This is a good try and certainly will work for larger demand of water.

3.3 Regeneration of forest

Disinfection and distillation of water as mentioned above are useless unless water is obtainable. One of the causes of shortage of water is deforestation. About 70,000km^2 of forest is being lost from the world. The area of Slovenia is 20,273km^2. There is no simple way to solve this problem. We must plant trees and raise them for 20 years or longer. Then a forest will start recovering. Politicians and governmental officers in many countries know this. Some of them have tried very hard. A successful result, however, is scarcely reported.

The authors like to introduce a successful project [6] carried out by a Japanese medical doctor, Dr. Yasuo Abe. He created an excellent system to raise trees and started planting 25 years ago. His system has been working so well that it is worth explaining the method in this paper, because it is applicable to any part of the world.

He is a pediatrician and used to be a dedicated mountain climber. Since 1974, he had worked as a volunteer doctor visiting Nepal several times a year for ten years. He saw so many children dying. They drink contaminated water, suffer from diarrhea and severe dehydration and are infected by all sorts of germs, and consequently die. He was convinced that he could not help those children unless forests are regenerated and fresh water becomes obtainable.

He started his project first by studying forestry in Shinshu University in Japan for 2 years. On the other hand, he did an extensive survey and talked with local people in order to decide the types of the trees to be planted. He chose a village, Tupche, which had completely lost their forest many years ago. He began from an activity to make villagers understand how important the forest is, and made a planting plan together with them. The trees chosen are all domestic trees including fruit trees.

On May 22nd in 1990, he went to the village with 5,000 nursery trees that he had ordered in advance and bought from Nepali Institute of Forestry. He and villagers worked together and planted 5000 trees.

Everybody knew that a half of the trees just planted would be eaten by their goats, cows and wild animals and that another half would be dried out and die during the dry season of five months period. A Nepali scholar told Dr. Abe that in Nepal only 0.5% of planted tree can survive till the next year.

In order to overcome this difficulty, he created a brilliant system. The system was simply a card. The card was named Plantation Card (called Green Card by villagers because the colour of the card was green). On the front side of the card,

Name of Card Holder
Name of Village
Date of Planting

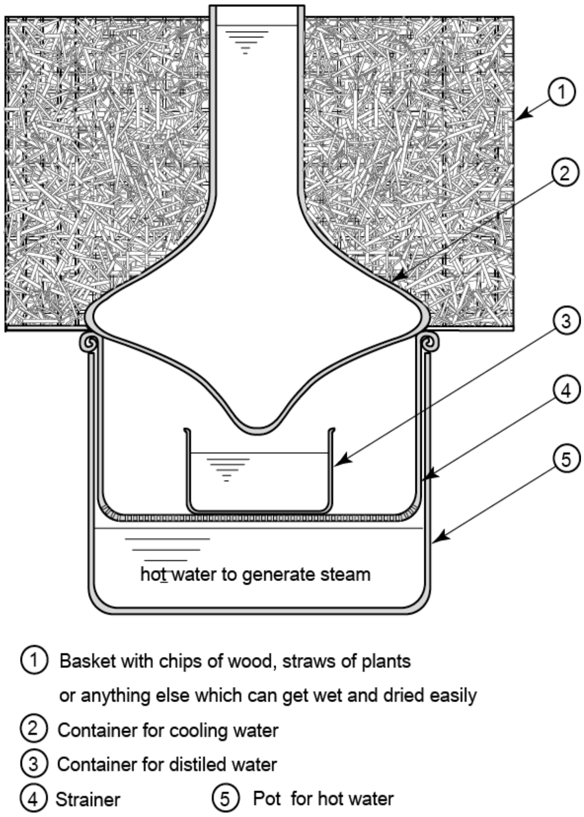

Figure 6 Distillation equipment

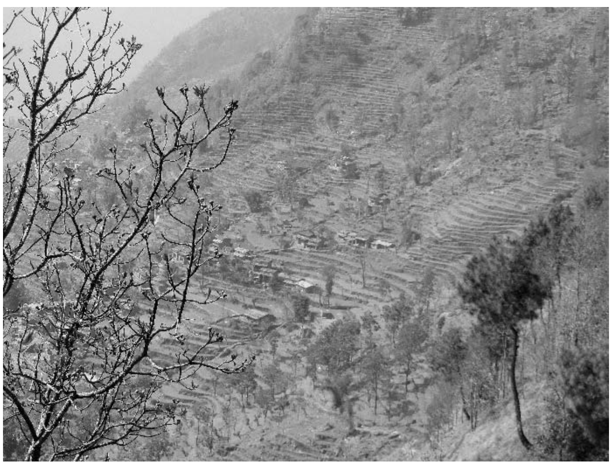

Figure 7 A typical village that lost their forest

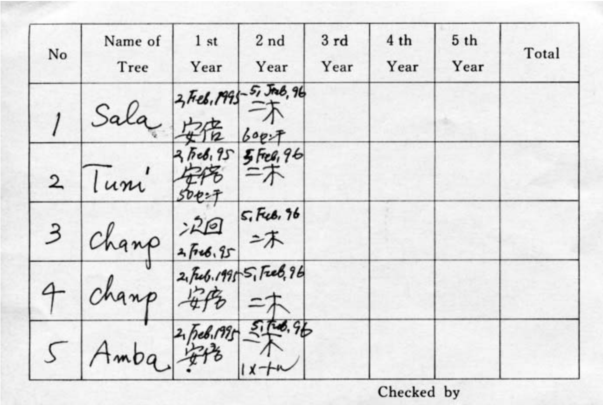

No	Name of Tree	1 st Year	2 nd Year	3 rd Year	4 th Year	5 th Year	Total
1	Sala	2,Feb,1995 安倍	5,Feb,96 二木 60センチ				
2	Tuni'	3,Feb,95 安倍 50センチ	5,Feb,96 二木				
3	Champ	[illegible] 2,Feb,95	5,Feb,96 二木				
4	champ	2,Feb,1995 安倍	5,Feb,96 二木				
5	Amba	2,Feb,1995 安倍	5,Feb,96 二木 1メートル				

Checked by

Figure 8 The plantation Card handed to villagers

Name of Dr. Abe and his address were printed. On the back side, a table shown in **Figure 8** was printed.

When a person is given a plant/plants, he receives this card. His tree is numbered and the name of tree is written in the second column. Dr. Abe confirms the planting and writes the date of plantation in the column of the first year and signs his name under the date. Everyone receives this card for every five trees. If the tree could survive one year later, Dr. Abe will write the date of confirmation and signs.

This method was proved to be an excellent idea. Dr. Abe found the next year, for his surprise, that 93% of 5,000 trees survived. Each villager had his/her own trees. Some groups built walls surrounding their areas. A girl who planted the nursery around her house built a small hedge using branches with thorns. In the dry season, everybody worked hard to water the trees every day. Many of them had to spend one hour to carry up buckets filled with water. Everybody took care of trees with love and pride. This is the beauty of this system.

This project has been going on for the last 24 years. Some of the trees grew really big as shown in **Figure 9**. Area of forest is being extended year by year covering 6 villages. The numbers of trees planted exceeded 500,000. In the forest thus re-born a spring has appeared. In the forest a little far from a village, even a tiger was eye witnessed. Forest Center, a bridge, water tanks and even a Gompa (a temple) were built for people. Two persons were sent to Japan, trained there and have been appointed as full time workers for the forest. Nursery trees are being grown by the Forest Center. All trees are self-supplied now

Dr. Abe has spent all of his earnings to this project. Volunteers in Nagano prefecture are helping him through an NGO. Their activity involves school children who collect used paper packs of milk from their homes and sell them for recycling. "Milk packs turn into forests in Nepal" is their slogan.

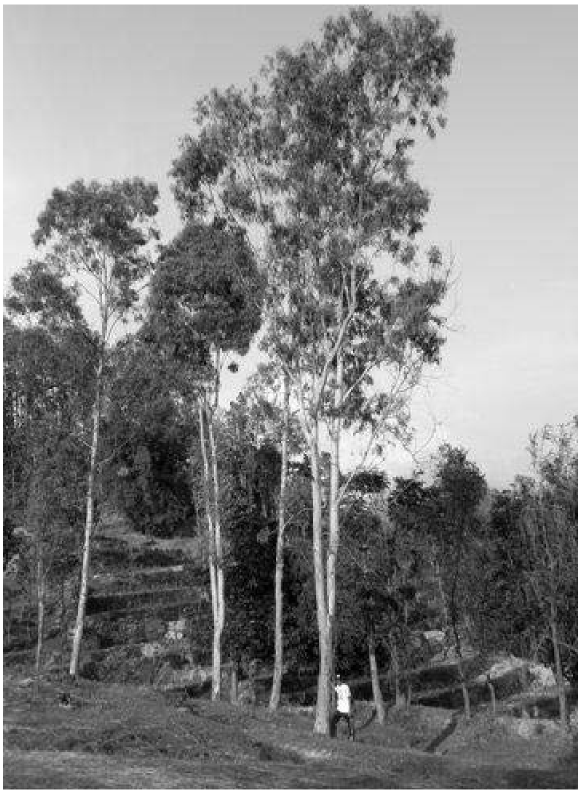

Figure 9 Trees planted 24 years ago

4 Shelter home

As we discussed in the former sections, many people are losing their houses. At present, about 1.5 billion people including 2 million refugees have no house. This number will increase to at least 3.5 billion in few decade. We have to supply them with shelters and toilets.

Specification for shelter is not so severe.

1) not too heavy
2) occupies a little volume when folded
3) cheap
4) good heat insulation ability
5) good anti-ultraviolet performance
6) easy to assemble and reassemble
7) recyclable or burnable after use

The authors like to propose one of the simplest shelter homes as like as shown in **Figure 10**. A sphere has the biggest rate of the volume to the surface area. Since the house with the shape of sphere is difficult to make and transport, the shape of a soccer ball is employed.

A soccer ball consists of 12 pentagons and 20 hexagons. If we make 10 panels of 1 pentagon connected to 2 hexagons, and 2 panels of a pentagon, as shown in **Figure 11**, we can assemble a shape of soccer ball. Connection is made by rubber bars that have two grooves on both sides. The gap coincides with the thickness of the panels.

Suppose the length of every side of pentagons and hexagons is made 400mm, we can build a shelter with the height of 3m. For the material of the panels, a hard plastics with air babbles in it is probably the best. That is because it is light and it has the high heat insulation characteristics.

If we make this shelter using the panels with 10mm thick, we will have a quite strong and durable shelter with good heat insulation. When it is folded, we can pack all parts, 12 panels and 40 bars, in 2m in length, 800mm in width and 120mm in thickness. The net weight is about 95kgf. Three men can deal with it without lifting machine.

5 Electricity and power assist

5.1 Mini-hydraulic power station

We need electricity. Some countries cannot have enough number of power stations. Some others have the stations but cannot deliver the electricity, because they have not enough money to

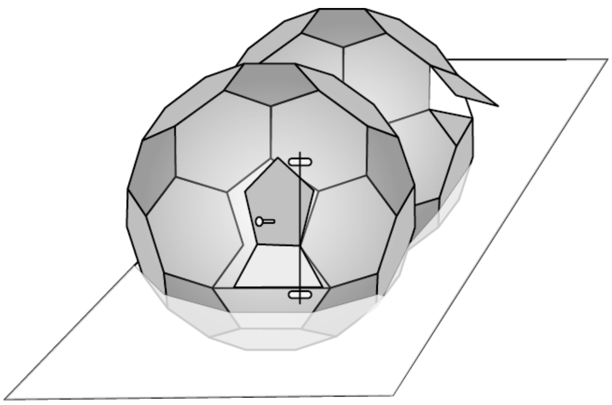

Figure 10 Soccer ball shelter

build a wire network or the wires are stolen.

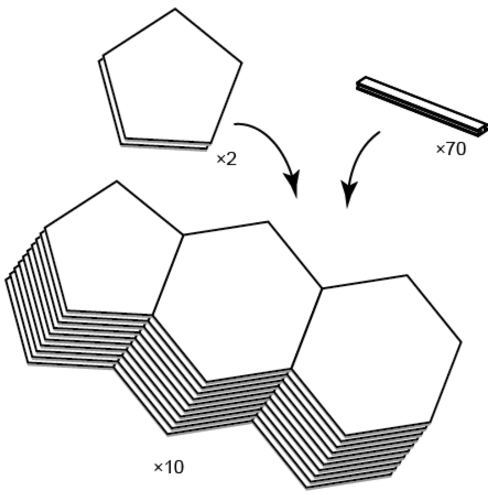

Figure 11 Parts needed for one shelter

It is ideal that each village has its own power station. Solar voltaic is ideal in that sense. But it costs too much. Therefore, it is a rational idea that each village has its own small hydraulic power station.

In ordinary hydraulic power station, Pelton turbine and Francis turbine are employed. These turbines have been used for a long time. But, they require at least 10m of head, which in turn a good size of dam is required.

Here, let us see the diagram shown in **Figure 12**. This is found in any textbook of hydraulic machines in university level. This shows that the water wheels of old days are exactly what we want. If we pour water of 4 m^3/sec on top of a water wheel with 4m in diameter, we can obtain 30kW. It is enough to supply the electricity to 200 houses at night and to operate a pomp to supply water for drinking or irrigation in day time.

In fact, the centre of Tsurumi city in Japan, a water wheel power station was built. It is called Kachuugawa Mini-hydraulic Power Station and is supplying 20kW to the city hall [7]. Companies specialized in the water wheel power generation have also been established.

5.2 Mini-excavator for farming

Farming is a hard job. Turning over the soil, particularly, requires farmers a great effort. The places where big cultivating machines are applicable is really limited in the world. It is not an exaggeration to say that farming is being carried out at small fields on slopes in most part of the world.

In such areas, a small but powerful excavator is a practical answer. An excavator shown in

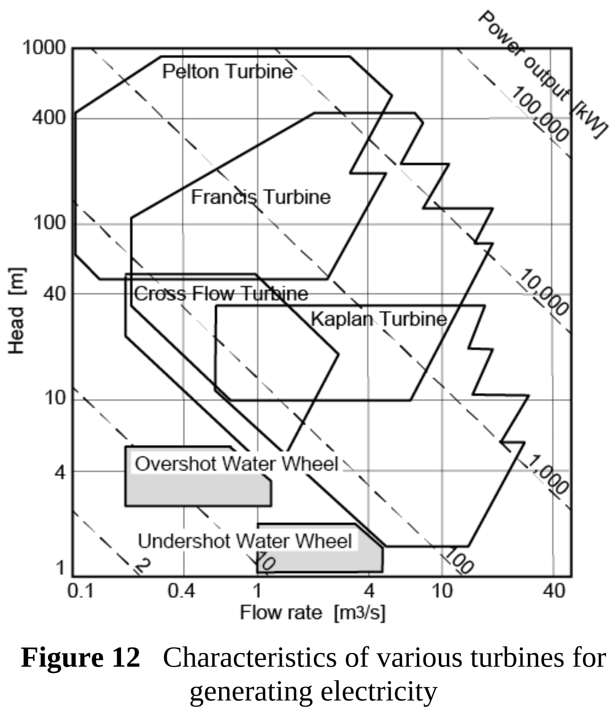

Figure 12 Characteristics of various turbines for generating electricity

Figure 13 A typical mini-excavator

Figure 13 is an example. It can be easily manoeuvred by one person, and transported on a small cart. But, again, it is too expensive.

We do not need a sophisticated machine like this. All what we need is a simple, tough and light machine. It seems that there is also a subject which some engineers have to tackle.

6 Conclusion

The population of the world is expected to become 10 billion in 2050, which is only 36 years from now. In many developing countries the growth of population overwhelms their economic growth. People will become poorer and poorer, and consequently about a half of total population will be living their hard lives. Whether you like it or not, it will come.

If we want to sustain or improve the present level of air pollution, food and energy supply, clean water or social factors as like as crime rate, what can we do? Some engineers have to assist those who live in slum-like environment.

Several ideas were listed in this paper.

1) The first thing we have to do is to supply those people with simple incinerators. It is very important for them and for the whole society that they have tidy environment and pride.
2) Efficient cooking stoves, which can generate heat from wooden chips, papers and dungs of animals, are necessary. The people in the arid regions can use parabolic thermal collectors.
3) Resources of safe water will become less and less. An example of distillation equipment is proposed.
4) We are losing the forest of about 70,000km^2 every year. The area of Slovenia is 20,273km^2. A project carried out by a doctor in Nepal is introduced. The very successful result proves that we can regenerate forests.
5) At the moment, about 1.5 billion people have no hose. An idea of shelter house is proposed.
6) Needs for mini-hydraulic power station and mini-excavator for farming are also pointed out.

The readers' comments, suggestions and new ideas from engineers' view point are truly welcome, which in turn can save the world.

References

[1] World Population Prospects: The 2012 Revision. In the Report issued by Population Division of the Department of Economic and Social Affairs of the United Nations Secretariat, http://esa.un.org/wpp/

[2] Mark R. Montgomery: The Place of the Urban Poor in the Cairo Programme of Action and the Millennium Development Goals, Panel on Urban Population Dynamics (2003), pXXIV-1.

[3] Mark R. Montgomery: The Place of the Urban Poor in the Cairo Programme of Action and the Millennium Development Goals, UN-Habitat (2003), pXXIV-2.

[4] UN Report: "Seven Billion and Growing", United Nations Department of Economic and Social Affairs, Population Division, Technical Paper No. 2011/3, p.26

[5] John Wilfrid Wright, "simple concentrating solar cooker for poor semi-desert countries", Spirit of Enterprise The 1993 Rolex Awards, BURI Buri Druck AG, Bern, 1994, pp.139-141.

[6] Garth Johnson, in his homepage: http://www.flickr.com/photos/extremecraft/5756879763/

[7] Yasuo Abe: "Pray for turning Nepali mountains into green" (written in Japanese), Shunju-sha, April 30th, 2002.

[8] The City Hall of Tsuru, Kachugawa Mini-hydraulic Power Station, http://www.city.tsuru.yamanashi.jp/forms/info.aspx?info_id=2681

Environmental loading reduction by bio-ethanol application to vehicle engine

T. Mori[1], and Y. Takasu[1]

[1] *Nagoya University, Japan*

Abstract

In addition to environmental problems such as global warming, it has been saying that fossil fuels of vehicle engines are limited. In this research bio-ethanol was paid attention and its usefulness was discussed, comparing with gasoline from the standpoint of energy balance. Furthermore in the case of applying bio-ethanol to car engine fossil energy consumption, carbon dioxide reduction and so on were discussed by simulations.

Keywords: environmental problem, bio-ethanol.

1 Introduction

Recently, environmental problems such as global warming become serious. Because much of transportation energy of cars, airplane and ships depends on fossil fuels, discharge of carbon dioxide cannot be restrained and aim of Kyoto Protocol on Climate change cannot be attained. Oil production in the world is uncertain based on the political unrest and oil price increases at all times. Therefore decrease of dependency of transportation energy on oil is recognized an urgent issue. Besides research development of bio fuel has an aim of an effective application of waste, it is expected as a recycle probable energy and means to decrease greenhouse gas.

In this research bio-ethanol which is one of bio fuels was paid attention and its usefulness was discussed, comparing with gasoline from the standpoint of energy balance. Furthermore in the case of applying bio-ethanol to car engine fossil energy consumption, carbon dioxide reduction were discussed by simulation.

2 Present condition and possibility of bio fuels as transportation energy

2.1 Background concerning about bio fuel

Figure 1 shows the present state of carbon dioxide circulation on the earth in 2008. Carbon contained in biomasses originates from carbon dioxide in the atmosphere in the growth process of plants by using solar energy. Even if biomasses burn, carbon dioxide in the atmosphere does not presume to increase and then biomasses are carbon-neutral energy. Therefore if biomasses are used as

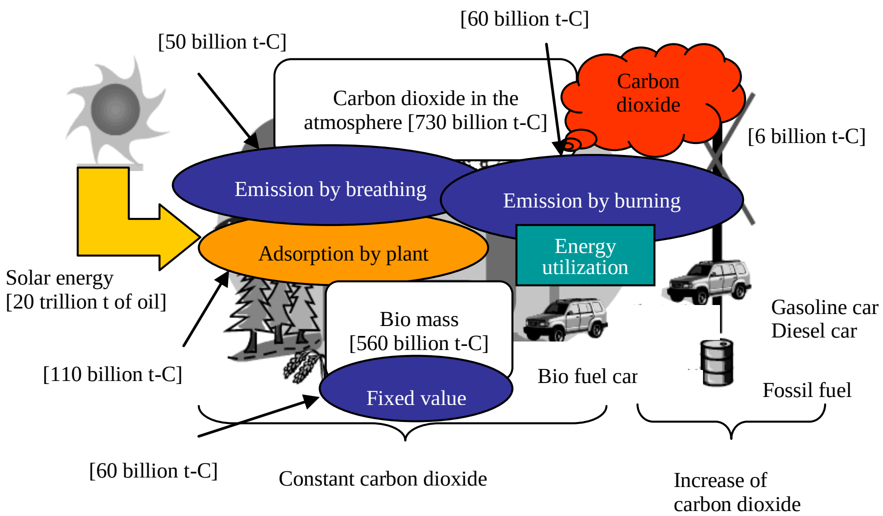

Figure 1 Circulation of carbon dioxide in the earth

alternative energy of fossil fuel, carbon dioxide in the atmosphere keeps constant, and it is an effective tool for provision against global warming. Especially if bio fuel is liquid and can be mixed easily in a liquid fossil fuel, existing internal combustion engines and existing commercial fuel distribution system can be utilized, they are expected as transportation energy among recyclable energies.

2.2 Worldwide tendency concerning about bio fuel

Figure 2 shows proceed of bio ethanol production in the world. After the annual production from 1980 to 2000 kept almost 15 billion *l*, it increased abruptly after 2000. This increased production

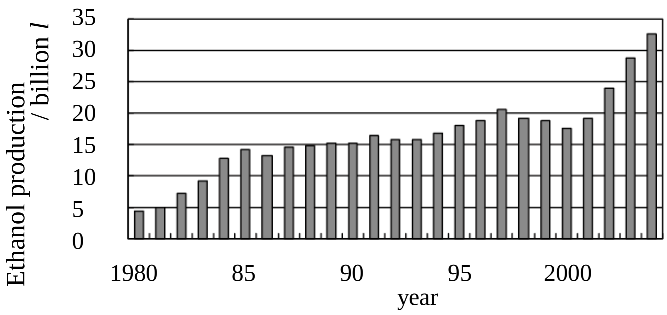

Figure 2 Bio ethanol productions in the world

responded the global environmental problem which connected to Kyoto Protocol on Climate change.

Figure 3 shows share of bio- ethanol production. Many nations attempted actively to introduce utility of bio fuels. In USA and EU promotion of agriculture and forestry, energy security and global warming control are attached importance. Furthermore in China bio fuel must be developed owing to increasing energy consumption with economic growth. In Brazil and ASEAN export of bio fuel and promotion of related industries are taken importance. On the other hand in Japan it has started only recently that significances and objects of introducing bio fuel are arranged and policies for promoting utilization of bio fuel are discussed.

When bio fuel is introduced as substitution of fossil fuel, the competition with utilization as food must be taken into consideration. The world population goes on increasing and is estimated to reach the peak of 9.2 billion persons. The present farmland is 14.5 billion ha which is 10 % of 145 billion ha of the land area all over the world. Expandable farming area in future is estimated 0.5 billion ha by the United Nations. Most of this area is necessary to satisfy increasing food demand, even if agricultural technologies are developed. Therefore a new production technology of bio fuel must be established. It is called as the technology of second generation bio fuel including cellulose bio ethanol. Bio masse materials until now are sugar cane, sugar beet and grains which are also food and can be transformed easily to bio ethanol. In future the second generation bio ethanol is potential for environmental protection material.

In Japan, of course the research of bio ethanol is considered to be important, bio ethanol is predicted about 6 billion *l*/year shown as in Table 1. In order to evade the competition to food, application of grass biomass and woody biomass are supposed. However import of bio ethanol is advantageous to production economically even taking transport cost.

Figure

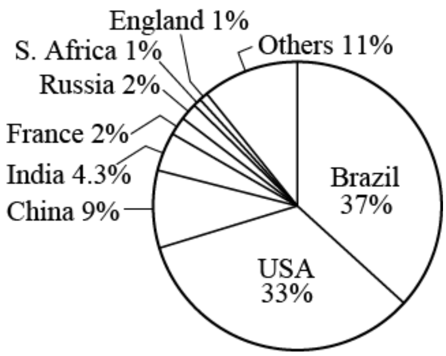

Table 1 Predicted production of bio ethanol in 2030 /billion *l*

material	
1. Saccharide, starch	0.05
2. Grass (rice, wheat straw)	1.8~2.0
3. Energy crop (rice, sugar beet)	2.0~2.2
4. Wood	2.0~2.2
5. Bio diesel	0.1~0.2
sum	6.0

3 Reduction effect of environmental load by bio ethanol

3.1 Recyclable energy and non-recyclable energy

Recyclable energies which are electric generations utilizing natural energies such as water power, solar power and wind power, bio ethanol and bio diesel are energies to be permanently supplied. On the other hand fossil fuel energies which are gasoline, light oil and kerosene made from crude oil, coal and natural gas, are generated in a long time of several hundred millions years and cannot be reproduced.

3.2 Comparison of environmental loading of bio ethanol and gasoline under consideration of LCA (Life Cycle Assessment)

3.2.1 Comparison of energy budget bio ethanol and gasoline in producing district such as Brazil

Although bio ethanol is recyclable natural energy, fossil energies are committed in the production process shown as Figure 4. Therefore it must be counted in consideration of an environmental loading.

Energy budget *E*s are given by the following expressions.

$E_B = B/F, \; E_G = G/F$

Where *B* and *G* are energy amounts of ethanol produced and gasoline produced, *F* is the energy amount of fossil energy charged to produce.

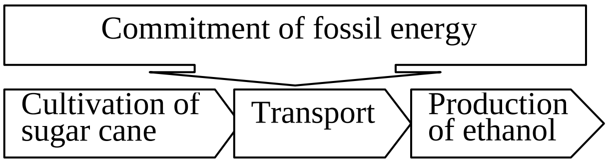

Figure 4 commitment of fossil energy in the production of bio ethanol

In cultivation of sugar cane 202 MJ/t of fossil energy is used, including indirect cost of fertilizer, weed killer and maintenance of equipment and machine and direct cost of farming and transparent machine. In production of bio ethanol from sugar cane 49 MJ/t of fossil energy is used, including indirect cost of chemical products and lubricants and maintenance of equipment and machines. Therefore commitment *F* of fossil energy is 251 MJ/t for creation of ethanol. Energy amount *B* obtained from produced ethanol is 1921 MJ/t. Consequently an energy budget of bio ethanol is given by,

$E_B = 7.6$

An energy budget of gasoline is given in many investigations,

$E_G = 6.7$

An energy budget of bio ethanol is better than that of gasoline, but a creation of bio ethanol must be taken a long time.

3.2.2 Comparison of energy budgets of bio ethanol and gasoline in Japan

In the case of the country which must import bio ethanol from other producing country, in the cost generating bio ethanol transport cost by a tanker between both countries must be counted. The transport cost between Brazil and Japan is 73 MJ/t and then total cost *F'* obtaining bio ethanol in Japan is 324 MJ/t.

The modified energy budget is given by

$E_B' = B/F' = 5.9$

This value is a little worse than the ethanol budget in Brazil and gasoline budget. Use of bio ethanol for alternative energy even in Japan is considered to be effective for solving environmental problem.

3.2.3 Comparison of fossil energy consumptions in utilizing as car fuel

When the same energy L is consumed, bio ethanol and gasoline use fossil energy of 0.17L ($=L/E_B' = L/5.9$) and 1.15L ($=L+L/E_G = L+L/6.7$). When utilization of car fuel is examined, environmental loading must be considered for not only fossil fuel but also bio fuel. The problem of fuel must be discussed not only at use, but also in production. Namely LCA (Life Cycle Assessment) must be considered.

4 Simulation of substitution from gasoline to bio ethanol

4.1 Contents of simulation

Under consideration of the forgoing discussion, simulations were conducted in order to evaluate the possibility of using bio ethanol as alternative fuel of gasoline. Two items are evaluated.

1. Possible ratio substituting gasoline to bio ethanol
2. Possible reduction of carbon dioxide by using bio ethanol

On 2008 in the world oil reserves are 1,138 billion bb*l* and oil is consumed by 85 million bb*l*/day and then oil should exhaust after 36 years.

4.2 Results of simulation

4.2.1 The case of Japan

Based on predicted production of domestic bio ethanol in Japan [1], shown in Figure 5, possible substituting ratio of bio ethanol will be 12.3 % until 2043 and it is energy of 4.4×10^9 GJ equivalent to 2 years consumption of gasoline.

Next if bio ethanol amounts to be imported is 3 times domestic produced amount, 49.0 % amount of gasoline can be substituted in 2043 and 8.6 years of gasoline consumption can be substituted until that year.

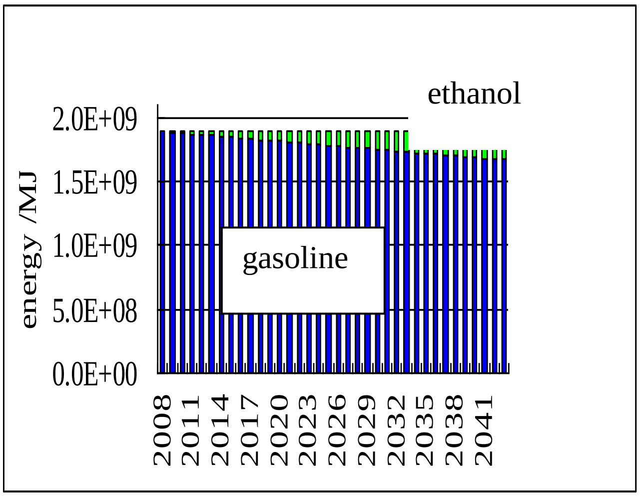

Figure 5 Possible substituting ratio of bio ethanol

In the second place possible carbon dioxide reduction is discussed in the case of E10 where 10 vol% bio ethanol is mixed to gasoline. Parameters of general gasoline car shown in Table 2 are used in order to calculate this problem.

The mileage of E10 is estimated as follows,

$$10 \times 0.9 + 6 \times 0.1 = 9.61 \text{ km}/l$$

Both cases using gasoline and E10 are compared with when the car is driven 100 km. used amount of each fuel is calculated by

Amount of gasoline = 100/10 = 10 *l*

Amount of E10 = 100/9.6

In both cases amount of gasoline used are

10 *l* in 100% gasoline

100/9.6×0.9 = 9.375 *l* in E10

Consequently amounts of emitted carbon dioxide are given by,

$2.4 \times 10 = 24$ kg in case of 100% gasoline,

$2.4 \times 100/9.6 \times 0.9 = 22.5$ kg in case of E10.

Reduction of emitted carbon dioxide per 100 km drive becomes 24-22.5=1.5 kg and reduction rate is 1.5/24=0.0625 by applying E10.

Table 2 Parameters of general gasoline car

Mileage of gasoline	10 km/*l*
Mileage of ethanol	6 km/*l*
Coefficient of CO_2	2.4 $kgCO_2/l$

All mileage in Japan reaches 445 billion km based on statics [2], and then all reduction of emitted carbon is $4.45 \times 10^{11} \times 1.5 \times 10^{-2} = 6.675 \times 10^9$ kg=6.675 Mt.

Another estimation of reduction of emitted carbon dioxide can be conducted based on the calories of gasoline and E10 shown in Table 3. Amount of E10 for energies of 1,820 PJ is $1{,}820 \times 10^{15}/(33.3 \times 10^6)$ =5.47 trillion *l*. Amount of gasoline in E10 of 5.47 trillion *l* is $5.47 \times 0.9 = 4.92$ trillion *l*. Therefore reducing gasoline consumption is 5.27-4.92 =0.35 trillion *l*. Corresponding reduction of carbon dioxide is given 8.3 trillion t which is near to the previous value.

Table 3 Energy consumed in a year and calories of fuels

Gasoline consumption by car	
	5.27 trillion *l*
	1,820 PJ
Calorie of gasoline	34.6 MJ/*l*
Calorie of E10	33.3 KJ/*l*

For using mixed fuel of gasoline and ethanol as car fuel, under consideration of combustion process of car engine and engine efficiency, E10 has been developed. However if a new car engine is developed, emission of carbon dioxide can be decrease. Therefore the following is discussed. Mixed ratio of gasoline and bio ethanol is assumed as $(1-m):m$. As bio ethanol is mixed by 100*m* %, the name of this mixed fuel is called by E100m.

The mileage of this fuel is calculated by

$$10 \times (1-m) + 6m = 10 - m$$

When the car is driven 100 km, consumed gasoline is

$$\frac{100}{10-4m} \times (1-m) = 50\frac{1-m}{5-2m}$$

Consequently amount of emitted carbon dioxide is given by

$$f(m) = 2.4 \times 50\frac{1-m}{5-2m}(1-m)$$

The derivation of *f*(*m*) with respect *m* is

$$\frac{1}{120}\frac{df}{dm} = -\frac{2(1-m)(4-m)}{(5-2m)^2}$$

As $0 \leq m \leq 1$, $-2(1-m)(4-m) \leq 0$ and denominator>0. Consequently, ratio of bio ethanol must increase as far as possible for decrease of carbon dioxide. The development of 100% ethanol engine car which has sufficient performance is expected.

Based on the discussion of heat energy and Figure 5 reduction of carbon dioxide in 36 years can be estimated, and the estimated value is shown in Table 4.

As mentioned above, fossil fuel is used in the production of bio ethanol and then emission of carbon dioxide must be considered in use of ethanol. Table 5 shows reduction of carbon dioxide under consideration of LCA.
The demand of Kyoto Protocol on Climate change can be resolved based on the forgoing

Table 4 Reduction of emitted carbon dioxide in 36 years

Domestic production	
Amount of ethanol	207 trillion *l*
Reduction of CO_2	304 trillion kg
Domestic production and import	
Amount of ethanol	828 trillion *l*
Reduction of CO_2	1220 trillion kg

discussion. However from now costs should be examined and infrastructures, facilities and production technologies of bio ethanol should be developed.

Table 5 Reduction of emitted carbon dioxide under LCA consideration

Domestic production	
Amount of ethanol	207 trillion *l*
Reduction of CO_2	249 trillion kg
Domestic production and import	
Amount of ethanol	828 trillion *l*
Reduction of CO_2	996 trillion kg

4.2.2 The case of the world

Figure 6 shows consumed calorie of gasoline which is assumed 85 million bbl/day and ethanol production calculated in calorie, in the world. In 2043, 34.62 % of energy consumed in the world can be substituted by ethanol. Amount of ethanol produced in 36 years is 4.27×10^5 PJ which is energy in 6.26 years.

Table 6 shows possible reduction of carbon technology dioxide in 36 years. Possible reduction of carbon dioxide of 29.6 billion t in 36 years is a little more than emitting carbon dioxide of 27.1 billon t in 1 year.

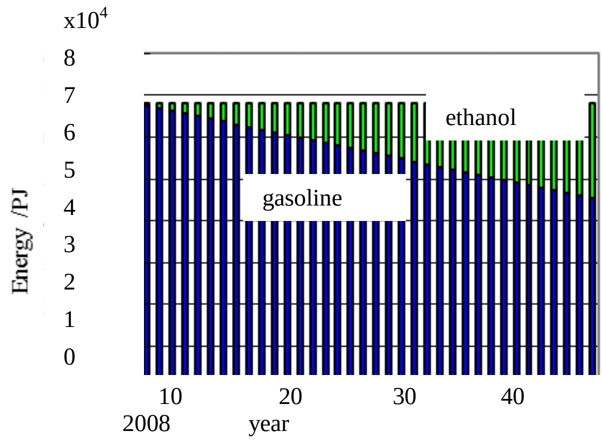

Figure 6 Possible substituting ratio of bio ethanol in the world

Table 6 Reduction of emitted carbon dioxide in 36 years in the world

Ethanol production	20.16 trillion *l*
Possible reduction of CO_2	29.6 billion t

5 Conclusions

Reduction effect of environmental loading by applying bio ethanol to car engine was discussed and the following was appointed.

(1) Biomass is an effective tool for provision against global warming.

(2) In production of even bio ethanol fossil energy is used and then carbon dioxide must be considered to be emitted in use of bio fuel.

(3) Energy budget of bio ethanol of 7.6 is larger than that of gasoline of 6.7.

References

[1] homepage of ministry of agriculture and forestry of Japan, http:/ /www.maff.go.jp /j /biomass/

[2] homepage of ministry of environment of Japan, http://www.env.go.jp/

[3] http://www.nedo.go.jp/index.html

Application of corundum based abrasives for abrasive waterjet cutting: disintegration properties and recycling potential

Pude, F.[1]; Grigoryev, A.[1]; Perec, A.[1]; Stirnmann, J.[1]; Wegener, K.[1,2]

[1] *Inspire AG, Corporation for Mechatronic Systems and Production Technology, Zurich, Switzerland; perec@inspire.ethz.ch*
[2] *Institute for Machine Tools and Manufacturing, Swiss Federal Institute of Technology (ETH), Zurich, Switzerland; info@iwf.mavt.ethz.ch*

Abstract

It is known from numerous publications that corundum based abrasives are used for cutting of extremely hard materials like e.g. ceramics by means of abrasive waterjets. Due to a reduced lifetime of the used focusing tubes this type of abrasive is only applied under special consideration of economic aspects. Caused be the limited application of this grain type the available amount of used abrasive is small at the involved cutting centers. For that reason a recycling process was never thought to be suitable. Nevertheless it is of scientific interest to observe the disintegration of these particles which have been interactive with mostly advanced materials. Garnet based abrasives are commonly classified in different grain size classes after sieving to evaluate their recycling potential. Based on a feasibility study this paper will present some results on achieved cutting data and shows also the geometrical change of the used focusing tubes. This was realized by non-destructive examination. The disintegration properties of the corundum based abrasive were monitored by sieving and optical test methods. Finally the obtained results were used to make a rough calculation for comparing the possible recycling process (cleaning, sieving, and drying) for corundum and garnet based abrasives.

***Keywords*:** abrasive, waterjet, corundum, grain size, recycling, disintegration

Life cycle assessment of ice abrasive water jet cutting technology

Andrej Zupančič[1], Marko Jerman[1], Andrej Lebar[1], Jon Baranda Jimenez[2], Ainhoa del Caso[2]

[1] *University of Ljubljana, Slovenia*
[2] PRYSMA, Spain

Abstract

The main water jetting technologies used by industry are pure Water Jet (WJ) and Abrasive Water Jet (AWJ). AWJ uses water with abrasive particles. The cutting power is obtained by transforming the hydrostatic energy of the water in a jet with sufficient kinetic energy as to disintegrate the material. The energy required to cut materials is obtained by pressuring the water to ultra-high pressures and focusing the water into high speeds through a sapphire orifice of small diameter.
The AWJ cutting technology is one of the WJ technologies that is more widely used in industry. It has been well proven that AWJ technology have energetic and economic efficiency for rough cutting as well as for the precise cutting of thin metallic sheet parts. However, the use of abrasives is not always possible, for example in applications such as the processing of hygroscopic and chemically reactive materials, as well as when working near high voltage, toxic or radioactive sources. Because of all this reasons a new technology of water jet cutting was developed. After upgrading water jet technology with some components, it was possible to generate ice particles in order to increase the cutting capacity. Developed technology is called Ice Abrasive Water Jet Technology (IAWJ) in IceJet (IJ) project. This project is a feasibility study funded by the European LIFE program within the thematic area of Environment Policy & Governance. The main objective of the IAWJ project is to demonstrate the technical feasibility of IAWJ cutting technology, to cut different types of materials with different characteristics, through the development of a pilot plant. It is known that manufactures are trying to achieve sustainability through changes in products, processes and systems. Sustainable technology researches provide techniques to balance the economic, social, and environmental needs of today with the prospects for the same - or better - quality of life for tomorrow's generations. One of the techniques to assess environment impacts associated with all the stages of product's lifetime is Life Cycle Assessment (LCA). It can help to avoid a narrow outlook on environment concerns. In this paper it will be described how the IAWJ technology effects the environment and compared with other water jet technologies with LCA analysis.

Keywords: Water jet, abrasive water jet, ice jet, sustainability and Life Cycle Analysis.

1 Introduction

There are several different techniques of cutting with a water jet. This are water jet, abrasive water jet and ice abrasive water jet technology. Water jet is widely used in industry for cutting, graving and removing metal or non-metal materials especially in airplane and nautical industry. Water jet technology is usually used for cutting soft materials or cleaning materials. To improve cutting efficiency are used mineral abrasive. It is added in mixture chamber. But in this technology 90% of waste is presented by abrasive. After all we have abrasive stacked in cutting surface. This is for example not acceptable in turbine paddle. Because of all this reasons a new technology of water jet cutting was developed, called ice abrasive water jet. The principal difference is that Ice Abrasive Water Jet (IAWJ) works with water ice particles while in AWJ technology the abrasive is mineral garnet. Therefore, the waste generated during the IAWJ cutting process will be drastically reduced. In the LIFE+ project has been first time carried out sustainability analysis in this area. LIFE + is program of the European Union to subsidize projects based on the development of environmentally friendly technologies. The purpose of the analysis is to compare three technologies together and analyze their environmental performance.

The main goal of IAWJ technology is to improve the existing technologies in terms of environmental compatibility. Technologies are usually compared by criteria such as price, material recovery, energy efficiency but Life Cycle Analysis method offers a general framework for evaluation. The analysis presents a systematic approach to evaluating the impact on the environment, resources and human health using the life cycle.

2 Water jet technologies

The cutting power is obtained by transforming the hydrostatic energy of water in a jet with sufficient kinetic energy to cut the material. The energy required to cut the materials is obtained by pressurizing the water to ultra-high pressures and conducting the water through a small diameter orifice made in sapphire in order to reach high speeds. Currently, the main water jet technologies used in industry are Pure Water Jet Technology (PWJ), Abrasive Water Jet Technology (AWJ) and developed technology. This is Ice Abrasive Water Jet Technology (IAWJ) [1, 5].

2.1 Pure water jet technology

PWJ technology (Figure 1) has lower cutting capacity than abrasive water jet technology, therefor material for cutting must be softer. The first applications of this technology were carried out in the early seventies to cut corrugated cardboard. Currently it is used for other applications such as cutting foams, rubbers and in food industry. Basically it is used in industrial processes where cutting with abrasive is not acceptable due to the possible contamination of the resulting material after the cut. Therefore, the application scope of PWJ is much smaller than the AWJ technology [1, 5].

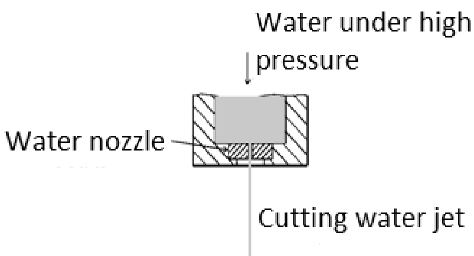

Figure 1 Pure water jet [7].

2.2 Abrasive water jet technology

AWJ cutting technology presented in figure 2 is a non-conventional machining process in which abrasive grains entrained in a high speed water jet collide with the work piece and erode it. A water jet is used to accelerate the abrasive grains and to assist the material removal process [1, 5].

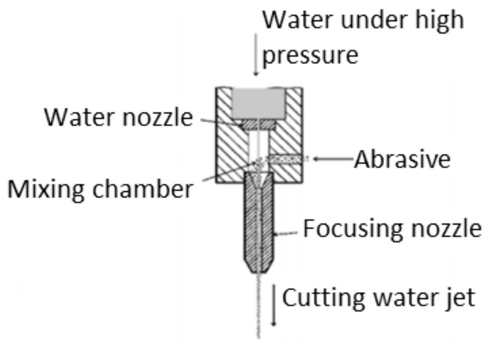

Figure 2 Abrasive water jet [7].

AWJ is currently used in cutting, engraving and milling of both metallic and non-metallic materials up to 120 mm thickness. In recent times this technology has become very important in naval and aerospace industries, where materials with different types of alloys and composites are widely used. These materials are difficult to manufacture by using conventional technologies. This technology is also used for cleaning and surface treatment of materials [1, 5].

2.3 Ice abrasive water jet technology

IAWJ technology is based on AWJ technology. Instead of abrasive grains in the mixture chamber the liquid N_2 is used to freeze the high speed water jet (figure 3) [1, 5].

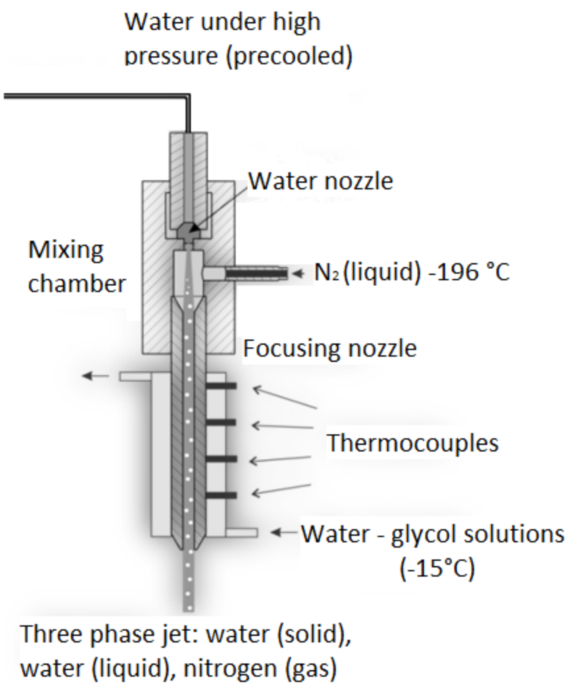

Figure 3 Ice abrasive water jet technology [5].

In cutting head temperature of water rises. To get good conditions for water to freeze, it needs to be cooled down to -20 °C (Figure 4). This gives us a good mixture of ice grains and water. Therefore a high pressure heat exchanger was designed and built [1, 5].

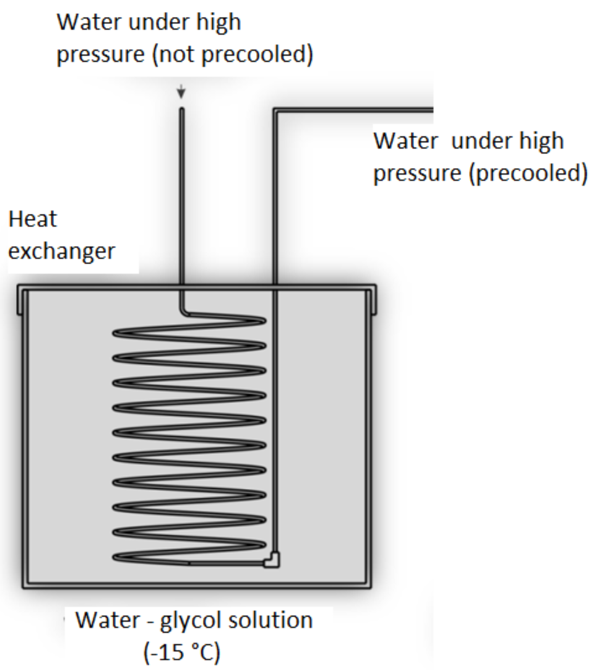

Figure 4 Pre-cooling of pressurized water in IAWJ [5].

3 Sustainability

As the environmental awareness increases, industries and businesses are assessing how their activities affect on the environment. Society has become concerned about the issues of natural resource depletion and environmental degradation. Many businesses have responded to this awareness by providing "greener" products and using "greener" processes. The environmental performance of products and processes has become a key issue, which is why some companies are investigating ways to minimize their effects on the environment. Many companies have found it advantageous to explore ways of moving beyond compliance using pollution prevention strategies and environmental management systems to improve their environmental performance. One such tool is Life Cycle Assessment. This concept considers the entire life cycle of a product (Curran 1996) [1, 5 and 6].

4 Life cycle assessment

Life Cycle Assessment (LCA) is a "cradle-to-grave" approach for assessing industrial systems. Approach begins with the gathering of raw materials from the earth to create the product and ends at the point when all materials are returned to the earth. LCA is unique because it evaluates all stages of a product's life from the perspective that they are interdependent, meaning that one operation leads to the next. LCA enables the estimation of the cumulative environmental impacts resulting from all stages in the product life cycle, often including impacts not considered in more traditional analyses (e.g., raw material extraction, material transportation, ultimate product disposal, etc.). By including the impacts throughout the product life cycle, LCA provides a comprehensive view of the environmental aspects of the product or process and a more accurate picture of the true environmental trade-offs in product and process selection. When deciding between two or more alternatives, LCA can help decision-makers compare all major environmental impacts caused by products, processes, or services [1, 2, and 6].

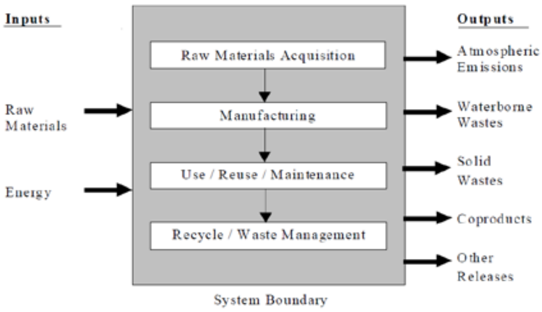

Figure 4 Life cycle Stages [2].

Figure 4 illustrates life cycle phases that can be considered in an LCA and measuring inputs/outputs. The LCA process is a systematic, phased approach and consists of four components: goal definition and scoping, inventory analysis, impact assessment, and interpretation as illustrated in figure 5 [1, 2, and 6].

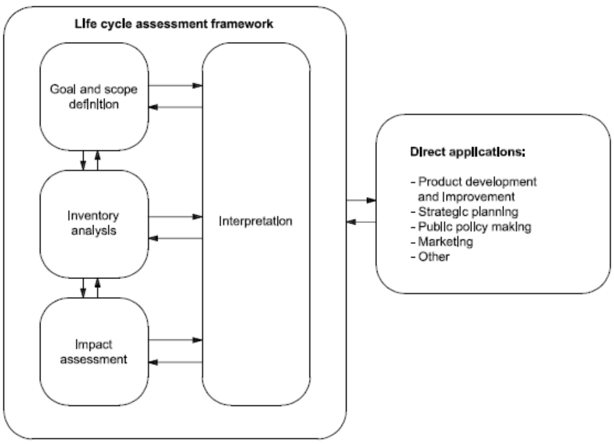

Figure 5 Phases of an LCA [2].

In the case of ICEJET, the LCA will be used as a tool for assessing the impact of water jet technology (PWJ, AWJ and IAWJ), to know and compare the environmental impacts of the three technologies from cradle to grave approach. The final objective is to have more environmentally relevant information, especially in the niches in which the different technologies may overlap [1, 2, and 6].

4.1 Goal Definition and Scoping

Define and describe the product, process or activity. Establish the context in which the assessment is to be made and identify the boundaries and environmental effects to be reviewed for the assessment [1, 2, 6].

In this chapter also defined that the Ecoindicator 99 methodology in its hierarchic perspective has been followed. Ecoindicator is database of numbers that express the total environmental load of a product or process. With appropriate LCA software it is possible to calculate additional indicators. Hierarchy perspective is used because is widely accepted by scientific community and it is considered by default in Ecoindicator 99 in the data base Ecoinvent © v2.01 (2009). It means that test measure three types of environmental damages. These are human health, ecosystem quality and resources. All types are then divided into several sub-sections [2].

4.2 Life Cycle Inventory

A Life Cycle Inventory Analysis (LCI) means building a flow model of a technical system. The model is an incomplete mass and energy balance of the system, which only takes into account the flows with environmental relevance. LCI activities include [1, 3, 6]:

1. Construction of the flowchart according to the "System boundaries" decided in the object and scope section.

2. Data collection for all the activities of the product system together with its associated documentation. Results of data collection for all technologies are presented on figures 6, 7 and 8.

Initial unit process	# BBDD	Input/output	Quantity	Unit
STAGE OF OBTAINING RAW MATERIALS, MANUFACTURING, AND ASSEMBLY				
6	8310	steel product manufacturing, average metal working	1385	kg
STAGE OF TRANSPORTATION				
9	1943	transport, lorry >16t, fleet average	1574,745	tkm
11	1968	transport, transoceanic freight ship	8503,9	tkm
STAGE OF USE				
13	8311	chromium steel product manufacturing, average metal working	10,582	kg
16	1840	polyvinylchloride, at regional storage	39,360	kg
18	1847	synthetic rubber, at plant	51,304	kg
20	478	sand, at mine	1478476,8	kg
21	2526	EUR-flat pallet	1478,4768	unit
22	1943	transport, lorry >16t, fleet average	1118763,395,	tkm
24	1968	transport, transoceanic freight ship	14597001,450	tkm
25	7207	electricity, low voltage, production RER, at grid	2974016	kWh
29	2288	tap water, at user	723168	kg
30	2085	process-specific burdens, inert material landfill	1995943,68	kg
STAGE OF DISPOSAL				
37	2082	disposal, steel, 0% water, to inert material landfill	1385	kg
40	1943	transport, lorry >16t, fleet average	85,870	tkm

Figure 6 Collected data for AWJ in each stage of LCA analysis [3].

Initial unit process	№ BBDD	Input/output	Quantity	Unit
STAGE OF OBTAINING RAW MATERIALS, MANUFACTURING, AND ASSEMBLY				
1	8311	chromium steel product manufacturing, average metal working	0,292	kg
STAGE OF TRANSPORTATION				
3	1943	transport, lorry >16t, fleet average	0,332004	tkm
5	1968	transport, transoceanic freight ship	1,79288	tkm
STAGE OF USE				
6	8311	chromium steel product manufacturing, average metal working	0,584	kg
8	7207	electricity, low voltage, production RER, at grid	669600	kWh
9	2288	tap water, at user	910656	kg
STAGE OF DISPOSAL				
10	2082	disposal, steel, 0% water, to inert material landfill	0,292	kg
12	1943	transport, lorry >16t, fleet average	0,018104	tkm

Figure 7 Collected data for PWJ in each stage of LCA analysis [3].

Initial unit process	№ BBDD	Input/output	Quantity	Unit
	STAGE OF OBTAINING RAW MATERIALS, MANUFACTURING, AND ASSEMBLY			
1	8339	copper product manufacturing, average metal working	90,2019919	kg
3	8310	steel product manufacturing, average metal working	128,758365	kg
4	8311	chromium steel product manufacturing, average metal working	143,64687	kg
	STAGE OF TRANSPORTATION			
11	1943	transport, lorry >16t, fleet average	412,284417	tkm
13	1968	transport, transoceanic freight ship	2226,408373	tkm
	STAGE OF USE			
17	8311	chromium steel product manufacturing, average metal working	1,064	kg
24	300	nitrogen, liquid, at plant	80352	kg
25	402	ethylene glycol, at plant	555	kg
26	7207	electricity, low voltage, production RER, at grid	716204,16	kWh
27	2288	tap water, at user	1795028	kg
	STAGE OF DISPOSAL			
28	2082	disposal, steel, 0% water, to inert material landfill	362,6072269	kg
38	1943	transport, lorry >16t, fleet average	22,48164807	tkm

Figure 8 Collected data for IAWJ in each stage of LCA analysis [3].

3. Calculation of the inputs and outputs (environmental loads) such as use of natural resources and pollutant emissions of the system in relation to the functional unit. This is an accumulative process, often iterative. While collecting the data, the knowledge on the systems itself increases. Thus, sometimes the decisions taken while defining the goal and scope need to be reviewed. The results of the inventory is an LCI which provides information about all inputs and outputs shown as elementary flows to and from the environment, for all the unit processes involved in this study. Calculations are presented on figure 9 and 10.

Selected LCI Result		AWJ	PWJ	IJ corrected
Category	Subcategory			
air	NMVOC (kg)	5817672816	270526973	283174047,4
resource	land occupation (m2a)	786639,1676	41432,1391	44916,53261
air	CO2, fossil(kg)	8194219,201	1687523,85	1845250,648
air	nitrogen oxides(kg)	18844,31792	2959,75756	3245,534336
air	sulphur dioxide(kg)	26952,40499	5195,14619	5728,631859
air	particulates, < 2.5 µm(kg)	2145,098048	419,141506	460,4030818
water	BOD	9336,456685	755,588053	838,6434965
soil	cadmium	1,595423247	0,00232746	0,175178326

Figure 9 Summary of selected LCI results of all technologies [3].

Selected LCI results Additional		AWJ	PWJ	IJ corrected
Category	Subcategory			
air	Methane (kg)	16868,53957	3281,29341	3596,971749
total	oils, unspecified (kg)	5559,973141	433,186042	483,2315685
air	N20 (kg)	223,8219876	46,2310819	50,7208012
air	particulates, >2.5 um and <10 (kg)	672,4111194	108,502177	121,3833943
air	particulates >10 um (kg)	5345,866883	1132,71645	1242,158886
air	Lead (kg)	3,249612395	0,65254132	0,722267892
air	Zinc (kg)	13072,79785	9,07046226	1664,432096
total	heat, waste (MJ)	117663830,7	23896505,7	26197520,91
air, radioactive	radon (+ radium) (kBq)	3291289663	728312686	802239277,9
air, radioactive	noble gas (kBq)	1723343859	381578467	421565401,1
air, radioactive	Aerosole (kBq)	12401,13249	2752,31583	3045,684442
air, radioactive	Actinides (kBq)	2440,609747	531,711799	589,3444482
water, radioactive	Radium (kBq)	308464,6546	63954,1	71477,3018
water, radioactive	Tritium (kBq)	76911756,65	17030146,6	18808419,86
water, radioactive	Nuclides (kBq)	286494,676	63554,8887	70421,83765
water, radioactive	Actinides (kBq)	103935,7976	21280,6272	23454,41355
resource	Water (m3)	72169,03888	15060,0535	16560,85705
air	carbon monoxide (kg)	4644,791646	584,985895	645,8288981
air	Particulates (kg)	8162,813353	1660,35403	1823,88955
resource	carbon, biogenic, fixed (kg)	90982,9927	895,54247	977,0422003

Figure 10 Summary of additional LCI results of all technologies [3].

4.3 Life Cycle Impact Assessment

The stage of an LCA called life cycle impact assessment (LCIA) aims at describing the environmental consequences of the environmental loads quantified in the inventory analysis. The impact assessment is achieved by "translating" the environmental loads form the inventory results into environmental impacts such as acidification, ozone depletion, effect on biodiversity, etc.

ISO 14040 determines a mandatory structure for this LCA stage [1, 4, 6]:

- Selection of impact categories, category indicators and characterization models,
- classification and
- characterization.

Values are in LCIA re-calculated from the results of selected LCI data with Ecoinvent database v 2.1 2009. A mass or energy balance is developed, including the relationship of each process with the processes "upstream". By addition of all the values associated to each process, the total final value is obtained for the entire unit process that is being evaluated. The value obtained from the database is multiplied by the functional unit value obtained for each stage in the process of the corresponding cutting technology. But before describing results it is important to understand established system boundaries stated in analysis. The cutting tests for AWJ technology have been performed in company IAMCUT using FLOW WMC-02 machine. For PWJ technology tests have been performed in IAMCUT using OMAX 2652A machine. IAWJ technology tests have been done in University of Ljubljana using prototype developed in Laboratory for alternative technologies. Because tests have been done in different location and machines, it means that comparison of the data obtained for three technologies need to be done. All technologies are based on PWJ technology. Machines have done tests of PWJ technology. Results of tests have been compared and conversion factor is 0,934. When calculating results is important to take into account this factor to make result correct [1, 4, 6].

For treatment of data obtained in the LCI, and the classification and characterization of the impacts produced for the LCIA, the following treatment procedure is followed: first the total values obtained for all the functional units of each of the unit processes are taken [1, 4, 6].

That value is multiplied by the value of the Ecoindicator 99 (H, A) found on the Ecoinvent v2.1 2009 database for that process in each of the corresponding cutting stages. "Points" are the reference unit for the calculation of impacts using this methodology, a single unit of measurement that allows comparisons between the various indicators and assessment of the main impacts of the three technologies.
Table 1 present results for all technologies. All three technologies present summary of the environmental impacts according to Ecoindicator 99 expressed in points and categorizations. On table 1 AWJ technology has 5.75 times higher environment impact than IAWJ and 6.29 times higher than PWJ [1, 4, 6].

Table 1 Summary of impact of three technologies according to Ecoindicator 99 [4].

TOTAL ECOINDICATOR 99-(H,A) [points]		AWJ	PWJ	IAWJ
ecosystem quality	acidification & eutrophication	10764,69	1774,97	1948,6
ecosystem quality	Eco toxicity	8294,98	1512,231	1662,35
ecosystem quality	land occupation	10634,08	847,35	928,45
ecosystem quality	total	29693,29	4134,51	4539,37
human health	carcinogenic	13346,26	2859,35	3180,83
human health	climate change	47109,13	9679,06	10583,83
human health	ionizing radiation	3018,378	667,79	736,26
human health	ozone layer depletion	18,36	2,2261	2,45
human health	respiratory effects	127562,21	22967,27	25230,36
human health	total	191050,720	36174,82	39732,89
resources	fossil fuels	264378,48	36721,58	39980,75
resources	mineral extraction	2586,66	492,03	581,16
resources	total	266964,51	37212,69	40561,04
total	total	487714,99	77524,27	84835,45

4.4 Life cycle interpretation

Life Cycle Interpretation is a systematic technique to identify, quantify, check, and evaluate information from the results of the life cycle inventory and/or the life cycle impact assessment. The results from the inventory analysis and impact assessment are summarized during the interpretation phase. The outcome of the interpretation phase is a set of conclusions and recommendations for the study. According to ISO 14040:2006, the interpretation should include [4]:

1. Identification of significant issues based on the results of the LCI and LCIA phases of an LCA,
2. evaluation of the study considering completeness, sensitivity and consistency checks and
3. conclusions, limitations and recommend.

A key purpose of performing life cycle interpretation is to determine the level of confidence in the final results and communicate them in a fair, complete, and accurate manner. The key points of the LCA analysis in LIFE+ project are summarized in the following aspects [4]:

1. The stage of use is the most pollutant step in any of the 3 cutting technologies studied.
2. In the stage of use, the main environmental impacts result from electricity consumption in the 3 cutting technologies studied.
3. In AWJ technology, the transportation of abrasive causes significant environmental impacts too, both due to highway and sea transportation and the need to use pallets to transport the bags with abrasive.
4. In IAWJ technology, the liquid nitrogen consumption also results in important environmental impacts. On the other side, the impacts resulting from the obtaining and manufacturing of stainless steel and copper are significant. These materials are required for the manufacturing of the accessory equipment for IAWJ technology.

5 Conclusion

In this paper three technologies were presented. Pure water jet, abrasive water jet and ice abrasive water jet. Pure water jet was developed for cutting soft materials. With upgrading PWJ to AWJ, cutting head was changed. Mixture chamber was added to mix high speed water with abrasive. This upgrade improves cutting capacity. But in the other hand AWJ cannot always be used, for example processing of meat products, the cleaning of sensitive surfaces as well as biomedical applications and etc. The principal difference is that IAWJ works with water ice particles while in AWJ technology the abrasive is mineral garnet. Therefore, the waste generated during the IAWJ cutting process will be drastically reduced. In the LIFE+ project the sustainability analysis in this area has been carried out for first time. For sustainability analysis LCA method was used. LCA method is a “cradle-to-grave” approach for assessing industrial systems. “Cradle-to-grave” begins with the gathering of raw materials from the earth to create the product and ends at the point when all materials are returned to the earth. With analysis we obtained a complete review of the environment impact throughout its entire life cycle of technologies. Three technologies and their environmental performance were analyzed.

The goals of this Life Cycle Assessment (LCA), established in the document “Objectives and scope”, are to compare the three water jet cutting technologies and analyze their environmental performance. The aim of the study is [4]:

1. To perform an inventory of all components in the three different cutting technologies (according to system boundaries established)
2. To compare the three different technologies with respect to environmental impact
3. To identify the stages in the life cycle which make the largest contributions to the total environmental impact.

Results of analysis show that from all phases, phase of use has biggest impact on environment at all three technologies. The biggest proportion of use presents the electrical consumption. In IAWJ, high environment impact has extraction, production and assembly phase of raw liquid nitrogen, copper and stainless steel. In AWJ technology big environment impact also presents transport of abrasive and the use of pallets. At the end the biggest environment impact has AWJ technology. In comparison with the results of cutting it can be said that the IAWJ technology is good enough in cutting ability of rubber and very organic oriented technology [1, 2, 3, 4].

References

[1] Zupančič A., Life cycle assessment of abrasive ice jet cutting technology, Slovenia, May 2013

[2] Ice Jet project consortium, LCA comparing three cutting technologies: Abrasive Water Jet (AWJ), Pure Water Jet (PWJ) and Ice Jet (IJ). OBJECTIVES AND SCOPE, Spain, December 2012

[3] Ice Jet project consortium, LCA comparing three cutting technologies: Abrasive Water Jet (AWJ), Pure Water Jet (PWJ) ad Ice Jet (IJ). LIFE CYCLE INVENTORY (LCI), Spain, December 2012

[4] Ice Jet project consortium, LCA comparing three cutting technologies: Abrasive Water Jet (AWJ), Pure Water Jet (PWJ) and Ice Jet (IJ). LIFE CYCLE IMPACT ASSESSMENT (LCIA), Spain, December 2012

[5] Jerman M., Pregled literature in zasnova merilnega mesta za obdelavo s kriogenim vodnim curkom, Ljubljana, 2011

[6] SAIC, Life cycle assessment: Principles and practice, Ohio, May 2006

[7] http://www.drustvo-tavo.si, retrieved on 03.07.2013

Range-Extender in electric vehicles – a revival of (highly optimized) two-stroke engines on a small scale

A. Nagel[1], S. Thäter[2], and R. Steinhilper[2]

[1] *Fraunhofer IPA, Germany*
[2] *Bayreuth University, Germany*

Abstract

The limited accumulator capacity of modern electric vehicles, which are driven by accumulator powered electric motors, is one reason why these systems do not prevail. To increase the range and the attractiveness of electric powered vehicles, the research project "MIHY - **Mi**niatur **Hy**brid" is handling the development of a modern range extender by using two-stroke engines (mechanical power: ~ 3 kW) on a small scale. To increase the over-all efficiency, thermal energy in the exhaust system has to be converted into kinetic energy. Therefore a laval nozzle accelerates the exhaust gas to supersonic speed, which is driving a subsequent, for the exhaust conditions specialized, turbine generator. Furthermore the whole exhaust system, including the turbine and the laval nozzle, is optimized for the resonance of sound waves in order to minimize the loss of fresh gas during the gas exchange in the two-stroke engine. So the sound waves, which are caused by the combustion, must reflect at the nozzle to a certain time to assure an optimal charge of the combustion chamber. Therefore the length of the exhaust system and the propagation delay are synchronized. At the piston outlet they provoke a local pressure increase, which forces unburned gases back to the piston. All relevant conditions like pressures and temperatures at different points, the crankshaft speed and angle, the flow speed, the generated electrical power are recorded by using high speed analyzing equipment and simulated by using CFD (Computational Fluid Dynamics). In this paper relevant calculations and the dimensioning of a revolutionary exhaust system for increasing the efficiency of a light weight two-stroke range extender are presented for the first time.

Keywords: MIT&SLIM2013, e-mobility, two-stroke engine, range-extender, hybrid vehicle, exhaust turbine, waste heat, CFD, simulation, high efficiency.

1 Introduction

E-mobility is deemed to be a big challenge of the automotive industry in the next few years. Advantages like the CO_2-savings and the noiseless driving emerge obviously. Based on the high acquisition costs und the limited range of those cars the potential customers are not willing to buy them. Because of the limited range of e-cars with an average range of 100-150 km only few customers are disposed to pay an additional price compared to the price of a conventional car. The technology of the lithium-ion-accumulators shows great potential according to the store capacity and a thereby related increased range of e-cars. The price of those accumulators will certainly fall over time to a competitive level [1]. Up till then Range-Extender will be a method of choice to configure e-mobility more competitive. For that reason the Bayreuth University develops a high efficient Range-Extender in the context of the research project "**Mi**niatur **Hy**brid" (MIHY).

2 Initial situation

To realize the research intense tasks within two and a half year (project duration of MIHY) an experienced partner is needed. The industrial partner in this project is "Webra Feinmechanik GmbH" (in the following WEBRA). WEBRA produces high performance model combustion engines for a reasonable price since 50 years. For this reason amongst others, it was decided that the following developments will be realized in a small scale. Advantages of this proceeding are the fast and cost effective development as well as the less difficult technology of model engines compared to the large scaled engines in modern vehicles. Afterwards the achieved results can be transferred to the big scaled engines and Range-Extender.

2.1 State of the art

Range-Extender are available in many different variants on the market. Especially, according to the mode of use, the classification of the operation mode (serial or parallel hybrid) of electric driven cars is relevant (cf. Figure 1).

The parallel hybrid operation mode provides the possibility to drive by electric motor and/or by combustion engine. Whereas the serial operation solely uses the combustions engine to charge the connected accumulator.

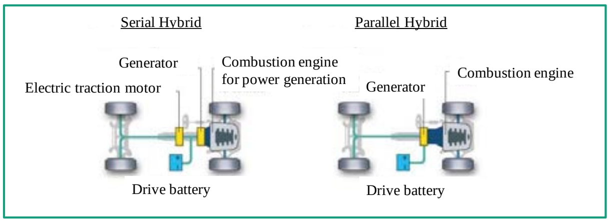

Figure 1 Hybrid drive modes [2]

This allows the use of significant smaller, lighter and load point optimised combustion engines. The Range-Extender of the MIHY-project is applied for this purpose. Furthermore the Range-Extender of this project is supposed to be more efficient than comparable systems by efficiency increasing developments.

Usually combustion engines are deployed for this purpose and are indicated by an average efficiency of approximately 40%. This value characterizes the available mechanical drive power. The remaining 60% of the deployed chemical energy of the fuel get lost by the cooling of the engine and by thermal energy of the exhaust gas [3]. The previous approach of the development of load point optimised combustion engines was limited to the improvement of the efficiency of the mechanical drive power. The concept of the MIHY Range-Extender however allows the partly usage of the remaining 60% energy losses, additionally.

2.2 Procedure

Starting point of the development is the two-stroke engine “Speed 150i” from the company and project partner WEBRA. The model combustion engine has a cylinder capacity of 25 ccm³ and a performance of 2.8 kW with 11,000 rpm. The engine runs with a fuel-oil-mixture. The engine modification to propane/butane gas operation is optional to ensure a flexible and comprehensive supply with fuel. An additional advantage of the gas-fuelled operation mode is the improvement of the emission levels (pollutant emissions and noise level) as well as the increase of the efficiency. This is the way to increase the efficiency of 40 % beside other arrangements e.g. the use of the energy losses in the cooling system and of the exhaust system. Consequently the following tasks have to be completed:

- modification of the engine to gas-fuelled operation
- utilization of the thermal and kinetic energy in the exhaust gas
- utilization of the energy losses of the cooling system

Figure 2 shows the schema of the above described concept of the MIHY Range-Extender to maximize the range of an e-car. The mechanical energy converted out of the combustion engine is used to drive a first generator which is connected to the crank shaft. To use the energy contained in the exhaust gas it is necessary to lead the exhausts primarily through a so called exhaust-power turbine which is linked to a second generator. The energy losses of the cooling system are processed in another way, but also those ones will finally be converted by a third generator into electric energy. With the help of an electronic control system the electric energy of the three mentioned generators are used to charge the drive accumulator of an e-car.

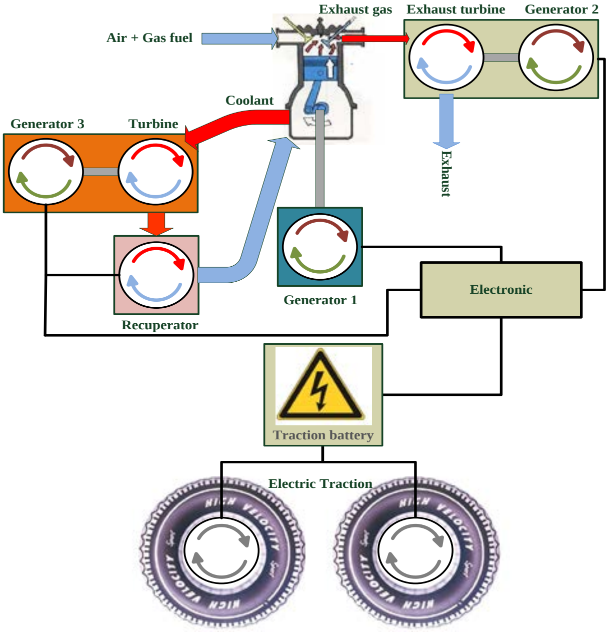

Figure 2 MIHY-concept

To accomplish the aimed targets, a step by step realization is intended. Initially the gas turbine and all necessary attachment parts will be dimensioned and constructed. These will replace the previous commonly used exhaust system (normally a silencer resp. tuned pipe). The utilization of the wasted energy of the cooling system and the conversion from petrol to gas operation will be implemented in a later state.

3 Overview of selected results

To use the exhaust energy, a range of preliminaries and calculations are necessary. Those are described in the following sections.

3.1 Range-Extender combustion engine

As already mentioned all developments are based on a 25 cm³ two-stroke engine of the company WEBRA. The reason is the extreme simple construction, modifiability high power-to-weight ratio and the low price. The achieved results during the MIHY-project can be accessed at later point in time and used to build a more powerful Range-Extender. This allows the support of the drive-accumulators of a four-person hybrid e-car with electric energy. Instead of using one large scaled Range-Extender, it is also possible to link four smaller MIHY Range-Extender to provide the needed performance. The operation method of the MIHY Range-Extender will be static at a constant rotational speed. Hereby the first thoughts about realization began. By the use of performance diagrams the possible engine power at a constant rotational speed of 5,000 rpm is determined. With an assumed efficiency of 40% the engine power is 1.3 kW [3]. Exact measurements and calculations of the efficiency take place during the project MIHY at a later point. Important for further steps is the determination of operating parameters like volume flow, pressure and temperature. By the chemical reaction equation the amount of primary energy (fuel), which is needed to achieve a performance of 1.3 kW at an engine efficiency (h_{engine}) of 40%, can be calculated (cf. Equation 3.1.1 and 3.1.2).

2 C_8H_{18} *+ 25* O_2 ® *16* CO_2 *+ 18* H_2O (3.1.1)

$$P_{chem} = \frac{P_{mech}}{\eta_{\text{engine}}} = 3.25\ kW \quad (3.1.2)$$

With a lower heating value of $H_{\text{u}} = 40 \cdot 10^3 \, \frac{\text{kJ}}{\text{kg}}$ and an air ratio of 14.7:1 the total air mass flow results to 1.27 g/s. Under normal conditions and an assumed exhaust gas density of $r_{gas} = 1.4\,\frac{\text{kg}}{\text{m}^3}$ this corresponds to a volume flow of approximately 0.9 l/s. Depending on the exhaust gas temperature and furthermore operating factors a volume flow of 2 l/s is achievable.

Important parameters of the exhaust gas are calculated by the help of the Otto-cycle (cf. Figure 3). Interesting are especially the conditions at point 4, which represent the pressure and temperature of the exhaust gas at this certain point. Taking the cooling losses as well as the gas-exchange cycle by the flush of fresh gas, as it occurs in two-stroke combustion engines, into consideration the conditions approx. 20mm behind the exhaust port results to:

- temperature: T = 191° C
- pressure: p = 2.8 bar

A comparison of those values with the literature shows a classification at the bottom edge of the possible. The literature refers values up to an exhaust gas temperature of 400° C and a pressure of 10 bar [3] [4].

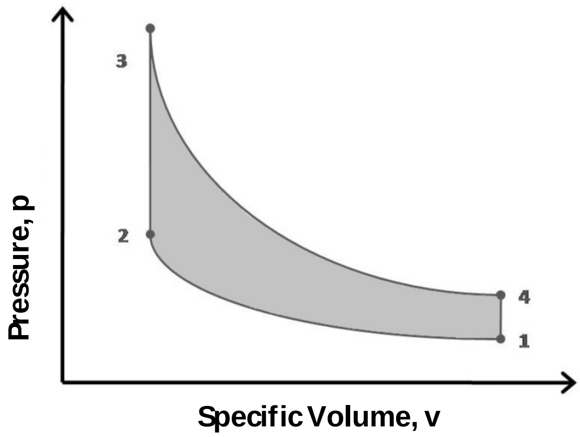

Figure 3 Otto-cycle

Important findings are the losses contained in the exhaust gas in form of thermal energy. For the considered model those are approximately 1 kW. This energy normally gets exhausted unused into the environment. In future those losses are supposed to be reduced by developing an exhaust-power turbine. Thereby the over-all efficiency of the MIHY Range-Extender is raised clearly.

3.2 Measurements at the exhaust system

The considerations and calculated values made in chapter 3.1, are verified by measurements. The used engine therefore is not the WEBRA “Speed 150i” but a related high-performance engine (product name: *Chung Yang R236*).

Temperature measurement

The temperature measurement at the exhaust port of the engine provides a maximum exhaust gas temperature of approx. 160° C (cf. Figure 4).

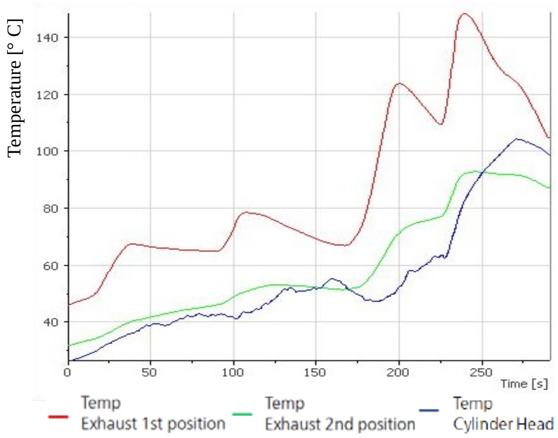

Figure 4 Temperature measurement

The undulated moving of the temperature profile is caused by rotational speed regulations during the experiment (Figure 4). From the moment t > 0 s the engine was running in idle speed. The rotational speed was raised continuously, held for 50 s and then raised stage-by-stage. The maximum rotational speed of 11,000 rpm was reached after t = 230 s with a consistent load. Therefore, it is possible to achieve the temperature of T = 190° C from the calculations of chapter 3.1.

The temperature measurement at the exhaust port and the tuned pipe outlet shows a DT of approx. 40° C. On the one hand this can be explained by the geometry of the tuned pipe which affects the pressure and temperature change; on the other hand, by heat losses to the immediate surroundings. For this reason a thermal insulation is applied to the resonance tube.

Low pressure measurement

When measuring the pressure ratio in the tuned pipe by a high sample rate (50 kHz) of the pressure sensor, it is possible to perform more precisely measurements compared to the slower temperature sensors. Consequently even procedures within an operating cycle can be detected by the pressure sensor. At 5,000 rpm one cycle takes 12 ms in time. With a sample rate of 50 kHz, ten measurements per cycle (every 1.2 ms) are made.

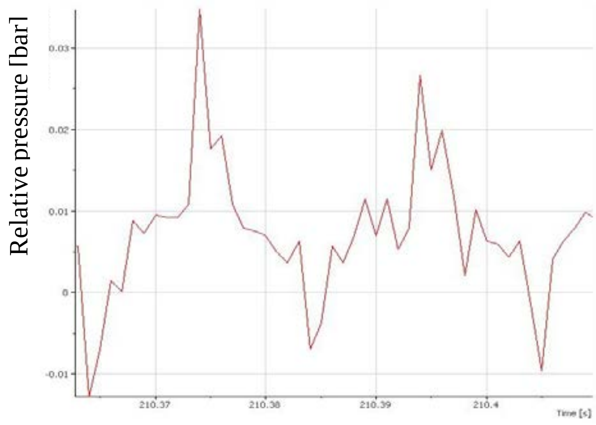

Figure 5 Pressure measurement

The relative pressure, which is measured with the pressure sensor, “DRTR-AL-10V-R10B” from *HYGROSENS*, shows periodic oscillations. An analysis of the length of the single peaks as well as a correlation by the help of the velocity of sound in the exhaust gas shows the resonance behaviour in the tuned pipe clearly. Hereby the relative pressure at the end of one stroke gets negative. This represents the exhaust back-pressure and therefore a decrease in pressure at the end of the tuned pipe (cf. Figure 5). The application of a tuned pipe at current state is essential. The maximum absolute pressure in Figure 5 is approx. 1.4 bar. The pressure measurements, the measured temperatures and the to be determined flow speed are the basis for the following laval nozzle.

3.3 Laval nozzle

By the given area of the exhaust port at the “Speed 150i” of 346 mm² and the adjusted rotational speed during first test runs, the exhaust gas velocity results to 2.7 m/s. For an effective use of the turbine this value is way too low. For this reason the flow velocity is raised by the help of a laval nozzle (cf. Figure 6). Due to their specific geometry it is possible to accelerate the exhaust far into the supersonic range. This happens by the transformation of thermal into kinetic energy.

The geometry dimensioning is achieved by the calculations of impulse and flow speed respectively, by values out of data sheets. Very relevant parameters are the area ratios inside the nozzle and at the outlet. This is ascertained by the existing pressure ratio, directly in front of the narrowest point of the laval nozzle and the external pressure [5].

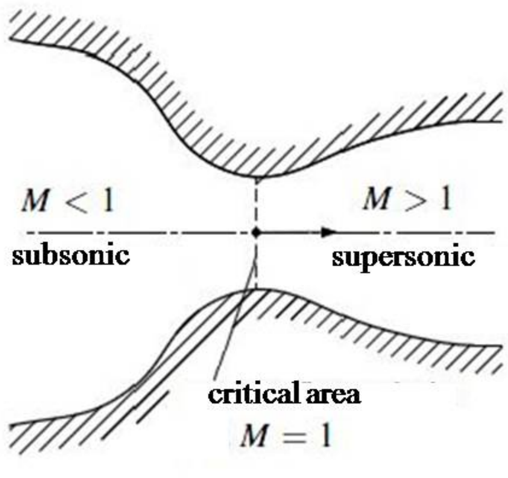

Figure 6 Principle of the laval nozzle [5]

By the temperature and pressure values from chapter 3.1 two limit cases of the nozzle geometry are picked. According to those the diameter of the tightest spot of the laval nozzle has to be between 5 and 15 mm. With those two inner diameters, (also called critical diameter) the scope for following more accurate determinations of the nozzle geometry is arranged. In this regard, exhaust gas is accelerated to Mach > 2 (approx. 700 m/s) at the nozzle outlet. This provides a very good basis for the efficient drive of the following exhaust-power turbine.

3.4 Construction

On the basis of up till now made considerations, calculations and measurements a construction of the tuned pipe, the laval nozzle and the exhaust-power turbine can be realized.

Tuned pipe

The tuned pipe for the „Speed 150i“ has to be adjusted to the present engine and its optimal operating conditions. By calculating the resonance times, most relevant dimensions of the tuned pipe are defined. In this case, the rotational speed is important. Caused by the low rotational speed of 5,000 rpm, the tuned pipe has a length of $l_r \approx 700$ mm. Further needed dimensions in Figure 7 can be calculated by formula or by empiric determined values. By dimensioning of those values the geometry of the resonance body is certain. The formula and the cone shaped geometry 12 and 14 (cf. Figure 7) apply for a range of various rotational speeds. With a fixed rotational speed as it is preset, the cone shaped courses could be omitted and a staged passage could be chosen.

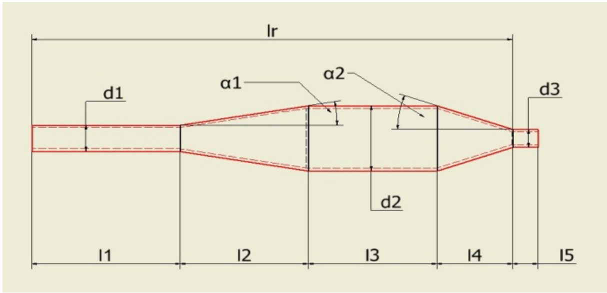

Figure 7 Dimensioning of the tuned pipe

From the previous measured values of pressure and temperature as well as the calculated values of the flow speed, exhaust pressure and exhaust temperature in front of the laval nozzle a first prototype was modelled by the help of the CAD-software *SolidWorks2013*®.

Laval nozzle

Directly to the tuned pipe, the laval nozzle is connected and represents the pre-stage of the turbine casing. The nozzle outlet is directed on the downstream located turbine wheel. As the critical inner diameter cannot be calculated exactly up till now, it is necessary to determine the value experimentally (Figure 8).

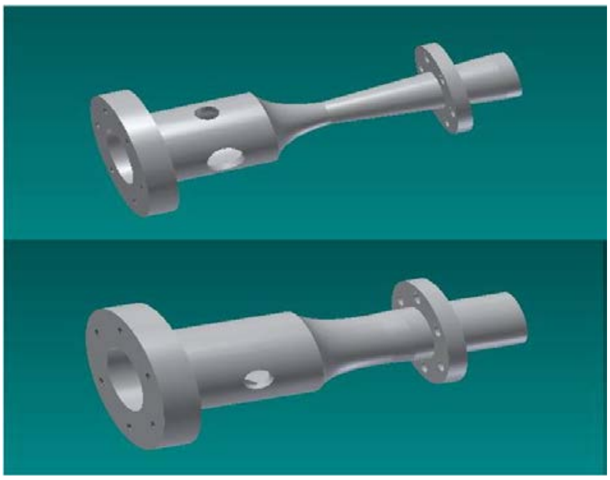

Figure 8 Laval nozzle with critical diameter of 5 and 15 mm

This process is important as the laval nozzle (a laval nozzle has six operating modes) is only working exactly with the right dimensioning. The dimensioning is dependent of the pressure ratio in front and behind of the nozzle and this, in turn, is dependent of the engine rotational speed, exhaust temperature and the pressure course of the downstream power turbine [8].

Exhaust-power turbine

The exhaust-power turbine is located directly behind the laval nozzle and is developed in several steps. After developing different possible designs, three most promising variants with the greatest potential are built in CAD-software, suitable for production and printed by the rapid prototyping method. Those can be analysed concerning their operating performance. Figure 9 shows the chosen version. The different variants are not named here.

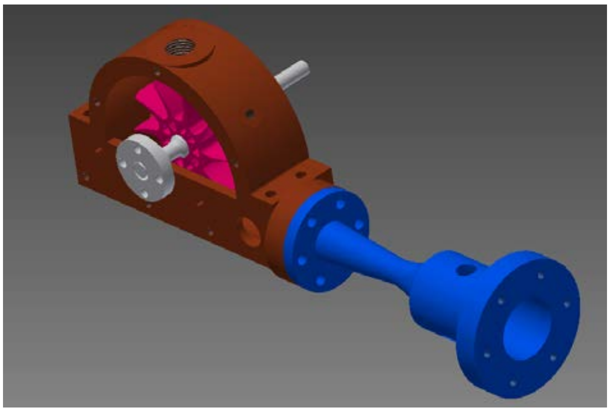

Figure 9 Exhaust-power turbine

Besides a simple and robust building technique the integration of pressure and temperature sensors as well as a flow speed sensor was also considered here. The whole construction is produced according to ISO-standards. Especially relating to screws and necessary tools, the variety of options was considered to be kept at a low level.

3.5 Simulations

According to the theoretical calculations of the laval nozzle the exhaust gas velocity should now result to 700 m/s in front of the exhaust-power turbine. To confirm the results, practical experiments and flow simulations with the help of CFD-software are executed. By different scenarios the estimation of the ideal dimensioning as well as about the actual flow velocities are possible.

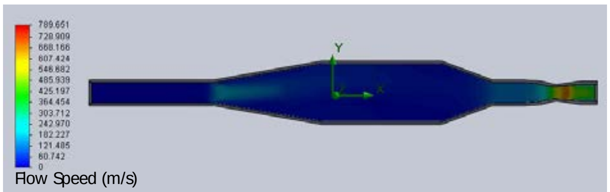

Figure 10 Flow speed in the exhaust system

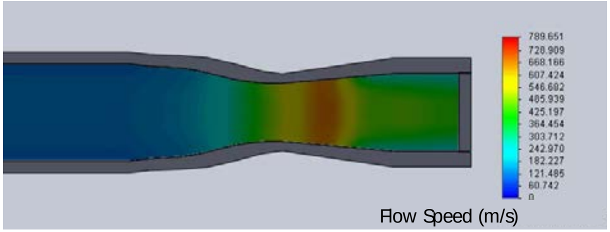

Figure 11 Flow speed in the laval nozzle

Figure 10 and 11 show the results of the simulation of the flow speed of the exhaust gas. In the area of the laval nozzle a yellow-red-coloring shows the intense sped-up. The maximum velocity of approx. 700 m/s is reached right after the narrowest section. At the narrowest section the velocity is Mach = 1. The velocity of sound c_L in the exhaust gas depends on the square root of the absolute gas temperature (cf. Equation 3.5.1) [6].

$$c_{\mathrm{L}} = \sqrt{k \cdot R \cdot T_{\mathrm{krit}}} \qquad (3.5.1)$$

Downstream the velocity decreases a little bit, but it stays above 400 m/s (cf. Figure 11, green area) and consequently in the supersonic range. This is the velocity the exhaust gas hits the wheel of the exhaust-power turbine.

The high flow velocity is reached by the transformation of the thermal into kinetic energy. Figure 12 shows this relation. In front of the laval nozzle the temperature is around 500 Kelvin. Downstream temperatures drop about approx. 200 Kelvin. The critical temperature is around 400 Kelvin.

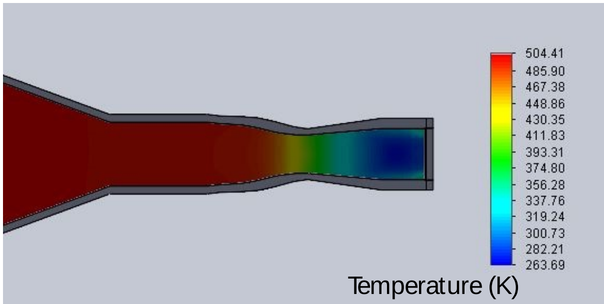

Figure 12 Temperature profile in the laval nozzle [7]

4 Current prototype

The realization of the present work from a first prototype to a complete system can be implemented in the next steps.

4.1 Complete System

All in chapter 3 specified components are shown in Figure 13. These include:

- motor flange,
- tuned pipe,
- laval nozzle,
- turbine case with turbine.

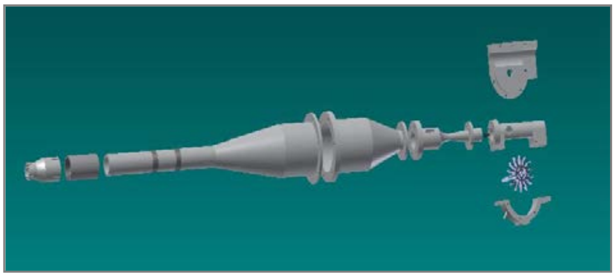

Figure 13 CAD model of the complete system

The construction is kept modular und guarantees a simple change of the components. Consequently different variants of the laval nozzle can be tested. The continuous development of single components is simplified.

The whole system, including the engine, has a maximum dimensioning of 800x100x150 mm. Later a more compact installation is planed, wich combines exhaust system, cooling circuit and engine bearer on a common square plate. The prototype is made out of steel and aluminum and is manufactured at the *Chair Manufacturing and Remanufacturing Technology* of Bayreuth University. Original pictures of the up-to-date prototype will not be published, because of patent protecting reasons.

4.2 Performance and efficiency

The most important point in dimensioning the exhaust-power turbine is the performance calculating. The determined parameters can be used to conclude on the improved over-all efficiency. The current calculating of the performance is done under following assumptions:

- lowest expected temperature before the laval nozzle (cf. Chapter 3.1)
- lowest expected pressure before the laval nozzle (cf. Chapter 3.1)
- flow speed behind the laval nozzle 400 m/s
- usage of the kinetic energy of the exhaust gas behind the laval nozzle by the exhaust-power turbine up to 60 %
- over-all efficiency of the turbine under load of 50 %

The last two headwords are assumptions to calculate the expected losses. Those decrease the value of the performance accordingly. Despite those assumptions an idling speed of the turbine wheel of n_{idle} = 88.000 rpm with a flow speed of $u_{exhaust\_gas\_in}$ = 400 m/s and a flow speed at the outlet of $u_{exhaust\_gas\_out}$ = 50 m/s of the exhaust gas could be determined (cf. Equation 4.2.1) [7].

$$n_{\text{idle}} = \frac{60 \cdot \eta_{\text{flow}} \cdot (\upsilon_{\text{exhaust\_gas\_in}} - \upsilon_{\text{exhaust\_gas\_out}})}{\frac{360^\circ}{\alpha} \cdot l} \qquad (4.2.1)$$

n_{idle}:	idling speed
$u_{exhaust\_gas\_in}$:	speed of exhaust gas flowing to turbine blades
$u_{exhaust\_gas\_out}$:	speed of exhaust gas flowing out from turbine
h_{flow}:	efficiency of the turbine
l, a:	flow length, angle of dip of exhaust gas over turbine blades

Thereby a theoretical performance of $P_{turbine\_max}$ = 922 W could be achieved. The difference between idling cycle and operation with load is defined with above named over-all efficiency of 50 %. At load i.e. linking the turbine to the electric generator the performance is added up to $P_{electric}$ = 411W. The efficiency of the exhaust-power turbine in relation to the whole deployed (cf. Chapter 3.1) chemical energy arises to $\eta_{turbine}$=14% [7].

The efficiency of the whole system can be calculated by summing up the single efficiencies of the engine and the exhaust turbine (cf. Equation 4.2.2).

$$\eta_{total} = \frac{P_{crankshaft}}{P_{chem}} + \frac{P_{turbine}}{P_{chem}} = 54\% \qquad (4.2.2)$$

The over-all efficiency of the system is increased by the exhaust turbine from initially η_{engine} = 40% to η_{total} = 54%. This efficiency exceeds commercial available Range-Extender powered with diesel fuel.

5 Summary and forecast

The given tasks and aimed goals of the research project MIHY are very extensive.

A methodical and strict procedure is necessary to achieve them. The results published in this paper are consequently only the first step to an optimized Range-Extender.

5.1 Summary of the previous results

The up to now achieved results during the project MIHY have a high potential for future developments. A disadvantage that hasn't been handled till now is the bad emission level (pollutant emissions and noise level) of two-stroke engines. Advantageously in contrast is the usage option of the thermal energy included in the exhaust gas. By the thermodynamic calculations and the flow conditions at the outlet of the engine, as well as the necessary transformation of thermal into kinetic energy, the usage of a laval nozzle got required. With an ideal adjusted geometry the exhaust gas is accelerated into the supersonic range (currently approx. 400 m/s).

The accelerated exhaust drives the exhaust-power turbine which supplies an electric generator that dispenses an electric performance of 411 W. The over-all efficiency of the system is raised to η_{total} = 54%. This exceeds occasionally the Range-Extender which are commercially available.

The fuel resistance of the power turbine, additional efficiency improvements, practical experiments and the compliancy of the exhaust standards are to accomplish.

5.2 Forecast and further approach

The further steps which are to accomplish during the research project MIHY are related to the gas modification of the engine "Speed 150i". The results achieved here, shall help to improve the emission levels as well as a rise of the temperature of the exhaust gas. This influences the performance of the turbine positively.

Furthermore as a part of the gas modification a direct fuel injection can be tested. This would decrease the losses by the flush of fresh fuel-air-mixture during the two-stroke cycle. The replacement would also affect the geometry of the tuned pipe, which could get simplified. The laval nozzle has to be adjusted, too. In the case of an ideal adjusted laval nozzle it could approximate to the proved principle of a radial turbine.

As an additional task to increase the over-all efficiency it could be tried to use the losses of the cooling and to convert it into electric energy.

Finally the produced electric performances of the crankshaft, the exhaust-power turbine and the cooling cycle are linked together and used to charge the drive accumulators. The realization of the given tasks and aimed goals should lead to a high efficient Range-Extender in a compact configuration, which can be tested in a radio-controlled car in the scale 1:5.

6 Acknowledgments

The project "Miniatur-Hybrid" („MIHY") is supported by the "Bundesministerium für Wirtschaft und Technologie", by decision of the German Bundestag as well as the „Zentrales Innovationsprogramm Mittelstand".

7 References

[1] Kolke, R. Dr.-Ing.; Gärtner, A.: Alternative Antriebe im Straßentest – Eine ADAC Studie, accessed 11.05.2013, online www.adac.de, 2012.

[2] MTB-Tech Group: Hybrid-Konzepte, accessed 11.05.2013, online https://www.mbtech-group.com/eu-de/spotlights/mbtech_hybrid/hybridkonzepte.html, 2009.

[3] Demuth, P..: Modell-motoren, Neckar-Verlag, Villingen, 1994.

[4] Merker, G. und Schwarz, C.: Grundlagen Verbrennungsmotoren, Vieweg+Teubner Verlag, Wiesbaden, 2012.

[5] Kalide, W.: Energieumwandlung in Kraft- und Arbeitsmaschinen, Carl Hanser Verlag, München Wien, 2005.

[6] Kalide, W.: Energieumwandlung in Kraft- und Arbeitsmaschinen, Carl Hanser Verlag, München, 1982.

[7] Will, F.: Entwicklung einer Abgasturbine für Zweitaktmotoren, Diplomarbeit, Universität Bayreuth, 2013.

[8] Settles, G.: High-Speed Flow Through a Laval-Nozzle, Penn State Gas Dynamics Lab, 2000.

Innovations and technologies

Innovation management opportunities in Slovenian manufacturing: an empirical analysis within low- and hi-tech companies

Borut Likar[1], Sašo Sukič[2], Janez Kopač[3], Marko Ropret[4]

[1]University of Primorska, Slovenia
[2]University of Ljubljana, Slovenia
[3]University of Ljubljana, Slovenia
[4]University of Primorska, Slovenia

Abstract

The aim of the paper is to identify the innovation factors and consequently possibilities for improvement the innovation management of Slovenian manufacturing companies. We analysed both the low- (henceforth referred to as: LMT) and hi-tech manufacturing companies (henceforth referred to as: HMT). The methods of data analysis consisted mainly of regression analysis (influential factor determination) and descriptive statistics within three identified groups of companies (Non-innovators, Innovation followers and Innovation leaders) so as to enable concrete guidelines for companies. The research results showed positive correlations between innovation inputs, innovation results and economic performance – this was largely confirmed both for LMT and HMT companies. More precisely, two groups of innovation factors mainly influencing innovation results (and consequently business performance) were identified: first, the financial innovation inputs, considering both the height and structure of innovation expenditure. Both within LMT and HMT companies, we noticed, that Non-Innovators and Innovation followers were spending mostly on machinery and equipment, but too little on R&D expenditure (compared to Innovation leaders). The second group of influential innovation factors, consists of the non-financial innovation factors, where considerable potential for improvement exists as well. As regards the LMT Non-innovators, in order to become innovation active – i.e. an Innovation Follower, one of the prerequisite factors is providing sufficient managers' support for innovation (innovating the management). The "shift" from Innovation Follower to Innovation Leader; however, requires ensuring a proper management of innovation within a broader LMT company context. As regards the HMT companies it was shown the Non-Innovators generally received sufficient management support for innovation, but a prerequisite for their improvements lies mainly in improving their opportunity identification activities. But to move from HMT Follower to HMT Leader, several additional non-financial factors must be improved. It must also be stressed that achieving Innovation leader status is much more difficult in case of HMT companies compared to their LMT counterparts (i.e. bigger adjustments needed by the Non-innovators and Innovation Followers). Therefore, in the short-term it may be most productive for national policy makers to support innovation within LMT companies, while in the long-term improving the situation within HMT companies must also be addressed.

Keywords: innovation, management, low-tech, hi-tech, opportunities, manufacturing, Slovenia

1 Introduction

According to the words of management guru Peter Drucker [1], every organization needs the following key competence: innovation. Research confirms the significant positive correlation between innovation and the economic results [2]. Despite the importance of this fact, Europe is consistently behind USA and Japan regarding reached innovative results [3, 4, 5]. A continuous progress is noticeable compared to USA, lately also compared to Japan, but a great gap between EU and these two developed regions still remains [5]. Furthermore, China, India and Brazil are becoming important global players in the field of research and development (R&R). Slovenia belongs (according the Summary innovation index (which shows the innovativeness of EU members and some other countries based on 29 indicators) to the group of countries that even falls behind the European average – so-called »Innovation followers« [5]. In order to achieve progress, research has to be made with emphasis on the study of systemic and systematic approach for the improvement of the existing state [6].

Until recently, in the manufacturing sector, a great part of research from the field of innovation management was directed towards the high technology companies [7]. The latter represented a synonym for the high value added and economic growth. Only recently researchers are starting to identify the meaning of technologically less intense branches for the innovativeness and the international successfulness of countries. Moreover, high and medium-high tech companies (hereinafter: HMT) as opposed to low and medium-low tech (hereinafter: LMT) in most of the developed economies include only a trivial share of GDP – even in the USA, that is a member of OECD with the highest share of high-tech production, they contribute less than 3% to the GDP [8]. In accordance with that, LMT represent an extremely important group of companies whose innovation and economic successfulness is essential for the economic prosperity in the country. At the same time, innovation potential of LMT and HMT in Slovenia is obviously not enough exploited. Frequent statistical indicators, such as the share of innovative active companies, show that the both branch groups are relatively close to the average of the countries EU-27, but actual innovative and economic results are distinctively below the EU average. A majority of the companies are Innovation followers, their innovation incomes from market novelties representing barely a half of EU-27 average [2]. Similarly, unfortunately applies for the reached economic results, which is seen in the much lower added value per employee. Economic subjects are trying to increase the level of innovation results with different, often partial approaches which are not effective.

The purpose of this paper is a holistic identification of factors that affect innovation and economic results in the manufacturing sector. Results in the low and medium-low technology firms and the high and medium-high technology firms, based on the scientific data, will represent the foundation for the rise of innovation and consequently economic successfulness. The structure of the paper is as follows: firstly we introduce the research methodology; then we present the specific findings which apply separately for LMT and HMT while the last part consists of the conclusions where we connect the research results and define the guidelines for a more successful innovation management in companies.

2 Research methodology

The research is based on the national data about the innovative activities of CIS (Community Innovation Survey). This data are particulary suitable for scientific analysis because of the participation of the majority of Slovenian companies and the application of the international standardised research methodology. Primary data (2004-2006 period) in the Slovenian medium and large manufacturing companies (624 units) was obtained by the Statistical Office of the Republic of Slovenia (SURS). Aforementioned data gathers primarily (regarding influential factors) the financial inputs of companies (costs of the internal RR, costs of the external RR, costs for the acquisition of machines, equipment and programming equipment, costs for the acquisition of other external knowledge, training costs, costs for the introduction of innovations to the market and other. We have also conducted an additional survey from the non-financial inputs point of view (62 questions on a 7-level scale; year 2008). These represent the potentially influential factors as regards the management innovation process (the vision and the strategic views of the encouragement of innovativeness, the organizational culture and climate, the role of management support, the innovation cooperation within a company and with the environment, the system of material and non-material rewards, the role of the protection of intellectual property, the training and the development of staff competencies, the identification of the opportunities and generation of ideas). To this data we have added financial information from the balance sheet gained from the AJPES base, information about the structure of employees from the SRDAP base.

All companies from the manufacturing sector were included in the case of SURS data and in the case of our research, we have included a sample of 86 manufacturing companies. For the conduction of the statistical analysis we have used (beside the basic statistics) the factor analysis, regression analysis, classification into groups and the Mann-Whitney statistical test (the latter was used only for the 2008 data, since it does not include the entire population). Financially measurable innovation results were used as fundamental measure as regards innovation results: RII – *Turnover from product innovations as a share of total turnover* and RMI - *Turnover from product innovations new to the market as a share of total turnover from product innovations*. Also, we have used the subjective evaluation of the total (financial and non-financial) benefit from innovations – *Average total benefit of the company from innovations* (Likert scale 1-7) (Likar and others 2011).

3 Results

We have come to the conclusion that different groups of companies (low and medium-low tech manufacturers and high and medium-high tech manufacturers) show different patterns as regards managing innovation. This means a different direction of the innovation policy is needed – on the company level as much as on the country level. Innovation levers that lead to the successfulness in the group of high tech manufacturers are not so optimal for the low tech manufacturers. Innovation policy has to be more adapted to the branch. Only branch-specific innovation policy can lead to success.

In the following text we will show the results of the separate analyses for both company groups (LMT, HMT): an identification of key innovation factors, based upon which it is possible to improve the innovation results in companies, later followed by the correlations of the innovation and the economic results of the company (basis: regression analysis and statistical tests/comparisons of factor average values).

3.1 The analysis in low and medium-low tech companies (LMT)

The group of low tech manufacturing companies is the largest among the branch groups in Slovenia, it gathers more than a half of all medium and large manufacturing companies included in the research (N = 422). The LMT branches are categorised on basis of Eurostat/OECD methodology [9], while thorough analyses follow in the forthcoming subchapters (3.1.1 - 3.1.3).

3.1.1 The relation between the financial inputs and innovation results

First let’s take a look at how a company can financially influence the share of innovative in total incomes (RII).

Interestingly, we have not identified a statistically significant influence of the innovation total investments on RII (Sig. > 0,1). But we have identified a statistically significant influence of the level of innovative investments on the variable that measures the successfulness of market novelties/RMI (stand. β =0,24). Consequently, there is a possibility that sufficient investments are prerequisite for the achievement of market novelties. With the further analysis of differently innovative companies we have confirmed that the level of financial innovative investments is of great importance, as is also the structure of these investments.

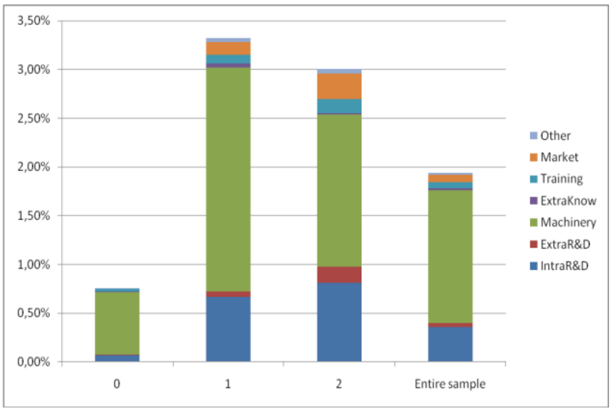

Figure 1 The height and structure of financial investments (branch group LMT).

The comparison of Innovation Followers and the Innovation Leaders within LMT shows that both groups of companies invest comparable amounts into innovation, approximately 3% of total turnover (Figure 1). But the Non-innovators invest a lot less – less than 1%. Clearly, only in the case of non-innovative companies (but not the Followers), a rise of financial investments is needed, which proves very interesting.

Differences regarding the relative structure of these costs are also important. Non-innovative companies direct their low innovative investments into the purchase of machines and equipment (84 %). The investments made by medium innovative companies (followers) into tech equipment are higher than those made by innovative leaders – they take up 69 % of all investments. But the leading companies do invest more intensively than both other groups into R&D (internal and external) (27 %), into training (5 %) and into marketing of innovations (9 %). Investments into machines and equipment take up 52% of all investments made by the innovative leaders; so fundamentally less than with the followers. The amount (EUR) of turnover created with 1 EUR invested into innovation clearly confirms the adequacy of investments made by the Innovation Leaders: the Leader companies generate 14,3 EUR which is 8,9x more than the Innovation Followers (1,6 EUR)! In other words, every EUR that was invested by the Laders is returned than 14x! This fact is especially interesting, as it does not demand raising the overall financial innovation investments!

3.1.2 The relation between the non-financial inputs and innovation results

First, let's take a look at how a company can improve the share of innovative revenues in total revenues (RII). A medium strong effect of the role of intellectual property (stand. β = 0,45) and the role of support of managers (stand. β = 0,36) prevails regarding the effect on RII. Among other process factors that statistically significantly and weakly affect the RII are (sorted by the strength of the influence): the organizational culture and climate (stand. β = 0,30), the vision and strategic aspects of encouraging innovation (stand. β = 0,29) and the training and the development of staff competencies (stand. β = 0,25).

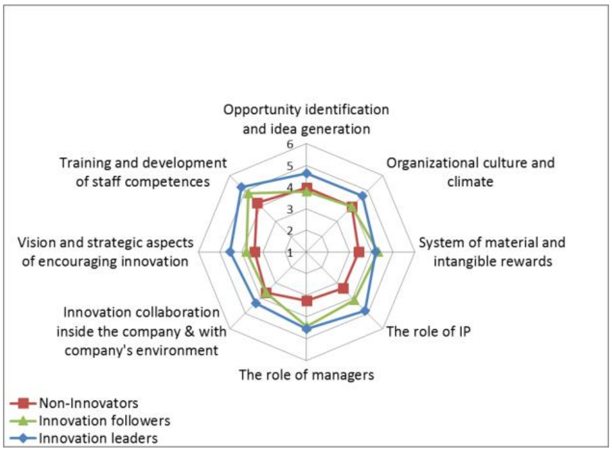

Figure 2 Non-financial investments of non-innovative companies, innovation followers and innovation leading companies (branch group LMT).

In order for a company to be innovation leading, it also has to be successful when it comes to commercialization of market novelties (and not just of innovations that are new for the company itself). The medium strong significant effect of organizational culture and climate (stand. β = 0,36) is the most important for the increase of the revenue share from market novelties (RMI). The effect of the role of protection regarding intellectual property (stand. β = 0,28) is somewhat weaker but still significant. But other innovation process factors are also not unimportant. All 8 factors turned out to have a positive and a significant effect on the total (material and non-material) benefit from innovation. The role of support of managers (stand. β = 0,57) once again stands out among the most important influential factors (strong effect), followed by the vision and the strategic views of the encouraging innovation (stand. β = 0,53) and the innovation cooperation within a company and with the environment (stand. β = 0,52). The following factors have a medium strong positive effect: the training and the development of staff competencies (stand. β = 0,49), the identification of the opportunities and genereation of inventions (stand. β = 0,41), the role of the protection of intellectual property (stand. β = 0,38), the system of material and non-material rewards (stand. β = 0,36). The factor of organizational culture and climate has a significant weak effect (stand. β = 0,27).

With applying the suitable systematics – upwards movement on the innovative chart – we can get to the clear guidelines for the transition from the non-innovative to the innovation leading company (Figure 2). Innovation followers (in comparison with the non-innovative companies) provide the support of managers for innovation (4,1 vs. 3,4) to a significantly greater extent (Sig. ≤ 0,10). At the same, we have also showed with the regression analysis that the factor significantly affects the ability to reach innovative results. One of the fundamental steps for the crossing from the non-innovative company to the innovative follower can therefore be seen in the »innovation of management« [10] before we can even talk about the management of innovation. But, an adequate management of additional factors, that does not just treat managers aspects, is needed for the crossing from the innovation follower to the innovation leading company. Significant differences (Sig. ≤ 0,10) show the need for the provision of more suitable organizational culture and climate (5,0 vs. 4,0); the results of the regression analysis confirm the importance of this factor. Innovation leaders (compared to the Followers) also have a better control of the factor of the identification of the opportunities and creation of inventions (4,8 vs. 3,8) and of the factor of the innovation cooperation within the company and with the company's environment (4,5 vs. 3,7), but those are less important factors (from the view of average value based on the leading companies and the results of regressive analysis). Some other factors are also potentially important (especially regarding the stand out of the value of leaders), but that can not be statistically confirmed.

3.1.3 The relation between the innovation results and economic successfulness

It is obvious that the innovativeness in the LMT group pays off. Innovation leading LMT are economically more successful than the Non-Innovators and the Followers. They are the most profitable: ROE adds up to 0,08 %, that is 33% more than Followers and Non-innovators. We also have to emphasize that the ROE of the Leaders is rising most quickly. If we take a look at the return on assets (ROA), we can notice, that the leaders (0,03) have a higher ROA than both other groups (even 50% higher). At the same time, the innovation leading companies reach a gross added value (27.199 EUR per employee) that is one third higher from the innovation inactive one. Innovation leaders have the fastest growth of net incomes: it adds to 1,78%, that is 18% more than the non-innovative and 45% more than the followers. The number of employees at the innovation leading companies is growing during the observing period (3%), meanwhile it decreases in case of the Followers (-3,60 %) and Non-innovators (-4,40 %). At the same time, even the Innovation leaders show unused potential - for example, the added value per employee in case of the Innovation leaders reaches only 60% of EU average.

3.2 The analysis in high and medium-high tech companies (HMT)

The group of high tech manufacturing companies includes 182 medium-large and large companies in Slovenia. The HMT categorization is in accordance with the methodology of Eurostat/OECD [9], while thorough analyses follow in the forthcoming subchapters (3.2.1 - 3.2.3).

3.2.1 The relation between the financial inputs and the innovation results

We have not identified a statistically significant influence of the level and structure of financial innovation investments on the share of innovation revenues in total revenues (RII). Yet, we have identified a significant influence of the costs of the acquisition of other external knowledge / total turnover (stand. $\beta = 0{,}27$), namely on the revenue share from market novelties (RMI). This finding shows the importance of the external knowledge and innovation cooperation in HMT companies for the achievement of market novelties. With the aforementioned factor one can explain 6,1 % the RMI variance (Adjusted R Square = 0,06). Considering that the most of effects were not significant, it is worth to remind of the relatively small number of HMT in our analysis (especially in comparison with the LMT) which can be one of possible reasons. At the same time, actual innovation patterns of companies clearly indicate that the financial investments are a factor connected with the innovation results, since the innovation leading companies differ from the Followers and Non-innovators regarding the level and the structure of these investments.

Namely, the group of Innovation leaders invest altogether the greatest financial inputs into innovation, almost 7 % of revenues, the group of medium innovative Innovation followers approx. 4,5 %, and the group of Non-innovators slightly over 1 % of revenues (Figure 3). Therefore the achievement of innovation leadership in HMT obviously also demands relatively high total financial investments! Besides the height of total investments, the optimization of the mere structure is an additional challenge. In addition to the important role of external knowledge, it is very important that the most innovative companies invest relatively less into machines and equipment, while at the same time more into training and into marketing of innovations. To be more precise, the Non-innovators spend 93 % of all expenditures for the acquisition of machines and equipment, Followers 40 % and the Leaders just 25 %. When it comes to the Non-innovators, investments into (internal and external) RR add up to barely 8% and regarding Followers and Leaders approx. 40 % of all innovation investments.

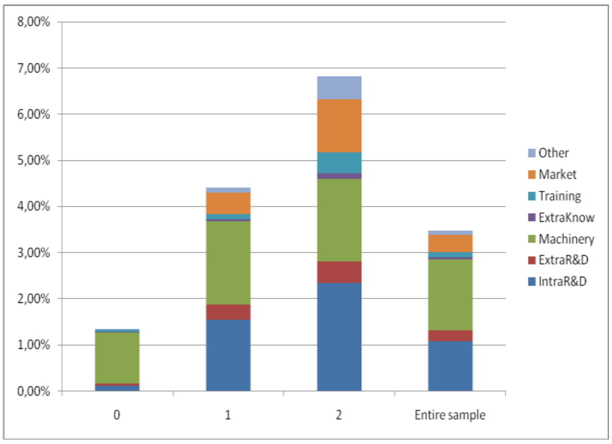

Figure 3 The height and structure of financial investments (branch group HMT).

The productivity (and the justification) of financial investments of the innovation leaders is clearly shown by the amount of revenues that the company makes with one EUR of innovation costs: that adds to 7,7 EUR when it comes to the Leaders, which is 4,1× more than the Followers achieve (1,9 EUR)! That means that every invested EUR of the

Leaders is returned almost 8x! Let's not forget; however, that this rise of productivity demands relatively high financial innovation investments with appropriate structure.

3.2.2 The relation between the non-financial inputs and innovation results

Based on the limitations of the sample that treats the process (non-financial) innovation factors of HMT (limited size and non-normality of distribution), the execution of regression analysis would not be justified. With the application of statistical tests, comapring the means we can establish (Figure 4); however, that the Leaders stand out when it comes to high attention to the innovation process factors (except the factor of the tole of managers), which indicates a positive correlation of these factors with the innovation results. Because of the low number of included HMT, the differences somewhat exceed the limit of statistical significancy (Sig. > 0,10), yet a thorough look reveals, they clearly make sense.

In the continuing text, we sistematically show where the differences in management of the non-financial inputs appear between the differently innovative groups of companies. Non-innovative HMT in comparison with the Followers do not pay enough attention to the identification of the opportunity and the creation of inventions (5,0 vs. 3,9). Interestingly, Non-innovators pay more attention than Followers to the system of material and non-material rewards (3,7 vs. 4,0), the role of IP (4,2 vs. 3,1) and the support of managers (4,2 vs. 5,6), while at the asame time also being more dependent on the innovation cooperation (that it is a less suprising finding) (4,1 vs. 4,4). Despite the formal support of managers and the established formal system of material and non-material rewards, the Non-innovators realize only smaller, from the financial effects point of view negligible innovations (since in the case of Non-innovators, following applies: RII = 0, RMI = 0!).

If we move higher on the »innovation ladder« - from a Follower to an Innovation leader – we can see that the Followers need a fundamentally larger attention especially regarding the three non-financial innovation factors: innovation cooperation within the company and with the environment (5,5 vs. 4,1), protection of intelectual property (6,0 vs. 3,1) and the provision of the system of material and non-material rewards (5,0 vs. 3,7).

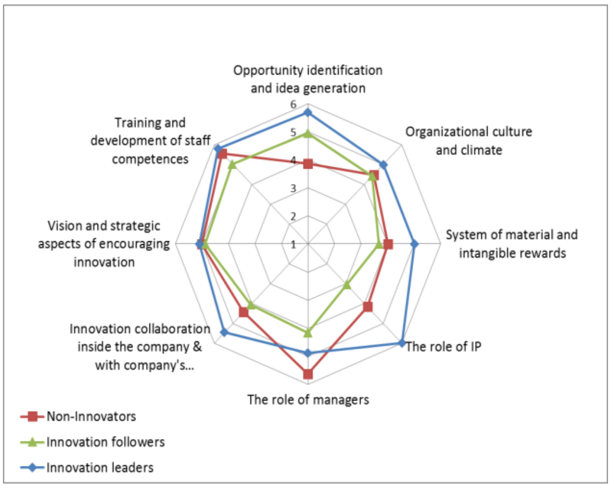

Figure 4 Non-financial investments of non-innovative companies, innovation followers and innovation leading companies (branch group HMT).

3.2.3 The relation between the innovation results and the economic successfulness

HMT indicate quite the contrary results, compared to the LMT: the most innovative companies are economically the least successful. The growth index of net revenues is the lowest in the group of Leaders - it adds up to 8,37 %, which is approx. 35 % less than in case of the Non-innovators and 42 % less than in case of the Innovation followers; similar results can be seen when it comes to the capital growth index. According to the revenues per employee, innovation leading companies (92.283 EUR) are 10 % above the Non-innovative and rank on the same level as Innovation Followers. At the same time, Innovation leaders, as the only among the three groups, record a negative average growth of revenues per employee (-2,54 %). All HMT record a decrease of ROE in the observed period, wherein the Innovation leaders have the biggest decrease – 34,81 %, which is 4x more than Non-innovative and 13x more than Innovation followers. At the same time, ROA of the innovation leaders (0,03) is the lowest – it adds to 70 % less than in the case of Non-innovators and 50 % less than in the case of Followers. Some indicators (capital, assets, pays) of the Innovation leaders have (in the period 06/07) grown above average, but in the entire observed period (06/08) the growth was below average. Of course there can be several reasons for the weak economic results of the Leaders. Based on the results of the research, it is possible that the HMT in Slovenia need such high financial investments for the achievement of

Innovation leadership that the profitability of a company is consequently low. Let's recall that the HMT Innovation leaders invest on average considerably more than innovation leaders, so low profitability of a company may be an obvious consequence. Certainly, the question of mass production appears and the Slovenian high tech companies do not reach it yet. High investments would without a doubt pay off, if they were accompanied by sales on a larger scale.

4 Conclusion

The crisis has hit Slovenia more than several other countries [11, 12]. If we take international findings into account, which say that the non-innovative countries are more subjected to crisis than innovative countries [13], we can look for important causes for the crisis in those findings facts.

Our research also indicates large structural differences regarding the innovation factors and results among companies from different branches. That is why, a separate treatment is needed for a more detailed analysis, not just on manufacturing and services level, but also within manufacturing (and services).

From a company's innovation management policy point of view, we can find an obvious correlation between the innovation inputs (financial and manufacturing) and the innovation results. The latter are statistically significantly correlated with the economic results. In other words; who correctly invests into innovation, is economically more successful. In order to achieve optimum results, two groups of influential factors are key and comparably important regarding influence on innovation results. On one hand, there are financial investments that have to be adequate not just regarding total amount, but also regarding structure. Therefore, it is not just important how much you invest but also where you invest in. Interestingly, Leaders invest less into machinery and equipment than followers and Non-innovators, but much more into R&D activities. The second group of influential innovation factors, consists of the non-financial inputs, concerning management of the innovation process. Here, in the low and medium-low technology companies for the crossing from the non-innovative company to an innovation active company (a Follower that generates innovation revenues, yet not optimum ones) the process factor of main importance is the support from the company's management. For the further improvements towards the innovation leading companies (those that have great innovation reveneus, especially from market novelties), the vision and support of managers have to begin to live in practice of the entire LMT business – a rise of following factors proves essential: training and the development of staff competencies, organizational culture and climate, innovation cooperation within the company and with the company's environment (the so-called concept of »open innovation«). High and medium-high tech manufacturers demand a different approach as regards the innovation process. Here, the non-innovative companies (compared with the Followers) first and foremost lack a systematic approach regarding the identification of innovation opportunities and the rise of the innovation cooperation level (not just within the company but also with the environment!). Also, the protection of intellectual property is extremely important for the transition from the Innovation follower to the Innovation leader.

As regards national innovation policy, an extremely important finding is, that more financial and non-financial investments into innovation are needed for successful innovation in the high and medium-high tech companies than in the low and medium-low tech companies. Therefore, additional encouragement of innovation in low- (and medium low) tech companies is urgent for the country. Especially as due to the many LMT companies, the improvement of innovativeness would positively impact the GDP. Productivity of innovation investments (regarding the achieved innovation revenues) of the low and medium-low tech manufacturers is considerably higher than in the case of high and medium-high tech companies. Of course the proposition does not mean, that it is not reasonable to invest into high-tech branches in Slovenia – they are absolutely important for the development of society, but fundamentally better management of many factors is needed for that.

References

[1] P.F. Drucker: The essential Drucker: selections from the management works of Peter F. Drucker, Elsevier, 2007.

[2] Likar, B., Fatur, P., Ropret, M., Trček, D., Markič, M., Bavec, C., Škafar, M., Rodman, K. Referenčni model inoviranja: zaključno poročilo o rezultatih raziskovalnega projekta. Koper: Fakulteta za management, 2011.

[3] Archibugi D, Coco A: Is Europe Becoming the Most Dynamic Knowledge Based Economy in the World?, Journal of Common Market Studies, Vol. 43, No. 3, str. 433-459, 2005.

[4] Likar, B. The influence of innovation, technological and research processes on the performance of Slovenia's woodworking industry. Wood research 53 (4): 115-20, 2008.

[5] UNU-MERIT. Innovation Union Scoreboard 2011. http://ec.europa.eu/enterprise/policies/innovation/files/ius-2011_en.pdf, 2012.

[6] Mulej, M. and Ženko, Z. Dialektična Teorija Sistemov in Invencijsko-Inovacijski Management, University of Maribor, Faculty of Economics and Business, Maribor, 2002.

[7] Heidenreich, M. Innovation patterns and location of European low- and medium technology industries. Research Policy 28, 483–494, 2009.

[8] Smith, K. 2002. What is the Knowledge Economy? Knowledge intensity and distributed knowledge bases. Maastricht: United Nations University.

[9] Felix, B. Statistics in focus. Science and technology. High tech industries and knowledge based services. European Communities, Luxembourg, 2006.

[10] Mulej M., Fatur P., Knez-Riedl J., Kokol A., Mulj N., Potočan V., Prosenak D., Škafar B., Ženko Z. Invencijsko-inovacijski management z uporabo dialektične teorije sistemov (podlaga za uresničitev ciljev Evropske unije glede inoviranja), Likar B (Ur.), Ljubljana: Korona plus d.o.o. – Inštitut za inovativnost in tehnologijo, 2008.

[11] Likar, B. Inovativnost se ne bo "zgodila". V: Vehovar, U. (Ur.), Dragoš, S., Hribernik, A., Ignjatović, M., Jaklič, M., Likar, B., Stanojević, M., Vehovar, U. Neosocialna Slovenija : smo lahko socialna, obenem pa gospodarsko uspešna družba?, (Knjižnica Annales Ludus). Koper: Univerza na Primorskem, Znanstveno-raziskovalno središče, 2010.

[12] Ložar, B. Sistematizacija inkrementalnih in prebojnih inovacij v Sloveniji, Analiza inovativnosti v slovenskem gospodarstvu, Gospodarska zbornica Slovenije, Tehnološka agencija Slovenije, 2009.

[13] Filippetti, A., Archibugi, D. Innovation in times of crisis: National Systems of Innovation, 2011.

Technology, design and innovation relations

M. Filiz[1]

[1]*University of Süleyman Demirel, TURKEY*

Abstract

In this study, design take place in which areas of our lives, in relationship with innovation and tecnology are discussed. In Tecnology, the emergence of creative ideas, how ideas can be applied in this respect, the way to show us how to design and innovation, explained.
Countries can continue with increased production without stopping; continuous employment achieve, increase of export capacity, the manufacturer and the state is of great importance for ensuring earnings.
Which is quite a lot of variety of products and services in the countries and companies to make a difference today, and in this race put out new work in order to pass one step ahead. The smallest value provided by the manufacturer should provide positive gains grew like a snowball.

Keywords: MIT&SLIM2013, Industry, design, technology, innovation

1 Introduction

Industry, the production of goods and services, technology, art, architecture, inventions, discoveries, inventions or in the production every goods and services tecnology used, design, innovation is everywhere that it is possible to talk about.
What is design? It can be briefly described as follows. What is available or when required to create a new goods and services of rendering its preferred embodiment is the creation of a suitable usage form.
Mankind is a designer in every period of life.
What is technology? For the delivery of products to the user a number of criteria for the design and the use of techniques that rational and economic purpose and a design tool.
Design without the technology, the technology is not without design. So we say Where in technology and design innovation, innovative side of it. Innovation new ideas, new ideas, new by taking steps new products, new services, new business formats and has a new outlook on life. Part of the design of a product innovation by innovation include operational.

2 Innovation-Technology Relationship

Creativity with a new perspective by looking at existing problems, taking into account the opportunities to use emerging technologies and market dynamics to generate new ideas detecting.
That means creativity, design and innovation, when taken together, practical and attractive offers for customers who use the goods and services in a given format. Design, for the purpose of mobilizing the creativity. This is the creativity of the user conveys the vehicle technology.
More simple words, all creative and new idea, it serves the development of a new design technology [1].
Design, the center of the innovation process. So, envisioned a new product, developed and transformed into a prototype moment. With the design, a new thinking and ideas within the framework of the meaning and value of creativity involved.
To examine the relationship between technology and innovation, innovation-driven innovation processes in different design (design-driven inovation) [2] described as follows (Figure 1).

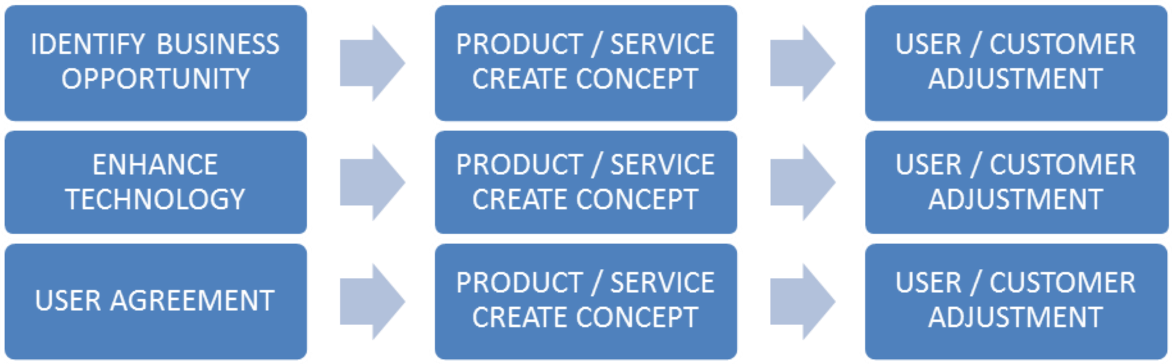

Figure 1 The relationship between technology and innovation

Principles of design-driven innovation, user-oriented approach as a principle of the system, grouped in four headings:

1) Innovation, people's lives and experiences on the construct: physical, cognitive, social, cultural and emotional interactions based on the experiences
2) Innovation is not just a product, the system as a construct
3) Organisational culture of design and innovation support level: cross-disciplinary team work, experimentation, etc.
4) apply a systematic design methods and processes [1].

3 Design-Technology Relationship

Design, science, technology, and provides a link between use. Products and services based on new technologies, enables the acceptance by the user. Technological innovation, the marginal benefit for low-tech sectors or industries, design, innovation itself is an effective trigger. Design always comes first from engineering.

Innovative firms, and design, both R & D spending is noteworthy. R & D, design and innovation activities of firms that invest in all, innovation is higher than the odds of making it. Using appropriate technology, an innovative idea or production of goods, can be a good R & D activities [3].

3.1 Place of Industrial Production Process of Innovation

Innovation in today's globalizing economy, is considered one of the most important factors determining competitiveness. I. The Industrial Revolution, ie, since the 18th century, the technology to produce a large extent the competitiveness of nations, effectively utilize and develop new technology-based solutions is related competencies [2].

Time needed to convert it to a marketable product, an invention of 3-5 years. Only 5% of patented inventions into marketable products to turn into-8, and only half of them can provide a significant benefit. Innovation, requires understanding and a different culture. This understanding of different cultures and a broad vision, open to change and development occurs in individuals [3].

Culture and understanding required for innovation
a) Large vision (different visual)
b) to take the risk
c) Creativity
d) to be open to change and evolve
e) the ability to query
f) Failure to tolerate
g) the value of the customer to know
h) Good communication skills
i) co-operation
j) Learning and knowledge management

Factors Affecting the Development of Innovation Culture
a) Education
b) The free flow of information
c) intellectual property system
d) The awarding of inventions and inventors
e) Supportive government policies
f) Supporting regulations
g) Adequate industrial, technological and R & D infrastructure
h) the culture of business innovation
i) Supporting efforts to Entrepreneurship
j) a positive approach despite failures
k) funding for innovation projects and easy access to financial resources [4].

3.2. Technological Innovation Managemen

A new or improved product, service, and manufacturing process development and as a result, the whole process of obtaining an income from commercial innovation. Innovation, innovation, and / or convenience, and continuity to bring an idea was born. Developed this idea into practice pouring the company to increase the competitiveness of the market and to ensure continuity, the results need to be evaluated.

Arising from the results of innovation again and again in order to ensure the continuity and the creation of a new examining returns, new thoughts arise, a new innovation process is activated [4].

Technological innovation management, labor and physical resources:

- the production of new knowledge
- New and improved products, production methods and ideas for the production of services
- Translation of ideas, prototypes work
- They are produced and distributed for use (removal of the market), and is directed to the organization.

4 Conclusion

Design is a critical innovation, actor and category. The role and importance is not sufficiently understood. The process of innovation technology, R & D complements. An innovation in its own right (design-driven innovation) source. Innovation leader countries and companies are aware of this. Innovation brings advantages to businesses, increased efficiency, and competitive advantage, ensuring payments imbalance, raising awareness of social responsibility, loyal customer base, the acquisition, institutionalization and provide branding businesses with R & D as a sort of orientation is possible.

Design innovation, technological development with innovation, R & D activities, to the development of the market provides the technological progress in size and are integral parts of a whole.

References

[1] Aksoy, M. (2005) "Continuous Innovation (Innovation), the Technological Capabilities Assessment", Technological Capability Değerlendirmesi.doc December 2005-1 -

[2] Er, A. (2009) "Design Technology and Innovation" Department of Industrial Design, Istanbul Technical University, 8 Technology Awards and Congress, TUBITAK-TTGV-Bulletins on June 25, 2009, Istanbul

[3] Gokce, S. (2010) "Innovation Concept and Importance of Innovation" Euphrates Development Agency, 16 July 2010

[4] Uzkurt, C. (2010) "Innovation Management: Innovation What, How, and How marketed?", Journal of Ankara Chamber of Industry, July / August 2010

The effect of systemic factors on the development of high-tech entrepreneurship in Slovenia

Sašo Sukič[1], Borut Likar[2]

[1]University of Ljubljana, Slovenia
[2]University of Primorska, Slovenia

Abstract

The paper presents an overview of financial and nonfinancial systemic factors in the field of high-tech entrepreneurship in Silicon Valley (USA) and in the area of Bangalore (India) in comparison to the Republic of Slovenia. Silicon Valley and the area of Bangalore are a synonym of a successful model for the development of high-tech entrepreneurship. Based on an empirical research, the paper compares the financial and nonfinancial systemic factors in these areas with the state in Slovenia and defines the most important factors which slow down the innovative and high-tech entrepreneurship in Slovenia. Said factors are: entrepreneurial spirit and culture, competitiveness, knowledge, development and innovation, finance, taxes, administration and infrastructure. The systemic factors analysis has shown that the majority of these factors hinder business operations of Slovenian companies, while the analysis has revealed some of systemic problems in the field of encouraging entrepreneurship. Limited access to finances and excessive bureaucracy acknowledge the already recognised problems of the Slovenian entrepreneurship. However, a special attention should be paid to the basic nonfinancial factor. Entrepreneurial spirit and culture represent a serious obstacle in the development of high-tech entrepreneurship by way of which the country's planners of the economic and innovation strategy are faced with an important warning since the said strategy is the basic term for the development of high-tech entrepreneurship which requires a change in the mindset and values. Based on the research results, it may be concluded that in the short term Slovenia cannot (yet) become Silicon Valley.

Keywords: innovativeness, entrepreneurship, systemic factors, Silicon Valley, Bangalore

1 Presentation of the problem

The area of high-tech entrepreneurship, such as Silicon Valley, is a synonym for innovation and development. It is characterized by certain key systemic factors for the development of such area. Similar is the area of Bangalore, which is currently one of the fastest growing business areas in the world. Sukič, Gider and Likar [1] stress that the path from an idea to concrete development of areas such as Silicon Valley and Bangalore, is not easy, since it proves important to consider both key systemic factors as well as the economic, social and cultural differences between the countries. Slovenia also endeavors to transfer the Silicon Valley ideas into its own environment. A representative high-tech enterprise in Slovenia is, save for notable exceptions, relatively underdeveloped. The state's strategic documents provide the thinking in the right direction; however, there is a long way to the actual of a country with developed high-tech entrepreneurship. Among the factors contributing to successful knowledge transfer, some recent findings may be identified, such as: superior RR on the "useful" areas, preparedness for interdisciplinary RR, networks among public institutions, industry and academia, as well as physical vicinity, which enables informal yet frequently very constructive networking. Innovation management at the strategic and operational level, organizational structures, such as offices for licensing technologies, focus on finding the values of RR, supported by clear policies, access to venture capital, and last, but not least, the tradition and history of successful commercialization of RR and geographic location [2] are also important. These are the factors that make a successful Silicon Valley and distinguish it from many less successful global followers. The scope of required potential in Slovenia is presented in more detail hereunder.

2 Systemic factors of high-tech entrepreneurship

This section presents the key factors of the development in Silicon Valley, area of Bangalore and Slovenia, followed by a comparison of systemic factors.

2.1 Key development factors

Over the past decades, the Silicon Valley has become the model for the development of high-tech companies around the world, irrespective of its relatively short 50-year history [3].

Likewise [3] indicate as the typical characteristics of the model of the Silicon Valley:
- confidence in entrepreneurship,
- key role of venture capital,
- critical role of research universities,
- large supply of highly-qualified researchers,
- benefits arising from company location,
- extensive role on free market with limited government interference.

Stremlau [4] summarizes Edward Yourdan, the software industry analyst, who claims that India has the opportunity to become an important factor in the global software market, which is not the greatest added value of Bangalore. The greatest added value is its people, i.e. highly-educated engineers and programmers, who are usually paid less than equally qualified professionals in most developed economies.

Highlighted as major systemic factors that facilitated the development and growth of Bangalore, may be in particular:
- highly-educated engineers and professionals,
- relatively cheap and English-speaking personnel,
- large investments of foreign multinationals in technology industries,
- support from research centers,
- technology parks with adequate infrastructure and attractive tax relieves.

In his study Sukič [5] notes that both areas are connected by many key factors that are essential for the growth and development of economic environment, although there are some differences in their development. While the growth of Silicon Valley began independently in harmony with the University of Stanford and the support of innovative ideas with venture capital, the growth of Bangalore caused liberalization of India, which led to the planned construction of high-tech area with direct foreign investments and investments of domestic private banks. The biggest difference between them is by all means the culture, since Silicon Valley developed in a spirit of free and egalitarian culture of the United States of America, while India represents the culture of different religions and disproportionate development of the country, which is, due to its size and development, becoming an increasingly important area of the world.

2.2 Comparison of systemic factors

In relation to the key systemic factors, Table 1 shows a comparison of the said factors in Silicon Valley (USA), the area of Bangalore (India) and in Slovenia. The data are based on reports from the Innovation Union Scoreboard 2010, Global Competitiveness Report 2010-2011 and Doing Business 2011. The data reveal that there is a substantial difference between Slovenia and Silicon Valley, while most factors in Slovenia are comparable to the area of Bangalore, Slovenian proves more developed in terms of infrastructure. The largest difference is noticeable in finances where Slovenia is lagging behind both the aforementioned areas. The fiercest comparison factor is tax system, as the systems differ among the countries.

Table 1: Comparison of systemic factors for the development of high-tech entrepreneurship in Silicon Valley, area of Bangalore and Slovenia (* Data for the United States, ** Data for India)

Systemic factor	Silicon Valley*	Bangalore**	Slovenia
Entrepreneurial spirit and culture	High	Medium	Medium
Competitiveness	High	Medium	Medium
Knowledge	High	Medium	Medium
Development and Innovation	High	Medium	Medium
Finance	High	High	Low
Taxes	High	High	Medium
Administration	Medium	Medium	Medium
Infrastructure	High	Poor	Medium

Source: [6], [7], [8].

The comparison of critical system factors, which are the most important for the growth and development of Silicon Valley and area of Bangalore, represent the starting point for the study of systemic factors among Slovenian high-tech companies.

3 Research Methodology

3.1 Presentation of research

Data analysis was conducted applying the quantitative research method. Data analysis represents the findings of the research on systemic factors that contribute to/or hinder the development of innovative works of Slovenian high-tech entrepreneurship and the assesment of their impact on the development and innovation in Slovenia. The data were collected by means of electronic questionnaires on a sample of eighty innovative and potential companies in Slovenia, which were selected based on three criteria, namely, financial data obtained from the Agency of the Republic of Slovenia for Public Legal Records and Related Services (AJPES), international awards for innovation and preservation of successful business performance of the Slovenian gazelles in the last three years. Some small and medium-sized enterprises were also added to the sample so as to complete the sample representation of potential companies. Out of 80 Slovenian companies, 27 companies responded to the questionnaire, i.e. the response was just over 33%. Six companies were excluded from the sample due to the lack in completed questionnaires. So the final total sample comprised of 21 companies.

3.2 Description of Research

The questionnaire was divided into the following three parts: (1) information on a company, (2) impediments in company's business operations, and (3) systemic factors affecting the development of entrepreneurship. In the first phase, the companies' respondents were to enter their basic data: firm's age, number of employees, net sales revenues, which industry branch a company is engaged in and which markets a company operates on. In the second phase, the companies made their own assessment of the obstacles posed in Slovenia from 1 (disagree) to 5 (completely agree). Listed obstacles were as follows. : excessive bureaucracy, low purchasing power of the population, shortage of skilled labour force, expensive labour force, poor infrastructure (roads, communications,...), lack of quality management, limited access to financial resources, introduction of new technologies, and introduction of new organizational forms. The responses of the companies were statistically processed by way of calculating the mean value of estimates. In the third phase of the questionnaire, the companies assessed - from 1 (unimportant) to 5 (very important) – the systemic factors that significantly influence the development of entrepreneurship: payment defaults, high taxes, lack of entrepreneurial and innovation culture, slow restructuring of productive and technologically advanced operations, lack of venture capital, excessive administration and bureaucracy, inefficient and sluggish judicial system, difficulty in dismissing employees, non-availability of adequately skilled labour force, inadequate competition protection. The survey continued by the companies responding to more detailed questions regarding the systemic factors that affect the development of entrepreneurship.

4 Results

The data on the companies show that the share of companies as per their entry into business operations was distributed pro rata from 1 year to more than 50 years, while the number of companies' employees was dominated by the companies with up to 10 employees (37%), and the company revenues with revenues amounting to up to EUR 2 million (52%). Most companies appertained to information and communications (33%), manufacturing (22%) and expert, scientific and technical activities (19%).

4.1 Obstacles in business operations

The following section shows the average evaluation given by the companies as regards the obstacles in business operations (Figure 1). The results highlight excessive bureaucracy (average score 3.91), followed by limited access to financial resources (3.82) and expensive labour (3.55) as the major obstacles.

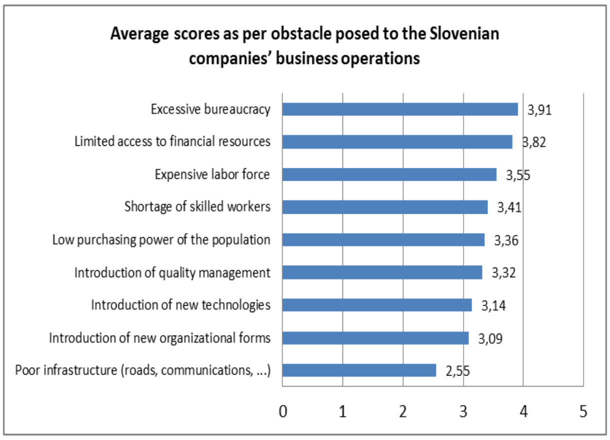

Figure 1: Average scores as per obstacle posed to the Slovenian companies' business operations

4.2 Systemic factors associated with the development of entrepreneurship

Deriving from the data analysis of systemic factors in Figure 2, it derives that companies indicate high taxes (average score 4.35), slow restructuring of productive and technologically advanced operations (4.19), excessive administration and bureaucracy (4.14), and inefficient and sluggish judicial system (4.14) as the most critical factor in the development and innovation of the Slovenian economy.

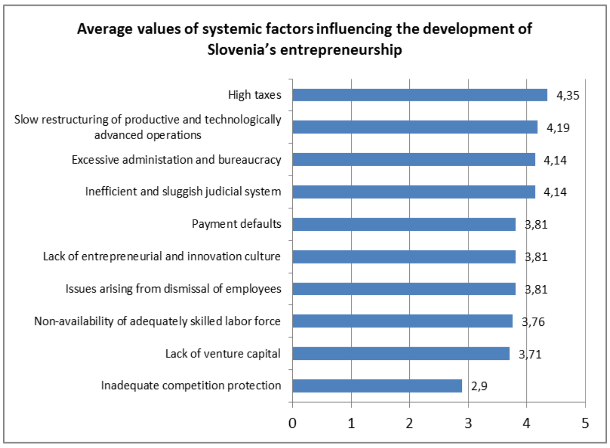

Figure 2: Average values of systemic factors influencing the development of Slovenia's entrepreneurship

4.3 Detailed analysis of systemic factors associated with the development of entrepreneurship

The most important findings of the research are given below.

• In Slovenia, being an entrepreneur is not a value (this is highlighted by 76% of respondents). These data stress the state of the entrepreneurial spirit and culture in Slovenia, indicating the reluctance of the environment to the entrepreneurship and the lack of creative and innovative ideas for development of companies with higher value added.

• The competitiveness of the Slovenia's economy on the world rankings is falling; according to the surveyed companies, the main reasons of said decrease are inefficiency of labour market (33% answers), market size (24%) and lack of innovation (19%).

• Slovenia ranks below the EU average in the number of patents [9]. The surveyed companies provide the following reasons for the aforementioned: high cost of patents, trademarks and models (29%), general opinion that companies do not need the protection of intellectual property rights (29%), non-innovative companies (24%) and administrative obstacles (18%).

• The share of population in Slovenia, which is involved in tertiary education, is at the top of the EU average. Irrespective of this, it is faced with inadequate structure of enrolment in tertiary education pursuant to the market needs [9]. The surveyed companies assessed the quality and competence of knowledge and skills of Slovenian graduates with marks from 1 (inadequate) to 5 (excellent). The average score was 3.68.

• Slovenian companies co-operate relatively poorly with educational and research institutions. In the last five years, 43% of the surveyed companies have regularly co-operated with educational and research institutions, once to five times 24% of the surveyed companies, occasionally 19% of the surveyed companies and never 14% of the surveyed companies.

• Beside the companies, an important role should be given to the research sphere; however, in Slovenia, there is a substantial problem of transfer of knowledge from research-development sphere into companies [10]. Hence, the lack of interest in participation in the research sector (43%) and inadequacy of ideas and transfer of the latter (38%) is highlighted by the surveyed companies as the main factors, which make this transfer impossible.

• Slovenian companies have a relatively large number of highly-qualified staff. Prevailing among the surveyed companies are the companies (62%) that have a workforce of more than 50% of the highly-qualified staff. Followed are by companies (19%), which have a workforce of only 11 - 20% of such staff.

• Slovenian companies invest relatively intensively in their development. Data from the survey show that 43% of the surveyed companies invest more than 30% of annual assets in research and development, 19% of the companies invest up to 3% of annual assets 14% of the companies invest 20-30% of annual assets 14% of the companies invest 11-19 % of annual assets and 10% of the companies invest 4-10% of annual assets. The survey showed that the most important sources of financing the development of companies are company's own sources of financing (57%), short-term bank loans (14%) and venture capital (14%). Such data are certainly not encouraging for the creation of new high-tech companies, as most of the corporate financing is associated with their own financial resources. The reason for this is the relatively underdeveloped financial sector. The surveyed companies assessed the development of the financial sector from 1 (very poor) to 5 (very good). The average score was 2.33.

• Considering the difficulties of the Slovenian banking system and the data on the increase of companies with financial resources coming from abroad, 62% of surveyed companies responded that they were not financed from abroad, 19% of the surveyed companies are financed with foreign capital in the amount of more than 40% and 19% of the surveyed companies are financed by foreign sources in the amount between 1-10%.

• Data on above-average work load reveal that 35% of the surveyed companies estimates that this impacts (negative) their business to a great extent, 35% of the surveyed companies recognized the medium impact, 20% of the surveyed companies indicated a great impact, while 10% of the surveyed companies do not recognize the effect.

• Companies that mentioned the problems with the administration are faced with it especially in the area of electronic commerce, tax, environmental and customs affairs, public procurement tenders, employment of foreigners and poor quality and support of e-government services.

• As a part of the construction of infrastructure Slovenia has started to invest intensively in infrastructure and technology parks that have facilitated the creation and growth of companies in the recent years. The surveyed companies assessed the level of development of the supporting infrastructure and technology parks in Slovenia, with scores ranging from 1 (unsatisfactory) to 5 (very good). The average score was 2.95.

5 Conclusion and discussion

The described research shows that Slovenia fails to have serious potential to become the next Silicon Valley in the near future, since the results of the survey clearly stress the need to change the key system factors in high-tech entrepreneurship in Slovenia, at both the enterprise level as well as the state level. Measures and changes in practice are required in Slovenia so as to allow the development and promotion of business environment, i.e. business environment which would be based on the integration of all key systematic factors and which would be accepted by entrepreneur entities [5]. It is necessary to commence eliminating the obstacles in practice at the most basic systemic factors, such as the development of entrepreneurial spirit and culture. Finally, the surveyed company assessed that entrepreneurship in Slovenia is not a value and that the entrepreneurship out of necessity dominates. Additionally, there are also problems of bureaucracy and administration, difficulties in obtaining finances and high taxes. Irrespective of the fact that companies are faced with the problem of a lack of research and the transfer of ideas from the research sphere to companies and inadequate quality and adequacy of knowledge and skills of Slovenian students, they are aware of the importance of co-operation with research sphere and they employ a high proportion of highly-educated staff and allocate a large proportion of their annual profit for the development. Creating the conditions for a successful transfer model of the Silicon Valley and the development of key systemic factors puts Slovenia before a big decision closely linked to its ability to instigate the change of systemic factors, which are essential for the restructuring of the economy and creation of high-tech and innovative companies. Otherwise, Slovenia shall merely witness, on one hand, the demise of companies, or, on the other hand, the success of Slovenian companies, which are considering withdrawing from Slovenia [1]. The findings are consistent with the results of nation-wide research [2], which found that Slovenian high- (and medium-high) technology sector is - according to innovation as well as economic performance - less effective than low- (and medium-low) technology sector. Furthermore, the most innovative companies in the high tech sector are less successful than the low technology. Therefore, the state should strive to intensively promote innovation in the low-tech industries, since the improvement of innovation in these industries shall contribute significantly to the Slovenia's GDP. This proposal does not entail that investing into high-tech industries in Slovenia is not sensible. On contrary, such investments are absolutely essential for the development of the society; however, it is primarily necessary to have better control of many factors. In the aforementioned research [1] certain factors are shown, predominately all those that are in the domain of the companies; the systemic factors at the state level are considered in the article of this research. We believe that it important to manage both for the comprehensive management of the innovation in the high-tech sector.

References

[1] S. Sukič, F. Gider, B. Likar: Ali Slovenija lahko postane evropska Silicijeva dolina?. Ventil 18 (1), pp. 72-78, 2012.

[2] B. Likar in sodelavci: Referenčni model inoviranja – model celovitega obvladovanja inovacijskih procesov v podjetju, Temeljni project. ARRS šifra: J5-0425-7097-08, http://www1.fm-kp.si/visintapl/datoteke/REFERENČNI%20MODEL%20INOVIRANJA_FINAL_HiRes.pdf, 2011.

[3] I. Cook, R. Joseph: Rethinking Silicon Valley: New Perspectives on Regional Development. Prometheus 19 (4), pp. 377-393, 2001.

[4] J. Stremlau: Dateline Bangalore: Third World Technopolis, Foreign Policy 102, pp. 152-168, 1996.

[5] S. Sukič: Možnosti za nastanek Silicijeve doline v Sloveniji. Diplomsko delo, Univerza na Primorskem, Fakulteta za management Koper, 2011.

[6] PRO INNO Europe*:* Innovation Union Scoreboard 2010. Http://ec.europa.eu/research/innovation-union/pdf/iu-scoreboard-2010_en.pdf, 2011.

[7] World Economic Forum: The Global Competitiveness Report *2010–2011*. Http://www3.weforum.org/docs/WEF_GlobalCompetitivenessReport_2010-11.pdf, 2010.

[8] The World Bank: Doing Business 2011. Http://www.doingbusiness.org/~/media/FPDKM/Doing%20Business/Documents/Profiles/Country/DB11/SVN.pdf, 2011.

[9] UMAR: Poročilo o razvoju 2011. Http://www.umar.gov.si/fileadmin/user_upload/publikacije/pr/2011/POR_2011s.pdf, 2011.

[10] Government of RS: Konkurenčnost slovenskega gospodarstva - pregled stanja in ukrepi za izboljšanje. Http://data.si/userfiles/data.si/dokumenti/Pdf%20dokumenti%20za%20objavo%20%28listine,%20zakoni,%20uredbe%20ipd%29/Konkuren%C4%8Dnost%20slovenskega%20gospodarstva%20-%20pregled%20stanja%20in%20ukrepi%20za%20izbolj%C5%A1anje.pdf, 2011.

Service Engineering for Prospective Vehicle Service Processes

A. Nagel[1], R. Steinhilper[2], S. Freiberger[2] and S. Thäter[2]

[1] Fraunhofer-IPA, Germany
[2] University of Bayreuth, Germany

Abstract

Garages are - concerning the vehicle service - faced with growing complexity in automotive mechatronics and on-board bus communication technology. Because of the necessity of profound technical knowledge and smart as well as cost efficient diagnostic tools for garages, Bayreuth University and Fraunhofer-IPA pick up the challenge and develop innovative service-processes for future requirements by the project "Kfz-Service Engineering 2020". In order to improve established service-processes and develop new service processes a wide variety of service cases had been inspected in garages. The ten most relevant service cases are selected by using an analytical hierarchy process. Future service cases of vehicles amongst others are in the context of electronic diagnostics, control units, electro mobility and automotive lightweight construction. To be able to find and analyze electronic faults, for example, new diagnostic tools have to be developed. New and innovative service processes have been developed for those purposes, which will be published for the first time in this paper. They include the development of test benches, diagnostic and repair tools as well as the installation of highly specialized service centres and remanufacturing companies, to ensure cost efficient vehicle services. The overall aim of the project "Kfz-Service Engineering 2020" is to enable garages to repair and to service modern vehicles as well as to remanufacture expensive automotive subsystems.

Keywords: MIT&SLIM2013, service engineering, remanufacturing, service case, service process, vehicle, e-mobility, garages, diagnosis tools

1 Introduction

Service is the nowadays common term for after sales service or maintenance. The definition of service engineering includes the systematic new development for all technical service processes. The products for which the technical service is provided and developed, is affected by several laws and goals of the service for consumer and capital goods. The service engineering, described in this paper is for prospective vehicle service processes which are developed in the research project "Kfz-Service Engineering 2020" (in the following: SE2020)

1.1 Background

The project SE2020 focusses on the requirements and tasks that have radically and significantly changed during one generation of automotive service engineering (Figure 1). This trend hasn't been even noticed to its full extent until now. Vehicles belong to those consumer goods which generate the greatest amount of service for predominant private customers.

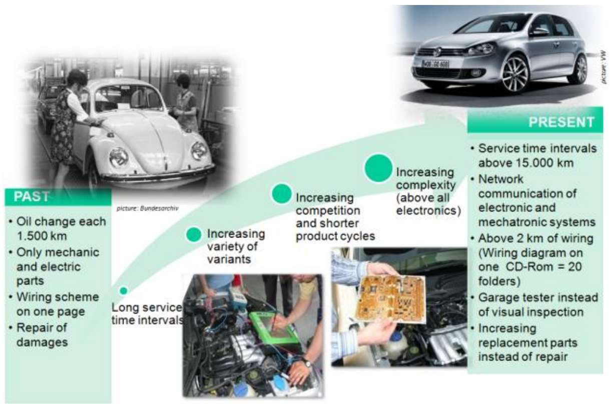

Figure 1 Past and present service requirements

A typical example is the replacement of faulty automotive components as engines, generators or control units.

Due to the tough competition in innovation and the battle of for customers of new vehicles, the product development times and product lifecycles are getting shorter and shorter in the automotive industry. The increasing requirement of customers, concerning safety and comfort, raises the complexity of today's vehicles. By the way in modern vehicles are up to 80 electronic modules integrated, which are mostly in charge of data collection, automotive control or regulation of mechatronic systems [1].

In consequence of the mentioned developments, the reliability of the automotives declines, which is proved by numerous vehicle recalls and documented in breakdown statistics [2]. Even with the latest available diagnostic methods, nowadays garages are barely able to localize the exact failure and to repair it. For the most parts it is merely possible to exchange the whole system, which increases the diagnostic effort as well as the spare part costs.

Additionally the original equipment manufacturers became an information monopole of cars respectively parts. This jeopardises the so far healthy competition on the vehicle market, e.g. by excluding independent garages. Europe does not hold a top position relating to a dynamic market and competition structure between the so called Original Equipment Service (OES) and Independent Aftermarket (IAM) [3].

Also in regard to sustainability the enhancement of technical services, as a part of vehicle attendance, implies extensive challenges but also high potential in two different ways.

On the one hand technical components in many cases do not achieve their technical age anymore, because of their shortened innovation cycle nowadays. Already many components are completely replaced by the next generation, before their possible mechanical service life has been reached, but the electronic does not represent the actual state of technology anymore. Only seldom cases succeed by modularity to continue using mechanical systems by upgrading with modern electronic units. A negative example indeed is the automotive: The average life cycle is up to 15 years compared with the innovation cycle of the electronics, which is 1 - 3 years [4]. Consequently that means to service a 6 year old vehicle, it is required to have the maybe third generation antiquated electronic available. Spare parts therefor are expensive, rare or not available. A replacement of old electronic components by a new one is in most cases not possible.

New service processes must be achieved for such systems by original equipment manufacturer, service centres and garages as a new value added service.

On the other hand - besides the depict repair of the defect component - another category of new service processes offers special potential:
Addressed is the remote diagnosis. Until now automotive garages handle with damages which are already existent or service a car to avoid defects (e.g. exchange of gear belt). According to the case of service the appropriate service application takes place. The remote diagnosis however enables the design of all new service processes. In this process at the vehicle e.g. the process parameters at the CAN-Bus-interface (**C**ontroller **A**rea **N**etwork) can be controlled and if they exceed a critical value a warning message can be send to a service-garage or to the mobile phone of the user. The service- garage is able to setup a wireless remote diagnosis with the car. Requirement for this purpose is of course the previous agreement of the customer. After the remote diagnosis an expert is able to evaluate, if there is a defect and if subsequent service process steps will avoid it. The customer in the future will not go to the garage after the defect is caused; instead the garage would request the customer in first instance to come for the service. The necessary hardware and software is currently developed by Fraunhofer. Its function is related to the so called “Emergency Call” systems [5].

1.2 Targets

The target of the project SE2020 (cf. Figure 2) is the (further) development of technologies and organizational form to:

1. identify and analyze new service cases (especially failure diagnoses and elimination plus efficiency deficits) as well as the development of associated new solutions,
2. manage the necessary knowledge, which means to provide the knowledge for the service provider and service recipient and to increase it by synergetic effects,
3. structure and design the service process systematically and to generate the economic advantage for the provider and recipient of the service by developing terms of references and indicator systems as well as,
4. generate new dimensions / new profiles of the vehicle services.

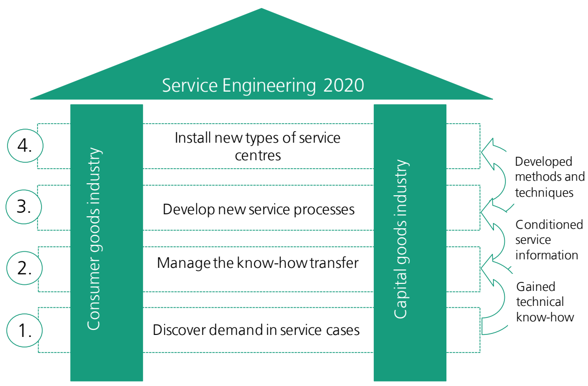

Figure 2 Objectives of SE2020

2 The project SE 2020

Chapter 2 gives a brief overview of the project consortium, the proceeding and the work packages of the project SE2020.

2.1 Project consortium

In order to achieve the targets for prospective vehicle service processes mentioned in chapter 1.2, a consortium of representatives from research as well as the chamber of crafts has been formed and assigned tasks according to their competence and experience. The consortium consists of the chamber of crafts Bayreuth and two German research organizations (Fraunhofer and Bayreuth University) with a profound background in the remanufacturing industry as well as in the field of service engineering. Additionally, the consortium is supported by numerous independent and authorized garages.

2.2 Proceeding and work packages

The project SE2020 is divided in a seven month phase I (pre phase) and a four year phase II (main phase). In phase I data of garages were collected through a technical questionnaire. The feedback reflects the current situation in the vehicle service sector. The results influence the focused systems of the project in phase II.

Furthermore, in order to achieve optimal results, the SE2020 project is splitted into four different work packages and milestones (cf. Figure 3).

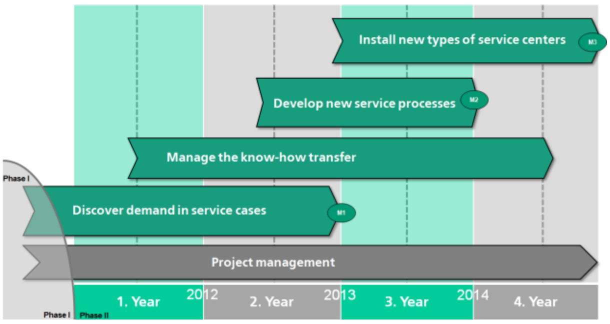

Figure 3 Work packages and milestones of the project SE2020

The current project status is the completion of phase I and milestone 1, which contains the analysis of 50 service processes of phase II in 50 different service cases in 25 garages, as well as the choice of ten service cases with the greatest demands for new service processes.

3 Project results

The results achieved in the project SE2020 are subjects of chapter 3. It has to be differentiated between results of phase I and phase II of the project SE2020.

3.1 Questionnaire regarding service cases

According to work package 1 (cf. Figure 2) 50 service cases have been recorded in 25 garages in detail. Therefor independent and authorised garages have been inspected. In phase I questions concerning the frequency of ten in advance picked automotive systems have been arranged. The determined results were extrapolated for whole Germany (cf. Figure 4).

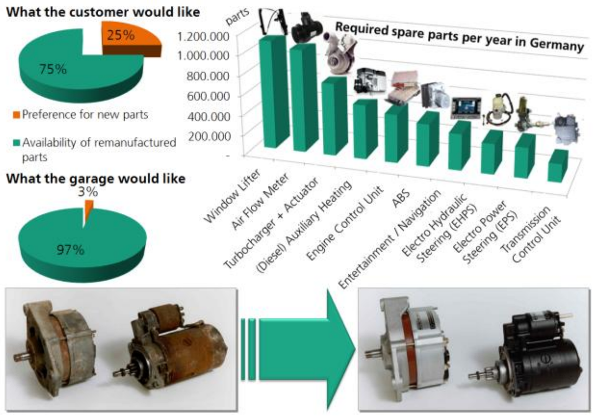

Figure 4 Service cases in Germany

For a qualitative collection of information to service cases a questionnaire with 20 questions has been developed. In this questionnaire questions relating to the garage, the kind of service case, the diagnosis tools and other questions have been included.

The service cases have been determined quantitatively by the record of the following data:

- measure of working hours
- appraisal of the material costs
- collection of technical data
- picture and video recording
- description of service process.

Figure 5 shows a comparison of labour costs with the material costs of the picked service cases.

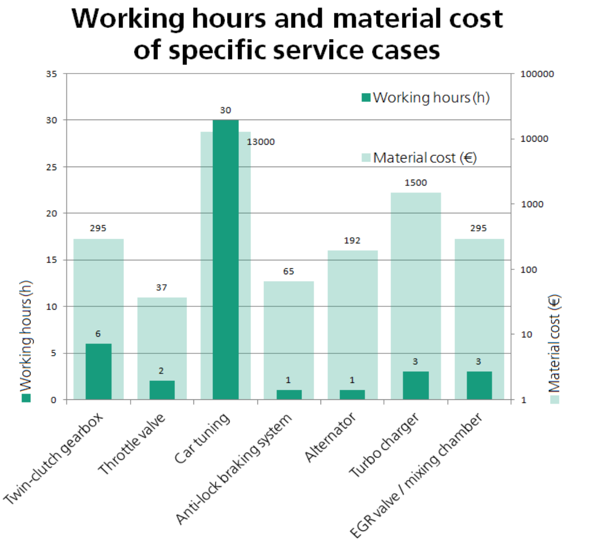

Figure 5 Comparison of working time and cost of materials

The established technical data contain information about the vehicle itself as well as detailed data of the defect systems plus diagnosis data. The description of the service process in a service case contains the procedure starting with the vehicle reception to the customer satisfaction with the service (cf. Figure 6).

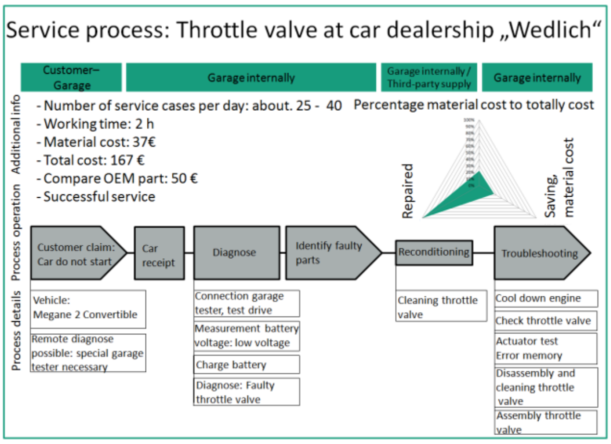

Figure 6 Example of a service process

3.2 Choice of ten service cases

The choice of the ten most promising automotive service cases is based on the economic collection of data in phase I, the detailed recording of 25 garages with the 50 service processes, the numerous expert discussions at the workshops, the technical / economical analysis of the service processes and of course the longtime experience of the project executing engineers and technicians of the crafts, the Bayreuth University and Fraunhofer.

A simple choice of the ten service cases on the basis of its occurrence does not include different influencing factors like the price, the amount of work or the sustainability. That's why for example the service case window lifter is playing no further part in this project as there is no need for a new service process. One kind of solution for the choice of adequate representatives offers the Analytic Hierarchy Process (AHP) as well as the Cost-utility Analysis. The Analytical Hierarchy Process is a basic approach of the decision theory. The mathematical method was developed in the 1970s from Thomas L. Saaty. The intent and purpose of this method is to include rational as well as intuitive alternatives in the process of decision [6]. In the process the person making the decision enforces paired comparisons which are used to define a priority of the ranking. For that reason initially the costs of the repair of single assemblies as well as the costs of the installation of remanufactured systems are compared with the costs of new systems.

The analysis shows for which systems a repair promises a high saving and for which the complete exchange has to be favoured. Besides the occurrence of service cases the listing of the relevant influencing factors illustrates only an extract. As a part of the AHP not only absolute factors also intuitive factors can be considered. For the evaluation of the service cases the following factors are taken into consideration as well:

- complexity
  - eligibility of the process for independent and authorised garages
  - needed tools / machines
  - qualification of the employee
- sustainability
  - relevance in the year 2020
  - conservation of material and energy
- demand
  - current sold numbers of products
  - acceptance of customer

In the first instance pair-wise comparison between the different criteria and a relative evaluation to each other took place. The pair-wise comparison is used to determine the relative importance of criteria in comparison to the others.

If two criteria are equal to each other the pair-wise comparison generates a 1. Is one criterion much more important than the other criteria the value shall be 9. The ranking between those factors is shown in Figure 7. Additionally it describes the savings, to figure their importance once more.

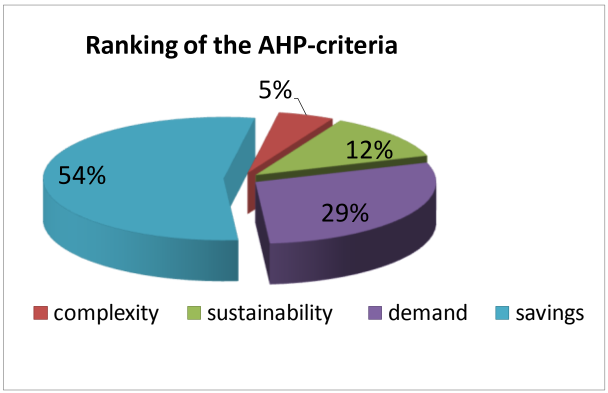

Figure 7 Ranking of the AHP-criteria

To finally dissolve the decision problem matrix a multiplication as well as a creation of eigenvectors is provided. Consequently the service cases can be compared by the criteria saving, complexity, sustainability and demand. After applying of the AHP on all service cases the most promising cases are defined to:

- direct-shift gearbox,
- camshaft sensor,
- generator,
- turbocharger actuating element,
- headlight,
- control unit (immobilizer),
- injector,
- wheel alignment,
- sporadic failures,
- engine control unit.

Numerous expert interviews in garages in phase II lead to a non relevance of some service cases for the project service engineering chosen by the AHP. These involve the camshaft sensor, generator, control unit (immobilizer), injector as well as the wheel alignment. On the other hand new service cases relating the "CAN bus" and the electro mobility have been added. Due to the high need considered by the automotive experts. In particular at independent workshops the necessary OBD-remote (**O**n **B**oard **D**iagnostics) diagnosis represents the third promising service-case which is supposed to be developed during the project service engineering 2020.

Furthermore the service cases in the field of EPS-steering, light weight construction and development of the *Wiki-CAN* forum are added. By the scientific evaluation of the 50 cases, taking the experience of the specialists into consideration are now the ten promising service cases available for the project service engineering 2020. Those are finally:

- direct-shift gearbox,
- remote diagnosis,
- electro-mechanical power steering,
- turbocharger actuating element,
- headlight,
- diagnosis *Wiki-CAN*,
- light weight construction,
- electro mobility,
- sporadic failures,
- engine control unit (ECU).

3.3 Service Process Electro-Mechanical Power Steering (EPS)

A service process that was chosen according to chapter 3.2 was the electro-mechanical power steering (EPS). If a defect at the EPS of a vehicle occurs, it gets signalized by a yellow or red warning light in the instrument cluster. In the case of a red light the garage has to be visited immediately. Up to now the process (shown in Figure 8) starts with the customer driving his car to the garage resp. getting his car towed to the garage. The diagnosis is made and the failure on the EPS is determined. So far the process is designed to change the complete EPS.

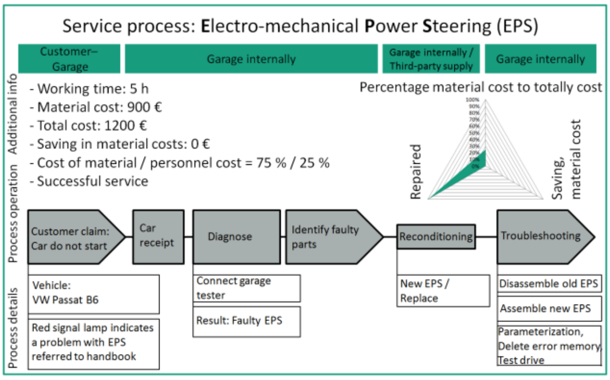

Figure 8 Service process: Electro-mechanical power steering (EPS)

The record of the existing service process results in an exchange of the overall system instead of a repair. As an exchange system a new system is generally used, because there are no remanufactured EPS available. Occasionally some pre used EPS are available. For this reason the financial savings between new systems and exchange systems was considered with 0 €.

With material costs that add up to 75% of the repair costs there are no savings possible. So one possible proceeding could be to change the service process towards a feasible repair of the EPS. Another possibility to economize the material cost would be to use a used or remanufactured steering. Under the assumption of reparability and the ability to remanufacture the new developed service process is shown in Figure 9.

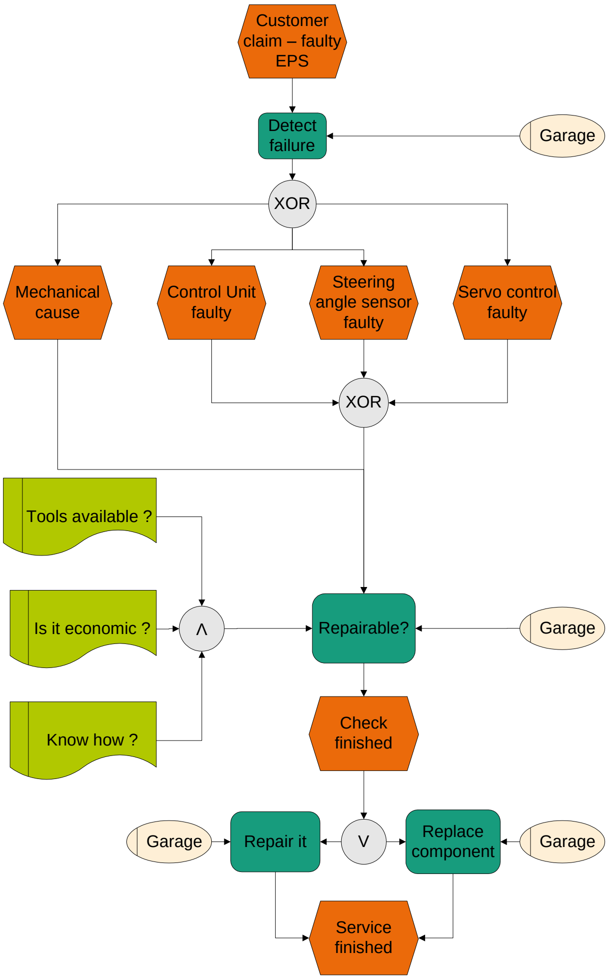

Figure 9 New developed service process for EPS

Currently nobody remanufactures the EPS, because of safety considerations - except of some manufacturers like "ZF Lenksysteme" which just started remanufacturing their own electrical steering.

In the context of the project SE2020 the possibilities to repair the EPS immediately in the garage and which arrangements for the remanufacturing in special service centres are needed is the next task within the project.

For the remanufacturing of EPS six steps of refabrication are necessary (cf. Figure 10). The entrance diagnosis of the mechatronic systems (to which the EPS belongs) is the first step in remanufacturing like Figure 10 shows.

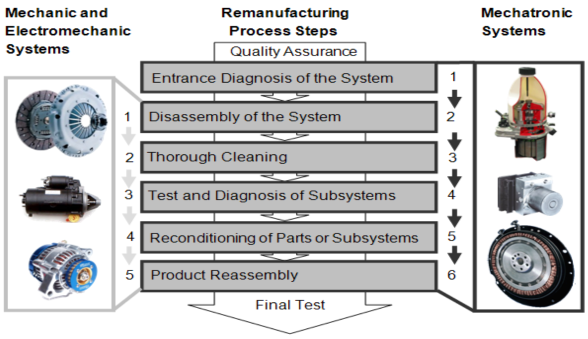

Figure 10 Remanufacturing process steps

An EPS has to comply with the technical safety demands after the remanufacturing has been accomplished. Relevant for this purpose is the guideline 701 156 / EWG article 3. The guide line 2005/64/EG of the European Parliament and Council from 26 October 2005 about the type-approval of motor vehicles with regard to their ability for reuse, recycling and recovery and the change of the guideline 70/156/EWG of the council includes additional provisions which are important related to the remanufacturing. Upon request the TÜV South Garching gave us in June 2012 following statement: "*Representative legal regulation: 70/311 EWG, 2007/46/EG. Reference to §38 of the German road traffic registration (StVZO); in practice the German Association for Technical Inspection (TÜV) is verifying the common way / time synchronization (wheel angle has to follow the steering angle directly) and the tendency of the wheels to reset*". The guarantee and liability of the remanufactured systems have to be given by the company that is remanufacturing the EPS. The remanufactured steering system has to be marked. In order that those requirements of the relevant named guide lines are achieved and especially that they can be approved a final test of EPS steering by the help of an EPS test bench is necessary. Figure 11 shows the developed test bench for EPS.

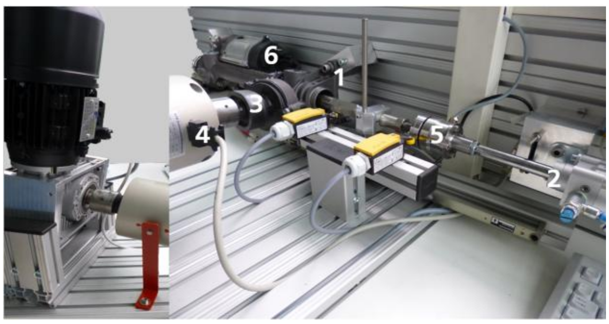

Figure 11 Test bench for the EPS

The test bench achieves the initial functional tests as well as the final functional test and diagnosis. For this reason the EPS is installed in testing position 1 of the test bench and is connected to an air cylinder (position 2) mechanically. The air cylinder simulates the performance of the wheels in relation to the vehicle speed, cross wind and other parameters. In position 3 steering thrust as well as steering motions at the steering shaft can be simulated. The torque sensor (position 4) and the force senor (position 5) are used to determine the torque and force. Additional parameters, like steering angle, steering angle speed, etc. can be recorded as well. The EPS-ECU (position 6) provides information about the CAN-Bus, which allows reliable conclusions about operating parameters (e.g. rotation speed, operation mode, steering assistance torque) of the EPS asynchronous motor. The test bench is regulated by the help of the individual customizable software *LabVIEW*® and hardware modules of “National Instruments”. The test bench was developed during the project SE2020 and can be applied for the following duties:

- initial test
- final functional test
- communication with EPS steering module
- calculation of steering gear tightening
- measuring of torque, supporting torque and steering moment, angle and speed
- simulations of loads
- characteristic diagrams measurement
- verification of the used parameter set

The measured data can be visualized and saved in a data bank as well as compared with each other for I/O-tests. The test bench was developed for the second and third type of EPS steering generation of the VW Passat B5 and B6.

3.4 Service Process *Wiki-CAN*

Wiki-CAN was developed within the project SE2020. The purpose of it was to enhance the diagnostic process of service-processes, which are in the context with the CAN-Bus of vehicles. Of course many, but not anyone, of the authorized repair garages have the necessary garage tester for such tasks. Independent repair garages have the problem not to own a garage tester for each vehicle model. For those one it would be helpful to have one analyzing “CAN bus” tool for all vehicle models. With the help of *Wiki-CAN* it is now possible to use a very cost-efficient “CAN bus” interface, which is connected between the OBD-plug of the vehicle and the notebook [7]. The in-house developed public domain software, which is running on a notebook, can be used to upload or download CAN-messages. The uploaded messages can be transferred to the so called *Wiki-CAN* forum and shared with other users, which are working on the same problem, control unit or vehicle. In this forum it is possible to find information about the meaning of the uploaded CAN-messages. It is also possible to download CAN-messages from other users from the forum and to playback these messages to a connected control unit, independent of the vehicle. In this way the *Wiki-CAN* helps to improve the diagnosis service processes. It has to be mentioned, that the *Wiki-CAN* service process is getting better the more people take part of it and its related forum. Wiki-CAN, as well as the forum can be accessed online at this address: http://www.kfz-service-engineering-2020.de/wikican-forum/. A “wiki” with detailed instructions is also available (cf. Figure 12).

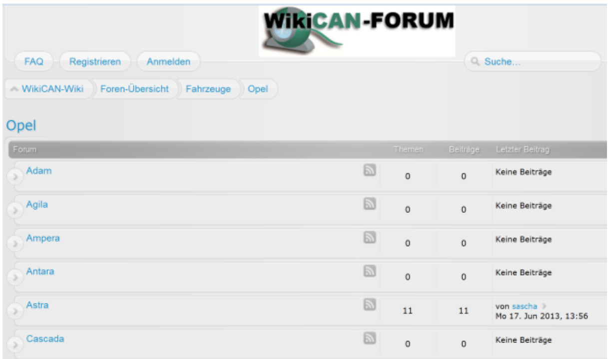

Figure 12 Service process: *Wiki-CAN*

4 Conclusion

This paper publishes for the first time the results of the first half of the project “Kfz-Service Engineering 2020”. The results of a survey of 50 service cases in garages are shown first. On the basis of this data the ten most relevant service cases are selected. According to the experts, those ten cases represent the most eminent potential in the field of service in the automotive service sector. Especially in the field of electro-mechanical steering and turbocharger actuators new service processes have been developed. This includes the construction of test benches which have met a brisk demand among different companies from the automotive remanufacturing industry.

But also in the sector of the remote diagnosis, the diagnose service process *Wiki-CAN*, light weight construction and e-mobility interesting new solutions have been achieved. The development of a repair kit for LED headlights is about to be finished and different knowledge, training and instruction guides have been created for example for the Toyota *Prius*® or the Mitsubishi *i-MiEV*®. The actual project progress for the residual service processes can be seen at the German web page www.se2020.de (cf. Figure 13).

Figure 13 German project web page for SE2020

5 Acknowledgments

The project “Kfz-Service Engineering 2020” is supported by a funding from the Bavarian Federal Ministry of Economics, Infrastructure, Transport and Technology.

6 References

[1] S. Freiberger: Prüf- und Diagnose-technologien zur Refabrikation von mechatronischen Systemen aus Fahrzeugen, Shaker Verlag, Aachen, 2007.

[2] R. Brauch, C. Zach: Autoelektronik und Zuverlässigkeit – Erfahrungen aus Fehlerstatistiken. In: Elektrotech. Inftech. 123(10), pp.451-453, 2006.

[3] A. Kampker: Elektromobilität, Springer Vieweg, Berlin, 2013.

[4] U. Raubold: Lebenszyklusmanagement in der Automobilindustrie, Gabler Verlag / Springer Fachmedien Wiesbaden GmbH, Wiesbaden, 2011.

[5] G. Meyer, J. Valldorf: Advanced Microsysems for Automotive Applications 2010, Springer Verlag, Berlin, 2010.

[6] T. Saaty, L. Vargas: Models, Methods, Concepts & Applications of the Analytic Hierarchy Process, Springer Verlag, New York, 2012.

[7] S. Freiberger, A. Nagel, R. Steinhilper: WebCAN for Remanufacturers - A New Automotive CAN-Bus Tool - Analyzing and File Sharing Application. 9th Global Conference on Sustainable Manufacturing, St. Petersburg, Sep 2011.

Upgrade of abrasive flow machining process for controllable creation of micro geometry and polishing of surface in tooling industries

F. Pušavec, J. Kenda, and J. Kopač

University of Ljubljana, Slovenia

Abstract

In the field of polishing, hand polishing has the largest comprehension. On account of nowadays different requirements such as: reducing of finishing time, process control and the ability to predict the effect, etc. hand polishing has to be replaced with superior process. An alternative is two way abrasive flow machining (AFM). In comparison with hand polishing, AFM is very efficient process, suitable for finishing external as well as internal surfaces, which are often complex and out of reach. In this paper, the influence of the process on surface roughness and micro geometry of injection mold, for manufacturing of plastic convex gears, are investigated. The hardened tool steel AISI H11 injection mold parts, before being processed with AFM, have been pre-machined by wire electrical discharge machining (WEDM). Due to AFM drawbacks, the novel two way abrasive flow machining with movable mandrel has been proposed and used. Results of the work show that the application of AFM is capable to remove WEDM damaged surface and produce polishing surface. Moreover, the novel upgrade of AFM process can control also the micro geometry of the finished surface. In this way an injection mold has been made with surface roughness bellow $R_a = 0.1$ um, and the convex shape in the range of 5 um. The convex shape of final product – plastic gear is offering significant improvement of gear performance, energy efficiency in operation as well as its fatigue life, prolonged for more than two times. As a contribution, a novel AFMmm has been presented with the capability to synergistically shape and polish the geometry of the final product on a micro level.

Keywords: abrasive flow machining, finishing, surface integrity.

1 Introduction

The current industry is facing accelerated demands for higher quality of surfaces and higher added-value products. High-performance materials with specific property requirements (in terms of better functional properties, decreased cost and sustainability) and the ability to process them efficiently are crucial for new product development in many relevant industrial sectors such as aeronautics, automotive, railway, machine-tool and others.

The idea is well defined and implemented in the other fields (architecture, civil engineering, etc.), but there is a huge lack of those principles implemented into the manufacturing/finishing systems and technologies [1]. Concerning finishing processes, they constitute important manufacturing activity that contributes to the growth of EU as well as global economy, especially by the highly growing automotive and aerospace industry. Manufacturing process demands approximately 15% of the total manufacturing cost for finishing operations. When the surface roughness value is less than one micron the cost of surface finishing operation again increases sharply. In the manufacturing/finishing industry, still the ordinary hand polishing procedure is used, and presents one of the most time-consuming, expensive, health problematic and environment polluting solutions. The solvents and cleaners applied to metal parts and solutions used in polishing generate significant amounts of waste as well as small particles that enter the workers respiratory organs. Polishing solutions also often contain heavy metals. Cleaners often appear in process wastewater, while solvents containing hazardous air pollutants (HAPs) and volatile organic compounds (VOCs) can be emitted into the air, released in wastewater, or disposed of in solid form. Additionally, in many cases, hand polishing is also an unsuitable procedure due to high inability to assure constant roughness, constant thickness of removed material, adequate geometry after finishing, etc. Although these drawbacks trigger both cost and regulatory requirements, they can be addressed successfully through sound pollution prevention and manufacturing best practices, such as those provided with innovative abrasive flow machining (AFM). Therefore, the goal of the research is to develop a sustainable & innovative AFM finishing system and technology, based on new concepts of clean and dry polishing with innovative combination of AFM flowing abrasive polymer and movable/rotatable mandrel simultaneously (AFMmm) that show high potential in improvement of their a) environmental impact, b) energy consumption, c) operational safety, d) personal health, e) waste management, and f) manufacturing costs [2].

In the last few decades, ultrafine-grained and high surface integrity materials have attracted considerable interest, since these high performances surface materials have higher mechanical and fatigue properties in comparison to conventional hand polished or ground counterparts. The ordinary hand polishing procedure, is actually one of the most time-consuming and expensive solutions. In many cases, hand polishing is an unsuitable procedure due to high demands for constant roughness, constant thickness of removed material, adequate geometry after finishing, etc. Additionally, for many applications entire components are not necessary to have high integrity specification, and the mere optimization of the material surfaces through improved integrity (roughness, texture, residual stresses, etc.) greatly enhances the properties of the materials for such applications. This is due to the fact that the majority of failures such as fatigue fracture, fretting fatigue, wear and corrosion, etc., are very sensitive to the structure and properties of the material surface, and in most cases material failures originate from the surface. However, some research works on AFM of a range of materials have shown encouraging possibilities for producing (1) much thicker layers with nanostructures on the surface, lower heat affection on the material on the surface, and (2) more compressive residual stresses on the surface (which are favorable), combined with this kind of processes. Thus, the capability of product enhancement thanks to the use of AFM process, to obtain products that withstand longer fatigue life, better corrosion resistance, etc., stands as a challenge with real possibilities.

1.1 AFM

The abrasive flow machining (AFM) is actually a polishing technique (finishing method) that uses the flow of a pressurized abrasive polymer media for removing workpiece material (figure 1) [3, 4]. AFM represents performance enhanced process and can be used for polishing, deburring, removing recast layers, etc. [5]. It is suitable for finishing external as well as internal surfaces, which are often complex and inaccessible. It is specifically appropriate for parts with complex geometry and high demands for surface integrity. Despite of the advantages, the AFM process is still not widely and generally used in the real industrial finishing applications. Therefore, further development is inevitable. The reason for this is in the current state of development, which is still on a low level and on the other side high complexity of this process. Because of this, the project goal is to develop the system to such a stage that it will be reliable, economical and ready for use in real EU manufacturing industry applications. The paper so shows some possibilities for raising the AFM on wide area of industrial levels and sectors.

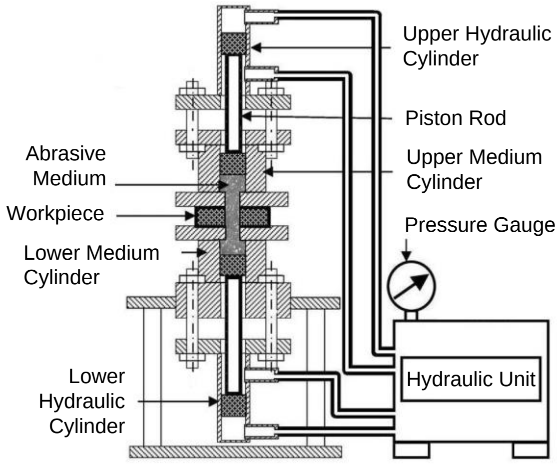

Figure 1 Scheme of the abrasive flow machining process (AFM).

2 AFM and gear manufacturing

The research presented in this paper was carried out on workpiece made of heat treated steel grade that is used in injection molds that could be coated with TiN, TiCN, TiAlN, CrN, etc. coatings enable longer injection mold life. The purpose of the research was to investigate the influence of AFM process parameters on surface roughness and important micro geometry of the injection mold, to results in desired surface integrity of the final plastic products (convex shaped gears).

In the manufacturing of tools for injection molding, in general, the finishing process is destroying the geometrical characteristics. And with this also the tolerances of final product are affected. The problems with geometrical tolerances can lead even to non-functionality of the final product. This can be to some extend solved with development of performance predictive models of AFM that assure the possibility for optimizing the process setup, parameters, geometry as output, roughness, etc. The aim of this work is to apply this methodology on gear injection mold, for reduced roughness, prolongation of tool life, and decrease of noise in gear operation (enhanced product performances).

Plastic gears have been used for more than 50 years, while there usage is exponentially increasing. The advantage of plastic material in such applications goes on account of novel plastic materials with improved technical properties: hardness, wear, stiffness, damping of vibration and no need of lubrication, in parallel with lower manufacturing costs, what put them ahead from metal gearing. Plastic gears are nowadays used in variety of applications, like: domestic appliances, modules for automotive industry, mechatronic components, etc. (figure 2). Anyway, performing the search of standards from the field, there are in minority covering the plastic gearing. There is a German standard VDI 2545 that covers strength of the plastic gearings, while the general specifications are analog to metal ones and are listed in VDI 2545, ISO 6336 and DIN 3990 [6]. Regarding the plastic materials for these applications, there is a huge lack of coverage. Standards like AGMA 909-A06, ANSI/AGMA 1006-A97 and ANSI/AGMA 1106-A97 cover specifications of gear injection molding process, however just related to the geometry.

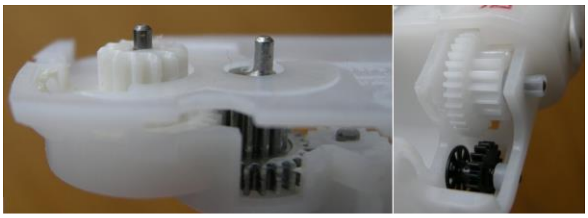

Figure 2 Example of plastic gearing.

In general plastic materials are sensitive to high temperatures and significant heat expansion. This can contradict the tolerances in the process of injection molding. To contradict these issues, the molds have to be manufactured with high quality, focused to surface integrity. To assure this high quality, the standard procedure of WEDM (wire electrical discharge machining) is in most cases not sufficient any more and further finishing process has to be performed [7]. Additionally, if take under the consideration that new high performance gears, that are coming into the usage in high tech product, which are not any more 2D geometry, but have convex shape teeth, the alternative finishing process are desired. One of solutions to assure such geometry of gearing is AFM, used as finishing process after WEDM rough manufacturing technique.

3 Novel AFM upgrade – AFMmm

One of the major problems with the AFM process, concerning finishing performances, is to get uniform finished surface roughness, uniform material removal rate on entire finished surface, required workpiece geometry/micro geometry, residual stress profiles, etc. [8].

That problems rise when the workpieces have relatively large cross-section of the shape. In this case the undesired variation of velocity, through the cross section, will appear. In the current state-of-the-art the problem is to some extend solved with the adjustment of abrasive fluid viscosity, but then this polishing media has limited performances (cannot then be used universally also for small cross sections). The consequences of this problem are two:

- With increased cross-section of the workpiece, the speed of polishing media decreases and this results in lower abrasive flow machining process efficiency.
- Friction between the workpiece surface and the polishing media may lead to nonuniform distribution of polishing media velocity on polishing workpiece cross-section (the lowest velocity in the contact zone of abrasive media and workpiece surface. This again results in lower process efficiency.

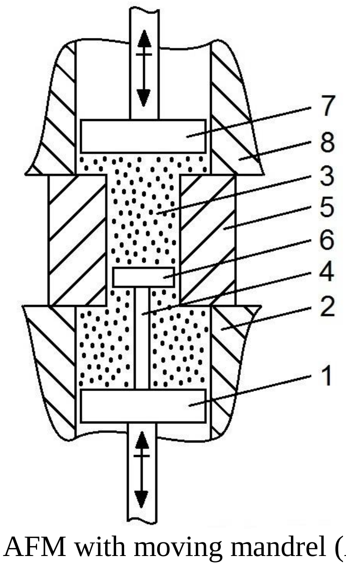

Figure 3 AFM with moving mandrel (AFMmm).

The problem of nonuniform polished surface and nonuniform material removal can be solved by using a movable/rotatable mandrel (patent pending, [9]). AFM with movable/rotatable mandrel (AFMmm) is achieved higher polishing media speed at the site of polishing and therefore higher efficiency of the process. At the same time is achieved drastically smaller pressure difference between the inflow and outflow of the polishing media on the workpiece as a result of the relatively small height of the attached part on the movable mandrel. Small pressure difference has negligible influence on the abrasive flow machining process. The AFMmm principle is shown on figure 3, presenting system of abrasive flow machining on the principle of movable mandrel, where is to the piston 1 attached rigid movable mandrel 4 that guides the part 6 through the workpiece.

As a feasibility study, numerical model has been testly composed by finite element modeling of the abrasive fluid flow (AFM). Additionally, the FEM analysis of AFMmm and its variants have been performed. The results of undesired pressure drop and velocities are shown on the following figures 4-6. In all the cases it can be seen that the pressure drop is with AFMmm principle drastically reduces, what is an advantage. Additionally, from the velocity results it can be seen that the velocity can be controlled on the desired positions with the mandrel. Normally the mandrel is set so that the velocity is increased and so efficiency and quality of the process are increased.

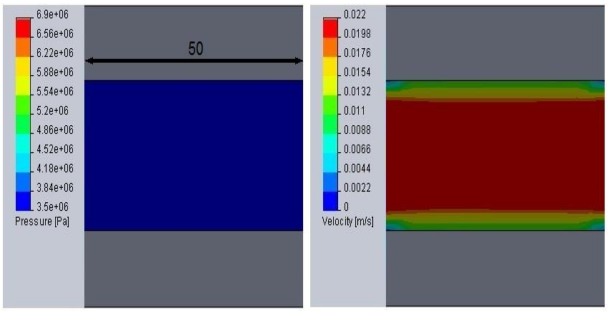

Figure 4 Abrasive flow machining: Δp = 0.17 MPa, v = 0.0105 m/s.

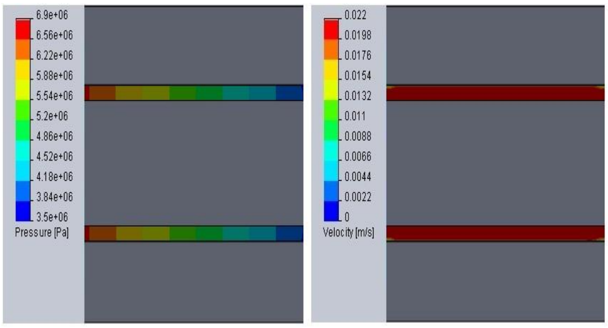

Figure 5 Abrasive flow machining with a constant diameter mandrel: Δp = 3.40 MPa, v = 0.022 m/s.

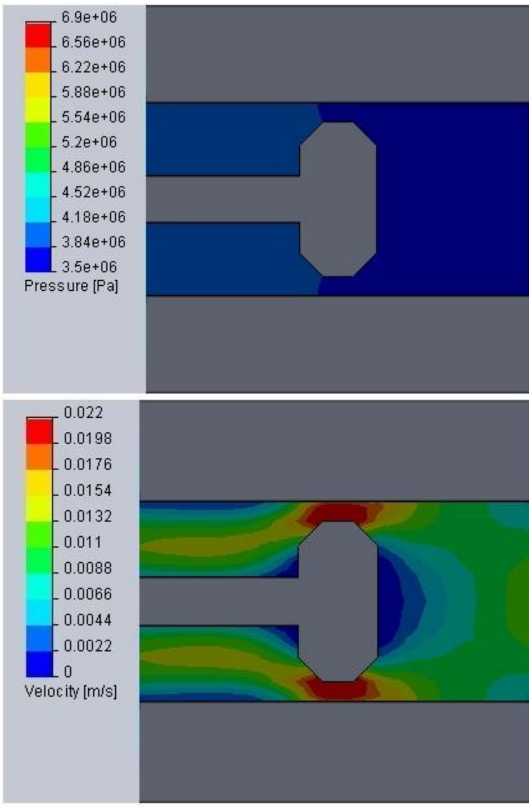

Figure 6 Abrasive flow machining with moving mandrel:
Δp = 0.49 MPa, v = 0.022 m/s.

4 Simulation of AFM in finishing of gear injection molds

Most of the research performed on AFM has focused on the analysis of the process on the surface roughness and productivity (quantity of removed material vs. time). The analyses are focused on the tool cavity for plastic gear injection process, while the aim is to reduce cycle time of finishing, further reduce roughness, assure constant effect of polishing along the profile as well as assure desired geometry/micro geometry of the cavity. In general, the AFM process has been used only for polishing and along the polishing media flow, due to the pressure drop, the efficiency of the process is reducing. With novel upgraded methodology of AFM, the micro geometry can be also controlled. This can offer production of finished convex/concave micro geometries. In concrete case, the purpose is to manufacture polished mold for convex gear tooth (figure 9 and 11).

For simulation of the velocity and pressure profiles along the flow of the polishing fluid through the cavity, the FEM (Finite Element Model) can be used [10, 11]. Therefore, the FEM model of AFM has been created. As on the AFM machine tool, the volume flow rate and inlet pressure can be set, they have been set as constants q_v = 0.00001693 m^3/s and pressure p_m = 3.5 MPa. The factors that directly relates to the productivity (removal of material per time) are the local pressure (normal force on the machined surface) and the velocity of the polishing media on the machined surface. In up to now AFM process, those two factors have not been controllable. With innovative idea of using fix/moving mandrels that can provide desired aperture for the polishing fluid flow, this can be controlled. In this way, while the specifications are to made convex gears with the 5 um size of convexity (the mold have to have concave shape), two different mandrels have been defined and simulated:

- constant diameter mandrel
- convex mandrel

Both mandrels, compared to the polishing process without it, are shown in figure 7.

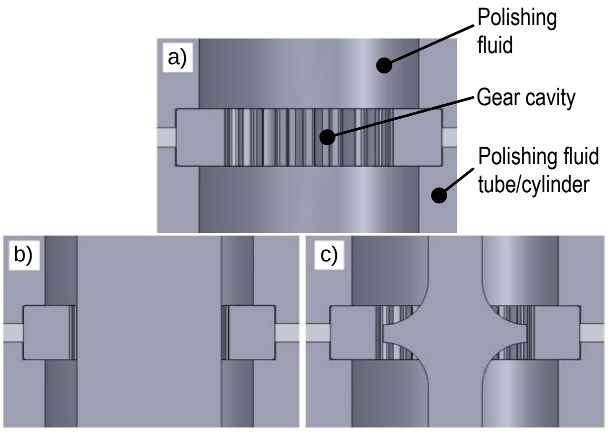

Figure 7 Polishing set-up: a) no mandrel, b) constant diameter mandrel, c) convex shaped mandrel.

The FEM results for all three cases are shown in figure 8. Results show that with adding the constant diameter mandrel to the injection mold, the velocity is increased for a factor of 7. While, there is still a huge pressure drop. However, for this specific case, we want non constant polishing efficiency along the polishing media flow. The efficiency has to be maximized in the middle of the gear width. With convex mandrel, the velocity profile can be obtained. Based on the FEM, it can be seen that at the inlet and outlet, the velocity is approximately 0.008 m/s, while in the middle, the mandrel is significantly increasing the velocity to 0.05 m/s. From this, higher volume of removed material is expected in this middle portion of the mold. With the optimization procedure, where the convex shaped mandrel has been defined, it can be seen that polishing is expected to be more efficient in the middle (high velocity), while the pressure drop between inlet and outlet can be neglected, Δp_m = 0.0768 MPa. Nevertheless, comparing polishing with and without mandrel (what will be discussed in next section), the cycle time to obtain polished surface can also be expected to be reduced for nearly 7 times (from 1650 s to 240 s).

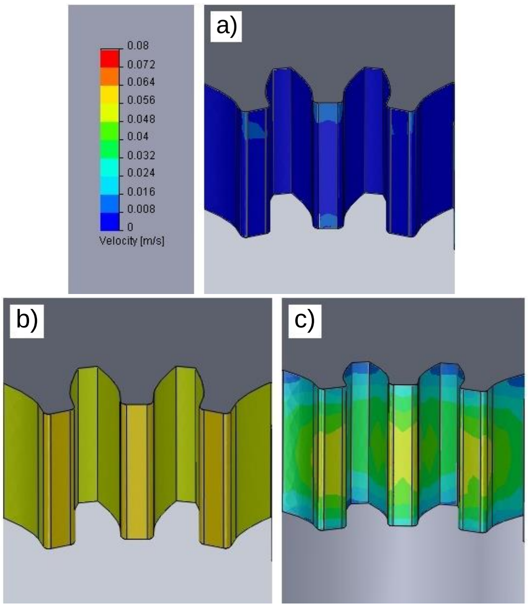

Figure 8 Distribution of polishing fluid velocities a) no mandrel, b) constant diameter mandrel, c) convex shaped mandrel.

5 Experimental procedure

Rough workpieces (shown in figure 9), have been prepared by wire EDM. The properties of workpiece, polishing machine tool and polishing fluid are listed in table 1.

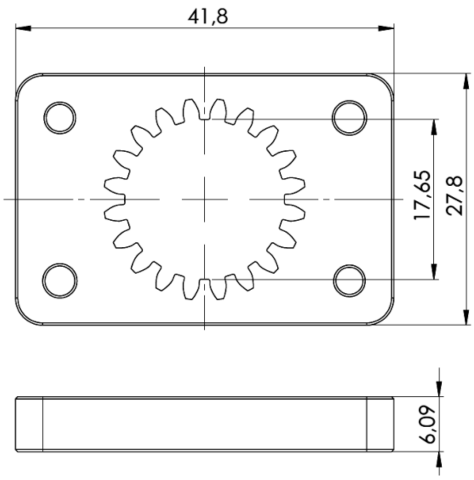

Figure 9 Gear injection mold for gears as final product.

Table 1 System parameters for AFMmm experiments.

	Parameter	Value
Workpiece	Material	AISI H11
	Hardness	53 HRc
	Roughness	R_a = 0.68 um
	Rough process	WEDM
Polishing parameters	Pressure	3.5 MPa
	Volume flow rate	1.693e-5 m^3/s
	Nr. of cycler	1
	Cycle time	240
Polishing fluid	Abrasive	Boron carbide
	Abrasive size	133-172 um
	Mass portion	57 %
	Temperature	40 °C
	Dynamic viscosity	2650 Pas

5.1 Surface roughness results

The surface roughness measurements have been performed on eight different positions and two different heights of the cavity (mold) for injection of gears. Results are shown in figure 10. From the results it can be seen that the process of AFMmm is very efficient. In first 120 s, the majority of polishing process is done. From R_a = 0.68 um we can obtain fine finishing surface with R_a = 0.07 um.

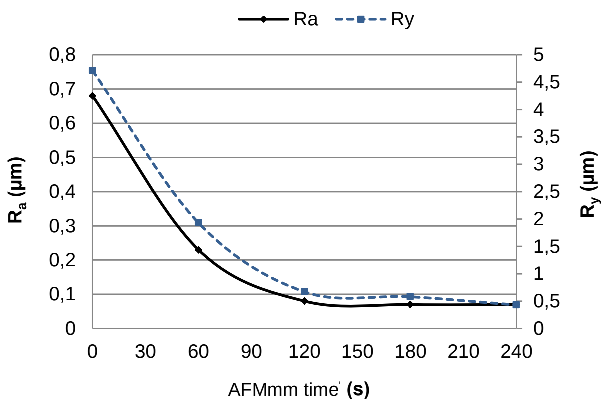

Figure 10 AFMmm influence on roughness vs. time.

5.2 Geometry results

One of the main objectives of this case study, besides roughness, is to obtain concave shape of mold (to assure convex shape of gear). To quantify result, the profiles of gear teeth have been measured. The coordinate measuring system has been used. And the profile, shown on figure 11, has been constructed from 55 measuring points.

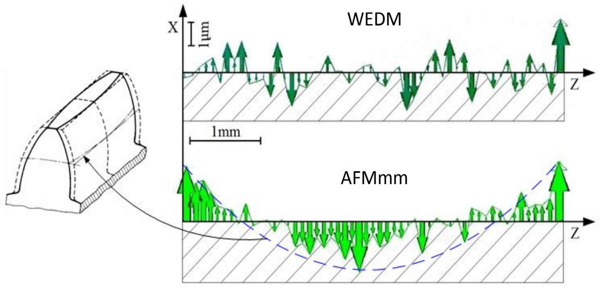

Figure 11 Shape of profile on tooth face after WEDM and AFMmm.

From those micro-geometry results, it can be seen that WEDM treated surface has straight line of gear tooth and on it superimposed high surface roughness. Adding AFMmm finishing process to WEDM as post operation, in first line significantly reduce roughness and assures desired concavity. The concavity of cavity is so satisfactory assured with appropriate regulation of polishing fluid velocity and pressure on the way through the mold. The size of convexity is approximately 5 um.

5.3 Durability tests

To test the efficiency of such gears, durability tests have been performed. With polished convex shaped injection mold, the plastic gear have been injected and tested. Durability test set up is shown on figure 12. For transparent evaluation the durability has been compared for WEDM and WEDM+AFMmm prepared mandrels and corresponding gear as products. According to standard VDI 2545 and preliminary tests [12], the mechanical load and rotational speed of gears have been set in all cases to 0.33 Nm at 1100 rev/min respectively. It has been observed, that plastic gears with polished and convex surface can resist double the life of unpolished (conventional) gears. The conventional gears have resisted 1.5 million cycles, while carefully prepared convex shaped and polished gears, went up to 3.4 million cycles. Also the temperature during testing has been measured. At smooth convex gears the temperature was on average 7 deg Celsius lower than in case of conventional ones. Therefore, it can be claimed that polished and convex gears can reach longer fatigue life on account of lower thermal loads, smother running.

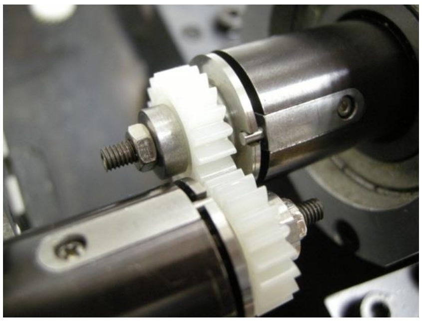

Material: PA6, ULTRAMID B3S (Basf)
Gear geometry: modul = 1 mm, 20 teeth, width 6 mm
load: moment = 0.33 Nm, rpm = 1100 1/min
Tool geometry: evolvent,
No lubrication

Figure 12 Couple of gears in durability tests.

6 Conclusion

The term finishing in this work refers to the application of Abrasive Flow Machining/Polishing process (AFM) with novelty - movable/rotating mandrels (AFMmm), to improve functionality of the final product and its performances. It is going for a new type of sustainable polishing process that is performed dry and clean, and is capable to replace conventional polishing processes, as well as is capable to be used in advance material and geometry processing technologies. So far, there are no systems/products available on the market integrating flowing of an abrasive laden viscoelastic polymer and moving/rotating of mandrel simultaneously and so enhance overall process and product performances.

In this work, the preliminary case-study has been carried out, to quantify an impact of AFMmm technology (improved innovative abrasive flow machining process) on improvement of treated workpiece surface and the workpiece micro geometry. The objective is to make convex gear tooth polished geometry with the convexity height of 5 um, with the aim of gear transfer efficiency.

In case-study roughness and micro geometry of the plastic gear injection mold matrix before and after finishing operation, was analyzed. It has been shown that finishing time in the case of AFMmm technology, compared with conventional AFM, is reduced more seven times.

Moreover, alternative AFMmm can significantly decreases roughness (for approx. nine times) and provides the improved cambered shape of gear tooth which is equable all over the finished surface. The cambered shape is the result of AFMmm media flow orientation and so beneficially influence plastic gears life time. Plastic gears life time is longer for approx. 125 %. From a quantitative point of view, it appears that AFMmm generates cambered shape with a maximum distance between points (convexity) of 5 μm.

The work shows that AFM finishing system and technology that actually presents clean and dry polishing, with innovative combination of AFM flowing abrasive polymer and movable/rotatable mandrel simultaneously and controlled, has high potential in improvement of a) environmental impact, b) energy consumption, c) operational safety, d) personal health, e) waste management, and f) manufacturing costs and g) final product performances.

References

[1] F. Pusavec, P. Krajnik, J. Kopac: Transitioning to sustainable production – Part I: application on machining technologies. Journal of Cleaner Production, vol. 18, no. 2, pp. 174-184, 2010.

[2] J. Kenda: Karakterizacija in napovedovanje učinka poliranja orodnega jekla z dvosmernim abrazivnim tokom. PhD disertation, University of Ljubljana, 2013.

[3] J. Kenda, J. Kopac: Abrasive flow machining as a sustainable polishing process. 1st International Conference of Sustainable Life in Manufacturing, Turkey, pp. 110-131, 2010.

[4] W.B. Perry: Abrasive flow machining - principles and practices. Non-traditional conference proceedings, pp. 121-127, 1989.

[5] J. Kenda, F. Pusavec, G. Kermouche, J. Kopac: Surface Integrity in Abrasive Flow Machining of Hardened Tool Steel AISI D2. Procedia Engineering Procedia Engineering, vol. 19, pp. 172-177, 2011.

[6] S. Beermann: Estimation of lifetime for plastic gears. AGMA Conference, vol. 1, pp. 1-17, 2007.

[7] M.T. Antar, S.L. Soo, D.K. Aspinwall, D. Jones, R. Perez: Productivity and Workpiece Surface Integrity When WEDM Aerospace Alloys Using Coated Wires. Procedia Engineering Procedia Engineering, vol. 19, pp. 3-8, 2011.

[8] M.R. Sankar, J. Ramkumar, V.K. Jain: Experimental investigation and mechanism of material removal in nano finishing of MMCs using abrasive flow finishing (AFF) process. Wear, vol. 266, no. 7-8, pp. 688-698, 2009.

[9] J. Kenda, F. Pusavec, J. Kopac: Arrangements and methods for abrasive flow machining. Patent pending, Slovenian Patent Office, 2013.

[10] Y.A. Çengel, J.M. Cimbala: Fluid mechanics : fundamentals and applications. McGraw-HillHigher Education, Boston, 2006.

[11] A.J. Fletcher, J.B. Hull, J. Mackie, S.A. Trengove: Computer modeling of the Abrasive Flow Machining process,. Proceeding of International Conference on Surface Engineering, pp. 592-601, 1990.

[12] A. Pogačnik, M. Kalin: Parameters influencing the running-in and long-term tribological behaviour of polyamide (PA) against polyacetal (POM) and steel. Wear, vol. 290–291, no. 0, pp. 140-148, 2012.

The Challenges for Effective Management in the Realm of Digital Working - a Discussion Paper

Paul Levy, Senior Lecturer, CENTRIM, University of Brighton UK

and

Professor Mihael Junkar, Faculty of Mechanical Engineering, University of Ljubljana, Slovenia

Abstract

The paper explores the critical issues for sustainable working in the digital realm. Largely a discussion paper, we draw on informal interviews with digital workplace and intranet managers and explore specific challenges for intranet and HR (Human Resource) managers in the realm of digital working.

Opening Remarks - Digital Working Metaphors

The notion of “place” has become easily ported into the realm of digital working. The Digital workplace” continues the tradition of borrowing metaphors from the physical world to make practical sense of digital working. This tradition is based on the notion that we, as humans, are beings in time and space, and therefore the use of physical metaphors will help us to navigate our way in the non-physical or “virtual” realm. In the early days of business and personal computers, we therefore had the “desktop”, the “inbox” and the “folder”. Ironically, the use of these particular metaphors largely resulted in the transposition of already existing bad office practice and bureaucracy to computer experience and we soon had the black comedy of cluttered desktops on PCs, over-full inboxes and folders that were full of chaos! That legacy still lasts to today and even the “cloud” is really just an online metaphorical physical space for clutter.

The evolution of work based systems also drew upon the worlds of communication science and robotics and words such as “intranets” sat alongside words such as “portal”. Science fiction, space, cybernetics, biology and art have all been blundered along with attempts to make up new mashed up words, often laced with humour and a certain kind of open disrespect for the more formal language our parents use. So we have “Twitter” and “Yammer” and “Facebook”.

Human beings have always been able to create language for “things” in physical space-time. It is a phenomenon worthy of further study that the “digital” realm borrows so heavily and often clumsily from the physical and that we are unwilling or unable to create genuinely new language to capture what goes on in digital working. Is this because the digital “world” is so much like our physical that physical labels apply well and easily; or could it be that the true nature of digital experience of human beings is that it is a fundamentally alien realm and that we are unable to grasp it? Is it more a state or set of states of more or less dimmed or alert consciousness and that physical language can’t easily lay hold of it? There might actually be no up and down, no in no in or out in the essential digital and we may need to find new words and sounds that are not drawn from physical imagery if we are to engage with it in conscious and ever more useful ways.

The digital might be an expression of consciousness, not of human physical action. Our computers may be to the digital realm, as a hammer is to a pool of water.

Pragmatism can lay hold of aspects of the digital, label it physically and even control aspects of it. Physical metaphors can render the digital more understandable to the layperson. Yet the nature of human clumsiness and our inability to retain more than a few thoughts at any one time will always mean that digital processing can "perform" in all kinds of more effective and unique ways without our direct participation. Currently the digital realm is being thoroughly limited by the limitations of human beings in physical space-time. The imposition of physical metaphors are likely to severely limit what the digital realm can offer physical beings in terms of our economic and social activity. Simply put, the use of physical metaphors to shape and "capture" digital potential and possibility will engender mediocrity of the most profound kind. In fact this is happening already the the development of the digital into productised prosthetic "gadgets" strikes me as repetitive, uncreative and disappointing.

The digital realm is a thing of itself and it has many alien qualities. Humanising it will limit it in both benevolent and disappointing ways. It may chain the waking monster or it may create an emergent will for it to break free and turn on its "masters". Science fiction has much to say here.

In the corporation the concept of the "digital workplace" is taking hold – a mostly physical transposition of the digital. And now everyone is wondering how you control what your employees are doing if you can't see them physically in an office? Do you real time observe their digital work, or do you watch them through Big Brother cameras? Will your boss be able to see what you are seeing at will through your Google Glasses?

I'd like to suggest that the digital has a role to play that is entirely different, and most of what it can offer, is not in terms of a "place" at all.

The digital can become a realm of processing. Here human interaction with it is based on conscious needs and also is often inspired by the processes themselves as they demonstrate and involve new forms of (possibly wonderful, possible insidious) alien intelligence. They may just rewrite the rules of physical working and living.

Process engaging with process, not in a "place" but in a flow, or set of flows. The digital work process will start to evolve its own laws of nature that might be closer to music and eloquence, to evolution and involution. The digital realm may throw up new senses, both for itself and its processes but also for human beings. New diseases may arise – new states of sleep and stupor, new forms of hypnosis and nervous conditions. The spectrum of colour that lies beyond the human eye will come into play more and more, and quantum computing may begin to redefine space and time itself. The digital work "place" will only be a place in terms of human beings' attempts to make full sense of what is happening. And of course, some humans may attempt to "go in", linking up their nerve endings and brains with the digital, creating new hybrid forms of human and digital life and consciousness – the cyborg.

The notion of the "digital workplace" is essentially a failure of imagination. Such failures have often served the corporation well for decades, especially during times of paradigm shift. Often we try to impose understanding and control of the new by naming it in terms of the old. It creates both functionality and a kind of blindness and deafness.

What's unique about the digital world is that, even as it is being humanly created, its potential is regularly stretching the bonds we create for it. We are making an egregore – a thing that has beingness that lies beyond or tired and limited metaphors. Most digital processes are still control through human input and clumsy functional mastery. But that isn't going to last much longer. And when the ghost in the machine wakes up – it is unlikely to respect our version of time and space.

The Implications for Human Resources Management

We recently undertook informal interviews with HR (Human Resources) directors in large corporations in the UK. They collectively identified the following areas for development of HR in digital working: – extending induction of new employees to include the realm of digital working – this includes the "culture" as well as induction into the portal and the virtual working processes – integrating intranet governance more explicitly into disciplinary procedures – identifying much more explicitly the skills and competencies needed to work excellently in the realm of digital working – this includes a trading and development agenda as well as clearer criteria for promotion – much more Conscious job description and specification – there's an unhelpful and unclear line between 'comms' and intranet/DW – developing governance and clearer people management skills concerning virtual meeting, BYOD (bring your own device) and working off premises – an emerging skill set around confidentiality management and professionalism in the use of social media and public platforms – developing an agenda for leadership in the realm of digital working

Challenges for HR in the digital working realm

The challenges for HR are specific in places and vague in others… Specific: – does HR need to develop procedures to embody specific behaviours that represent professional practice, over and above what previously existed. For example: – in the upholding of confidentiality, the right in certain cases to anonymity, in clearer guidelines on acceptable and unacceptable "behaviour" in forums, in Yammer and also externally in terms of interaction digitally with customers and suppliers (cross-cultural etiquette also comes into play here) – is an employee responsible for the behaviour or outcome of an automated program ? Facebook are currently under fire for auto placing adverts from companies such as Marks and Spencer into inappropriate pages. Apparently internally heads have rolled. In terms of your second question… What is the role of comms? Is it to manage the intranet as a communications device? What is the role of the intranet team? Is it to deliver the key communications platform for the business? If so, why does comms sit sometimes under HR in the organogram? – especially if a big part of the comms function is also externally focused on sits under a marketing role?

When intranets evolve into fundamental and business critical working processes, they move beyond both IT and HR into business operations.

When the realm of digital working begins to digitalise physical working on fundamental business and operational processes, then newer functions emerge. I remember when HR was called "Personnel" and was largely about hiring and firing, contracts and promotion etc.

Then it was renamed as HR – actually HRM – Human Resources Management. This then included issues such as induction as well as training and development.

Then HRM became HRD – Human Resources Development and started to focus on multi skilling, leadership and management development, and helping to create the "learning organisation. HR has morphed and shown itself able to.

Now, when the intranet clearly sat within IT and a “comms” function, HR was about putting policies and some HR processes onto the intranet. But that was really a transposition of “Personnel” practice.

As elements such as learning became digitized into distance learning, then HRM began to be bound up with the intranet. I’d suggest that the “D” in HRD remains largely outside of the intranet realm at present – at least according to the directors I spoke to. But what about when the intranet evolves into an entirely new beast – a realm of digital working where some core processes aren’t even carried out by humans? Then the H in HR starts to become a partial representation of process reality in the business. Does HR need to morph once more to capture the true essence of human and non human activity within the business? It will at least need to further get to grips with the human risks, skills and learning opportunities at the human-digital borderland.

The senior managers I spoke to saw the intranet as increasingly coming under the banner of a newer process management/leadership function. There might by HRM and DPM (Digital process management) – they might be under HR – they might not.

Conclusion

The role of HR is evolving, just as the role of the intranet manager is, and needs to, evolve.

HR is no longer only about employees but also about how human beings behave. Human behaviour models in digital working are at an early stage of development. Governance has largely been about policing and control, largely because human behaviour models in the realm of digital work are fairly unknown and unpredictable. As HR evolves it will need to understand digital collaboration better along with the human to gadget/platform interface. Concepts such as work stretching and different employment relationships based around freelancing and emergent, temporary working will need to be further developed and implemented. HR’s role in change management and in creating digital work cultures also need attention. Finally, more negative aspects such as digital work burnout and distraction and future shock will become more relevant.

HR is going to have to change ahead of the date of digital working evolution.

Reference

Further information and source material can be found on our digital blog, Digital Inferno, at
http://digitalinferno.wordpress.com

Process modelling and measurements

METHOD OF MEASURING THE WATER JET DIAMETER

Jesús Gil Cano[1], Andrej Lebar[2], Mihael Junkar[2] and Marko Jerman[2]

[1] *University of Cartagena, Spain.*
[2] *University of Ljubljana, Laboratory for Alternative Technologies, Slovenia.*

Abstract

In this paper we present a new method of measuring the water jet (WJ) diameter using the digital image acquisition and processing with digital manipulation of the photography. The experimental setup was built on the machine for ice jet experiments, in order to evaluate new measurement method and to compare the novel photographic method with the method which makes use of the load cell to measure the WJ diameter.
The images were processed by fitting a custom Gaussian function to the specific rows of image. Function was fitted to five image rows which correspond to five different distances from the water nozzle. At the precisely same distances also radial dependence of WJ force was measured.
It was found, that the method using digital camera and computer evaluation of image can yield good results which are in good correspondence with measurements of WJ diameter obtained by the load cell. It also showed that due to possible implementation in industry applications, it would be useful as a quick, easy and affordable technique. The main advantages of such method are that the equipment can be cheap and, as the method is contactless, it doesn't get destroyed over time.

Keywords: Water Jet (WJ), Ice Jet (IJ), Jet Diameter, Imaging processing, Macro photography.

1 Introduction

Abrasive water jet (AWJ) technology was first commercialized in the late 1980's as a pioneering breakthrough in the area of non-traditional processing technologies. AWJ machining is a rapidly developing technology used in industry for a number of applications, such as cutting, shaping and milling [1].

Abrasive water jet (AWJ) is non-conventional machining processes, where material is removed from a work-piece using a multitude of small abrasive particles [2]. One of the drawbacks of the AWJ technology is that the use of abrasives in the industrial environment is not always possible, because there are kind of applications such as the machining of hygroscopic and chemically reactive materials, as well as when working near high voltage, toxic and radioactive sources; even in process of meat products, the cleaning of sensitive surfaces and biomedical applications [2].

Another disadvantage of the AWJ technology is that it produces a lot of waste product that consists mainly of the mineral abrasive. The latter is being added to the high speed water jet in order to increase its efficiency. These particles also get stuck inside the work piece, thus contaminating it [3]. One of possible solutions is to substitute abrasive particles in AWJ with ice crystals and thus get rid of the majority of material in the waste sludge.

The effectiveness of the use of ice particles as a substitute for abrasives was demonstrated [4], it was also demonstrated that the measured water droplet diameters and consequently the diameters of the created ice particles are comparable to the ones used in mineral abrasive [5].

Previous experiments in the field of quality of the jet and measurement of the jet diameter have been done by different research groups. Researches [6] have been researching cost efficient methods for measuring the jet diameter using two different component one being a non-contact led micrometer and the other a class 2 lasers. Both methods were effective. Another researches [7] also successfully used a high speed camera for jet analysis in their research.

In this research, we want to study phenomenological analysis of the water jet, combining digital image processing with digital manipulation of the photography, and modifying process parameters such as pressure, water temperature and diameter of the water nozzle. In order to verify the effectiveness of this new measurement method, the results were compared with results from the method that has already been established. The main advantage is that low cost equipment is required, and that the jet shape can be easily and quickly acquired.

2 Experimental setup

The measurement system used to perform the experiments is presented in the block diagram in Figure 1.

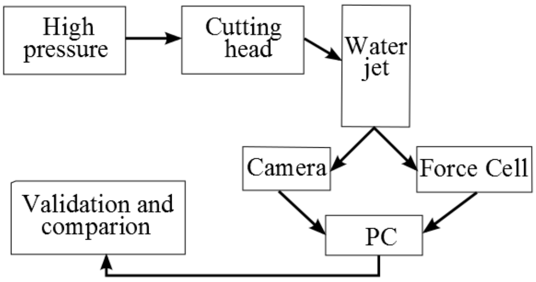

Figure 1: Block diagram of the measurement system for jet measurements**.**

To carry out this research we used the Ice Jet prototype machine, several modifications in the work ambient have been done, and several additional tools had to be created to get the maximal quality of the photos and consequently more accurate analysis results. Figure 2 shows the layout of the measurement equipment for both researches.

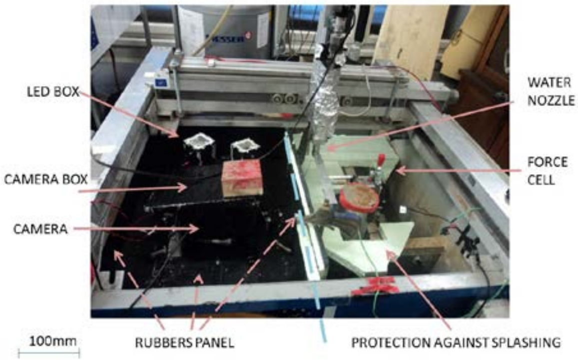

Figure 2: Experimental setup of the working area.

The force method uses a load cell to measure forces. This method has already been verified and was used as reference for the verification of the imaging method. On the left side of Figure 2 is the imaging method equipment. It is composed of photographic equipment with a lighting system and a digital camera. Components were protected against water. In order to minimize the reflection of the light some rubber panels were used. Positioning of lights and camera was achieved with a mechanical system that was able to get the focus of the light and the camera in the water jet.

In order to get homogenous illumination of the measured area with as less volume as possible, a couple of high power (10.5W each) LED were used. The brightness of the LED was 1100 lumen, which it is the total amount of visible light emitted by the LED source, and the cool white correlated color temperature (CCT) was 5600K. These values are enough to lighten the entire length of the water jet and to get an adequately sharpphotos. In the other hand, a camera with a resolution of 8.2 megapixel and with maximum resolution of 2336 x 3504 pixels was used.

2.1 Positioning and Calibration

The LED lights have to be positioned symmetrically and the camera has to be set on their axis of symmetry to insure proper image quality. The center of the focus of the light has to coincide with half of the length of the jet and the distance between LED lights has to be long enough not to bother the field of camera view. In Figure 3 the final position of the lighting equipment is shown.

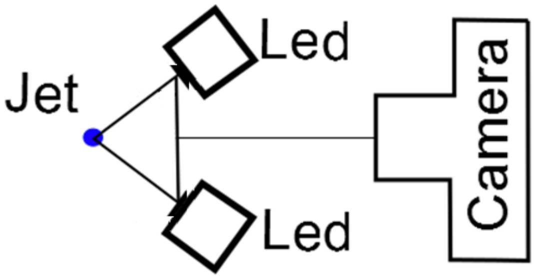

Figure 3: Positioning of the illumination equipment.

Image calibration was done using a ruler with the surface positioned along the center plane of the water nozzle from which it was possible to determine the pixel to millimetres ratio on each picture.

The ruler was also used to prevent the distortion of the photo and to have the reference of the jet position, since it was easier to focus the camera. Figure 4 shows this system.

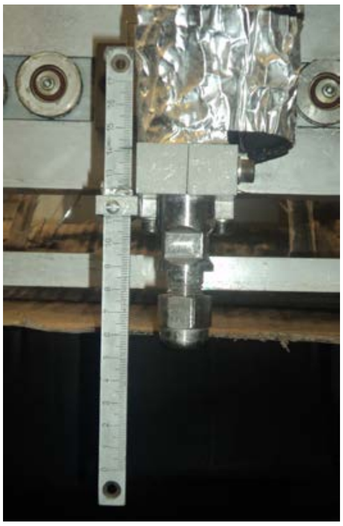

Figure 4: Image calibration system.

The graph in Figure 5 shows the absolute value of derivative of brightness from y axis. Non-equal height is causet by the non-uniform illumination of the ruler. Also the markers on the ruler are not equally black. The calibration was performed once, because the distance between the jet and the camera was kept constant.

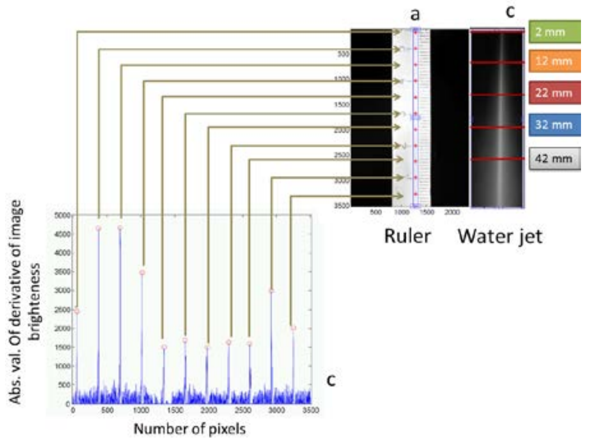

Figure 5: Calibration performed with the ruler. (a) It was placed along the center of the water nozzle. This allowed us to determine the pixel to millimeters ratio on each picture during the experiment (c).

2.2 Model function selection

False color representation reveals the internal structure of jet. A Gaussian funtion was used to describe this structure [8].

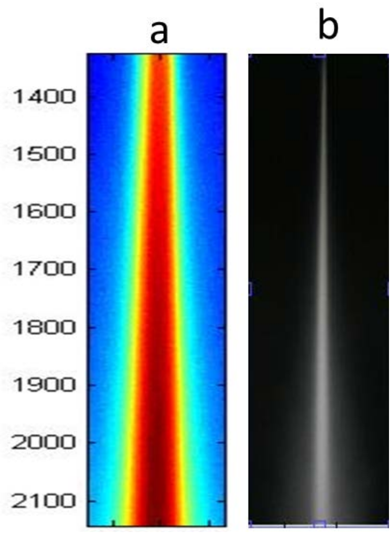

Figure 6: Different representation of internal structure of the jet.

An observation of the jet shape in the Figure 7 implies that a good correlation with Gaussian curve is expected. In each image of the jet the parameters of the Gaussian function were calculated by mean value of the non-linear function fitting. In the equation of the figure 7, the parameter μ is the mean value or the position of the center of the pear and σ is its standard deviation or the width of the shape. The influence of these parameters on the shape of the Gaussian curve is shown in Figure 7.

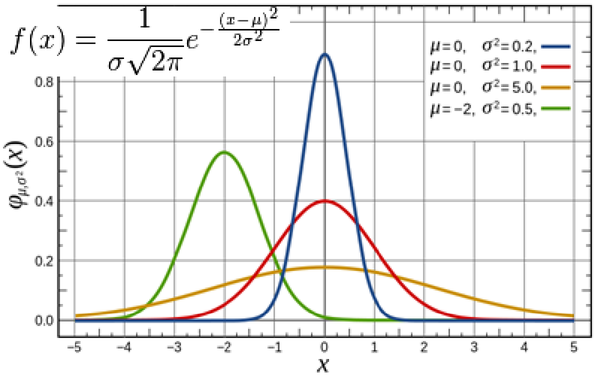

Figure 7: Plots for different parameters of Gauss function.

In the Figure 8 the radial dependence of the relative brightness at five different radial distances are shown. The interval value between the measurements is 10 mm. The values presented in this figure are derived from one of the experiments done. This interval of measures was chosen to compare them with the force method measurements.

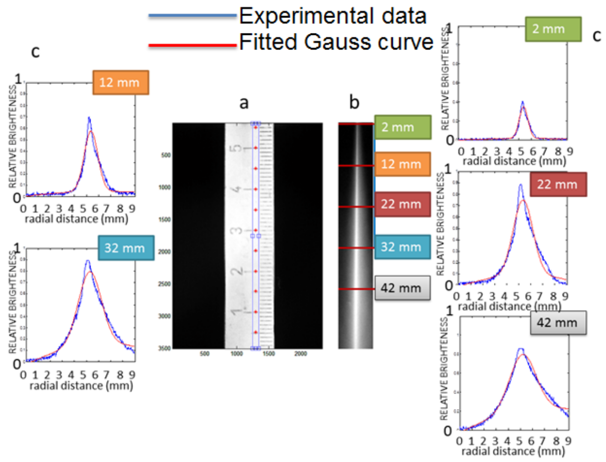

Figure 8: Illustration of typical relation between jet relative brightness and radial distance. Calibration ruler (a) jet image (b), Gaussian curves (c).

2.3 Validation of the method

Validation and composition between jet shape measurement by imaging method and jet pressure measurement were done simultaneously. Both methods have been studied with the same conditions of water temperature, water nozzle diameter and pressure.

To be able to compare the two methods, it is necessary to find a factor which binds the two solutions due to the fact that the analysis results of the measurements are obtained in a different manner. The force method permits to directly acquire the value of the diameter of the water jet, while the imaging method provides the relation between jet relative brightness and radial distance.

Figure 9 points out the correlation between both methods. The asterisks represent the average of all widths of the Gaussian function and all force diameters from all experiment, and the equation of the figure 9 depicts the calibration curve.

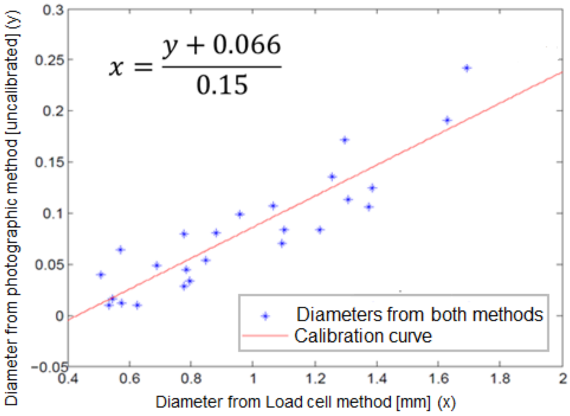

Figure 9: Calibration curve where the parameter "x" is the diameter from the load cell method and "y" is the diameter from the photographic method but uncalibrated.

2.4 Verification of the results

To validate this calibration curve several examples were done. The same parameters of the camera were used such as shutter speed and exposure value (ISO) while modifying process parameters such as pressure, water temperature and diameter of the water nozzle. The graphics shown in the figure 10 represent one of the experiments done and it can see how both curves follow the same linear tendency.

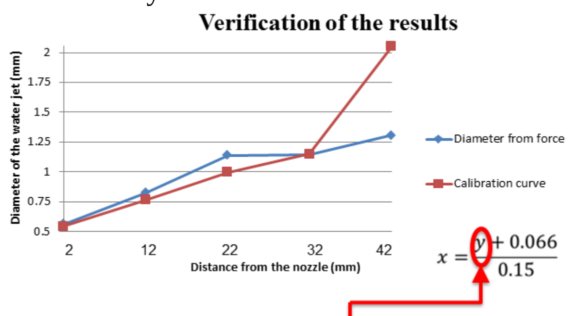

Distance from the nozzle (mm)	Average of uncalibrated diameter measurement [Uncalibrated] (y)	Diameter from force method (mm)	Calibration curve (mm) (x)
2	0.015	0.56	0.54
12	0.048	0.82	0.76
22	0.083	1.13	0.99
32	0.106	1.14	1.15
42	0.242	1.30	2.05

Figure 10: Calibration curve and average force measures, with 200 MPa of pressure, 0.20 mm of the diameter of the water nozzle and with 23ºC of water temperature.

3 Conclusion

A method and instrument capable of measuring the water jet diameters was developed. Measurement experiments show the validity of the proposed method. We have shown that there is a linear relation between the jet diameter and the width of radial dependence of image brightness and that it is possible to define the jet diameter using the new method. The photographic method is much faster than the force method. Using the newly developed method, the geometry along the whole length of the jet can be obtained at once, while using the force method only the measurement at a discrete distance from the water nozzle in can be measured at once. The developed method is noncontact which means that there is no wear of the instruments.

Acknowledgment

This work is supported from the University of Ljubljana, Laboratory for alternative technologies.

References

[1] Marko Jerman; State of the art report on Ice Jet Technology, Life.

[2] Version 2 ME, IIT Kharagpur. Module 9 (Non-conventional Machining).

[3] Marko Jerman and Henri Orbanić; Ice Jet Machining technology for the greener tomorrow.

[4] E. Geskin, L. Tismenetskiy, F. Li, "Development of Ice Jet Machining Technology", NJIT, *8th American Water Jet Conference*, 1995, pp. 671-680.

[5] E. Geskin, L. Tismenetskiy, F. Li, "Development of Ice Jet Machining Technology", NJIT, *8th American Water Jet Conference*, 1995, pp. 671-680.

[6] E. Geskin, L. Tismenetskiy, F. Li, "Development of Ice Jet Machining Technology", NJIT, *8th American Water Jet Conference*, 1995, pp. 671-680.

[7] E. Geskin, L. Tismenetskiy, F. Li, "Development of Ice Jet Machining Technology", NJIT, *8th American Water Jet Conference*, 1995, pp. 671-680.

[8] M. Jerman, A.Lebar, M. Junkar; Measurement and modeling of the water jet shape.

Modeling of the main cutting force in high-pressure jet assisted turning process by genetic algorithm

V. Pucovsky[1], D. Kramar[2], M. Sekulić[1]

[1] *University of Novi Sad, Serbia*
[2] *University of Ljubljana, Slovenia*

Abstract

Genetic algorithms present an efficient way of machining processes modelling. They have proven this on numerous occasions so it was assumed that they can be used in this advanced machining system. Inconel 718 was machined with high-pressure jet assisted turning process and the main cutting force F_v was measured. Model for calculating the cutting force F_v depending on process parameters was used to, with genetic algorithms adapt constants figuring in this function so that modelled results were as much as possible closer to experimental values.

Keywords: high-pressure jet assisted turning process, main cutting force, genetic algorithm, modeling.

1 Introduction

With everyday increasing demand of the market, each branch of the industry is trying to meet those demands in order to gain profit. Meeting this goal is not always easy. Sometimes it's not all about working hard but rather working smart. Machining industry, as one of the main driving forces in modern world, has to keep up with contemporary technical and technological trends. Many times, just to be in line with market demands, it has to set up new trends. This radical type of influence has to be supported with adequate knowledge base and scientific guidance. Content of this paper has, although in small dose, injected that much needed scientific contribution to the practical realization of machining industry. Combining two highly potential tools from engineering branch, authors managed to improve existing machining process and thus hopefully save both financial funds and resources.

On the one side there is a machining technology that already showed its ability and had secured its place in modern machining shops. Turning process with assisted high-pressure jet coolant is a modern way to improve classical machining technology. With added feature of high pressure coolant it expanded the use of classical machining range and now can be also used on hard to machine materials.

On the other side lies a powerful artificial brain with its algorithms being improved almost on a daily basis. Genetic algorithms, as a subgroup of evolutionary algorithms, had already shown their potential in machining industry and new usage is still being discovered.

This paper presents a modelling of the main cutting force values during high-pressure jet assisted turning process. Modelling is done with genetic algorithms, as a type of artificial intelligence. Comparison is than made between experimentally obtained data and modeled results [1].

2 Experiment and Modeling

The experimental work was carried out at the Laboratory for Machining, the Faculty of Mechanical Engineering in Ljubljana. The experiments were conducted in longitudinal turning process on conventional lathe, fitted with a Hammelmann high-pressure plunger pump of 150 MPa pressure and 8 l/min capacity. The fluid used was the Vasco 5000 cooling lubricant from Blaser Swisslube Inc., a 5,5% emulsion without chlorine on the basis of vegetable oil mixed with water (pH 8,5-9,2). The jet was directed normal to the cutting edge at a low angle (about 5-6°) with tool rake face. As an input data five process parameters were varied: diameter of the nozzle D_n (mm), diststance between the impact point of the jet and the cutting edge d (mm), pressure of the jet P (MPa), cutting speed v_c (m/mm) and feed rate f (mm/rev).

All experiments were carried out using the nickel-based alloy Inconel 718 supplied as bars (145 mm diameter x 300 mm long) with hardness between 36 and 38 HRC by orthogonal arrays with three levels (coded by: 1, 2 and 3), Table 1. A PVD TiAlN-coated carbide tool (grade P25) SNMG 12

04 08-23 has been chosen. The cutting tool was mounted on the static dynamometer (Kistler® 9259A). The measurement chain also included a charge amplifier (Kistler® 5001), a data acquisition hardware (NI® USB-6218 BNC) and a graphical programming environment (NI® LabVIEW) for data analysis and visualization. Subject of this study is to modeling dependence of the main cutting force F_v on the input data five process parameters by genetic algorithms.

Table 1 Machining parameters and their levels

Symbol	Parameters	Levels		
		1	2	3
A	Diameter of the nozzle, D_n (mm)	0,25	0,3	0,4
B	Dist. between the impact point of the jet and the cutting edge, d (mm)	0	1,5	3,0
C	Pressure of the jet, P (MPa)	50	90	130
D	Cutting speed, V_c (m/min)	46	57	74
E	Feed rate, f (mm/rev)	0,2	0,224	0,25

For modelling purposes only 20 instances were used (Table 2) and remaining 7 (Table 2) were used for evaluation of model. As a modeled function, linear regression model (Equation 1) will be used.

$$F_v = C_1 + C_2 \cdot D_n + C_3 \cdot P + C_4 \cdot v + C_5 \cdot f + C_6 \cdot P \cdot v \qquad (1)$$

Within this paper genetic algorithms will be employed to search for an optimal values of constants C_1, C_2, ... C_6 for which modeled equation will give the smallest deviation from experimentally obtained data. Genetic algorithms are, as mentioned above, a part of evolutionary algorithms which means that their main principle is based on theory of evolution resp. survival of the fittest. On the beginning of the process 1000 individuals are randomly created. These individuals are actually possible solution for the problem and contain constants C_1, C_2, ... C_6. Next step is to incorporate all those constants to Equation 1 and send every result to the fitness function for evaluation. Fitness function is a measure of success for each individual and is directly involved in direction of further population development. Fitness function is actually an average of percent errors (Eq 2) for all instances with one solution of constants:

$$\Delta = \sum_{i=1}^{20} \left| \frac{E_i - M_i}{E_i} \right| \cdot 100 [\%] \qquad (2)$$

where E_i is an experimentally obtained value of the main cutting force and M_i is its modeled value. After an evaluation, 40 of the top ranked are automatically transferred to the next generation. This step is called elitism and is necessary in order to preserve the best genetic material. Next, potential parents for the next generation of individuals are created. This is done by putting into effect so called tournament selection. 80 individuals are randomly selected from current generation and the best one is placed into the mating pool. This step is repeated until enough parents are selected to form 80% of the next generation which are created by crossover of individuals from mating pool. Remaining individuals are created with direct mutation of their predecessors. Mutation is employed in order to insert fresh genetic material in population and prevent an algorithm to get stuck in local minimum. After 1000 generations the best solution contained constants which implemented into Equation 1 creates an Equation 3.

3 Results

Values of process parameters, used to model the resulting function, implemented into Equation 3 will make the following results (Table 2).

Mentioned resulting equation will be:

$$F_v = 37{,}758 + 8{,}015 \cdot D_n + 11{,}757 \cdot P + 19{,}936 \cdot v + 41{,}232 \cdot f - 0{,}185 \cdot P \cdot v \qquad (3)$$

Table 2 Data used for experiments and results of the main cutting force obtained both experimentally and modeled by Equation 3 (modelling data).

No	D_n (mm)	d (mm)	P (MPa)	v (m/min)	s (mm/o)	F_v, exper. (N)	F_v, model (N)	Error (%)
1	0,25	0	50	46	0,2	1280	1128	11,9
2	0,25	0	90	57	0,224	1508	1295	14,1
3	0,25	0	130	74	0,25	1400	1274	9
4	0,25	1,5	50	46	0,25	1350	1128	16,4
5	0,25	1,5	90	57	0,2	1150	1293	12,4
6	0,25	1,5	130	74	0,224	1370	1273	7,1
7	0,25	3	50	46	0,224	1150	1127	2
8	0,25	3	90	57	0,25	1295	1295	0
9	0,25	3	130	74	0,2	1235	1272	3
10	0,3	0	50	57	0,2	1245	1245	0
11	0,3	0	90	74	0,224	1265	1350	6,3
12	0,3	0	130	46	0,25	1320	1390	5,3
13	0,3	1,5	50	57	0,25	1385	1248	9,9
14	0,3	1,5	90	74	0,2	1145	1349	17,8
15	0,3	1,5	130	46	0,224	1190	1388	16,6
16	0,3	3	50	57	0,224	1055	1246	18,1
17	0,3	3	90	74	0,25	1460	1352	7,4
18	0,3	3	130	46	0,2	1390	1388	0,1
19	0,4	0	50	74	0,2	1375	1427	3,8
20	0,4	0	90	46	0,224	1305	1260	3,4
							Δ→	**8,23**

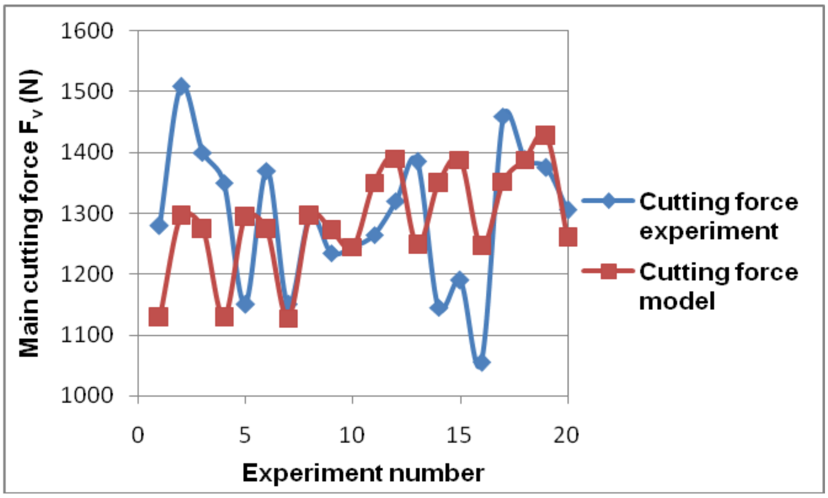

Figure 1 Graphical comparison between modelled and experimental data, used for modelling of the main cutting force F_v

Table 3 Data used for experiments and results of the main cutting force obtained both experimentally and modeled by Equation 3 (only verification data).

No	D_n (mm)	d (mm)	P (MPa)	v (m/min)	s (mm/o)	F_v, exper. (N)	F_v, model (N)	Error (%)
1	0,4	0	130	57	0,25	1320	1345	1,9
2	0,4	1,5	50	74	0,25	1250	1429	14,3
3	0,4	1,5	90	46	0,2	1275	1221	4,2
4	0,4	1,5	130	57	0,224	1465	1345	8,2
5	0,4	3	50	74	0,224	1187	1428	20,3
6	0,4	3	90	46	0,25	1160	1260	8,6
7	0,4	3	130	57	0,2	1450	1344	7,3
							Δ→	**8,87**

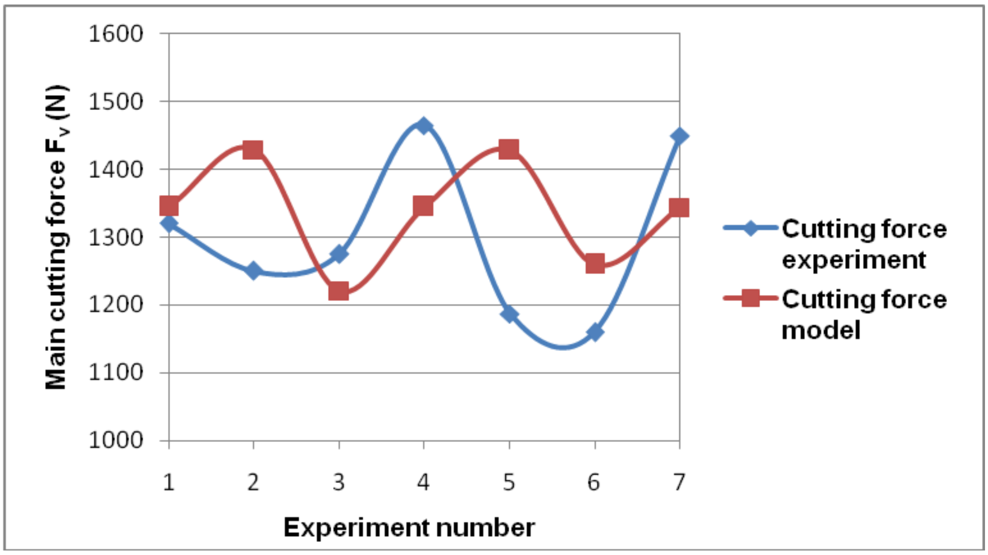

Figure 2 Graphical comparison between modelled and experimental data, used only for verification of the model, of the main cutting force F_v

As can be seen the average percent error is 8,23% which is, taking in consideration an amount of data used for modelling, acceptable value. Graphical representation of these values, and direct comparison between experimental and modeled data, is shown in Figure 1.

Remaining 7 instances, which were not used for modelling purposes, are now employed to judge the quality of yielded model. As presented in Table 3 the average percent error in this case was 8,87% which is near to that in Table 2. This indicates that the model is adequate and valid. Figure 2 presents a graphical representation of results from Table 3.

4 Discussion

Yielded results generated average percent error of 8,23 resp 8,87%. These results, by authors opinion, are acceptable because of couple of factors; data used for modelling is scarce and the model of the function (Eq 1) is simple linear type which offers very little flexibility. Despite of these limiting factors obtained results are independent and can be used without the use of computer.

5 Conclusions

Generated results, as mentioned in previous chapter, are in acceptable range. Further improvement can be done by increasing the quantity of experimental instances. Also various types of equations for modelling of cutting force can be tried and hopefully find some model which will suite this purpose better.

References

[1] V. Pucovsky, P. Kovac, M. Tolnay, B. Savkovic, D. Rodic: The Adequate Type of Function for Modeling Tool Life Selction by the Use of Genetic Algorithms. Journal of Production Engineering, pp. 25-28, Vol. 15, (1), 2012.

[2] D. Kramar, M. Sekulic, P. Kovac, M. Gostimirovic, J. Kopac: The Implementation of Taguchi Method for Quality Improvement in High-pressure Jet Assisted Turning Process. Journal of Production Engineering, pp. 23-26, Vol. 15 (2), 2012.

[3] D. Kramar, M. Sekulic, Z. Jurkovic, J. Kopac: The Machinability of Nickel-based Alloys in High-pressure Jet Assisted (HPJA) Turning. Metalurgija, pp. 512-514, Vol 52 (4), 2013.

[4] D. Kramar, J. Kopac: High Pressure Cooling in the Machining of Hard-to-Machine Materials. Strojniski vestnik – Journal of Mechanical Engineering, Vol. 55 (11), 2009.

A novel method for material machinability evaluation

B. Sredanović[1], G. Globočki - Lakić[1], Đ. Čiča[1] and S. Borojević[1]

[1]*University of Banjaluka, Faculty of Mechanical Engineering, RS, Bosnia and Herzegovina, Corr. author address: sredanovic@gmail.com*

Abstract

Definitions of machinability have an important role in material machining. Material machinability is most often defined by different criterion. Criterion is based on the output cutting parameters: cutting forces, tool wear, machined surface quality, chip shape, vibration and etc. Some material may have a good machinability according to one criterion, but very low when the other criteria is considered. The goal of developing a novel method is to take into account several criteria simultaneously. Experimental researches are performed, and material machinability in metal cutting is analyzed.

Keywords: machinability, evaluation, method.

1 Introduction

Managing with production technologies requires a lot of knowledge about several elements, such as: workpiece materials, tool materials, geometry, machine tool, machining conditions and etc. This managing is more complicated because relations between mentioned elements [1]. In metal cutting technology knowledge about machining of different material has an important role [2]. Based on this knowledge, it can be concluded about process economy, process sustainable and etc.

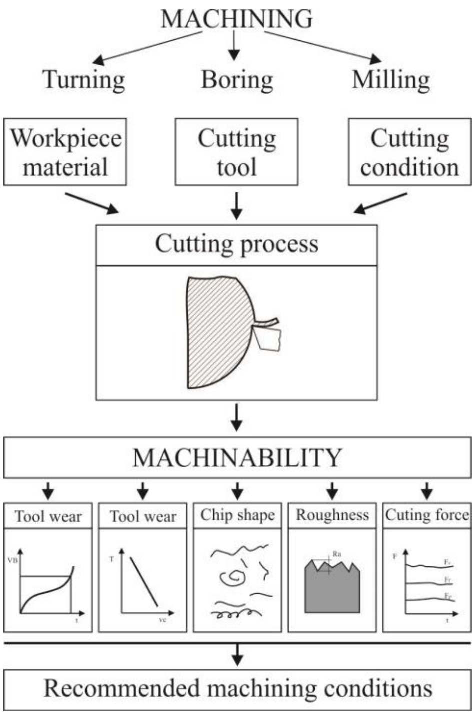

Figure 1 Material machinability definition [3]

Behaviour of materials during machining with different process and conditions can be explained with material machinability [4]. Material machinability is complex technological category. It is relative category because analyse of machinability of different materials requires minimum two materials or two combinations (same material but different cutting conditions).

Material machinability is defined as easiness of material machinability with different tools and conditions in economical frames. Machinability depends on the workpiece material, tool material, cutting geometry, process conditions, etc. The goal of machinability testing is finding the optimal conditions of material processing and effective management of cutting process (Figure 1).

2 Material machinability evaluation

Material machinability is defined over the main criteria - the output parameters of cutting process which depend on the input cutting parameters [1]:

- tool wear,
- surface roughness,
- cutting forces,
- energy consumption,
- cutting temperature,
- tribological parameters,
- chip shape,
- material removal rate and etc.

Machinability is usually defined over machinability indexes, without units, as the relative estimate of machinability [2, 3, 4]. These calculated indexes are used as coefficients for cutting speed and feed. It can be concluded that machinability is defined by one criterion only.

Main problem in machinability estimating is that some material may have a good machinability according to one criterion, but very low to other criterion. Complete definition of machinability or “absolute” or “universal” machinability is based on the consideration of many criteria simultaneously [1 - 4].

On example, *Boulger* proposed that the machinability is expressed through economy of the process with use of special machinability test [5]. *Lee* and *Shaffer* have suggested that it can be defined by the thermodynamic number [5]. *Enache* has developed the global model of machinability which containing more criteria [6]. *Rao* and *Gandhi* used the principles of the matrix and graph theory for defining the absolute materials machinability, named “matrix model” [7].

2.1 Novel method for machinability definition

In this paper, a novel method of machinability definition, which is based on vector analysis, is introduced. It considers several machinability criteria. Proposed method requires three axes rectangular coordinate system. Each axis in system represents some of mentioned criterion (Figure 2).

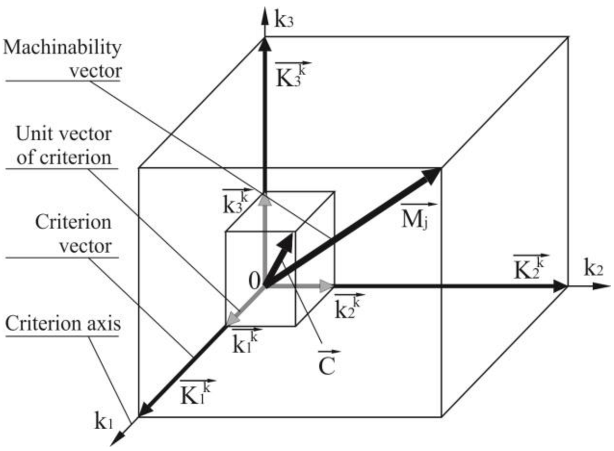

Figure 2 Machinability vector definition

As real criterion value can be take values calculated by model or measured values in experiment [8]. For analyzed group of material or material/conditions combination, there are different real criteria values (*j*), from minimum to maximum value:

$$r_i = \left(r_{i\min},...,r,...,r_{i\max}\right) \qquad (1)$$

The real criterion values must be normalized because differences of units of machinability criterion and different orders of magnitude of machinability criteria values. On example, there are differences in value of cutting forces and surface roughness. Results of real criterion normalisation there are named criterion values (K_i). Real criterion value normalization is performed in order from 0 to 1.

For criterion which increasing of values decrease the machinability, normalization is performed by:

$$K_i = \frac{r_i - r_{i\min}}{r_{i\max} - r_{i\min}} \qquad (2)$$

For criterion which decreasing of values increase the machinability, normalization is performed by:

$$K_i = \frac{r_{i\max} - r_i}{r_{i\max} - r_{i\min}} \qquad (3)$$

In previous equations r_{imax} is maximum value of criterion, r_{imin} is minimum value of criterion and r_i is observe value of criterion.

In mentioned coordinate system, criterion values (K_i) are set on the corresponding axis. Each axis has a corresponding unit vector ($\overrightarrow{k_i^{ko}}$) which length corresponds to minimum criterion value (infinite length). Sum of unit vectors gives control vector ($\vec{C}$), which direction determines the best uniformity of machinability criteria or the best machinability (Figures 2).

Based on the criterion values and the corresponding unit vectors, the criterion vector which lies in the appropriate coordinate axis is formed as scalar product of unit vector and criterion vector:

$$\overrightarrow{K_i^{KO}} = \overrightarrow{k_i^{ko}} \cdot K_i \qquad (4)$$

Machinability vector is sum of all individual criteria vectors, and can be calculated and formed for each material in group or each combination material/condition:

$$\overrightarrow{M}_j = \sum_{i=1}^{n} \overrightarrow{K_i^{KO}} \qquad (5)$$

In general, material which machinability vector has less intensity and closing smaller angle with a control vector has better machinability. The size of the parallelogram area formed by the machinability vector and its control vector is related to machinability of materials (Figure 3).

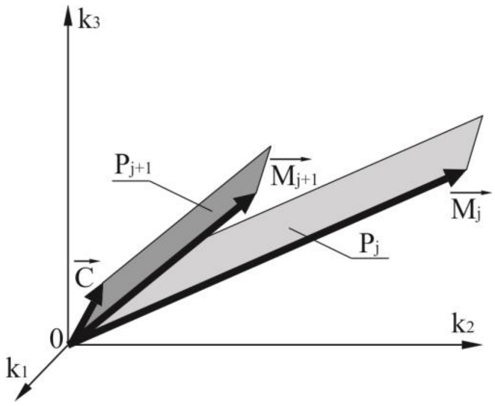

Figure 3 Area of the parallelogram related to machinability of materials j and j+1

On other hand, material with a smaller area defined by the parallelogram has better machinability in compare to material with a larger parallelogram surface area. Size of parallelogram area can be expressed through the value of vector product between machinability vector and control vector:

$$P_j = \left|\vec{C} \times \vec{M}_j\right| = \left|\vec{C}\right| \cdot \left|\vec{M}_j\right| \cdot \sin\angle\left(\vec{C}, \vec{M}_j\right) \quad (6)$$

It can be concluded that universal machinability (M_u) is inversely proportional to the area of parallelogram formed by machinability vector and control vector. Based on established relationships, on equations (5) and (6) and equation for sinus value [9], it can be written in final form:

$$M_u = P_j^{-1} = \left(\sqrt{K_1^2 + K_2^2 + K_3^2} \cdot \sqrt{\left|1 - \frac{(K_1 + K_2 + K_3)^2}{K_1^2 + K_2^2 + K_3^2}\right|}\right)^{-1} \quad (7)$$

Previous equation has two parts: first part represents the influence of criteria values on machinability and the second part shows the influence of criteria values uniformity on machinability [10, 11, 12].

3 Case studies on material machinability evaluation

Case studies were performed for materials in different machining conditions, cutting tool, process, lubrication technique and etc. Experimental studies were performed, data results were modelled and material machinability was analysed [13, 14]. Material machinability was compared on different developed models [5, 6, 7].

3.1 Case study one

In this case, experimental procedure and machinability evaluation was performed on group hard-to-machine steels. During experimental measurement same turning condition was used.

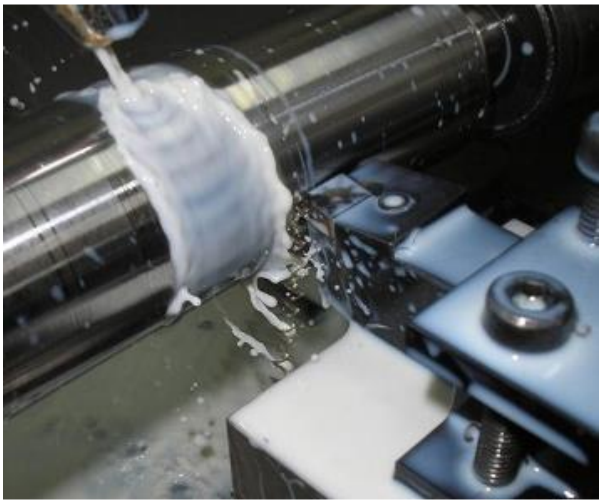

Figure 4 Experimental measurements in case study 1

Process output parameters were monitored: main cutting force (F_c), feed cutting force (F_f) and passive cutting force (F_p); flank tool wear (VB) and intensity of tool wear (I_{VB}); and arithmetic average height (R_a) as the surface roughness parameters. Experiment was performed on universal lathe with good stiffness and geometry accuracy (Figure 4). For machining of group of hard-to-machine steels was used HM carbide cutting tool, with the following cutting conditions: cutting depth a_p = 1 *mm*, feed rate f = 0.18 *mm/rev* and cutting speed v_c = 130 *m/min*. All experiments were carried out using cutting fluid with 3% emulsion of vegetable oil.

Table 1 Results and calculations for case study 1

Material DIN	F_c [N]	I_{VB} [μm/min]	R_a [μm]	Matrix method	**Vector method**
55NiCrMo	725	21	6.8	232	372
S6-5-2	726	19	6.6	344	433
90MnCrV8	654	15	5.9	1050	1327
36CrNiMo4	516	14	6.2	1516	2274
X210Cr12	659	16	6.3	709	707

In this case, crucial process output parameters that describe cutting processes were monitored. For calculation of machinability evaluation values by different models, cutting force, intensity of flank tool wear and surface roughness were used (Table 1).

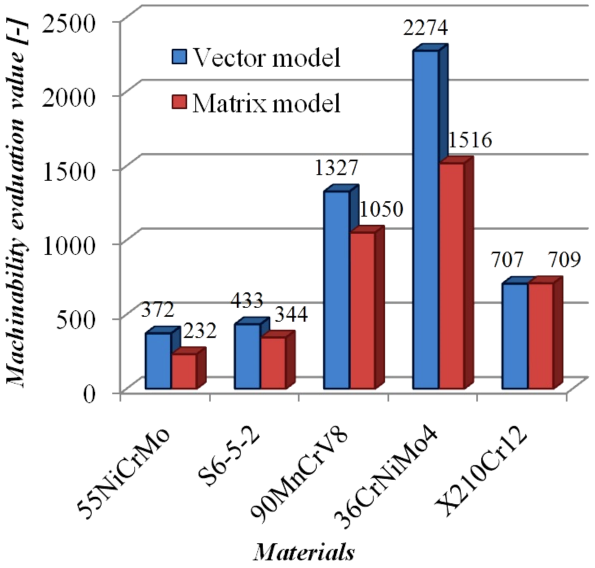

Figure 5 Evaluation values by novel vector model and *Rao-Ghandi*'s matrix model for case 1

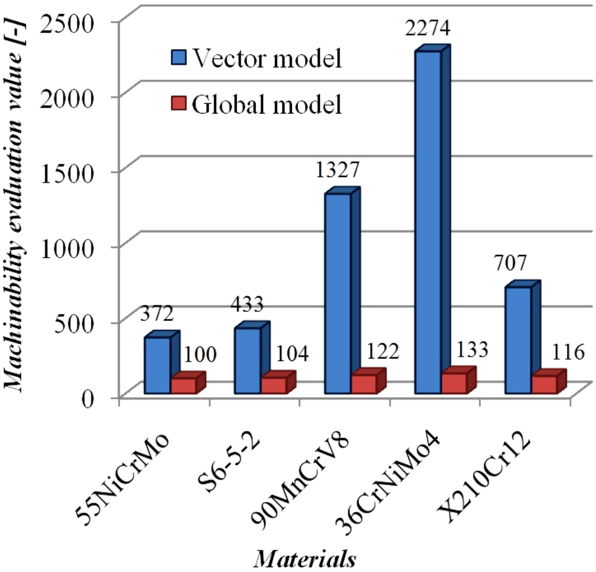

Figure 6 Evaluation values by novel vector model and *Enache's* global model for case 1

On Figure 5 and 6 were shown calculated machinability evaluation values, obtained by novel matrix model and early developed models, *Rao-Ghandi*'s matrix model and *Enache*'s global model. Order tendency of outputs for newly model corresponds to previously developed models. It can be concluded that new model outputs have good matching with matrix and the global model outputs [15]. From diagraph can be concluded that hard-to-machine steel 36CrNiMo4 has the best machinability in comparison with other steel from group. The worst machinability has steel 55NiCrMo.

3.2 Case study two

In this case, experimental procedure and machinability evaluation was performed on one material but different cutting condition. During experimental measurement different lubrication techniques in turning, standard (flooding) and high pressure jet assisted machining (HPJAM), was used [16, 17].

Process output parameters were monitored: main cutting force (F_c), feed cutting force (F_f) and passive cutting force (F_p); flank tool wear (VB) and intensity of tool wear (I_{VB}); arithmetic average height (R_a) as the surface roughness parameters and chip shape.

Workpiece material used in experimental research was the construction carbon steel C45E. Tensile straight of this material is $\sigma = 820\ N/mm^2$, module of elasticy $E = 2 \cdot 10^3\ MPa$, and hardness of steel is 45 HRc.

Experimental research was performed on conventional lathe with maximum spindle speed $n_{max} = 2240\ rev/min$, and feed $f_{max} = 1.6\ mm/rev$. Carbide cutting tool SNMG 1204 08 NMX for semi-turning was recommended cutting tool by manufactures. Tool holder was PSDN 2525 M12, with inclination angle 45°. All experiments were carried out using cutting fluid with 3% emulsion of vegetable oil also.

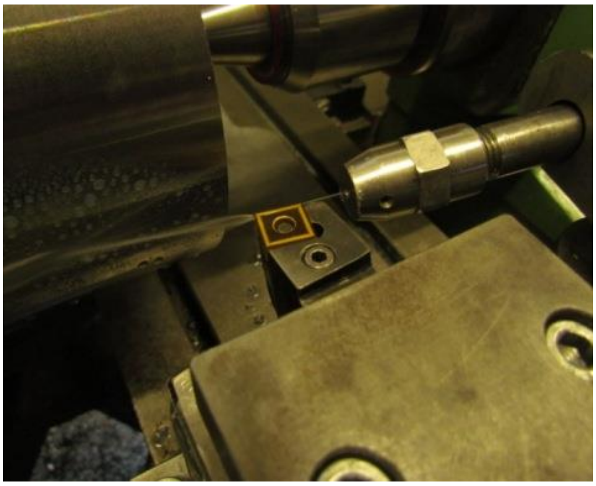

Figure 7 Initial jet in HPJAM turning of C45E

In HPJAM conventional lathe was fitted with high pressure plunger pump. Pressure was set at $p_{HP} = 50\ MPa$ and flow rate at $Q_{HP} = 2.0\ l \cdot min^{-1}$. Standard sapphire nozzle with diameter

d_{HP} = 0.4 *mm* commonly used in water jet cutting applications was installed on the distance of H_n = 30 *mm* from tool cutting edge in order to assure its use in the core zone of the jet and avoid variations in the diameter of the jet and radial distribution of the pressure. The jet was directed normal to the cutting edge and ψ_{HP} = 30° from clearance face at a low angle (about 5° - 6°) with the tool rake face.

In this case was performed a great number of experiments, with flooding and HPJAM cooling and lubrication techniques. There are analyse a few results which obtained with the following parameters: depth of cut a_p = 2.0 *mm*; feeds f = 0.28 and 0.40 $mm \cdot rev^{-1}$ and cutting speed v_c = 320 $m \cdot min^{-1}$.

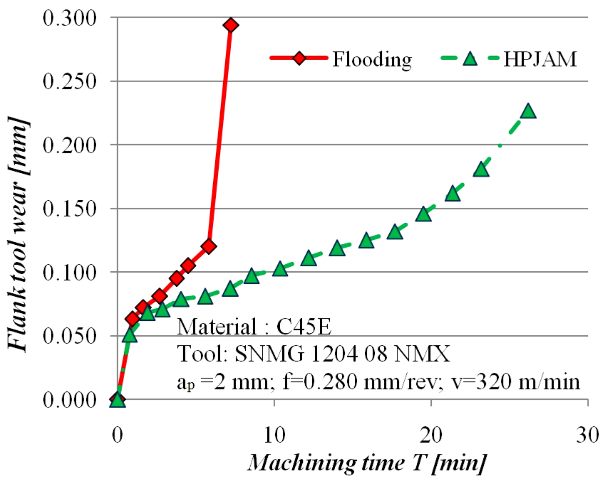

Figure 8 Flank tool wear for different cooling and lubrication techniques

In this case, experimental studies have shown that the use of HPJAM has a positive effect on the cutting process [17, 18, 19]. In using of HPJAM tool life is increased for 4 times (Figure 8). Also, feed cutting forces and passive cutting forces decreased by 8%.

Table 2 Results and calculations for case study 2

Combinations of input parameters	F_c [N]	I_{VB} [μm/min]	R_a [μm]	Matrix method	**Vector method**
Flooding f=0.28	1137	27	3.55	940	1629
Flooding f=0.40	1599	32	4.23	255	384
HPJAM f=0.28	1142	8	3.82	1480	2161
HPJAM f=0.40	1569	9	4.26	483	589

For calculation of machinability evaluation values, cutting force, intensity of flank tool wear and surface roughness were used (Table 2).

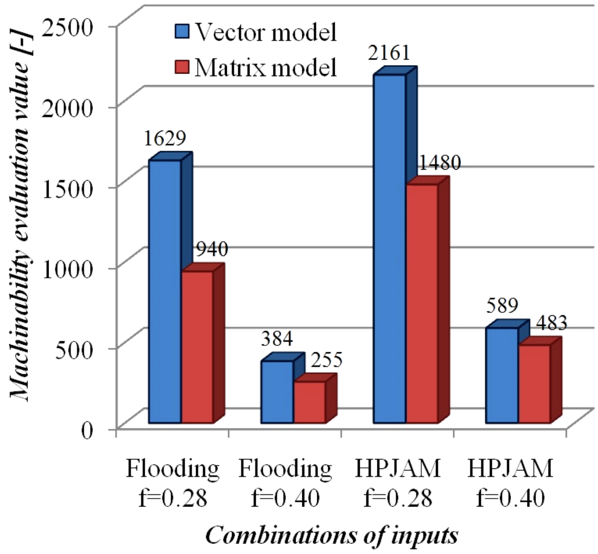

Figure 9 Evaluation values by novel vector model and *Rao-Ghandi'*s matrix model for case 2

On Figure 9 and 10 calculated machinability evaluation values for same material and different condition (cutting parameters and cooling and lubrication techniques). From diagraph can be concluded that turning with smallest feed and HPJAM technique gives better machinability in any case. This conclusion are available in other experimental research which performed by other authors. Also, order of novel developed model outputs model has a good matching with different model outputs.

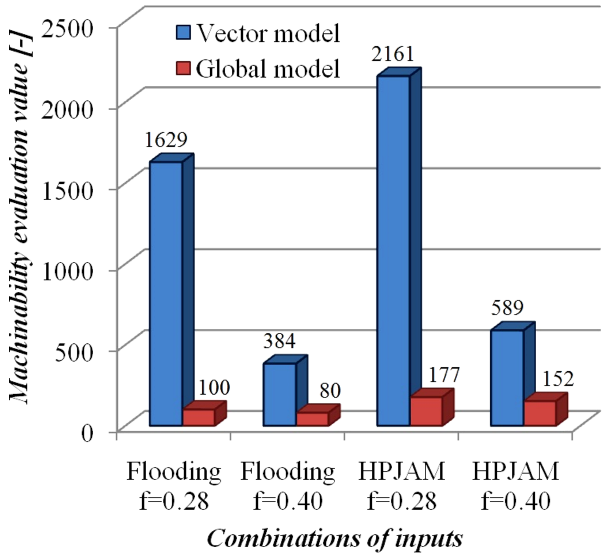

Figure 10 Evaluation values by novel vector model and *Enache's* global model for case 2

Conclusions about the machinability of materials and processing can be archived in using the various machinability criteria [20]. As machinability criteria there was used cutting energy, material removal rate (MMR) and level of chip shape acceptable.

Figure 10 Flank tool wear and chip shape for flooding (above) and HPJAM (below)

Parameterisation and normalisation of some machinability criteria in metal cutting is specific problem. The biggest problem is occurs in non-measurable parameters, as a chip shape. Chip shape is very significant indirect parameter of metal cutting process. In this paper the standard classification and acceptable estimating for chip shape was used.

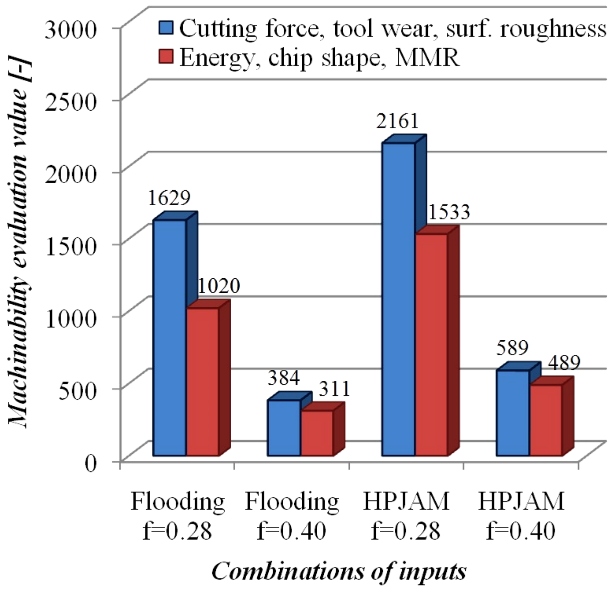

Figure 11 Machinability evaluation values for different criteria

After parameterisation by assessment of chip shape (Figure 10), real criteria normalisation and calculation of machinability evaluation value was done. On Figure 11 machinability evaluation values for criteria different types was calculated. From graph can be concluded that estimation of machinability can be performed with indirect parameters of cutting process as a chip shape, MMR and etc. In this case, turning of C45E with combination HPJAM technique with f = 0.28 *mm/rev* gives the best machinability, as it was concluded in previous analysis of this experimental results.

4 Conclusion

The novel developed method for machinability evaluation was shown a good matching with early developed models. At least, in vector model, number of criteria was not limited, because as the number of criteria can take more than tree. Machinability criteria can be of different type (direct and indirect) and obtained different cutting operation and processes. As input in model can be used different tool-workpiece-condition combination. Developed method can help in selecting of the best mentioned combination and in successful managing in metal cutting technology. If there are large number of different mentioned combinations, machinability assessment will be more accurate.

In both cases which presented in this paper, calculation of machinability evaluation values was given similar results to results in studies of different researchers. Calculation and analysis shows that some processes, as turning with HPJAM technique, provide the better “universal machinability”.

In the future research developed model in terms of using greater number of machinability criteria will be investigated. Also, special software with data bases, for managing in real metal cutting processes, will be developed.

5 Acknowledgments

This research is the result of a bilateral project BI-BA/12-13-001 between Slovenia and Bosnia and Herzegovina with collaboration between Laboratory for Cutting from Faculty of Mechanical Engineering in Ljubljana and Laboratory for cutting technologies and machining systems from Faculty of Mechanical Engineering in Banja Luka.

References

[1] W. Grzesik: Advanced machining processes of metallic materials: theory, modelling and application, Elsevier B. V., Netherland, 2008.

[2] G. Globočki – Lakić: Obrada rezanjem – teorija, modeliranje, simulacija, Mašinski fakultet Banja Luka, BIH, 2010.

[3] J. Kopač: Cutting forces and their influence on the economics of machining. Journal of Mechanical Engineering, vol. 48, no. 3, pp. 121-132, 2002.

[4] E. Kuljanic, M. Sortino, G. Totis: Machinability of difficult machining materials, 14th International Research - Expert Conference "Trends in the Development of Machinery and Associated Technology" TMT 2010, pp. 1-14, Mediterranean Cruise, September 2010.

[5] E. W. Theile, K. J. Kuding, and et.: Comparative machinability of brasses, steel and aluminum alloy: CDA's universal machinability index, Publication of CDA, New York, USA, 1990.

[6] S. Enache et al.: Mathematical model for the establishment of material machinability, Annals of CIRP, vol. 44, pp. 79-82, 1995.

[7] R. V. Rao, O. P Gandhi: Diagraph and matrix methods for machinability evaluation of works material, Int. J. of Machine Tools & Manufacture, vol. 42, pp. 321-330, 2002.

[8] S. K. Ong, L. C. Chew: Evaluating the machinability of machined parts and their setup plans, International Journal of Production Research, vol. 38, pp. 2397–2415, 2000.

[9] E. Krayzig: Advanced Engineering Mathematiscs, John Wiley & Sons, New Jersey, USA, 2006.

[10] B. Sredanovic, G. Globocki - Lakic: Quality monitoring of production systems and processes in form of vector of power, Proc. of 9th Int. Scientific and Practical Conference - Research, Development and Application High Technologies in Industry, Saint Petersburg, Russia, pp. 418-420, April 2010.

[11] B. Sredanović, G. Globočki - Lakić, B. Nedić, Đ. Čiča: New approach in deffining of universal macinability in cutting, 37th JUPITER conference with international participation, Belgrad, Serbia, May 2011.

[12] G. Globocki - Lakic, B. Sredanovic, B. Nedic, Dj. Cica, D. Catic: Development of mathematical model of universal material machinability, Journal of the Balkan Tribological Association, vol. 17, no. 4, pp. 501-511, 2011.

[13] G. Globocki - Lakic, S. Borojevic, Dj. Cica, B. Sredanovic: Development of Application for Analysis of Machinability Index, Journal Tribology in Industry, Volume 31, No.1&2, pp. 57-60, 2009.

[14] G. Globocki - Lakic, B. Nedic, B. Ivkovic, V. Golubović - Bugarski, Dj. Cica: Possibility of Determination of Material Machinability Over Tribological Parameters by Use of Tribometer Block on Disk, Proc. of 9th CIRP International Workshop on Modelling of Machining Operations, pp. 307-312, Bled, Slovenia, May 2006.

[15] D. Kramar, B. Sredanović, G. Globočki - Lakić, J. Kopač: Contribution to material machinability definition, Journal of Production Engineering, vol. 15, no. 2, pp. 27-32, 2012.

[16] V. Sahma, M. Dogra, N. Suri: Cooling techniques for improved productivity in turning, Int. J. of Machine Tool & Manufacturing, Vol. 49, pp. 435-453, 2010.

[17] D. Kramar: High-pressure cooling assistance in machining of hard-to-machine materials (in Slovene), PhD thesis, University of Ljubljana, 2009.

[18] C. Courbon, D. Kramar, P. Krajnik, F. Pusavec, J. Rech, J. Kopac: Investigation of machining performance in high-pressure jet assisted turning of Inconel 718: an experimental study, Inter. J. of Machine Tools & Manufacture, vol. 49, pp. 1114-1125, 2009.

[19] D. Kramar, J. Kopac: High pressure cooling in the machining of hard-to-machine materials, Journal of Mechanical Engineering, vol. 55, no. 11, pp. 685-694, 2009.

[20] B. Sredanović: Development of universal machinability model based on cutting procees parameters, (in Serbian), MSc thesis, Faculty of Mechanical Engineering Banja Luka, Bosnia and Herzegovina, 2012.

Further development of the spatial cutting tool wear measurement system

L. Čerče[1], F. Pušavec[1], J. Dugar, and J. Kopač[1]

[1] *University of Ljubljana, Slovenia*

Abstract

The tool wear evaluation has a very strong impact on the product quality as well as efficiency of the manufacturing process. This paper presents the further development of an innovative and reliable direct measuring procedure for measuring spatial cutting tool wear. The influence of the orientation of measurement head according to the measurand was examined. Based on the analysis of measurements accuracy and the amount of captured reliable data, the optimal setup of the measuring system was defined. Further a special clamping system was designed to mount the measurement device on the machine tool.
To test the measurement system tool life experiment were performed, where cutting tool wear was measured directly on machine tool. The results showed that novel tool wear diagnostic represent objective estimation, performed on a machine tool that provides higher productivity and quality of the machining process.

Keywords: Spatial cutting tool wear, Wear diagnostic on machine tool, Optical triangulation..

1 Introduction

Machining performance of material is very important in terms of material processing and quality of final product. Based on the machining performance optimal machining parameters are usually determinate. The term machining performance refers to the ease with which a metal can be machined to an acceptable surface finish, and is hardly measured/evaluated. It is defined by the following criteria: cutting tool wear, cutting tool life, cutting forces, power consumption, chip formation, machined surface integrity and geometrical accuracy of the machined surface.

Criteria, such as cutting force, roughness, energy consumption, integrity and geometrical accuracy of the machined surface can be objectively determined by exact measurements, while cutting tool wear is in practice measured manually and on a subjective level [1]. Most frequently, cutting tool wear is measured with the use of toolmakers microscopes to help determine the range of wear (flank face).

In addition to poor precision of this method, the problem is in three-dimensional nature of wear, which cannot be fully analyzed with 2D based measurements/measurement principles. It can be concluded that research on defining and analyzing tool wear in three dimensions is still of great significance.

A survey of the literature indicates that many different approaches have been applied for tool wear prediction [2-5], contrary direct measuring techniques make an assessment of tool wear by either evaluating the worn surface by optical methods (microscope), or measuring the tool material loss by radiometric techniques. Direct methods require to periodically interrupting the cutting process. Optical methods use optical equipment like the toolmaker's microscope, optical microscope, scanning electrical microscope, charged coupled devices (CCD cameras), white light interferometry etc. [7-11].

The main disadvantages of mentioned methods is the inability of measuring crater depth KT (spatial geometry) and/or needs to preform them off line of the machining process.

In one of our previous works [12] spatial tool wear measurement system has been presented which is able to measure crater depth KT on-line on the machine tool. In next chapters, optimisation of this measurement system and test on a case study will be presented.

2 Measuring system

The measuring system consists of a high-accuracy 2D profile laser displacement sensor Keyence LJ-G015 with proper controller Keyence LJ-G5001 [13] and motorized linear translation stage Standa 8MT173-DCE2, as is seen on figure 1 and 2.

With movement of the profile sensor across the cutting tool and the support of developed software (LabVIEW application), the profile data are grabbed and prepared in a matrix form for further evaluation/analyses.

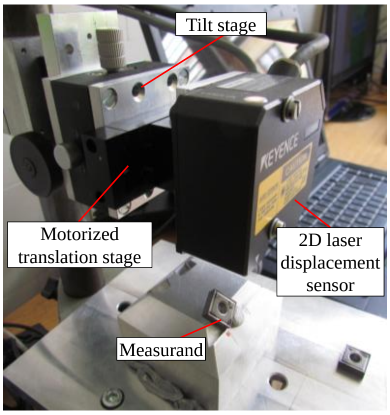

Figure 1: Measuring system

Laser displacement sensor measure the distance from measurement head to the points projected on the measured object. In this way Z-coordinate of point cloud are measured. X-coordinate is defined by the specification of the laser displacement sensor [13], while Y-coordinate represents linear stage feed direction.

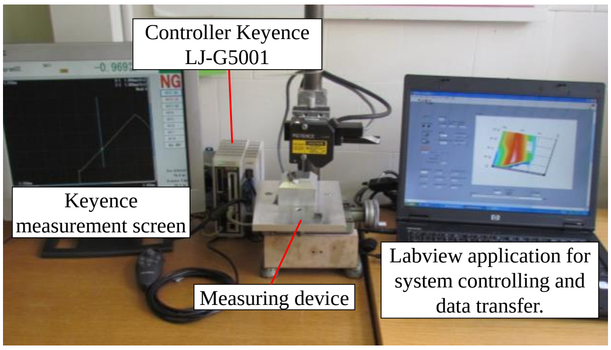

Figure 2: Measuring interface and controller

3 Experimental work

In experimental work the influence of the orientation of measurement head according to the measurand was examined. The aim of the optimization is to find the optimal orientation of measurement head that capture as large amount of data from the rake face, cutting edge, and primary and secondary flank face.

For this proposes a special clamping system has been designed. Cutting insert is fixed on a prismatic holder and can be rotated about it axis for angle α. The prismatic holder can be rotated for angle γ. The measuring head was fixed on a tilt stage, which rotates for angle β (Figure 3).

The extreme positions of the measuring system were experimentally defined on base of needed data quality. Cutting insert was rotated from 12° to 30° while prismatic holder from -25° to 15°. The measuring head was rotated from -5° to 5°.

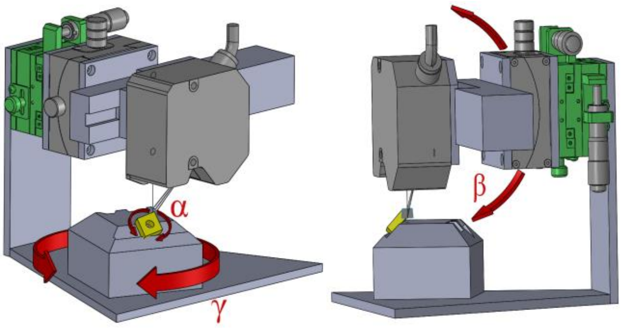

Figure 3: Special clamping system

The general full factorial design consisted of 75 experimental runs, taken at 5 levels for angles α, γ and 3 levels for angle β. For each captured point cloud the surface was reconstructed, trimmed to the volume of 2.4 x 2.4 x 1mm.

The number of triangles in a single measurement presents an estimator of the quality of the measurements.

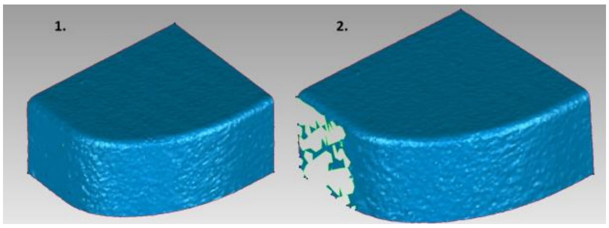

Figure 4: Comparison of two measurement meshes

Figure 4 shows a comparison between two measurements. The first measurement was done under the conditions α= 12 °, β= -5° and γ= -15 ° while the second α= 12°, β = -5° and γ= -5°. From the results we can assume that changing the angle γ for 10° drastically deteriorated measured surface on the secondary cutting edge. There are actually no measured points.

Because of the smaller incident angle there is scattering of laser beam, so the amount of captured data in this area is smaller.

All measurements were individually compared with the reference measurement, measured on a professional measuring device Alicona IF-Edge Master with 5µm lateral resolution. From the obtained deviation results following estimators were calculated (table 1):

- number of triangles
- maximal / minimal deviation,
- mean value of the deviation,
- mean value of the of negative deviations,
- mean value of the positive deviations and
- number of segments for which deviations are in the range of ± 0.008 mm in %.

Table 1: Input and output parameters for statistical evaluation

Input				Output						
#	α [°]	β [°]	γ [°]	Number of triangles	Maximum deviation [mm]	Minimal deviation [mm]	Mean value of the deviation [mm]	Mean value of the positive deviations [mm]	Mean value of the of negative deviations [mm]	Part of deviations which are in the range of ± 0.008 mm [%]
1	12	-5	-25	42122	0,046	-0,309	-0,001	0,006	-0,007	74,57
2	12	-5	-15	38842	0,119	-0,194	0,000	0,004	-0,004	83,19
3	12	-5	-5	37385	0,089	-0,025	0,001	0,005	-0,004	82,10
4	12	-5	5	36966	0,249	-0,162	0,002	0,010	-0,006	74,02
…	….									

Table 1 is presenting just 4 of 75 results. Based on input and output parameters the empirical regression models were developed. To analyse the quality of those models ANOVA has been performed and found out that significant correlation can be made only for prediction of “Number of triangles” and “Part of deviations which are in the range of ± 0.008 mm”.

Booth models have been used for optimization of the measurement head position. The optimization was based on overall desirability function [14], were each solution is valuated from 0 to 1, higher it is, better it is. The optimal combinations scored 0.638, with angles α=16°, β= -5° and γ= -21. In Figure 5, result of geometrical comparison with referential measurement is shown. With the use of this setup 91.11% of measurements results are in the range of ± 0.008 mm, while the number of triangles is 45310.

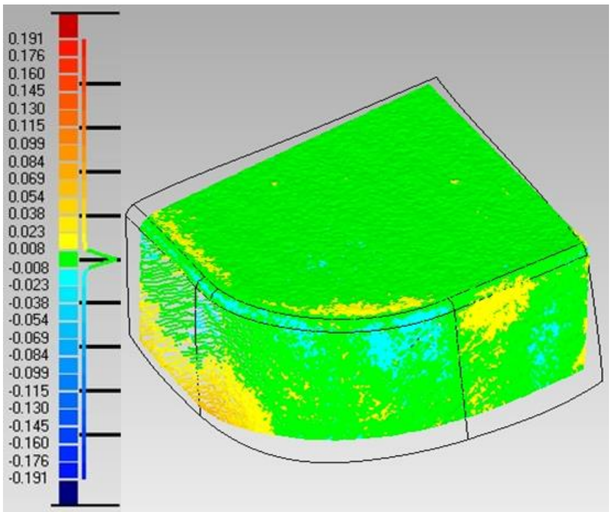

Figure 5: 3D deviation results of the optimal setup (α=16°, β= -5° and γ= -21°, D=0.638)

4 Case study

The optimization procedure of the key parameters was tested in machining environment. For this purpose a special clamping system has been designed that simulate the previously obtained optimal setup and can be mounted on the machine tool. The measurement system is mounted on MORI SEIKI SL-153 CNC lathe as can be seen on Figure 6. This provided a quick measurement of tool wear on the machine tool. It is ensured that the measuring device is placed in such a way, so that it is accessible and ready to implement measurements at any time (without removing cutting insert). At the same time the measuring device does not interfere with other processes, executed by the machine tool during its operation. In this way, we can implement the measurement that includes far more information about tool wear without having to take out the cutting tools, as it is necessary when it comes to the measurement with a toolmaker’s microscope.

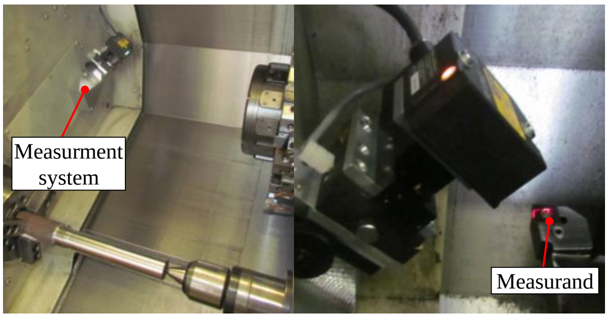

Figure 6: Measurement system mounted on Mori Seiki machine tool

The presented measurement system has been tested by determining the machining performances of bearing steal material 100Cr6, which has been heat treated to a hardness of 63 HRc in the longitudinal turning. The initial workpiece diameter was 40 mm and length 310 mm. Machining tests were conducted on a Mori Seiki SL-153 turning center. Commercially available Walter CNMA120412-T02020 cutting inserts with grade WAK20 were used with PCLNR 2020K 12 tool-holder. The experiment was performed with no cooling/lubrication fluids.

The cutting parameters have been defined according to the producer recommendations and were a_p=0.7 mm, v_c=50 m/min and f_n=0.15 mm/rev. These parameters were defined based on maximizing the material removal rate with an industry acceptable tool life of 10-15 min.

The workpiece was machined longitudinally at intervals over a length of 20 mm. Resaults of correspodning tool wear is presented in figure 7.

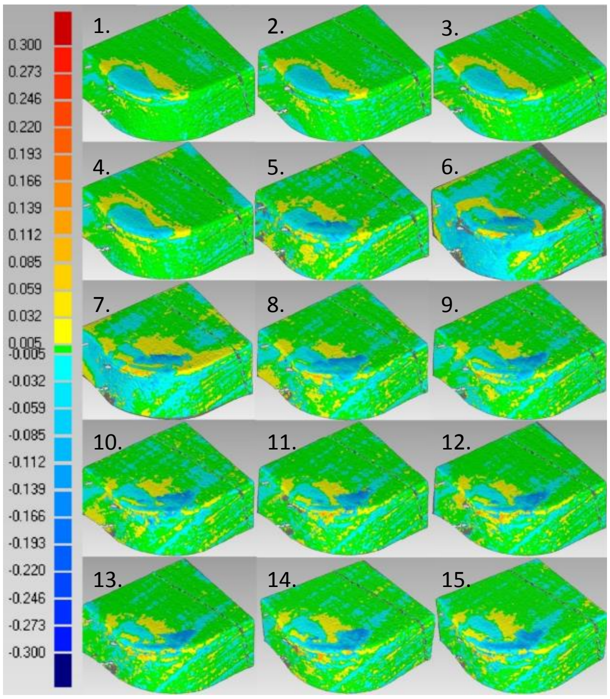

Figure 7: 3D deviation results

After each operation, the measurement procedure is carried out in the following order:

1. Machine tool moves the cutting insert to the measuring area.
2. Machine tool operator starts the measurement on PC measuring interface.
3. Laser displacement sensor captures the first profile.
4. Motorized linear stage Standa 8MT173-DCE2 move the measurement head for predefined ΔY.
5. By repeating steps 3 and 4 gradually the system captured a large number of 2D profiles and stores theme in internal memory of Keyence LJ-G5001 controller.
6. When the last profile is measured, the system transfer data from the Keyence LJ-G5001 controller to PC and move the translation stage to zero position.
7. Machine tool moves the cutting insert to the working area.

The measurement itself is executed in approximately 20 seconds (at 3 mm length measurement and ΔY = 0.005mm).

A total of 15 repeated measurements were performed. Figure 7 is showing the progression of wear on flank and rake face, BUE and chipping of cutting edge. The increase of crater wear depth is evident with growing darker blue color.

The maximum crater wear depth KT after the last experiment was in a range between 0.021 mm and 0.086 mm (figure 8). From the results it is also clearly visible the progression of chipping on cutting edge.

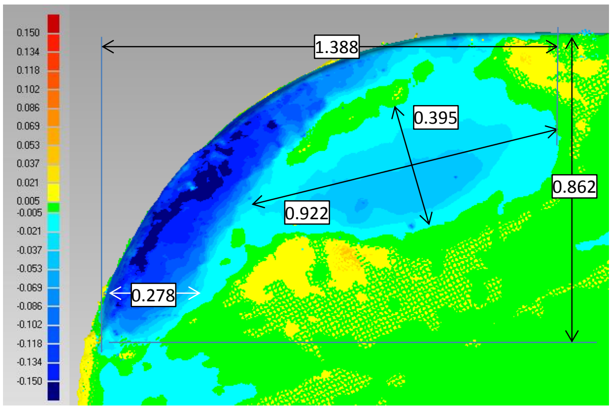

Figure 8: Measurement of crater wear and chipping with spatial tool wear measurement system

Additionally, presented measurement of crater wear, obtained with spatial measurement system, was compared to the conventional measurement made with toolmakers microscope (figure 9).

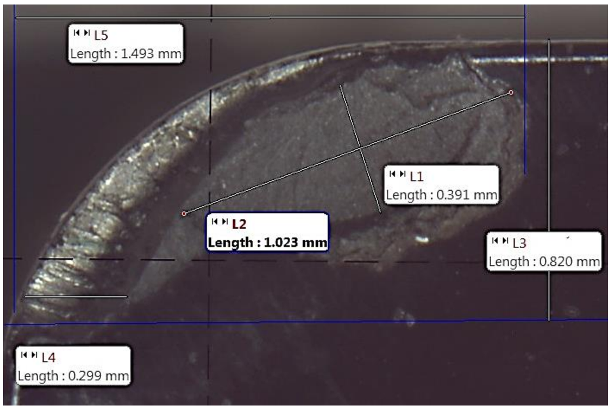

Figure 9: Measurement of crater wear made with toolmakers microscope

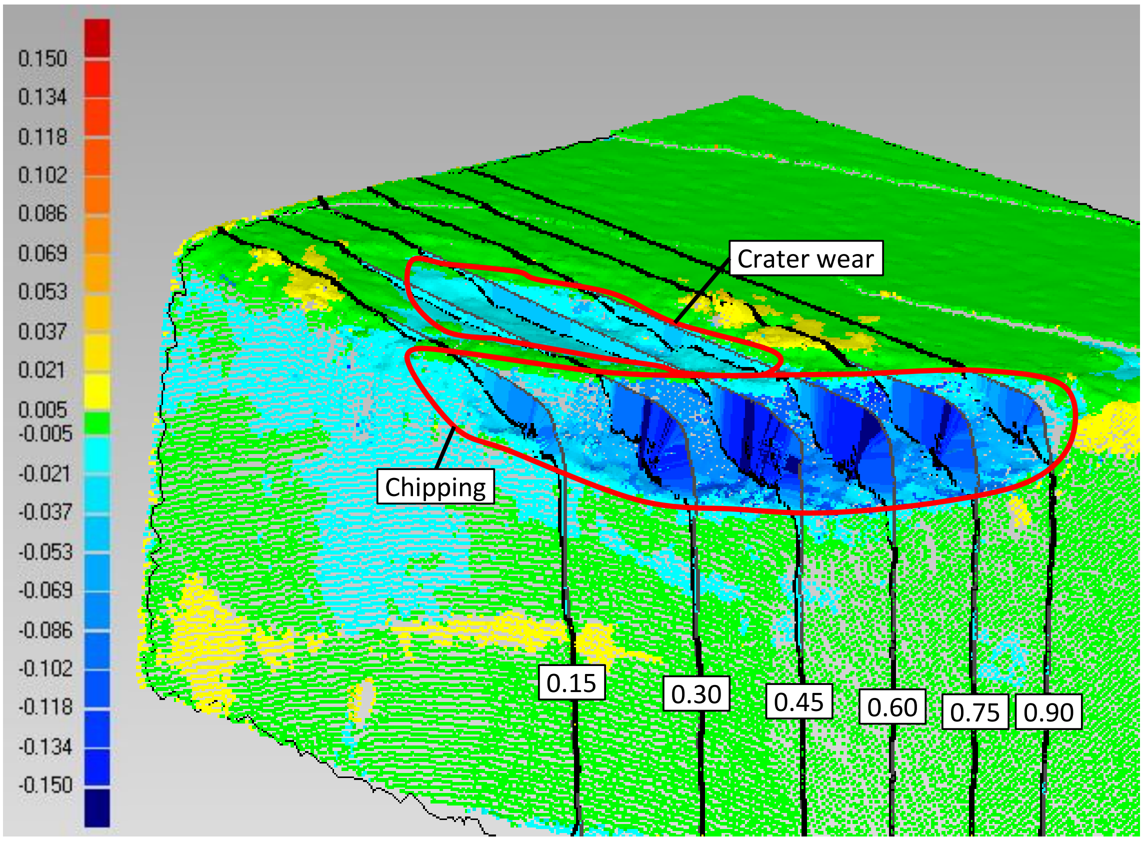

Figure 10: Chipping, crater wear and cross sections parallel to secondary flank face

From these measurements carried out with spatial tool wear measurement system (Figure 8), it is evident that the length of crater wear is 0.922 mm, the crater wear width is 0.395 mm. With the use of toolmakers microscope the length of crater wear is 1.023 mm, the crater wear width is 0.391 mm. The results show a good correlation between the measurements carried out with spatial tool wear measurement system and toolmakers microscope. Some minor variations in measurements may be attributed to the subjective nature of measuring with toolmakers microscope. This error may also occur due to the precision of determining the lower limit of the wear formation, since the microscope image does not reveal the depth of wear.

Whit the use of spatial measurement system, the limit of the wear formation can be accurately determined. Depth of flank wear can be seen from the comparison of cutting inserts cross-sections (Figure 10). From cross-sections becomes clear that the depth of flank wear (VB) where chipping occurs is in the area from 0 to 0.150 mm, and the width of wear goes from approximately 0.3 mm to 0.1 mm.

Such critical tools wear negatively effect on roughness and tolerances of produced parts.

5 Conclusions

In this work further development of spatial tool wear evaluation system is presented. The influence of incident angles of the scanning process was examined. Based on the analysis of measurements accuracy and the amount of captured data, the optimal setup of the measuring system was defined. Further a special clamping system was designed to mount the measurement device on the machine tool.

To test the measurement system, machining experiment was done, where cutting tool was measured directly on the machine tool. The results had been compared with the result obtained with conventional measurement method, with the use of toolmakers microscope. From the results of the measurements we can say that the proposed spatial tool wear measurement system offers high resolution and accuracy 3D dimensional deviation measurement. It outperforms traditional 2D deviation methods both in accuracy, efficiency and reliability. Another huge benefit of this method is the fact that the measurement can be performed very quickly, without removing the cutting tool from the machine tool. Obtained measurement data are realistic 3D models of the cutting tool, where we can clearly see what the existing conditions of the cutting tool are.

Future work will be focused on developing computational procedures for the analysis of 3D deviation data provided. The objective is automatic diagnostics and early alert pointing to possible tool damage, excessive local tool wear, tool misalignment and other possible causes for tool breakage and stop of the process.

References

[1] W. Grzesik, Advanced Machining Processes of Metallic Materials, Elsevier B.V., 2008.

[2] J. Kopač: Odrezavanje; Teoretične osnove in tehnološki napotki, 2008.

[3] K.C. Ee, A.K. Balaji, I.S. Jawahir, Progressive tool-wear mechanisms and their effects on chip-curl~chip-form in machining with grooved tools: an extended application of the equivalent toolface (ET) model, Wear, vol. 255, 2003, p. 1404-1413.

[4] G. Byrne, D. Dornfeld, I. Inasaki, G. Ketteler, W. Konig, R. Teti, Tool Condition Monitoring (TCM) - The Status of Research and Industrial Application, CIRP Annals - Manufacturing Technology, vol. 44, Issue 2, 1995, p. 541-567.

[5] E. Govekar, J. Gradišek, I. Grabec, Analysis of acoustic emission signals and monitoring of machining processes, Ultrasonics 38, vol. 1–8, 2000, p. 598–603.

[6] E. Dimla, Sensor signals for tool-wear monitoring in metal cutting operations--a review of methods, International Journal of Machine Tools and Manufacture, vol. 40, Issue 8, 2000, p. 1073-1098.

[7] S. Kurada, C. Bradley, A review of machine vision sensor for tool condition monitoring, Comput. Ind., vol 34, 1997, p. 52-72.

[8] J. Jurkovič, M. Korošec, J. Kopač, New approach in tool wear measuring technique using CCD vision system, International journal of machine tools & manufacture, vol. 45, 2005, p. 1023-1030.

[9] T. G. Dawson, Thomas R. Kurfess, Quantification of tool wear using white light interferometry and three-dimensional computational metrology, International Journal of Machine Tools and Manufacture, vol. 45, Issues 4-5, April 2005, p. 591-596.

[10] W.H. Wang, Y.S. Wong, G.S. Hong, 3D measurement of crater wear by phase shifting method, Wear, vol. 261, Issue 2, 31 Julij 2006, p. 164-171.

[11] A. Weckenmann, K. Nalbantic, Precision Measurement of Cutting Tools with two Matched Optical 3D-Sensors, CIRP Annals - Manufacturing Technology, vol. 52, Issue 1, 2003, p. 443-446.

[12] L. Čerče, F. Pušavec, J. Kopač, Spatial cutting tool wear evaluation, Journal of Production Engineering, Vol. 15, no. 2, p. 10 - 14, 2012.

[13] High-accuracy 2D Laser Displacement Sensor, LJ-G Series, User`s manual 2010

[14] Raymond H. Myers, Douglas C. Montgomery, Christine M. Anderson-Cook, Response Surface Methodology: Process and Product Optimization Using Designed Experiments, 3rd Edition, 2009

3D foot surface scanning for the purpose of foot orthotics production

Karlo Obrovac[1], Toma Udiljak[2], Jadranka Vuković Obrovac[3], Josip Nižetić[4], Alan Mutka[2]

[1] University of Osijek, Croatia
[2] University of Zagreb, Croatia
[3] Ortogen d.o.o, Croatia
[4] Cognitus d.o.o, Croatia

Abstract

Orthopedic and generally individual insoles are often used for the treatment of deformities, and other pathological conditions that manifest themselves in the foot, or to improve the performance of people who spend a lot of time standing or walking. Insoles are intended to reduce the burden resulting from the ground reaction, to improve propulsion and stability of walking, and to compensate the deficit due to static deformity or present pathology. [1] Numerous studies have shown the benefits of individual approach to making insoles towards application of over the counter ones. Among the most important parameters on which to base the development of insoles or molds is implementation of volumetric measurements. Volumetric measurements in the classical approach are based on taking footprints in wet sand or clay. Over time, these methods have been upgraded and now are in use polyurethane foam boxes in which foot is immersed, and later poured gypsum solidification gives grounds for mold. In addition, the classical approach often encounters using plaster bandages wrapping around the foot to form "slipper cast." By pouring plaster into this structure and its solidification we also get mold. These methods are still often found in use in orthotic practice. With the development of digital technology, this practice have begun to introduce new solutions that improve the practice by saving time of making insoles and reducing the discomfort which the patient may have during the measurement process. The application of digital measuring technology enabled CAD/CAM manufacture of orthopedic insoles (or molds). Although there are numerous solutions present in the market, there is still a great need for more accessible devices that enable wider application in practice.

Keywords: CAD/CAM, foot orthotic, 3D scanner

1 Introduction

First digitizers were used to create the most challenging orthotics, and to create socket for the prosthesis, and were based on the contact principle. However, the measurement process is extremely long lasting, and its result was often infused with artifacts. Therefore the results have not been used as a surface over which were implemented corrective procedures. Instead, they were used for topographical measurements which were the base for modifications of templates in CAD program. This methodology is even today frequently encountered in practice. After the initial enthusiasm by applying three-dimensional digitization, in practice, because of aforementioned, occurred skepticism about the use of these devices. The cost and time were only slightly lower, and there were no major shifts in other aspects of the application of these systems, which would justify the high price of initial investment. Over time, there has been progress in sensor technology, as well as their prices fall, and as a breakthrough laser technology through the application of LED laser module. This enables broader use non-contact digitization devices in the industry and in many other areas such as the protection of cultural heritage [2]. The first of such devices in orthotic practices were based on the use of ultrasonic probes, and were mostly used for the digitization of plaster casts of body parts. Further advancement of technology has opened the possibility to define easily available devices. By applying these non-contact systems, it is possible to carry out measurements of the existing mold or impression of the body in the proper material or the measurement is carried out by direct imaging of the body part of interest. Advantages of this contactless acquisition regards of the contact principle are numerous; in terms of digitizing the plantar aspect of the foot, these methods allow for quick and easy shooting with the ability to record the surface of the foot in the corrected position, with semi- or fully weight bearing position. Further progress of optics and digital cameras, have emerged more compact devices which give satisfactory results, concerning the accuracy,

recording speed, and convenience of use. These devices are usually based on the triangulation principle.
Digitizing devices used in orthotic practice in most cases are the devices for general purpose although there are those that are specifically designed for particular use. Here it is worth noting device from Amfit company [3] based on the contact principle and devices from companies Vorum research [4], and Polhemus [5].

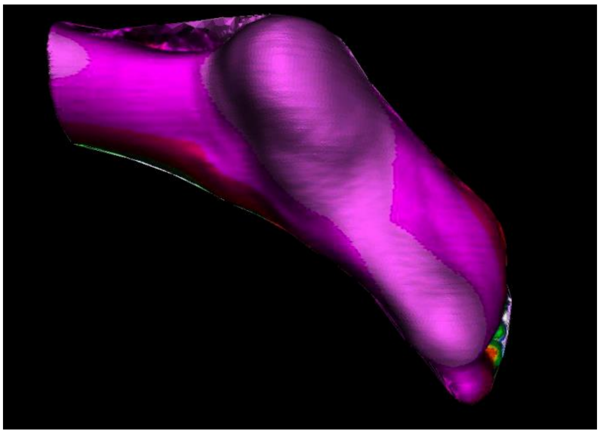

Figure 1. Foot plantar surface directly scanned with Gray code projection based system

The leading problem why the use of this approach has not yet surpassed the classic approach lies in the fact that these devices are high-priced and not available for a wider range of users, and because of the questionable viability of applying such technology. Therefore, they are most often found in use within major orthotic laboratories, where in addition to scanning surface of the foot, figure 1, they are used to scan other body parts. Defining easily available digitization devices represents a large area of research and opens the door for the introduction of digital technology in orthotic practice [6].

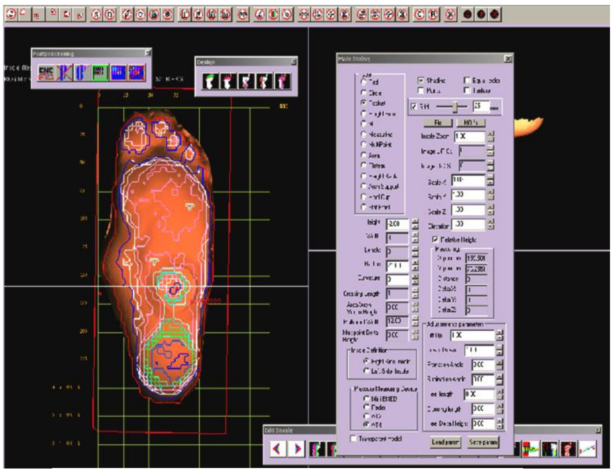

Figure 2. Foot orthotic CAD design

2 Our contribution

In our approach, our desire was to unite the needs of users in a single solution and define the unit to be in an accessible way to allow customers to introduce their practice with a methodology of the contactless recording of the surface of the foot, and through this approach to provide CAD/CAM production of orthopedic insoles, figure 2 and 3.

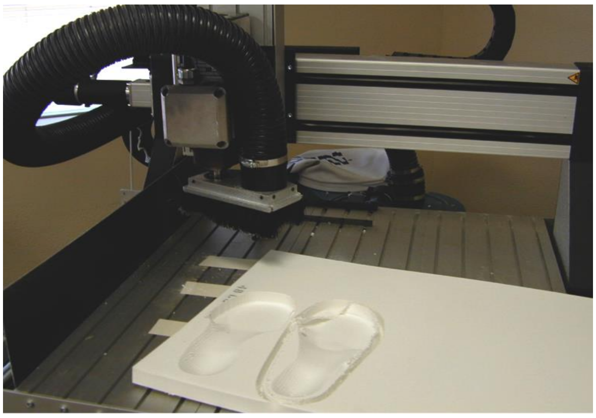

Figure 3. CAM foot orthotic production

Our work is based on the use of commercially available hardware with a minimum of additional equipment. The primary reason for this lies in the fact that this made it easy for assembly, its multiplication if the need dictates, and easy replacement of components in case of failure. In addition to the above, device must have a simple calibration procedure, adequate accuracy and speed of operation, and intuitive working environment. The device must also be easy to use, and its use must require minimal training time. Over the many years of work, we have defined more devices based on different principles, which are subjected to a practical test to verify satisfaction of initial application.

3 Applied hardware

As basic hardware are selected:
1. digital network cameras
2. digital SLR cameras
3. laser line modules (generators)
4. digital projectors
5. flat-bed scanners

This choice was the result of a number of facts during the optimization process. As one of the most important result of this procedure is decision to exclude, from further consideration, any development procedure involving the use of moving parts or combinations in which the laser line generator was fixed on a CNC machine. This was due to a significant reduction in costs associated with the controller, mechanical components cost, increasing robustness to exclude mechanical components that are cheaper editions sensitive to the effects of external influences, and simplified certification procedure, figure 4.

4 Metodology

A number of principles has been taken in consideration that would be the functional basis for future assembly:

1. Stereophotogrametry with projection of the random pattern
2. The application of white light interferometry
3. The scanning with binary Gray code Projection
4. The scanning with stripe projection generated with laser line generator or digital projector
5. The method of the foot scanning based on structuring a light source from flat-bed scanner.

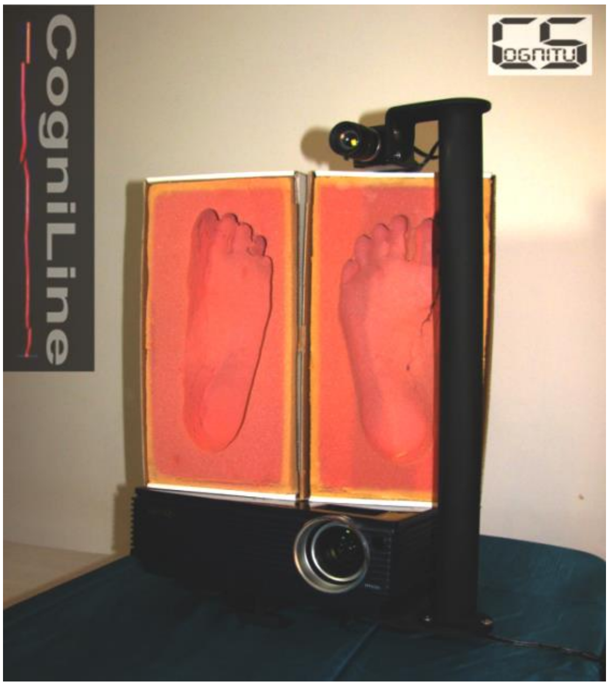

Figure 4. Our projector/network camera based digitizer

During the development process, we identified the advantages and disadvantages of each principle and considered the initial set of requirements. From there, application of the stereophotogrammetry with a projection of randomized pattern onto observed object was a method that allowed the fastest results because it is enough to capture two images from the two projections (we used a device that enabled manual linear shift of camera for a given amount, what allowed to preserve parallelism of optical axes between two camera positions). In addition to above principle we consider the use of stereophotogrammetry with cameras whose optical axes are not parallel, i.e. the principle of finding positions of points in space - based on epipolar geometry. However, method for applying correlation algorithms for the best pixel correspondence in the second picture requires significant time for search, and is sensitive to changes in brightness, due perspective changes, which further compromises the process of finding corresponding points in two images. In another system we used white light interferometry as a base principle.

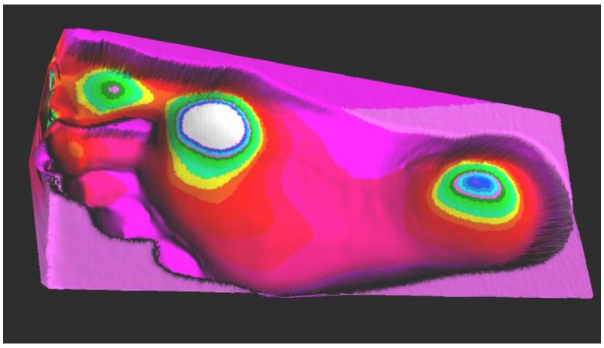

Figure 5. Foam box scanned with with system based on the white light interferometry

Interferometry method with projection sinusoidal pattern is also carried out very quickly (to implement it is sufficient to capture three object images, with the phase shift of the 120 °). [7] The result is the very detailed point cloud, figure 5. The method is highly sensitive to possible object shifts (even very small), and so if it is not implemented very quickly (what requires short exposure, and the special requirements to hardware) this may generate a significant artifacts. The method also depends largely on the conditions under which the recording is conducted and result also depends on the intensity of each pixel on the filmed object. In terms of non - laboratory light from secondary sources can greatly affects the final result. Still, device based on this method can be used if there are satisfactory lighting conditions in which the measurement is carried out, to capture objects that do not move while shooting, and if the object is uniformly colored. Method is under the given circumstances suitable for scanning of feet impressions in polyurethane foam, previously made plaster casts of the feet, plaster "slipper casts”, finished insoles, molds and shoe lasts. Particularly good results are obtained with uniformly colored surface of the object, which can be easily achieved by applying a thin layer of powder on the surface using an appropriate spray.

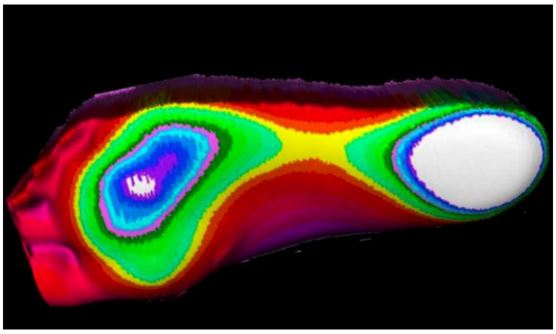

Figure 6. Foam box scanned with Gray code projection based system

Applying the projection of structured light in the form of binary pattern (Gray code) [8] as a principle showed very satisfactory results, figure 6. The method allows for simple calibration procedure and for a relatively small number of acquired images to obtain dense record of spatial samples of recorded surface. The principle allows to be used with a digital projector and available digital cameras (in our devices we use digital SLR cameras) that can be easily programm controlled.
Method, however, in spite of its advantages, also depends on the lighting conditions of the room in which the recording is conducted. This is particularly important for the module that calculates specific binary code for particular projected stripe. Device based on this principle gives very satisfactory results in the spaces with lighting from diffuse sources and with medium intensity. Such a requirement can be achieved in a significant number of institutions where the foot scanning is carried out for the purpose of orthotics production.
In the institutions where there are no such conditions, and where these measurements are conducted more frequently due to the large number of patients, it is necessary to define a methodology which enables scanning with attention to be paid to the frequent and large changes in light intensity. For this purpose, we define digitizing device based on the projection of the stripe light pattern of greater intensity using a digital projector or using the laser line generator, figure 7.

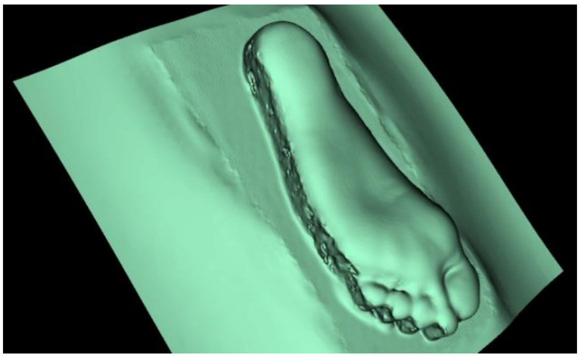

Figure 7. Foam box scanned with projector generated stripes projection

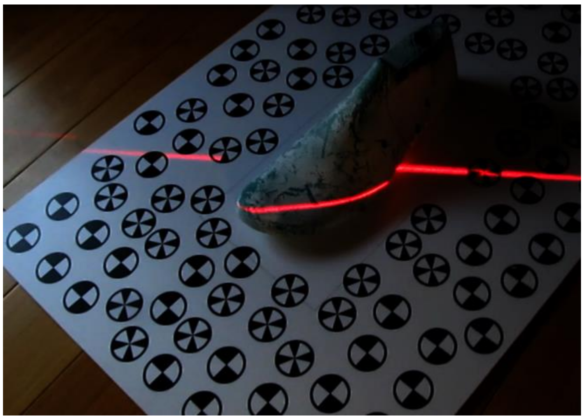

Figure 8. Shoe last scanning using laser line projection hand held device

Digital projector enabled illumination of the object with linear pattern programmed to moves across its surface, which is simultaneously registered with a digital camera. With a given intensity of the applied light pattern, this acquisition can be implemented quickly, and without the need for significant exposure adjustment. In addition to a digital projector, as a line source, it is possible to use a laser line generator. In most of the existing systems that use of laser line generator, we find mechanical components (linear axis or rotation table) where for each projected line, conditions under which the object is illuminated with light pattern, are known.

Figure 9. Dorsal aspect of the foot digitized with hand held laser line projection based device

In regards of our initial idea, we wanted to avoid the use of mechanical components. Due to that fact we defined a device that would be based on the use of digital cameras and laser line generator mounted onto handle, figure 8. Handheld device allows for free hand motions and filming a scene with an object illuminated from laser module at the same time registering the calibration object, which would later define the parameters of rotation and translation, ie. camera position in space. During the calibration procedure plane with a laser beam is defined, relative to the coordinate system of the camera, and with the known parameters of the position of the camera in space in relation to the calibration device, it is possible to integrate all the spatial sections of the projected laser beams (laser planes) and the object obtained during recording in a single cloud of points that defines the topography of the observed object. This way, it is not necessary for the use of expensive gyroscopic devices or special manipulators. Mentioned methodology allows for fast acquisition of large amount of data, and is robust to external influences. In general handheld scanners are less sensitive to changes of the scanned surface slope [9], figure 9. Device allow for fast scanning of the plantar and dorsal aspect of the foot and lower leg, figure 10. The device can also be used for the digitization of plaster molds and the shoe lasts.

Figure 10. 3D mesh generated from point cloud acquired using hand held laser line projection based device after performed denoising procedure

Finally, during our research the need for defining a device that would allow for digitization of the plantar aspect of the foot in a very cheap and fast way have emerged. For this purpose, we considered the possible use of the flatbed scanner and with the requirement not to any hardware modification should be performed. Flatbed scanners are often used for the feet scanning, but in the most of the cases they can only accurately define outer contours and in general provide only foot image. Until the introduction of our method there was no existing principle that in a satisfactory manner, and with the use of such devices would define the spatial geometry of the scanned foot surface. For this purpose, we use of opaque grid foil which is placed on the scanner glass and on whose upper surface plantar aspect of the foot is placed during the scanning. The light changes and the shadows from grid stripes on the foot surface are registered in the cleft sections and are related to the changes in the height. With the known calibration parameters, and the procedure of depth undistortion, it is possible to carry out the reconstruction of the surface using the interpolation through a set of profiles. The obtained result meets the required needs for design and production of orthopedic insoles, figure 11.

Figure 11. Foot scanned with the flat bed scanner /grid based system

4 Application

The results obtained from these measurements undergo testing, in terms of defining deviations of accuracy; by comparing the results obtained from the implementation of measurements of the same object with those acquitted using a reputable device with high nominal accuracy. Sum of the differences between the results obtained by our measurements from the data obtained with mentioned devices ranged from 4% in the method based on a flat-bed scanner and grid to 0.25% of the results obtained using the interferometry method. Developed devices are subject to constant upgrading and improvement of algorithms in terms of increasing the speed and accuracy of recording and the supporting functions necessary for the function of each of scanning module. All of the above systems are in practical use and proven robustness and adequate quality for the design and production of orthopedic insoles, figure 12 and 13.

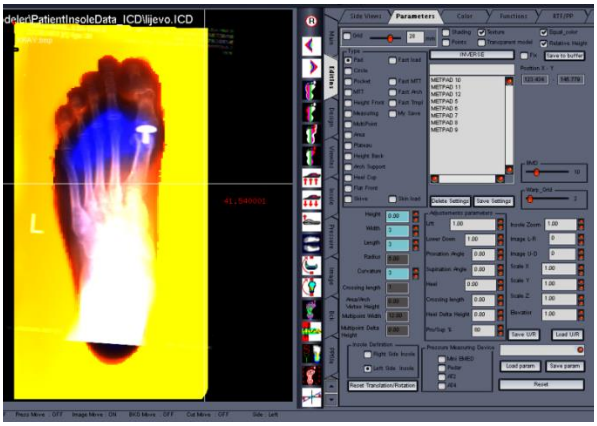

Figure 12. The plain radiograph superimposed to the foot surface, allows for accurate surface adjustments

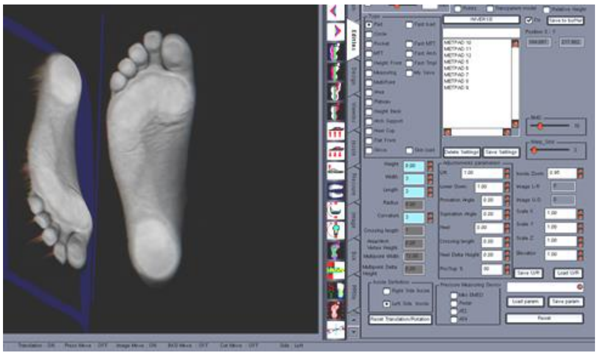

Figure 13. Foot orthotic CAD design allows for hyper realistic visualisation of the scanned surface

5 Conclusion

The paper reviewed developed devices used to implement digitization of the feet, and for the needs of orthopedic insoles production. Our goal was to create a device that will introduce digital measurement techniques in a orthotic practice in easy and affordable manner. While there are many solutions on the market that are made for the said purpose or can be used for the same purpose, and that give a satisfactory results, their cost is still a limiting factor that prevents their wider use. Therefore we decided to define our own solutions that would give a satisfactory result in terms of price/quality, and that on the robust and reliable way allow user to obtain adequate results. Our work has shown that with use of the aforementioned hardware and applied methodologies, there were significant differences in the obtained results, and some combinations, in practical terms, indicate characteristic advantages and disadvantages. Therefore, the appropriate combination of hardware and methodology is result of specified requirements of particular location.

References

[1] Udiljak,T., Granberry, WM., Obrovac, K., A New Approach to Foot Orthosis Design and Manufacture, World Manufacturing Congress WMC 2001, Rochester NY

[2] Levoy, M, The digital Michelangelo project, Second International Conference on 3-D Digital Imaging and Modeling (Cat. No. PR00062),1999.

[3] http://www.amfit.com/products/contact-digitizer

[4] http://www.vorum.com/common/english/pdfs/FW_scanners_YETI.pdf

[5] http://www.polhemus.com/?page=Scanning_Fastscan

[6] Scott Telfer, James Woodburn,The use of 3D surface scanning for the measurement and assessment of the human foot, J Foot Ankle Res. 2010; 3: 19.

[7] H. Y. Liu, W. H. Su, K. Reichard, and S. Yin, "Calibration-based phase-shifting projected fringe profilometry for accurate absolute 3D surface profile measurement," Opt. Comm. 216, 65-80 (2003).

[8] Gühring, J., 2000, Dense 3D surface acquisition by structured light using ot-the-shelf components. In Videometrics and Optical Methods for 3D Shape Measurement, Volume 4309, p.220-231. - strukturirano svjetlo

[9] D. Koutny, D. Palousek, T. Koutecky, A. Zatocilova, J. Rosicky, and M. Janda, 3D Digitalization of the Human Body for Use in Orthotics and Prosthetics,World Academy of Science, Engineering and Technology 72 2012,p.1634

An investigation into roller burnishing process

B. Zabkar[1], J. Kopac[1]

[1] *University of Ljubljana, Slovenia*

Abstract

Plastic deformation processes have been used to modify the surface roughness and integrity properties by generating fine grain size gradients in the surface region of many materials. These fine grained materials often exhibit enhanced surface integrity properties and improved functional performance (wear resistance, fatigue life, etc.) compared with their conventional coarse grained counterparts. Burnishing is a superficial plastic deformation process used as a surface smoothing and surface enhancement finishing treatment after some machining processes that eliminate secondary operations. In roller burnishing, a hard roller is pressed against a rotating cylindrical workpiece and parallel to the axis of the workpiece. Burnishing is a cold forming process, in which the material near a machined surface is displaced from peaks to fill the valleys of the surface profile. Roller burnishing is an economical process, which can be effectively used in many industrial fields. In the present work, various experiments are conducted to investigate the effect of burnishing force, burnishing feed and pre-machined surface roughness on surface roughness of roller burnished bearing steel.

Keywords: Roller burnishing, surface roughness, process parameters.

1 Introduction

The properties of machined components such as surface integrity, fatigue strength and load bearing capacity are becoming increasingly important. The burnishing process is considered as cold forming finishing process which has positive influence on surface integrity. Most significant impacts of roller burnishing are increased surface hardness and decreased surface roughness. The process also transforms tensile residual stresses, present in the surface zone after turning, into compressive residual stresses [1]. The burnishing process is applied to cylindrical workpieces of both, external and internal surfaces and does not involve material removal. Under certain conditions, this process provides a manufacturing alternative to grinding, precision turning and honing operations. In most cases, burnishing process is performed on the same lathes where workpieces were machined [1].

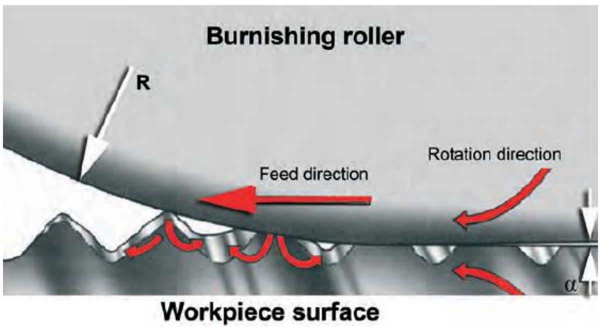

Figure 1 Roller burnishing process [2]

Figure 1 show how the surface's peaks are pressed down, almost vertically, into the surface and the material then flows into the valleys between the peaks. The resulting smooth surface occurs not because the peaks are bent into the surface, but because the material at the workpiece surface is plastically deformed and the material flows, eliminating surface roughness [2].

The curved arrows pictured at the material's surface demonstrate how the material is displaced into the valleys between the peaks. Plastic deformation increases the roller's contact with the surface in that the applied rolling pressure (or burnishing force) affects the peaks that lie ahead of the roller's current position while causing the peaks at the point of contact to flow. The region found between the arrows labeled "rotation direction" demonstrates how the material's surface is shaped during the burnishing process. The roller suppresses the plasticized material, preventing it from flowing backwards against the feed direction, while clearance angle α ensures that the surface is not over-burnished [2].

Advantages of roller burnishing:
1. Produces mirror-finish surfaces.
2. Increases surface hardness, decreases friction and wear.
3. Provide compressive residual stresses
4. Consistent dimensional tolerance and repeatability.
5. Single pass operation which requires short cycle time.

The principle of roller burnishing is transferring the force applied on a roller to the surface in a certain path. During the rotation action the contact area is so small that hertz type pressure occurs on material surface. This provides low energy and rolling force requirement. Roller burnishing process is done below the recrystallization temperature therefore the residual stresses are not released. The real crystal structure contains various irregularities that should come first to the slip formation, because the maximum stress occurs on these locations. If the load on the crystal is big enough, it will start to move and dislocation can be moved.

Figure 2 presents a diagram of roller burnishing process for a spherical roller. The first contact to the machined surface occurs in Section (A). In section (B) the yield strength of the surface is exceeded and plastic deformation takes place. Pressurized depth can be seen here as (D). After the material has been subjected to the maximum compressive strain, in section (C) it begins to elastically relieve (E) through the finishing zone finally leaving with a smooth surface and a compressive residual stress of significant peak value. The stresses formed on the material during the compression decrease towards the center. [3]

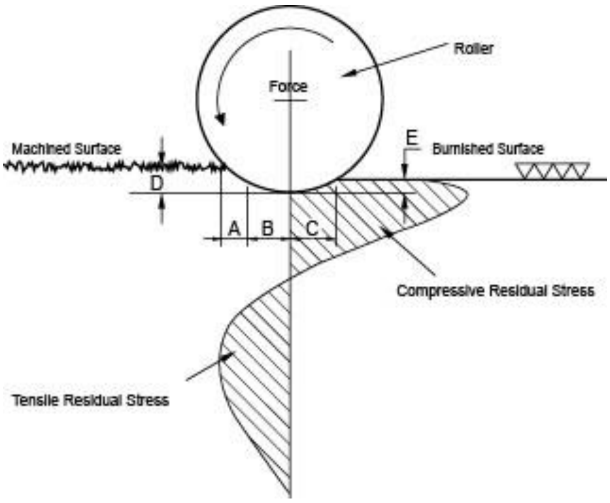

Figure 2 Roller burnishing process [3]

2 Roller burnishing tools

There are several types of tools depends on the application of use. Some of them are single roller tools that consist of a tool body equipped with a tool shank, a spring assembly that allows the roller head to move with no play and very low friction, and a gauge that indicates the burnishing force as measured by spring deflection. Single roller tools are designed to machine a wide variety of irregular surfaces, including specific contours, fillets, and grooves. These tools can be used for burnishing internal and external cylindrical surfaces of different diameter dimensions. Burnishing force is variable, and accurately measured [2].

Figure 3 Single roller tool [2]

Multiple roller tools are designed to machine external pins and internal cylindrical bores. Tool automatically collapses when retracted to prevent surface damage [2].

Figure 4 Multiple roller tool [2]

3 Influential parameters

Surface roughness after the roller burnishing is dependent on the contact pressure of roller and feed rate. These are the variable process parameters. Contact pressure is defined as the quotient of the burnishing force and the contact area between the roller and the workpiece. The contact area is affected by the clearance angle α between the roller and workpiece, roller diameter and fillet of roller.

3.1 Input parameters

Roller burnishing is a cold forming process where a compression stress is applied to the workpiece surface. Therefore material mechanical properties have big influence on output results of the process. Especially yield strength of material.

Input surface roughness Ra_i also affects the achieved surface quality. The values of R_Z may vary from 5 and 50 micrometers. Typically, the value of R_Z is 5 to 15 micrometers [4]. The best pre-treatment of the surface is achieved through the choice of turning feed rate that is less than half the radius of the cutting insert.

3.2 Geometry conditions

Roller must be placed in relation to the workpiece in that way, there is a clearance angle α between the roller surface and the surface of the workpiece. The size of the clearance angle is usually between 0,5 and 1,5°. It also depends on the workpiece material, harder than the material of the workpiece is, greater than the clearance angle. If the angle is too small the surface quality decreases, because it could be over-burnished.

We can achieve the same finish result with bigger or smaller roller diameter *d*. For a large roller we need to increase burnishing force. This can cause bending if we are dealing with longer workpieces. Therefore, we use smaller diameter rollers for machining thin walled workpieces that can not be clamped enough firmly. In other cases, we rather use large diameter rollers.

Depending on the material of the workpiece, the roller fillet *r* is 1 to 5mm. For most of the steels the situable fillets are from 1 to 2mm.

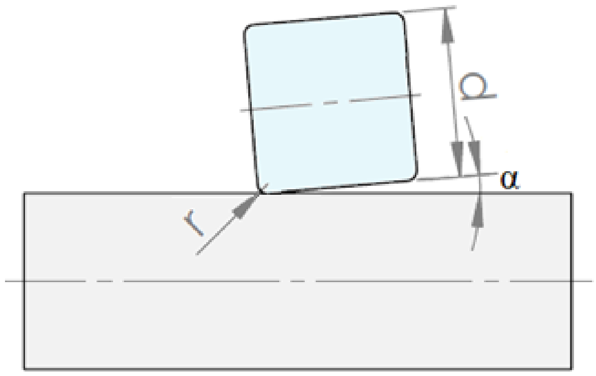

Figure 5 Geometry of burnishing process

3.3 Process parameters

The burnishing force *F* is an important factor in the burnishing process. If the force is too small, the required surface quality is not achieved. Higher burnishing forces can lead to cracking and peeling of the workpiece surface, as in the surface layer the tensile strength of the material is exceeded and microstructure fracture is achieved.

Feed rate *f* has big impact on the quality of the surface after burnishing process. It is also linked to the changes in the clearance angle of the roller α. When working with larger clearance angle means that feed rate value should be reduced if we want to achieve required surface quality.

Burnishing speed *v* does not have significant influence on the surface roughness, because roller burnishing is a cold forming process that is running below recrystallization temperatures and under this conditions velocity of transformation does not affect material’s yield strength [5]. Moreover, there are guide values which depend on the design tools and the size of the workpiece.

In some experimental studies, the number of passes *n* is presented as an influential parameter on the final surface roughness. In principle, the roller burnishing increases surface hardness, so the question appears if it is reasonable to roll surface with multiple passes because after first tool passage, the surface is already hardened. Too many passes can also result peeling of the workpiece surface.

4 Experimental work

Specimens were turned and burnished on a lathe model Mori Seiki SL-153. The workpiece material was AISI 52100 (100Cr6) bearing steel in normalized condition of hardness 220 HV. We used two workpieces with nine sample lengths, which were turned to different input roughness values. Diameter of specimens after fine turning was 43,6 mm. Roller burnishing tool consists of radial roller bearing INA NUTR 1542X and thrust roller bearings INA 81104-TV, by which the backlash in the feed direction of the tool is compensated. Hardness of the bearing outer tread surface is 60 HRC. The tool was clamped into the lathe revolver using a Kistler 9129AA dynamometer.

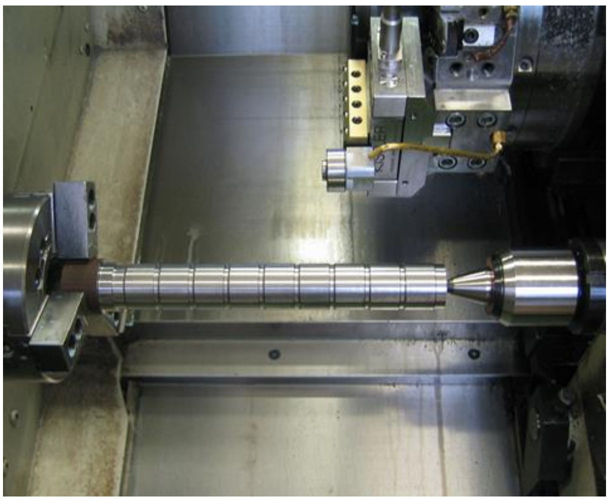

Figure 6 Experimental setup

4.1 Design of experiments

Using the Taguchi orthogonal matrix, we defined constant and variable factors (parameters) and their levels.

Constant parameters of roller burnishing:

- Clearance angle: $\alpha = 1.3°$
- Roller diameter: d = 42 mm
- Roller fillet: r = 1 mm
- Burnishing speed: v = 150 m / min
- Number of passes: n = 1

Variable parameters of roller burnishing:

- Burnishing force: F = 600, 1200, 1800 N
- Feed rate: f = 0.1, 0.2, 0.3 mm / rev
- Input surface roughness: Ra_i = 0.39, 0.96, 3.44

Assuming that there are no factor interactions, the Taguchi L_{18} orthogonal array has been used.

4.2 Results and discussion

Table 1 shows the results of experiments carried out in this research. Analysis of the results was performed in the program Minitab 16.

Table 1 Experimental conditions and results

No.	F [N]	f [mm/rev]	Ra_i	Ra
1	600	0,1	0,39	0,15
2	600	0,2	0,96	0,31
3	600	0,3	3,44	0,50
4	1200	0,1	0,39	0,12
5	1200	0,2	0,96	0,20
6	1200	0,3	3,44	0,43
7	1800	0,1	0,96	0,10
8	1800	0,2	3,44	0,18
9	1800	0,3	0,39	0,22
10	600	0,1	3,44	0,20
11	600	0,2	0,39	0,26
12	600	0,3	0,96	0,46
13	1200	0,1	0,96	0,12
14	1200	0,2	3,44	0,22
15	1200	0,3	0,39	0,31
16	1800	0,1	3,44	0,11
17	1800	0,2	0,39	0,14
18	1800	0,3	0,96	0,23

Analysis of the results gives us the values of signal to noise ratio for each parameter, and the influence of parameters on the output measured value Ra. Figure 7 shows the influence of each parameter on surface roughness. From the graphs can be seen that the most significant factor is feed rate (f), followed by the burnishing force (F) and the input surface roughness of the workpiece (Ra_i). Larger slope of the line connecting the levels of the parameter means that factor is more influential.

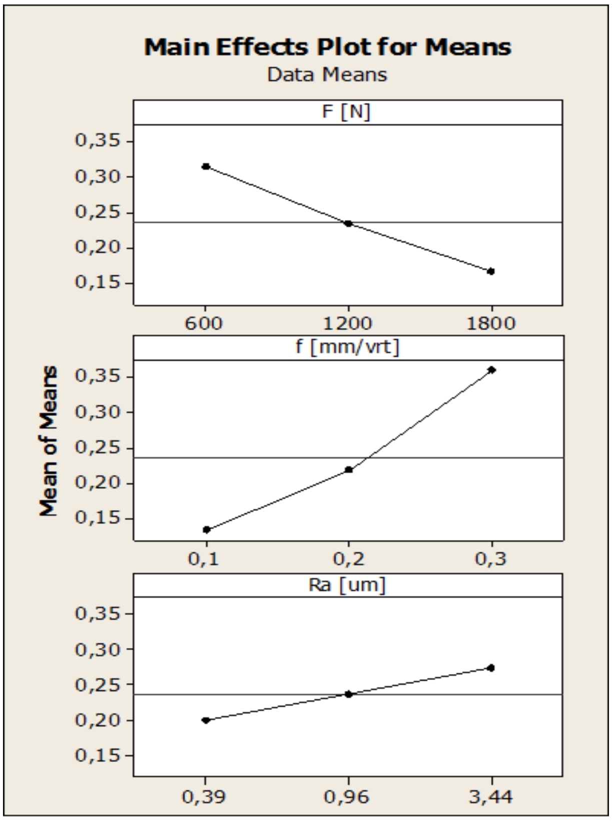

Figure 7 Influence of parameters on output surface roughness Ra

5 Conclusion

Many factors affect the result of roller burnishing process. It is important to find optional burnishing conditions. The purpose of this study was to examine the influence of three input parameters: burnishing force, feed rate and input surface roughness on the response surface roughness. The best response results were obtained at the lowest value of burnishing feed. Feed rate is also the most significant factor in the roller burnishing process.

References

[1] S. Świrad: The surface texture analysis after sliding burnishing with cylindrical elements. Wear, 2010.

[2] Ecoroll catalogue, http://www.ecoroll.de

[3] http://www.yamato.com.tr/roller_burnishing3.html

[4] Yamasa roller burnishing catalogue, http://yamasa.com.tr

[5] J. Puhar: Mehanska tehnologija: Preoblikovanje - postopki. I/1. Fakulteta za strojništvo, Univerze Edvarda Kardelja, 1990.

Industrial session

Mass production of the Step Lock Bolt

N. Sase[1], T. Takahashi[1] and K. Tamura[2]

[1] *Toyama National College of Technology, Japan*
[2] *University of Toyama, Japan*

Abstract

Screw fasteners have been widely adopted in almost all industrial products. Screw fasteners can be produced easily, be applied where strong fastening force is needed, be fastened by a simple tool and be made to loosen at any time. It has been known, however, that loosening of screw fasteners causes troubles occasionally. A great deal of time and money has been expended for the inspection and maintenance of the tightness of screw fasteners. In order to solve this problem, we invented an anti-loosening screw fastener named Step Lock Bolt (SLB). The SLBs, which have some steps on their screw helixes, provide high anti-loosening performance without sacrificing the advantages. In this study we propose a mass production method of the SLB screws. The screws should be produced by a rolling process in the same way as conventional bolt screws from the viewpoint of productivity. The procedure of the rolling process of M8 SLBs is reported. And an evaluating system of the SLB screw helixes at the production site is proposed, together with a convenient device for this purpose. These inventions enable the mass production of the SLBs by the rolling process. It is proved that the rolled SLBs provide high anti-loosening ability.

Keywords: Screw fastener, loosening, rolling process, on-site inspection, anti-loosening, bolt and nut

1 Introduction

Screw fasteners have a history of more than 600 years since their invention. They have been widely adopted in various industrial products because of their large clamping force, an easy fastening process and their high productivity. Their use has been still increasing.

Their inherent and inevitable fault is, however, that they will loosen eventually by vibration. Sometimes it can result in serious troubles. For preventing the troubles, a great deal of time and money has been expended for the inspection and maintenance of the tightness.

In order to solve the problem, we invented an anti-loosening screw fastener shown in **Figure 1**. It is named Step Lock Bolt (SLB) which has high anti-loosening ability[1]. In spite of the high anti-loosening ability, however, it has been thought to be difficult to produce them in mass production scale, because of a complication in tool settings.

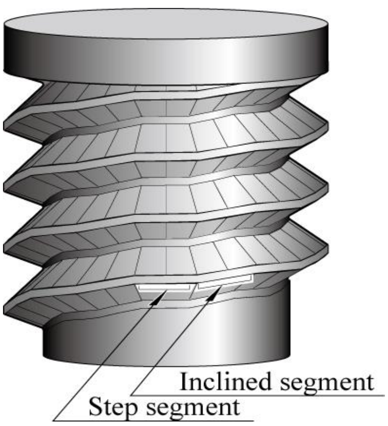

Figure 1 Step Lock Bolt (SLB)

In this study a production method of M8 SLBs by a flat-die rolling process is considered. The procedure and the required accuracy for the process are examined carefully, and a measurement and inspection method of the SLB screw helixes at the production site is proposed. Those are evaluated based on the anti-loosening ability of the SLBs.

2 Anti-loosening mechanism of the SLB

The structure of an SLB is shown in **Figure 1**. A segment that has no lead angle is called “step segment”, and a segment that has a lead angle is called “inclined segment”. The number of the step segments in a pitch varies depending on the diameter of the screw, usually from 3 to 10 segments, sometimes more.

The loosening of a screw fastener is caused by a two-stage process, the first one is the torsion of the bolt and the second is the slip at the bearing surface[2]. The bolt torsion is the direct cause of loosening. Therefore, if the torsion of the bolt does not occur, any slip at the bearing surface cannot cause loosening.

When a conventional bolt is fastened, the clamping force is supported by the inclined surface of the nut as shown in **Figure 2(a)**. The bolt easily slips off on the slope by the applied external force. This slip leads to the torsion of the bolt.

The clamping force of the SLB is, on the other hand, supported by its step segments as shown in **Figure 2(b)**. There is no slipping component force along the lead angle. Although the relative slip along the flank angle occurs, the torsion of the bolt will never be caused. In other words, the SLB does not have to be prevented from loosening because it never originates the cause of loosening due to its structure.

The anti-loosening performance of the SLB was tested by applying a cyclic load perpendicular to the bolt axis. The result is shown as the variation of the clamping force with the number of oscillations in **Figure 3**.

The conventional bolt starts loosening immediately after the test begins, and loses its clamping force by about 100 oscillations. On the contrary, the SLB keeps its clamping force even after 5,000 oscillations, although a slight loosening can be seen in the beginning. It is clear that the SLBs have high anti-loosening ability.

3 Rolling process of the SLB

For the mass production of the SLBs, we decided to employ a flat-die rolling process because designing and machining the dies as well as adjusting the rolling conditions are easier than those in other methods.

In the rolling process of conventional bolts, the clearance between the dies is adjusted, in the y direction in **Figure 4,** for controlling the major diameter of the screw. The relative position in the z direction is adjusted for matching the screw pitch.

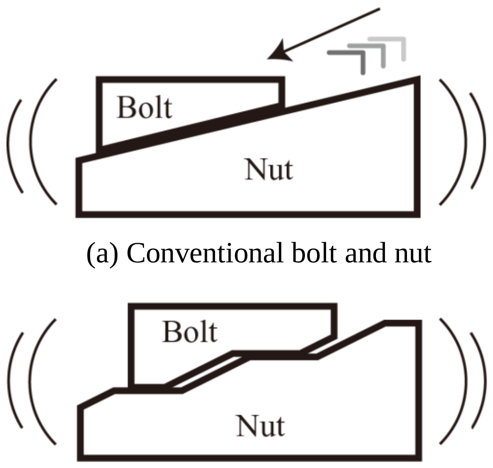

Figure 2 Loosening and anti-loosening mechanism

In case of the SLBs, another adjustment is required. In **Figure 4**, the step segments of the blank and the dies are indicated by the grey segments. When the blank rotates 180 degrees, the step segments on the blank, which are formed by one die, must fit to those on the other die. Therefore, the adjustment of the traveling die position in the x direction is also necessary. Furthermore, the mutual affection of these adjustments makes the SLB rolling more complicated.

Though these adjustments are necessary, once they are completed, SLBs are produced in the same way as the conventional bolt production. We examined the durability of the dies by carrying out the rolling of M8 SLBs for 150,000 times without any fine tuning during the test. It was found by this test that the shape of the rolled threads was quite stable and neither abrasion nor chipping was observed on the die threads.

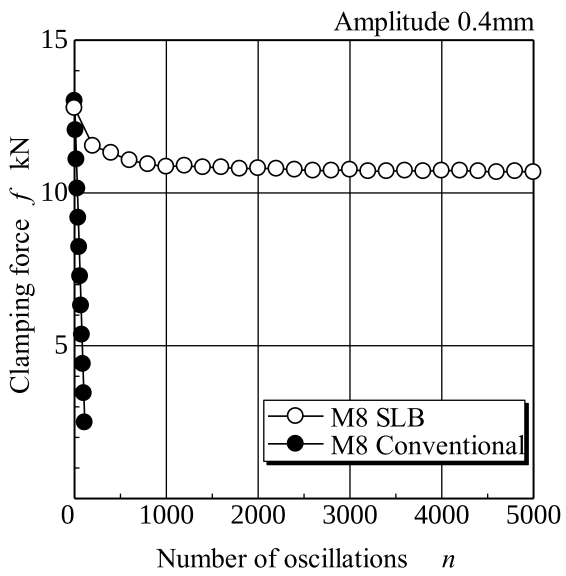

Figure 3 Anti-loosening performance of the SLB

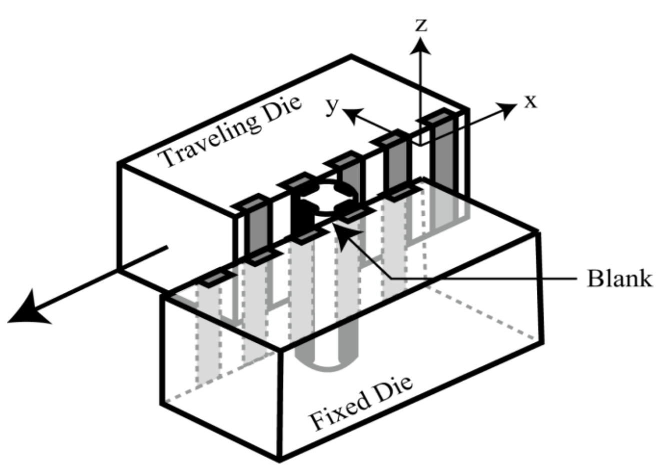

Figure 4 Rolling process of the SLB

4 Procedure of the SLB rolling

The authors attempted a great number of experimental rolling with several types of SLB dies in various conditions, and examined the shapes of the rolled screw helixes. It was found from these experiments that the SLBs could be produced accurately and systematically by a rolling process. The rolling should be done by pursuing the following procedure exactly.

i) When an SLB is designed, the geometrical specifications including the diameter, the pitch, the number of step segments in a turn, the length of each segment, the number of inclined segments and the length are determined. The diameter of a blank to be rolled, d_b, is calculated based on the indented volume of material and the bulged volume.

ii) The dies are designed and made on a hypothesis that the top surfaces of both dies exist in the same plane. Suppose that a step segment is formed by the fixed die and reaches the traveling die after a half turn of the blank, the segment must meet the same pattern on the traveling die. The step segments on the traveling die must be engraved at the same height as the fixed die. This is an important point for designing the SLB dies.

Therefore, when the dies are set on a machine, a good attention should be paid to keep the top surfaces of both dies in the same plane, parallel to the x-y plane.

iii) The die clearance D_c in the y direction has to be set next. The die clearance at the supplied point (where a rolling starts) is decided by the smoothness of the initial forming at the first contact of a blank with dies. But the clearance D_c set and measured under static condition and the D_c during rolling are different. It is affected by the rigidity of machines and the relative geometry between the diameter of the blank and the set D_c. In order to find an appropriate D_c, a special measurement is needed as follows:

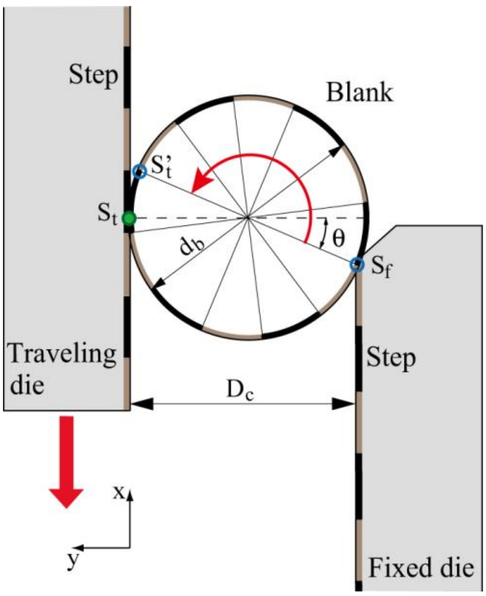

Figure 5 Dies adjusting in SLB rolling

Figure 5 shows the relative location of a blank and dies at the instance when a rolling has just started. It is assumed that there is no relative slip between a blank and dies. Plastic deformation of the blank by the traveling die starts at the point S_t, and the one by the fixed die at S_f. After a half turn of the blank, the arc length deformed by the traveling die will be a half circle, $\pi \cdot d_b/2$. The length by the fixed die, on the other hand, will be shorter than $\pi \cdot d_b/2$ by $\theta \cdot d_b/2$.

If we repeat several test rollings and record the initial set value of D_c, the theoretical value of $\theta \cdot d_b/2$, the actual length of $\theta \cdot d_b/2$ and the smoothness of rolling, we can estimate the best clearance for steady rolling.

iv) The die clearance at the finishing point can be decided based upon the completeness of forming at the crest of the screw thread as the same work as the conventional screw rolling.

v) Finally, when the number of steps in a pitch is an even number, the points on the blank S_f and S'_t, that is the opposite point of S_f, should be the same step pattern as shown in the figure, although the lead is shifted by a half pitch to the z direction. The starting point on the traveling die S_t can be calculated geometrically. Then the traveling die position in the x direction should be set precisely at the calculated position.

Following the above procedure the designed screw helixes with stepping lead are produced reliably. The mass production of the SLBs becomes realistic and practical.

5 Measuring and evaluating the SLB helix shape

The anti-loosening performance of an SLB depends on the shape of the step segments on the screw helix. In order to verify the adequacy of rolling conditions the shape has to be measured easily, quickly and accurately. The authors developed a portable measuring device for M8 SLBs as shown in **Figure 6**. It is palm-sized and 1.7 kg in weight. A rolled SLB is set in the internal screw of the device and is rotated by a handle. A variation in the screw lead is measured by a linear gauge and the rotating angle by a rotary encoder. The data is recorded every 50ms on a data logger.

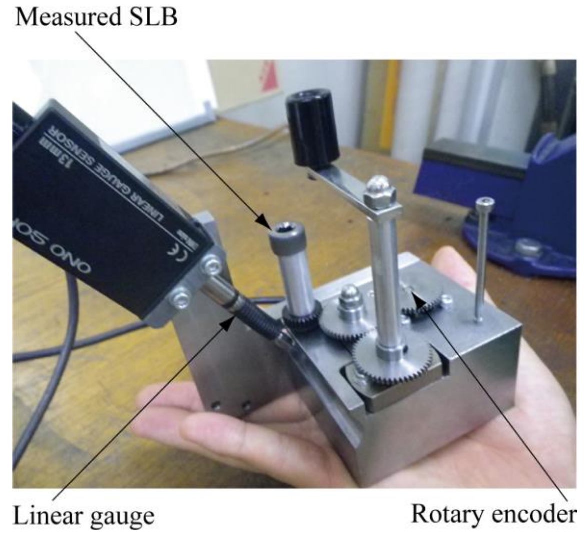

Figure 6 Measuring device for the SLB helix

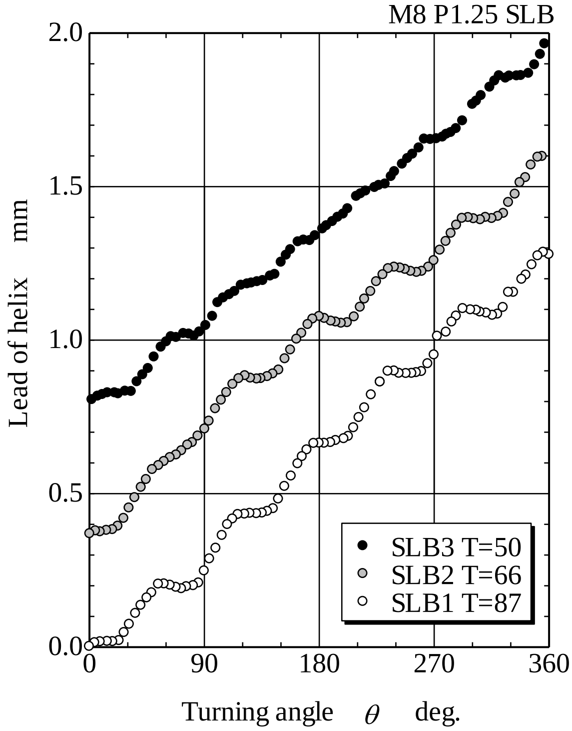

Figure 7 Lead of helix of the SLBs

On the measurement of conventional bolt screws, the value obtained from the linear gauge does not vary across the turning angles. In case of SLB's, the value changes with the turning angles, showing triangular waveforms. The value of the linear gauge is converted into the displacement in the axial direction of the bolt. When the average inclination of the helix is added to the displacement, the lead of the SLB helix is obtained.

Figure 7 shows the examples of the measurements of M8 SLBs with the pitch of 1.25mm produced in various conditions. It is clear from the figure that the SLB1, which is produced in an appropriate condition, has six distinct step segments in a pitch. On the other hand, in the helix of the SLB3 some step segments are barely observed. A change in the rolling conditions makes a big difference in the shape of the screw helix.

The measured helix shape must be evaluated objectively to decide if the rolling condition is suitable. The most important factors in the SLB helix shape for anti-loosening ability are the length and the angle of the step segments. The authors devised a method to evaluate the helix shape based on these two factors. The method is a scoring system as explained below.

Firstly, the difference of the leads between two consecutive data is taken and divided by the circumferential length between the two data. The obtained value shows the local inclination between two points on a helix thread.

Secondly, we introduce a threshold in order to judge if the inclination at an interval is considered to be on the step segment or not. When the inclination at an interval is smaller than the threshold, the interval is accepted as a part of a step segment and is given an evaluation score. The bigger score is given to the smaller inclination, in other words, to a flatter interval. When it is larger than the threshold, the interval is judged as a part of an inclined segment and is given zero score.

Thirdly, all the scores of every interval from 0° to 360° are added up. It is defined S_a. On the other hand, an ideal SLB with perfect step segments with 0 inclination is assumed. We can calculate the score of the imagined SLB in the same way. The value is defined S_i. If we introduce a factor T defined by

$$T = (S_a / S_i)\cdot 100,$$

T represents the quality of an SLB. As the thread shape of a rolled bolt approaches the ideal one, the value T becomes closer to 100.

The evaluation factor T thus determined for the 3 examples are as shown in **Figure 7**. The factor T seems to be indicative of the anti-loosening ability of the SLBs.

6 Change in the helix shape

The traveling die position in the x direction is also a sensitive factor for forming good step segments on the helix. Hundreds of SLBs were produced under various traveling die positions, and examined based on the change in the helix shape and the evaluation factor T.

The specifications of the SLBs examined were as follows: the screw is M8 with the pitch of 1.25mm, the allowable major diameter is 7.760−7.972mm, which corresponds to the medium quality of ISO standards. The material is chrome molybdenum steel. They are produced by the rolling machine THI-10 made by Sanmei works Co., Ltd. All of the rolled SLBs were quenched in 360 HV.

The average of the evaluation factor *T* of rolled screws and the standard deviation σ of the factor are shown in **Figure 8**. The traveling die position of zero on the x-axis is the reference position, which is calculated geometrically as mentioned in Section 4.

On the contrary to our expectation the SLBs with good shape of helix were able to be produced under a wide range of the traveling die position from -1.80mm to +0.8mm, not only at the reference position. The standard deviations are very small in this range. It means that, no matter where the die is in the x direction, a smooth rolling will be pursued. This phenomenon is considered as follows;

Although the initial relative position of both dies doesn't exactly match with each other, their positions are naturally harmonized during the later stage of a process. Therefore, the blank must be slipping on the dies little by little during the process. Then the blank is getting into the right position automatically because the required energy for plastic deformation is least there.

However, burrs and chips are noticeable on the screw thread produced at 0.4mm or more away from the reference position. The traveling die should be adjusted at the reference position with a tolerance of ±0.20mm.

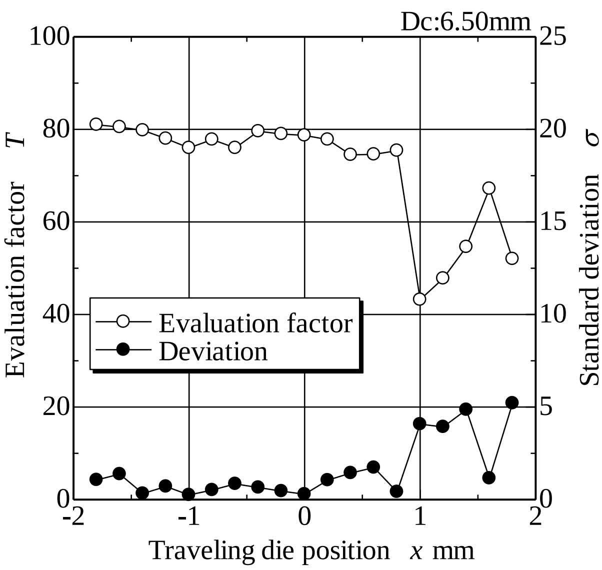

Figure 8 Change in evaluation factor

7 Anti-loosening ability with the helix shape

In order to investigate the relation between the quality of the helix shape and its anti-loosening ability, SLBs with various shapes of helix were produced, and evaluated by the system developed in the former section.

The anti-loosening abilities are examined by the displacement-based loosening device [3] given in **Figure 9**. This device rocks (or vibrate in other words) a testing screw fastener in the direction perpendicular to the bolt axis at the constant amplitude throughout a test. The amplitude is 0.4mm and the frequency 5Hz in this study. The initial clamping force of the testing fastener is constant at 12.79kN that is 80% of the maximum clamping force. The grip length is 27mm. The nut material is structural steel of the tensile strength 400−510MPa. The screw thread and the bearing surfaces are lubricated with molybdenum disulphide MoS_2. When the number of oscillations has exceeded 5,000 and the fastener is confirmed not to be loosened yet, the test is discontinued.

Some examples of the results of the loosening tests are shown in **Figure 10**. It is found from the figure the SLBs with the evaluation factor of 84 and 73 keep their clamping forces high even after 5,000 oscillations. (Initial loosening is observed in the beginning of every test. This is a common phenomenon to every sort of screw fastener and unavoidable.) Even the SLB with the factor of 50 can keep a high clamping force until 2,000 oscillations and 40% of the initial clamping force at 5,000. These results show that the higher the evaluation factor of an SLB is, the higher anti-loosening ability is provided. It is also clear that the SLBs with the evaluation factor of 70 or higher have an exceptional ability to prevent loosening.

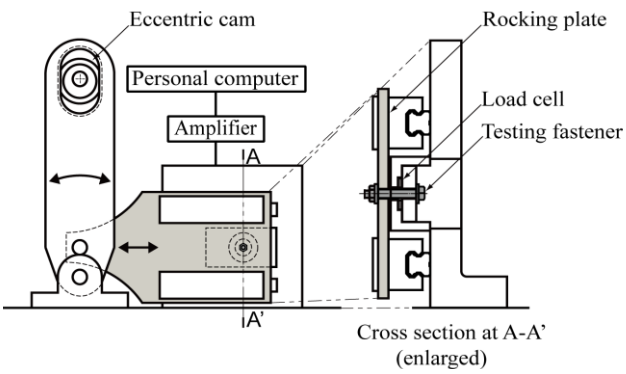

Figure 9 Displacement-based loosening device

Loosening of screw fasteners are, in many cases, caused by a deficiency of the initial clamping force. On the assumption that the initial clamping force is not applied adequately, a series of loosening tests was carried out in smaller clamping forces to the SLBs. The average evaluation factor of the tested SLBs is 78.

As shown in **Figure 11** the SLBs don't loosen in the smaller initial clamping forces, even in 2.9kN that is 20% of the maximum clamping force. As mentioned above the SLBs produced properly have extremely high anti-loosening ability. Most troubles caused by loosening of screw fasteners would be prevented by the SLBs.

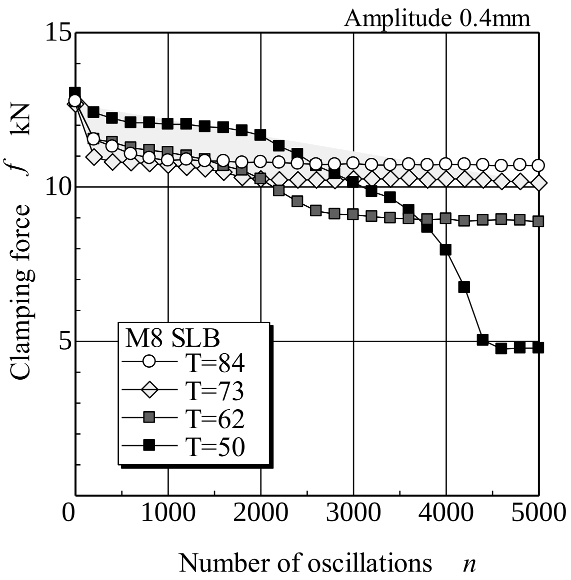

Figure 10 Change in anti-loosening ability with quality of screw helix

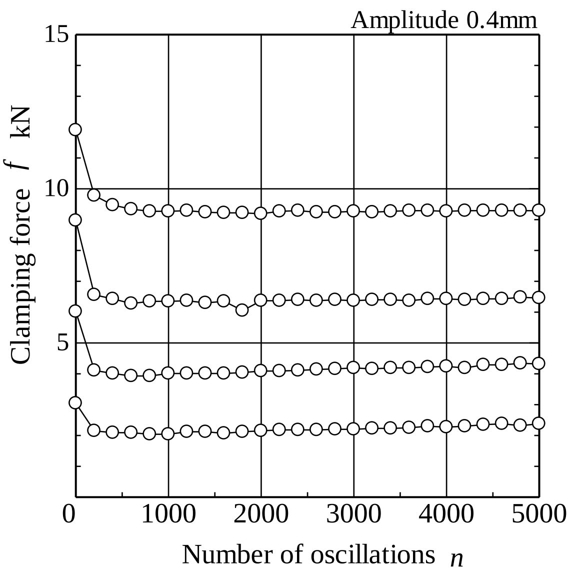

Figure 11 Anti-loosening ability with initial clamping force

8 Conclusions

It has been confirmed that the step-lock-bolt, SLB, has high anti-loosening characteristics. The next to be done is to establish a convenient procedure to produce it in a mass production scale. In this paper, a production method and a quantitative evaluation method were discussed and loosening tests was pursued. The following conclusions were obtained.

(1) A flat-die rolling process is appropriate to produce SLBs in mass production. Because some careful adjustments in setting the dies are requested, a procedure is proposed. By following the proposed procedure the SLBs are able to be produced accurately.

(2) A rolled screw has to be checked if the step segments are accurately formed. A device which can evaluate the helix shape based on the length and the angle of the step segments was developed.

(3) Hundreds of SLBs were produced and examined. The result showed that, once the dies are set fulfilling the key conditions, good SLBs are rolled unfailingly in stable manner.

(4) The SLBs produced by a flat-die rolling have high anti-loosening ability even when the clamping force is not high enough.

Acknowledgements

The authors would like to thank Mr. M. Nishoji and Mr. Y. Yamazaki for their assistance on the production and the measurement of the SLBs. We also wish to acknowledge valuable advice and reviewing this paper to Prof. H. Fujii of Gifu University.

References

[1] N. Sase, K. Nishioka, S. Koga and H. Fujii: An Anti-loosening Screw Fastener Innovation and Its Evaluation. In Journal of Materials Processing Tech., Vol. 77/1-3, pp. 209-215, 1998.

[2] H. Fujii and N. Sase: Have We Ever Prevented Screw Fastener from Loosening?. In Proc. of the CSME FORUM 96, Vol.1, pp.15-24 Toronto, Canada, 1996.

[3] N. Sase, S. Koga, K. Nishioka and H. Fujii: Evaluation of Anti-loosening Nuts for Screw Fasteners. Journal of Materials Processing Tech., Volume PRO 056/1-4, pp.321-332, 1996.

Innovative technologies

Electronic product cleaning by using various CO_2 based cleaning technologies

M. Bauer[1], S. Schweinstig[1], S. Thäter[2] and R. Steinhilper[2]

[1] *Fraunhofer IPA, Germany*
[2] *Bayreuth University, Germany*

Abstract

Regarding the automotive industry, the trend of substituting mechanical products by mechatronic and electronic ones becomes apparent. Correspondingly, the requirements for the industrial sector of remanufacturing have to be adapted, too. Modern electronic products are coated with sealants like silicone gels in order to protect them against external / environmental influences and undesirable access. Therefore, the demand for clearly defined specific processes increases. Here, especially the topic of technical cleanliness has to be considered. The research project eCleanER is exploring new cleaning technologies and equipment to remove these sealants by using various CO_2 based cleaning technologies. Beside the relatively high technical effort, cleaning with CO_2 shows lots of advantages. Used in solid phase as ice pellets or as snow it is an environment-friendly (lightly) abrasive cleaning medium. Modern processes using CO_2 in supercritical phase provide a good solubility of organic substances. Moderate temperatures as well as a simple regeneration of the loaded gas through expansion shall be mentioned.
Initial findings, in the field of electronic products cleaning, on the applicability of CO_2 in various forms like CO_2 pellets, CO_2 snow and supercritical CO_2 are presented in this paper.

Keywords: MIT&SLIM2013, remanufacturing, electronic, cleaning, CO_2 pellets, CO_2 snow, supercritical CO_2, technical cleanliness.

1 Introduction

Remanufacturing is the industrial recycling process to restore used products to an “as good as new” condition [1][2]. The worldwide remanufacturing industry represents about 100,000 companies with a turnover of approximately 100 billion Euros [1][3]. By applying a second product life cycle for individual products, remanufacturing saves up to 95% of material as well as energy consumption in comparison to the production of new products [2]. Due to less material and energy consumption the remanufactured products can generally be offered about 45% to 65% of equivalent prices of new ones [2].

In the production of new complex automotive products, the process step cleaning is one of the challenging tasks. It is important to achieve a defined technical cleanliness level to assure the quality of, for example, adhesive bonding. The achieved approaches and procedures for characterizing the state of technical cleanliness made it to the comprehensive standardization document VDA Volume 19. The cleaning processes in the production of new products are constantly adjusted.

In remanufacturing the cleaning process is also an important task. The challenges especially in remanufacturing of mechanical products in context of cleaning and technical cleanliness were taken up and explored in the research project CleanER - cleaning engineering for remanufacturing. These results already have been published in the paper "Technical cleanliness in Remanufacturing - an ambitious task" as well as in the PhD-thesis "Technische Sauberkeit in der Refabrikation" [4][5]. These results cannot be transferred one-to-one to the field of electronic products. This is due to complex contaminations such as sealants or extremely sensitive components, for example wire bonds on circuit boards.

To ensure a sustainable remanufacturing of electronic products, they must be thoroughly cleaned. This occurs during step 3 of the six-step remanufacturing process chain of mechatronic systems according to Steinhilper, which is shown in Figure 1 [6].

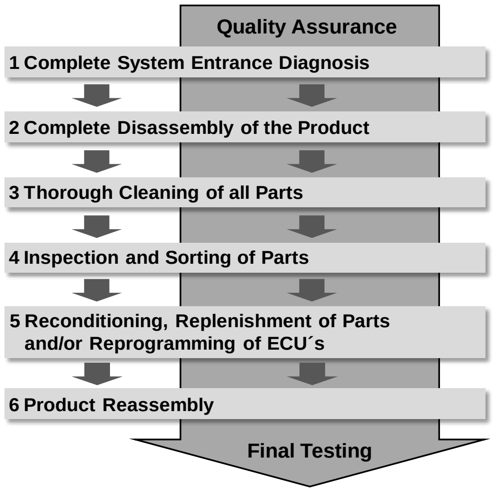

Figure 1 Remanufacturing process chain of mechatronic systems [6]

Unfortunately, there is currently no established cleaning process which ensures a thorough removal of different sealants.

Therefore, within the German research project eCleanER (electronic component cleaning engineering for remanufacturing), which is founded by the German Federal Ministry of Economics and Technology, scientists at Bayreuth University and Fraunhofer are developing innovative cleaning processes for remanufacturing electronic products like engine control units.

2 The research project eCleanER

In the following two subsections the project eCleanER is shortly introduced.

2.1 Project scope & work packages

Within the scope of the research project eCleanER innovative cleaning processes and technical services for cleaning as part of industrial remanufacturing will be developed. With respect to Figure 2 the project aims are in detail to determine the requirements for technical cleanliness of electronic products, to develop cleaning processes, to create technical cleanliness and to analyse the cleanliness of remanufactured electronic systems.

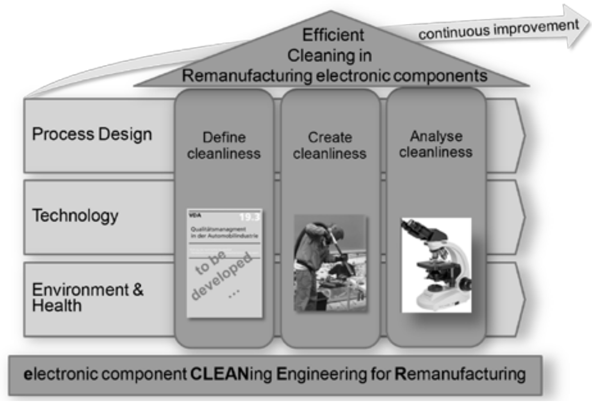

Figure 2 Scope of research project eCleanER

In order to achieve advanced and sustainable results, this research project is divided into seven work packages (Figure 3).

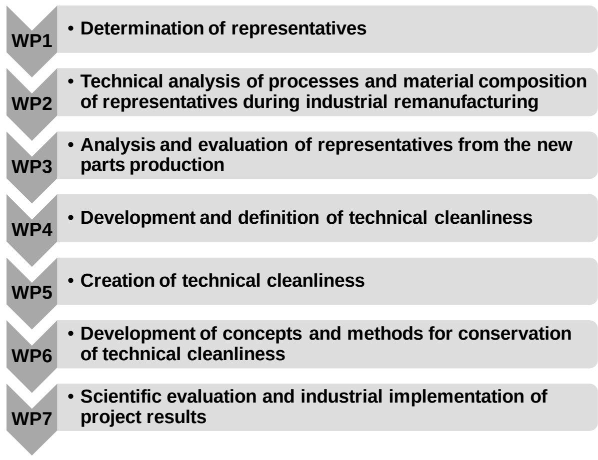

Figure 3 Work packages of the research project eCleanER

2.2 Project consortium

Facing the challenges in technical cleanliness for electronic products, a consortium of representatives from science and industry with different focus of the know-how has been formed. The consortium consists of two research institutions, Fraunhofer and Bayreuth University with extensive knowledge in the field of remanufacturing, process development and cleaning technologies. One cleaning machine manufacturer, one chemical laboratory as well as two remanufacturing companies are completing the project consortium. Additionally, the consortium is supported by the European Remanufacturers organization and an international magazine well known in this specific sector. A selection of project results will be presented in chapter 3.

3 Selected project results

The removal of unknown contaminations is a very ambitious task. Furthermore, there are a lot of different sealants in the field of automotive control units. Therefore, ten representative sealants are chosen and their substances are analysed. These results have been already published and can be found in the NEWTECH 2013 [7].

Concluding these results, the most interesting sealant is a sticky, transparent silicone gel which mostly can be found on modern ceramic hybrid circuit boards. Influencing the adhesive forces between this sealant and the circuit board by using various temperatures in the permitted range of automotive electronic components (-40 °C to 120 °C) brings no lasting effect. But a temporarily influence on the cohesive forces in the sealant can be obtained. To take advantage of this temporary embrittlement, besides the thermal influence a mechanical force is needed.

3.1 Cleaning by CO_2 pellets

The processes which combines both is the dry ice blasting. Similar to other forms of lightly abrasive blasting processes, small solid particles are transported by compressed air at extremely high speeds. But different to particles made of sand or plastic, the dry ice, with a temperature of approximately
-78 °C, sublimates instantly upon impact. Thereby a large volume of heat from the sealant is absorbed and it embrittles. Besides to the mechanical impact of following particles, the rapid phase change from solid to gas causes small shock waves to the sealant. A further surplus lies in the instant sublimation of dry ice particles. The resulting gas is non-toxic and causes itself no residues on circuit boards.

The influence of this process to a silicone sealant can be seen in Figure 4.

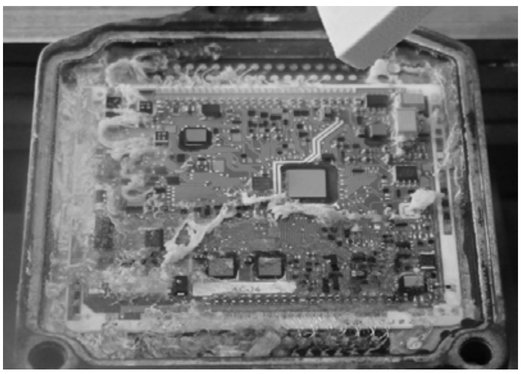

Figure 4 Usage of dry ice to remove a silicone gel sealant

In this experiment dry ice pellets with a diameter of 5 mm and a length of 10 mm were used. In the flexible tube and jet nozzle the pellets are bursting to nearly spherical particles with an average diameter of 3 mm. The pressure range of the compressed air lasts from 3 bar up to 8 bar. Very good results in removing the silicone gel can be achieved at the initial pressure of 3 bar. The use of a higher pressure is not recommended. As can be seen in figure 4, the mechanical impact of the dry ice particles harms various components on the circuit board. Especially small wire bonds in the upper area of the circuit board cannot withstand this impact. In addition, some other small components like resistors or capacitors have been blasted away. At higher pressures the obvious harm to the circuit board is no longer tolerable. Using a so called scrambler, which is milling the dry ice pellets to nearly spherical particles with an average size of 1 mm up to 2 mm shows no positive effect. The mechanical impact is still too heavy for some components. Besides these obvious harms, the thermal impact on the components must not be underrated. By using a thermographic camera the temperatures of the components and the circuit board during the experiment are recorded.

Some components are cooled down to temperatures around -50 °C, which are out of the permitted temperature range. A thermal harm to these components cannot be excluded.

3.2 Cleaning by CO_2 snow

Components on circuit boards in the field of automotive control units are subjected to a constant miniaturization. Latest ceramic hybrid circuit boards are using integrated circuits without housings. The connections are realized by tiny wire bonds made of gold with a diameter of approximately 15 µm. Due to this trend the mechanical impact on components on circuit boards during cleaning processes has to be dramatically decreased. Also the contamination through other particles and substances has to be avoided at any price. Furthermore the bare components cannot withstand this thermal impact as it can be seen at the dry ice process.

However, the good cleaning results achieved by the experiments with dry ice pellets are the basis for further experiments. For a gentle process design, following parameters are adjusted:

- mechanical impact,
- thermal impact,
- amount of external contaminations.

Using a CO_2 snow process is an inevitable consequence. Due to the fact, that instead of solid dry ice pellets, liquid CO_2 is used, much smaller particle sizes are formed. Using compressed air as a transport medium with a pressure of 3 bar, a reduced mechanical impact on the components results. Liquid CO_2 brings another advantage. A smaller volume of heat is needed during the phase change from liquid to gas. This leads to a reduced thermal impact. Furthermore liquid CO_2 out of a cylinder or a gas bottle is very pure. If needed, it can be offered with an extreme high purity. The overall amount of external contaminations can be degreased.

The influence of CO_2 snow to a silicone gel sealant on a modern hybrid ceramic circuit board can be seen in Figure 5. The process removes the sealant in an appropriate time and achieves good cleaning results. Using small injector nozzles even a partial removal of sealants is possible. The cleaning process of an area of 50x50 mm sealed by a silicone gel sealant, takes 2 minutes. About 95% of the sealant can be removed. The missing 5% are caused by complex geometries. If needed, a finishing by hand can lead to a complete cleaning.

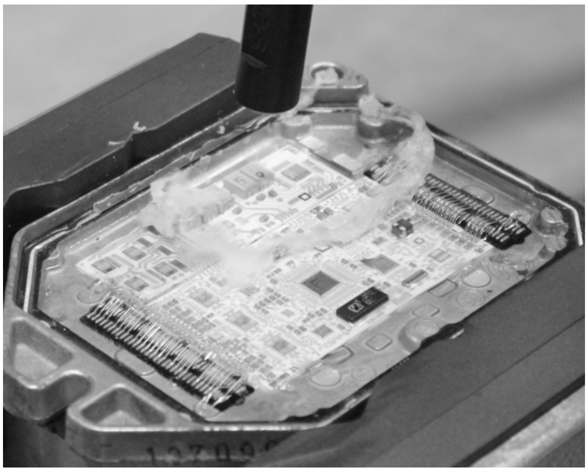

Figure 5 Usage of dry ice to remove a silicone sealant

Due to the smaller particles, the mechanical impact causes less damage to components on circuit boards. No components like resistors or capacitors are blasted away and thicker wire bonds with a diameter of about 500 µm can mostly withstand this impact. Only a few ones have been blasted away. Nevertheless, to insure the functionality all wire bonds in a section have to be renewed. Through further adjustments the mechanical influence can be decreased. Nevertheless, small golden wire bonds with a diameter of about 15 µm cannot withstand this mechanical stress.

As described, the volume of heat needed during the phase change from liquid to gaseous is low compared to the amount of the heat needed for the phase change from solid to gaseous. So the thermal impact on the components is also reduced. During the experiments the temperature is recorded by a thermographic camera. A scope of these recordings can be seen in Figure 6. Area 1, in this figure, shows the cleaned area. The cooling-down of the circuit board and its components is tolerable and in the permitted temperature range defined for automotive components. In Area 2, removed and displaced sealant can be seen. The initial state is shown in area 3.

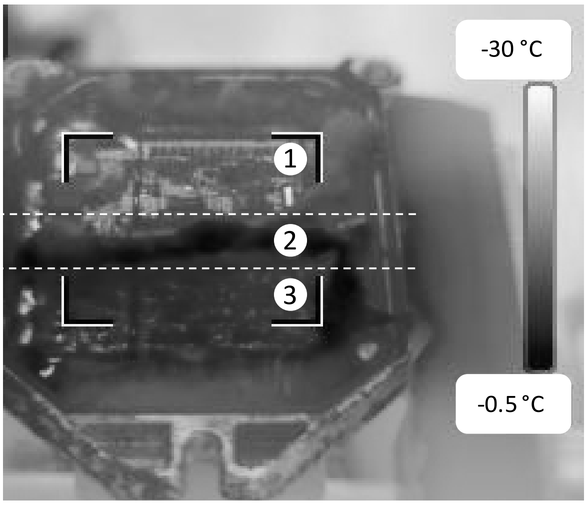

Figure 6 Thermograpic recording during the cleaning process by CO_2 snow

Using CO_2 snow offers a wide range of good opportunities in the field of silicone gel sealant removal from circuit boards. Control units up to the production year 2010 are mostly using wire bonds with diameters of about 500 µm. Hence the CO_2 snow process can be seen as a temporary solution. For the cleaning of newer control units, other processes and further developments are needed.

3.3 Cleaning by supercritical CO_2

Reducing the mechanical impact, keeping the thermal impact at a low level and keeping external contaminations in mind the number of possible processes decreases dramatically. In addition, the primary task, the removal of this wide variety of complex sealants is already a challenging task. Building on the results with classic solvents, solvent mixtures and the previous described experiments, the next step has to be the use of supercritical CO_2.

Supercritical CO_2 is formed above the critical temperature of 304.13 K (30.98 °C) and the critical pressure of 73.75 bar. The supercritical temperature and pressure range can be seen in Figure 7 [8].

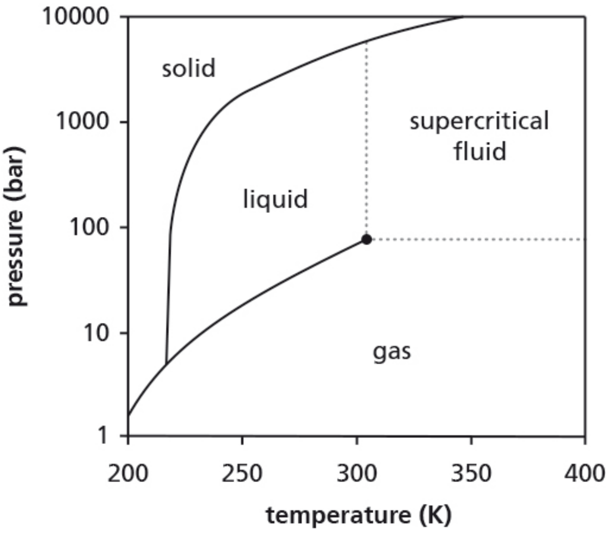

Figure 7 Carbon dioxide pressure-temperature phase diagram [8]

Supercritical CO_2 performs midway between gaseous and liquid. Furthermore it becomes a powerful nonpolar, environmental friendly solvent. Hence it is also called a “green solvent”. Nowadays it is already used for decaffeinating coffee and other tasks, mostly in the food industry.

The mechanical stress for pressure resistant components is negligible as well as the thermal impact. The characteristics of supercritical CO_2 as a solvent can be adjusted by modifying its temperature and its pressure. To enlarge the solubility of sealants different so called modifiers like ethanol or acetone can be added. An advantage of supercritical CO_2 is its flowability like a gas. Thus it reaches even small and complex geometries. If needed, a mechanical component can be added to the cleaning process by using ultrasonic oscillators.

First experiments, with silicone sealants and pure supercritical CO_2 around the supercritical point have been made. No influence of supercritical CO_2 in this configuration on silicone gels could have been observed.

In the wide range of possible options the project consortium of the eCleanER project is working to find the best parameters for removing sealants from modern circuit boards.

4 Conclusion

The cleaning process in the field of remanufacturing becomes more and more important and challenging. Especially in context of remanufacturing of electronic control units. The cleaning process has to fulfill high requirements regarding the mechanical and thermal impact on components as well as the overall input of external contaminations. Besides these high requirements, automotive electronic control units come up with an enormous variety of complex sealants as protection against mechanical, thermal and chemical influences.

The project eCleanER faces these challenges and does researches in various processes for a gentle removal of a widespread as possible range of sealants. Cleaning with dry ice is a process with a high mechanical and thermal impact on components. Despite good results regarding the removing of sealants, the caused damages to circuit boards are not tolerable. Using CO_2 snow during the cleaning process achieves also good results regarding the removal of silicone gel sealants. Furthermore the mechanical and thermal impact is less damaging. This process is a good solution for control units with a production year before 2010. Newer control units are highly miniaturized, their wire bonds are very fragile regarding mechanical stress and some integrated circuits are installed without housing.

In the field of remanufacturing new cleaning processes have to be developed to fulfill the high requirements of the future. One possible solution might be the adopting of the supercritical CO_2 process. These challenges are taken in project eCleanER.

5 Acknowledgements

The research project eCleanER is supported by a grant from the German Federal Ministry of Economics and Technology to Bayreuth University and Fraunhofer. The support is gratefully acknowledged.

References

[1] R. Steinhilper and U. Hudelmaier, Erfolgreiches Produktrecycling zur erneuten Verwendung oder Verwertung: Ein Leitfaden für Unternehmer. Eschborn: RKW, 1993.

[2] W. Hauser and R. Lund, The Remanufacturing Industry: Anatomy of a Giant; A View of Remanufacturing in America Based on a Comprehensive Survey Across the Industry. Boston, Massachusetts: Department of Manufacturing Engineering, Boston University, 2003.

[3] M. Haumann, Variantenmanagement in der Refabrikation. Aachen: Shaker, 2011.

[4] M. Junkar, J. Kopač, P.R. Levy, and O. Colak, Eds, MIT & SLIM 2011: Proceedings of the 11th International Conference on Management of Innovative Technologies & 2nd International Conference on Sustainable Life in Manufacturing, Fiesa, Slovenia, September 25th - 27th, 2011. Technical cleanliness in Remanufacturing - an amitious task. Ljubljana: TAVO, Slovene Society for Abrasive Water Jet Technology, 2011.

[5] S. Schweinstig, Technische Sauberkeit in der Refabrikation. Aachen: Shaker, 2012.

[6] R. Steinhilper, B. Rosemann, and S. Freiberger, Eds, LCE 2006: Product and process assessment for remanufacturing of computer controlled automotive components, 2006.

[7] M. Bauer, R. Steinhilper, S. Schweinstig, and S. Thäter, “Advanced Manufacturing Engineering and Technologies: Electronic Component Cleaning in Remanufacturing,” Stockholm, Schweden, Oct. 2013.

[8] M. O. Balaban and G. Ferrentino, Dense phase carbon dioxide: Food and pharmaceutical applications. Hoboken, N.J: Wiley-Blackwell, 2012.

Radio Frequency Communication – A new (service-) interface for electronic control units

R. Steinhilper[1], J. Kleylein-Feuerstein[2] and A. Reger[1]

[1] *University of Bayreuth, Germany*
[2] *Fraunhofer IPA, Germany*

Abstract

Mechatronic assemblies include electronic control units (ECUs) in general. These ECUs provide the functionalities of the assemblies via their firmware. In premium class vehicles there are up to 100 ECUs. During the entire product life cycle it is indispensable for manufactures and customer service to communicate with the implemented microcontroller. Currently communication works throughout service- or internal installed interfaces. Therefore it is necessary to open the case or to use a suitable plug for a successful data exchange. To enable a wireless communication, the new (service-) interface Radio Frequency Communication (RFCo) will be developed. Additional it will be possible to supply the microcontroller in the ECU wireless with voltage, which means wires and plugs are no longer required for communication. Besides the space saving, the RFCo interface enables a lot of innovative possibilities. For example, it will be possible to install a country-specific firmware on packed mechatronic assemblies before their distribution. Consequently only assemblies with the latest firmware will be delivered and variant diversities in production processes can be reduced. This results in a reduction of process times and production costs, while the customer satisfaction increases simultaneously.

Keywords: MIT&SLIM2013, wireless interface, electronic control units (ECUs), microcontroller, firmware, communication, radio frequency

1 Introduction

1.1 Initial situation

Several studies estimate a market share for embedded systems, containing electronic control units (ECUs), about 98% of all computer systems. Besides the automotive industry, main ECU applications can be found in aerospace technology and consumer electronics [1].

Currently ECUs have to be connected to flash the firmware with a high expenditure of time. Different firmware versions in various languages are increasing the variant diversity in early production stages as shown in Figure 1. Due to this fact the value added curve and the capital commitment increases early in the production process as well.

In order to cut costs and to reduce capital commitment, it is necessary to separate the variants as late as possible.

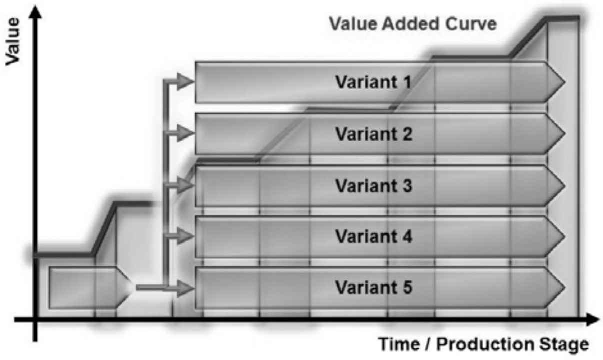

Figure 1: Variant diversity in early production stages.

Future customer requirements will further increase the variant diversity. There will be not only a demand for the latest software release, but also an individual configuration like display color and design as purchase options. In automotive and consumer market there are an enormous cost pressure, high quantities and a high rate of variant diversity. Especially the variant diversity is a cost driver and represents a very huge challenge for industrial engineering.

Such a solution has to be found, one hand to satisfy the customer demand, on the other hand to reduce the variant diversity.

1.2 About (service-) interfaces for electronic control units (ECUs)

Depending on use case, there are several prospects of service-interfaces for ECUs. To promote the benefits and disadvantages, some systems are presented hereinafter.

On-board diagnostics (OBD): In current vehicles ECUs are linked with various bus systems (e.g. Controller Area Network (CAN), Local Interconnect Network (LIN), Ethernet, FlexRay) which allow an easy access for vehicle diagnostics. In automotive engineering, OBD systems were introduced to meet exhaust regulatory requirements. Occurring errors are divided in codes and saved on ECU sustainable. These error messages could be read out in garages via standardized interfaces by skilled service personal. The data rate is highly influenced by bus system and the network length. For example, with CAN bit rates up to 1 Mbit/s are possible at network lengths below 40 m. Decreasing the bit rate to 125 kbit/s allows network distances up to 500 m [2]. In recent years there is a trend to include on-board check routines elements outside the electrical system. Increasing oil change intervals, wear measurement, traffic and road condition monitoring are recorded to reduce service or breakdown costs [3]. One application for these new services is the *Car Connect Device* from Delphi. The *Car Connect Device* records driving information over the OBD connector and saves the data in a cloud service [4].

Serial Interfaces: In the early sixty years the RS-232 interface was developed which is still in use for serial data transmission today. Because of electromagnetic susceptibility the differential serial data transfer standards RS-422 and RS-485 with common mode rejection are used. Up to the present day, the RS-standard is widely used throughout the world for ECU communication. With RS-232 data rates up to 1 Mbit/s are possible with a transmission distance of 15 m. Using RS-422 or RS-485 data rates up to 10 Mbit/s could be achieved.

Universal Serial Bus (USB): Perhaps the best-known interface is USB. Like RS-232, it was developed for the communication of computers with peripheral devices and is a widely used interface for ECUs today too. Influenced by cable quality, data rates up to 4000 Mbit/s are possible with the USB 3.0 standard.

Local Area Network (LAN): The most common standard for wiring LAN is the Ethernet standard. It is characterized by a high data throughput up to 10 Gbit/s and a cable length up to 100 m (IEEE 802.3an).

Beside the presented and other standardized systems, there are a lot of manufacturer-specific systems as well. These interface systems differ in technical specification, but there is always a need for a mechanic connection.

1.3 About wireless (service-) interfaces for electronic control units

The maximum range of wireless interfaces is highly influenced by environment conditions.

Wireless Local Area Network (WLAN): WLAN works at 2.4 GHz or 5 GHz band in general. With the standard IEEE 802.11h a maximum data throughput of 54 Mbit/s could be reached. By using Multiple Input Multiple Output (MIMO) technology data rates of 300 Mbit/s could be achieved in the standard IEEE 802.11n. Typical ranges are 25-40 m indoor and up to 100 m outdoor.

Infrared: The basic requirement for data transmission is a line of sight between transmitter and receiver. The standards for infrared interfaces were defined by the Infrared Data Association (IrDA). By using the Serial Infrared (SIR) standard, data rate up to 115.2 kbit/s could be reached, but very high rates up to 1 Gbit/s with Giga-IR are possible as well. The application range is limited to a few meters.

Bluetooth: The Bluetooth standard operates at the Industrial, Scientific and Medical (ISM) band at 2.4 to 2.485 GHz using the spread with frequency hopping at 1600 hops/s. Bluetooth is now increasingly establishing itself as a replacement for the Infrared interface. Depending on transmitting power, rages up to 100 m are possible.

The described (service-) interfaces are compared in table 1.

Table 1 comparison of existing wired and wireless (service-) interfaces.

system	nominal range	max. data throughput
wired ECU interfaces		
CAN	40 m	1 Mbit/s
RS-232	15 m	1 Mbit/s
USB (3.0)	3 m	4 Gbit/s
Ethernet (802.3an)	100 m	10 Gbit/s
wireless ECU interfaces		
WLAN (802.11h)	100 m	54 Mbit/s
WLAN (802.11n)	100 m	300 Mbit/s
Bluetooth (2.5 mW)	10 m	1 Mbit/s
SIR	1 m	115.2 kbit/s
Giga-IR	1 m	1 Gbit/s

2 Project wireless (service-) interface for electronic devices

2.1 Project scope

Goal of the project is to develop a wireless (service-) interface for devices with ECUs. The new interface is called Radio Frequency Communication (RFCo). One possible implementation is shown in Figure 2. In this implementation RFCo consists of a Radio Frequency Identification (RFID) tag and an additional memory. The RFID tag has an interface like Serial Peripheral Interface (SPI) or Inter-Integrated Circuit (I^2C) to communicate with the memory and the microcontroller. With this setup it is possible to send data from the RFID reader/writer to the microcontroller. The opposite direction from the microcontroller to the RFID reader/writer is also possible.

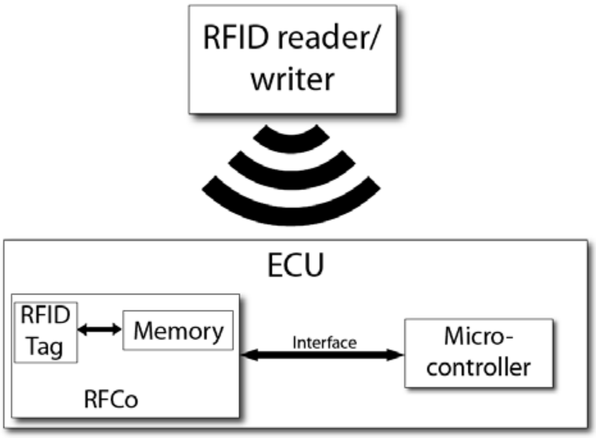

Figure 2 Possible implementation of RFCo.

Devices with electronic control units are, for example:

- Automotive assemblies (motor, transmission, steering, anti-lock braking system (ABS) and air conditioning)
- White goods (fridges, freezers, coffee machines and electric cookers)
- Consumer electronics (TVs, digital cameras and mobile phones)
- Industry machines and facilities (manufacturing robots and assembly facilities)

The required technical parameters of RFCo are shown in Table 2.

Table 2 Technical parameters required for RFCo.

parameter	value
range	1 [m]
data transfer	wireless
energy transfer	non wireless and wireless
data transfer rate	100 [Kbit/s]
number of connections to microcontroller	maximum 6
size	3 [cm²]

RFCo should be developed for three different operation purposes.

Operation purpose one: The ECU is not connected to a power supply. RFCo gets the power from a RFID reader/writer. The data sent to RFCo will be saved in an external memory. Besides RFCo the memory is also supplied by the RFID reader/writer. An external energy harvesting unit is needed for buffering the required memory energy. If the ECU is connected to a power supply the saved data is transferred to the microcontroller. One possible application for this operation process could be the parameterization of the ECU.

Operation purpose two: The ECU is not connected to a power supply. It will be possible to read and write data directly to the microcontroller. For this purpose it is not necessary to contact the ECU mechanically. Besides RFCo the microcontroller is also supplied by the RFID reader/writer. An external energy harvesting unit is needed for buffering the required memory and microcontroller energy. One possible application for this operation process could be the flashing of the ECU.

Operation purpose three: In the third operation purpose the ECU is connected to a power supply. RFCo is supplied by the ECU. The RFID reader/writer only transfers the data. One possible application could be the reading of the error memory.

For the project wireless (service-) interface for electronic devices a prototype with RFCo will be developed. The prototype will be implemented in an automotive ECU. Features of the prototype are:

- Reading error memory
- Sending and reading data
- Flashing microcontroller
- Parameterizing ECU

2.2 Proceeding and work packages

In order to achieve optimal results the project “wireless (service-) interface for electronic devices” is separated into seven work packages. The project duration is from 1st of October 2012 to 31st of March 2015. The work packages of the project are shown in Figure 3.

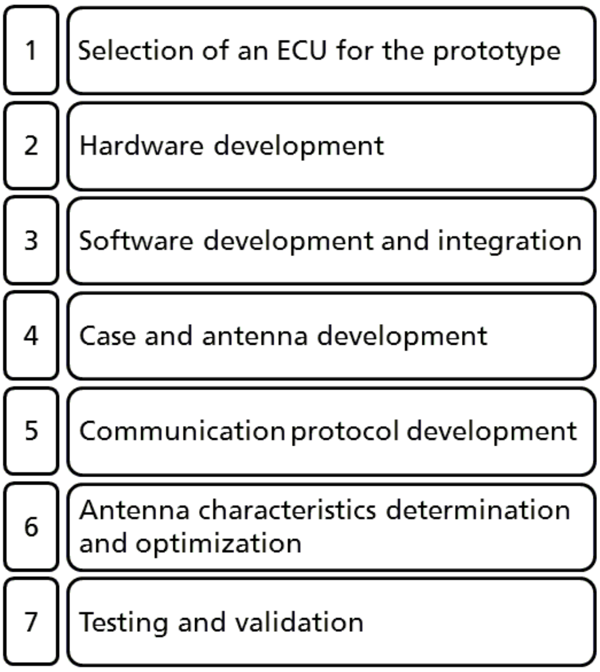

Figure 3 Work packages of the project wireless (service-) interface for electronic devices.

A selection of the first project results will be presented in chapter 3.

2.3 Project consortium

The consortium consists of two project partners.

The Fraunhofer Project Group Process Innovation located at Bayreuth, Germany has an extensive background in the mechatronic prototype development as well as remanufacturing. The Project Group Process Innovation will develop the RFCo hardware including the antenna design. Another task of the Project Group Process Innovation is the measurement of the antenna characteristics.

UG Systems located at Bamberg, Germany is a small enterprise, which is developing customized software and test systems. UG Systems will choose a prototype ECU and will develop the software as well as the communication protocol.

Both partners will be responsible for the testing and the validation of RFCo, including the final acceptance and demonstration of the prototype.

3 First project results

3.1 Hardware

RFCo consists of a RFID tag and an additional memory. The first step in the hardware development was to choose a RFID tag with the right microcontroller interface. For choosing the RFID tag it is necessary to know in which frequency range the tag should work. Therefore the possible frequencies (125 KHz, 13.56 MHz, 868 MHz and 2.45 GHz) were compared to each other. All other frequencies are reserved for other services, so it is not allowed to use them. At 125 KHz the maximum allowed power is 0.5 W and the range is about 0.8 m. For RFCo both values are insufficient. At 2.45 GHz there are many reflections so the transmittance is very low. Due to this fact 2.45 GHz could not be used, because RFCo should also work with electronic devices which are built in cases. The other two possible frequencies 13.56 MHz and 868 MHz are compared in Table 3.

Table 3 Comparison between the different frequencies.

parameter	13.56 MHz	868 MHz
range	1,5 [m]	4 [m]
worldwide	yes	no
maximum power	2 [W]	4 [W]
transmittance	good	medium
RFID mode	passive	passive and active

Besides the frequency it is also important that the RFID tag has a microcontroller interface. There are different interfaces like SPI, I^2C, CAN or LIN. The most common used interfaces are SPI and I^2C.

Matched with the technical parameters shown in Table 2 the RFID tag could work with 13.56 MHz or 868 MHz and should have a SPI or I^2C interface. For the Project wireless (service-) interface for electronic devices two RFID tags with different parameters were chosen.

RFID tag one: The Fujitsu *MB97R804B* tag has a SPI interface and works with 868 MHz. The tag also includes 4 KBytes Ferroelectric Random Access Memory (FRAM). Compared to other memories like Electrically Erasable Programmable Read-Only Memory (EEPROM), FRAM has distinct lower power consumption. The tag also needs an external antenna. For the test schematic a chip antenna, the Fractus *EZConnect (FR05-S1-R-*

0-105), was chosen. For an optimal reading and writing rate as well as a maximum power transfer an impedance matching between the tag and the antenna was needed. The antenna impedance ($Z_{Antenna}$) should be the same as the complex conjugate impedance of the *MB97R804B* (Z_{IC}). This impedance at 868 MHz is given with Z_{IC} = 36.6 – j247 Ω. In the test circuit the matching network consist of a defined wire length, inductivity and capacity. For the matching network the calculated values defined in the Fujitsu Semiconductor User Guide - FM3 Adapter Board are used [5]. In the next step a schematic and a layout was created. The developed prototype of the Printed Circuit Board (PCB) is shown in Figure 4. On the PCB there is the *MB97R804B* (1), a pull up resistor (2), a capacity (3), the matching network (4) and the *FR05-S1-R-0-105* (5).

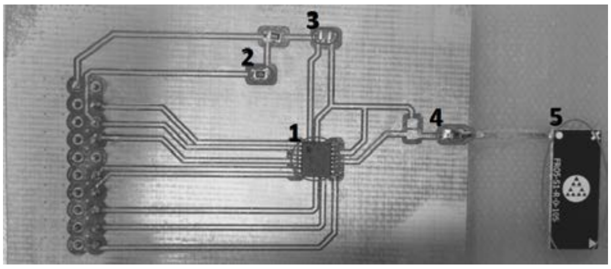

Figure 4 Developed PCB for the *MB97R804B.*

RFID tag two: The NXP *SL34011* tag has an I²C interface, works with 868 MHz and has an included 3 KBytes EEPROM memory. An external antenna is also needed. That means for the *SL34011* a matching network must be developed, too. The only known impedance was the *SL34011* impedance (Z_{IC}) from the datasheet, with Z_{IC} = 14 – j192 Ω at 915 MHz. For 868 MHz the impedance was unknown, so to assure that the circuit will work optimal the defined reference layout from NXP was used. The antenna reference designs are given in the NXP semiconductors: UCODE I2C PCB antenna reference designs [6]. Based on these values a schematic and a layout for the *SL34011* with an antenna for medium reading distance was developed. The developed PCB is shown in Figure 5. On the PCB there is the *SL34011* (1), PCB antenna (2) and pull up resistors for the I²C interface (3).

Besides the RFID tags also a RFID reader/writer device is needed. For the both RFID tags the *UHF RFID Starter-Kit Basic v2* from Beta LAYOUT is used. The kit contains a writing and reading module for 868 MHz with different antennas (near and far field). The maximum transmission power is 0.5 W.

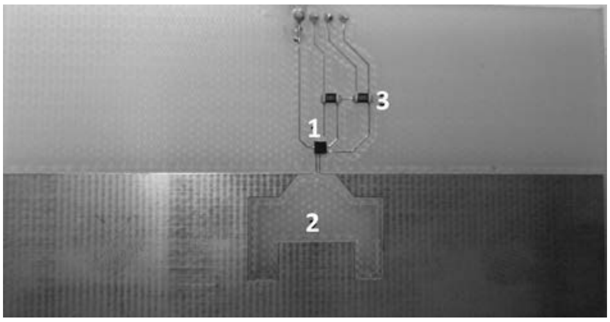

Figure 5 Developed PCB for the *SL34011* PCB.

3.2 Experimental setup

With the described hardware from 3.1 different experimental setups were built. One experimental setup is shown in Figure 6. It consists of a far field antenna, a RFID reader/writer, a Joint Test Action Group (JTAG) interface, a *STK 500* with an *ATMEGA 16* and the *MB97R804B* PCB from Figure 5.

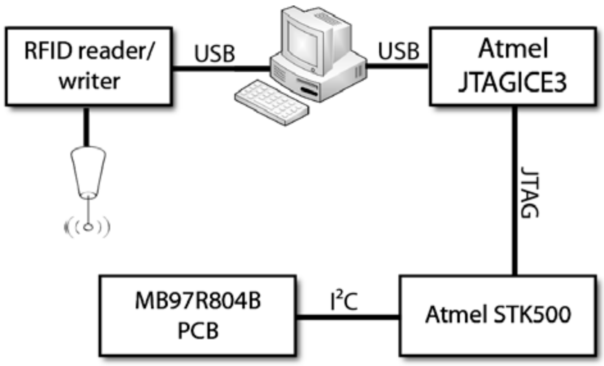

Figure 6 Experimental setup with the *MB97R804B* PCB.

With this test setup it is possible to transfer data between the RFID reader/writer and the microcontroller. It is also possible to emulate operation purpose one and three described in 2.1.

4 Conclusion

If RFCo development has finished, there are many opportunities to use this new wireless (service-) interface for electronic devices. Two applications are described here.

On the one hand it is thinkable that electronic devices get their current and country-specific firmware packed directly before their distribution. That means only devices with the newest firmware will be delivered.

On the other hand it is possible that the manufacturer could use RFCo direct in the production process of ECUs. Current ECUs will be contacted mechanically to flash them with the intended firmware. With RFCo there is no mechanical contact needed any longer.

Due to this fact the new wireless (service-) interface for electronic devices, RFCo, results in a reduction of process times and varieties, see Figure 7. This will lead to a reduction of production costs, while the customer satisfaction increases simultaneously.

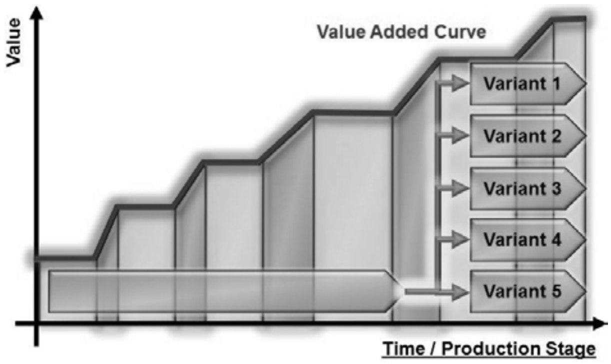

Figure 7: Reduction of variant diversities in early production stages.

The next step will be to build up the experimental setup with a better RFID reader/writer. Therefore a RFID reader/writer from KATHREIN, the *RRU4-ELC-E6* was ordered with one mid- and one wide-range antenna. This RFID reader/writer is made for industrial applications and has a maximum transmission power of 2 W. In addition an energy harvesting unit will be implemented in the existing PCBs, to realize the operation purpose two, described in 2.1.

After realizing these steps a complete ECU will be designed which supports the three operation purposes. Based on this ECU a demonstrator for RFCo will be built.

5 Acknowledgments

The project wireless (service-) interface for electronic devices is supported by a grant from the German Federal Ministry of Economics and Technology to Fraunhofer.

References

[1] J. Kohl: Effiziente Diagnose von verteilten Funktionen automobiler Steuergeräte. Technische Universität München, pp 15-17, München, 2011.

[2] W. Zimmermann, C. Schmidgall: Bussysteme in der Fahrzeugtechnik. Vieweg + Teubner, pp 133-141, Wiesbaden 2011.

[3] H.Braess, U. Seiffert: Handbook of automotive engineering. SAE International, Warrendale, 2005.

[4] Delphi introduces Unique Plug-and-Play Connectivity Service – Consumers Can Quickly Lock & Unlock Doors, Locate, Track and Monitor Vehicles via Mobile Devices. Delphi Press Release, Las Vegas 2013.

[5] Fujitsu Semiconductor User Guide: FM3 Adapter Board ADA-FM3-100PMC-RFID-TAG-1. Fujitsu, p. 9, Langen 2012.

[6] NXP Semiconductors: UCODE I2C PCB antenna reference designs. NXP, p. 27, Hamburg 2012.

Numerical simulations: An Indispensable Tool in Piezoelectric Micropumps Research

Borut Pečar[1*], Dejan Križaj[2], Danilo Vrtačnik[1,3], Drago Resnik[1,3], Matej Možek[1,3], Uroš Aljančič[1,3], Tine Dolžan[1], Slavko Amon[1,3]

[1]University of Ljubljana, Faculty of Electrical Engineering, Laboratory of Microsensor Structures and Electronics, Tržaška 25, SI-1000 Ljubljana, Slovenia

[2]University of Ljubljana, Faculty of Electrical Engineering, Laboratory for Bioelectromagnetics, Tržaška 25, SI-1000 Ljubljana, Slovenia

[3]Centre of Excellence Namaste, Jamova 39, SI-1000 Ljubljana, Slovenia

[*]Corresponding author: Tel. +386 1 4768 303, Fax +386 1 4264 630, e-mail address: borut.pecar@fe.uni-lj.si (B. Pečar)

Abstract

A complete three dimensional time domain electro-mechanical-fluid model is proposed that enabled: virtual prototyping of micropumps, detailed insight into devices operation at various frequencies, analysis of basic pumping effects, analysis of excitation signal wave-forms influence on micropumps operation and optimization of several design parameters such as optimal height and width of the throttles. The proposed model takes into account main physical effects such as inertial fluid flow, no-slip boundary conditions and hyperelastic material model for the PDMS.

Keywords: micropumps, piezoelectric actuation, numerical simulations

1 Introduction

Design, fabrication and characterization of microfluidic devices have been emerging as important research topics of the microsystem technology. Micropumps are significant components for delivering fluid and samples in microanalysis systems. Micromachined pumps are classified by actuating principles (piezoelectric, pneumatic, thermopneumatic, thermomechanic, electrostatic) or pump principles (reciprocating, peristaltic, electrohydrodynamic, electroosmotic, ultrasonic) [1, 2, 3].

An effective description and an accurate understanding of any pumping mechanism are critical, especially on the micro scale. With the existence of a comprehensive and adaptable model, accurate preproduction predictions of performance can be realized. Optimal geometries and operating parameters may be determined without the need for expensive prototyping.

Two dimensional (2D) numerical simulation models of diffuser type micropumps were first presented by Cui et al. [4] and Al-Hourani et al. [5]. 3D simulation models are more difficult to build compared to 2D models as they require more computer resources and are more difficult to solve. Additional difficulties encountered in 3D simulations are in simulations of large structures with small details (for instance check valves) that require careful meshing and solving strategies. Fan et al. [6] were able to show that the pumping efficiency at actuating frequencies over 7.5 kHz depends not only on the actuating frequencies and maximum membrane deflection, but also on its shape. Yao et al. [7] have built a coupled 3D model of a diffuser type micropump. They reported an increased numerical complexity of the model at higher actuating frequencies. An alternative to numerical modeling is to design microfluidic devices using electric circuit analogy, as recently reviewed by Oh et al. [8]. This approach however requires significant simplifications of the geometry as well as the physical phenomena.

In the present work, practical results from numerical modeling are presented. We applied numerical device simulation software, to develop a complete three dimensional model of the prototype pumps and to simulate its operation by solving a complete set of equations describing electro-fluid-solid mechanics coupling. Numerical simulation software, based on finite elements analysis Comsol Multiphysics (ver. 4.2) was used for this purpose [9].

2 Numerical simulation model

Numerical device simulation using finite elements discretization has been used for modeling operation of the pump and optimization of crucial design parameters. For this purpose a fully coupled three dimensional time dependent electro - structural mechanic - fluidic numerical simulation model is proposed. In the simulation model three differential equations are coupled and solved for seven unknowns: electric potential, three structural mechanics displacement components and three components of fluid flow velocities.

Numerical simulation software Comsol Multiphysics (Ver. 4.2a) has a special module for simulation of MEMS structures that includes piezoelectric materials. In the following a brief description of relevant equations, boundary conditions, material parameters and a solution strategy is given.

Fluid flow is described by the Navier-Stokes equation: (1)

$$\rho\frac{\partial v}{\partial t}+\rho(v\cdot\nabla)v=\nabla\left[-pI+\mu\left(\nabla v+(\nabla v)^T\right)\right]+F$$

where the left hand side represents contribution of the force acting on a differential volume of a fluid and the inertial force. v is the fluid velocity, ρ density, p pressure and μ dynamic viscosity. The above equation describing conservation of momentum needs to be solved together with equation of mass continuity which for incompressible fluid reads

$$\nabla\cdot v=0 \qquad (2)$$

Deformation of a structure due to movement of a piezoelectric actuator is modeled by structural mechanics equation for displacement vector u

$$f_{\mathrm{u}}=\rho\frac{\partial^2 u}{\partial t^2}-\nabla\cdot\sigma \qquad (3)$$

where f_u is a force acting on a differential volume and σ is a stress tensor. Stress σ and strain ε tensors are related through equation $\sigma=c_E\varepsilon$, where c_E is the elasticity matrix (determined with Young modulus of elasticity and Poisson ratio). In case of piezoelectric materials the stress also depends on the electric field E through electromechanical coupling matrix e: $\sigma=c_E\varepsilon-e^T E$. PDMS is a rubber like material and is most appropriately described by a hyperelastic model. In this work a Mooney-Rivlin two parameters hyperelastic model based on strain energy density is used [16]. Also, when piezoelectrics are mechanically deformed they induce electric charge which is written as $D=e\varepsilon+\varepsilon_0\varepsilon_{rS}E$ where D is the electric displacement vector and e_{rS} is the relative permittivity matrix. Strain tensor is further related to displacement gradient through

$$\varepsilon=\frac{1}{2}\left[(\nabla u)^T+\nabla u\right].$$

Electric field is given by a Gauss law

$$\nabla\cdot D=\rho_e \qquad (4)$$

where ρ_e denotes the volume electric charge density (in our case equal to zero). A voltage driving signal is used to deform the piezoelectric therefore a relation $E=-\nabla V$ is required with V being electric potential. Equations (1) to (4) are solved for fluid velocities, structural deformations and electric potential together with supporting relations described in the text.

3 Results

A strip-type (ST) MT pump has been proposed and operation analyzed through numerical simulation [10]. Such pumps enable compact parallel operation of several separate liquids what is of great interest in various LOCs (Lab on Chip). Simulations revealed that in this type of pumps, fluid flow is largest at largest deflection rate of the piezoelectric actuator, which occurs when the driving sinusoidal voltage signal changes sign. Similar to excitation signal, also fluid volume rate follows sinusoidal shape. However, due to different deformations of the membrane close to the throttles, a positive total fluid volume flow is achieved. From Figure 1, operation of a MT pump can be deduced as follows: Between the excitation signal and the volume flow rate at output is about a quarter period phase difference, meaning that largest volume outflow rate occurs during time of maximal rate of change of membrane deflection which occurs at times when the excitation signal changes sign. In the first quarter period, the membrane moves up and the fluid flows inside the pumping chamber. Simulations show that during this time frame more volume is pumped from the outlet side than from the inlet side resulting in negative fluid flow (shown in Figure 1 with dashed line).

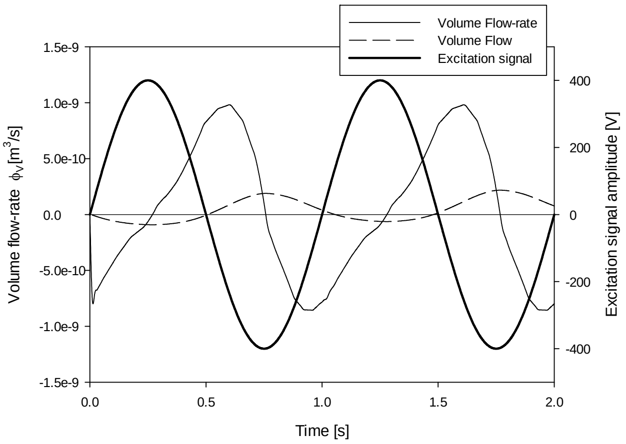

Figure 1. Time dependent fluid flow at the channel outlet, as a consequence of 1 Hz 400 V sinusoidal excitation signal.

Micropump operation details were analyzed through 3D graphs of structural deformations, pressure distributions and vectors of fluid velocity for selected time frames (Figure 2). Inside each frame a volume flow-rate at inlet and outlet at specified times is presented as well. Volume flow-rate is computed as a surface integral of a normal fluid velocity at selected cross-sections and expressed in ml min^{-1}. For positive applied excitation signal the middle part of the membrane (together with a PZT) moves upwards while the part of the membrane not covered by the PZT moves downwards. This enables widening (opening) of the channel cross-section at the left throttle and narrowing (closing) of the channel cross-section at the right throttle.

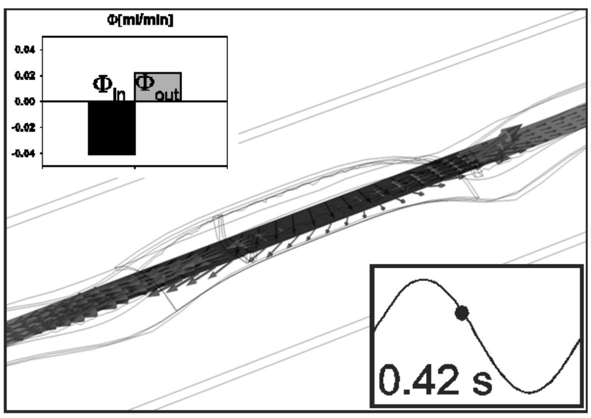

Figure 2. Structural deformations, pressure distribution and fluid velocity (vectors) for selected time frames (1 Hz, 300 V).

Figure 3 shows simulated responses of strip-type micropump on two excitation wave-forms (200V, 50Hz). Bold line represents the input excitation function, continuous and smooth enough to ensure convergence towards systemic solution. Thin line represents simulated instantaneous output flow-rate response while dotted line represents simulated pressure response at one selected point near under the micropump membrane. Simulated pressure response at selected points near under micropump membrane could become valuable indicator of micropump design suitability and might aid predict medium cavitation in real-life micropump systems.
Uncontrolled membrane fluctuations in case of saw-tooth excitation were the result of inappropriately chosen membrane and piezoelectric actuator thicknesses. In such case, incomplete deformation and uncontrolled membrane fluctuations also caused poor micropump flow-rate performance.
It was demonstrated, that membrane fluctuations could be reduced and micropump performance improved just by proper adjusting of membrane and actuator thicknesses to the actuator length.

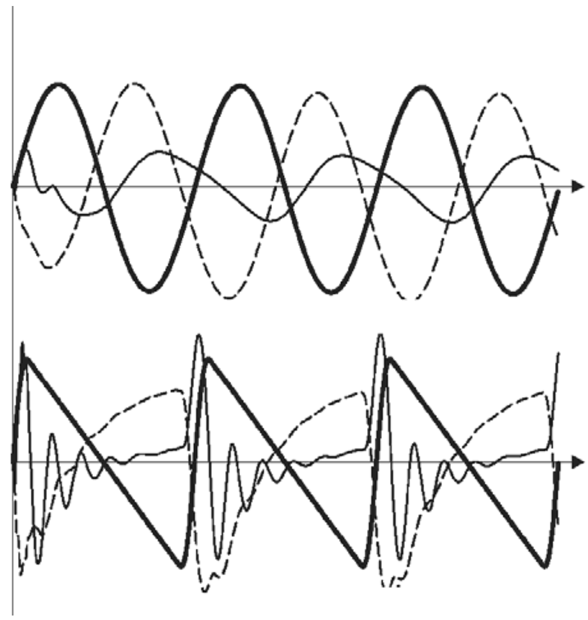

Figure 3. Response characteristics for two 200V / 50 Hz excitation wave-forms for strip-type micropump. The bold line is excitation wave-form, thin line is outlet instantaneous flow-rate, dashed line is the pressure near and under the micropump membrane.

Numerical simulation enabled virtual prototyping of the proposed device, enabling detailed insight into device operation, at various frequencies, revealing basic pumping effects, role of the excitation signal amplitude and backpressure as well as optimization of several design parameters such as optimal height and width of the throttles (Fig. 4).

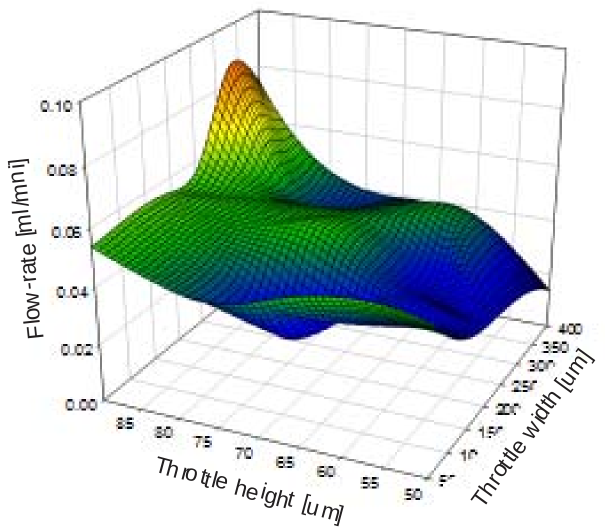

Figure 4. Numerical optimization of strip-type micropump: Outlet flow-rate vs throttles dimensions.

4 Conclusion

A complete three dimensional time domain electro-mechanical-fluid flow equations coupling enabled virtual prototyping, optimization and detailed analysis of prototype micropumps operation. The proposed model takes into account main physical effects such as inertial fluid flow, no-slip boundary conditions and hyperelastic material model for the PDMS. Micropump operation details were analyzed through 3D graphs of structural deformations, pressure distributions and vectors of fluid velocity for selected time frames. Excitation wave-form influence on micropump operation was studied in detail by simulating micropump outlet flow-rate responses on two excitation wave-forms (200V, 50Hz). Simulated pressure responses at selected points near under micropump membrane were found as valuable indicators of micropump design suitability which might aid predict medium cavitation in real-life micropump systems.

Acknowledgments

Authors would like to thank the Slovenian Research Agency/ARRS and Ministry of Education, Science and Sport for their support of this work.

References

[1] S. Shoji, M. Esashi. Microflow Devices and Systems J. Micromech. Microeng. 4, 157, 1994.
[2] P. Gravesen, J. Branebjerg, O. S. Jensen, Microfluidics a Review, J. Micromech. Microeng. 3, pp. 168-182, 1993.
[3] M. Elwenspoek, T.S. Lammerink, R. Miyake and J. H. J. Fluitman. Towards Integrated Microliquid Handling Systems. J. Micromech. Microeng. 4, 227, 1994.
[4] Cui, Q.; Liu, C.; Zha, X.F. Simulation and optimization of a piezoelectric micropump for medical applications. Int. J. Adv. Manuf. Technol. 2008, 36, 516–524.
[5] Al-Hourani, S.; Hamdan, M.N.; Al-Qaisia, A.A.; Ashhab, M.S. Fabrication and Analysis of Valve-less Micro-pumps. JJMIE 2011, 5, 145–148.
[6] Fan, B.; Song, G.; Hussain, F. Simulation of a piezoelectrically actuated valveless micropump. Smart Mater. Struct. 2005, 14, 400–405.
[7] Yao, Q.; Xu, D.; Pan, L.S.; Melissa, T.A.L.; Ho, W.M.; Peter, L.V.S.; Shabbir, M. Full Coupling Simulation of a Membrane Micropump. In Proceeding of NSTI Nanotech 2006—The Nanotechnology Conference and Trade Show, Boston, Massachusetts, MA, USA, 7–11 May 2006; Volume 2, pp. 598–601.
[8] Oh, K.W.; Lee, K.; Ahna, B.; Furlanib, E.P. Design of pressure-driven microfluidic networks using electric circuit analogy. Lab Chip 2012, 12, 515–545.
[9] Comsol Inc. Microfluidics Module User's Guide©; COMSOL AB: Tegnergatan 23, Stockholm, Sweden, May 2011; pp. 75–77.
[10] Pečar, B.; Vrtačnik, D.; Resnik, D.; Možek, M.; Aljančič, U.; Dolžan, T.; Amon, S.; Križaj, D. A Strip-Type Microthrottle Pump: Modeling, Design and Fabrication. *Sensors* 2013, *13*, 3092-3108.

Process chain for microreactor monomere replication in polymer

I. Sabotin, J. Valentinčič

University of Ljubljana, Slovenia

Abstract

Microreactors are flow-through systems containing three-dimensional structures with extremely small inner dimensions between ten to several hundred micrometers. An important part of a microreactor is a micromixer which mixes the introduced reactants in order to enable desired chemical processes. This paper deals with manufacturing process chains for producing a microreactor monomere using two types of bottom grooved micromixers, namely staggered herringbone micromixer (SHM) and slanted groove micromixer (SGM). Prototype designs were produced with micro EDM milling and experimentally tested. Appropriate process chains for tool production were identified and a direct one was realized consisting of micro milling and micro EDM milling technologies. Finally, the process parameters for microinjection moulding of polystyrene (PS) were selected for mass production of micromixers.

Keywords: microreactor, micromachining, EDM, micromilling, microinjection moulding, micromixer

1 Introduction

Miniaturization is a recent trend in analytical chemistry and life sciences as well as in non-silicon micromachining technologies [1,2]. In the past two decades, miniaturization of fluid handling and fluid analysis has emerged in the interdisciplinary field of microfluidics. A sub-domain of microfluidics is the field of microreactor technology. Microreactors are most commonly understood as flow-through systems containing three-dimensional structures with extremely small inner dimensions between ten to several hundred micrometers. Due to the small amount of chemicals needed and high rate of heat and mass transfer, these systems are an extremely efficient tool for organic synthesis as well as for process intensification [2,3]. Rapid mixing is essential in many microfluidic systems used in biochemistry analysis, drug delivery, sequencing of synthesis of nucleic acids as well as in microreactor systems [2,3,4]. Micromixers can be integrated in a microfluidic system or work as stand-alone devices.

Two well-known passive micromixer geometries are so called slanted groove mixer (SGM) and staggered herringbone mixer (SHM) [4]. The oblique grooves serve to transport fluid from the apex of the groove structure to the downstream edges of the microchannel. At the edge the fluid turns upwards towards the channel ceiling which results in a helical motion transversal to the primary flow of the fluid, causing exponential increase in the interface surface and consequently shortening the diffusion path length (Fig. 1).

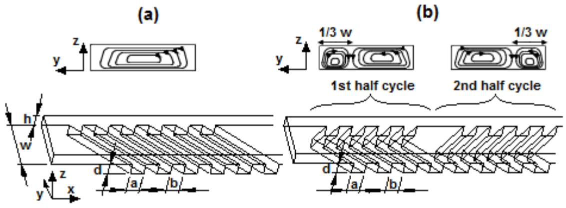

Figure 1 (a) Typical geometry of SGM and the schematic representation of streamlines in the channel cross-section. (b) Geometry of SHM and schematic representation of double helical motion caused by the groove geometry [11].

SGM and SHM geometry is readily fabricated using micro systems technologies, more precisely standard soft lithographic methods [4]. This technology can easily produce sharp corners, but high aspect ratio (depth/width) requires longer processing time. The SHM reported in the literature have a lot of shallow and narrow grooves on the bottom of the mixing channel. Additionally, lithographic methods are limited in terms of the type of material that can be used. On the other hand, micro engineering technologies can produce high aspect ratio features in a wider range of materials, in our case high aspect ratio grooves, but each feature requires additional time to be machined. The process chain proposed here allows the machining of materials with better mechanical properties, which is useful for manufacturing of mould inserts.

It is obvious that the micromixer design can be optimized for the machining technology used. Bottom grooved micromixers optimized for manufacturing with micro engineering technologies have significantly less grooves which are much deeper compared to micromixers fabricated by standard soft lithographic methods **Error! Reference source not found.**. This paper describes the technological activities related to enabling the mass production of a successful micromixer prototype design. The prototype is briefly presented and the differences in features on the prototype and the tool insert are emphasized. Various process chains for machining features on a tool insert for microinjection moulding are discussed. A direct tooling approach is found as the most appropriate and suitable process steps are selected to machine the tool insert. Finally, the microinjection process parameters are defined for a successful mass production of micromixers.

2 Prototyping and verificationion

The design of micromixers given in Fig. 2 was optimized by means of computer fluid dynamics (CFD) modelling, which implements finite element method (FEM) for solving incompressible Navier-Stokes equations and convection-diffusion equations at steady state **Error! Reference source not found.**. Prototypes were machined in steel X2CrNiMo17-12-2 with mirror like polished surface and sealed by means of a polymethyl methacrylate (PMMA) cover layer. Fastening with several screws ensured no leakage. Both micromixer prototypes have a similar mixing performance (Fig. 3), but the manufacturing of the bottom structure is more challenging in the case of SHM. Both micromixers prototypes were machined on a Sarix SX 200 micro EDM milling machine. When having deep grooves as shown in Fig. 3(b), air bubbles are formed in the micromixer, which is not acceptable. Hence, the depth d was reduced from 100 µm to 75 µm (verification results for this depth are not shown).

The performance testing was performed by using two syringe pumps (PHD 4400, Harvard apparatus) to introduce two coloured water phases into the micromixer. One phase was coloured blue (Water blue, 5 g/l) and the second one red (Congo red, 0.5 g/l). These coloured aqueous solutions provide a good contrast due to high solubility and large extinction coefficient of the dye.

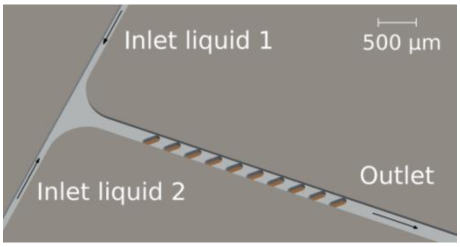

(a) SGM design of micromixer

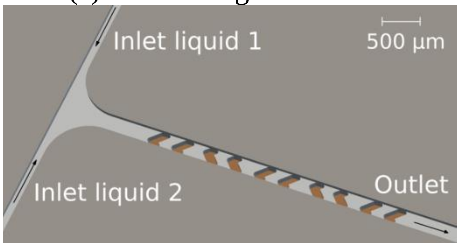

(b) SGM design of micromixer

Figure 2 Two designs of bottom grooved micromixers

A CCD camera (Image source DFK 22) was attached to an optical microscope with 100 times magnification and resolution of 4 µm per pixel. The inflow for each phase was set to 1.9 µl/min, which corresponds to an average fluid velocity of 6.3 mm/s. The results of the simulations were verified via comparison of the course of the interface between the two phases as obtained by simulation and experimentally.

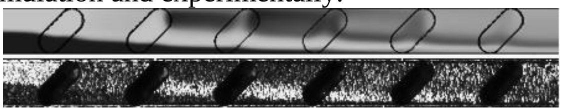

(a) SGM design, d = 100 µm

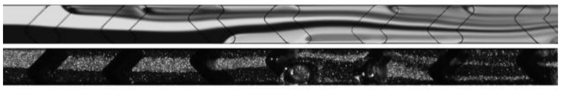

(b) SHM design, d = 100 µm

Figure 3 Two designs of bottom grooved micromixers

3 Process chain for tool insert

To implement microreactor technologies for large scale production, a lot of small components need to be assembled in a matrix to enable high volumetric flow and productivity comparable to conventional reactor systems. Bottom grooved micromixers can be massively produced by polymer embossing techniques or microinjection moulding. In both cases a tool needs to be fabricated to transfer its shape to the polymer. Depending on geometry, dimensions and surface characteristics of the micromixers' features and on the mould insert requirements in terms of mechanical strength and durability, different approaches and related process chains can be chosen for the fabrication of the tool. When material removal processes are used for the generation of the geometry, two main approaches can be distinguished with respect to tool manufacturing, as shown in Fig. 4.

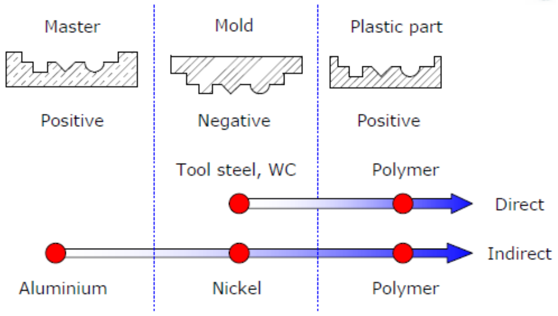

Figure 4 Direct and indirect process chain

The direct approach consists in the application of material removal processes for the realization of the mould insert from a substrate of the intended tool material. *The indirect approach* involves the use of material removal processes for the generation of the opposite geometry of the tool on a suitable substrate (e.g. Aluminium) followed by electrodeposition of Nickel and removal of the initial substrate (e.g. by selective dissolution). As the part is characterized by small cavities (channels and grooves) on a relatively large flat surface, the mould insert (opposite geometry of the part) is characterized by thin protrusions on a large flat surface. Direct machining of such a tool insert involves removal of a large amount of material.

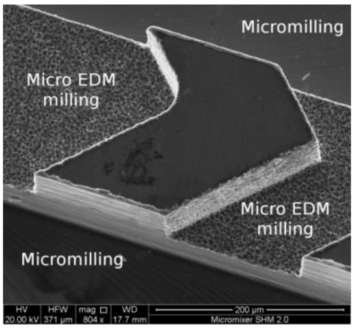

Figure 5 Image of a tool segment for microinjection moulding of SHM micromixer

A direct two-step process chain was selected for the realization of the mould insert. For the generation of the smaller features on the tool insert, namely the inclined features inside the channels, micro EDM milling was selected due to the possibility of using tool electrodes with diameters down to 15 μm, making this process compatible with the dimensional requirements of such features. However, the low material removal rate that characterizes the micro EDM milling process represents a considerable limitation when larger material volumes have to be removed. Therefore the aluminium substrate was prepared by means of a preliminary operation consisting in the generation of the channel protrusions by mechanical micro milling. The tool insert (Fig. 5) was thus produced on two machines, namely a Kugler Micromaster for micromilling and a Sarix SX 200 for micro EDM milling.

4 Microinjection moulding

The two micromixers are aimed to be used for synthesis of ionic liquids, which are used as solvents in chemical reactions due to their insignificant vapour pressure, non-flammability, thermal, chemical and electrochemical stability. Therefore, fluorinated ethylene propylene (FEP) is an ideal material for micromixers fabricated by microinjection moulding. FEP has a very good chemical resistance, similar to polytetrafluoroethylene (PTFE), and it can be processed by injection moulding, which is not the case for PTFE. Both materials contain fluorine which is quite aggressive to most standard machine tools; nickel based tools are used for injection moulding of such materials. Since the micromixers are still in the development phase, polystyrene (PS) was selected as a polymer to fabricate micromixers. PS is not aggressive to steel, but its chemical resistance is much lower when exposed to ionic liquids; still high enough for testing the manufacturing process chain. The experiments were carried out on a 15 kN injection moulding machine (Battenfeld Micropower 15).

As it is common practice, the process parameters were selected in several steps in order to obtain complete filling of the mould and a good product quality. Four injections with various process parameters were performed to find the proper parameters to fill the cavity of 700 mm³ (Table 1). Ten shots were made to ensure that the process was stable before the samples were collected.

Table 1 Process parameters of microinjection moulding

Parameter	Trial 1	2	3	4
Plunger speed (mm/s)	60	60	70	60
Holding pressure (MPa)	10	7	10	10
Mould temperature (°C)	60	60	60	60
Holding pressure time (s)	3	3	3	8
Cooling time (s)	4	4	4	9

Geometrical features important for micromixer functionality are lateral width of the groove a, groove depth d and reliable replication of the short arm of SHM grooves.

In Fig. 6 the sections of polymer parts produced by process parameters given in Tab. 1 are presented. From qualitative inspection of the figures it can be seen that the injection by the first trial yield the best results. The grooves on the edges are sharper in comparison to other trials (shown by white circle in Fig. 6(a)). A reduction of holding pressure to 7 MPa (Fig. 6(b)) resulted in less filling of the groove ridge (tool cavity between two consecutive grooves denoted). In Trial 3, an increase of plunger speed to 70 mm/s and keeping the holding pressure at 10 MPa exhibit even less filling of the groove ridge (Fig. 6(c)). It can also be observed that both the groove lateral dimension and the rounding at the groove edges at the side walls increased. Especially the roundings hinder the SHM micromixer functionality since the shorter groove arm becomes even shorter and less active in transporting the fluid laterally. In Fig. 6(d), the results of Trial 4 are presented. The groove edges on the left side of the groove are noticeably distorted due to increased holding pressure and cooling time.

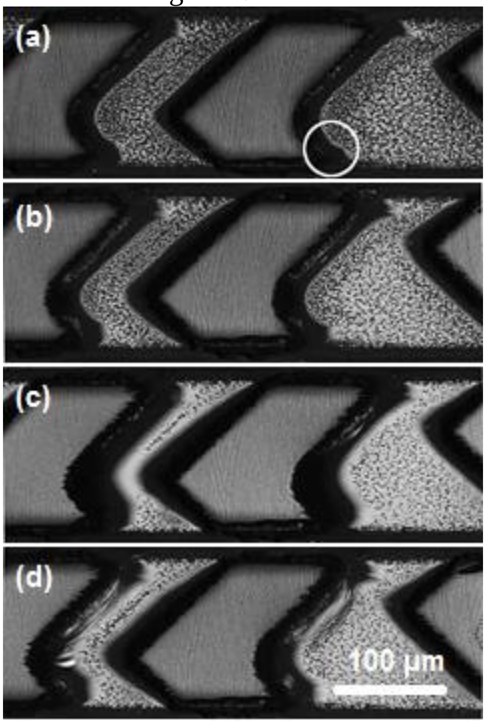

Figure 6 Microinjection moulded trials

Table 2 Comparison of measured dimensions of features for machined tool and the polymer part (Trial 1).

Feature	Tool [µm]	Polymer part [µm]
w	201 ± 2	231 ± 4
h	49 ± 1	49 ± 1
a	149 ± 2	180 ± 4
d	75 ± 1	76 ± 1

For the polymer micromixer verification purposes the parts resulting from process parameters of Trial 1 were used and the comparison in measured features between the tool and the polymer part are presented in Table 2. The dimensions were measured on five different places of the same part. Mean value and standard deviations are given.

5 Conclusions

The design of bottom grooved micromixers depends on the fabrication technology. Micromixers produced by soft lithographic processes have a lot of shallow grooves whereas those produced by micro engineering technologies have less and deeper grooves. The depth of the groove is limited by the occurrence of air bubbles in the micromixer.

The process selection for manufacturing of the bottom grooved micromixer prototype, where only a small volume of the material needs to be removed, is relatively straightforward. Manufacturing the tool insert for microinjection moulding requires either an indirect process chain or a lot of material to be removed. Indirect process chain requires nickel deposition and dissolving of aluminium master from the nickel mould, which is time consuming and thus causes additional costs. Hence, the tool insert was produced via direct process chain utilising micromilling and micro EDM milling.

Acknowledgements

Part of this work was carried out with the support of the European Community. We appreciate the support of the European Research Infrastructure EUMINAfab (funded under the FP7 specific programme Capacities, Grant Agreement Number 226460) and its partner Cardiff University.

References

[1] Alting L, Kimura F, Hansen HN and Bissacco G. Micro Engineering, Annals of the CIRP, Vol. 52, (2003), pp 635-658.
[2] Hessel V, Lowe H and Schonfeld F. Micromixers – a review on passive and active mixing principles, Chem. Eng. Sci., Vol.60, No.8-9, (2005), pp 2479-2501.
[3] Cvjetko M and Žnidaršič-Plazl P. Ionic liquids within microfluidic devices, in Ionic Liquids: Theory, Properties, New approaches, Ed. Kokorin A, Intech, (2011).
[4] Stroock AD, Dertinger SKW, Ajdari A, Mezić I, Stoone HA and Whitesides GM. Chaotic Mixer for Microchannels, Vol.25, Science, (2002), pp 647-651.
[5] Sabotin I, Tristo G, Junkar M., Valentinčič J. Two-step design protocol for patterned groove micromixers. Chem. eng. res. des. (2012).

Design of vario-therm tempering systems for injection moulding of micro-parts

D. Kobold[1], A. Glojek[1], and A. Hančič[1]

[1] Slovenian Tool and Die Development Centre

Abstract

In the past few years, injection moulding technology for production of micro polymer parts has developed intensively. Products complexity, quality and tolerances reached extremely high demands. In addition, requirements for decreasing cycle time have been constantly grown. The cycle time of producing micro polymer parts is usually, in contradictory to expectations, quite long. The reason for this is mainly mould tempering. The mould has to be heated over the recommended temperature otherwise filling of the cavity is not sufficient. After moulding phase rapid cooling is required to enable ejection of the part as soon as possible. It means that injection moulding technology for producing micro polymer parts is significantly dependant on tempering of the moulds. Mould tempering influences also on quality of micro parts. In the paper study of design and testing different vario-therm system is presented. Process optimisation is defined by use of numerical simulations and experimental moulding of developed micro featured spiral. As the most important results process parameters suitable for micro injection moulding, comparison and crucial benefits of tested vario-therm tempering systems is examined.

Keywords: MIT&SLIM2013, injection moulding, micro polymer parts, vario-therm tempering.

1 Micro-injection moulding technology requirements

Micro injection moulding is a replication technology used for producing large scale series of micro parts from polymer materials. Basically micro injection moulding process design is similar to the conventional moulding process, but due to dimensions of micro parts having width and length much larger than the thickness, specific moulding parameters are required. Usually at least one dimension of micro part measure less than 1 mm.

Consequently filling of thin walls from technology aspect is difficult, therefore for micro injection moulding low material viscosity, high strength, toughness and impact resistance of material, short injection time and high solidification speed to prevent deposition in the mould are required [1, 2, 3].

To achieve efficient production of micro parts, special design of moulds and accurate small screw diameter injection moulding machines are strongly recommended. During micro moulding process, control of various process parameters (injection time and speed, packing pressure, melt temperature, clamping force etc.) are required. Moreover, proper tempering of mould is crucial because it affects material flow and can enable efficient filing of cavity [2, 3]. Actually, cycle time as well as melt solidification also depends on mould tempering.

Due to wide range of process parameters needed to be considered at micro injection moulding use of final element methods (FEM) can give enormous support. Determination of the main moulding parameters, material flow and prediction of the shrinkage can give huge support at micro part or mould cavity design.

In the paper results of performed experimental and FEM study dealing with development of micro moulding technology for industrial use are presented. Results enable better understanding of micro injection moulding technology and are directly applicable in industry practice.

2 Description of performed work

As it was mention before tempering of the mould for micro injection moulding has vast influence on producing micro polymer parts [1, 2, 4]. As shown Figure 1, tempering of the mould for micro moulding takes 80 % of whole cycle time [2]. At conventional process the mould cooling time compared to injection and ejection time is much smaller [2].

Product surface area of micro parts is large compared to products volumes, which results in rapid heat loss from the molten material as the cavity fills, and this requires high injection speeds and high mould temperatures to avoid premature solidification and incomplete products [3]. For that reason mould for injection moulding of micro parts usually have to be heated over the recommended temperature. On the other hand, to achieve as fast as possible ejection of the parts, additionally rapid cooling have to be also realised.

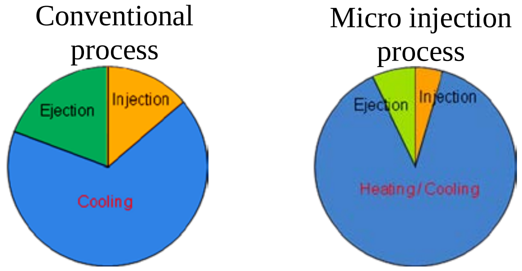

Figure 1 Moulding cycle time distribution [3].

Consequently, tempering of the micro mould consists of both heating and cooling and has enormous impact on cycle time. Efficient heating and cooling reduces the cycle time, therefore productivity is significantly increased. On the other hand, uniform cooling improves part quality by reducing residual stresses and enable maintaining dimension accuracy and stability of parts as show Figure 2.

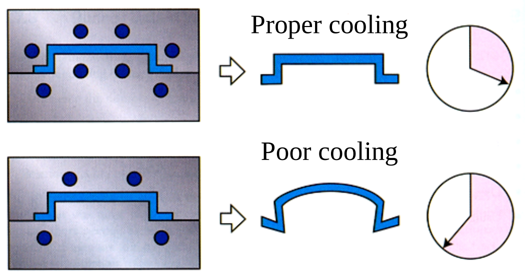

Figure 2 Potential mistake caused by insufficient cooling [3].

There is big lack of study dealing with determination of micro injection moulding process parameters, material behaviour and applicability of FEM simulations. To make step forward in this field, extensive experimental and FEM study were performed. Results and explanations of designed studies are presented below.

2.1 Experimental and FEM study design

To study influence of process parameters on material flow at micro injection moulding mini mould dimensions 130 x 80 x 75 mm for moulding spiral was developed (see Figure 3). Mould design enabled exchanging of cavity inserts which were fabricated for testing different types of vario-therm tempering systems.

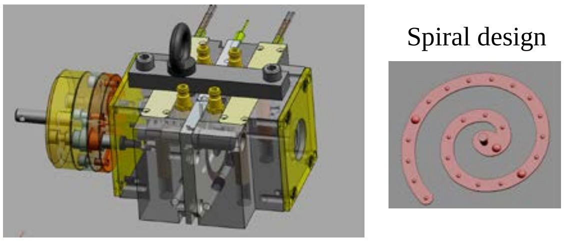

Figure 3 Mini mould for injection moulding spiral.

The spiral features thickness of 0.4 mm and length of 240 mm. Runner length was 21.5 mm with maximal diameter of 3.9 mm and taper angle of 1°. Half of the spheres were located at a distance of 10 mm enabling determination of material flow length.

Mini mould was actually designed to test five different vario-therm tempering systems:

1) Heating with hot water and cooling with cold water (conventional procedure).
2) Heating with the resistance heaters and cooling with cold water.
3) Heating with the ceramic heaters and cooling with cold water.
4) Heating with use of steam and cooling with cold water.
5) Heating and cooling with use of Peltier actuators and help of hot or cold water.

Installation of different vario-therm system was realised with use of exchangeable inserts having made cooling channels and features for locating heaters. Temperature of the mould was continuously measured with thermocouples on the fixed side, ejection side and on cavity plate of the mould.

The control of operating vario-therm tempering system was automatic and adjusted with operating parameters of moulding machine through external controller. A scheme for control operation of the vario-therm tempering system designed for electric heaters is shown in Figure 4.

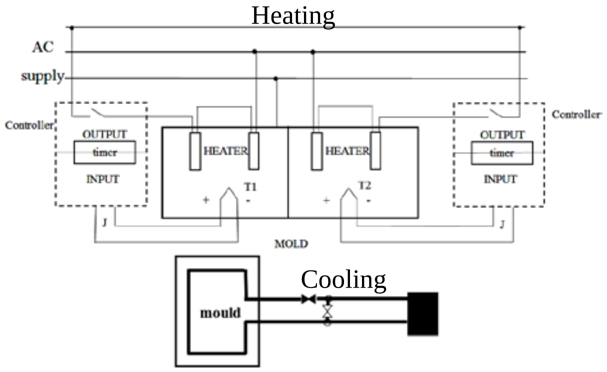

Figure 4 Scheme of the vario-therm tempering system operation control.

All listed vario-therm tempering systems were designed and produced with an aim to define what kind of tempering is the most suitable for micro injection moulding process and which vario-therm tempering system has the best heating versus cooling response. Tests were performed with use of Arburg Allrounder 170S moulding machine.

To determine response of vario-therm tempering systems temperature change on fixed side T_{n1}, ejection side T_{n2} and in cavity plate T_m located on ejection side of the mould were measured.

On the basis of measured responses the most efficient vario-therm tempering system were selected and after that used for further experimental investigation of injection moulding process by injection moulding of spiral.

For injection moulding of spiral at process parameters listed in the Table 1 polymer material PP CaC 40% (commercial name: Polifor 12CA/40 HD Natural SOFTER) was used.

Aim of these tests was to define influence of mould temperature (T_{mould}) on material flow and check how accurate can be the predictions of material flow with FEM simulations.

Table 1 Injection moulding process parameters.

Process parameters	Material parameters	T_{mould}
$P_{injection}$ = 2500 bar $V_{injection}$ = 150 mm/s $P_{packing}$ = 1000 bar (switch point at cavity pressure of 250 bar) $T_{packing}$ = 4 s	PP 40 % $CaCO_3$ T_{melt} = 220 – 235 °C $T_{ejection}$ = 108 °C	20 °C 40 °C 60 °C 80 °C 100 °C 150 °C

In experimental moulding of spiral process the material parameters listed in first and second column of Table 1 has been taken as constants, only T_{mould} has been changed according to values listed in the third column.

Actually, at conventional injection moulding of PP 40 % $CaCO_3$ mould temperature from 20 °C to 60 °C and ejection temperature of 100 °C is recommended. But in reality, vario-therm tempering process above the mould temperature of 100 °C has to be established.

At each different T_{mould} five replications were performed. That enabled evaluation of deviations and determination of average value of spiral flow length. Average value of flow length was used for comparison with FEM predicted values.

FEM simulations were carried out by using Autodesk Simulation Moldflow Insight software. Material characteristics were derived from the used Moldflow software database. Material characteristics of PP 40 % $CaCO_3$ has been previously intensively studied therefore are in Moldflow database well described. The fact is that they are obtained for conventional injection moulding process therefore performed study also gives an answer if material characteristic determined for macro level are suitable also for simulating micro injection moulding.

The second crucial parameter in FEM simulations is mesh. Tree-dimensional type of mesh was used. Per minimal thickness of 0.4 mm 12 final elements were used. Maximal size of final element did not exceed 1.2 mm (see Figure 5).

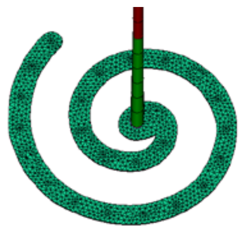

Figure 5 Tree-dimensional meshed spiral.

More detail explanation of experimental and FEM study is described in next chapter.

3 Analysis of results

Efficiency of vario-them tempering systems responses is represented diagrams in Figure 6. From the plotted diagrams the differences can be distinguished between temperature changes versus time of heating and cooling of the mould.

It is clear that ceramic heaters having power of 4 x 400 W performed best. Resistance heaters having power of 4 x 250 W needed more time to heat the mould to the maximal temperature. Heating with steam also performed well especially at the beginning of the heating due to latent temperature of steam.

Otherwise, heating with steam is not energy efficient because it needs powerful steam generator. Namely, it is necessary to make rapidly steam from water which has room temperature. At presented study steam generator reached power of approximately 2400 W.

Heating with Peltier actuators performed a little bit better than heating only with hot water (100 °C). Due to insufficient power of Peltier actuators, heating without support of hot water is useless. However, Peltier actuators make possible to achieve very efficient heating of cavity surface but on the other hand present an insulation layer for hot water heating.

For cooling down the mould cold water of 20 °C was sufficient enough for all the tested vario-therm tempering systems. Cooling with

Peltier actuators is even little bit more efficient as cooling only with water especially when is applied close to cavity surface, but on the other hand it is hard to achieve enough power of Peltier actuators for efficient industrial use [2].

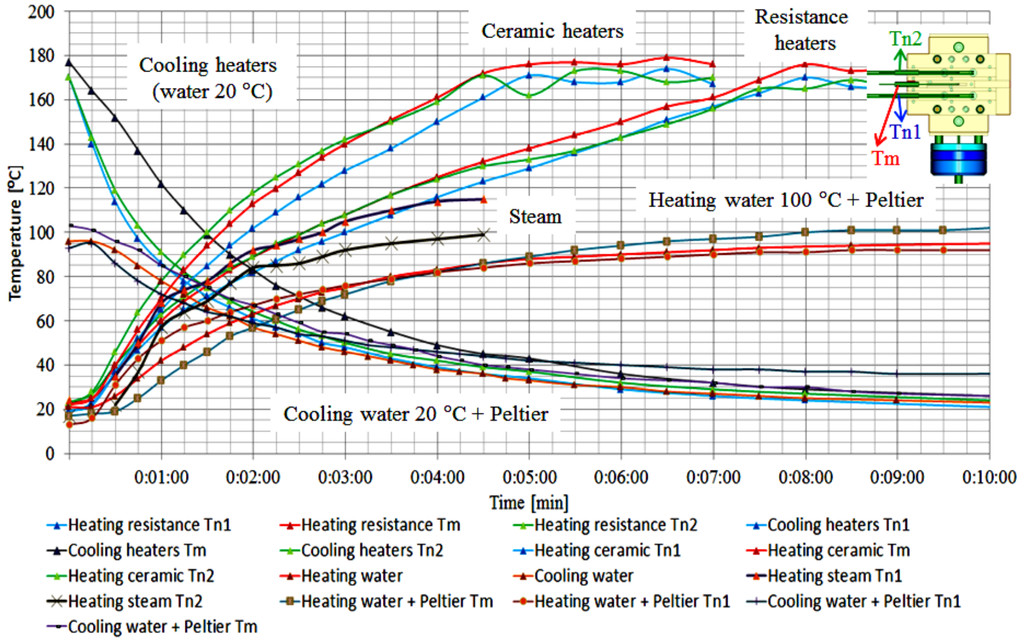

Figure 6: Vario-therm tempering systems responses.

Table 2 shown temperature gradients for heating, while in Table 3 are listed temperature gradients for cooling.

Ceramic heaters used for further studies enabled to heat mould from 20 °C to 100 °C in 2 minutes while resistance heaters needed 3 minutes to heat mould to 90 °C. Also steam performed quite well since measured temperature gradient is similar to resistance heaters. However, heating with steam is much more expensive as heating with resistance or ceramic heaters because it is needed expensive and powerful steam generator and expensive regulation of heating/cooling circuit, therefore this system is recommended only for bigger multi cavities moulds designed for producing large series of micro products.

Table 2 Temperature gradients of tested vario-therm tempering systems at heating.

	0,5 min	1 min	2 min	3 min
Resistance heaters ΔT	25	45	71	90
Ceramic heaters ΔT	34	61	98	123
Water ΔT	13	27	46	56
Steam ΔT	23	49	69	82
Water + Peltier ΔT	8	23	44	58

Cooling with cold water temperature of 20 °C enabled in 1 minute cool down of 180 °C mould for 54 °C. Recommended temperature for ejection PP 40 % $CaCO_3$ material is 100 °C. That means approximately 1 minute cooling period was applied at moulding of spiral at mould temperature of 150 °C. Heating with use of ceramic heaters took 3 minutes which means that cycle time was 4 minutes long.

Table 3 Temperature gradients of tested vario-therm tempering systems at cooling.

	0,5 min	1 min	2 min	3 min
Water (180 °C to 20 °C) ΔT	27	54	88	105
Water (100 °C to 20 °C) ΔT	11	24	42	52
Water + Peltier (100 °C to 20 °C) ΔT	9	21	38	50

For micro moulding of spiral the ceramic heaters and cooling with cold water was used. Comparison of spirals' flow lengths obtained at process parameters listed in Table 1 is shown in Figure 7.

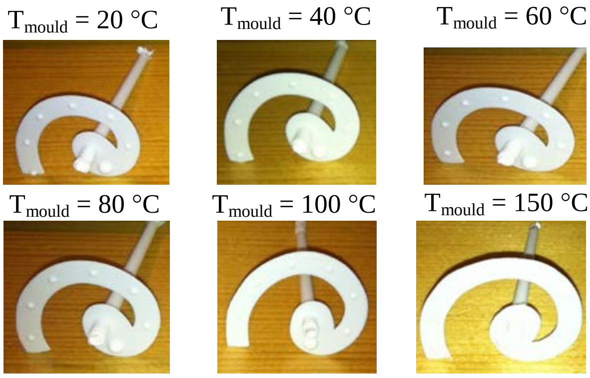

Figure 7 Comparison of spiral flow length.

For each different initial mould temperature FEM simulations were also performed. Results are presented in Figure 8 where comparison of FEM predicted and experimentally measured flow lengths are shown respectively.

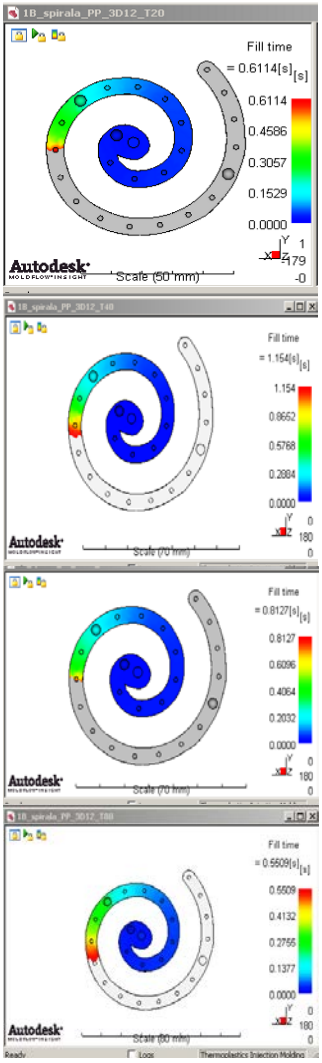

T_{mould} = 20 °C

Flow length:
- Experiment: 70.2 mm
- FEM: 120 mm

T_{mould} = 40 °C

Flow length:
- Experiment: 72.6 mm
- FEM: 121 mm

T_{mould} = 60 °C

Flow length:
- Experiment: 72.6 mm
- FEM: 121 mm

T_{mould} = 80 °C

Flow length:
- Experiment: 74.8 mm
- FEM: 130 mm

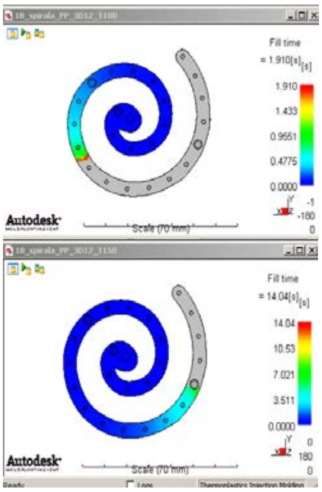

T_{mould} = 100 °C

Flow length:
- Experiment: 77 mm
- FEM: 136 mm

T_{mould} = 150 °C

Flow length:
- Experiment: 95 mm
- FEM: 199 mm

Figure 8 Comparison of spiral flow length.

It is very clear that mould temperature significantly influencing flow length and that FEM simulations' results are not close to experimental measurements. Inaccuracy of flow length prediction with FEM simulation exceeds 40 %.

Additionally, three different types of FEM computing methods and mesh types such are Midplane, Dual Domain and 3D-mash [3] with 6 final elements per thickness have also been tested. According to the obtained results applied changes in FEM models did not bring any improvements to prediction of flow length.

Diagrams in Figure 9 represent influence of mould temperature on flow length. It is clear that mould temperatures over the 100 °C influence flow length increase significantly. It is also clear that inaccuracy of FEM results is constant in respect to the mould temperature. Obviously the problem is in material properties which were derived from MoldFlow software. Material characteristics, approximations of heat transfer coefficient and rheology are at micro moulding much different as at conventional moulding process.

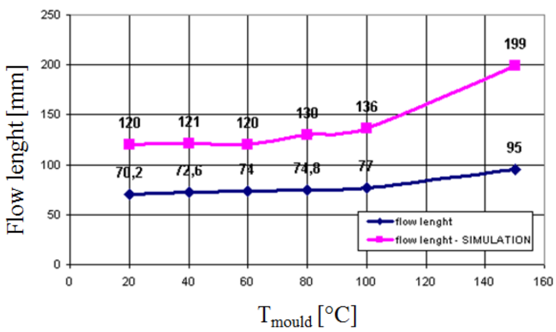

Figure 9 Evaluation of flow length versus mould temperature.

4 Conclusions

Vario-therm systems are recommended for micro moulding of complicated micro parts. Proper tempering enable producing dimensionally accurate parts with improved material flow. However, vario-therm process needs to be designed according to selected material and part dimensions. It is also clear that injection moulding cycle at vario-therm tempering exceed 3 to 4 minutes. Long cycle times have significant impact on micro parts price.

Also very important at the micro moulding technology is the issue of FEM simulations. Obtained results do not fit experimental results sufficiently. At this field a lot of new studies have to be performed which can make possible to better understand and model material behaviour at micro moulding process.

According to obtained results presented in the paper presented assumptions were obtained and can be used as guidelines for further development of FEM models. Clear is that the numerous approximations traditionally made for conventional injection moulding simulation may become invalid for micro moulding.

One example of this is the heat transfer coefficient used to model the heat flux across the interface of the polymer and mould metal [5]. Values typically used in conventional injection moulding are derived from experiments performed on typical cavity thicknesses above 1 mm [5]. These heat transfer coefficient values may not be appropriate in a simulation of the packing phase of micro injection moulding. Usually a constant heat transfer coefficient is assumed, but it cannot describe the flow through micro channels and its standard value suitable for simulation of macro parts differs substantially from values indicated for micro injection moulding [5].

Moreover, one of the main limitations encountered in micro moulding simulations relates to the fact that rheological data used in current packages are obtained from macroscopic experiments and that a no-slip boundary condition is employed with the consequence that wall slip cannot be predicted. On the other hand, standardized micro capillary rheology testing equipments and procedures are currently not available. Moreover, surface tension, neglected in macro moulding, plays an important role on the filling of micro structures but is not taken into account.

However, it is recommended that for micro moulding parts which more typically have length and width scales similar to their thickness scales three-dimensional simulation models are preferred [5].

Nevertheless, set FEM models based on tree-dimensional meshes did not give sufficient results which could be used for more efficient development of industrial micro injection moulding applications.

5 Acknowledgements

Part of the presented results was obtained within Minanotech – Micro injection mould development with efficient use of nanotechnology project financially supported by Mnt-Era.net initiative through collaboration of Slovenian Ministry of Higher Education, Science and Technology (MHEST) and The Austrian Research Promotion Agency (FFG).

References

[1] I. Catic, M. Rujnic-Sokele, M. Sercer: Influence of cavity materials on the cooling time of molding. Proceedings of 63rd Annual Technical Conference & Exibition 2005, pp. 961-965.

[2] B. Žagar: Razvoj tehnologije temperiranja s termoelektričnimi moduli in uporaba v predelavi polimernih materialov. Doktorska disertacija, Ljubljana, 2009.

[3] J. Shoemaker. Moldflow Design Guide, A Resource for Plastic Engineers. Hanser Munich, 2006.

[4] J. Shoemaker, K. Hayden, P. Engelmann: Designing the Cooling System: What´s the Relationship between Mold Material Selection, Water Line Spacing and Mold Surface Temperature Variation. Proceedings of the 64th Annual Technical Conference & Exhibition, ANTEC, Charlotte, 2006.

[5] F. S. Costa, G. Tosello, B. R. Whiteside: Best practice strategies for validation of micro moulding process simulation. Polymer Process Engineering 09: Enhanced Polymer Processing, pp. 331-364, 2009.

Advanced technologies

Powerled Life Test System

B. Uslu[1] and İ.S. Üncü[2]

[1] Mehmet Akif Ersoy University, Turkey
[2] Süleyman Demirel University, Turkey

Abstract

There have been revolutionary developments in the lighting methods and techniques with developing technology. Ten years ago, incandescent lighting lamps were used. However, today the compact fluorescent lamps are used instead. In recent years, the powerled used lighting products have been commercially available and promising. Although powerleds theoretically promise long life, reliability and energy saving –compared to the other luminaire products-, the estimated life and reliability cannot be achieved because of the situations in application such as the quality of driver circuit, temperature problems and led product quality. The estimated life of powerleds were analyzed in a different point of view except current systems. The structure of phosphorus of white powerleds was studied and the rest of led lifetime was interpreted.

Keywords: MIT&SLIM2013, Led, powerled, lighting, led lifetime.

1 Introduction

LEDs that were used first as signal and sign displayers in simple electronic circuits have started to become high power luminaries and used with the developments in recent years. LEDs, have many advantages because of their strucrural features compared to lighting luminaires which are alternatives of LEDs. The most important of them is lifetime. Current luminaires have a lifetime between 2 000 and 20 000 hours, however LEDs' lifetime is about 100 000 hours. In addition, LEDs are seen as future's lighting luminaire by many firms and experts due to their reliability, chromaticy and structural advantages.

Though the lifetime of 100 000 hours sounds great, this data should be tested whether it is wrong or not. However, it seems impossible to test this. 100 000 hours mean about 11-12 years and it is not economic and applicable to make LEDs work such a long time and evaluate. Because of this, the lifetime of LEDs is calculated by using different kind of aging models and statistical analysis.

Accelerated life methods are used in evaluating the lifetime of LEDs. In this method, the lifetime process of LEDs is being accelerated by operating much more electrical and thermal aging that LEDs will ever meet in their lifetime. Therefore, the lifetime of LEDs is determined according to statistical methods by examining the electrical, thermal and luminance ratings of LEDs [1].

In this study, the lifetime of LED lighting products and evaluation of the rest of the lifetime have been calculated by studying phosphor layer with the image processing methods.

2 Method

LEDs produce one wave light. White light is got with the combination of a few different wave lights. Therefore, white light cannot be produced with just LED directly. The production of white light with LED is done by powering on 3 different LEDs (red, blue, green) at the same time or by covering LED chip which spreads ultraviolet light with phosphor layer as shown in Figure 1 [2],[3]. This method is generally used in the production of white light.

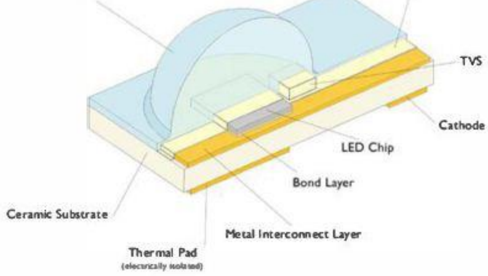

Figure 1 Powerled structure [2]

The chemical structure of covered phosphor layer changes in time by the effect of temperature and electrical current and loses its chromatic and luminance features [3]. The lifetime of powerleds has been calculated by evaluating the degradation rate on phosphor layer with image processing techniques. The degradation of phosphor layer has been done by aging LED luminaires gradually - according to determined aging rates- in prepared test box seen in the temperatures in Figure 3.

The temperature in box has been measured by four DS18B20 sensors and temperature measuring software and recorded.

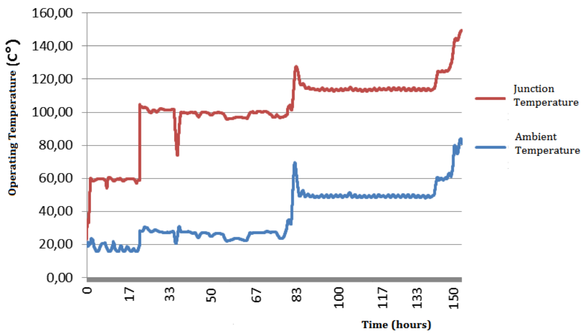

Figure 2 Powerled operating temperature

2.1 Powerled test box

The powerled test box which is 100cm wide, 80cm high and 40cm deep and has two parts as seen in details in Figure 3 has been manifactured in order to control and measure electrical, optical and temperature ratings.

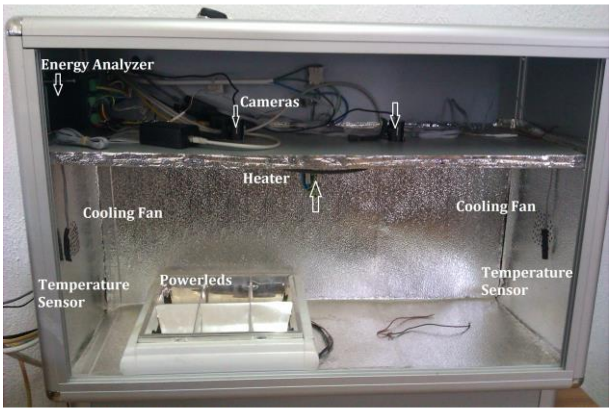

Figure 3 The powerled test box in details

The upper part of this test box has measuring sensors and devices, and below is the part that will be equipped with powerled luminaire. The above and below part of the test box have been devised as wooden and light-proof in order to prevent the effect of external lights to measuring sensors. An aluminium layer and thermal insulation in the part that LEDs placed, have been made to control and stabilize the inside temperature and to prevent temperature changings due to external effects.

The test box has been devised so that it can measure and compare the electrical, thermal and optical ratings of two lighting luminaires at the same time.

In order to provide aging and stabilize the temperature in the box, a heater and a cooling fan have been tied into the test box and a temperature control circuit with pic control have been used to control. The system of powerled lifetime test box block diagram seen in Figure 4

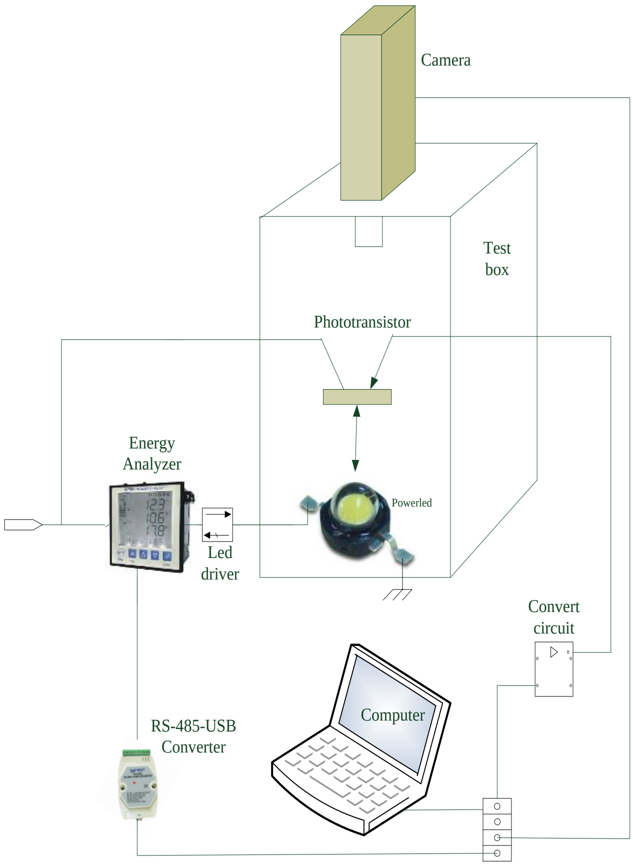

Figure 4 The system of powerled lifetime test box block diagram

2.2 Powerled monitoring software

The images taken by high-resolution cameras have been monitored instantly with the software seen in Figure 5 and the luminance image of a powerled lamp has been taken in every 5 minutes.

Apart from this software, the phosphor layers images of powerled have been recorded in every 50 hours with the USB microscope

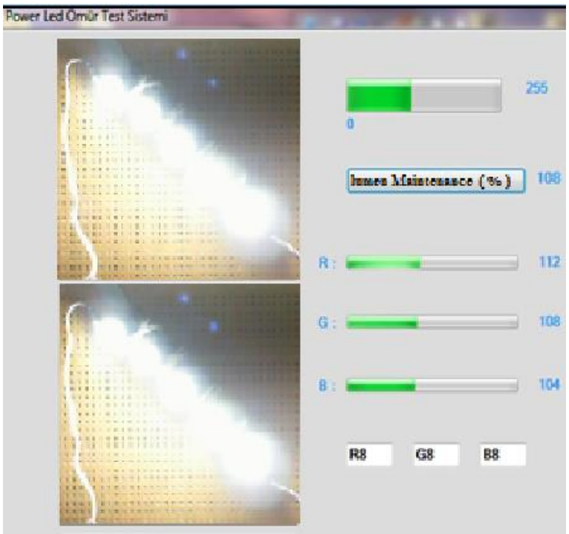

Figure 5 Powerled monitoring software

2.3 Aging models

Accelerated life-degradation test and step stress accelerated life-degradation tests which are used in aging electronic equipment are performed for powerleds because of their semi-conductor structure [1].

2.3.1 Accelerated life-degradation test (ALT-ADT)

In this method, 3 groups of materials that will be used in aging are formed. There will be 10 pieces in each group. And aging test in different levels is applied to evaluate lifetime. Aging stress can be the temperature and also other ratings about lifetime (Figure 6). Each group consists of 10 pieces and each group is worked in the stable stress level adjusted before [5]. The ratings are used in different statistical methods and a prediction is done.

Figure 6 Applying graphic of the accelerated life-degradation test [5]

2.3.2 Step stress accelerated life-degradation test (SSALT-SSADT)

In this method, one group of materials that will be used for in aging is formed and stress ratings are applied gradually. Each group should consist of 10 pieces and the stress rating is not stable in this group. The stress level is increased gradually and data is collected (Figure 7). The data is evaluated with statistical methods and lifetime is found out [5].

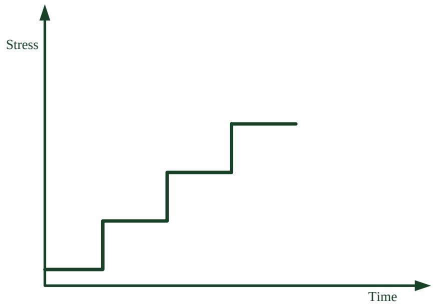

Figure 7 Applying graphic of step stress accelerated life-degradation test [5]

2.4 Applying the experiment

5 powerleds with 1 watt is worked during 150 hours intermittently without using cooling layer according to the accelerated life-degradation method. The photos of the powerled lamp have been taken in every 5 minutes and recorded using the software prepared in this study. Also, before turning on the LEDs, the phosphor layer of the powerleds has been illustrated by USB microscope at 50, 100, 150-hour intervals.

2.5 Powerled's electrical values

PowerLED's current, voltage and power values are shown in figure 8. During operation, neither current, voltage nor power value changes observed.

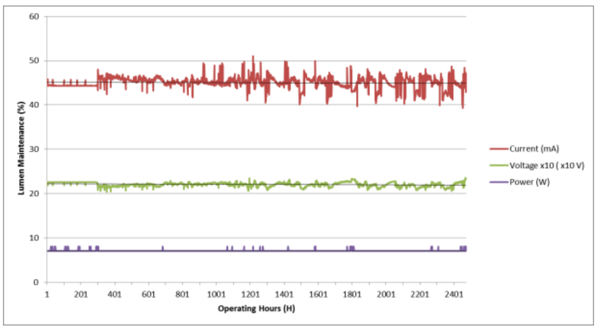

Figure 8 PowerLEDs electrical values

3 Findings

3.1 Measuring luminance

The temperature ratings have been increased gradually to provide aging powerleds (1). During aging process the phosphor layer on LED chip has been examined and illustrated. And luminance data over the image has been digitized with high-resolution cameras and image processing techniques. The luminance ratings of powerled in figure 9.

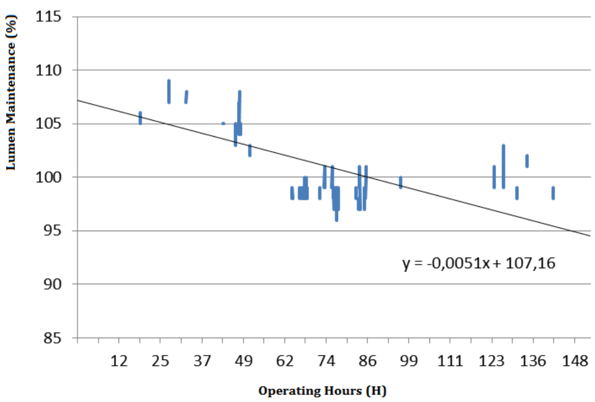

Figure 9 The luminance ratings of powerled

3.2 The phosphor layer of powerled

The recorded photos of the phosphor layer are seen in Figure 10.

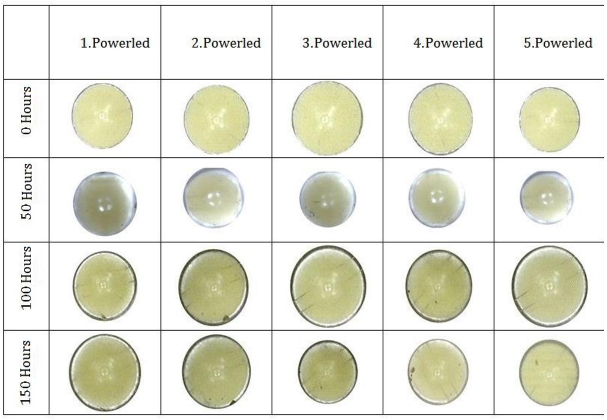

Figure 10 The photos of powerled phosphor layer

The phosphor layers of all LEDs have been arranged as shown in Figure 11. Colour histograms have been defined with the software to monitor chromatic changes of powerleds.

Figure 11 Chromatic changes of phosphor layer

Some chromatic changes have occurred around the phosphor layer in time and also some fractures and cracks as seen in Figure 12. This situation causes chromatic changes on the colour of phosphor in image.

Figure 12 The fractures and deformities on the phosphor layer

This chromatic change and deformities are about working hour of LED. The changes that happened in time on the surface of the powerled are seen in Figures 13, 14, 15 and 16 at fifty hours intervals.

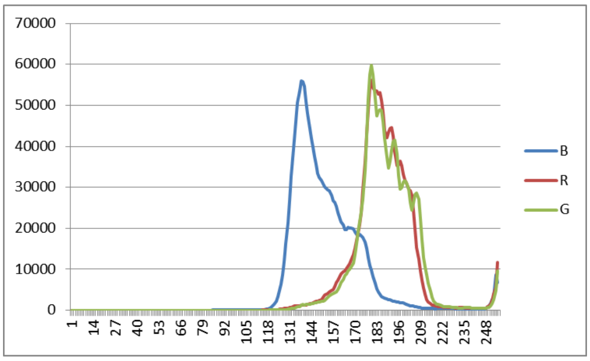

Figure 13 The colour histogram of the phosphor layer of the powerled that worked for 0 hours

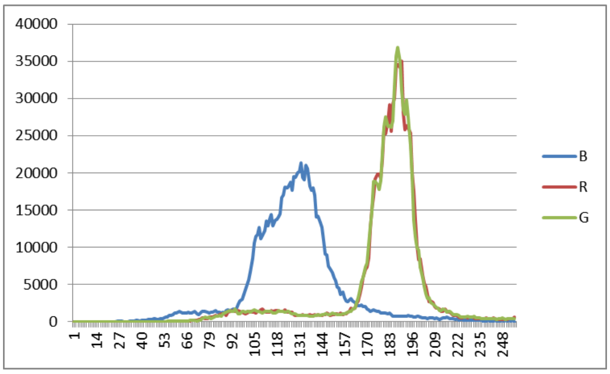

Figure 14 The colour histogram of the phosphor layer of the powerled that worked for 50 hours

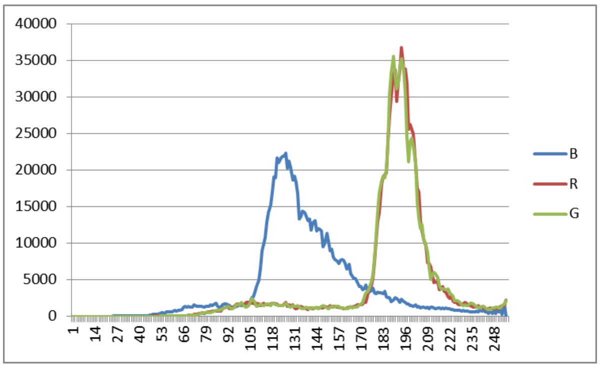

Figure 15 The colour histogram of the phosphor layer of the powerled that worked for 100 hours

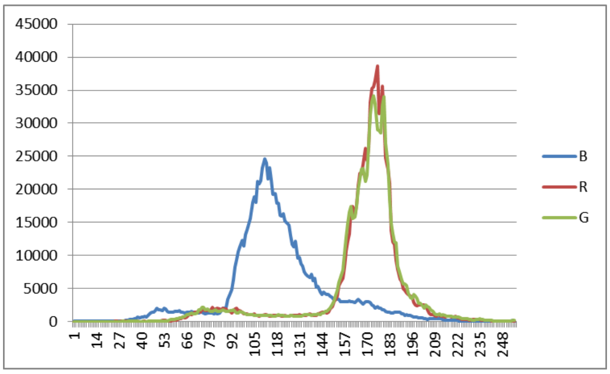

Figure 16 The colour histogram of the phosphor layer of the powerled that worked for 150 hours

When the tables above examined carefully some changes in the rates among the colours are seen in Figure 17.

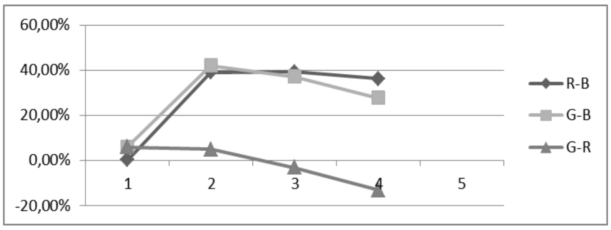

Figure 17 The change rate among the phosphor layer colours

4 Results and Discussion

When the images compared, it seen that the phosphor layer has had local chromatic changes. In addition to general chromatic changes, it has been found out that there are much more chromatic changes around the die. This situation has been evaluated and the amount of chromatic changes in the phosphor layer has been found out comparing the colour rates of the phosphor layer in the first image to the ones in the other images.

According to the result of this study it has been found out that there has been a decrease in the luminance ratings of the powerled by 12,5%, when it is powering on for 150 hours in accelerated aging conditions. Moreover, there has been a decrease in the blue colour of the phosphor layer by 40% and this causes a whiteness or darkness in the phosphor layer.

According to first 150 hours of operation no remarkable change in powerLED's current, voltage and power values are observed.

By the help of this study, it is indicated that powering on and lifetime of powerleds can be redefined by using developing image processing techniques.

Moreover, chemical changes occuring in phosphor layer should be considered. So, it will be better for reliability and evaluation of data.

References

[1] Cai, M., Yang, D.G., Koh, S., Yuan, C.A., Chen,W.B., Wu,B.Y., Zhang, G.Q., 2012. Accelerated Testing Method of LED Luminaries. Thermal, Mechanical and Multi-Physics Simulation and Experiments in Microelectronics and Microsystems (EuroSimE), 13th International Conference on, , 1-6, 16-18 April 2012

[2] Technical Datasheet DS56, Luxeon, PHILPS, 2008.

[3] Mottier, P., 2009,LEDs for Lighting Applications. ISTE Ltd, pp. 14-16, London

[4] Cree, 2011, "Hot binning", Droop, TM-21 and other 'Fum' LED Topics, pp. 13-18

[5] Jinsuk, L., Ryan, E., Changwon, S., Wesley, J., 2010. Stes-Stress Accelerated Degradation Testing (SSADT) For Photovoltaic (PV) Devices and Cells, Workshop on Accelerated Stress Testing & Reliability (ASTR), IEEE 2010, Denver, CO 6-8 October, 2010.

Chip Formation Analysis of High Pressure Jet Assisted Machining of Ti-6Al-4V

L.Yünlü[1], O. Çolak[1], C. Kurbanoğlu[2]

[1]*Suleyman Demirel University, Department of Manufacturing Engineering Isparta, Turkey*
[2]*Medeniyet University, Department of Mechanical Engineering Istanbul, Turkey*

Abstract

Titanium alloys find wide application in many industries, due to their unrivalled and unique combination of high strength-to-weight ratio and high resistance to corrosion. The machinability of titanium alloys is impaired by their high temperature chemical reactivity, low thermal conductivity and low modulus of elasticity. In this paper, we have focused on the effect of chip formation in high pressure jet assisted turning of Ti-6Al-4V. Experiments were performed under conventional (0,6 MPa) and high pressure cooling (15MPa and 30MPa) conditions using CNMG coated carbide tool insert. In this study, we have investigated the effect of chip formation in machining of Ti-6Al-4V. The experiments were carried out using a Computer Numerically Controlled machine (CNC lathe). Different value of cutting speeds and feed rates have been selected in order to study and observe the kind of chip formed. The cutting speeds selected in the experiment are 50, 70 and 90 m/min, while the feed rates range as 0.15, 0.1 and 0.2 mm/rev. The depth of cut is kept constant at 2 mm. The chips collected from all these machining parameters were taken to several chip preparation processes and then examined using scanning electron microscope. Discontinuous, chips were generated when machining with high pressure coolant, while continuous chips were generated when machining with conventional coolant.

Keywords: High Pressure Jet Assisted Machining (HPJAM), Chip Formation, Titanium Machining

1. Introduction

Titanium alloys have been widely used in the aerospace, biomedical, automotive and petroleum industries because of their good strength-to-weight ratio and superior corrosion resistance. However, it is very difficult to machine them due to their poor machinability [1]. Advanced material such as Ti-6Al-4V titanium alloy has been increasingly used for high performance application for oil and gas, aerospace and medical industries etc. However, machining of such alloy presents a great challenge due to the high temperature generation at the tool-chip interface, which lead to rapid tool wear within a short time [2]. Therefore, cutting performance of Ti-6Al-4V alloy can be improved enormously by controlling the tool-chip and tool-workpiece interfacial temperature rise and frictional effects through the use of a coolant [3, 4]. The use of a high-pressure coolant supply during machining is one of the many ways to dissipate extensive heat generation in the cutting zone [5]. Machining with high pressure coolant supply enables the coolant flow to traverse the machined surface faster, significantly increasing heat transfer of the coolant, penetrating deep into the cutting area and achieving high chip breakability through increased chip curl [6].

The formation of serrated chips (or shear-localized chips) is a typical characteristic of the machining of titanium alloys [7, 8]. These kinds of chips are favored for machined components as continuous chip get tangled and are not appropriate for automated processes. However, segmentation is also believed to be a critical aspect due to periodic variations in the cutting forces that increase tool wear rates and degradation of the machined surface finish. However, the causes and effects of chip segmentation in titanium alloys have received important attention in the aim of selecting the optimal cutting conditions to improve the production and increase both the tool life and surface quality [9,10].

2. Chip Formation Model

The study of chip formation was began in the 1930s and 1940s, based on the work of Taylor and

Mallock [10]. Since then, various Scientifics research worldwide of the industrial production, (companies aeronautic, automotive, orthopedic…) have made different chip classifications, depending microstructure, cutting speed, feed rate, depth of cut, angle of the cut, etc. [11]. Segmented chip formation is a two stage process in which workpiece material is plastically deformed ahead of the tool causing it to bulge [12]. When a critical strain level is reached catastrophic failure occurs and a shear band is formed extending from the tool tip to the workpiece surface. The resulting chips consist of moderately deformed chip segments separated by narrow bands of intensely sheared material [13]. Such a chip formation model is shown in Figure 1, 2. The direction of localized shear ϕ_{seg} can be obtained from measurements on micrographs of chip cross-sections. The instantaneous value of the shear angle ϕ may vary during the upsetting phase but reaches a value of ϕ_{seg} for the catastrophic shear phase. At higher cutting speeds this variation reduces so it can be assumed that $\phi \approx \phi_{seg}$ and hence the segment thickness $d_{ch} = d$ remains constant during the upsetting phase. The shear within each segment thus occurs along planes parallel to the adjacent shear bands [14].

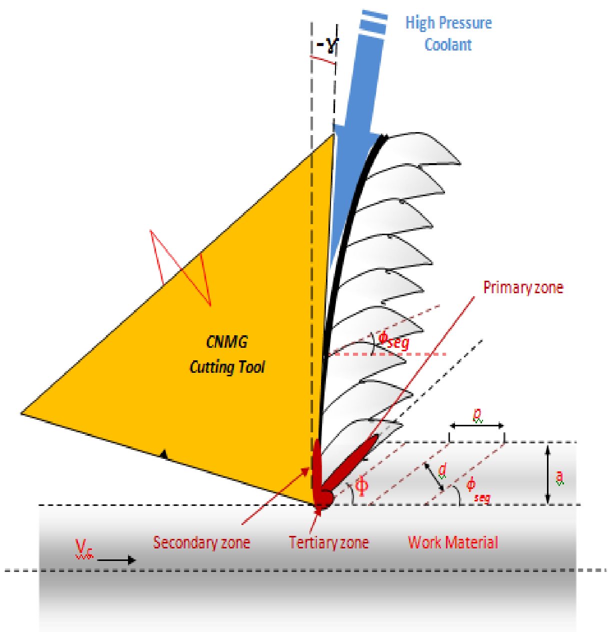

Figure 1. Schematic diagram of the serrated chip during the high pressure assisted machining.

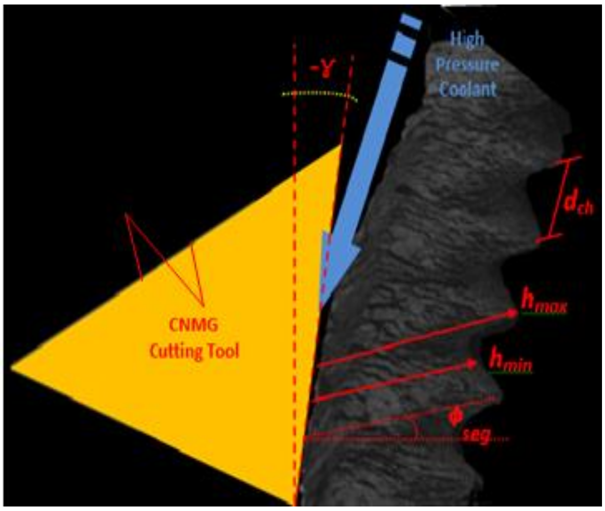

Figure 2. Serrated chip shape from experiments showing the measured parameters.

3. Analysis of the chip segmentation

Chip formation and its morphology are important features of metal machining and yield important information on the cutting process itself [9]. In order to analyze the chip morphology completely, the chips are examined under a microscope SEM. The chips were collected and polished to measure the thicknesses $h_{\max}$, $h_{\min}$ and d_{ch} the distance between each segments and ϕ_{seg} the inclination angle, as seen in Figure 1 from the values of $h_{\max}$ and $h_{\min}$, the degree of segmentation G was evaluated by:

$$G = \frac{h_{\max} - h_{\min}}{h_{\max}} \quad (1)$$

The classical model of continuous chip formation in orthogonal cutting envisages a thin shear zone inclined at an angle ϕ to the direction of cut. The chip compression ratio λ_h is defined as:

a: depth of cut,

h_c: average chip thickness,

$$h_c = \frac{h_{\max} + h_{\min}}{2} \quad (2)$$

$$\lambda_h = \frac{h_c}{a} \quad (3)$$

As As described in the introduction part, the shear angle ϕ and the inclination angle of a segment ϕ_{seg} are differentiated as shown in Figure 1 and 2. The angle ϕ_{seg} is actually measured on the collected chips while the shear angle ϕ cannot be. The angle ϕ represents the initial shear similar to the one that describes the formation of a continuous chip in the primary shear zone. Nevertheless, it may be possible to have an order of magnitude for ϕ by a geometric analysis as suggested for example by Genteand Hoffmeister [7]. Considering that an element of volume, characterized by the angle ϕ, the length p and the width d (cf. Figure 1 and 2), is the source of a segment with the inclination ϕ_{seg} and the width d_{ch}, by applying the condition of incompressibility in plastic deformation, we obtain the balance equation:

$$ap = \frac{ad}{\sin\phi} = d_{ch}\left(\frac{h_{\max}}{\cos\phi_{seg}} - d_{ch}\tan\phi_{seg}\right) \qquad (4)$$

Finally, with the assumption that the values of d and d_{ch} are close ($d_{ch} = d$), the initial shear angle ϕ may be estimated by the following equation:

$$\phi = \arcsin\left(\frac{a}{\left(\frac{h_{\max}}{\cos\phi_{seg}}\right) - d_{ch}\tan\phi_{seg}}\right) \qquad (5)$$

The frequency of serration f can be defined, as being the number of segments produced per unit time [9,13]. This frequency was obtained for a continuous chip as follows:

$$f = \frac{number\ of\ segments}{time\ of\ cutting} \qquad (6)$$

4. Experimental Procedure

The experiments were conducted on ALEX ANL-75 CNC lathe machine that is equipped with variable spindle speed from 50 to 4000 rpm and a 15 kW motor drive that is equipped with the high-pressure plunger pump of maximum 35 MPa pressure and 21 *l/min* volumetric flow rate capacity (Figure 3) [14].

The cooling/ lubrication fluid (CLF) used in the experiments was the chemical-based 5% concentration water soluble oil (Swisslube Blaser BCool 650). The high pressure CLF was injected between the cutting tool and formed chip back surface, at a low angle (about 5 to 6° with the cutting tool rake angle), as is shown in Figure. 3

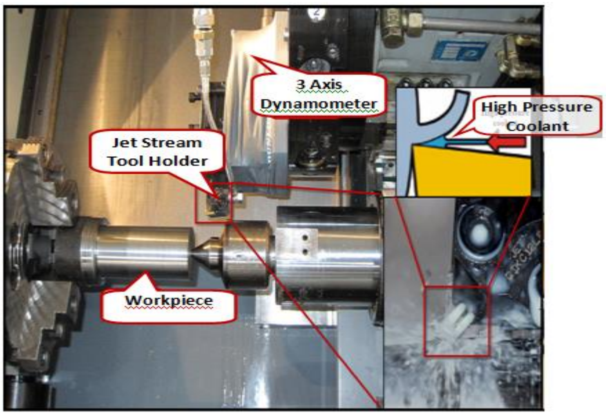

Figure 3. Experimental set-up, and the detailed view of high-pressure injection system [12]

The experiments designed based on Taguchi L9 orthogonal array at three different cutting speed, feed rate and pressure levels with a constant depth of cut. The cutting parameters used in this work and experiment results are given in Table 3. A (Ti,Al)N+TiN coated carbide cutting tool CNMG0812 has been chosen for the experiments. The tool has $r\varepsilon$ = 0.8 mm nose radius. It was mounted on a SECO Jet stream PCLNR tool holder, which results in cutting rake angle, γ_a =-6°, back rake angle, γ_b = –6°, approach angle, *Kr* = 95°, and *d* = 0.8 mm nozzle diameter. All experiments were performed on machining Titanium alloy (63.5 mm diameter and 300 mm long). The standard chemical composition and mechanical properties of the workpiece are given in Table 1 and Table 2.

Table 1. Chemical composition of Ti-6Al-4V / Wt.%

Al	Fe	O	Ti	V
6	Max 0.25	Max 0.2	90	4

Table 2. Mechanical properties of Ti-6Al-4V

Hardness [HRC]	Yield strength [MPa]	Tensile strength [MPa]	Elongation [%]	Thermal conductivity [W/m-K]	Specific heat capacity [J/kgK]	Density [g/cm^3]
36	950	850	14	6.7	526.3	4.43

Table 3. Ti-6Al-4V Cutting parameters and experiment results.

Exp.	V_c [m/min]	f [mm/rev]	P [MPa]	hmax [um]	hmin [um]	dch [um]	ϕseg [degree]
1	50	0,1	0,6	278,11	75,12	85,87	25,94
2	50	0,15	15	280,88	49,66	103,56	24,25
3	50	0,2	30	311,2	48,78	121,48	21,84
4	70	0,2	0,6	217,79	89,07	156,76	31,23
5	70	0,1	15	206,94	111,14	137,56	28,7
6	70	0,15	30	213,11	98,43	141,61	26,23
7	90	0,15	0,6	121,51	120,87	213,11	37,18
8	90	0,2	15	143,31	113,4	241,7	35,09
9	90	0,1	30	104,63	159,44	193,4	32,79

5. Result and Discussions

The different machining parameters produced different chip morphologies, as shown in Figure. 7. The effects of feed rate and cutting speed on minimum and maximum chip thickness are summariesed in Figure 4. The maximum chip thickness (h_{max}) increases as the feed rate increases and the cutting speed decreases. The rate of increase in maximum chip thickness associated with feed rate is much smaller compared to that associated with cutting speed (Figure 4a). The minimum chip thickness (h_{min}) increases as the feed rate decreases and the cutting speed increases. The rate of decrease in minimum chip thickness associated with feed rate increase is much smaller compared to that associated with cutting speed decrease (Figure 4b).

The change of the distance between of chip segments (d_{ch}) according to cutting speed and feed rate is given in Figure 5. The mean distance between chip segments increases with increasing feed rate and cutting speed.

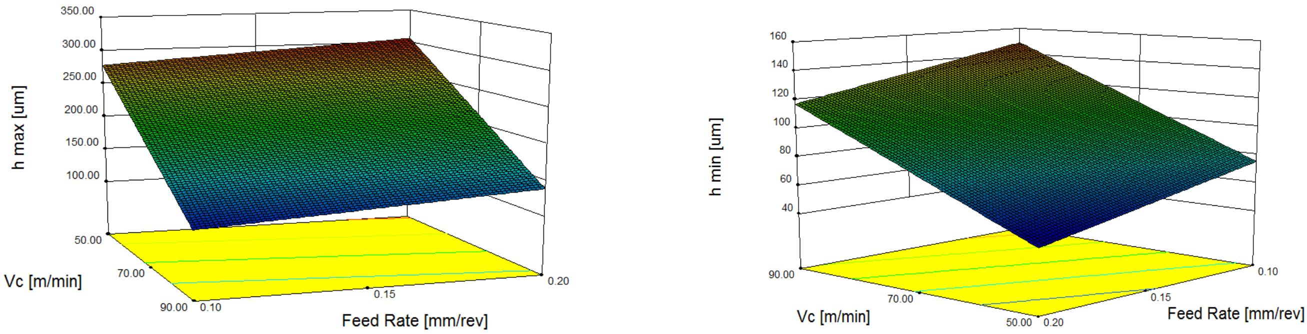

(a) (b)

Figure 4. The change of the (a) maximum and (b) minimum chip thickness according to cutting speed and feed rate.

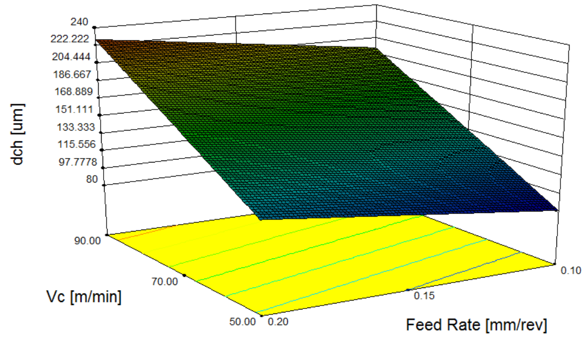

Figure 5. The change of the distance between of chip segments (d_{ch}) according to cutting speed and feed rate.

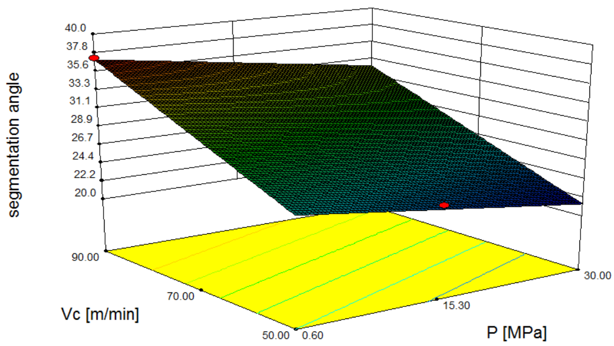

Figure 6. The variation in chip segmentation angle (ϕ_{seg}) with cooling pressure and cutting speed.

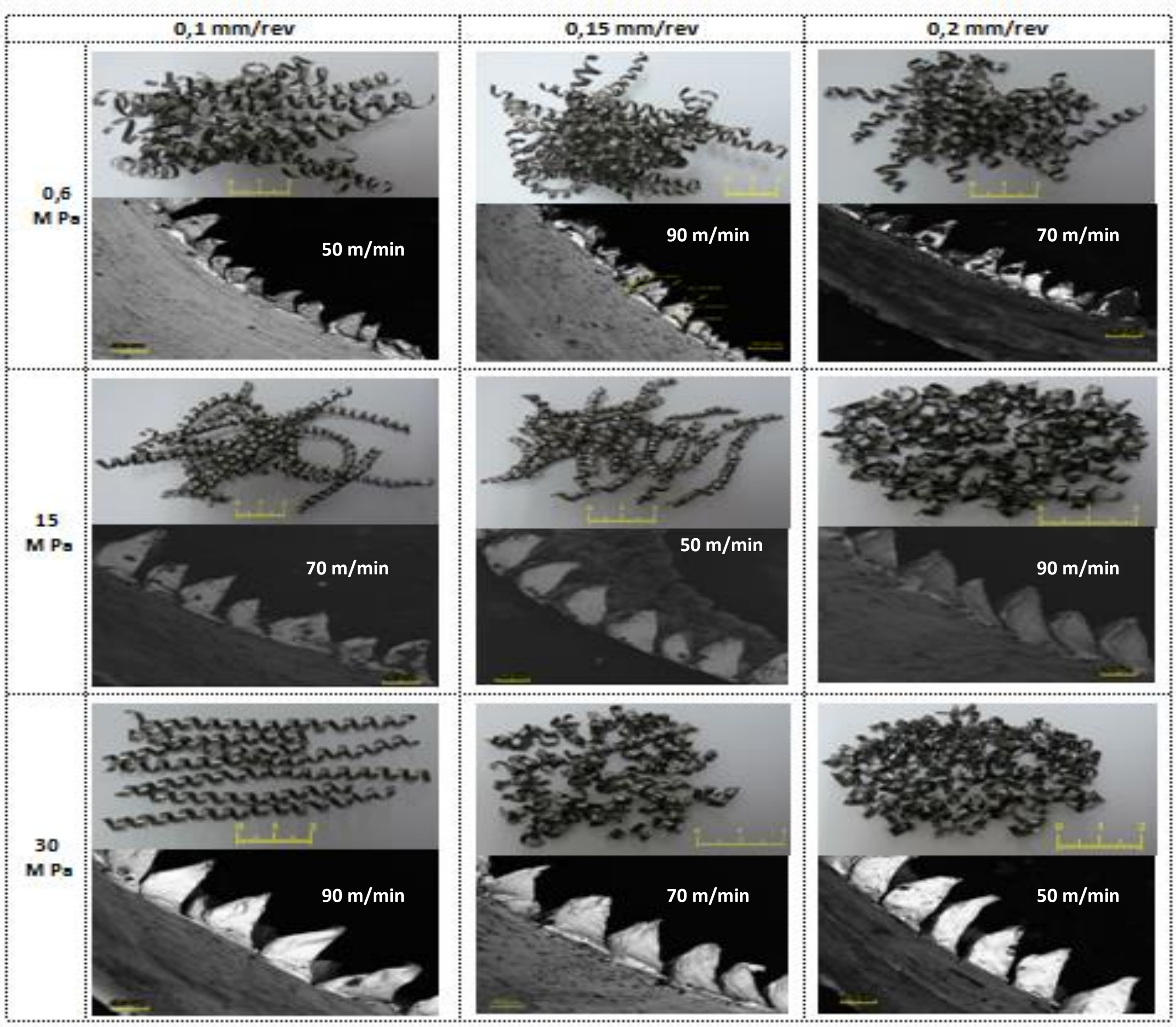

Figure 7. SEM photos of cross-section of chips

The change of the chip segmentation angle according to cooling pressure and feed rate is given in Figure 6. The chip segmentation angle increases with decreasing cooling pressure and increasing cutting speed.

The Chip formation, which has been obtained as the result of the cutting experiments applied in all cutting speeds, has been appeared same as the Merchant's model [9]. Serrated chip formation occurred at all tested feed rate and cutting speed. With increasing cutting speed, $h_{\min}$, ϕ_{seg}, d_{ch} increases and $h_{\max}$ decreases. However, with the increase of high pressure coolant majority of heat formed during the machining is thrown away by the chip. This situation causes the formation of long sawteeth and the curling of the chip with smaller diameter. As expected, the chip segmentation angle increases with increasing cutting speed and decreases with coolant pressure.

5. Conclusion

In this study, machinability of Ti-6Al-4V alloy was experimentally investigated, comparing conventional with high pressure cooling conditions on CNC lathe. During the experiments, maximum and minimum chip thickness ($h_{\max}, h_{\min}$), chip segments distance (d_{ch}) and chip segmentation angle (ϕ_{seg}) were recorded. The results were showed in 3d surface plots.

The following conclusions can be drawn from this work:

- When high-pressure coolant is employed, the high-pressure jet provoked the chip to bend and consequently induce chip breakage. This provides more space for the high-pressure coolant to penetrate the cutting region. During this stage, coolant may not only provide more lubrication to reduce friction at the contact interfaces but also act as a thermal barrier to restrict the heat transfer between chip and cutting tool.

- The feed rate, cutting speed and coolant pressure have a considerable influence on the appearance of the chip segments. Feed rate did not have any considerable effect on $h_{\max}$ and ϕ_{seg}. Similarly, coolant pressure did not have any considerable effect on $h_{\min}$ and d_{ch}.
- Discontinuous, segmented chips were generated when machining with high pressure coolant, while long continuous chips were generated when machining with lower pressure and conventional coolant.

References

[1] R. S. Pawade,Suhas S. Joshi, Mechanism of Chip Formation in High-Speed Turning of Inconel 718, Machining Science and Technology, 15: 132-152., (2011).

[2] A., B. Mohd Hadzley, R. Izamshah, A. Siti Sarah and M. Nurul Fatin, Finite Element Model of Machining with High Pressure Coolant for Ti- 6Al-4V alloy. Malaysian Technical University Conference on Engineering & Technology. (2013).

[3] Davorin Kramar, Janez Kopač, High Pressure Cooling in the Machining of Hard-to-Machine Materials, Journal of Mechanical Engineering 5511, 685-694. (2009).

[4] Nambi Muthukrishnan, Paulo Davim, Influence of Coolant in Machinability of Titanium Alloy (Ti-6Al-4V) Journal of Surface Engineered Materials and Advanced Technology, 1, 9-14, (2011).

[5] Suresh Palanisamy Stuart D. Mc Donald, Matthew S. Dargusch, Effects of coolant pressure on chip formation while turning Ti6Al4V alloy International Journal of Machine Tools & Manufacture 49, 739–743., (2009).

[6] Miroslav Neslušan, Michal Šípek, Jozef Mrázik, Analysıs Of Chıp Formatıon Durıng Hard Turnıng Through Acoustıc Emıssıon Materials Engineering 19, 1-11, (2012).

[7] G.A. Oosthuizena, G. Akdoganb, D. Dimitrovc, N.F. Treurnichtd, A Review of the Machinability of Titanium Alloys.

[8] S, M. Brandt, M.S. Dargusch, Characteristics of cutting forces and chip formation in machining of titanium alloys International Journal of Machine Tools & Manufacture 49, 561–568, (2009).

[9] G. Sutter, G. List. Very high speed cutting of Ti–6Al–4V titanium alloy–change in morphology and mechanism of chip formation” International Journal of Machine Tools & Manufacture 66: 37–43, (2013),

[10] A. Daymi, M. Boujelbene, S. Ben Salem, B. Hadj Sassi, S. Torbaty, Effect of the cutting speed on the chip morphology and the cutting forces, Archives of Computational Materials Science and Surface Engineering 1/2 77-83., (2009).

[11] A. Gente, H.W. Hoffmeister, C.J. Evans, Chip formation in machining Ti6Al4V at extremely high cutting speeds, CIRP Annals-Manufacturing Technology 50, 49–52, (2001)

[12] P. Dahlman Comparison Of Temperature Reduction In High-Pressure Jet-Assisted Turning Using High Pressure Versus High Flow Rate of Engineering Manufacture April 1, vol. 216 no. 4 467-473, , (2002)

[13] S. Belhadi, M.A. Yallese, K. Bouacha and N. Kribes, Chip Segmentation Effect On Cutting Forces Variation,

[14] Oğuz Çolak, Investigation on Machining Performance of Inconel 718 under High Pressure Cooling Conditions. Journal of Mechanical Engineering 58, 683-690., (2012).

[15] Fuat KARA, Kubilay ASLANTAS, Adem ÇİÇEK, Ortogonal Kesme İşleminde Kaplama Malzemesinin Talaş Morfolojisi üzerinde etkisinin araştırılması 2. Ulusal Tasarım İmalat ve Analiz Kongresi (2010), Balıkesir.

[16] M. Cotterell, G. Byrne, Dynamics of chip formation during orthogonal cutting of titanium alloy Ti–6Al–4V CIRP Annals - Manufacturing Technology 57, 93–96., (2008).

[17] Shane Y. Hong, Irel Markus, Woo-cheol Jeong, New cooling approach and tool life improvement in cryogenic machining of titanium alloy Ti-6Al-4V, International Journal of Machine Tools & Manufacture 41 2245–2260, (2001).

[18] Taguchi, G., Konishi, S. Orthogonal Arrays and Linear Graphs. American Supplier Institute., (1987).

Experimental Study on Machinability of AISI H13 Tool Steel

B. Yalçın[1], K. Kıran[2], E. Aykan[1], O. Çolak[2]

[1] *Süleyman Demirel University, Faculty of Technology, Department of Manufacturing Engineering, Turkey*

[2] *Süleyman Demirel University, CAD/CAM Research and Application Center, Turkey*

Abstract

AISI H13 tool steel has widely been used in industry especially to manufacture moulds/dies due to its good resistance. This paper presents an experimental study on rough turning of AISI H13 tool steel in order to investigate influence of machining parameters and coating grades on machining performance. Experimental design was made as full factorial at three different cutting speed, feed rate levels and two different coating grades. CVD-Ti(C,N) + Al_2O_3 + TiN and PVD-Oxide coated tungsten carbide tools were used and machining performance measures such as cutting forces, surface roughness and tool life were measured during the turning tests. The experimental results have shown that cutting forces and surface roughness for both coating grades have exhibited similar trends but CVD-Ti(C,N) + Al_2O_3 + TiN coating grade has provided longer tool life about 8 times higher than the other one at high cutting speed.

Keywords: Machinability, Tool life, Turning, Coating grade

1 Introduction

The manufacturing process of dies/molds is one of the most demanding tasks in manufacturing industries. Complex workpiece geometries, high material hardness as well as short lead time are among the main obstacles. At the same time, quality requirements become more and more important due to intensified competition and quality awareness [1].

A wide range of tool steels are employed to produce machined moulds and dies. In forging and die casting, the choice is generally hot work tool steels (AISI Group H series) which can withstand the relatively high working temperatures involved, typically 315–650 ^{o}C [2]. One of them that is frequently used in manufacturing industries is chromium based AISI H13 hot work tool steel. This steel possesses good resistance to thermal softening and heat checking, high hardenability, high strength and high toughness resulting in increased production rates and longer tool life. Therefore it is widely utilized on the production of hot work dies, such as forging dies, extrusion dies, die casting dies e.t.c (the hardness of AISI H13 varies with its application for different type of dies) [3-6].

The machining of tool steels has great importance in manufacturing industry. Thus, many researchers have conducted numerous investigations on machinability of AISI H13 with various cutting tools and machining parameters. Ghani *et al.* [7] have carried out an experimental work to investigate performance of P10 TiN coated carbide inserts when semi-finishing and finishing end milling of hardened AISI H13 tool steel (50±3 HRC). Xiong *et al.* [5] have studied on turning of AISI H13 hardened steel with WC–5TiC–10Co ultrafine cemented carbides. They investigated effect of cutting parameters on the tool life and tool wear mechanism. Axinte and Dewes [8] performed an experimental study to research effect of cutting parameter on surface integrity during the high speed milling of hardened AISI H13 tool steel using solid carbide ball nose end mills coated with TiAlN. Özel [9] has conducted a research on the influence of edge preparation in cubic boron nitrite (CBN) cutting tools on process parameters and tool performance by utilizing practical finite element (FE) simulations and high speed orthogonal cutting tests. The study shows that the presence of a chamfer affects the cutting forces and temperatures while no significant change in chip formation. Numerical simulation of hard machining AISI H13 tool steel was made by Umbrello *et al.* [4]. They developed hardness-based flow stress and fracture models for machining AISI H13 tool steel. Qian and Hossan [10] also performed numerical simulations of high-speed orthogonal machining by using CBN inserts.

This study investigates the rough turning of AISI H13 tool steel at various cutting parameters and tungsten carbide tools coated with CVD (Chemical Vapor Deposition)-Ti(C,N) + Al_2O_3 + TiN and PVD (Physical Vapor Deposition)-Oxide. The experiments were designed as full factorial at three different cutting speeds (V_c), feed rates (f) and two coating grades. The turning tests were conducted at dry cutting conditions and the depth of cut (a_p) was kept constant. Machining performance measures namely cutting forces, surface roughness and tool wear were recorded during the experiments.

2 Experimental work

A full factorial experimental design was performed in order to investigate influence of machining parameters on cutting forces and surface roughness. Machining parameters and their levels were given in Table 1.

Table 1 Machining parameters and levels used in the experiments

Level	**I**	**II**	**III**
V_c [m/min]	250	350	450
f [mm/rev]	0.15	0.25	0.35
Coating grade	CVD-Ti(C,N) + Al_2O_3 + TiN	PVD-Oxide	-
a_p [mm]	1.5	-	-

The experiments were made on ALEX ANL-75 CNC lathe machine that is equipped with variable spindle speed from 50 rpm to 4000 rpm and a 15 kW motor drive. The cutting forces, F_c, F_f, F_p, and surface roughness, R_a, were measured by using a three component piezoelectric dynamometer (Kistler 9722-A) mounted on the turret of lathe and surface profilometer respectively. The experimental layout is shown in Figure 1.

The two types of cutting insert, WC-CNMG120408PM-GC4205 CVD-Ti(C,N) + Al_2O_3+TiN and WC-CNMG120408MM-GC1115 PVD-Oxide coated tungsten carbide, supplied by Sandvik Coromant were tested at dry cutting conditions. All the experiments were carried out using the AISI H13 tool steel without hardening (hardness 20-22 HRC) supplied as bars (100 mm diameter and 270 mm long).

3 Experimental Results and Discussion

Base on the experimental plan, totally 18 experiments were carried out for both coating grades. Linear regression models for cutting forces and surface roughness were generated using experimentally obtained data. The test results with respect to cutting speed and feed rate are presented in Figure 2, 3, 4 and 5. From the plots of cutting forces we can see that all the cutting force components increase with rising feed rate as expected.

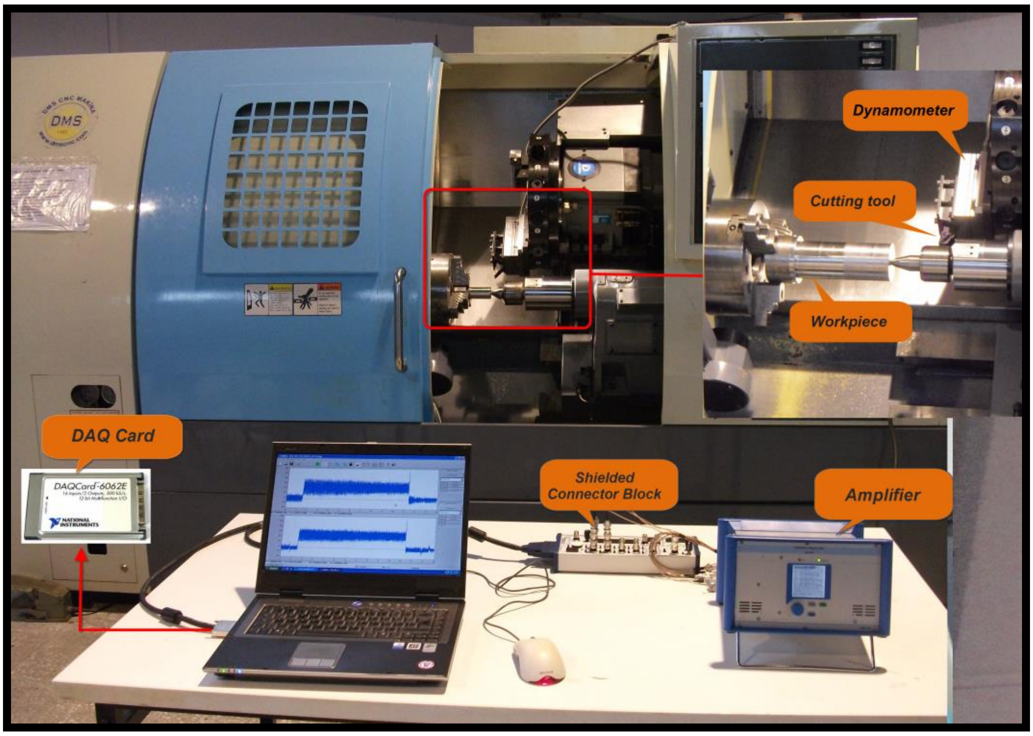

Figure 1 Experimental layout

This is resulted from increasing in contact area between workpiece and cutting tool. As can be also seen that cutting speed has a little decreasing effect on some cutting force components. This is due to softening of workpiece material emerged from high cutting temperature.

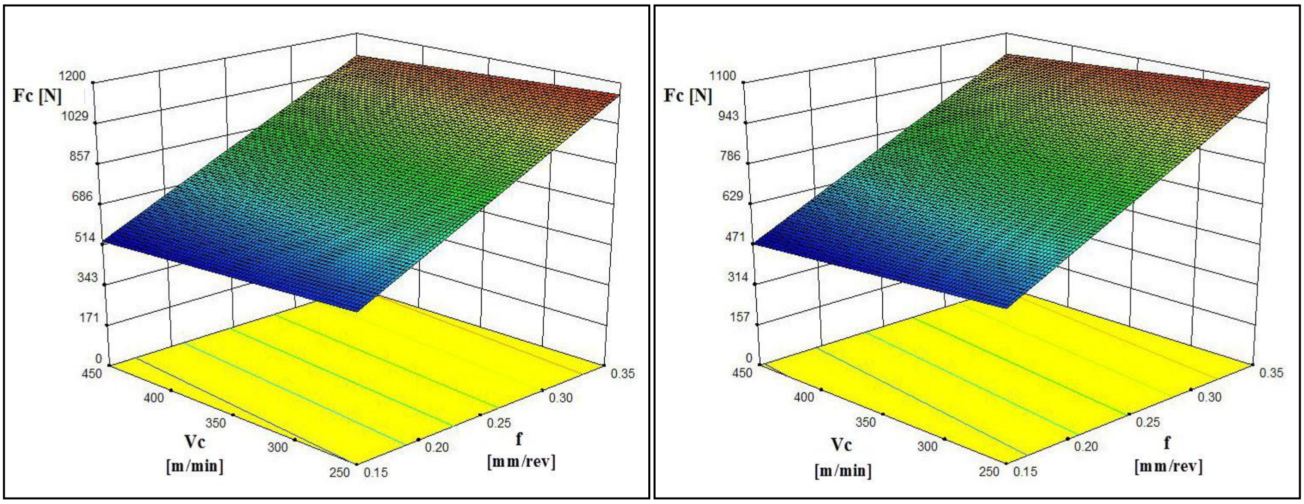

Figure 2 Main cutting force results for CVD-Ti(C,N) + Al_2O_3+TiN and PVD-Oxide coated tungsten carbide tools respectively

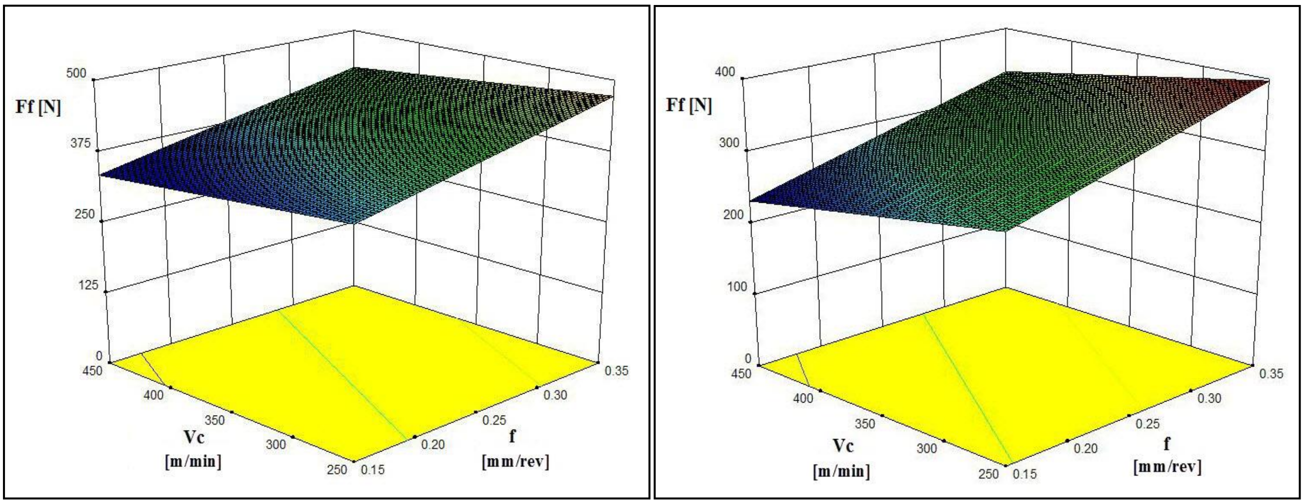

Figure 3 Feed force results for CVD-Ti(C,N) + Al_2O_3+TiN and PVD-Oxide coated tungsten carbide tools respectively

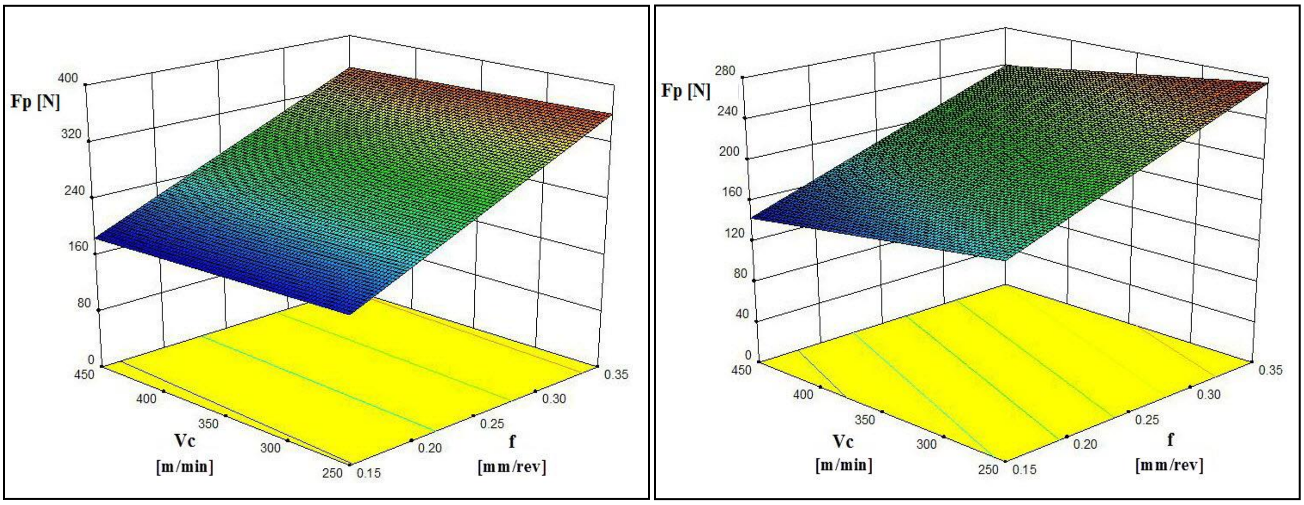

Figure 4 Passive force results for CVD-Ti(C,N) + Al_2O_3+TiN and PVD-Oxide coated tungsten carbide tools respectively

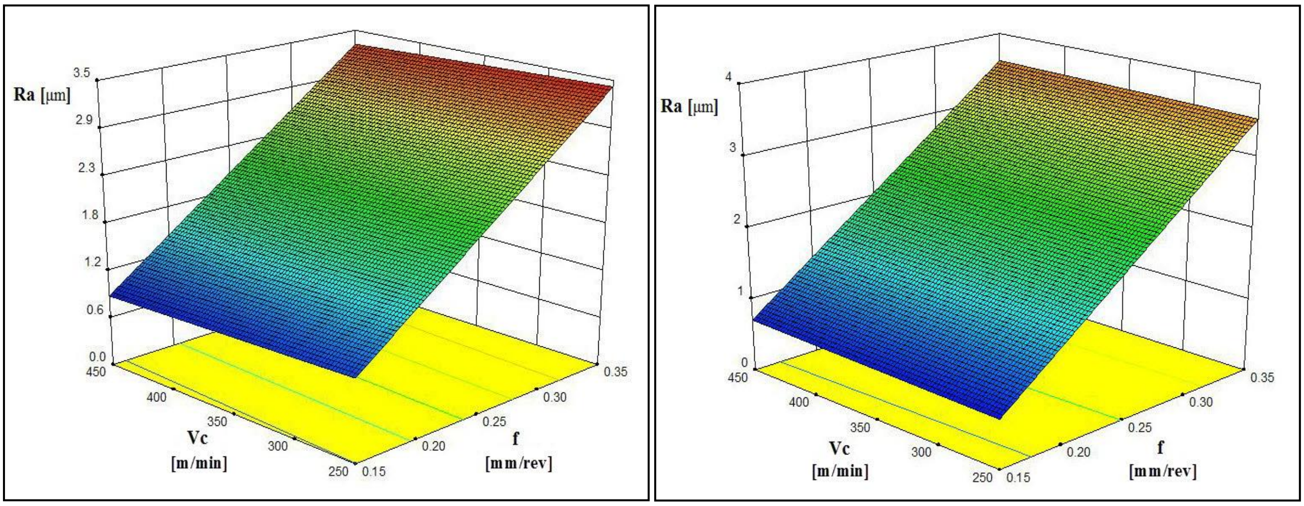

Figure 5 Surface roughness results for CVD-Ti(C,N) + Al_2O_3+TiN and PVD-Oxide coated tungsten carbide tools respectively

Figure 5 indicates surface roughness results for both coating grades. It is shown that surface roughness is strongly affected by feed rate. It is well known that the theoretical geometrical surface roughness is primarily a function of the feed for a given nose radius and changes with the square of the feed rate value [11]. It is also clearly observed that cutting speed does not have considerable influence on surface roughness. Comparing the plots each other, similar trends can be seen for both CVD-Ti(C,N) + Al_2O_3+TiN and PVD-Oxide coated tungsten carbide tools. But cutting force components for CVD-Ti(C,N) + Al_2O_3+TiN coating grade are a bit higher than the other one. The properties of coating grades can probably responsible for this difference.

In turning, to avoid the catastrophic tool failure that cause damage in tool, workpiece or machine tool, the useful life of a tool can be defined in terms of the progressive wear that occurs on the tool rake face (crater wear) and/or clearance face (flank wear). The flank wear is frequently used to define the end of effective tool life because of its major negative influence on dimensional accuracy and surface finish of the component as well as the stability of the machining process once a certain level is reached [12]. Thus, the flank wear (VB_B=0.3 mm) is defined as the tool life criterion in the present study. Obtained tool life results are given in Figure 6 for both coating grades.

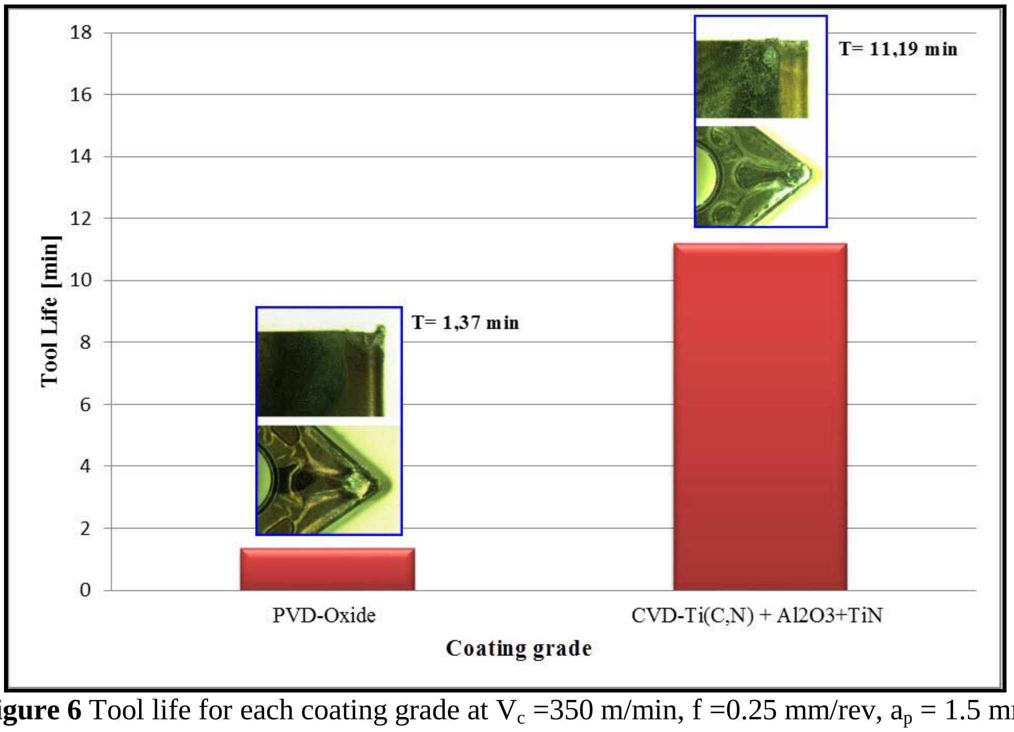

Figure 6 Tool life for each coating grade at V_c =350 m/min, f =0.25 mm/rev, a_p = 1.5 mm

It is shown that CVD-Ti(C,N) + Al_2O_3+TiN coated tungsten carbide tool has about 8 times longer tool life compared with the other one. PVD-Oxide coated tungsten carbide tool has exhibited poor cutting performance at those machining parameters. Hence, one more tool life test were executed at V_c =50 m/min, f =0.2 mm/rev, a_p = 2 mm to discover the problem, and the tool life is measured as 17.79 minutes at these parameters. We have figured out the fact that high cutting speed that increases temperature of cutting edge causes lower tool life when machining with PVD-Oxide coated tungsten carbide tool.

4 Conclusions

In this study rough turning of AISI H13 tool steel was investigated at various cutting parameters and tungsten carbide tools coated with CVD -Ti(C,N) + Al_2O_3 + TiN and PVD-Oxide. The influence of machining parameters and coating grades on cutting forces, surface roughness and tool life were determined by performing a series of experiments. Base on the results, it can be concluded that cutting forces and surface roughness for both grades showed similar trends. But cutting force components when machining with CVD-Ti(C,N) + Al_2O_3+TiN coated tungsten carbide tools are a bit higher than the other one. This can be due to the properties of coating grades. On the other hand, CVD-Ti(C,N) + Al_2O_3+TiN coating grade has provided about 8 times longer tool life than PVD-Oxide at given parameters. This poor tool life of PVD-Oxide coating grade is due to cutting speed resulting in high temperatures in the cutting zone. Thus, tool flank wear reaches quickly to defined tool life criteria. It should be utilized at lower cutting speeds in order to be prolonged tool life.

Acknowledgements

This work was supported by Unit of Scientific Research Projects of Süleyman Demirel University, Turkey (project 2547-M-10).

References

[1] H. Yan, J. Hua, R. Shivpuri. Flow Stress of AISI H13 Die Steel in Hard Machining. Materials and Design, 28, pp. 272–277, 2007.

[2] H. Coldwell, R. Woods, M. Paul, P.Koshy, R. Dewes, D. Aspinwall. Rapid Machining of Hardened AISI H13 and D2 Moulds, Dies and Press Tools. Journal of Materials Processing Technology, 135, pp. 301–311, 2003.

[3] J. C. Outeiro, D. Umbrello, J. C. Pina, S. Rizzuti. Modelling of Tool Wear and Residual Stress during Machining of AISI H13 Tool Steel. AIP Conf. Proc. 908, pp. 1155-1160, Portugal, 17-21 June, 2007.

[4] D. Umbrello, S. Rizzuti, J.C. Outeiro, R. Shivpuri, R. M’Saoubi. Hardness-Based Flow Stress for Numerical Simulation of Hard Machining AISI H13 Tool Steel. Journal of Materials Processing Technology, 199, pp. 64–73, 2008.

[5] J. Xiong, Z. Guo, M. Yang, W. Wan, G. Dong. Tool Life and Wear of WC–TiC–Co Ultrafine Cemented Carbide during Dry Cutting of AISI H13 Steel. Ceramics International, 39, pp. 337–346, 2013.

[6] A. G. Jaharah, I. A. Choudhury, H.H. Masjuki, C. H. Che Hassan. Surface Integrity of AISI H13 Tool Steel in End Milling Process. International Journal of Mechanical and Materials Engineering (IJMME), 4, pp. 88-92, 2009.

[7] J.A. Ghani, I.A. Choudhury, H.H. Masjuki. Performance of P10 TiN Coated Carbide Tools when End Milling AISI H13 Tool Steel at High Cutting Speed. Journal of Materials Processing Technology, 153–154, pp. 1062–1066, 2004.

[8] D.A. Axinte, R.C. Dewes. Surface Integrity of Hot Work Steel after High Speed Milling-Experimental Data and Empirical Models. Journal of Materials Processing Technology, 127, pp. 325–335, 2002.

[9] T. Özel. Modeling of Hard Part Machining: Effect of Insert Edge Preparation in CBN Cutting Tools. Journal of Materials Processing Technology, 141, pp. 284–293, 2003.

[10] L. Qian, M. R. Hossan. Effect on Cutting Force in Turning Hardened Tool Steels with Cubic Boron Nitride Inserts. Journal of Materials Processing Technology, 191, pp. 274–278, 2007.

[11] K. Bouacha, M. A. Yallese, T. Mabrouki, J. F. Rigal. Statistical Analysis of Surface Roughness and Cutting Forces using

Response Surface Methodology in Hard Turning of AISI 52100 Bearing Steel with CBN Tool. Int. Journal of Refractory Metals & Hard Materials, 28, pp. 349–361, 2010.

[12] J.A. Arsecularatne, L.C. Zhang, C. Montross. Wear and Tool Life of Tungsten Carbide, PCBN and PCD Cutting Tools. International Journal of Machine Tools & Manufacture, 46, pp. 482–491, 2006.

Feeding the ultrasonic devices used in boats with solar energy by using logic switching method

R. Abdulla[1], F.G.K. Abdulla[1]

[1] *Suleyman Demirel University, Turkey*

Abstract

The marine industry is evolving constantly as many of the countries have shore. In order to be durable for years; boats' hull are generally made of fiber or steel. For preventing the corrosion of the boat and making the surface of the boat below sea uniform and smooth; it is painted. These paints used are toxic and are produced to keep marine organisms away from the boat. However full efficiency can not be achieved and they also harm the environment. Accordingly; to remove the marine organisms that cause extra friction and increase the fuel consumption; motorized equipments, acid and cleaning systems that require arm strength are used. These methods help to clean under the vessel a little but they also result in loss of time. To eliminate such problems; various systems are tried and finally with the help of ultrasonic waves; marine organisms are disturbed and prevented from sticking onto boat's surface. Ultrasonic antifouling systems are generally operated when the boat is on hold in marines or ports. Some of the boats do not have battery and some have portable battery. As a result; to protect the "boat on hold" from marine organisms; a device fed by solar energy must be installed. In this study; the environment friendly ultrasonic systems which take its operating energy from the battery of boats are aimed to be operated with solar energy. With the help of logic switching system, solar energy is used and the feeding of battery which will operate the ultrasonic device is completed.

Keywords: Ultrasonic antifouling, environment, solar energy, boating industry.

1 Introduction

Nowadays ultrasonic technology is increasingly well-known and used in many areas [1, 2]. Because of the difficulty and high cost of the traditional cleaning process, ultrasonic technology also started to be used in marine industry. The installation of this eco-friendly device is completed when it is installed in the interior of the boat which does not have any contact with water. The operation of the system is based on the principle of conversion of high voltage ultrasonic waves into mechanical movement with piezoelectric transducers and the mechanical movement transmitted [2] to boat's hull.

In existing ultrasonic systems, supply is provided from boat's battery. However it is not possible for boat's without battery. Therefore, to solve the problem of feeding the device, solar energy - an inexhaustible supply of renewable energy [3] can be used. Thus, an automatic selection between the battery of the boat and the battery fed by solar energy is done with a simple switching circuit and the operation of ultrasonic device is provided. Logic switching method is used for this.

Logic switching circuits are widely used in the protection or control of electronic systems [4]. In this study , with the help of microprocessor and relay that is used as switching element, automatic selection of the energy source necessary to run the ultrasonic device is provided either from boat's battery or the battery fed by solar energy.

2 The Design Of Circuit

2.1 Choice of components

Some of the main circuit components used in this study are as follows.

Pic16f88: Voltage control programming is done with this microprocessor. This 18 pin microprocessor is chosen on purpose as it provides enough number of pins in generating ultrasonic waves and overcoming other tasks.

20MHz crystal: It supports the selected operating frequency of microprocessor. High operating frequency allows high processing speed and generating precise frequency.

5V Relay: This circuit component works as a switch allowing passage of solar energy if input voltage in normally open (NO) pin is greater than the rated coli voltage of relay.

12V Relay: This circuit component works as a switch allowing passage of solar energy or energy from the boat's battery depending on input voltage in NO pin.

7805 Voltage Regulator: It is used to provide 5V that microprocessor and other circuit components need.

Resistors: They act as a voltage divider for the energy from solar power. In this way, a voltage in the range of 12V is controlled without using the voltage reference pins of microcontroller.

2.2 Circuit

At this stage, the control of the voltage input with a programme and the auto-selection of solar energy is implemented.

In Figure 1, the circuit diagram and the batteries that feeds the circuit are shown. One of the battery is the boat's and the other one is the solar energy. Energy supply from solar energy fed battery providing the required voltage needed for the circuit is the main goal. 5V or 12V is needed for the output of the circuit. These voltages provide the supply for microprocessor and other necessary circuit components.

In order to benefit from solar energy optimally, automatic switch is required (Figure 2). The switch controlled by microcontroller decides whether allow passage of solar energy or not. For make it happen, the voltage from the battery fed by solar energy is read with the help of microcontroller. The energy coming from this battery, supply 5V reference voltage to microcontroller with the help of voltage divider consisting of two resistors. This results in simple circuit and computation for programmer. In the circiut the voltage value of AN0 pin of microcontroller, which is configured as analog input, is read and determined. Accordingly, by considering the proper threshold limit value (0.2V is chosen for the study), if the voltage value read by microcontroller is smaller than 12V - threshold value;

- AN1, the digital output of the microprocessor is set to 1.Thus the output will be 5V.This output set the RL1 switch to the Normally Open (NO) pin and the common output of relay (COM) becomes(5V. As the NO pin of RL2 relay will be 5V, there will be no change and the input of 7805 voltage regulator will be fed by boat's battery (Figure 3a).

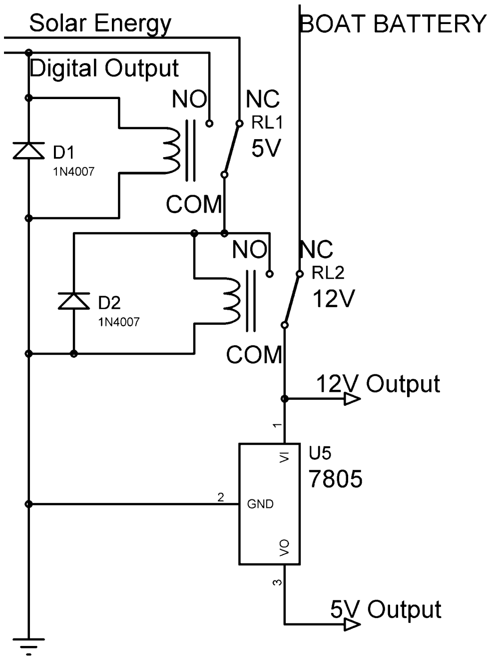

Figure 1 Energy source selection.

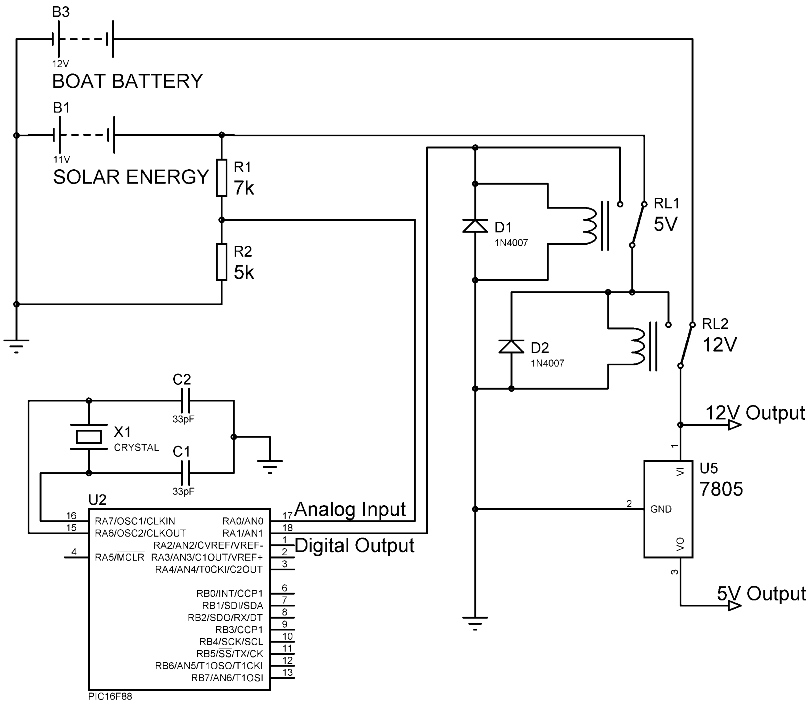

Figure 2 The circuit scheme.

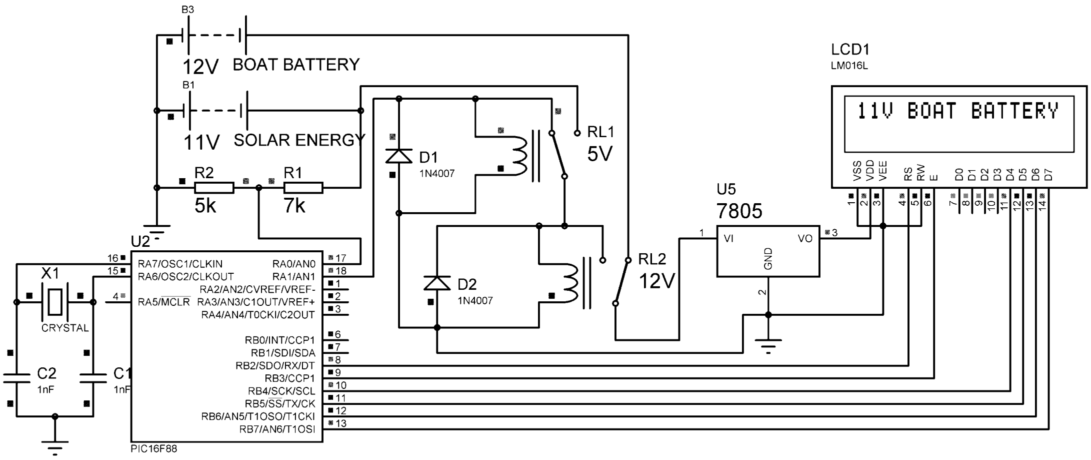

a)

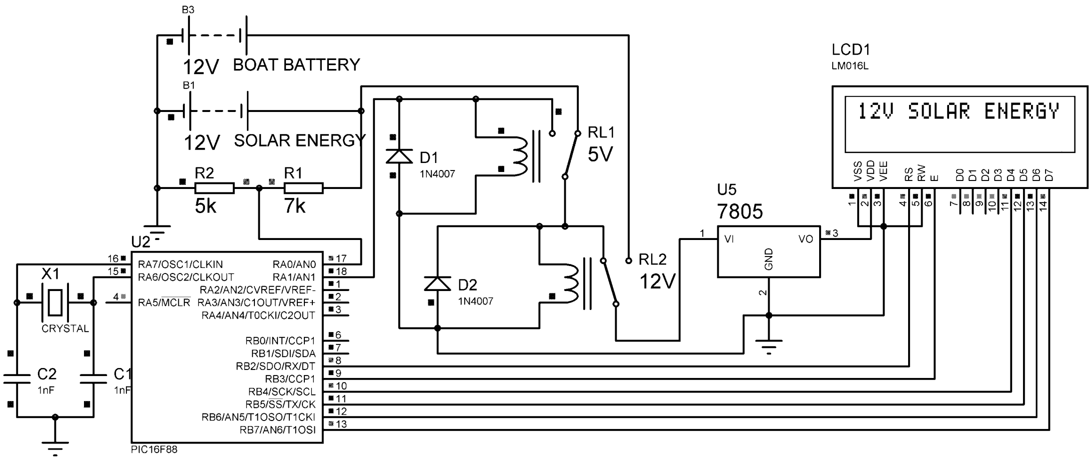

b)

Figure 3 a) Boat battery is switched, b) Solar energy is switched.

if the voltage value read by microcontroller is greater than 12V - threshold value;
- AN1, the digital output of the microprocessor is cleared. Thus the output is 0V. This output doesn't make any changes on RL1 relay. Therefore the COM output is 12V fed by solar energy. As the NO pin of RL2 relay will be 12V, relay will be switched to NO pin. Thus COM of RL2 will be 12V supplied by solar energy (Figure 3b).

2.3 Pseudocode

The basic functioning of the programmed designed circuit is as in the following pseudocode.

start program
configure pin AN0 as analog
configure pin AN0 as input
configure pin AN1 as output
determine threshold value
start infinite loop
read ADC from AN0 pin
control result
if control < 12V-threshold value
Set AN1 //i.e. boat battery is in progress
else
clear AN0 //i.e. solar panel is in progress
write result to LCD
jump to loop
end

Corresponding pins are shown in Figure 4.

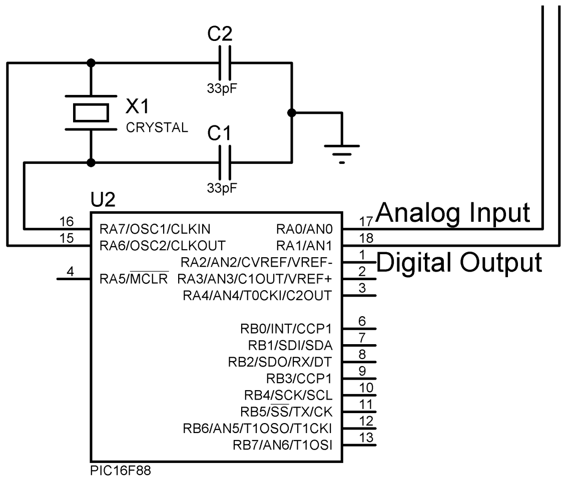

Figure 3 Microcontroller's input - output pins.

3 Conclusion

To feed the ultrasonic devices which are used in boats and supply the needed energy from boat's battery with alternative eco- friendly solar energy is a must. In the study, with the help of logic switching method auto-selection of the feeding energy is performed for a boat which has both battery and solar panels. With this system, required levels of output voltages have enabled generating ultrasonic waves. Consequently, the environment friendly ultrasonic systems take the needed operating energy from the battery fed by solar energy.

References

[1] K.S. Suslick: The Chemical Effects of Ultrasound. Scientific American, pp. 80-86, Feb., 1989.

[2] I. Ay, N. Anaç: Ultrasonik Yöntemle Parça Temizleme. IV. Mühendislik-Mimarlık Sempozyumu, Balıkesi Üniversitesi, pp. 229-241. 11-13 Sep., 2002.

[3] Q. Fang, L. Canbing: Design of Transmission Line Solar Ultrasonic Birds Repeller. Power Engineering and Automation Conference (PEAM), 2011 IEEE, Vol:1,pp. 217-220, 8-9 Sep., 2011.

[4] C.E. Shannon: A Symbolic Analysis of Relay and Switching Circuits. Trans. of AIEE, Vol. 57, pp. 713-723. 20-24 Jun. 1938.

Technologies for tube sampling in nuclear power plant heat exchangers

J. Valentinčič[1], M. Resnik[1], M. Frankovič[1]

[1] *University of Ljubljana, Slovenia*

Abstract

This paper deals with the problem of taking samples of stainless steel tubes from heat exchangers in nuclear power plants. Sometimes, these heat exchangers may also be referred to as steam generators. Maintenance of such heat exchangers assumes periodical tube sampling to determine the degree of degradation. There are many obstacles and requirements due to limited access and possible radiation. These narrow tubes must be cut from inside out in depths up to 10 meters with minimal or zero debris left in the system. Additionally, the damage of the surrounding tubes has to be avoided. The end of the tube is rolled into a tube holding plate, thus loosening up of that end is also required in order to successfully extract the tube. After examining the existing patents electro thermal solutions were chosen for this application. Main reason is that they can be used for both, cutting and extracting the tube.

Keywords: Heat exchangers, steam generators, nuclear power plants, tube sampling, electrical discharge machining (EDM).

1 Introduction

Nowadays nuclear power plants contribute an important part of electrical energy all over the world. Maintenance is crucial to avoid power losses, break downs, and other unnecessary costs. Therefore, maintenance intervals are carefully planned and maintenance should always be on schedule. Among various tasks, the tubes inside a heat exchanger have to be examined. Random tube samples are taken to determine the state of degradation and study the wear mechanisms of these tubes. Based on the examined samples, the heat exchanger is either confirmed to be further used or it is determined for replacement. Furthermore, they help to predict problems and improve the design of heat exchangers. Main problem that occurs on site is limited access and difficult working environment, often inside the radioactive zone in the nuclear power plant.

In this paper, requirements for tube cutting from inside out will be presented together with the overview of already patented solutions.

1.1 Tube specifications

Tubes are exclusively made of stainless steel because of its wear and corrosive resistance. There are many different sizes of tubes used in heat exchangers, identified by outer tube diameter and wall thickness. The most common types of tubes used are shown in Table 1.

Table 1 Tubes used in heat exchangers

Material	X5CrNi18-10 (A 213 Tp 304)
Dimensions (diameter x wall thickness)	12.7x0.71; 12.7x0.72; 25x0.7; 25x1.25; 19x1.25; 19x1.35; 25.4x3.2

1.2 Other specifications

The chosen principle should be able to cut all specified types of tubes as fast as possible. Tube can be accessed from one side only and there are only 2 meters between tube end and the wall. Cutting head should be able to be placed as deep as 10 meters inside the tube and work without interruptions. The part of tube that stays inside is plugged but never the less, debris from the cutting process is highly unwanted. Maximum size of debris should not be above 0.1 millimeter in diameter.

Another requirement that needs considering is getting the rolled in part of the tube loosened up to enable the tube to be pulled out of the supporting plate. This is achieved by heating the tube and cooling it down afterwards. Since the tube is rolled in a supporting plate, it cannot expand outwards due to the heating. In the cooling phase, the tube shrinkage occurs.

2 Solutions overview

In this section, patented solutions that are interesting for our application will be presented and new solutions will be proposed. They can be divided into two main groups on the basis of how the material is removed.

2.1 Mechanical solutions

Mechanical solutions are using cutting edges to remove material.

2.1.1 Tube cutting apparatus and method

Rotating head is attached to a flexible shaft [1]. When shaft rotates the cutting edge comes in contact with the tube wall. Cutting edge includes serration which defines two cutting teeth where chips are being formed: Figure 1.

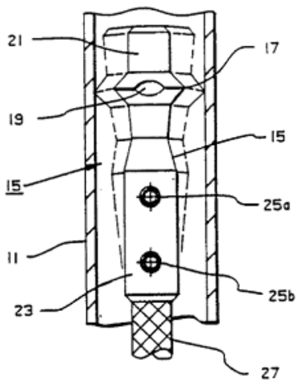

Figure 1 Tube cutting apparatus [1].

2.1.2 Movable cutting edge

Cutting knife has one cutting edge and is forced out against the wall with a spring. It is inserted inside the tube by being rotated counter clockwise. The cutting begins with rotating the head clockwise.

2.1.3 Eccentrically mounted cutting knife

This solution is based on a cutting knife mounted on a shaft eccentrically placed inside the tube housing. When shaft rotates, knife is in partial contact with the tube. When a certain section is cut, tube housing is gradually rotated so that the next section can be cut. This process goes on until the tube housing does a full circle and the tube is cut around entire circumference.

2.1.4 Grinding

Instead of a cutting insert a simple abrasive disk is used. Rotating disk causes radial force that forces the disk in contact with the tube inner wall. Disk wear is easily compensated but the cut is not an ideal circle. The debris left over is smaller than debris from other mechanical solutions.

2.2 Electro thermal solutions

These solutions use electric energy to heat and remove material, similar as in electrical discharge machining. Some solutions use individual discharges while others use a continuous arc.

2.2.1 Internal tube cutter

Rotating head is mounted to the shaft under an angle so that contact is ensured between the head and the tube [2]. Coolant must be present. Because of an electric circuit between both, an arc occurs: Figure 2.

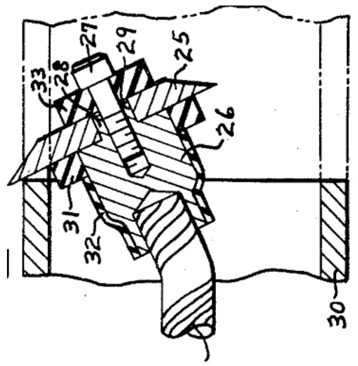

Figure 2 Internal tube cutter [2].

2.2.2 Apparatus for electric discharge machining of holes

This apparatus is designed to make vertical holes between horizontal planes or holes using electrical discharge machining [3]. By rotating the electrode around the tube it could be cut in half. It uses a hard drawn copper wire as an electrode and a stainless steel tube as housing (Figure 3).

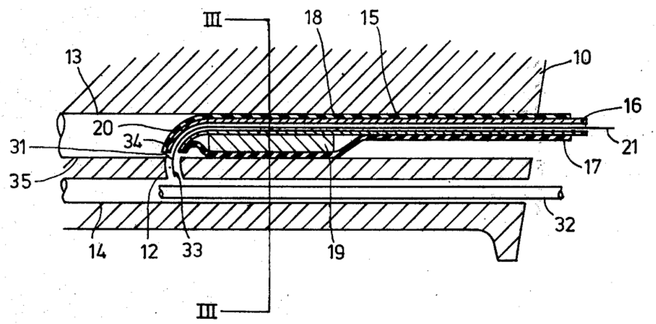

Figure 3 Apparatus for electric discharge machining of holes [3].

2.2.3 Electron discharge machining apparatus and method

This patent includes both, cutting and pulling out the tube [4]. There is an electrode on a rotating shaft and a complex mechanism for centering the electrode. Another mechanism enables the electrode to be moved closer to the tube wall with purpose of starting and maintaining the arc (Figure 4).

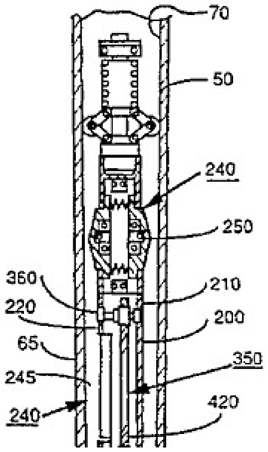

Figure 4 Electron discharge machining apparatus [4].

2.2.4 Inner wall tube disintegrator

Powerful electrical source is used to disintegrate the tube and relax the tube from a boiler tube sheet [5]. Solution is highly complex. An electrode is rotated at the end of a flexible cable (Figure 5).

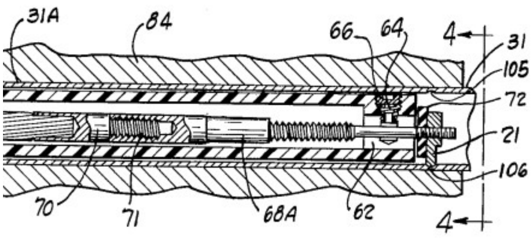

Figure 5 Inner wall tube disintegrator [5].

2.2.5 Remotely actuated metal disintegration machining apparatus

This is a solution patented by Westinghouse, designed to access the places inside the tube through bends [6]. This patent includes a solution for positioning the electrode at a desired remote location by a vibration feeder (Figure 6).

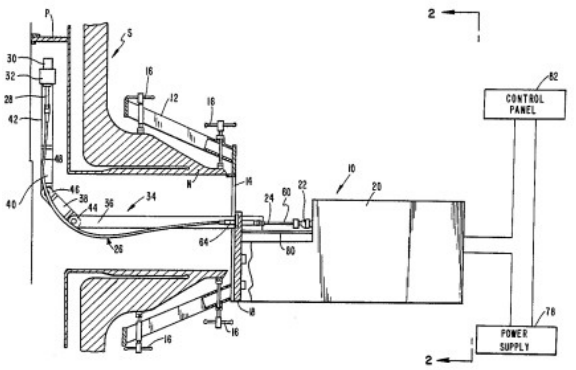

Figure 6 Remotely actuated metal disintegration machining apparatus [6].

2.2.6 Device for cutting the wall of tubular piece by EDM

Here, axial movement of a simple cone is transformed into a radial movement of the electrode [7]. Servo system controls the gap between the electrode and the tube. Deionized water is used as dielectric. Therefore the tube must be appropriately plugged (Figure 7).

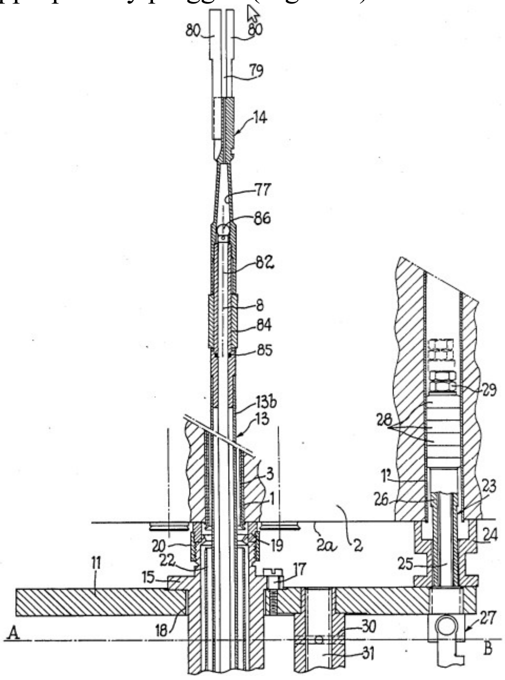

Figure 7 Device for cutting the wall of tubular piece by EDM [7].

2.2.7 Portable device for cutting the inside wall of a tube by a continous arc

The last of solutions is using a powerful electrical source such are TIG welder, 12V battery or other, and is more similar to a disintegrator than an EDM [8]. This solution uses a rubber spacer to force the rotating wolfram electrode against the tube wall: Figure 8.

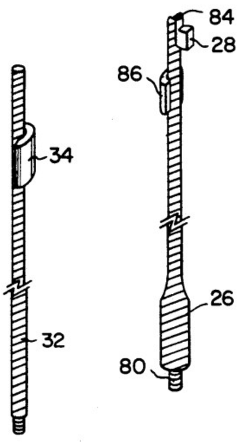

Figure 8 Portable device for cutting the inside wall of a tube by a continous arc [8].

3 SWOT analysis

To decide which solution fits our requirements best a SWOT analysis was conducted. Strengths and weaknesses from internal origin and opportunities and threats from external origin were carefully evaluated.

3.1 Mechanical solutions

In Table 2 the SWOT analysis of mechanical solution for tube cutting can be found.

Table 2 SWOT of mechanical solutions

Strengths	Weaknesses
- multiple solutions - simple material removal - fast cutting - well known process	- deformation due to head rotation - getting the cutting head in and out - cutting edge wear resistance
Opportunities	**Threats**
- cheap - patentable	- particles left in the system

3.2 Electro thermal solutions

In table 3 the SWOT analysis of electro thermal solutions is shown.

Table 3 SWOT of electro thermal solutions

Strengths	Weaknesses
- mechanical properties of the tube are unimportant - debris is small enough	- presence of coolant or dielectric - complexity - slow process - energy consumption - electrode wear
Opportunities	**Threats**
- good chances of developing an useful solution	- expensive - avoid already patented solutions

4 Conclusions

After considering all possible solutions, the electro thermal solution proved to be the best. It meets the requirements better than mechanical or any other solution.

TIG welding machine can be used as a power source for both, cutting and heating of the tube with intent to extract it. Another alternative for heating is with induction, using an internal water cooled copper coil.

The cutting head must be as simple and robust as possible. It should be cost effective and easy to replace, in order to replace is after each cut.

In future work, EDM and TIG principle of cutting welder will be examined. A great benefit would be if the cut can performed without the dielectricum or shielding gas.

References

[1] Evans, David. “Tube cutting apparatus and method”. Patent 4,779,496. 25 October 1988.

[2] Cammann, Fred. “Internal tube cutter”. Patent 2,942,092. 21 June 1960.

[3] Dudden, Derrick. “Apparatus for electric discharge machining of holes”. Patent 3,995,134. 30 November 1976.

[4] Cole, William. “Electron discharge machining apparatus and method”. Patent 5,543,599. 6 August 1996.

[5] Cammann, Fred. “Inner wall tube disintegrator”. Patent 4,476,368. 9 October 1984.

[6] Zafred, Paolo. “Remotely actuated metal disintegration machining apparatus”. Patent 4,584,452. 22 April 1986.

[7] Chamming’s, Pierre. “Device for cutting the wall of tubular piece by electrical discharge machining”. Patent 4,916,282. 10 April 1990.

[8] St. Louis, Daniel. “Portable device for cutting the inside of a tube by a continuos arc”. Patent 5,077,456. 31 December 1991.

Application of Vortex tube for tool cooling

Miroslav Duspara[1], Borut Kosec[2], Marija Stoić[3], Davorin Kramar[4], Antun Stoić[1]

[1] Mechanical Engineering faculty in Slavonski Brod,
[2] Faculty of Natural Sciences and Engineering, Ljubljana
[3] College of Slavonski Brod,
[4]Faculty of Mechanical Engineerig, Ljubljana

Abstract

The environmental pollution and health hazards of traditional tool cooling technique applied for machining processes will be evaluated and compared with new acceptable alternatives, based on six main sustainability aspects: cost, environment impact, energy consumption, waste management, safety and personal health. The innovative technique with the analytical predictive models has to be developed for industrial applications. This technologies show high potential of productivity increasing while assuring sustainability principles. The introduction of dry machining is one of sollution of today's metal cutting industry that tirelessly endeavours to reduce machining costs and impact from chemicals in the environment. Modern tool tips are already capable of maintaining their cutting edge at higher temperatures, but even with these improvements in tool materials, the cutting edge will eventually break down. Applying cold air to the tool interface of these modern tool tips will also extend their tool life reducing the cost of metal cutting.

Keywords: Dry machining, air-cooling, principle of work of vortex tube

1 Introduction

The vortex tube was discovered by Ranque [1] and first described in detail by Hilsch [2]. Vortex tubes are now commercially used [3] for low-temperature applications, e.g. to cool parts of machines, to set solders, to cool electronic control cabinets, to chill environmental chambers, to cool food, to test temperature sensors, and they are also applied to dehumidify gas samples [4].
Recently it has been proposed that vortex tubes could be used as components in refrigeration systems replacing the conventional expansion nozzle in order to increase the efficiency [5].
The coolants in refrigeration systems pass through a thermal cycle in which the pressure may well drop below atmospheric.

ADJUSTABLE SPOT COOLER ADVANTAGES

- ► No moving parts.
- ► Quiet
- ► Driven by air not electricity.
- ► Small and light weight-portable.
- ► Low in cost compared to most others
- ► Superior design and performance
- ► Maintenance free operation
- ► Made of durable stainless steel and metal parts, no cheap plastic parts
- ► Adjustable temperature range
- ► Generators are interchangeable
- ► System uses strong magnetic base

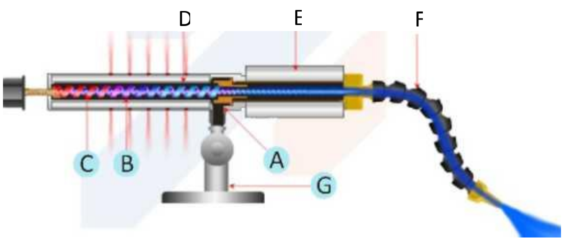

Figure 1 Vortex tube [6]

Figure 1 shows adjustable Spot Cooler- Compressed air enters at point (A) into the vortex tube component of the spot cooler. The vortex tube splits the compressed air into a hot (B) and cold (C) stream of air. The hot air from the vortex tube is vented to the atmosphere at point (D) after being muffled to reduce noise. Cold air enters into the muffler (E) and then distributed through the hose distribution kit (F) and onto the item being cooled. A strong magnet (G) holds the spot cooler in place. The temperature of the cold air is controlled by an adjustable knob.

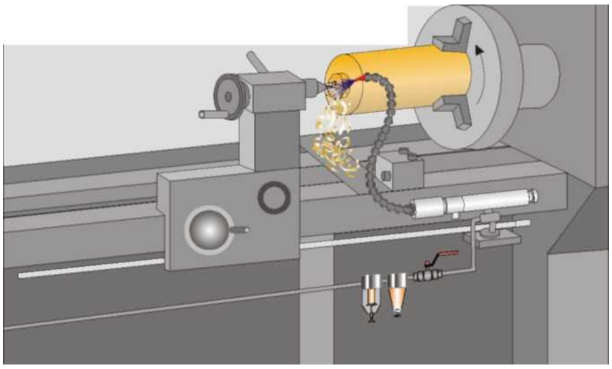

Figure 2 Using vortex tube for cooling turning process [6]

2 Principle of work of vortex tube

The flow rate and temperature in a Vortex Tube are interdependent. When you open the adjusting valve at the hot end, the cold air flow decreases and the temperature drops. As you close the valve the cold air end flow increases and temperature rises. The percentage of the total input air that exits the cold end is termed the "cold fraction". Depending on inlet air temperature a cold fraction of between 60% and 80% produces the optimum combination of flow and temperature drop for maximum cooling effect, when using an H generator. Lower cold fractions produce colder air but do not cool as well because of reduced flow. Most industrial applications require the 60% to 80% setting and the H generator for optimal cooling. In some instances such as cooling laboratory samples, testing circuit boards and other "cryogenic" applications, a 'C generator is used which limits the cold end flow rate to lower levels and produces very cold temperatures. To set the Vortex Tube to the desired temperature simply insert a thermometer at the cold end and adjust the hot end valve.

The inlet nozzle is tangential to the vortex generator and therefore can provide a high speed rotating airflow inside the vortex generator. Subsequently, there is a radial temperature gradient increasing from the inner core of the tube to the outside wall of the tube. This is primarily because of the potential energy of compressed air converting to kinetic energy due to the forced vortex caused by the external torque near the tangential air inlet. Therefore the high-speed swirling flow inside the tube and away from the walls is created. The existing air inside the vortex hot tube is normally at the atmospheric temperature and so, when the rotating flow enters the vortex tube it expands and its temperature drops to a temperature lower than the ambient temperature. The difference between these two temperatures will lead to a temperature gradient along the tube producing colder peripheral air than the core air. As a result, the central air molecules will lose heat to those in the outer region as shown in Fig. 3.

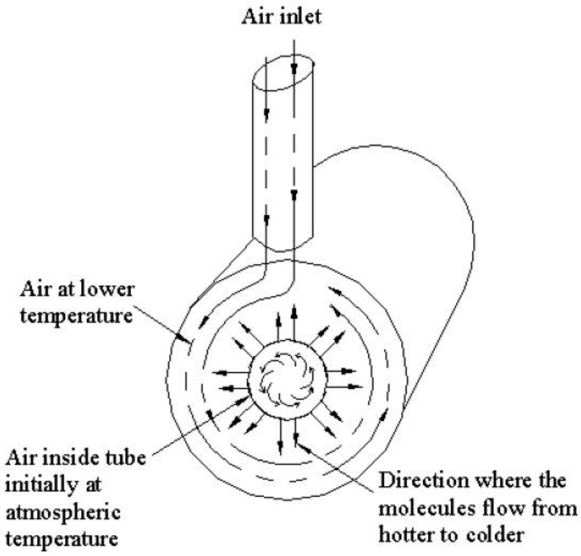

Figure 3 Radial heat convection in vortex tube due to the expansion of the compressed air [7]

It is notable that this system is a dynamic system due to the nature of the airflow in the tube and so will not reach equilibrium. Hence the peripheral air has a higher kinetic energy (hotter) than the inner air (colder). The existence of a major pressure gradient due to the forced vortex in the radial direction will provide a centripetal force for circular swirling and therefore it will lead to a high pressure at the tube wall and low pressure at the centre. When the air enters to peripheral region (A), as it expands, the outer air will be cooled due to its expansion. Consequently, the inner core air (B) will get warm because it is compressed by the expansion of the peripheral air.

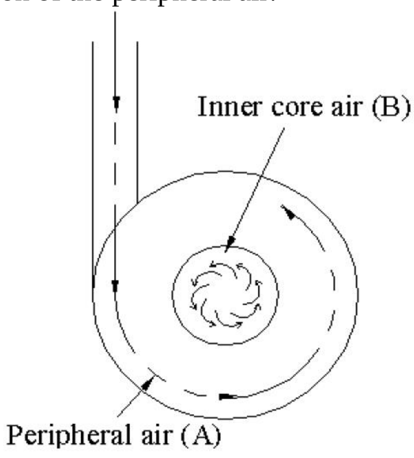

Figure 4 Schematic positions of the peripheral and inner core air [7]

Heat is then transferred from the inner core (B) to the outer core (A).
As the inner air is being compressed, it naturally tries to push against the periphery by expanding. Work is therefore done on the outer core air, which then gets heated and the difference in pressures results in the expansion and contraction of the air, which causes work to be done on the peripheral air. Work is therefore done on the outer core air, which then gets heated and the difference in pressures results in the expansion and contraction of the air, which causes work to be done on the peripheral air. Therefore, heat is transferred radially outward as shown in Fig. 4.

2.1 Temperature of hot/cold side on vortex tube

The vortex tube with atmospheric inlet pressure was operated for a variety of cold gas fractions Y= j_c/j_0. The temperature measurements are shown in figure 5.

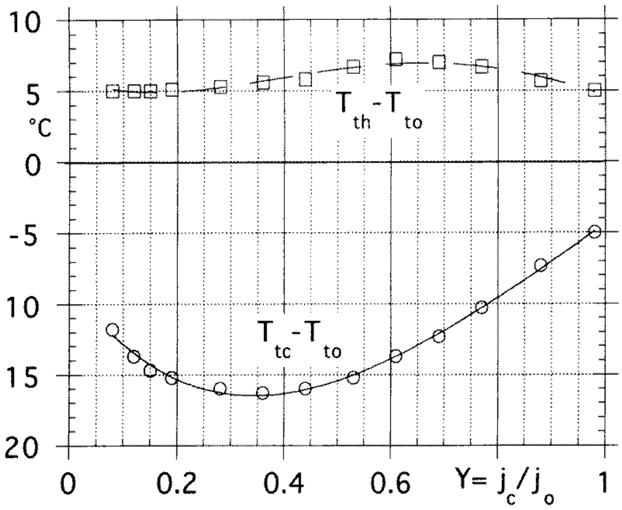

Figure 5 Exit temperatures for vortex tube with atmospheric inlet pressure [8]

Clearly the temperature splitting effect is obtained. The cooling is well developed, but it appears as if the heating is not quite as pronounced. We have lately become aware that varying the moisture content of the ambient air will change the thermal capacity of this working fluid significantly and hence contribute to variations of the temperature change. This effect could easily amount to several degrees and it should be more pronounced in the hot flow component than in the cold stream.
To put the temperature measurements into perspective several high-pressure curves for the same vortex tube are given in figure 6.

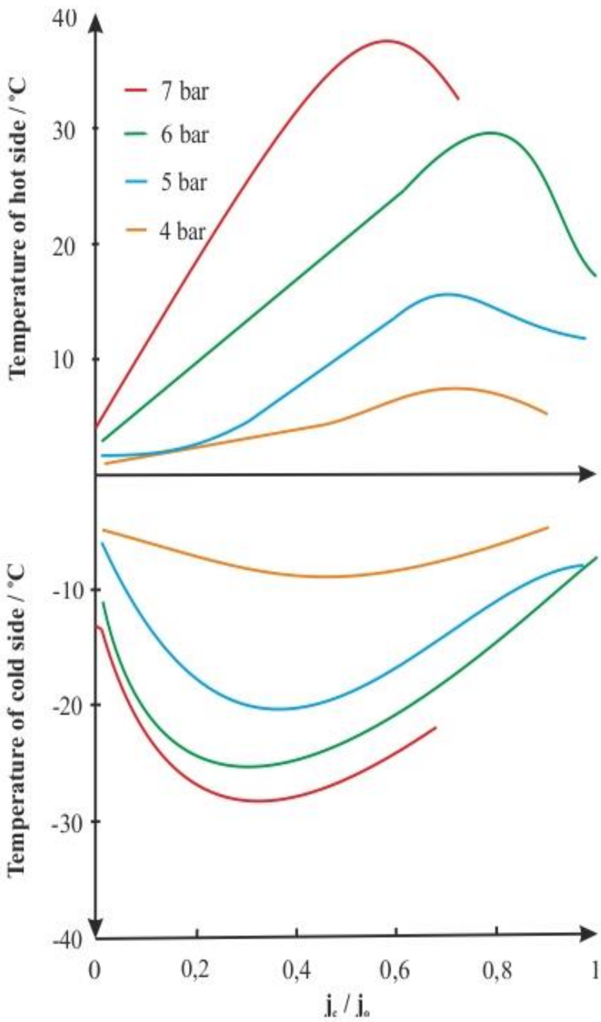

Figure 6 Total temperature separation for vortex tube operated with compressed air [8]

3 Effect of air-cooling on tool life

It is known that all the wear mechanisms increased at elevated temperatures reducing the tool life [9]. The application of cold air to the tool tip is shown to reduce the temperature at the tool tip enabling the tool tip to have a longer tool life [10]. The effectiveness of the air-cooled system can be shown when a comparison is made between the wear for a dry cut and an air-cooled cut for one minute and seven minutes of machining. Figures 7a-d show the flank wear as seen under a microscope.

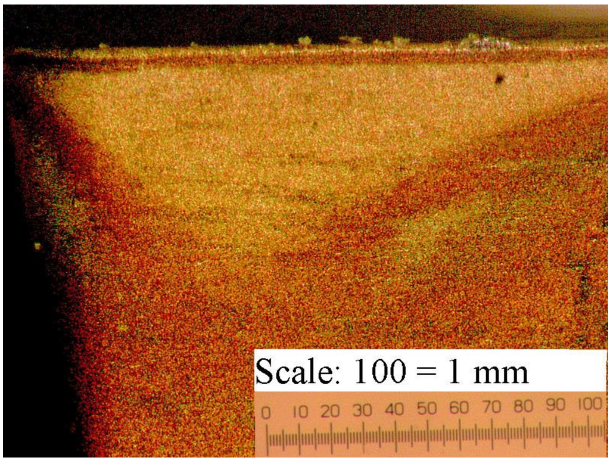

Figure 7a Picture showing flank wear for a dry cut after 1 minute of machining at a cutting speed of 190 m min-1 and feed rate of 0.23 mm/rev with a 2 mm depth of cut [7]

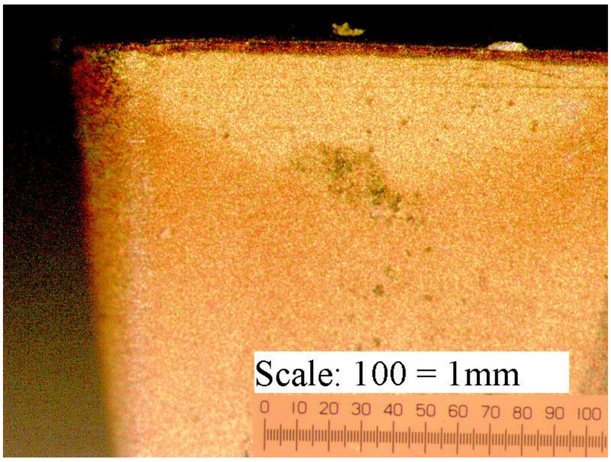

Figure 7b Picture showing flank wear for an air-cooled cut after 1 minute of machining at a cutting speed of 190 m min-1 and feed rate of 0.23 mm/rev with a 2 mm depth of cut [7]

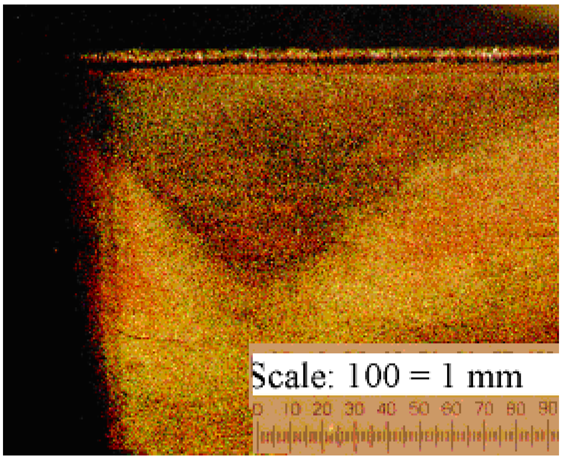

Figure 7c Picture showing flank wear for a dry cut after 7 minute of machining at a cutting speed of 190 m min-1 and feed rate of 0.23 mm/rev with a 2 mm depth of cut

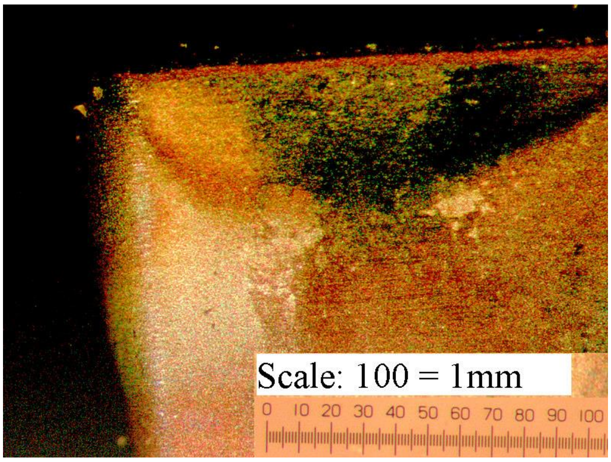

Figure 7d Picture showing flank wear for a air-cooled cut after 7 minutes of machining at a cutting speed of 190 m min-1, and feed rate of 0.23 mm/rev with a 2 mm depth of cut

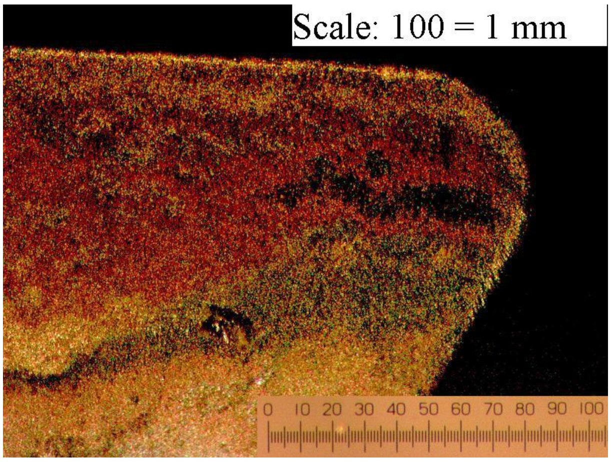

Figure 8a Picture showing top rake face wear for a dry cut after 7 minutes of machining at a cutting speed of 190 m min–1, and feed rate of 0.23 mm/rev with a 2 mm depth of cut [7]

The development of the flank wear was shown to take longer to develop when the cooled air was applied to the cutting zone as shown in Fig. 7d.

After seven minutes of dry machining the top rake face is starting to develop crater wear, at 0.5 mm from the flank face as shown in Fig. 8a. Further dry machining will accelerate this rate of wear. At this stage the tool radius shows no sign of wear and the top flank edge has no observable notches.

The air-cooled tool tip shows no visible sign of tool wear on the top rake face and the flank wear is also substantially reduced. Observation of the chips produced during dry and air-cooling indicated that much of the heat was being dissipated from the cutting zone.

Figure 9 shows the chips produced during the dry and air-cooled tool tip test. The left hand chips produced during dry cutting and the right hand produced during air-cooling.

Figure 9 Picture showing chips produced by a 2 mm depth of cut at 0.23 feed rate, and cutting speed of 190 m min-1 [7]

4 Conclusion

The results obtained from using compressed air combined with the vortex tube have shown that this method of cooling the tool interface is effective and compares exceedingly well with traditional cooling methods. The temperature recoded during air-cooling was found to be 60°C which is 40 °C cooler than that obtained during traditional wet machining and 210 °C cooler than dry machining as shown by Fig. 10. These temperatures were measured 1 mm from the tool interface and for that reason the temperatures recorded at this position are considerably reduced from that of the tool interface.

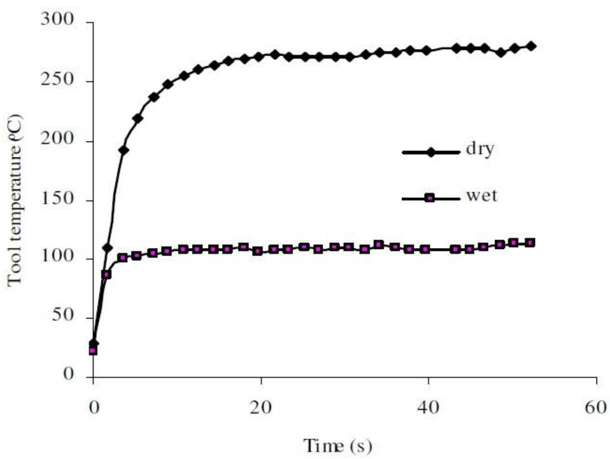

Figure 10 Temperatures recoded at the tool tip for dry and air-cooling [7]

The most convenient method of determining the effectiveness of the air-cooling is by determining the tool life, as it is known that there is a relationship between tool life and the wear mechanisms that are shown to increase at elevated cutting temperatures. Inspection of the tool tip using a microscope confirmed that the tool wear is reduced when being air-cooled, resulting in longer tool life. The vortex tube air-cooling systems proved to be effective at dissipating the heat from the tool tip, proving that air-cooling is an effective method of cooling tool tips. Therefore, whenever dry machining is the preferred method of metal cutting, aircooling should be incorporated as there are no associated environmental issues and will extend the life of the tool.

References

[1] Ranque G J 1933 Exp´erienesd sur la detente giratoire avecproductions simultanes d'un echappement d'air chand etd'un echappement d'air froid J. Phys. Radium IV (7) 112–14

[2] Hilsch R 1946 Die expansion von gasen im zentrifugalfeldals k¨alte prozess Z. Naturforsch. 1 208–14

[3] Swirl Tubes Norgren 5400 South Delaware, Littletown, Colorado; Vortex Tubes Exair products, 1250 Century Circle North, Cincinnati, OH, 45246, USA; Vortex Tubes Vortec Corp, Cincinnati OH, USA

[4] von Linde R 1950 Einrichtung zum abk¨uhlen einesverdichteten gases German Patent 926729 (24 October 1950)

[5] Keller J U 1993 J. Kl Klima Luft K¨alte Heizung 21 300–4

[6] http://www.nex-flow.com/vortex_tube.htm (15.07.2013)

[7] Brian Boswell and Tilak T Chandratilleke; Air-Cooling Used For Metal Cutting, American Journal of Applied Sciences 6 (2): 251-262, 2009

[8] B Ahlborny, J Camirey and J. U. Keller; Low-pressure vortex tubes, J. Phys. D: Appl. Phys. 29 (1996) 1469–1472.

[9] Young, H.T., 1996. Cutting temperatures to flank wear. Wear, 201: 117-120.

[10] Cook, N., 1973. Tool wear and tool life. ASME Tran. J. Energy. Ind., 95: 931-938.

Burr Formation after Face Milling of Compacted Graphite Iron used in Diesel Engine Blocks

M. O. dos Santos[1-3], G. F. Batalha[1], M. Stipkovic Filho[1-2] and E. C. Bordinassi[3]

[1] Laboratory of Manufacturing Engineering – Dept. of Mechatronics & Mechanical Systems Eng. Polytechnic School of Engineering - University of Sao Paulo - Av. Prof. Mello Moraes, 2231 São Paulo – SP – Brazil

[2] Universidade Presbiteriana Mackenzie – School of Engineering - Rua da Consolacao, 930 Sao Paulo – Brazil

[3] Dept. Mechanical Engineering – Instituto Mauá de Tecnologia – Praca Maua, 1 Sao Caetano do Sul – SP – Brazil

Abstract

Since the growing demand in the use of engine cylinder blocks of Compacted Graphite Iron (CGI), especially in diesel engines, and the cost spent on machining lines with deburring processes, this work aims to investigate the burr formation mechanisms during face milling of CGI, in a similar face of an engine cylinder block (6- cylinder in line). Carbide inserts were used in a 100 mm of diameter milling cutter. A Complete Factorial Planning was used to determine de quantity of experiments, varying the cutting speed, the feed rate, the depth of cut, the flank wear and the exit angle of the tool cutter from the workpiece. The burrs measurement was performed in seven different positions of the workpiece exit edge. The tool wear and the exit angle of the tool from the workpiece interfered significantly in the burr height. It was observed the decrease of the burr height with the increase of the feed rate and with the decrease of cutting speed and cutting depth. Through the software STATISTICA 8.0 values were obtained for main effects and interactions, along with confidence intervals and standard error. Finally, the adopted plan allowed the development of an empirical model capable of predicting the burr height.

Keywords: Compacted Graphite Iron, CGI, Face Milling, Burr, Cutting Parameters, Diesel Engines.

Introduction

The growing demand of the companies to expand their markets, by reducing costs and adding value to the product has been accompanied by solutions committed to the reduction of environmental pollution, such as reducing emissions of air pollutants and noise. In this context, the automotive industry and its suppliers have increasingly seeking to improve their processes and products as well as develop new materials and technologies to achieve a compromise between profits and low environmental impact [1].

A typical example of this can be viewed in the diesel engines manufacturing, where recent technological developments, both in performance and in reducing the emission of pollutants and noise, are the result of higher working pressures and temperatures, causing in the block engine major mechanical stress, which may cause premature breakage.

The gray cast iron, traditionally material used in the manufacture of diesel engine blocks, in the current levels of its development, only resist the efforts of high pressure from fuel combustion by increasing the sectional area of the material, an undesired situation. To avoid this situation, vermicular cast iron or CGI (Compacted Graphite Iron), with its mechanical properties intermediate to those of gray cast iron and nodular, is gaining force in the automobile industry [2].

However, such superior properties of this material imply a higher cost compared to machining of gray cast iron, mainly due to process times and higher tool wear. Thanks to these problems has been intensively researching the machinability of this material, so that it may be increasingly closer to gray cast iron.

Despite numerous studies involving machining processes in engine blocks, there are still many problems to obtain the final product within optimum parameters of tolerance and finishing surface. Among them may be cited the lack of quality at the edges of machined workpiece, a problem that takes into account the burr formation.

Burr is an undesirable protruding material out from the workpiece that is formed in front of the cutting edge due to the plastic deformation involved during machining [3]. Their size depends on the process and the machining operation, the material, cutting conditions, the cutting tool material, among others.

Besides being very harmful during the machining provoke premature wear of the tool, also cause geometric distortions in the machined surfaces difficult the assembly between components and endangers the physical integrity of workers and hinder or prevent the deployment of automated manufacturing. Thus, the occurrence of burrs in the manufacturing process is indispensable to use a deburring operation to remove them and to give to the finished part the design dimensional tolerance.

Despite the importance of the subject in machining there are few studies on the mechanisms that lead to the burr formation. There is more research on the deburring than with the aim of studying the mechanisms governing their formation to seek a way to avoid them or at least minimize them.

Among the research related to the burr formation, there were many researchers who have worked in their classification. In some cases the mechanism of burr formation was used, in others they were classified according to the cutting edge of the tool that generate the burr. The shape and burr direction were also criteria used to classify them.

In according with [4] three basic mechanisms of burr formation: a lateral deformation involving material flux to the free surface of the workpiece; chip bending to the same cut direction as the tool reaches the workpiece face and tensile rupture of the material located between the chip and the workpiece. According to these mechanisms they classified the burrs in four types: *Poisson* burr, *rollover* burr, *tear* burr and *rupture* or *cut-off* bur, as showed in Figure 1 [4].

In according with [5], after face milling stainless steel AISI 304 classified the burrs in five different types: Knife-type burr, Secondary-type burr, Burr breakage, Curl-type burr and Wave-type burr. According to [6], many studies have been conducted in an attempt to minimize the dimensions of burrs, since the appearance of these is inevitable in all machining operations.

Another researcher [7], has analyzed that the dimensions and geometric description of the burrs may be considered its height and its thickness. To measure these two quantities can be used since simple dial indicator to complex image analyzers. It is known that the thickness of the burr has an irregular profile making it a little more difficult to measure [8].

The Figure 2 shows the height and thickness of a burr, where t_b is the thickness of the root of the burr, t_{min} is the minimum thickness, $t_{máx}$ is the maximum thickness and h is its height.

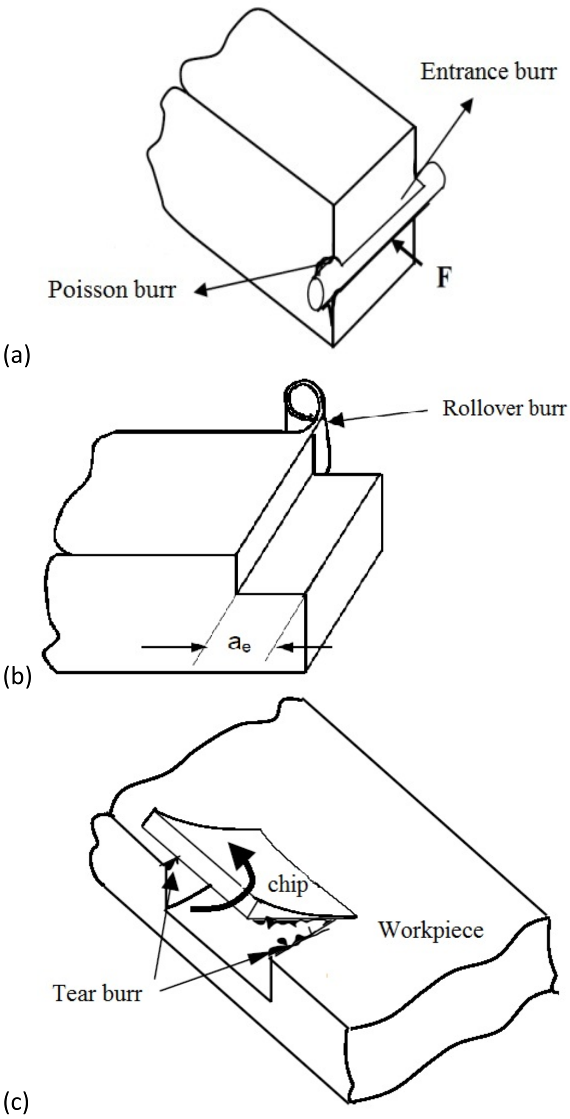

Figure 1. (a) *Poisson* burr; (b) *roll-over* burr; c) *Tear* burr [4].

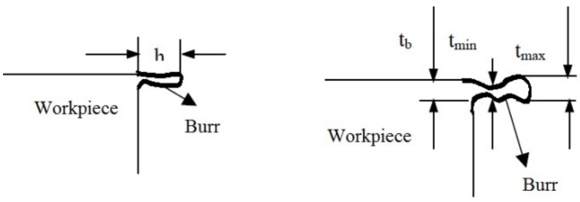

Figure 2. Burr dimensions scheme [7].

To simplify the analysis of the complex mechanisms of burr formation, the majority of researches on the subject use the orthogonal cut due to its geometric simplicity and to reduce the number of variables involved [9].

In orthogonal cutting, burr occurs in three stages: initiation, development and forming. The burr formation starts when the cutting tool is approaching to the end of the workpiece (Figure (3)), giving large deformation at its edge, creating a bulge, if the material is ductile and partial or total detachment edge, if the material is brittle [6].

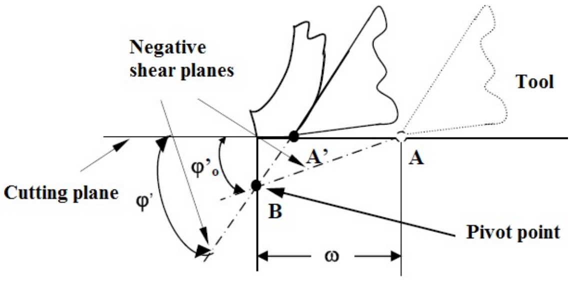

Figure 3. Geometric variables and the displacement of the cutting tool from point A to point A' and rotation of negative shear plane around B [6].

According to [6], the early formation of burr occurs at the instant that the chip formation ends when the cutting tool reaches the point A. Thus the energy that was intended for the chip is transferred to the burr formation. The displacement of the cutting tool from point A to point A' causes rotation of negative shear plane around the pivot point B. Occurs then the change of shear angle for your final condition (ϕ'). From this point burr formation occurs.

As studied by [10] is necessary to differentiate the investigations related to the formation of burrs in machining of research on how to minimize them. Gilespie et al. [4] in their work had already observed that the burrs cannot be avoided by changing machining parameters alone as feed rate, cutting speed and tool geometry.

These cutting parameters directly influence the formation of burrs and therefore must be taken into account in the analysis of the mechanisms of their formation. These parameters are in the foreground in influencing the burr formation and their dimensions can be minimized significantly by choosing appropriate cutting data [10].

Experimental Methodology

The machining tests aimed the measurement of the generated burr. They consist of the face milling of a workpiece with similar face to the flame face from an engine block of compacted graphite iron FV450 (Fig. 4), ISO 16112/2006 JV450, = 246HB Brinell hardness, yield stress = 355 MPa, elongation = 0.4%, using carbide interchangeable inserts.

Figure 4. Workpieces prepared for the machining tests.

The metallurgy laboratory from the Maua Institute of Technology, through some samples from the workpieces, has conducted analyzes of the each workpiece checking its graphite morphology and matrix structure, as shown in Figure 5.

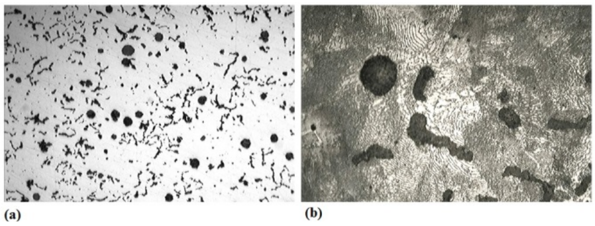

Figure 5. (a) Micrograph showing the morphology of graphite form III = 85%, and size 4-5, form IV = 5% and size 4-5, forms V+VI = 10% and size 5-6 (Magnification: 65x / without etching). (b)Micrograph showing the pearlitic matrix. Magnification: 325X / etching: 3% Nital.

The Figure 6 shows the workpiece ready for the tests in the machining center. Each plate is made of four linear surfaces of 240 mm, 56 mm of width and 14 mm of height useful for machining.

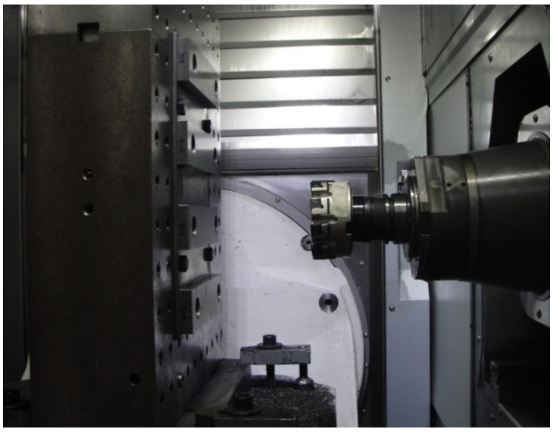

Figure 6. Workpiece set at a bracket on the table

of the machining center to perform the tests.

The machine tool used was a universal machining center GROB G550, cone HSK63, with 12,000 RPM rotation, 52 kW and 82.8 N.m. The machine is installed at the by B.GROB Brazil Center for Technology Application (CTA) (Fig. 7).

Figure 7. Machine tool GROB G550.

An Ingersoll face milling cutter VF2V 100R00 with 100 mm of diameter and capacity of 10 teeth was used. It consists of eight inserts with geometry for roughing and the other two with straightener's geometry as shown in Figure 8 (a). The rough cemented carbide inserts used Fig. 8 (b) also Ingersoll, type NNE324-10, and straighteners Fig. 8 (c) type YDA323L101.

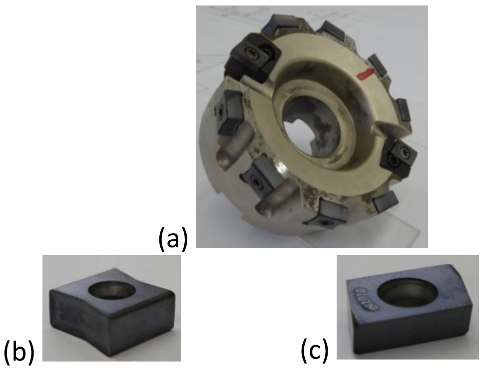

Figure 8. (a) Face milling cutter, (b) Rough insert NNE324-100, (c) Straighteners insert YDA323L101.

The device of the straighteners inserts have adjustable in the axial direction to ensure flatness between them and rough inserts and also ensure good surface finish. The straighteners inserts are controlled by the axial height of 0,015 mm above the other eight rough inserts, whereas in the radial direction are 0.10 mm apart. This regulation does not allow straighteners inserts the basic function of chip removal, but only eliminate the peaks, giving a better finish to the milled plane.

Tests were performed to relate the main parameters of machining processes (cutting depth, feed rate, cutting speed, flank wear and exit angle of the tool from workpiece), with the burr height. In Figure 9 there is an indication of the machining direction and the division of the workpiece edge in seven segments for burr height measurement.

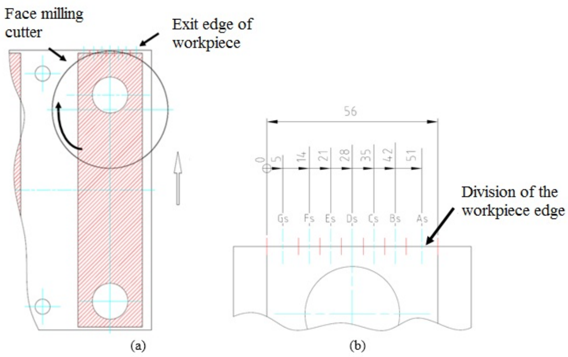

Figure 9. (a) Indication of machining direction; (b) Division of the workpiece edge in seven segments for burr height measurement.

The four controllable parameters: cutting speed, feed per tooth, depth of cut and flank wear were considered as input variables, while the burr height (h) is the output variable. Table 1 shows the four factors with their respective levels adopted in the complete factorial planning.

Table1 - Variables of factorial planning

Factors	Vc [m/min]	fz [mm/tooth]	Ap [mm]	$V_{B\ max}$ [mm]
1 (min.)	130	0,05	0,3	0
2 (max.)	190	0,1	0,7	0,3

The number of tests was determined through the Complete Factorial Planning $\mathbf{2^k = 2^4 = 16}$ tests. On a single test is obtained two test responses (h), one for each level of the output angle of the cutter tool, being $\theta_{mín} = 160^o$ and $\theta_{máx} = 180^o$, as Figure 9. Therefore, in the planning must be obtained thirty-two responses (h). Three replicates were performed for each test, totalizing 24 + 3x16 = 64 tests and 128 responses.

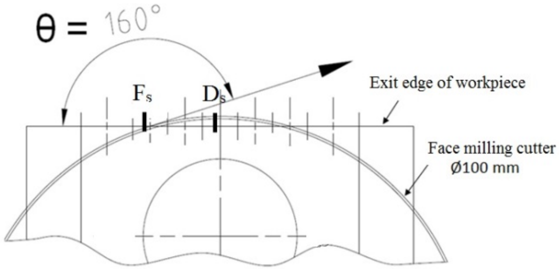

Figure 10. Description of D_s and F_s points for burr height measurement

Table 2 shows the sequence of milling tests performed, combining all parameters.

Table 2. Tests sequence

Vc [m/min]	fz [mm/tooth]	ap [mm]	Trial.
130	0,05	0,30	1
190	0,05	0,30	2
130	0,10	0,30	3
190	0,10	0,30	4
130	0,05	0,70	5
190	0,05	0,70	6
130	0,10	0,70	7
190	0,10	0,70	8
130	0,05	0,30	9
190	0,05	0,30	10
130	0,10	0,30	11
190	0,10	0,30	12
130	0,05	0,70	13
190	0,05	0,70	14
130	0,10	0,70	15
190	0,10	0,70	16

After each machining condition, the burr height on the exit edge piece was measured by the profilometer by Hommelwerke, model Wave System WL-120 installed in the metrology department from B. GROB Brazil, as Figure (11).

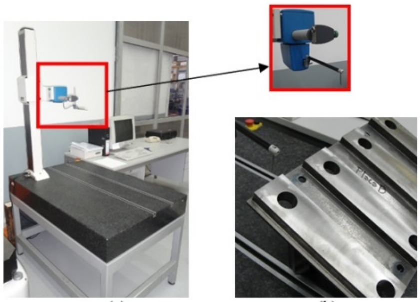

Figure 11. Profilometer used to measure the burr height formed in the tests.

In Figure 12 it's verified the procedure for collecting the burr profile formed, which through the WL-120 software is possible to treat the image of the burr profile and quote it with accuracy of ±0,1µm.

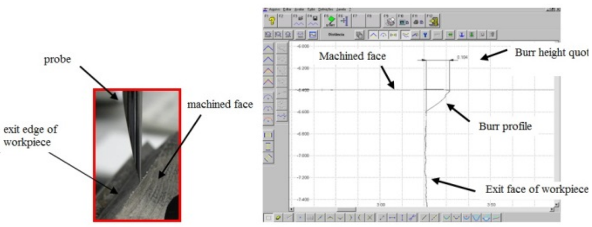

Figure 12. Burr height measurement Procedure after each test completion via interface WL-120.

Results

Due to the clockwise milling cutter, the teeth enter by the exit edge of the piece between the segments A_s and D_s and leave by the segments D_s and G_s, generating a combined output of the workpiece edge: entrance and exit of teeth cutter. It was considered the burrs generated between the segments A_s and D_s input burrs and the burrs generated between the segments D_s and G_s, output burrs. Because of the greater height of the burrs formed on the segment D_s, the exit edge of the piece, these burrs are considered outbound.

Through the tests, particularly in conditions of high tool wear, was noticed the presence of burr with two different morphologies: curl-type and knife-type (Fig. 13), as [5]. Parameters such as the exit angle of the tool from the workpiece, and even the cutting tool wear, among other less influential define the type of morphology generated at the edge of the workpiece. It was observed that the shape was characteristic as stretching burr (*tear*), according to the classification provided by **[4]**.

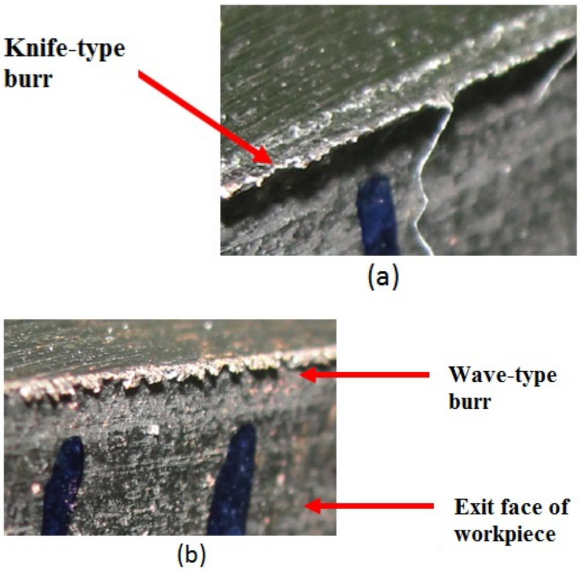

Figure 13. Analysis of burr formed during the tests 15^{th} (a) and 13^{th} (b), for V_{Bmax}=0.3mm.

The burrs heights obtained in the G_S to A_S region, for the test 13^{th} using wear inserts ($V_{B\ max}$=0,3mm) are showed in the Fig. (14).

It can be noticed from Fig. 13 the larger dimensions of burrs formed in the region of output burr than the region of the inlet burr at the exit edge of the workpiece. This is due to the effect of the displacement of the cutter on the inlet region to provide a deformation in the material and a large portion of this deformation is distributed over the workpiece material itself, preventing the expansion of the same, which makes the size of the burr lower. The same does not occur in the output region, since deformation of the material will extend beyond the edge, forming a burr much higher.

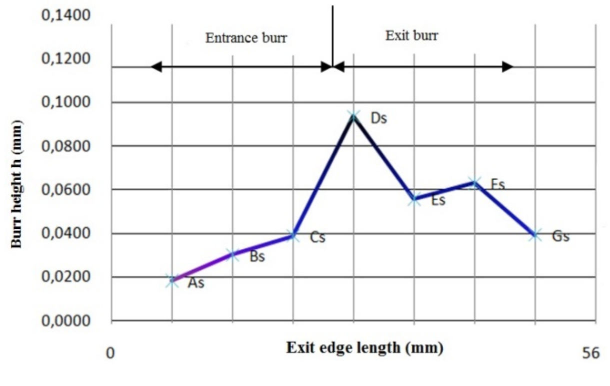

Figure 14. Variation of the burr height at the output edge formed during the 13th test.

Analysis of the results confirms that generally, the segment D_S output angle equal to 180 °, shows larger burrs than the other segments (A_S to G_S) which confirms the results found by **[11]** which defined the region D_S as the critical point of the leading edge of the engine block. The reference **[12]** justify the increase of the burr height at this point due to the progressive approach of the cutting tool to the end of the workpiece edge, then the edge undergoes plastic deformation when on it operates at higher shear force, causing the reduction of thickness cutting and folding of the chip accordingly.

Factor analysis was applied to the results and allowed it to indicate the influent parameters on the average burr height, in which utilized a confidence index equal to 95%. Therefore, the software STATISTICA 8.0 was used.

The Fig. 15 illustrates the average effects of V_C, f_Z, a_p, θ e V_{Bmax} on the burr height *h* using the complete factorial planning.

From the results, was observed that the tool wear presented results with burr heights higher because these promote greater lengths of contacts in the chip tool interface which cause increases in machining efforts, in power consumption and cutting temperature, which facilitates the deformation of the material without the same emphasis to the edge of the workpiece, forming burrs with larger dimensions than those found in milling with new tools.

It was noticed that for small cutting depths, such as in this work, the cutting action occurs manly by the secondary edge of the cutting tool, then generating the primary burr, which possesses an increased dimension proportional to the depth of cut until a boundary transition. The transition boundary from primary to secondary burr was not observed among the parameters evaluated in this experiment. The increased of the depth cut generated a small increase in the burr size.

In face milling of medium carbon steel AISI 1040 (hardness of 180HB), **[13]** observed a decrease of 50% in burr height, while its cutting speed was doubled, while **[8]** noticed only fluctuations of the burrs dimensions, not being clear its decrease with the increase of cutting speed.

In the present study, although insignificant, there was a small reduction of the burrs height by increasing the cutting speed, but without statistical significance, compared to the observed high dispersion.

The increase in the cutting speed reduces friction at the interface chip tool. The reduction of this friction provides similarly, a corresponding increase in primary shear angle, reducing the degree of discharge and consequently plastic deformation in the primary shear plane.

Changes in feed rate provide variation in cutting force, temperature and plastic deformation of the material. During the milling, for small feed rate, the compression generated by the cutting tool on the material edges generates a large plastic deformation. This deformation provides an increase in the burr size. As much as the feed rate increases, it becomes clear the increase in chip thickness sheared, providing a reduction in the plastic deformation and consequently the burr height. The same as **[11]**, in this work was observed good significant of the feed rate, with its negative effect, it means, while the feed rate increases the burr height decreases.

Through Figure 16 it can be seen that significant effects within the confidence range of 95% had been tool wear and the exit angle of the tool from the workpiece. While the most significant interactions were cutting speed with depth of cut, cutting rake angle and feed rate, where these interactions was influenced to a lesser extent by the cutting speed, which was already noted, has little linear influence on burr formation. Then tool wear was the most important parameter in the burr formation, followed by feed rate and rake angle of the workpiece.

In the construction of the empirical model, where the burr height is a function of five variables, being $h = f(Vc, fz, ap, V_{Bmax}, \theta)$, the model that best predicts the burr height as a function of this variables, with the standard error coefficient estimated in ± 0.001625, can be estimated by the Eq (1):

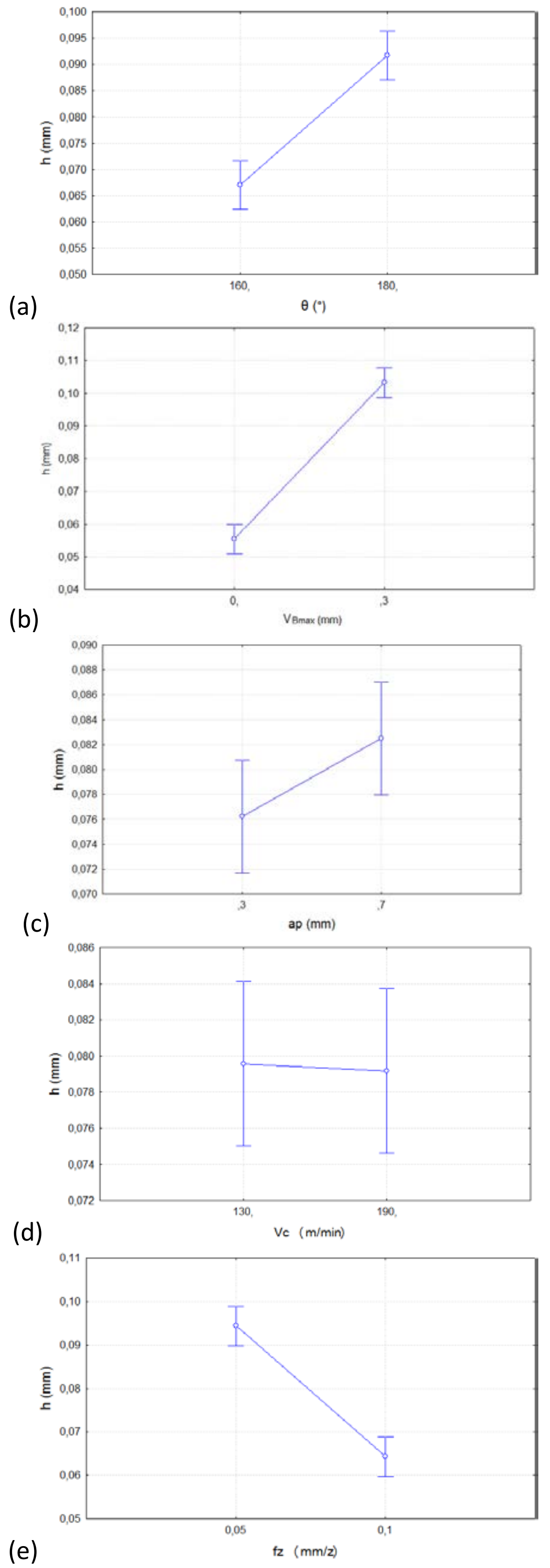

Figure 15. Effects of average factors on burr height through complete factorial design, depending on the parameters (a) angle θ, (b) maximum flank wear (c) depth of cut (ap) (d) cutting speed (e) feed per tooth.

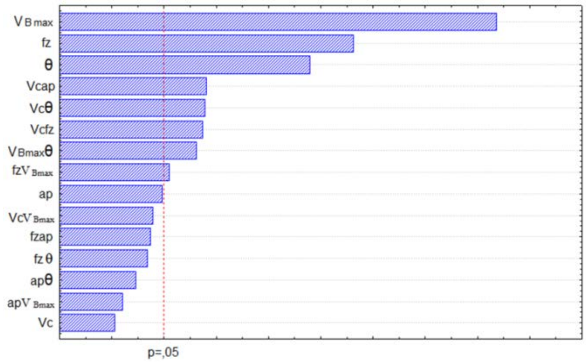

Figure 16. Pareto diagram for the main effects and interactions on the burr height h.

$$\hat{h} = 0.07937 - 0.015052.\mathrm{f}_z + 0.0239.V_{Bmax} + 0.012342.\theta + 0.005630.V_c.\mathrm{f}_z - 0.005870.V_c.a_p + 0.005806.V_c.\theta - 0.003590.\mathrm{f}_z\, V_{Bmax} + 0.005253.V_{Bmax}.\theta \quad (1)$$

Briefly, residues between the measured and estimated values can be analyzed by the graphs of Figure 17. The residues left by the tests distributed normally and random, as is noted in Fig 17.a. The amounts of residue for the tests are shown in Figure 17b.

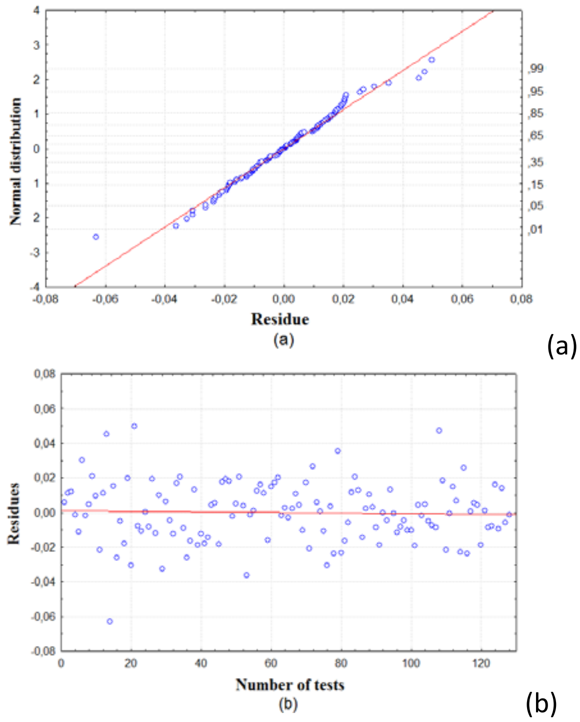

Figure 17. Residual between the measured and estimated values. a) - Normal distribution of the residue, b) - Residual values for 128 responses.

Conclusions

The following conclusions can be drawn from the present investigation:

- In general, with the cutting parameters investigated, the increase of cutting speed (v_c), the increase of feed per tooth (f_z) and the reduction of depth of cut (a_p) promoted the decrease of burr height (h).
- The burrs have their increasing heights from the end of the edge to the center thereof.
- The output burrs have larger dimensions than the input burrs.
- The cutting speed had become less influential in burr dimensions in relation to the other used cutting parameters.
- Wear cutting tools provides greater burrs than those presented by new tools.

Acknowledgements

The authors are gratefully acknowledge to Tupy Fundições for providing the work material, to Maua Institute of Technology (IMT) for the micrograph analyzes, to Iscar Brazil for providing the cutting tool and inserts, and to B. GROB Brazil for supporting with the machine tool.

References

[1] Santos, M. O., 2012, Study of Burr Formation after Face Milling of Compacted Graphite Iron used in Diesel Engine Blocks, 155p. (In Portuguese) Master dissertation – Polytechnic School of Engineering - University of Sao Paulo, Sao Paulo, Brazil.

[2] Guesser, W. L. 2009, Mechanical properties of cast irons (In Portuguese). São Paulo, Brazil: Ed. Edgard Blucher, 336p.

[3] Palman, S.; Müller, S. & Bechler, M., 2011. Marktübersicht Entgrattechnik für Werk stücke im Automobil Powertrain. Bereich. 52 p. Projektarbeit – Hochschule Kempten – University of Applied Sciences. Germany.

[4] Gillespie, L. K. & Blotter, P. T., 1976. The Formation and Properties of Machining Burrs. Journal of Engineering for Industry – Transactions of the ASME, v 98 Ser B, n 1, p. 66-74

[5] Lin, T. R., 2000. Experimental Study of Formation and Tool Chipping in the Face Milling of Stainless Steel. Journal of Materials Processing Technology, v. 108, n. 1, p. 12–20.

[6] Ko, S.L. & Dornefeld. D.A. 1996. Analysis of Fracture in Burr Formation at the Exit Stage of Metal Cutting. Journal of Materials Processing Technology, v. 58, n. 2-3, pp. 189-200.

[7] Kishimoto, W., Miyake, T., Yamamoto, A., Yamanaka, K., & Tacano, K., 1981. Study of Burr Formation in Face Milling. Bull. Japan Soc. of Prec. Eng., vol.. 15 n. 1, pp. 51-52.

[8] Da Silva, L. C., 2004. Study of Burr Formation in Face Milling of Gray Cast Iron Motor Block Using Inserts of Ceramic and PCBN. 176 f. Master dissertations (In Portuguese) Federal University of Uberlândia. Uberlândia MG- Brazil.

[9] Hashimura, M., Dornfeld D. A., 1995. Analysis of Three Dimensional Burr Formation in Oblique Cutting. Annals of the CIRP. vol 44, n.1, pp., 27-30.

[2] Aurich, J.C.; Dornfeld, D.; Arrazola, P.J.; Franke, V.; Leitz, L. & Min, S., 2009. Burrs-Analysis, Control and Removal. International Conference on Burrs, CIRP Annals – Manufacturing Technology. V. 58, n.2, pp. 519-542

[11] Da Silva, L. C., 2011. Behavior of the Burr in Face Milling of PH 13 8Mo Stainless Steel. 190 f. (In Portuguese) Doctoral Thesis – Federal University of Uberlândia. Uberlândia MG, Brazil.

[12] Chern, G.L. & Dornfeld, D.A., 1996. Burr / Breakout Model Development and Experimental Verification. Transactions of the ASME - Journal of Engineering Materials and Technology. Vol. 118, n. 2, pp. 201-206. doi:10.1115/1.2804887.

[13] Olvera, O. & Barrow, G., 1998. Influence of Exit Angle and Tool Nose Geometric on Burr Formation in Milling Operations. Proceedings of The Institution of Mechanical Engineers Part B - journal of Engineering Manufacture, vol. 212, n. 1, pp. 59-72.

Groove rolling of a round bar

T. Pepelnjak[1], S. Štarkel[2]

[1] *University of Ljubljana, Slovenia*
[2] *Štore Steel d.o.o., Slovenia*

Abstract

Steel making plant having great diversity of 350 different rolled profiles, bars and strips in their production program produces also 50 dimensions of round steel bars. Due to demanded geometrical accuracy with the bars roundness as one of the most difficult attainable parameter the production of round bars demands high knowledge in technology of groove rolling. Therefore, the process of rolling set-up gets quite complicated. The existing process is based on use of computer program for groove design and calculating rolling parameters, called Wicon, but it gives only rough values needed for rolling mill settings. Hence, to get the proper settings, calibration experts still have to rely on their experiences. In the paper, the procedure of the rolling mill set-up is presented. The positioning of the produced bar dimension with diameter of Ø32 mm rolled with groove shapes determined by Wicon was analysed and positioned into prescribed tolerance field. Finally, the guidelines for further research work were stated in order to improve the bar tolerances and stabilize the rolling process.

Keywords: hot rolling, process set-up, Wicon program

1 Introduction

Production of rolled feedstock having different shapes for various manufacturing applications is known for decades. Since this technology is performed in hot stage with several technological parameters it is still very comprehensive and difficult to optimise. Since trial rolling of each shape is still indispensible various computer programmes for calculation of rolling mills are in use. In particular difficult and technological complex is hot groove rolling of round bars and wires where theoretical knowledge needs to be supported also with practical experiences of workshop personnel.
The rolling of bars and profiles with profile mills is called groove rolling where the calculation of parameters on mills are far more complicated as it is the case in flat rolling. Furthermore, the majority of works dealing with rolling process is oriented to flat rolling process and only minor part of research activities deals with groove rolling.
Minimal difference between the circumferences of the mill pair is called roll gap which determine the reduction of the profile during the rolling on the observed mill pair. The shape and size of this gap is influenced by the elastic deformation of the roll mill combined with the mill displacements due to clearances of the rolling system – so called "jump" [1] – Figure 1. Therefore, the roll gap is increased regarding to its initial values at the beginning of the rolling process [2].

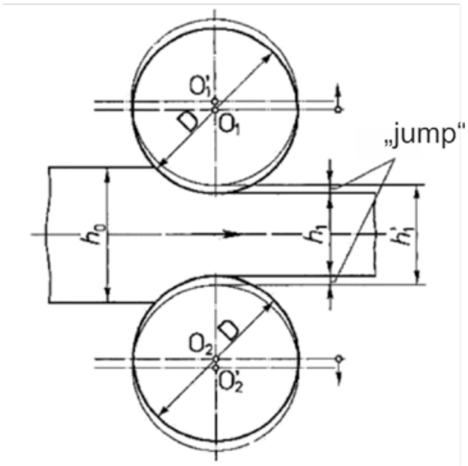

Figure 1 Rolling gap and "jump" [1].

2 Groove rolling set-up

The set-up of groove rolling process consists of:

- Determination of necessary reduction of cross-section (initial to final shape)
- Determination of the bar's shape reduction for each rolling pass
- Determination of necessary mill pairs, their numbers and shapes
- Determination of rolling gaps and rolling speeds for each rolling pass.

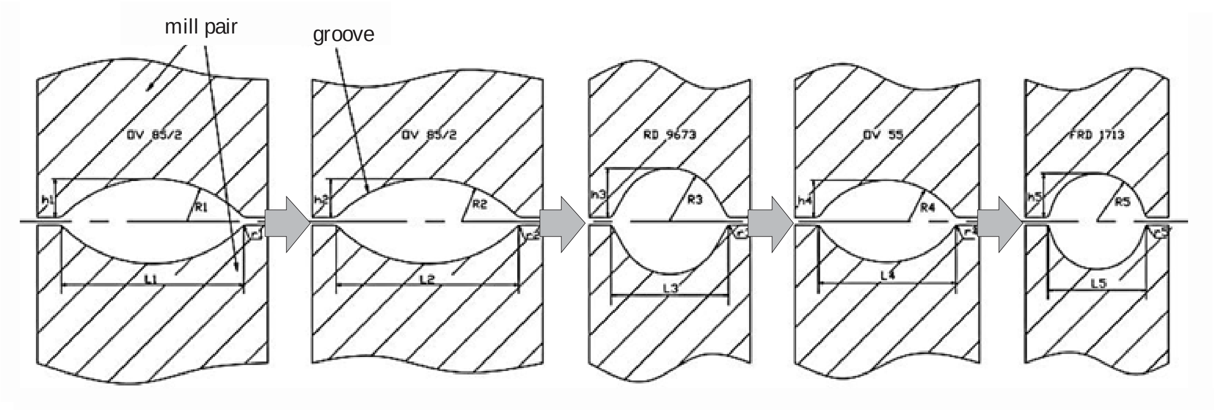

Figure 2 Sample of a groove multi-pass rolling line / courtesy Štore Steel

The set-up of the entire multi stage rolling mill is calculated in reverse order from the final product shape to the initial rolling profile. According to the literature [1] due to the temperature decrease during the rolling process the allowed cross-section reduction is from 30-35% at the beginning of the multi-stage line while it decreases down to 10 to 15% at the final stage. The changes of a groove shapes for a multi-pass line are presented on Figure 2 [3].

While the initial contact between rolling mills and workpiece material has less influence on the rolling process at flat rolling this cannot be stated for the groove rolling. The cross-sectional stress strain condition at groove rolling is very complex and non-uniform demanding also the alternating loading of the rolled material. This can be assured by horizontal and vertical positions of the rollers on the multi-stage mill – Figure 3 [4, 5].

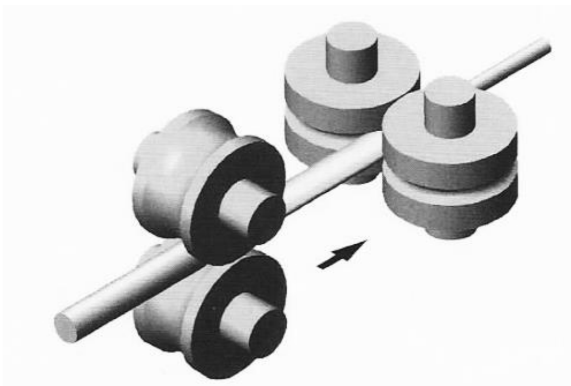

Figure 3 Multi-stage groove rolling concept [5].

Lee et all [4, 5, 6] have analysed shape optimisation of the roller pair during groove rolling and effect of roll gap adjustment on exit cross sectional shape. They have analysed proper tool geometry set-up – Figure 4 - for minimisation of rolling errors and defects appearing during the hot forming process. Furthermore, they have calculated the shapes of the rollers for horizontal and vertical setup of the tool. The influence of strain rate vector on bar rolling was analyzed by Deng et all. [7] while Kwon et all. have analyzed the influence of rolling process on material homogenization and grain refinement during the bar rolling process [8].

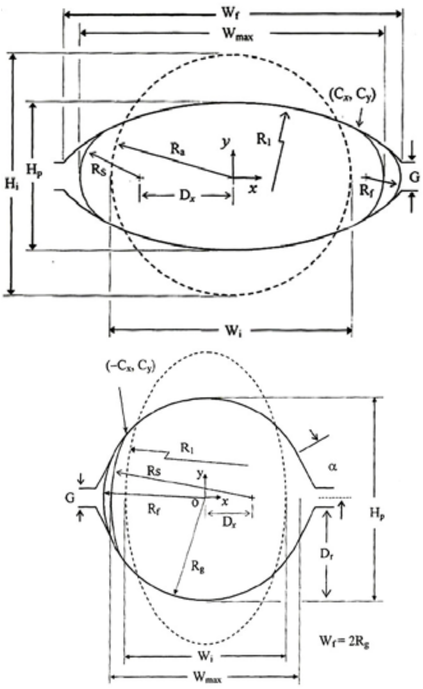

Figure 4 Shape of horizontal roller (middle) and shape of the vertical roller (bottom) [4].

3 Rolling of Ø32 mm bar

The groove rolling process was analysed for round bar having 32 mm in diameter and tolerances according to the DIN EN 10060 standard. Material for the bar was 1.1191 (C45E according to DIN). Parameters of groove rolls were analysed and determined by the computer programme Wicon [9] used for calculation of tool geometry. The program calculates following parameters:

- G_{teo} Theoretical size of the roll gap
- v_{teo} Theoretical output velocity of the rolled bar
- D_{teo} Theoretical diameter of the rolls
- W_{teo} Theoretical width of the profile
- H_{teo} Theoretical height of the profile
- λ_{teo} Theoretical R-factor.

Theoretical R-factor noted also with parameter λ represents the ratio between the input and output cross-section of the rolled specimen for each individual sequence of the conti-rolling line

$$\lambda = \frac{A_0}{A_1} = \frac{l_1}{l_0}.$$

Calculation of the geometry for the entire rolling line was performed for forming of a bar having diameter of Ø32 mm from a squared profile of 72x72 mm with roundness of 10 mm on the corners. The Wicon program has calculated rolling in nine passes out of which five are with horizontal rolls and four with vertical rolls. The rolls are positioned as follows:

1 horizontal – 2 horizontal – 3 vertical – 4 horizontal – 5 vertical – 6 horizontal – 7 vertical – 8 horizontal and 9 vertical.

The calculated circumferential rolling speeds of the mill tool pairs varies from 0.88 m/s for the first rolling sequence up to 4.25 m/s for the ninth pair of the rolling mill. The conti-rolling line used for bar rolling is presented on Figure 5 while the entire set-up of the geometry for the calculated rolling line is presented on Figure 6.

The calculated values of roller dimensions and kinematics for conti-rolling line were base for manufacturing of individual pair of rollers. Therefore, bars produced by determined geometry and proper set-up of roller speeds have to express dimensions within the prescribed tolerance field.

Figure 5 Conti rolling line / courtesy Štore steel [6].

Experimental verification of hot rolled round bars was analysed by measurements of 18 bars with dimensions of Ø32x5000 mm. In order to minimise the influence of initial bar grip at individual pair of rollers the bar diameter was measured 200 mm form each end of the bar and on the middle of each bar. The 54 acquired measurements in two perpendicular directions have resulted in following average values:

Measuring point 1 (begin of the bar):

- Vertical position: 32.23 mm
- Horizontal position: 32.07 mm

Measuring point 2 (middle of the bar):

- Vertical position: 32.25 mm
- Horizontal position: 32.09 mm

Measuring point 3 (end of the bar):

- Vertical position: 24 mm
- Horizontal position: 32.08 mm

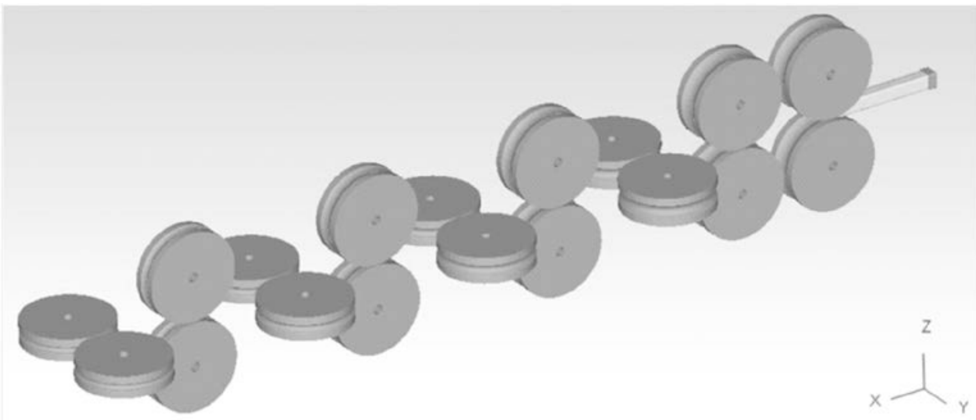

Figure 6 Set-up of the rolling line for production of bars having with Φ 32 mm in diameter

Average value of all measurement in horizontal position is 32.08 mm while the average value for the vertical position is 32.24 mm respectively. Prescribed tolerances for roundness at hot rolling of the analysed bar diameter are 0.9 mm. The produced material is within tolerance field and very similar to those predicted by the Wicon programme – Table 1.

Table 1 Roundness of the analysed bar Ø32 mm.

	Heigth [mm]	**Height [mm]**	**Roudness [mm]**	**Diameter Mean value [mm]**
Calculated value (WICON)	32.04	31.99	0.05	32.02
Measured value	32.24	32.08	0.16	32.16

4 Conclusions

The hot rolling process of round bars with groove rolling is complex forming procedure influenced by several parameters. The help of computer programs like Wicon already enables faster set-up of rolling process but the start-up of production process due to various parametric influences on rolling gap, "jump", temperature decrease along the conti-rolling line etc. is not well defined.

Currently there is still lack of knowledge when fine tuning of the entire conti-line is performed and this operation is influenced by the operator's knowledge and experience. In future research work the industry express needs on process optimisation and proper set-up of individual rolling phases oriented towards decrease of used energy for rolling process being in line with guidelines of sustainable production.

References

[1] F. Gologranc: Forming: part 2, Bulk Forming. Ljubljana: Univerza v Ljubljani, Fakulteta za strojništvo, 1999. ISBN 961-6238-22-1. (in Slovene)

[2] Rolling mill roll deflection (online). 2010. (used 18.6.2013). https://en.wikipedia.org/wiki/File:Rolling_mill_roll_deflection.svg.

[3] Case of a groove rolling line. Courtesy Štore Steel d.o.o., 2013

[4] Y. Lee: Rod and Bar Rolling: Theory and Applications. New York: Marcel Dekker, Inc., 2004. ISBN 0-8247-5649-5.

[5] M. Awais, H.W. Lee, Y.T. Im, H.C. Kwon, S.M. Byon, H.D. Park: Plastic work approach for surface defect prediction in the hot bar rolling process Journal of Materials Processing Technology, Vol. 201, Iss. 1–3, 26 May 2008, 73-78

[6] S.M. Byon, D.H. Na, Y. Lee: Effect of roll gap adjustment on exit cross sectional shape in groove rolling - Experimental and FE analysis, Journal of Materials Processing Technology, Vol. 209, Iss. 9, 1 May 2009, 4465-4470

[7] W. Deng, D.-W. Zhao, X.-M. Quin, X.-H. Gao, L.-X. Du, X.-H. Liu: Linear Integral Analysis of Bar Rough Rolling by Strain Rate Vector, Journal of Iron and Steel Research, International, Vol. 17, Issue 3, March 2010, 28-33

[8] H.-C. Kwon, Y.-T. Im: Process design for refinement and homogenization of microstructure in bar rolling, Journal of Materials Processing Technology, Vol. 167, Iss. 2–3, 30 August 2005, 273-282

[9] Computer programme WICON, http://www.wicon.se/. (14.9.2013)

[10] Conti-line in use. 2010. Courtesy Štore Steel d.o.o.

Microcontroller enabled real time monitoring of energy efficiency in micro EDM milling process

G. Tristo[1], A. Lebar[2], G. Bissacco[3], J. Valentinčič[2]

[1] *University of Padua, Italy*
[2] *University of Ljubljana, Slovenia*
[3] *Technical University of Denmark, Denmark*

Abstract

Energy resources consumption is an important issue, which is addressed by the concept and methods of sustainable development. In the domain of production engineering the importance of machining process energy consumption measurement is twofold. On the one hand it can be used as a machining process performance monitoring tool, and on the other hand as energy costs optimisation tool. In the paper energy monitoring was performed on a micro electrical discharge machining device. Electrical current was measured by means of a Hall sensor. Electrical signals were online processed and saved to the database by means of microcontroller system which is described in detail. Topographies of machined work-pieces were measured and analysed with respect to the measured electrical energy in order to calculate the material removal volume per unit of consumed electrical energy.

Keywords: Electricity consumption monitoring, microcontroller, micro EDM milling.

1 Introduction

Sustainability has become an important issue in all spheres of life. This will be the case for many years to come, or at least until we find an as yet unknown solution. Sustainability focuses on safeguarding natural resources against exploitation, in the name of productivity and competitiveness, by manufacturing and service organizations. Public sector and non-profit organizations are also at fault. It is a major concern in many countries and is leading to strict regulations regarding the impact of products and services during their manufacturing, use and disposal.

Companies around the world have shown interest in environmentally friendly manufacturing. Companies have been under increasing pressure to seriously think about their sustainable business practices both in manufacturing and services. The pressure promoting sustainable business practices is both external (government regulations, profit and not-for-profit organizations) and internal (strategic objectives, top management vision, employee safety and well-being, cost savings, productivity and quality).

In this paper, a mini framework for developing sustainable business development through sustainable production operations is presented. The energy consumption of the micro EDM milling process related to the energy consumed only by a dielectric unit will be analysed. The novelty presented here is the design, build, and use of a cheap acquisition system based on a microcontroller board Arduino Uno to monitor energy consumption of micro EDM milling process.

Anastas and Warner define green chemistry as “the design, development, and implementation of chemical products and processes to reduce or eliminate the use and generation of substances hazardous to human health and the environment” [1]. One could define green manufacturing, green marketing and green supply chain in a similar way [2].

Sustainability is about building a society in which a proper balance is created between economic, social and ecological aims. Sustainability can be pursued at different levels: business, product design, supply, production, distribution, remanufacturing/recycling. Production sustainability includes managing the processes with sustainable input such as energy, people, equipment and machines with the objective of reducing waste, rework, inventory and delays as well as reducing carbon footprint.

With rising to new records of prices per kWh and the introduction of taxes related to Green House Gas (GWP) emissions, energy is being considered by industrial enterprises as a valuable resource which requires to be strategically planned and managed with more and more sophisticated optimization strategies. Accordingly to recent studies [3], electricity monitoring in manufacturing companies should be performed in 3 levels or orders: factory, department, and unit process. Examining the lower level, energy bills can be sensibly eased reducing machine tools energy wastes. To accomplish this task different approaches are available, from product design optimization and life cycle management to production plant scheduling and tool machine ecodesign. What all these approaches have in common is the requirement of complete transparency of energy usage among the entire manufacturing facilities, which means that it is necessary to implement a detailed grid of meters to characterize energy consumption over time, plus an informatics system capable to log data from meters, process it and visualize human readable results in support to management and decision making.

In addition, power metering systems can report a wide range of parameters to characterize voltage quality, which is very important especially in applications that are sensitive to voltage sags, surges and disturbances. As a matter of fact, electricity is probably unique in being a product which is manufactured, delivered and used at the same instant of time [4] hence it is important for the company to monitor if contract claims are respected by providers as with any other variable input.

2 Measuring the electrical energy consumption

In general, the electrical energy consumption is calculated by Eq. 1:

$$E = \int_0^t P(t)\,dt, \tag{1}$$

where $P(t)$ is an electric power as a function of time t. Instant power P is a product between instant voltage U and instant current I. When using AC (sinusoidal) current supply to power linear, also known as Ohm loads, the power used on a load can be simply calculated by Eq. 2:

$$P = V_{\mathrm{RMS}} \cdot I_{\mathrm{RMS}}, \tag{2}$$

where root mean square (RMS) value of some arbitrary quantity x is calculated by Eq. 3:

$$x_{\mathrm{RMS}} = \sqrt{\frac{1}{n}\sum_{i=1}^{n}(x-\bar{x})^2} \tag{3}$$

But most of the production machines consist of several subsystems with linear, capacitive and inductive loads. In this case, a simple calculation using Eq. 2 gives the apparent power and not the real power. To calculate energy consumption at a given time, the sum of instant power (Eq. 4) over the observed time is calculated using Eq. 1.

$$P(t) = V(t) \cdot I(t), \tag{4}$$

3 Micro EDM

Material removal in Electrical Discharge Machining (EDM) is performed by means of electrical pulses between tool and workpiece electrodes. In EDM machines the electrical discharges are provided by a generator, but other electrical components are required in order to perform precision micro machining. Setup

3.1 Sarix SX-200

The machine that has been selected for the energy efficiency investigations in this work is a Sarix SX-200 (**Figure 1**), state of the art in micro electrical discharge machining, capable of performing micro EDM milling, drilling, die-sinking and grinding operations.

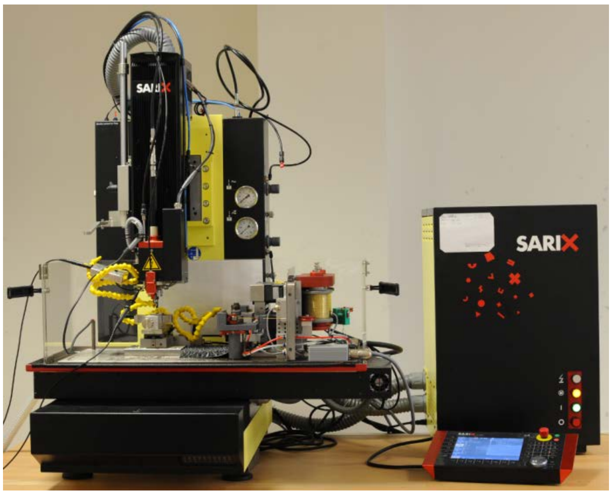

Figure 1. Sarix SX-200 micro EDM milling machine

The machine is made of three main sub systems with different electrical elements: the main C structure with motors, actuators and other equipment to perform machining, the control unit (SX-CU) with generators and logic boards to drive the process and the dielectric unit (SX-DA) for filtering, cooling and pumping the dielectric liquid. The flushing of dielectric liquid, which in this case is low viscosity hydrocarbon oil, is provided by a pump directly on the machining area through a hose.

The focus of this paper is only SX-DA unit which is connected to the SX-CU only for communications purposes and is connected to the power grid through with a separate plug. SX-DA is equipped not only with the necessary electrical pumps, one for flushing and one for cooling and filtering the dielectric, but also with the auxiliaries such as power supply, electro valves, temperature and pressure sensors, logic boards, SX-CU communication interface board, relays, safety switches, and circuit breakers.

In Table 1 are listed the machining parameters that were used during the energy consumption monitoring.

Table 1. Machining parameters

POL [-]	-	-
WIDTH	4.6	μs
FREQ.	130	kHz
CURR.	50	A
VOLT.	130	V
GAIN	50	-
GAP	100	-

3.2 Microcontroller

The most useful information about the energy consumption of SX-DA unit with details about its subsystems is provided by measuring, recording, processing, and displaying the energy consumption of main subsystems as given in Table 2.

To this end, it is necessary to build a system capable to read analogue signals from current and voltage sensors, convert them to digital values, perform mathematical operations, store the results in a database, and finally display the relevant information in human readable format. Other secondary but important requirements of the system are related to its costs and ease of use, in order to encourage its application in small and medium industries. Costs and dimensions of the system should be reduced to minimum, while the flexibility should be high enough to easily adapt it to different machines. Results should be remotely accessible and, of course, invasiveness over machine operation must be avoided.

To satisfy these requirements, a system has been designed and made by necessary number of current and voltage sensors, connected to a microcontroller board to process signals from sensors, Ethernet connection for data transfer, and a web server to store and display results, as in **Figure 2**.

A microcontroller board chosen for this work is an Arduino Uno, which sports an Atmel ATmega328 microcontroller clocked at 16 MHz, 2 KB SRAM and 6 analogue inputs with 1024 levels analogue to digital converter at a nominal sampling rate of 10 MS/s. Ethernet shield has been added to both Arduino Uno boards to be able to send data through existing Ethernet network to the remote server.

Current sensors have been selected from commercially available options that are based on Hall-effect integrated circuits, which are available in different sizes. In this system, two types of ACS 712 sensors were used: the first type with the peak current of 5 A and the second type with the peak current of 20 A. Voltage sensors instead have been assembled in-house and are based on a voltage divider circuit, in order to simply scale down the voltage signal from 220 V AC (Table 2: A1-CH2, A2-CH1, A2-CH2) and 12 V DC (Table 2: A2-CH3) to the range of 0 to 5 V that is accepted by the microcontroller Analog-to-Digital Converter (ADC). All current and voltage sensors, as well as Arduino Uno boards were powered by a dedicated 9 V power supply unit with additional 5 V voltage regulator to stabilize the DC voltage required by all the elements of the system.

Results from the data elaborated with Arduino are sent over Ethernet to a remote server using UDP protocol. On the server, incoming data was read out, stored and visualized on a graphical user interface by a script written in Processing language.

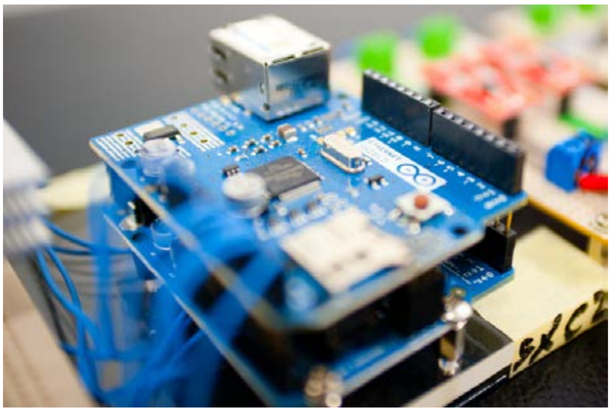

Figure 2. Arduino Uno microcontroller board and Ethernet Shield as were used in the experiments

Table 2. List of main electrical components in SX-DA unit and their allocations to Arduino based monitoring system

Component	Description	Microcontroller	Channel
MAIN	Main plug of dielectric unit SX-DA	A1	CH2
P1	Pump: low pressure flushing circuit	A2	CH1
P2	Pump: dielectric cooling and filtering circuit	A2	CH2

3.2.1 Clock Speed

Arduino Uno AVR RISC-based 8 bit microcontroller has a clock speed of 16 MHz, which theoretically should give enough computational power to sample current and voltage signals, perform calculations and send elaborated data to the server. However the programming language is not optimized for floating point calculations, hence operations with variables can occupy the microcontroller for several clock cycles, reducing the number of samples per second.

3.2.2 SRAM

Arduino Uno microcontroller board is built around the ATmega328 chip, which has 2 KB SRAM. This means that the maximum number of elements that can be stored in memory is very limited. As an example, if we want to store in memory unsigned long elements that are 4 bytes in size having a total of 2048 byte SRAM available, no more than 512 variables can be initialized. This is just a theoretical estimation, the actual limit is lower. In any case it is evident that it is not possible to use SRAM to store values for a long period of time, it can be used as a small buffer but the data must be saved into a remote server.

3.2.3 Data transfer protocol

The data elaborated by the microcontroller is sent to a computer that will store and display it to the user in a human readable format. Cheap microcontrollers as is Arduino Uno are not able to perform multiple operations in parallel; as a consequence it is important to minimize data transfer time because the time spent to send data to the remote server corresponds to a sort of blackout in sampling the signals from the sensors. As far as transmission protocols Arduino Uno offers different possibilities as communication through USB and Ethernet. The maximum speed of the serial port is limited to 115.2 kbps and it is not suitable for connecting many Arduino boards to the same computer, it is a better solution to use Ethernet protocols as HTTP, TCP/IP or UDP adding an Ethernet Shield to Arduino. In this case not only the transmission speed is drastically increased with its nominal transfer rate of 10 Mbps but the connection between microcontrollers and server is extremely simplified, with the added possibility to supplant complicated wired connections with a wireless router. Among the available protocols over Ethernet, UDP trading a little of data transmission reliability for a substantial increase in data transmission speed.

3.2.4 Analogue to digital converter

The analogue to digital converter (ADC) of the ATmega328 microcontroller by default is capable to convert analogue signals at a rate of about 10 Ksps, which is sufficient in sampling a voltage/current signal characterized by a frequency of 50 Hz. However in practice conversion rate of the ADC is different than sampling rate of the system, which is affected by data transfer time, computational load between analogue channel readout, especially when manipulating floating numbers and number of channels that are read. As a matter of fact, the 6 analogue inputs/outputs of the microcontroller board are multiplexed and hence read successively, with two important negative outcomes: first, when reading the signals from multiple sensors the sampling rate decreases to a fraction; secondly, channels are not read simultaneously but there is a short time interval between each channel readout.

It is evident that an increase in ADC speed, or conversion rate, would be doubly beneficial in diminishing the influence on results of the issues described above. Interestingly it is known [5] from the ATmega328 datasheet that the ADC by default is under clocked at 125 KHz, while it can withstand clock frequencies up to 200 KHz without any side effect, or 1000 KHz with a marginal loss in resolution. After setting the prescaler of the ADC clock to 32, which corresponds to a clock speed of about 500 kHz, it was possible to acquire during the experiments from 850 to 1150 S/s, depending on the number of channels and the complexity of calculations.

In order to monitor energy and power, voltage and current sensors are required. Voltage sensor is a voltage divider circuit, while current sensors are commercially available breakouts that are developed around Allegro Microsystem ACS712 integrated circuit. Amplitude and offset trimmers of the output signal have been adjusted to fit the range accepted by Arduino analogue input pins, with the assistance of an oscilloscope.

The nominal resolution of Arduino Uno internal ADC is 10 bit, which corresponds to 1024 levels on a measured range, and the accepted voltages at the input ports are in the range of 0÷5 V. This translates in a resolution of about 0.6 V for voltage sensors, since complete sine wave needs to fit into the measured range of the microcontroller input and amplitude voltage equals to $\pm 220\sqrt{2}$. Following the same procedure, the resolution of current measurements is 0.014 A for 0÷5 A current sensors and 0.055 A for 0÷20 A current sensors.

3.1 Arduino software

As any software in general the Arduino script written in C programming language accepts some values as inputs, processes them, and finally makes available the results at the output. The inputs in this case are signals between 0 V and 5 V originating from current and voltage sensors that are connected to the analogue input/output pins. The Arduino software has to accomplish the following tasks: to read analogue values as fast as possible, to perform the necessary calculations to obtain the desired values, and finally to send them to the server.

The microcontroller board is equipped with 6 analogue inputs. One of them is allocated to a voltage sensor and the other five are available for current sensors. Voltage and current values required to calculate real power have to be acquired in the very same instant, but as previously introduced when discussing about the ADC, in Arduino the analogue inputs are multiplexed and as a consequence they are not read simultaneously but successively. However if the analogue channels are read fast enough relatively to the frequency of the input signal this difference can be neglected. This is very important to properly calculate instant power (Eq. 4). The microcontroller's algorithm cycles between three main loops:

1. a loop to acquire all the values from the ADC (all channels subsequently)
2. a loop to perform calculation on the acquired values
3. a loop to send the data to the server This was done intentionally to reduce the time discrepancy between voltage and current signals by acquiring them as close as possible and to reduce the "blackout time" by optimizing data transmission.

In the first loop analogue channels are read and converted to digital values as fast as possible. Values are stored into variables. In the second step calculations are performed. Variables are scaled according to the prior defined calibration gain and offset factors to the physical values. Calibration factors, for each sensor are determined as described later in **section 4.3**. As mentioned before, the SRAM is not capable to store a large number of variables and data transmission is not fast enough to send a live stream of values, hence real power, RMS of voltage and RMS of current are calculated with running algorithms continuously at maximal sampling rate (Eq. 5), and results are sent to server with a time interval of 1 second.

$$RMS_{i+1}^2 = RMS_i^2 + \frac{\left(Val_i - RMS_i^2\right)^2}{i} \qquad (5)$$

$$P_{i+1} = P_i + \frac{V_i * I_i - P_i}{i} \qquad (6)$$

In the formulas given as Eq. 5 and 6 above, V_i and I_i are instant values of voltage and current respectively, $V \cdot I$ is instant power, P is real or average power, RMS can represent voltage or current RMS depending on the value assigned to Val. The Eq. 5 and 6 are derived as follows:

$$\begin{aligned}
\bar{x}_n &= \frac{1}{n}\sum_{i=1}^{n} x_i = \frac{n-1}{n}\frac{1}{n-1}\left(\sum_{i=1}^{n-1} x_i + x_n\right) \\
&= \frac{n-1}{n}\frac{1}{n-1}\sum_{i=1}^{n-1} x_i + \frac{n-1}{n}\frac{1}{n-1}x_n \\
&= \frac{n-1}{n}\left(\frac{1}{n-1}\sum_{i=1}^{n-1} x_i\right) + \frac{1}{n}x_n \\
&= \bar{x}_{n-1} + \frac{1}{n}(x_n - \bar{x}_{n-1}),
\end{aligned}$$

where x can be rms of voltage or electric current [6].

Other values that are calculated and stored in memory are: number of samples which contribute to the average values, microcontroller time reference at the beginning of the analogue inputs sampling and number of periods of the sampled sine wave signals. Every second identification number, time reference, number of samples, voltage RMS, voltage frequency, and for each current channel frequency, current RMS, real power, are converted with a predefined pattern into a binary packet that is then sent to the server. While these values are sent to the server, the information from sensors are lost, but using UDP data transfer protocol it was possible to limit the blackout time to only 3÷5 milliseconds.

3.1.1 Server

Since raw data is processed in Arduino and results are transmitted to the server every second, data throughput is moderate, and consequently server hardware requirements are also moderate. For this work an Acer Aspire 5738 laptop with 2 GHz Intel Core2Duo processor and 4 GB of RAM was used.

Data is sent by both Arduino boards to server through an Ethernet connection using UDP protocol at a predefined UDP port. The software on the server that manages the incoming data was written in Processing programming language, because of the similarities with Arduino programming language. The software listens to the predefined UDP port and once a packet of binary data is received the variables are decoded and stored in a formatted text file. Results can be monitored in real time through the graphical user interface and processed using Matlab for further analysis.

3.2 Calibration

Calibration of voltage and current sensors was performed using a multimeter as reference. Dedicated software was made for both server and Arduino to calculate the offset of the analogue signal, and then to estimate the gain matching the two RMS values read from the multimeter and the sensor.

Alternating current (AC) in general is varying through all the sensor range and depending on the setting of the trimmers on sensor breakout can show a response curve that is not perfectly linear at the extreme values. For this reasons current sensors have been calibrated in Direct current (DC). A calibration circuit was made with a variable 0 to 12 V power supply capable to provide up to 6 A and a suitable high power resistor in order to dissipate from 0 to about 5 A, which is the range of currents sensed during experiments. The calibration procedure was applied at different current values as in **Figure 3** for each sensor, with ranges of nominal current values that depends on sensor application, and repeated 5 times. At the end, the coefficients of the calibration function were obtained fitting the results. The response curve is not completely linear, but highly repeatable. Hence, the polynomial fit was used. For the sensor which calibration curve is shown in **Figure 3**, the function of the fitted curve is given as Eq. 7.

$$current = -2.29 + 0.005 + ADC^2 * 1.5 * 10^{-8} - ADC^3 * 4.64 * 10^{-11} \quad (7)$$

In **Figure 3** example of data from calibration procedure relative to sensor A2-CH2 for SX-DA dielectric flushing pump, tested in a range from -2 to +2 A, which shows a perfectly linear response curve.

4 Experiments

Energy consumption of the machine was measured while performing a pocketing operation of a circular cavity with a diameter and depth of about 527 µm and 30 µm respectively, on a block of plastic mold steel in milling configuration and with a tungsten carbide tool electrode. Given that technological parameters don't have any direct influence on the power consumption of the SX-DA unit, only one set as reported in **Table 1** was tested. The test was repeated 9 times. Energy consumption was calculated from the data recorded on the server by the acquisition system described in previous sections. The main variables that are stored in the database about every one second for each channel are the time reference of the record, voltage RMS, current RMS and real power.

In order to be able to expand this work in future, by comparing results relative to different working conditions and process parameters, the results have been related to unit of material removed. The volume of material removed has been measured after the experiment with an optical profilometer.

4.1 Geometrical characterization of the microfeatures

The geometries of each of the 9 blind holes machined during the experiments (**Figure 4**) have been characterized using a Sensofar PLµ Neox confocal microscope, by acquiring a 3D reconstruction of the microfeature and hence by measuring the diameters and depths with Image Metrology SPIP software. It was then possible to calculate the volume of material removed during the µEDM process as reported in **Table 3**.

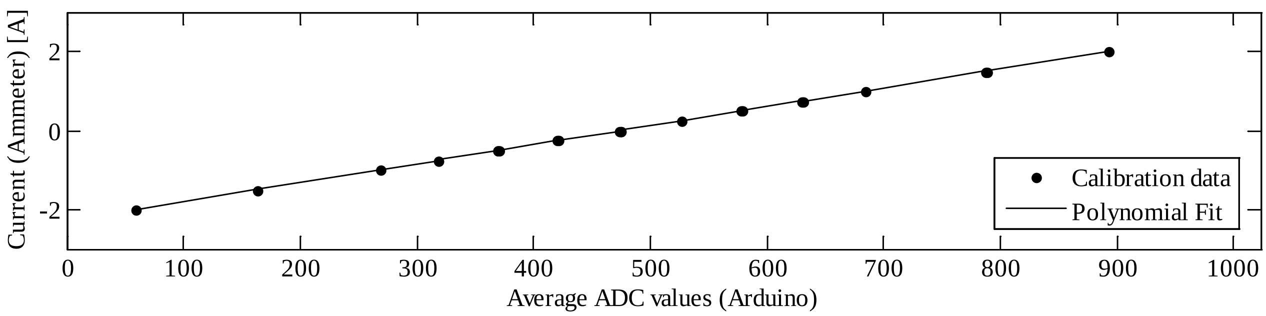

Figure 3. Calibration curve for current sensor

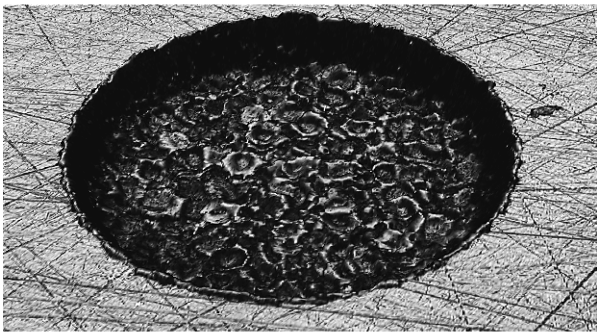

Figure 4. Confocal image of a blind hole machined by µEDM, having a diameter of 527.6 µm and a depth of 30.3 µm.

4.2 Machining time

The power consumption monitoring system has been started before the machining process was launched and stopped after the tool electrode was cut at the end of each experiment. For this reason several information was recorded that was not related to machining, while to evaluate for instance the efficiency of the process it is important to select the data relative to the machining. The machining timeframe, and consequently the time that was required to remove the material of the blind hole, were retrieved with a script in Matlab by using the flush pump as indicator of the status of the machine. As a matter of fact the flushing of dielectric is turned on at the beginning of machining and then it is stopped at the end of the operation. The flushing pump is then turned on again to cut the tool electrode at the end of each experiment, as it is possible to notice in **Figure 6**. In average for the 9 experiments the machining operation was lasting about 413 seconds, as reported in **Table 3**.

4.3 Energy consumption

The values stored in the database were processed in Matlab, using the time references defined in **Section 4.2**, in order to calculate relevant indicators that can eventually be used to compare the energy efficiency of different machining operations. Real power has been averaged through the machining time, energy consumption has been calculated as described in **Section 2** and finally the energy consumption per unit of volume of material removed has been gathered from the geometrical characteristics of the machined holes and energy consumption. Results are reported in **Table 3** and **Figure 5**.

4.4 Discussion of results

The results reported in tables and figures introduced in previous sections show a good repeatability of the measures (**Table 3**), which is a necessary requirement for the reliability of the acquisition system.

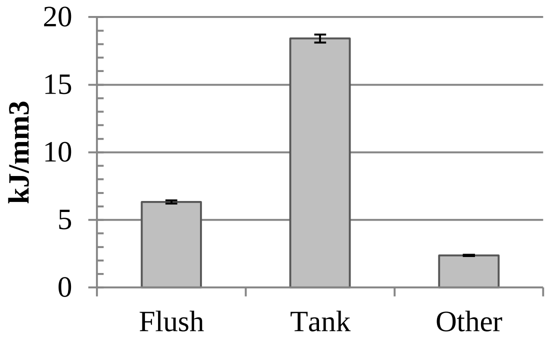

Figure 5. Average energy consumption per unit of volume of material removed relative to the subsystems of the dielectric unit

The measured average real power of 292 W, relative to the tank pump, is compatible with the manufacturer specifications, which rate the power consumption to 300 W.

The chart in **Figure 5** can be used to compare operations which are different for machining parameters, working conditions or even technology. This capability is of paramount importance in enhancing the sustainability of industrial processes. For instance, this system enables process parameters optimization for sustainability, based on objective data.

Plots like that in **Figure 6**, updated in real time, can give valuable information about the on-going process, enabling sophisticated analysis and providing necessary data for critical decision making.

5 Conclusions

A low cost system, consisting in a number of Arduino microcontroller boards with Ethernet Shields, voltage and current sensors and a server, has been developed for the real time energy monitoring of a µEDM machine tool. Custom software has been developed for both the Arduino boards and the server to calibrate the sensors and to acquire, process, store and display data. Sensors have been calibrated across all the operative range. The system has been applied and tested for the measurement of the overall energy required to machine a cylindrical pocket with the µEDM machine, and the energy consumed during the process by some of the machine sub systems. The geometrical characteristics of the blind holes have been measured with an optical profilometer. The data collected in the database was analysed and related to the volume of material that was removed, in order to calculate the energy per unit of volume of material removed.

In conclusion, the proposed system for real time monitoring of energy consumption has proved to be able to deliver valuable and actual information about the process with satisfactory repeatability.

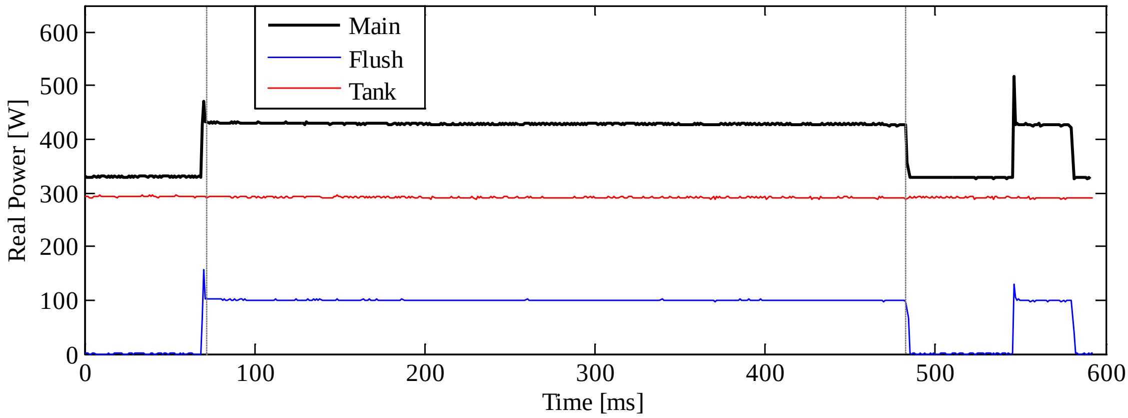

Figure 6. Real power data as recorded by the acquisition system of the SX-DA unit. The activity of the pump that flushes the dielectric on the workpiece was used as reference to identify the machining operations along the acquisition timeframe

Table 3. Geometrical characteristics of the blind holes and time, real power, energy required by the dielectric unit and its main subsystems during their machining

Rep. n.	M. time s	Radius mm	Depth mm	Volume mm^3	Main W	Flush W	Tank W	Main kJ	Flush kJ	Tank kJ
1	412.5	0.2636	0.0298	6.5	429.0	99.5	290.2	177.0	41.1	119.7
2	412.5	0.2626	0.0300	6.5	430.6	100.9	292.1	177.5	41.5	120.5
3	412.5	0.2629	0.0304	6.6	429.0	100.2	291.0	176.9	41.2	120.0
4	412.5	0.2629	0.0300	6.5	429.8	100.4	291.8	177.2	41.4	120.4
5	413.5	0.2638	0.0303	6.6	430.9	100.8	292.7	178.2	41.7	121.0
6	412.5	0.2628	0.0301	6.5	429.4	100.4	291.7	177.0	41.3	120.3
7	412.5	0.2638	0.0305	6.7	428.2	99.8	290.8	176.5	41.1	120.0
8	412.5	0.2637	0.0290	6.3	431.4	101.1	292.7	177.8	41.6	120.7
9	412.5	0.2632	0.0299	6.5	429.1	100.1	291.7	177.0	41.3	120.3
AVG	*412.6*	*0.2633*	*0.0300*	*6.5*	*429.7*	*100.4*	*291.6*	*177.2*	*41.4*	*120.3*
STD	*0.3*	*0.0005*	*0.0004*	*0.1*	*1.1*	*0.5*	*0.9*	*0.5*	*0.2*	*0.4*

6 Bibliography

[1] P.T. Anastas, J.C. Warner (Eds.), Green Chemistry: theory and practice, Oxford University Press, Oxford (1998)

[2] A. Gunasekaran and A. Spalanzani, “Sustainability of manufacturing and services: Investigations for research and applications,” International Journal of Production Economics, vol. 140, no. 1, pp. 35–47, Nov. 2012.

[2] E. O’Driscoll and G. E. O’Donnell, “INDUSTRIAL POWER and ENERGY METERING – A STATE-OF-THE-ART REVIEW,” Journal of Cleaner Production, Oct. 2012.

[3] D. J. Start, “A review of the new CENELEC standard EN 50160,” in IEE Colloquium on Issues in Power Quality, 1995, vol. 1995, pp. 4–4.

[4] J. Oxer and H. Blemings, Practical Arduino: Cool Projects for Open Source Hardware. Apress, 2009, p. 456.

[5] A.Lebar, L. Selak, R. Vrabič, P. Butala: Online Monitoring, Analysis, and Remote Recording of Welding Parameters to the Welding Diary, Journal of Mechanical Engineering 58(2012)7-8, 444-452

Linguistic model for estimation of surface roughness in milling

F. Čuš[1], and U. Župerl

[1] *University of Maribor, Faculty of mechanical engineering, Slovenia*

Abstract

This main goal of this paper is to presents a new method for surface roughness (R_a) prediction in end-milling by using initial cutting parameters and measured cutting forces signals. End milling machining process of hardened die steel with carbide end mill was modelled in this paper using the adaptive neuro fuzzy inference system (ANFIS) to predict the effect of machining variables (spindle speed, feed rate and axial/radial depth of cut) on surface roughness. In this paper we also discussed the developement of an ANFIS system that provide a linguistic model for the estimation of surface roughness from the knowledge embedded in the artificial neural network. The predicted surface roughness values determined by ANFIS were compared with experimental measurements. The comparison indicates that the performance of this method turned out to be satisfactory for evaluating Ra, within a 6% mean percentage error and 96% accuracy rate.

Keywords: Estimation, Surface roughness, Milling, ANFIS.

1 Introduction

Many parameters influence surface roughness in milling. Feedrate, cutting speed and tool geometry are controllable parameters, while tool wear, vibrations and workpiece/tool variability are uncontrollable. In manufacturing the relationship between process characteristics and surface roughness is difficult to capture. This is due to the complexity of the relationship between surface roughness and process characteristics. Therefore, an in-process method based on prediction model is required for the real time monitoring process.

Several models have been proposed to estimate the surface roughness. These include classical statistical approaches as well as fuzzy systems and neural networks. For instance researchers [1,2] developed an approach based on the least-squares regression for estimating surface roughness in machining while [3] have, respectively, used fuzzy pattern recognition for monitoring surface roughness over a limited range of cutting conditions. The capacity of artificial neural networks to capture nonlinear relationships in a relatively efficient manner has motivated a number of researchers to pursue the use of these networks in developing surface roughness prediction models. But in such models, the nonlinear relationship between sensor readings and surface roughness embedded in a neural network remains hidden and inaccessible to the user [4]. In this research we attempt to solve this situation by using the ANFIS system to predict the surface roughness. This model offers ability to estimate surface roughness as its neural network based counterpart but provides an additional level of transparency that neural networks fails to provide. It uses training examples as input and constructs the fuzzy if–then rules and the membership functions of the fuzzy sets involved in these rules as output. In this model, we adopted two different types of membership functions for analysis in ANFIS training and compared their differences regarding the accuracy rate of the surface roughness prediction.

2 Experimental design

In order to develop the surface roughness prediction model, experimental results were used. The experiments with the end milling cutter were carried out on the CNC milling machine (type HELLER BEA1). Material Ck 45 and Ck 45 (XM) with improved machining properties was used for tests. The solid end milling cutter (R216.24-16050 IAK32P) with four cutting edges, of 16 mm diameter and 10° helix angle was selected for machining. The corner radii of the cutter is 4 mm. The cutter is made of ultra fine carbide grade coated with TiN/TiCN coating. The coolant RENUS FFM was used for cooling. The cutting forces were measured with a piezoelectric dynamometer (Kistler 9255) mounted between the workpiece and the machining table. The data acquisition package used was LabVIEW. The surface roughness was measured by 7061 MarSurf PS1 Surface Roughess Tester. The set up can be seen in Fig. 1. The experiments were carried out for all combinations of the chosen parameters [5], which are radial/axial depth of cut, feedrate, spindle speed and tool wear. Other parameters such as tool diameter, rake angle, etc. are kept constant. Three values for the radial/axial depth of cut have been selected for use in the experiments: R_{D1} = 1d, R_{D2}=0.5d, R_{D3}=0.25d; A_{D1} = 2mm, A_{D2}=4mm, A_{D3}=8mm; d- cutting parameter (16 mm). In the experiments the following values for feedrate and spindle speed were varied in the ranges from 0.05-0.6 mm/tooth and 125 –350 min^{-1}, respectively. In this way two sets of data groups were generated, one for learning and other for estimation tests.

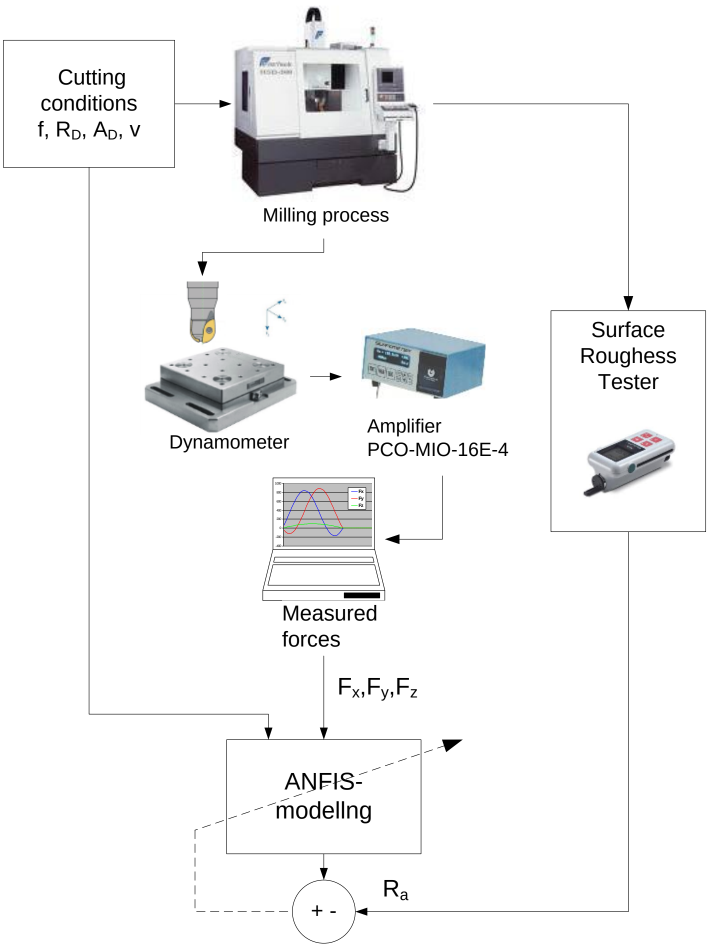

Figure 1 Experimental set-up.

3 ANFIS architecture

By given input/output data set, the ANFIS method constructs a fuzzy inference system (FIS) whose membership function parameters are tuned (adjusted) using either a backpropagation algorithm alone, or in combination with a least squares type of method. This allows fuzzy systems to learn from the data they are modeling. FIS Structure is a network-type structure similar to that of a neural network, which maps inputs through input membership functions and associated parameters, and then through output membership functions and associated parameters to outputs. FIS Structure is a network-type structure similar to that of a neural network, which maps inputs through input membership functions and associated parameters, and then through output membership functions and associated parameters to outputs. ANFIS applies two techniques in updating parameters. For premise parameters that define membership functions, ANFIS employs gradient descent to fine-tune them. For consequent parameters that define the coefficients of each output equations, ANFIS uses the least-squares method to identify them. This approach is thus called Hybrid Learning method since it combines the gradient descent method and the least-squares method. ANFIS modeling process starts by obtaining a data set (input-output data pairs) and dividing it into training and checking data sets. The training data set is used to find the initial premise parameters for the membership functions by equally spacing each of the membership functions.

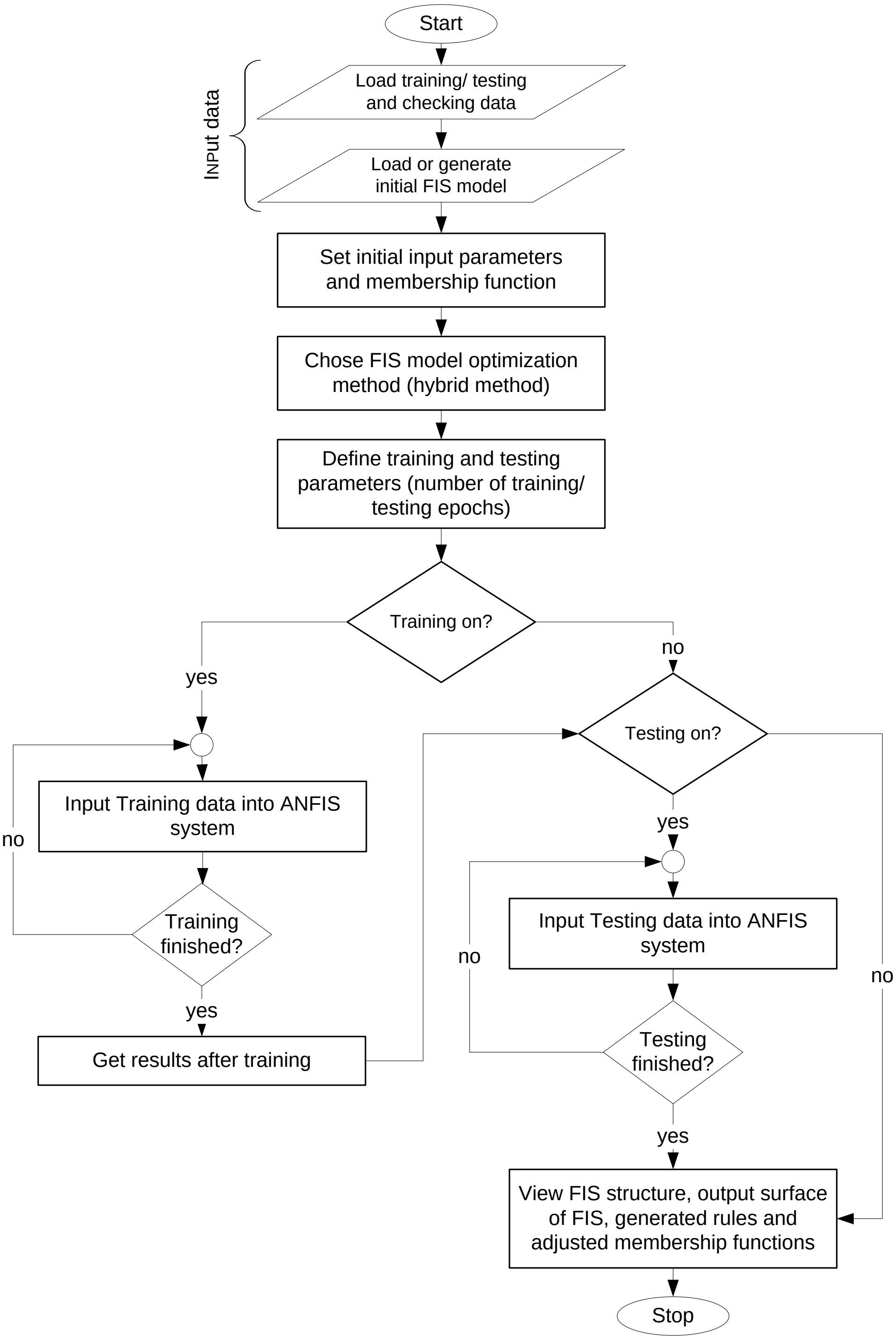

Figure 2 Flowchart of surface roughness prediction of ANFIS system

A threshold value for the error between the actual and desired output is determined.

The consequent parameters is found using the least-squares method. Then an error for each data pair is found. If this error is larger than the threshold value, update the premise parameters using the gradient decent method as the following (Q_{next}=Q_{nov}+η_d, where Q is a parameter that minimizes the error, η the learning rate, and d is a direction vector).

The process is terminated when the error becomes less than the threshold value. Then the checking data set is used to compare the model with actual system. A lower threshold value is used if the model does not represent the system.

Fig. 2 shows the flow chart for predicting the surface roughness via ANFIS. Fig. 3 shows the fuzzy rule architecture of ANFIS when the triangular membership function and the trapezoidal membership function is adopted, respectively. The structure shown in Fig. 2 consist of 36 fuzzy rules.

During training in ANFIS, 160 sets of experimental data were used to conduct 350 cycles of learning.

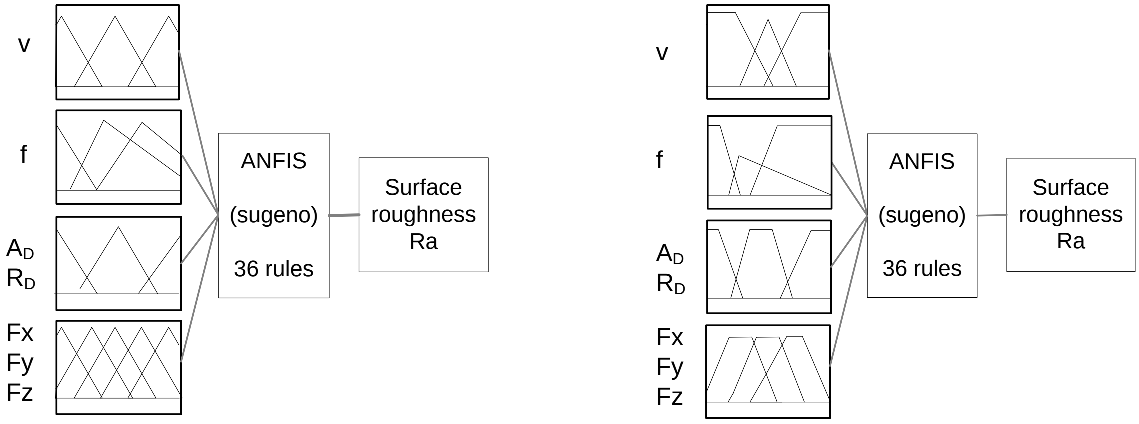

Figure 3 Architecture of fuzzy ruls for the triangular and the trapezoidal membership function.

4 Discussion of results

In conclusion, predicted surface roughness was found significantly sensitive to the measured cutting forces, especially the thrust cutting component. A total of 100 sets of data were selected from the total of 150 sets obtained in the end milling experiments [5] for the purpose of training in ANFIS. The other 50 sets were then used for testing after the training was completed to verify the accuracy of the predicted values of surface roughness.

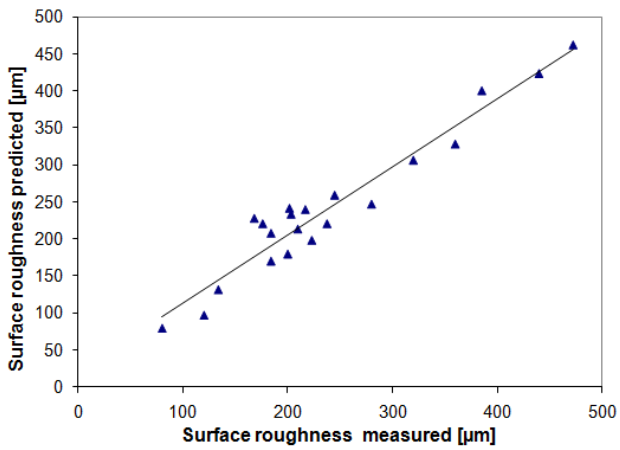

Figure 4 Scatter diagram of measured Ra and predicted for testing data using the triangular membership function.

The average error of the prediction of surface roughness is around 4% when triangular membership function is used in ANFIS. The accuracy is as high as 96%. The prediction accuracy of ANFIS when the triangular membership function is used is higher than that when the trapezoidal membership function is used. Fig. 4 shows the scatter diagram of the predicted values and measurement values of the surface roughness of 50 sets of testing data when triangular membership functions are used in ANFIS. It shows that the predicted values of surface roughness between 100 and 170 all follow the 45. line very closely. In other words, the predicted values are not far from the experimental measurement values.

5 Conclusion

In this contribution ANFIS system is used to predict the surface roughness in end-milling process. The experimental results indicate that the proposed ANFIS model has a high accuracy for estimating surface roughness with small computational time. The surface roughness values predicted by ANFIS are compared with the measurement values derived from the 150 data sets in order to determine the error of ANFIS.

References

[1] B. Ozcelik, M. Bayramoglu: The statistical modeling of surface roughness in high-speed flat end milling, International Journal of Machine Tools and Manufacture, Vol.46, pp. 1395-1402, 2003.

[2] W.A. Kline, R.A. DeVor, I.A. Shareef: The prediction of surface geometry in end milling, ASME J. Eng. Ind, Vol. 104, pp. 272-278, 1982.

[3] M. Alauddin, M.A. El Baradie, M.S.J. Hashmi: Computer-aided analysis of a surface-roughness model for end milling, J. Mater. Process. Technol., Vol.55, pp. 123–127, 1995.

[4] A. Sokolowski: On some aspects of fuzzy logic application in machine monitoring, Engineering Applications of Artificial Intelligence, Vol.17, pp. 429-437, 2004.

[5] F. Cus, J. Balic: Selection of Cutting Conditions and Tool Flow in Flexible Manufacturing System, The International Journal for Manufacturing Science & Technology, Vol.2, pp. 101-106, 2000.

Robot milling of welded structures

J. Tratar[1], J. Kopač[1]

[1] *Laboratory for Cutting, University of Ljubljana, Slovenia*

Abstract

Under the influence of sustainability and in search of new low-cost solutions for mechanical processing technologies robots present new intriguing way of modern machining applications. Evolving robot programming equipment offers new applications that can be implemented with existing robot hardware technology. Milling with robots is one of them and represents a relatively new and promising direction of multi-axis machining. In this article we present robot multi-axis milling of robot spatial welded pyramid out of VAC 60 material and machining of the weld stud. We used KUKA anthropomorphic robot, in all machining applications, that is available to us at the Faculty of Mechanical Engineering in Ljubljana, with an attached motor spindle unit. Robot milling of welded structural steel has been successfully completed. That indicates the possibility of using robotic manipulator for machining harder materials with a proper selection of the processing parameters and sufficiently loose tolerances of the finished product.

Keywords: robot, milling, steel

1 Introduction

In a time of constant progress, well spread automatisation and findings of a new and more economically feasible technologies, there arises a question, how to find at least a partial replacement for large, unwieldy and very expensive CNC machining centers.

As IFR (International Federation of Robotics) stated in 2011 there has been more than a million industrial robots operating in the world. Annual sales are despite the situation in the global markets since 2010, when there were 78,000 robots sold worldwide, estimated at about 10 % growth. That indicates growing trend of the robotics in industrial automation and the fact that the use of robots also spread to areas where they previously could not be noticed.

One of the possible partial modern replacements of expensive large CNC machining centers seems to be industrial six axis anthropomorphic robots (Figure 1). The development of software in the past few years enabled the robots to be no longer used only in conventional purposes of manipulative ("pick and place") operations and montage applications. Development also opened a new horizon of possibilities including the use of a robot as a multiaxis CNC machine centre.

However this new sustainable way of machining might be intriguing, it is important to know that milling with robot is less accurate than with conventional CNC machine centres and not suitable for all materials. It is because of the segmental robot structure that robots have lower stiffness than conventional CNC machines [1, 2, 3]. In most cases the robot is only suitable of processing softer materials, such as various foam, wood (wood composites), and some metals.

Despite all shortcomings, robots prove to be outstanding when machining very large workpieces and because of high flexibility even appropriate of rapid prototyping large workpieces. Robots can have quite large workspace (depending on the type of the robot). In our work we use KUKA KR 150L110 robot which has a reach up to 3500 mm.

Robots are intriguing by economic aspect because of low initial investment and very low maintenance and running costs [4, 5, 6].

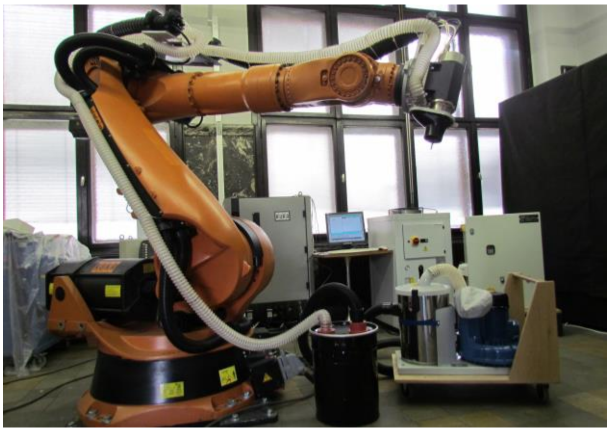

Figure 1 Robot machining cell.

For the purpose of this article we decided to use the robot manipulator for processing (milling) steel workpieces and welded structures. We tried to proof the assumption that it is possible to robot weld optional spatial forms and raw workpieces and rough machine them with two different robots or even with the same robot manipulator with attached weld gun and motor spindle.

2 Materials and parameters

We used the KUKA robot manipulator to rough mill welded pyramid and weld around the cap to make it suitable for bottoming.

Material used for welding was VAC 60 1mm thick wire. Weld material properties were similar to the structural steel. The pyramid welding programme was programmed in a virtual environment (Robot studio) and implemented on a small ABB robot with attached welding gun. We used CMT (Cold Metal Transfer) welding equipment to create hollow steel pyramid. ABB welding robot was not used in following milling applications.

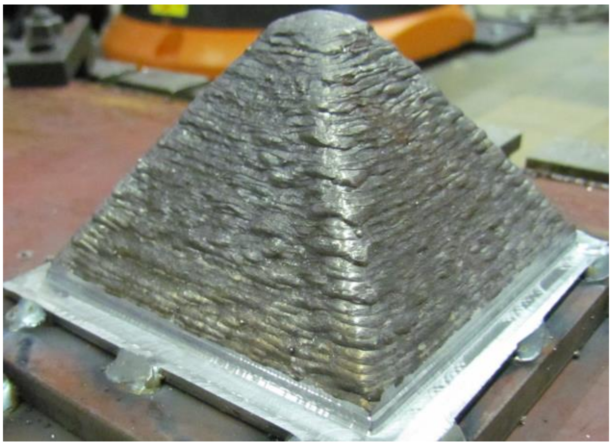

Figure 2 Robot welded pyramid.

Wall of the pyramid has been welded by two layers (two parallel welds). The thickness of each weld was approximately 9 mm ± 0.5 mm. The dimensions of welded sides were 93 mm and a height of the pyramid was 65 mm (Figure 2).

The cap with a diameter of 32 mm was welded by hand with the same material as a pyramid (60 VAC). The outer diameter of the weld was 45 mm and the height of the weld 6 mm (Figure 3).

Processing parameters and cutting forces were determined by milling tests on a pre-established welded block out of the 60 VAC material. To measure cutting forces Kistler dynamometer has been used. We also measured surface roughness with roughness meter Mitutoyo.

We used six blade carbide cutters with a blue coating (AlTiN and corner phase of 0.5 mm at an angle of 45 °) for all milling purposes. The diameter of the tool was 12 mm.

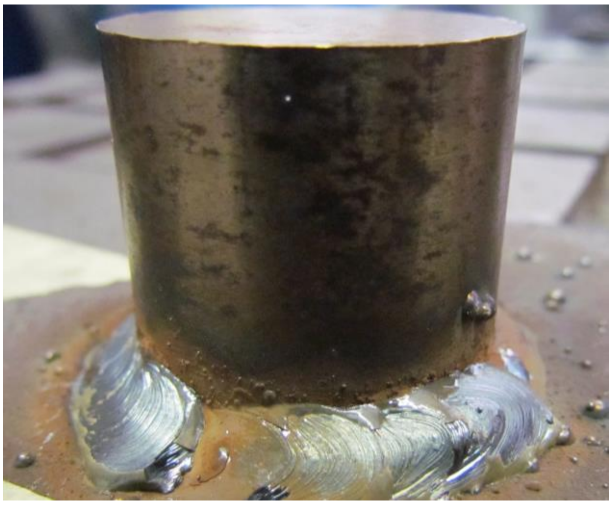

Figure 3 Hand welded cap before robot milling

Climb milling strategy has been used with two stepover values (A_p); 60% (7.2 mm) of the diameter of the cutting tool and 40% (4.8 mm) of the diameter of the cutting tool. Depth of cut was variable because we wanted to maximize productivity of the cutting process (P) and maintain satisfactory properties of the newly formed surface.

In all cases feed of the robot manipulator remain the same, 1200 mm / min and the spindle speed 5000 min^{-1}.

There are depth of removal (A_p), measured value of the surface roughness (R_a), the corrugation (R_y) and calculated productivity of the cutting process (P) shown in following table 1 and table2.

In the case of 4.8 mm lateral removal (A_p) we chose to use the 0.4 mm depth in the rough milling and 0.1 mm for the final treatment (Table 1). The same depths were used for 7.2 mm lateral cutting (Table 2).

Selected parameters were used for the production of two sides of the pyramid, and the other two parameters in Table 2 for the other two sides. All the toolpaths were programmed with Robotmaster program.

Table 1 Cutting, lateral withdrawal (A_e) 4,8 mm

A_p (mm)	R_a (µm)	R_y (µm)	P (mm^3/min)
0,4	2,4	34,3	2304
0,1	2,1	31,9	576

Table 2 Cutting, lateral withdrawal (A_e) 7,2 mm

A_p (mm)	R_a (µm)	R_y (µm)	P (mm^3/min)
0,35	2,1	43,8	3024
0,1	1,9	41,3	864

3 Implementation

Programming of the robot tool path is almost the same as classic three and/or more axis CAM programming of conventional CNC machines. Differences occur only in the final stages of programming, where additional simulations and calculations to check singularities, availability and collisions are carried out. For the production of the final product (Figure 4), we used a model of the equilateral pyramid with 90 mm long sides and a height of 58 mm.

We chose simultaneous 5 axis one-way strategy with parameters as described earlier. Milling was performed using one-way strategy because we longed to avoid vibrations that occur when changing the milling direction in material in milling with robot. Excessive wear occurs in the sharp edges of the tool path when machining in the workpiece because of vibrations which are caused by poor rigidity of the robot.

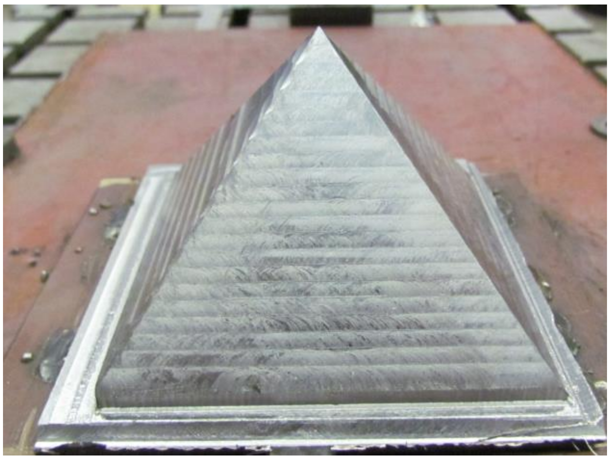

Figure 4 Robot 5- axis machined pyramid.

Pyramid workpiece was positioned on the working table at the distance of x = 1470 mm and y = 1205 mm from the robot base to achieve best results. Than workpiece has been clamped and processed (Figure 4). Workpiece was machined in about 80 minutes.

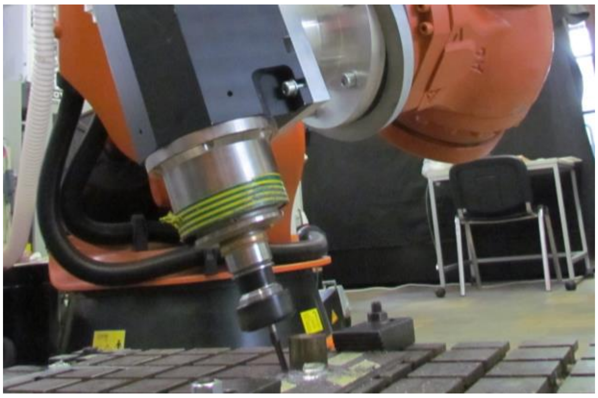

Figure 5 Multiaxis robot machining.

The same procedure has been used to machine the plug. We used four flute ball cutter with diameter of 6 mm coated with TiAlCN coating to carry out all milling operations. Due to the circular shape of tool path cutting speed was limited to 850 mm/min. Machining was completed within 10 minutes. We used co-spiral a strategy of milling without intermediate lifting of the cutting tool (Figure 5 and Figure 6).

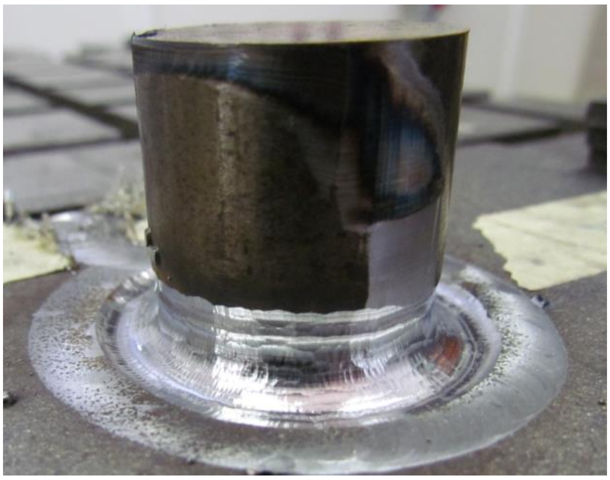

Figure 6 Multiaxis machined plug.

4 Results and discussion

Robotic manipulator allows very wide range of mechanical processes which can be carried out. Anthropomorphic robot has six degrees of freedom, so it can be used in any multiple (five) axis machining, as well as in the conventional three-axis machining operations.

After performed machining processes, we made measurements of the pyramid by the coordinate measuring machine DEA Diamond Model 2.1. Repeatability of the measuring machine is 0.35 mm, the linearity error ± 2.5 +4 L/1000 (L [mm]). Aligning of the measured piece was done by rule 3-2-1 (plane, line, point). Performed measurements showed that the pyramid workpiece has been machined in ± 0.5 mm overall accuracy.

The tool wear has also been observed during milling process. Due to the lower stiffness of the robot (in comparison with conventional CNC machines) vibration occur during the milling process, especially in the sharp edges of the tool paths, which greatly affected tool life. Therefore, it is necessary to properly program tool paths with properly chosen parameters in order to avoid excessive wear or even tool breakage.

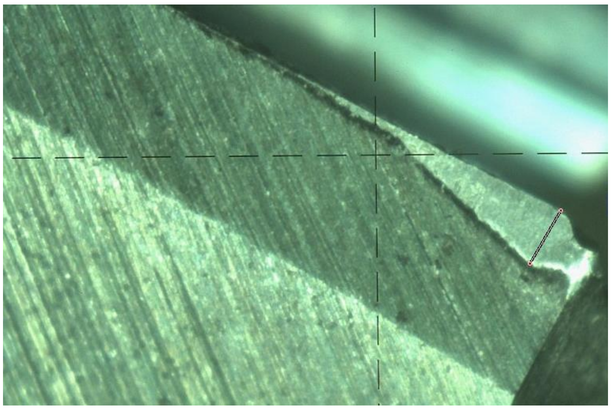

Figure 7 Cutter flank wear.

Figure 7 presents a microscope Mitutoyo image of the cutting edge of milling cutter with a diameter of 12 mm, which has been used to machine the pyramids and in the previous milling tests to define parameters.

Visible abrasive flank wear can be noticed (length of the line is 24 μm) with fracture of the tool edge in corner stage.

Tool has been than used for the processing of another pyramid and examined on the microscope (Figure 8).

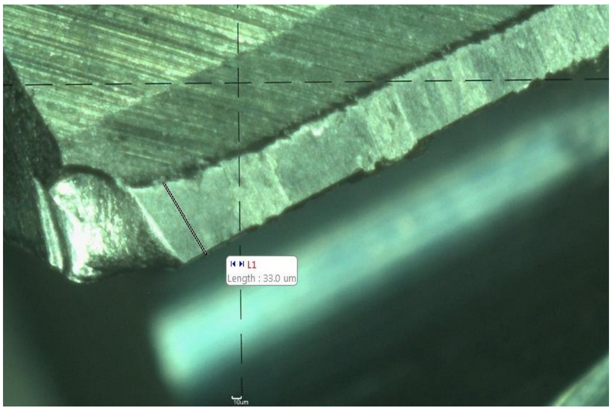

Figure 8 Cutter flank wear after all operations

Visible progressive abrasive wear (33 μm), and fracture edge of the stage tool can be noticed. Build up edge has appeared, tears on the cutting edge of the tool can be clearly seen. Fracture increased at the edge of the tool stage.

5 Conclusion

The robot manipulator in general can be used to mill softer materials such as; various prototype foam, plastics and wood. It is also possible to machine welded structures and welds in almost all shapes and sizes, for which the requirements for tolerances are a bit loose.

Anthropomorphic robot manipulator can be well adapted to machine complex workpiece shapes due to high flexibility and the six degrees of freedom. As such, it can effectively machine workpieces that other machines are not able to process because of limited reach or too complex shapes of the workpiece. Mostly robots can be successful and cost-effective replacement of hand finishing labour such as; grinding, milling or welding, even at an angle, or the inside of welded pipes and other complex structures where more demanding adaptive multi axis machining is needed. In our work we have been using two robots, smaller for welding and large for milling. With appropriate designed machining head attached to the top of the robot manipulator we could combine both operations in a single robot. Such preparation would save both costs as well as processing time and could be implemented for robotic cells which could replace manual labour of welding and milling, potentially grinding.

Robotic manipulators are attractive alternative to conventional and special machines for applications in multiple axis processing and will in future present significant part of modern production.

References

[1] International Federation of Robotics (www.ifr.org)

[2] J. Tratar, P. Kržič, J. Kopač: Uporaba robota v tehnologiji z odrezavanjem. Ventil, Vol. 17, No. 6, pp. 522-526, 2011.

[3] P. Kržič, D. Eržen, J. Duhovnik, J. Kopač: Offline programiranje industrijskih robotov s programom Mastercam. Orodjarstvo 2008-zbornik posvetovanja, Portorož, Slovenija, pp. 53-57, 2008.

[4] E. Abele, M. Weigold, S. Rotherbucher: Modeling and identification of an industrial robot for machining applications. CIRP Annals-Manufacturing Technology, 56, pp. 387-390, 2007.

[5] KUKA, Datasheet and manuals.

[6] C. Bates: Move over machine tools here come robots. American Machinist, 2006.

Machine Vision Control of Industrial Robot Assembly via Serial Interface

M. Pipan[1], E. Adrović[1], and N. Herakovič[1]

[1] *University of Ljubljana, Slovenia*

Abstract

The use of machine vision in automation and assembly became a standard in recent years. Machine vision is used for object recognition and orientation, fault detection and other tasks. Industrial robots are connected to machine vision with the use of special robot software for online programming. The on-line control algorithms are encrypted and therefore on-line programming can only be achieved with this software that enables communication between machine vision hardware and robot controller. In this paper a simplified method for connecting machine vision software, in MATLAB via serial port, to industrial robot controller is proposed. With the right structuring of communication algorithm and the use of external sensors we achieved semi-real time control of industrial robot assembly for manipulation of randomly placed objects.

Keywords: machine vision, industrial robots, serial communication, objects recognition.

1 Introduction

Connecting computers to industrial robot controllers enables the use of different tools for robot path optimization, simulation, haptic control, use of machine vision, CNC programs for large scale machining of softer materials, etc. [1]. Communication is usually done via serial port or LAN port. With the use of this synchronization PC becomes master and robot a slave [2]. For this kind of control fast communication protocols are used.

We propose an alternative approach where communication is done with the use of serial communication directly with the main robot program. The program reads strings and changes position variables accordingly. The robot controller is behaving as a master, while PC is a slave component that sends detected object position and orientation to the robot controller on demand. For this concept to work, we developed two way communication control algorithm in MATLAB (for machine vision object position and orientation with serial communication protocol) and tested its accuracy and repeatability. The machine vision detected objects have different heights and with the help of an additional limit switch on the vacuum gripper we achieved the task of placing all objects on specific locations with the same orientation independent of their original position. Objects were white wooden blocks with dimensions of 150x100x50 mm.

2 Test setup

We used a PC with FireWire communication for image acquisition from a CCD camera DMK 21F04 from IMAGINGSOURCE with a zoom lens. The camera gives grayscale images with resolution of 640x480 pixels which with used focal length gave a resolution of 1 pixel = 0.653 mm.. The MATLAB (programming environment for technical computing) was used for image acquisition and processing. After position and orientation was extracted the data was sent via serial communication to robot controller. The industrial robot used in this experiment was MOTOMAN HP20 with a NX-100 controller. The end effector of the robot was a vacuum gripper with limit switch for object sensing (Figure 1).

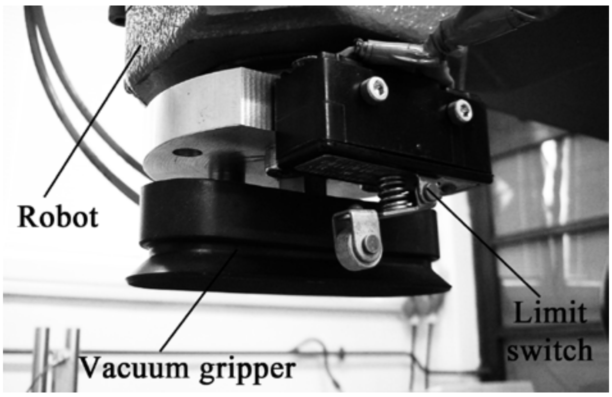

Figure 1 Robot end effector with vacuum gripper and limit switch.

This switch was used for object height determination that was used for object placing technique. The communication protocol for NX-100 controllers is fixed to 9600/8N1and cannot be changed [3]. The limit of communication speed exists to prevent third-party master PC control. Communication speeds for official programs via serial are 100 times faster.

3 Control algorithm

Control algorithm consists of three parts. First part is a machine vision object detection algorithm that uses blob analysis of binary image, which was obtained with CCD camera. The second part is a communication algorithm with defined protocol for a robot to pc communication. It consists of the following tasks: waiting for a start command, sending machine vision analysis results to robot and repeating the loop if necessary. The third part of the algorithm is a robot program that sends to PC a demand for object orientation parameters and also according to obtained height of the object chooses the right path for placing objects to specified destination in such a way, that all placed objects have the same orientation.

3.1 Machine vision algorithm

Machine vision algorithm for object detection is based on blob analysis. This is done with a MATLAB function *bwlabel()* [4] for blob detection. This routine detects objects in binary image by finding a single white pixel. After that it analyses all 8 or 4 neighbors and labels them as the same object if the pixels are white. The black pixels are ignored. In this way the whole image is processed and different object labeled. After blob detection we used *bwareaopen()* [4] function for removing small objects and *regionprops()* [4] for object feature extraction of position and orientation angle of blobs. The next step is to transfer this data from pixels to mm so that they can be sent to robot. The Figure 2 shows a block diagram of the vision algorithm.

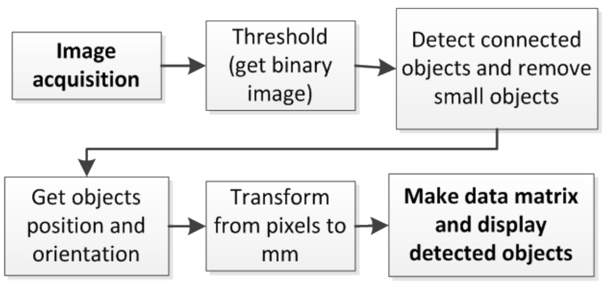

Figure 2 Machine vision algorithm diagram.

The last step is generation of a data matrix of labeled objects that consists of the index number of the object, x and y coordinates of object’s center and angle of object. The program displays detected objects with object data as shown in Figure 3.

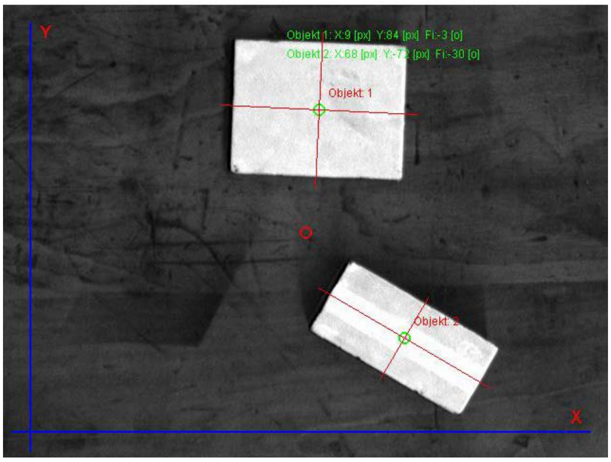

Figure 3 The displayed detected objects with coordinates and orientation.

The center of coordinate system is in the image center to minimize error due to image distortion towards the edges. Also the focal length was chosen in such a way, that we get relatively small area (430 x 314 mm) so that errors due to image distortion are minimized.

3.2 Communication algorithm

Communication algorithm in MATLAB is based on 9600/8N1 communication speed with 8 bits, no parity and 1 stop bit. The COM port for communication is an integrated port on the PC motherboard. The program starts with defining the communication parameters. After serial port definition the program waits for a start command from the robot which is a string ‘START’ in the ASCII format. After the start command is received image acquisition and object feature analysis starts. If there are no object detected ‘STOP’ command is send. When data matrix with objects coordinates is generated the first object is selected (the upper left object) and coordinates are converted to 22 byte string. First 7 characters represent x-axis, followed by a comma separation character, another 7 characters are for y-axis, followed by a comma separation character and the last 5 characters represent the object angle. We define coordinates with 7 characters because that is demanded by the robot controller. The sent string looks like this: ‘0022000,0065000,01200’. It represents the coordinates x = 22 mm, y = 65 mm and angle δ=12°. Than the string is send to robot COM port and the robot picks up the object and places it to a destination position. After the data is sent, the program checks if there was more than one object detected. If there was only one object detected, than it sends the robot command to stop the program and return to home position. If number of detected objects is larger than 1, than the program returns to standby mode and waits for robot controller to send a demand for object coordinates. A block diagram of the MATLAB communication protocol is shown in Figure 4.

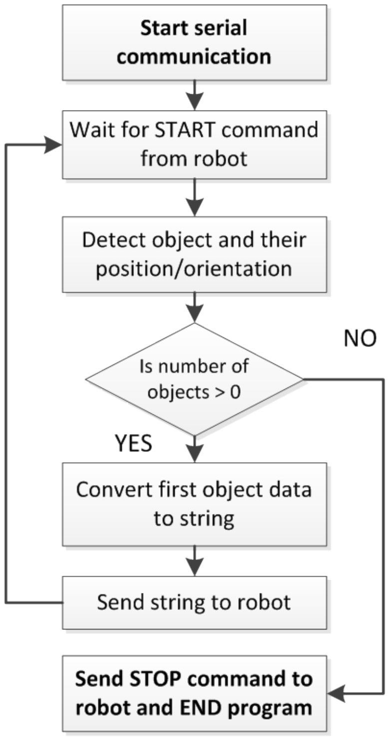

Figure 4 MATLAB serial communication protocol scheme.

3.3 Robot program

The last part of the system is a program that runs on the NX-100 robot controller. In the beginning of the program we define all static coordinates and variables:

- Robot position for waiting while objects are being detected.
- Robot home position when no objects are detected.
- Three different protocols for object placement for all possible block placements.
- Variables for coordinates *x*, *y* and angle *fi* that will be changed by the data acquired via serial communication.

In the next step the robot arm is moved to 'WAIT' position that doesn't block the camera view. If it gets a signal that machine vision program is idle and is waiting for command, it sends the command for the start of object coordinates and orientation analysis. The robot controller waits for 22 characters of data. The data is than logically processed and all three variables are changed according to received data. The robot moves to the new coordinates and starts descending in *z* direction until the limit switch stops it. The fourth variable of object height is than saved. Now vacuum gripper is activated and the placing protocol, chosen by the object height, is performed. After successful placement of the object the robot returns to its 'WAIT' position if there are more objects present. If there are none, it goes to home position. The schematic representation of the robot program for pick and place task of unorganized objects is shown in Figure 5.

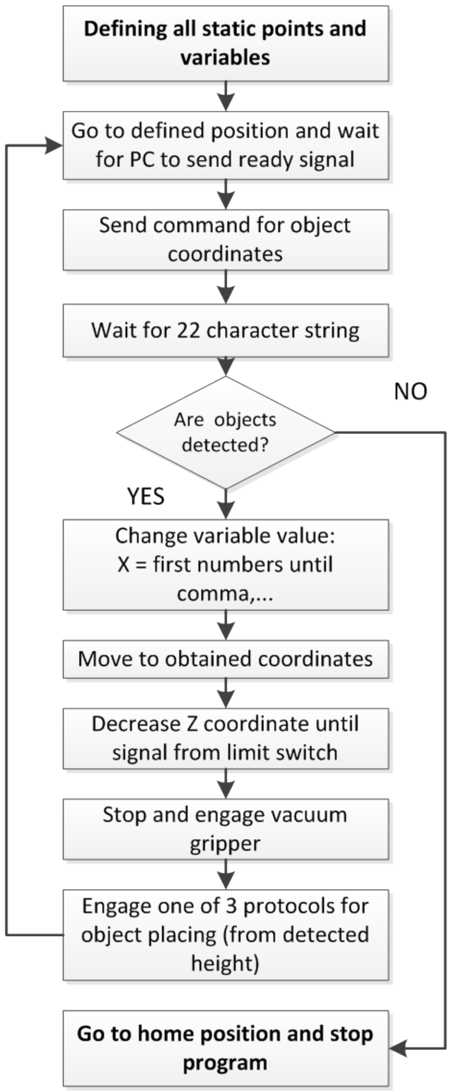

Figure 5: Schematic of NX-100 program for pick and place task of unorganized objects.

4 Experiment

In the first testing phase we calibrated the computer and robot coordinate system and tested the accuracy of machine vision position detection with a spike mounted as an end effector as proposed by paper [5]. The accuracy and repeatability of positioning was ±1 pixel or ±0.65 mm. Experiment was carried out with the use of two blocks that were put on a workbench in different ways to test all positions and orientations. There were two blocks positioned on the workbench at all times so the assembly didn't stop until we stopped adding the blocks. In the end we tested the whole detection area with all possible orientations of objects. Thirty objects were tested and all were successfully detected and picked up.

Three different placing protocols worked without a flaw. Also the presence of smaller objects on the workbench didn't interrupt the object detection due to use of a filter for smaller objects. The pick and place task during a testing phase is presented in Figure 6.

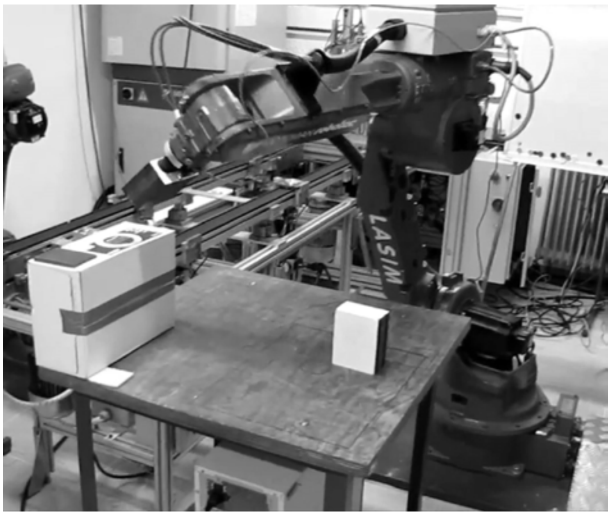

Figure 6: Pick and place task of randomly positioned objects.

5 Conclusions

Use of third-party programs for robot assembly control can be achieved with some limitations. The limitations are:

- Limit of communication speed.
- PC can only work in slave mode.
- The robot controller program has to be designed in a special way that is more time consuming.
- There must be a large amount of time/programming optimization for achieving optimal and fluent work flow.

The machine vision algorithm used in this paper is very basic and has some limitations. The two main limitations are the requirement that there must be a high contrast between the background and the objects (light/dark) to successfully use threshold transformation and the second limitation is that if the objects are one on top of another or touching each other the machine vision would detect only one object.

Overall we proved that with correct programming syntax and structure, we can achieve fluent detection and can pick up objects without any time delay due to communication problems. The master/slave configuration between the robot controller and the PC worked flawlessly and can be in the future upgraded with the use of advanced machine vision algorithms. Also instead of using a PC we will try to implement microprocessors with peripherals for CCD camera connection and serial communication support.

References

[1] N. Herakovič: Computer and Machine Vision in Robot-based Assembly. Strojniški vesnik – Journal of Mechanical Engineering 53, pp 858-873, 2007.

[2] E. Adrovic, M. Pipan, N. Herakovič: Sodelovanje dveh ali več robotov. VENTIL 18, pp 134-138, 2012.

[3] Yaskawa. NX100 INFORM MANUAL, http://www.ro.feri.uni-mb.si/predmeti/robotizacija/inform.pdf, visited: august 2013.

[4] H. Moore: MATLAB for engineers 3rd edition. Pearson Education Inc., New Jersey, USA, 2012.

[5] S. Ming, A. Dong, W. Yagunang: Calibration of Machine Vision System for Nondestructive Detection of Plants. The International Federation for Information Processing Volume 259, pp 1311-1314, 2008.

ICEJET: Environmental technology pilot plant for drastically reducing waste produced by abrasive water jet cutting techniques

LIFE 08 ENV/E/000167

Achieved goals

1. Production of ice particles with both prototypes. Ice particles generation with water and liquid nitrogen inside the prototype 1 in order to inject them to the water jet before performing the cut. Generation of particles in the water jet with prototype 2 injecting directly liquid nitrogen to the jet.
2. Cooling the high pressure pipe before the cutting head also with both prototypes. In both prototypes is necessary to cool down the water in the high pressure pipe. Using different technologies this has been achieved in both test stations, being more needed in the technology 2.
3. Testing both prototypes to make the first trial with the new technology. First tests have been carried out using both technologies, but the developed technologies are quite unstable because of the importance of the temperatures and so the tests have not been very conclusive.

Next steps

Combination of both prototypes to see if with the high capacity of the technology 1 of producing ice particles and with the way technology 2 cools down the water in the high pressure pipe, more conclusive tests could be carried out.

IceJet technology 1 Responsible Tecnalia

In order to generate ice particles in the proper way, many previous test were carried out.
- **Atomization tests**: to set the value for the parameters to obtain the desired size and amount of particles.
- **Transport system tests:** particles need to reach the cutting head in optimal conditions that is why different ways of transporting them have been tried. Thermocouples to control the temperature of ice particles.
- **Additional cooling system tests:** in the high pressure pipe to cool down the water before it enters the cutting head. Thermocouples have also been used to control the temperature of the water.

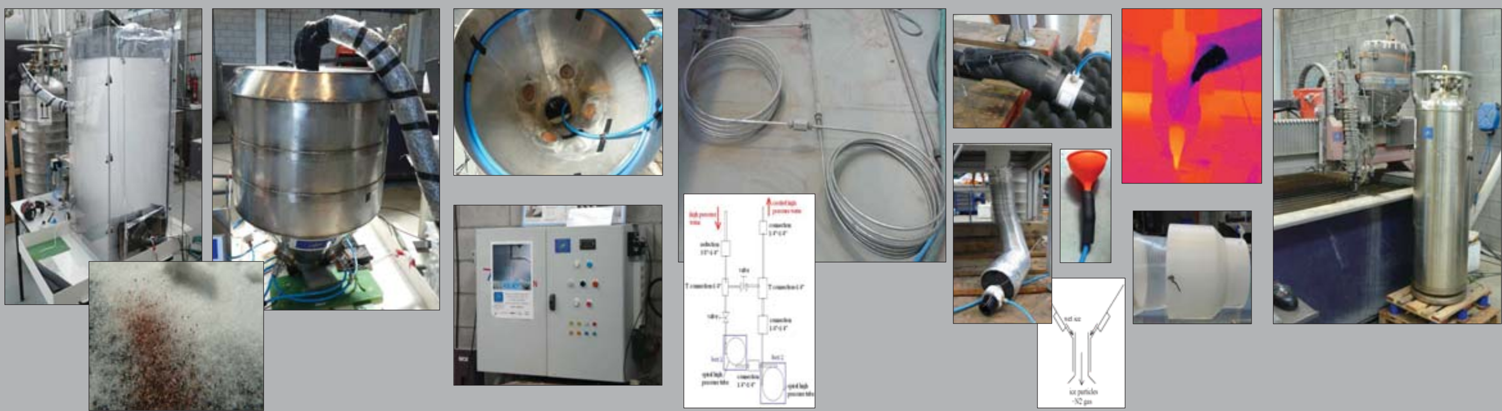

IceJet technology 2 Responsible UL / LAT

- **LN injection for generation of ice particles:** modified cutting head with gas release vent to stabilize the mass flow of LN to cool the jet more efficiently. Pressures used for the media that was injected into the cutting head must be at least of 1bar.
- **Monitorization:** Temperatures measured inside the glycol water solution tank, on the collimation tube before the orifice and on the focusing nozzle.
- **High pressure pipe cooling system**: achieved to cool down the high pressure water to at least -15ºC

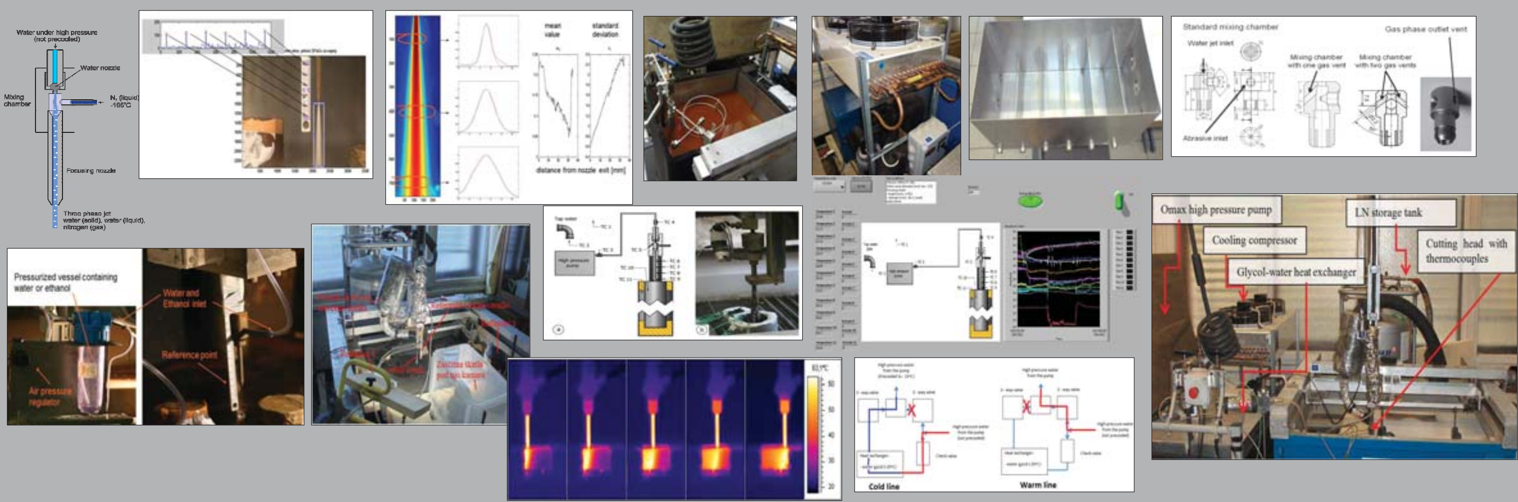

Authors: M. Jerman1, A. Lebar1, I. Etxeberria2, A.Suarez2
1University of Ljubljana, Laboratory for Alternative Technologies, Ljubljana, Slovenia; 2TECNALIA, Technology Corporation, Basque country, Spain

Advanced rapid technologies

Cutting graded materials with milling

T. Irgolic[1], F. Cus[1]

[1] *University of Maribor, Faculty of Mechanical Engineering, Slovenia*

Abstract

Professional paper shows the general characteristics of graded materials, their previous industrial use and potential use of graded materials in the future. In any case, today the use of graded materials is increasing and moving from the laboratory environment into everyday use. However, the subsequent processing of the graded material remains the big unknown, and represents a major challenge for researchers and industry around the world. It could be said that the study of machinability of these materials is in its infancy and in this area are many unanswered questions. Machinability problem of graded materials was undertaken at the Faculty of Mechanical Engineering in Maribor. After a radical study of the literature and potential machining processes of graded materials, we started with the implementation of cutting processes on the workpiece. This professional paper presents the first results of the analysis, which will be used for further research and machinability study of graded materials.

Keywords: milling, graded material, LENS

1 Introduction

Graded materials (FGM - Functionally Graded Materials) are in intensive use for last two decades. The first concepts of graded materials were conceived in 1984 during the development of the Japanese space program. Their main feature is the non-homogeneous microstructure through whole structure, where every layer has its own microstructure and different mechanical properties.

The most frequently represented scopes of the graded materials are [1, 2, 3]:

- Aerospace,
- Military industry,
- Medicine,
- Optoelectronics.

In any case, by reducing manufacturing costs in the future is expected that list of areas where graded materials are used will be much bigger. The greatest advantage of graded materials is their surface functional quality.

However the properties of graded materials also depend on the properties of the base material. In most cases, hardness of graded material may vary. Surface layer is the hardest and hardness usually linear fall to the softest zone of material, which is in the region where basic material and graded layer are mixed, shown in Figure 1 [4, 5].

The most common reasons for using graded materials are:

- High surface hardness,
- Good surface wear resistance,
- Different graded structures dampen vibrations

Special case of graded materials represents partially graded materials that do not have distinct layers with different chemical compositions, but they have a homogeneous chemical composition of the modified microstructure. The mechanical properties of these materials are comparable with the properties of the graded materials with distinct layers with different chemical composition [6].

The largest groups of graded materials are as follows:

- Bioactive graded materials,
- Tool steel with C, V, Cr and Ti gradients,
- Materials with self-lubricating ability,
- Graded materials with high temperature resistant surface layer.

2 Properties of functionally graded materials

Graded materials are very innovative product in the field of technology. Also very innovative is their production. The most common methods of manufacture graded materials are as follows:

- The application of thin film coatings (PVD, CVD)
- Powder metallurgy,
- Centrifugal method of manufacturing graded material,
- Additive fabrication (SLS, LENS, SLM).

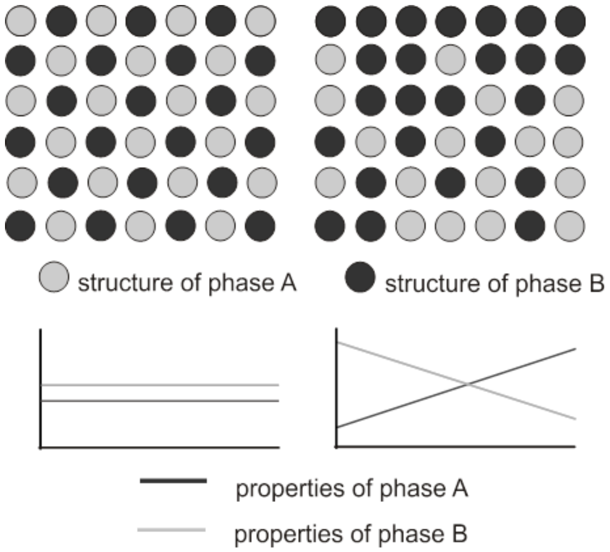

Figure 1 Comparison between the inhomogeneous material and the graded material with characteristic layer

LENS technology is the most frequent technology for the production of graded materials and graded layers which are welded on basic material. Deposition process is made by laser which melts basic material and by nozzle which supply the whole process with metallic powder.

After the deposition process on the surface, the pool of molten material is originated in which additional metal powder is added. Added metal powder is mixed with the basic melt and mixed with it and then converted to the solid state as the result of heat translation [1, 4, 5].

After the solidification of the base and additional material the line shaped coating is reached. It takes a lot of individual line shaped parallel coatings (single layer), as well as a large number of successive layers to finish the entire surface.

Benefits of using LENS technology are as follows:
- Fast creation of graded materials,
- A wide range of metallic materials,
- Low heat input,
- Fine-grained microstructure,
- The whole process of adding material is computer controlled,
- Low probability of cracking,
- Controlled protective atmosphere.

The biggest problem of metal graded materials is their subsequent treatment. It is very hard to machining and remove rough and steady surface. Because of that grinding is still in use for material removal instead of milling.

Schematic presentation of LENS technology is shown in Figure 2.

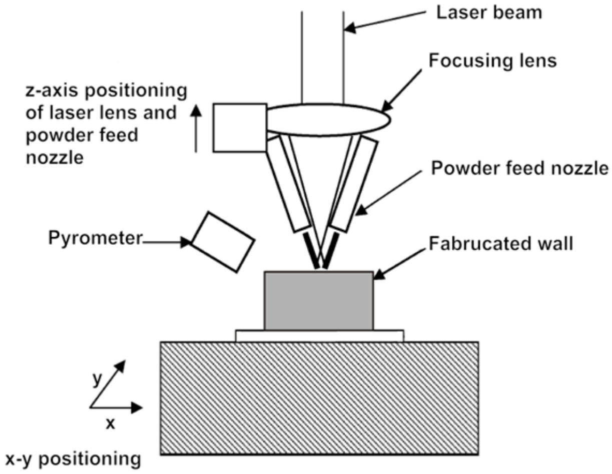

Figure 2 Schematic presentation of the most important components on the laser head of LENS technology machine

In comparison with milling is grinding slowly cutting process and material removal in time unit is much smaller. This is the main reason why Laboratory for cutting processes at the Faculty of mechanical Engineering in Maribor decided to completely replace grinding of graded material with milling process. Experiment realization and first results of the analysis are presented in chapter 4.

3 Production of graded materials

Test parts used in the experiment were produced with the machine Optomec LENS 850-R. Basic characteristics of the machine are shown in Table 1.

Table 1 Machine characteristics of Optomec LENS

Properties	Value
Working area	900x1500x900 [mm]
Max. motion speed	60 [mm/s]
Max. speed of layer deposition	500 [g/h]
Max. laser power	1000 [W]

Test parts with graded layers were made with machine Optomec LENS 850-R which is shown in Figure 3.

Figure 3 The machine Optomec LENS 850-R

Operational parameters for the production of test parts on machine Optomec LENS 850-R are shown in Table 2.

Table 2 Optomec LENS 850-R work settings

Machine settings	Value
Power	580 [W]
Feed rate	10 [mm/s]
Amount of filler material	5,8 [g/m]
Number of layers	4
Spacing between layers	0,4
Mark of filler material	1.3343

4 Experiment realization

Milling of workpieces made of graded material was on CNC milling machine Heller BEA 01.

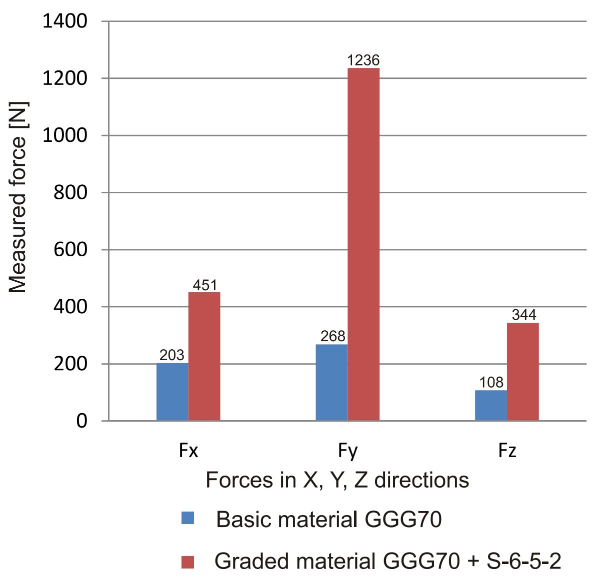

Figure 4 Comparison of the average forces in the X, Y and Z directions in milling basic and graded material

Material GGG70 (hardness 23 HRC) was used as the basic material, while the mixture of the basic material and the feed material S-6-5-2 (hardness 65 HRC) was used for the making of the graded layer which was 2,5 mm thick.

Cutting parameters used in experiment were: spindle speed n = 3000 rpm, feed rate f = 200 mm/min and cutting depth ap = 0.5 mm. An example of the measured cutting forces F_X, F_Y and F_Z by milling basic and graded material are shown in Figure 4. It is obvious from the experiment that cutting forces F_X, F_Y and F_Z in X, Y and Z directions of coordinate system are much greater in milling graded material (mixture of GGG70 and S-6-5-2). Cutting forces were measured with the system shown in Figure 5 [7].

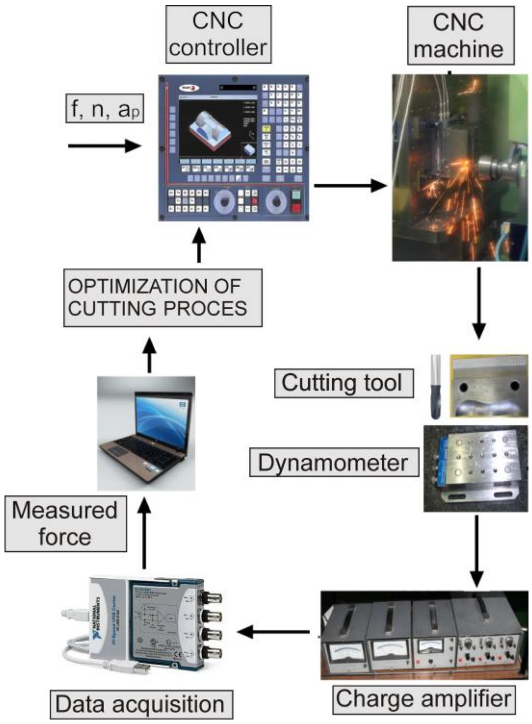

Figure 5 Cutting force measuring system

Milling on workpieces was performed with carbide ball-end mill cutters and end mill cutters manufactured by Sandvik Coromant. The geometry of the cutters used in our experiments is shown in Figure 6.

Figure 6 Ball-end mill carbide cutter and end mill carbide cutter manufactured by Sandvik Coromant

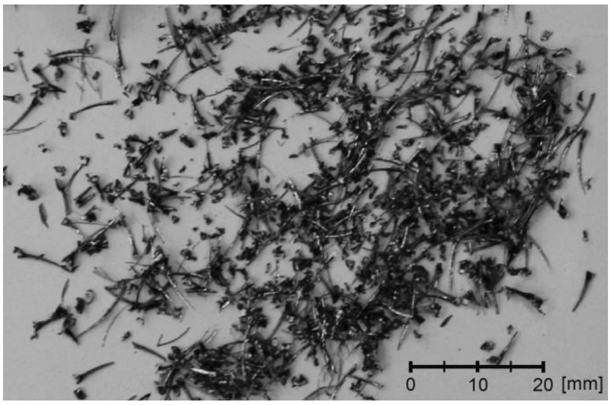

Figure 7 Shape and size of the chips generated in milling graded material

By milling graded materials, advantageous, short and broken chips were produced (Figure 7). Large tool wear have negatively influence on the quality of the machined surface.

After 25 minutes of machine treatment on the CNC machine, the cutting edge breakage on both cutters appeared (see Figure 8). Cutting with damaged cutter is unfavourable and surface quality is unacceptable, therefore can be considered that 25 minutes is maximum working time of this carbide cutters. After that time reached roughness is much worse and it does not achieve wanted characteristics.

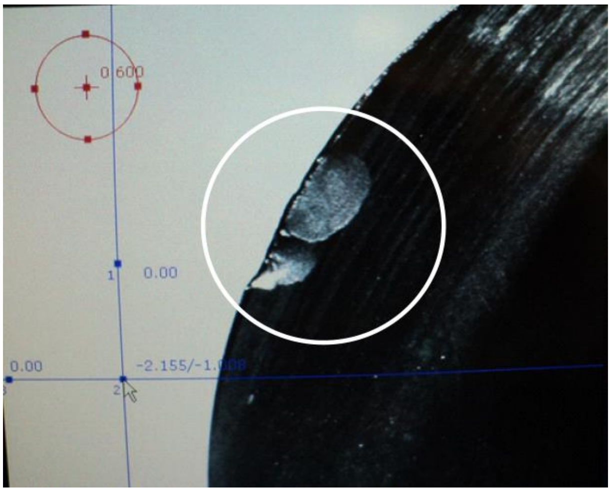

Figure 8 Cutting edge breakage on the ball-end mill cutter after milling graded material

5 Summary

Chips reached by milling graded material (mixture of GGG70 and S-6-5-2) are very advantageous because they are small and broken. They do not present any danger to cutting tool, CNC milling machine and operator. Large cutting forces by milling graded material are unpleasant features which lead to increased prime costs. Tool wear shortening and bad surface quality of graded layer can be considered as undesired costs which have negative impact on total costs.

Our wish for the future is to find the proper shape and geometry of cutters and suitable cutting parameters (cutting speed, feed rate, cutting depth...) for optimal milling process. With this optimal cutting parameters we want fully displace the grinding of graded material with milling, where material removal is greater.

In any case simulations and cutting experiments of graded materials are wished to be performed. Our goal is to introduce milling of graded material into daily production and replace grinding with more productive cutting process.

References

[1] Sekulic, M., Kovac, P., Gostimirovic, M., Kramar, D., Optimization of high-pressure jet assisted turning process by Taguchi method, Advances in Production Engineering & Management, vol. 8, 1 (2013) 5-12.

[2] H.-A. Bahr, H. Balke, T. Fett, I. Hofinger, G. Kirchhoff, D. Munz, A. Neubrand, A. S. Semenov, H.-J. Weiss, Y.Y. Yang.: Cracks in functionally graded materials. Materials science & Engineering. (2003), 2–16.

[3] Joshi, A., Patnaik, A., Gangil, B., Kumar, S.: Laser assisted rapid manufacturing technique for the manufacturing of functionally graded materials. 2012 Student Conf. on Eng. and Systems, (2012).

[4] Lijung, Song., Mazumder, J.: Feedback control of melt pool temperature during laser cladding process. Control system technology, 19 (2011), 1349-1356.

[5] Tadamalle, A.P., Reddy, Y. P., Ramjee, E., Influence of laser welding process parameters on weld pool geometry and duty cycle, Advances in Production Engineering & Management, vol. 8, 1 (2013) 52-60.

[6] Mallikharjuna R., Boddu., Robert G., Landers., Frank W., Liou.: Control of laser cladding for rapid prototyping – a review. Solid freeform fabrication proceedings, (2001), 460–467.

[7] Zuperl, U., Cus, F., Reibenschuh, M. Modeling and adaptive force control of milling by using artificial techniques. J. intell. Manuf., 23, 5, (2012) 1805–1815. doi: 10.1007/s10845-010-0487-z.

Combining additive and subtractive technologies to get optimized tool inserts

D. Homar[1], J. Kopač[1], K. Boivie[2], L. T. Gellein[2]

[1] *Faculty of Mechanical Engineering, University of Ljubljana, Slovenia*
[2] *Department of Production Technology SINTEF Raufoss Manufacturing AS, Norway*

Abstract

In last few years technologies for additive manufacturing of metal parts are improved to the point where it becomes capable to produce parts which have mechanical properties similar or even better than machined parts. This is the reason why these technologies have become useful to produce injection mould tool inserts with conformal cooling channel system. Conformal cooling can significantly improve productivity and quality of moulded parts, because cooling channels which are fully fitted to injection mould tool cavity, ensure more uniformly and more rapidly cooling. Additive manufacturing technologies does not have limitations of product shape due is built up in a layer by layer fashion. While geometry shape of cutting tools represent a big limitation to make parts with complex geometry. But additive technologies are still more expensive than machining technologies. The paper describes a hybrid manufacturing cell which consists of a machining machine and an additive manufacturing machine. The aim of this description is to present the benefits of two manufacturing processes to make one product. The hybrid manufacturing cell combines the advantages and eliminates the limitations of the two technologies.

Keywords: additive manufacturing, subtractive manufacturing, hybrid manufacturing, selective laser melting

1 Introduction and background

In the past, some researchers have tried to combine technologies for additive manufacturing and machining technologies, but their main purpose were make near-net shape and then milling on the end shape [1]. Other scientists divided CAD model of products into two or more modules, where some modules were produced by milling and another by additive process, subsequently assembled in end product [2]. In our case, 5 axis milling is combined with Selective Laser Melting (SLM) technology in hybrid cell. SLM is the process where the layer of metallic powder is melted and fused together layer by layer, with the high powered laser, direct from CAD data to create functional metal parts. Our goal is in order to part of product which is possible to produce with conventional subtractive process will be manufactured with 5 axis milling. Another part of product with a complex geometry, which is difficult, impossible or very costly to machine, it will be manufactured with SLM. Therefore the product will be split in two parts, with straight plane, before the processing. The base part, in most cases the biggest part, will be manufactured with milling and then the operator or robot will move the intermediate product from milling machine in machine for SLM. Subsequently, operator will fill building chamber with metal powder and then a machine will start building the second part of product from the upper surface, where the milling machine finished the its part of product. Hybrid cell is primarily intended for manufacturing injection moulding tool inserts with conformal cooling system. The conformal cooling system is a term for cooling channel which conform to the contours of the insert or cavity of injection moulding tool or tool for die casting. With conformal cooling system is achieved a better dimensional accuracy of the moulded part and reducing cycle time of injection moulding up to 40% [3, 4]. Every toolmaker wants to do the tool, with conformal cooling channel. But for conformal cooling system is decided by toolmaker only in special cases, due is not possible to do this system with conventional processes and additive manufacturing processes are too expensive for making entire tool. With hybrid cell, we want to do manufacturing moulds for injection moulding with conformal cooling channel cheaper, that it will be accessible for more toolmaker. Because with the CNC milling is impossible to produce certain geometric shapes, we decide that we combine this process with additive process in hybrid cell.

2 Benefits of hybrid cell manufacturing

With hybrid cell is combined benefits and eliminated handicaps of both processes. With powder bed additive manufacturing is possible to do any kind of geometric shape. But this process is not suitable for manufacturing big parts with relatively basic geometry, because is too time-consuming and too expensive for that kind of geometry. On the other hand conventional manufacturing achieve high production speed for massive parts. The highest downside of all additive manufacturing processes is bad roughness of surface due building the products layer by layer and this principle leave the stair on surface known as the stair-stepping phenomenon [5]. This stair is eliminated with finishing machining. The subtractive processes have a lot of material consumptions, but the additive processes have minimized material consumption. Because of these reasons, additive manufacturing is good options for production some part of the product where it is necessary to subtract a lot of material if a product is machined from cylindrical or cuboid of raw material. The cost of machining product increases with increasing the amount of subtracted material and with geometric complexity of products. But the cost of product, which is made with additive technology, increases with increasing the amount of added material, while the complexity doesn't affect the cost of product. On the figure 1 you can see that the cost depending on amount of subtracted/added material increase stepper for additive manufacturing than the machining.

Nowadays the materials, which are available for additive manufacturing, have excellent mechanical properties. Furthermore additive manufacturing of metal parts process can build the part in variable material composition. The biggest problem with additive technology is that it isn't very known by toolmaker or other technologist and because of this is very rarely used in manufacturing. Many technologists are very conservative, and with thus they are afraid to use new technology for manufacture products, which they produce up to the present by conventional processes.

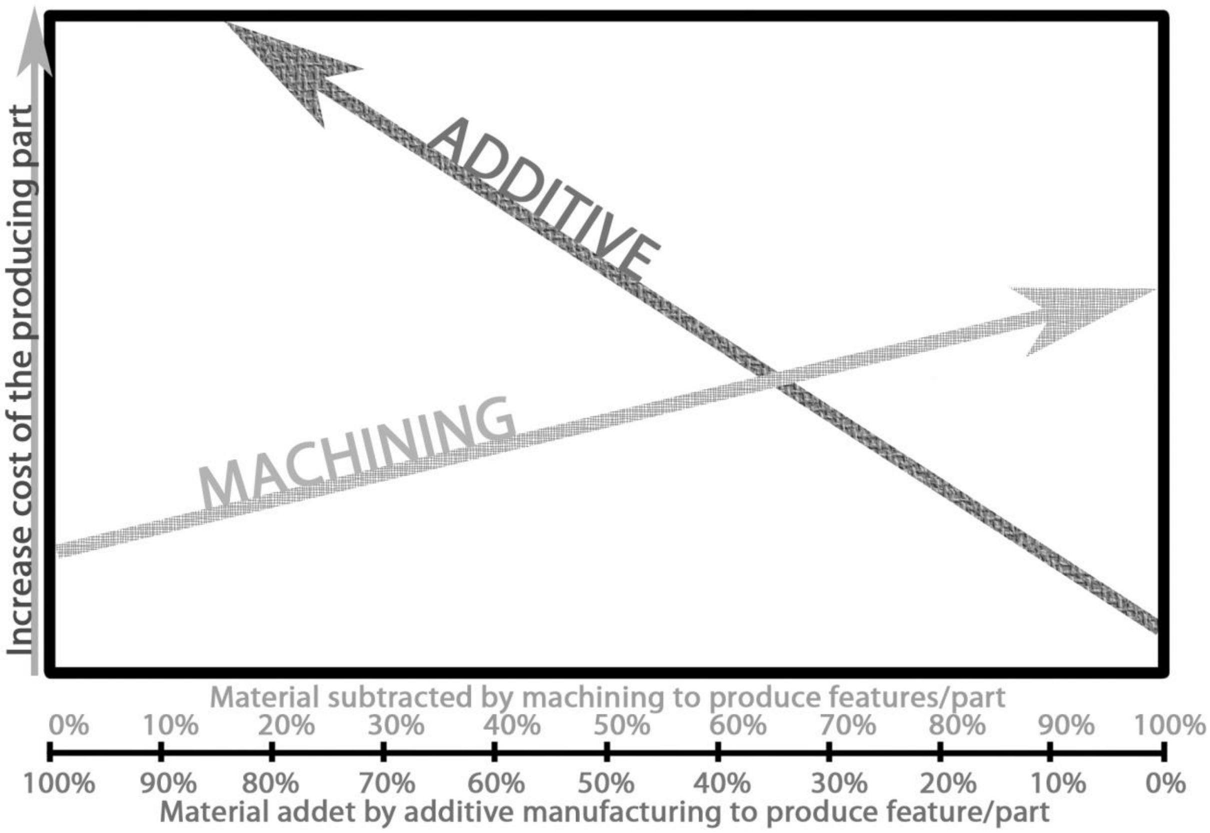

Figure 1. The graph shows increasing the cost for machined part and additive manufactured part depend on amount of subtracted or added material.

3 Workflow

Figure 2 shows the schematic workflow of the workpeace in hybrid cell, focusing on the manufacture injection moulding tool inserts. The basis for production on hybrid cell is that some part of product will be produced with technology, which is the most advantageous for geometry and for material of this part. Therefore, the base part, this is usually the bottom part of injection mould tool, where the geometry of this part is not complex and where the cooling system have only the straight holes, will be manufactured with conventional CNC machining from block of raw material. Another part of products where is curved channels of conformal cooling or another complex geometry is manufactured with additive manufacturing, due this geometry is not economical or possible to make with conventional process. Initially, the block of raw material must to be rigidly clamping on the CNC milling machine. Then the measurement system define the position of workpiece on the clamping system. After these the CNC milling machine can start with machining. On the end of the manufacturing any chips should be removed and cutting fluid be cleansed from the part. Then follows, clamping system with workpiece is positioned on machine for SLM and then operator fills the building chamber of SLM machine with metallic powder. Controller of SLM machine gets the data of X, Y and Z coordinates, and it can begin the AM building on the highest surface of workpiece. On the end of AM operation the part must be removed from the building chamber and all powder needs to be thoroughly removed before the heat treatment. Because demands for surface roughness of tool is very high, the product from SLM machine must be additional treatment on the end of hybrid manufacturing. Therefore, the part is clamped and positioned on CNC milling machine again and it is finish machined. On the end followed the grinding and polishing which for now won't be added in hybrid cell.

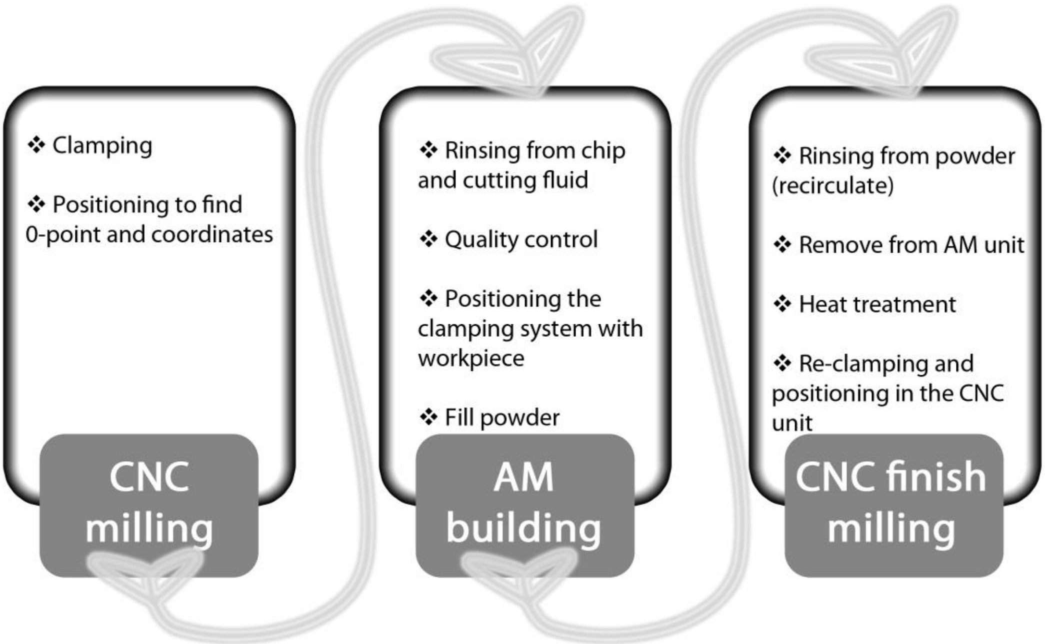

Figure 1. Schematic of workflow for the injection moulding tool insert in the hybrid cell.

4 Control, clamping and positioning system

The hybrid cell has to be controlled from common control system. This control system will manage the control systems of individual machine from central positions. Another of the most important part of a hybrid cell is the common clamping system. The 5 axis CNC milling machine has an integrated probe measurement system that will be used for positioning and also for quality control. But the additive manufacturing machine doesn't have measurement system, hence is important that have the common clamping system for milling machine and for additive machine. Measurement system on CNC milling machine specify position of workpiece on clamping system, subsequently operator or in the future that will be robot move this workpiece together with clamping system on additive manufacturing machine after the milling operation is finished. CNC controller on milling machine will pass the positioning data through a common control system on controller of additive manufacturing machine. Then additive manufacturing machine can start building the remaining part of an injection tool insert or other product.

We are developing the system for optimizing the manufacturing operational sequence (OMOS) based on defined product features. In other words, this system is the computer software which will automatically recognise which part of product have more advantages for some technology. Subsequently, this program will split the model in two or maybe more parts and it will save part for additive manufacturing in STL format and another part in STEP or similar format which is useful for machining.

5 Material

The best choice of material for making tools with additive manufacturing is basically variations of a maraging tool steal, DIN W.nr. 1.2709. This has among other merits the advantages that it does not harden significantly, during the building process. It is very recommended that the whole products is from same material, but is not necessary [6]. With same material it is eliminated the heat treatment between milling process and additive process. But the maraging tool steel, DIN W.nr. 1.2709. is not suitable for machining, for this reasons we use the Orvar Supreme steel from Uddeholm. In this case the milled part will have to be heat treated prior to AM-building and because of this it must be clamped and positioned again.

6 Conclusion

As described above, in order for the hybrid cell to be useful there are a number of requirements to be fulfilled. Even if the hybrid cell is still under development, provides several advantages or manufacturing the injection moulding tool inserts with conformal cooling channel or for a variety of different types of products. A hybrid cell will be interested by toolmaker if we will reach high level of integration and automation in a hybrid cell.

When we achieve all of this requirements listed above, it will be a lot of another opportunity for future work. Filling powder in building chamber on additive machine is very time-consuming manual process. But this process is very difficult to automate. Even more difficult is to remove loose powder after the additive machine finish job, because the metal powder remains in channel of conformal cooling or in another closed shape. Further, in the future more units, as the grinding machine or polishing machine, will be added in this hybrid cell.

References

[1] K.P. Karunakaran, S. Suryakumar, Vishal Pushpa, Sreenathbabu Akula, Low cost integration of additive and subtractive processes for hybrid layered manufacturing, Robotics and Computer-Integrated Manufacturing, Volume 26, Issue 5, October 2010, Pages 490-499, ISSN 0736-5845, DOI: 10.1016/j.rcim.2010.03.008.

[2] Olivier Kerbrat, Pascal Mognol, Jean-Yves Hascoet, A new DFM approach to combine machining and additive manufacturing, Computers in Industry, In Press, Corrected Proof, Available online 6 May 2011, ISSN 0166-3615, DOI: 10.1016/j.compind.2011. 04.003.

[3] Todd Grimm: User’s guide for rapid prototyping, United States of America, Society of manufacturing Engineers, 2004, ISBN 0-87263-697-6

[4] Gerd Pötsch, Walter Michaeli: Injection molding: an introduction, Munich, Carl Hansen Verlag, 2008, ISBN 978-1-56990-419-0

[5] S.O. Onuh, K.K.B. Hon, Optimising build parameters for improved surface finish in stereolithography, International Journal of Machine Tools and Manufacture, Volume 38, Issue 4, March 1998, Pages 329-342, ISSN 0890-6955, DOI: 10.1016/S0890-6955(97)00068-0.

[6] U, Artiček, S. Stepišnik, M. Milfelner, I Anžel, Povečanje produktivnosti orodij za brizganje plastike s pomočjo laserske tehnologije LENS, Vir znanja in izkušenj za stroko: zbornik foruma 4. industrijski forum IRT, pp. 49 – 54, Portorož, Slovenia, 11th and 12th june 2012 ;

Experiences from Small Prototype Workshop

P. Drešar[1], M. Jerman[1], A. Lebar[1]

[1] *University of Ljubljana, Slovenia*

Abstract

Abrasive water jet (AWJ) is a non-conventional machining process. It's most striking advantage is the absence of the heat affected zone. A broad spectrum of materials can be successfully machined with the AWJ machining, regardless of material brittleness, ductility or composition. Despite being superior also AWJ has its own intrinsic drawbacks. Characteristic striations on workpiece surface left after machining, taper of the cut, delamination of the composite materials and undesirable wetting of the sensitive material are problems which has to be addressed just in time in the workshop.
An overview of examples in a small prototype workshop is given regarding the materials, dimensions, handling problems and cost. It is interesting how experiences are combined with a model which is implemented in the AWJ machine software.
Suggestions are given for different possible upgrades and improvements of the AWJ machine to simplify operator's work.

Keywords: AWJ, nonconventional machining, cutting, taper, piercing

1 Introduction

Water jet (WJ) (Figure 1. a) and abrasive water jet (AWJ) (Figure 1. b) machining found its place in the industry due to superior machining performance. Various types of materials can be machined with great success. Potential of AWJ can be used at its best in the frame of prototype or small batch production, since workpieces are very different regarding the size, thickness and material composition.

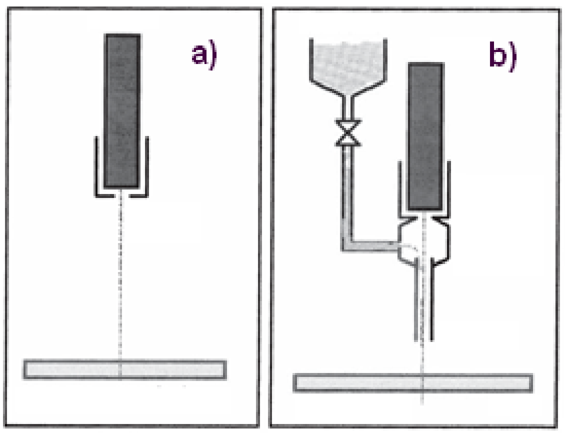

Figure 1. WJ cutting head a), and AWJ cutting head b).

Cutting tool in the AWJ machining is a high speed water jet. When needed an abrasive material is entrained in the jet in order to improve the material removal rate. “The tool” therefore remains always the same, regardless the workpiece material and travels towards the workpiece at the speed of nearly 900 m/s. Despite the multi-functionality of the machining process issues emerge permanently and which have to be addressed regularly.
In this paper it is reported on some challenges which emerged in the workshop, our perception of these challenges and the solutions implemented.

It was found out, that issues can be categorised in three several groups (Figure 1). In the first group there are issues connected with a workpiece size, in the second group are issues connected with defects and damage which occurs at the piercing and in the third group there are problems connected with clamping, positioning i.e. handling of the workpiece.

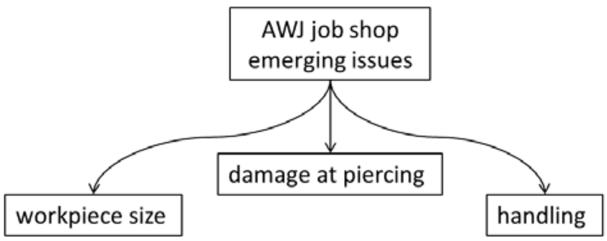

Figure 2. Issues categorised in three groups.

2 Workpiece size

When cutting workpieces of smaller dimensions, usual clamping with quick release bar clamp tool to the working table of the catcher tank is not possible. It is due to the fact, that the spacing of the supporting grid is too large to support very small pieces. In that case a vise clamp tool should be used (Figure 3).

Figure 3. Workpiece in the vise clamp tool.

Clamping in the vise clamp tool is usually rigid enough to achieve the tolerances usual for the AWJ machining. Special care should be applied in order that protruding (exiting) jet not damages the vise tool. Usually the finished workpieces are left on the supporting lamellae, but small pieces can be easily lost in the catcher tank. In order to avoid this from happening, a small bridge of material is added between the product and the waste material as it is shown in the Figure 4. Bridge material is after the machining braked on safe place where product can't be lost.
In the cases when workpiece surface is flat from the bottom side an double side adhesive tape can be used instead of the vise clamp tool.

The base material on which the workpiece is adhesively attached should be of precisely right material structure. It has to be rigid enough to give support but soft enough to enable WJ easy to transition. A polystyrene foam with commercial name Styrodur is very appropriate.

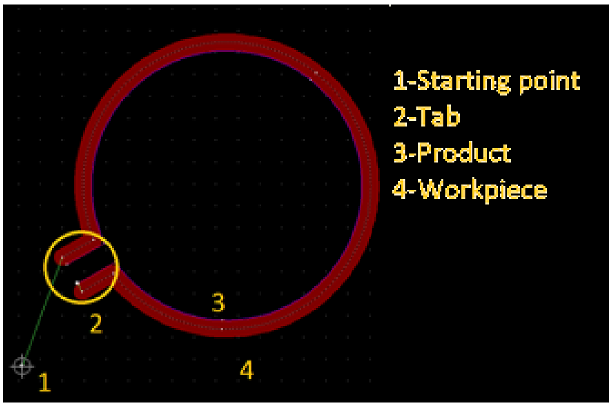

Figure 4. The bridge of material between the product and the waste material.

3 Damage by piercing

When machining the work piece from brittle materials or composites the defects can occur during the penetration of high-speed water jet through material. Damage on the brittle material is usually in the form of a fragment of detached material. Example of damage in brittle material is shown in the Figure 5.

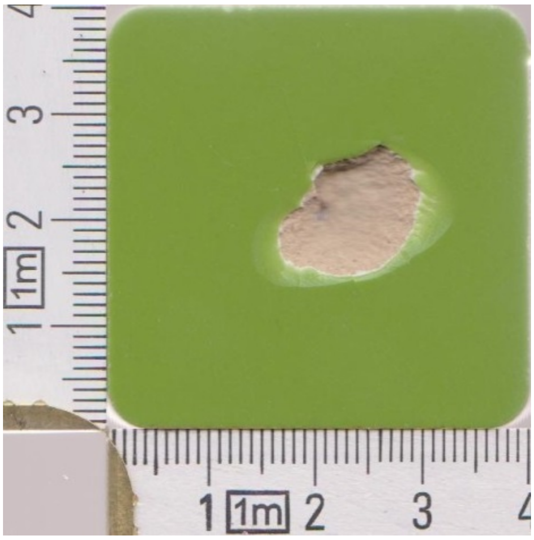

Figure 5. Example of piercing in ceramic material.

Damage in composite materials is usually inside the material, due to the delamination of layers of composite material. Example of damage in brittle material is shown in the Figure 6.
Damage is more expressed in the phase of piercing of workpiece material. Useful advice is therefore to avoid turning the WJ when cutting head is positioned over the workpiece material and start the cut on the edge of the workpiece as it is shown in the Figure 7.

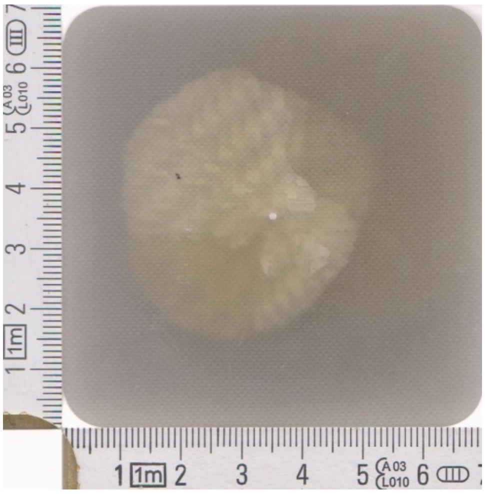

Figure 6. Example of piercing in fiberglass material.

If there is the demand to make a hole in the material it is advised to make a piercing in the middle of the waste material.

Figure 7. Cutting of glass. AWJ was turned on outside of the workpiece.

This strategy is feasible if there is enough material around the pierced hole. In the case that damaged material extend across the contour of the cut a bore has to be made in the waste material before the AWJ cutting start. In that case there can be problem of positioning when two different tools are used. Combination of two processes in one CNC machine is proved to be the solution.

4 Handling

One characteristic when cutting with AWJ is that there is no heat effected zone in the cutting zone. Therefore this kind of cutting is very appropriate for later metallographic analysis of the workpiece. Universality of such machining process enables cutting of different materials and their combinations. Furthermore it is possible to cut material with changing thickness along the contour. Because of these properties this process has proven successful at machining of intermediate products and used up products meant for further diagnostics such as shown in Figures 8 and 9. These kinds of workipeces are often of complex shapes which make it difficult to determine the point of origin of the cut as well as clamping to the work table. For the latter we usually use auxiliary material that is easy to machine and offers additional support during the cutting process. After this the operator can determine the point of origin form the characteristic point on the workpiece by means of visual inspection.

Figure 8. Workpiece meant for metallographic analysis.

Additional measure of precaution of the operator is needed when machining the wokrpiece where there is a possibility of defects during the cutting process. Such cases for example are the cutting of glass pieces or where the point of origin has to be determined either very precisely or for a series of intermediate products. The operator has to be careful to provide sufficient support for the workpiece so that the waste part doesn't chip off the product. In some cases extra care must be taken to prevent abrasive from damaging the surface of the workpiece and to prevent the water from evaporating which would leave a mark from the limescale on the surface.

Figure 9. Workpiece resting on the work table after the cutting process.

5 Conclusion

It is both evident and logical that working on prototypes is a very diverse task that demands an experienced operator with waste knowledge of different processes and materials. AWJ machine has proven to be an indispensable tool when trying to fulfil the variety of client demands but as described in the paper the software tools are not enough for such a versatile work. As was shown on different examples, the operator must be experienced enough to predict the possible complications. Because the series are usually small and unique it seldom happens that the operator will have the luxury of dealing with the same problem more than once. This demands that the person operating the machine is also very flexible and able to solve a variety of different technological problems.

Overall this paper provides the inside in the work of the AWJ machine operator. It shows the limitations and problems as well as the advantages that having a machine like AWJ in the workshop offers.

References

[1] http://www.intexglass.net/Water_Jet_Cutting_Machine.html

[2] B. Jurisevic, M. Junkar: Adaptive Control Constraint (ACC) of Abrasive Water Jet (AWJ) Cutting. In Proc. of 2nd Int. Conf. on Water Jet Machining, pp. 71-76, Cracow, Poland, 15-16 Nov., 2001.


New MV-series Wire-Cut EDMs
Grand Tubular
MV1200R/MV2400R
NUI
Natural
User
Interface
NUI - Easy operation
Intelligent AT
Intelligent AT -
Innovative automatic wire threading
MV2400R
MITSUBISHI
PFC
Precise Finish Circuit
PFC - Improved productivity
MV2400R
LLS
Long Life System
LLS system -
Energy savings,
low running cost
ODS
Opt Drive System
ODS -
Improved machining accuracy
Wire and Die Sinking Systems

TITAN®

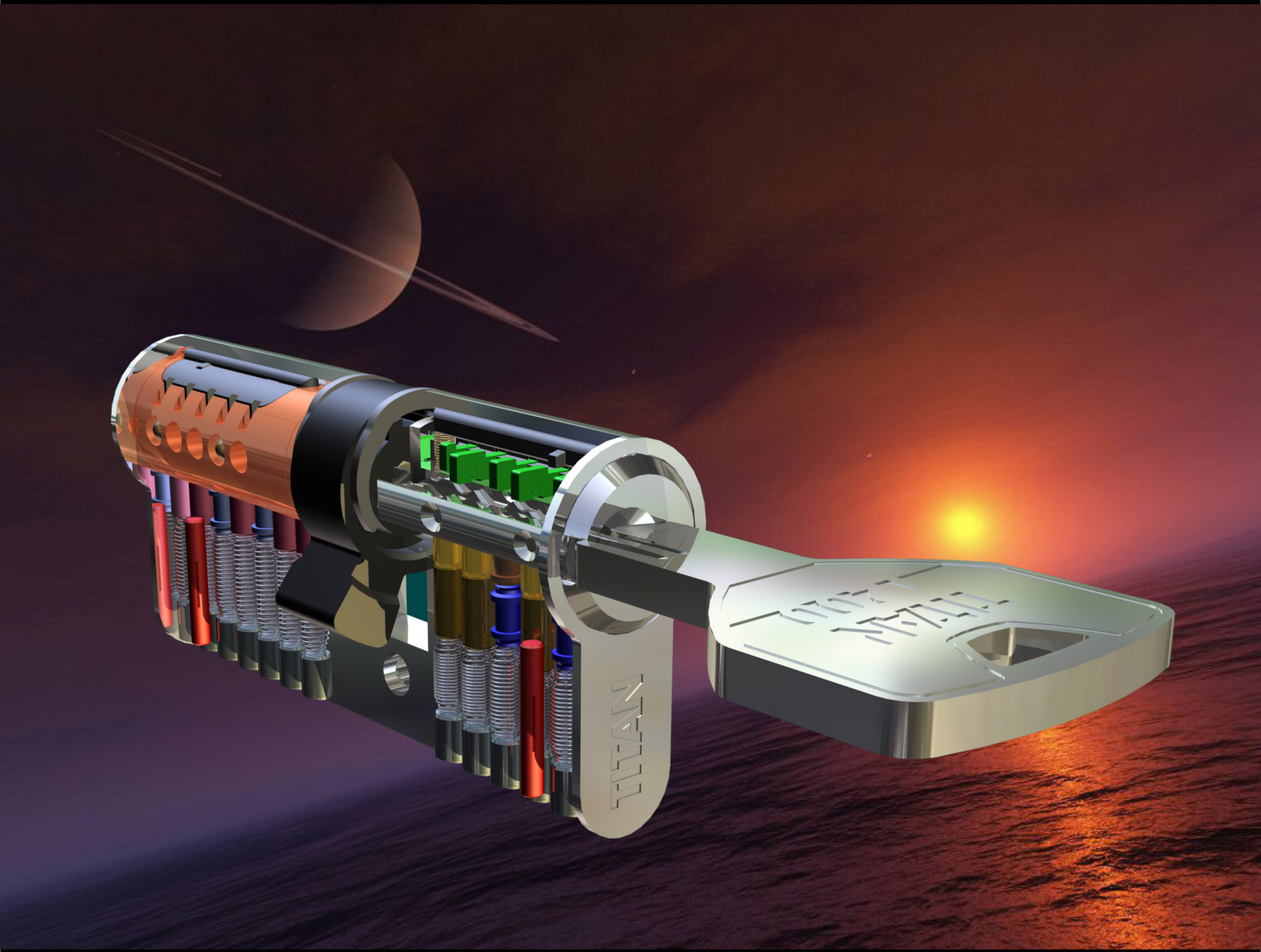

T250

innovation | technology | protection